AUTONOMIC NEUROSCIENCE EDITOR'S PICK 2021

EDITED BY: Vaughan G. Macefield and Joel C. Bornstein
PUBLISHED IN: Frontiers in Neuroscience

frontiers Research Topics

ISSN 1664-8714
ISBN 978-2-88971-060-7
DOI 10.3389/978-2-88971-060-7

About Frontiers

Frontiers is more than just an open-access publisher of scholarly articles: it is a pioneering approach to the world of academia, radically improving the way scholarly research is managed. The grand vision of Frontiers is a world where all people have an equal opportunity to seek, share and generate knowledge. Frontiers provides immediate and permanent online open access to all its publications, but this alone is not enough to realize our grand goals.

Frontiers Journal Series

The Frontiers Journal Series is a multi-tier and interdisciplinary set of open-access, online journals, promising a paradigm shift from the current review, selection and dissemination processes in academic publishing. All Frontiers journals are driven by researchers for researchers; therefore, they constitute a service to the scholarly community. At the same time, the Frontiers Journal Series operates on a revolutionary invention, the tiered publishing system, initially addressing specific communities of scholars, and gradually climbing up to broader public understanding, thus serving the interests of the lay society, too.

Dedication to Quality

Each Frontiers article is a landmark of the highest quality, thanks to genuinely collaborative interactions between authors and review editors, who include some of the world's best academicians. Research must be certified by peers before entering a stream of knowledge that may eventually reach the public - and shape society; therefore, Frontiers only applies the most rigorous and unbiased reviews.
Frontiers revolutionizes research publishing by freely delivering the most outstanding research, evaluated with no bias from both the academic and social point of view. By applying the most advanced information technologies, Frontiers is catapulting scholarly publishing into a new generation.

What are Frontiers Research Topics?

Frontiers Research Topics are very popular trademarks of the Frontiers Journals Series: they are collections of at least ten articles, all centered on a particular subject. With their unique mix of varied contributions from Original Research to Review Articles, Frontiers Research Topics unify the most influential researchers, the latest key findings and historical advances in a hot research area! Find out more on how to host your own Frontiers Research Topic or contribute to one as an author by contacting the Frontiers Editorial Office: frontiersin.org/about/contact

AUTONOMIC NEUROSCIENCE EDITOR'S PICK 2021

Topic Editors:
Vaughan G. Macefield, Baker Heart and Diabetes Institute, Australia
Joel C. Bornstein, The University of Melbourne, Australia

Citation: Macefield, V. G., Bornstein, J. C., eds. (2021). Autonomic Neuroscience Editor's Pick 2021. Lausanne: Frontiers Media SA. doi: 10.3389/978-2-88971-060-7

Table of Contents

frontiers in Neuroscience

REVIEW
published: 23 January 2019
doi: 10.3389/fnins.2018.01058

Sympathetic Nervous System Activation and Its Modulation: Role in Atrial Fibrillation

*Revathy Carnagarin[1], Marcio G. Kiuchi[1], Jan K. Ho[1], Vance B. Matthews[1] and Markus P. Schlaich[1,2,3]**

[1] Dobney Hypertension Centre, School of Medicine, Royal Perth Hospital Unit, Medical Research Foundation, The University of Western Australia, Perth, WA, Australia, [2] Departments of Cardiology and Nephrology, Royal Perth Hospital, Perth, WA, Australia, [3] Neurovascular Hypertension and Kidney Disease Laboratory, Baker Heart and Diabetes Institute, Melbourne, VIC, Australia

The autonomic nervous system (ANS) has a significant influence on the structural integrity and electrical conductivity of the atria. Aberrant activation of the sympathetic nervous system can induce heterogeneous changes with arrhythmogenic potential which can result in atrial tachycardia, atrial tachyarrhythmias and atrial fibrillation (AF). Methods to modulate autonomic activity primarily through reduction of sympathetic outflow reduce the incidence of spontaneous or induced atrial arrhythmias in animal models and humans, suggestive of the potential application of such strategies in the management of AF. In this review we focus on the relationship between the ANS, sympathetic overdrive and the pathophysiology of AF, and the potential of sympathetic neuromodulation in the management of AF. We conclude that sympathetic activity plays an important role in the initiation and maintenance of AF, and modulating ANS function is an important therapeutic approach to improve the management of AF in selected categories of patients. Potential therapeutic applications include pharmacological inhibition with central and peripheral sympatholytic agents and various device based approaches. While the role of the sympathetic nervous system has long been recognized, new developments in science and technology in this field promise exciting prospects for the future.

Keywords: autonomic nervous system, hypertension, neuromodulation, atrial fibrillation, sympathetic overdrive

OPEN ACCESS

Edited by:
Alberto Porta,
University of Milan, Italy

Reviewed by:
Michela Masè,
University of Trento, Italy
Raffaello Furlan,
Humanitas Research Hospital, Italy

***Correspondence:**
Markus P. Schlaich
markus.schlaich@uwa.edu.au

Specialty section:
This article was submitted to Autonomic Neuroscience, a section of the journal Frontiers in Neuroscience

Received: *03 September 2018*
Accepted: *31 December 2018*
Published: *23 January 2019*

Citation:
Carnagarin R, Kiuchi MG, Ho JK, Matthews VB and Schlaich MP (2019) Sympathetic Nervous System Activation and Its Modulation: Role in Atrial Fibrillation. Front. Neurosci. 12:1058. doi: 10.3389/fnins.2018.01058

CARDIAC AUTONOMIC NERVOUS SYSTEM (ANS) ANATOMY

The heart is extensively innervated and effectively regulated by the autonomic nervous system (ANS) through its sympathetic and parasympathetic branches (Kimura et al., 2012). The cardiac neural control occurs at multiple levels with each level capable of parallel processing of afferent neurotransmission and efferent cardiac sympathetic outflow (Esler, 2004). The ganglion cells of the ANS are located either inside (intrinsic) or outside the heart (extrinsic) and play an important role in cardiac function and arrhythmogenesis. The human cardiac intrinsic nervous system is made of ganglionated plexi (GP), which contain local circuit neurons of many types and chemo- and mechanosensory neurons that are distributed across the heart (Schotten et al., 2011). The GP are typically well innervated with both adrenergic and vagal nerve terminals and are accommodated

in the fat pads, which are located mainly around the pulmonary vein ostia. The extrinsic sympathetic innervation is mediated via the cervical, stellate (cervicothoracic), and thoracic ganglia. Parasympathetic extrinsic innervation is transmitted via the vagus nerve, although sympathetic fibers are located in vagal nerves and parasympathetic fibers in sympathetic nerves as well (Kawashima, 2005; Seki et al., 2014).

The extrinsic nerves run through the hilum of the heart along the great cardiac vessels and divide into seven epicardial subplexi, the intrinsic neural pathways of the ANS (Pauza et al., 2000). Small nerve fibers create a vast neural complex of small interconnecting efferent and afferent sympathetic, parasympathetic, and mixed nerve fibers, that contain the neurotransmitters, such as noradrenaline and acetylcholine, respectively, but some also include neuropeptide Y, somatostatin, vasoactive intestinal polypeptide, and substance P (Marron et al., 1994, 1995; Armour et al., 1997; Esler et al., 2006a; Tan et al., 2006; Deneke et al., 2011). The density of small fibers and ganglia is most significant in the posterior zone of the left atrium and surrounding the antrum of the left pulmonary veins (PVs) (Chevalier et al., 2005; Tan et al., 2006). The atria are mostly parasympathetically innervated, whereas the ventricles are primarily innervated by sympathetic nerve fibers (where only 16% of total cardiac ganglia reside) (Pauza et al., 2000; Kawano et al., 2003; Petraitiene et al., 2014). GP are clusters of ganglia from different subplexi and function as an intersection point of parasympathetic and sympathetic nerves and interconnect the intrinsic ANS (Armour et al., 1997; Hou et al., 2007; Malcolme-Lawes et al., 2013). The atrial GP are placed adjacent to the sinus node and PVs and are present in epicardial fat pads (**Figure 1**). Ventricular GP are located near the interventricular groove (Armour et al., 1997). The ligament of Marshall, the embryonic remnant of the left superior caval vein, close to the left superior PV is extensively innervated with parasympathetic and sympathetic nerves (Kim et al., 2000; Ulphani et al., 2007).

PATHOPHYSIOLOGY OF ATRIAL FIBRILLATION

Autonomic nervous system activation has been well-known as a central determining factor of atrial arrhythmogenesis, (Sharifov et al., 2004; Chen and Tan, 2007; Shen et al., 2011; Shen and Zipes, 2014). Studies involving modulation of the sympathetic limb of ANS demonstrated that suppression of sympathetic tone leads to a notable reduction in atrial vulnerability to AF induction and post-ablation AF recurrence (Linz et al., 2012; Pokushalov et al., 2012). The prevalence of AF increases with age, affecting around 0.5% of the general population under 40 years of age, >5% of the general population over 65 years of age, and >10% of the general population over 80 years of age (Sankaranarayanan et al., 2013). In young patients, there was a shift toward vagal dominance in lone AF and nocturnal paroxysmal AF predominantly (Jayachandran et al., 2000). In patients with paroxysmal AF and syncope, there is an abnormal neural response even during sinus rhythm, at which AF triggers vasovagal syncope (Brignole et al., 1993). It is also important to highlight that AF in younger patients is associated with higher mortality rate than matched controls. Patients admitted into the hospital with incidental AF had a worse prognosis when compared to patients without AF, with higher risk of all-cause mortality in the younger age group when compared to the over-75-year-old population (Andersson et al., 2013).

Atrial fibrillation promotes shortening of the atrial refractory period and AF cycle length during the first days of the arrhythmia, mostly due to downregulation of the Ca^{2+}-inward current and upregulation of inward rectifier K^{+} currents (Van Wagoner et al., 1999; Dobrev et al., 2005). Conversely, the structural cardiac disease leads to an extension of the atrial refractory period, demonstrating the heterogeneity of mechanisms causing AF in different patients (Schotten et al., 2011). Hyper-phosphorylation of various Ca^{2+}-handling proteins may contribute to increasing spontaneous Ca^{2+} release events and eliciting activity (Voigt et al., 2012, 2014), thus provoking atrial ectopic beats, and thereby AF. Interestingly, the instability theory of Ca^{2+}-handling has been recently challenged (Christ et al., 2014; Greiser et al., 2014), raising the hypothesis that Ca^{2+}-induced calcium release may mediate AF in structurally remodeled atria, demonstrating how a modified autonomic tone can cause AF (Nguyen et al., 2009).

Focal Initiation and Maintenance of AF

Haissaguerre et al. (2014) reported that a focal source in the pulmonary veins could initiate AF, and ablation of this source could eliminate recurring AF (Haissaguerre et al., 1998). The mechanisms of focal activity perhaps cover both triggered activity and local re-entry (Atienza et al., 2006; Patterson et al., 2007). Hierarchical organization of AF with rapidly activated zones promoting the arrhythmia has been demonstrated in individuals with paroxysmal AF (Mandapati et al., 2000; Sahadevan et al., 2004). However, it seems that the organization of these rapidly activated zones are less well demarcated in patients with persistent AF (Sanders et al., 2006).

The Multiple Wavelet Hypothesis and Rotors as Sources of AF

The multiple wavelets and organized sources theories, though unclear are the two principal proposed paradigms of AF perpetuation. Moe et al. (1964) proposed, through a mathematical model, that multiple wavelets randomly propagating through the atria are capable of perpetuating AF which in turn provoke wave breaks, and generates new daughter wavelets. Though AF would be sustained as long as the number of wavelets is beyond a critical level, it is still unknown whether these wavelets are driving AF or if they are simply passive, and result from the breakup of more organized waves. Whilst the multiple wavelet concept is supported by theoretical rationale (Moe and Abildskov, 1959), experimental and clinical data (Cox et al., 1991), optical mapping techniques identified that wavelets resulting from the breakup of high frequency organized waves were not capable of maintaining AF independently (Chen et al., 2000). In patients with longstanding AF, the fibrillatory waves are due to epicardial breakthrough of waves that propagate in the deep layers of the atrial wall providing a constant independent

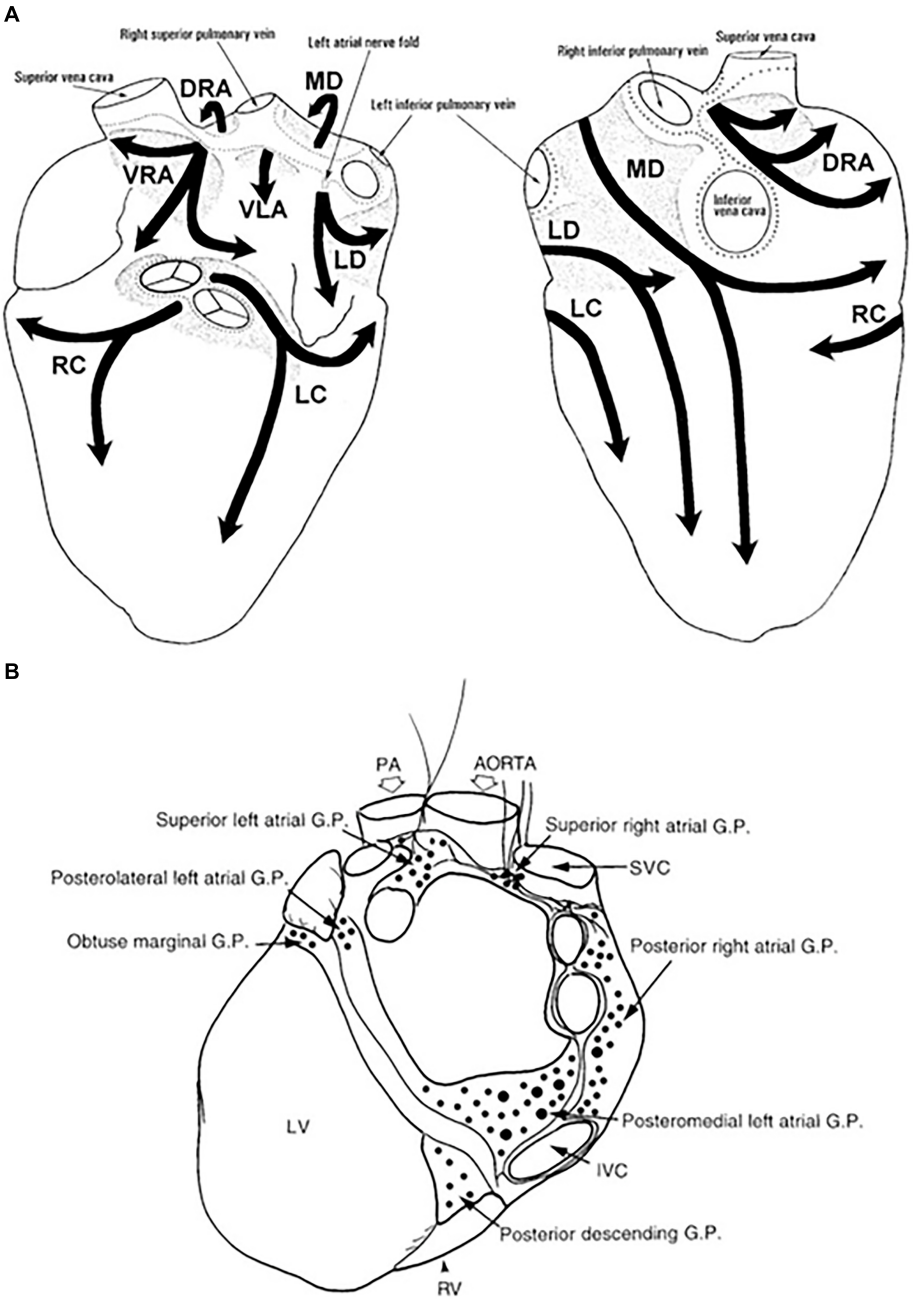

FIGURE 1 | Anatomy of the intrinsic autonomic nervous system. The extensive network of epicardial nerves on the atria and ventricles are divided in 7 subplexi: **(A)** Left is a posterior and right is an anterior view of the heart. Along these subplexi, ganglia are localized, conglomerated in ganglion plexi (GP) marked in light gray (Pauza et al., 2000). **(B)** The major atrial and ventricular GP from a posterior view of the heart (Armour et al., 1997). DRA, dorsal right atrial ganglionated subplexus; IVC, inferior vena cava; LC, left coronary ganglionated subplexus; LD, left dorsal ganglionated subplexus; LV, left ventricle; MD, middle dorsal ganglionated subplexus; PA, pulmonary artery; RC, right coronary ganglionated subplexus; RV, right ventricle; SVC, superior vena cava; VLA, ventral left atrial ganglionated subplexus; VRA, ventral right atrial ganglionated subplexus.

source originating over the entire epicardial surface (Allessie et al., 2010; de Groot et al., 2010). Early ablative termination of AF in the PV may not completely abolish the presence of PV antrum wavelets over time, which can in turn cause AF (Haissaguerre et al., 2005; Calkins et al., 2012) resulting in limited clinical impact (Beukema et al., 2008).

Studies showed the presence of high-frequency spiral wave-like activity emanating regularly from the left atrium, subsequently driving irregular fibrillatory conduction in the rest of the atria (Schuessler et al., 1992; Mandapati et al., 2000; Verheule et al., 2010) whilst complex signal morphologies were associated with areas of slow conduction, wave collision,

fibrillatory conduction, turning into wavelet pivot points and rotor meandering, or autonomic activation (Lu et al., 2008; Vaquero et al., 2008; Zlochiver et al., 2008). Localized source premise is based on experimental models in which organized re-entrant circuits, called "rotors" (Skanes et al., 1998; Vaquero et al., 2008) or focal impulses (Sahadevan et al., 2004) disorganize into AF. Jalife and co-workers clearly demonstrated that pacing-induced AF was due to the presence of a very rapid rotor (15–20 Hz) in the left atrium (Jalife et al., 2002). The CONFIRM trial demonstrated for the first time that localized sources in the form of electrical rotors and focal impulses are capable of sustaining AF in humans (Narayan et al., 2012). Furthermore, they also proved that brief ablation (Focal Impulse and Rotor Modulation, FIRM) of patient-specific AF-sustaining sources was able to terminate or consistently reduce persistent or paroxysmal AF prior to any conventional ablation in 86% of patients, and substantially increase long-term AF elimination compared to traditional AF ablation alone (Narayan et al., 2012). However, the results of the CONFIRM trial were limited to small series of patients with mixed AF types, so the actual role of stable rotors in more persistent forms remains to be proven. Further, in the absence of convincing evidence that human AF is driven by a single rotor, it is puzzling how we should interpret the CONFIRM study. In itself, this observation does not prove that human AF is driven by a single rapid source and the reported clinical success needs to be confirmed by other centers, especially in patients with longstanding persistent AF (Allessie and de Groot, 2014). Moreover, these studies utilize a low-resolution mapping system, which is not completely satisfactory in delivering mechanistic insights to draw conclusions (Ravelli and Mase, 2014). However, the high success rate of AF termination by targeting identified local sources strongly supports the hypothesis of rapidly organizing sources as key for the maintenance of AF.

CLINICAL CONDITIONS THAT MAY ACT AS PREDISPOSING FACTORS TO AF

Multiple cardiovascular diseases and associated conditions increase the risk of developing AF (**Table 1**), recurrent AF, and AF-related consequences. Diagnosing such conditions, as well as preventing and treating them are vital to prevent AF and its disease burden. Knowledge of these factors and their management is therefore important for optimal treatment of AF patients (Abed et al., 2013; Pathak et al., 2014). The ANS exerts significant control on both cardiac electrophysiology as well as conditions such as, hypertension which is often associated with exaggerated sympathetic tone and is the single most important clinical factor that accounts for around 80% of AF (Schotten et al., 2011). This is further complicated by the associated atrial remodeling and dilatation that increases the probability of repetitive firing or even the presence of episodic re-entrant activation circuits. Other clinical conditions commonly associated with AF include cardiomyopathy, valvular and coronary heart disease, heart failure, metabolic syndrome and diabetes, suggested to contribute to around 20–30% of AF cases (Psaty et al., 1997; Schoonderwoerd et al., 2008; Mahfoud et al., 2011; Schotten et al., 2011; Selmer et al., 2012; Schnabel et al., 2015; Vermond et al., 2015). These clinical pathologies induce electrical, structural and autonomic atrial

TABLE 1 | Cardiovascular and other conditions independently associated with atrial fibrillation.

Characteristic/comorbidity	Association with AF
Genetic predisposition (based on multiple common gene variants associated with AF)	HR range 0.4–3.2
Older age	HR:
50–59 years	1.00 (reference)
60–69 years	4.98 (95% CI 3.49–7.10)
70–79 years	7.35 (95% CI 5.28–10.2)
80–89 years	9.33 (95% CI 6.68–13.0)
Hypertension (treated) vs. none	HR 1.32 (95% CI 1.08–1.60)
Heart failure vs. none	HR 1.43 (95% CI 0.85–2.40)
Valvular heart disease vs. none	RR 2.42 (95% CI 1.62–3.60)
Myocardial infarction vs. none	HR 1.46 (95% CI 1.07–1.98)
Thyroid dysfunction	(reference: euthyroid)
Hypothyroidism	HR 1.23 (95% CI 0.77–1.97)
Subclinical hyperthyroidism	RR 1.31 (95% CI 1.19–1.44)
Overt hyperthyroidism	RR 1.42 (95% CI 1.22–1.63)
Obesity	HR:
None (BMI < 25 kg/m^2)	1.00 (reference)
Overweight (BMI 25–30 kg/m^2)	1.13 (95% CI 0.87–1.46)
Obese (BMI ≥ 31 kg/m^2)	1.37 (95% CI 1.05–1.78)
Diabetes mellitus vs. none	HR 1.25 (95% CI 0.98–1.60)
Chronic obstructive pulmonary disease	RR:
FEV1 $\geq 80\%$	1.00 (reference)
FEV1 60–80%	1.28 (95% CI 0.79–2.06)
FEV1 $< 60\%$	2.53 (95% CI 1.45–4.42)
Obstructive sleep apnoea vs. none	HR 2.18 (95% CI 1.34–3.54)
Chronic kidney disease	OR:
None	1.00 (reference)
Stage 1 or 2	2.67 (95% CI 2.04–3.48)
Stage 3	1.68 (95% CI 1.26–2.24)
Stage 4 or 5	3.52 (95% CI 1.73–7.15)
Smoking	HR:
Never	1.00 (reference)
Former	1.32 (95% CI 1.10–1.57)
Current	2.05 (95% CI 1.71–2.47)
Alcohol consumption	RR:
None	1.00 (reference)
1– 6 drinks/week	1.01 (95% CI 0.94–1.09)
7–14 drinks/week	1.07 (95% CI 0.98–1.17)
15–21 drinks/week	1.14 (95% CI 1.01–1.28)
>21 drinks/week	1.39 (95% CI 1.22–1.58)
Habitual vigorous exercise	RR:
Non-exercisers	1.00 (reference)
<1 day/week	0.90 (95% CI 0.68-1.20)
1-2 days/week	1.09 (95% CI 0.95-1.26)
3-4 days/week	1.04 (95% CI 0.91-1.19)
5-7 days/week	1.20 (95% CI 1.02-1.41)

AF, atrial fibrillation; BMI, body mass index; CI, confidence interval; FEV1, forced expiratory volume in 1 s; HR, hazard ratio; OR, odds ratio; RR, risk ratio. Adapted from Kirchhof et al. (2016).

remodeling which results in conduction abnormalities such as rapidly firing focus and multiple complex (Buch et al., 2003; Gami et al., 2007; Aizer et al., 2009; Chamberlain et al., 2011; Kim et al., 2014; Larsson et al., 2014) re-entrant circuits, thereby AF (**Figure 2**). In addition, increased renin-angiotensin-aldosterone system activity associated with sympathetic overdrive induced profibrotic cardiac signaling, atrial fibrosis and fibrillation (Kumagai et al., 2003; Ehrlich et al., 2006; Baber et al., 2011; Reil et al., 2012).

Autonomic remodeling may modify the reaction to ANS stimulation and the balance between the parasympathetic and sympathetic innervation (Coumel, 1996; Patterson et al., 2005; Furukawa et al., 2009; Ng et al., 2011; Shen et al., 2011). Increased sympathetic nerve density has been described in patients with permanent AF, but whether this is compensatory to increased vagal stimulation or causative of AF is unknown (Gould et al., 2006; Deneke et al., 2011). A heterogeneous increase in sympathetic innervation in the atria of dogs on rapid atrial pacing for long periods increases AF susceptibility (Jayachandran et al., 2000). Increased sympathetic and vagal nerve discharges before the onset of atrial arrhythmias in dogs with pacing-induced congestive heart failure by direct nerve recordings from the stellate ganglia and vagal nerves was also reported (Ogawa et al., 2007). Undeniably, atrial tachyarrhythmias in dogs presenting with congestive heart failure by fast cardiac pacing were prevented by prophylactic ablation of the stellate ganglion and the T2 to T4 thoracic sympathetic ganglia (Ogawa et al., 2007). In the same animal model of heart failure, Ng et al., also demonstrated increased sympathetic and parasympathetic nerve growth mostly in the pulmonary veins and the posterior wall of the left atrium (Ng et al., 2011).

In humans, PV ectopy, often originating from superior PVs, normally triggers paroxysmal AF (Haissaguerre et al., 1998). Animal and human studies have shown that stimulation of the GP close to PV triggers PV ectopies (Scherlag et al., 2005; Lim et al., 2011). In canine PVs, parasympathetic activation decreased action potential duration, while sympathetic activation increased myocardial cytoplasmatic (Ca^{2+}) (Patterson et al., 2005). Both components were necessary for early afterdepolarizations in PVs, consequently triggering AF. Ectopic activity in other highly innervated structures (ligament of Marshall) possibly also triggers AF (Chevalier et al., 2005; Scherlag et al., 2005; Tan et al., 2006). During catheter ablation procedures stimulation of the ligament of Marshall caused ectopic beats and triggered AF

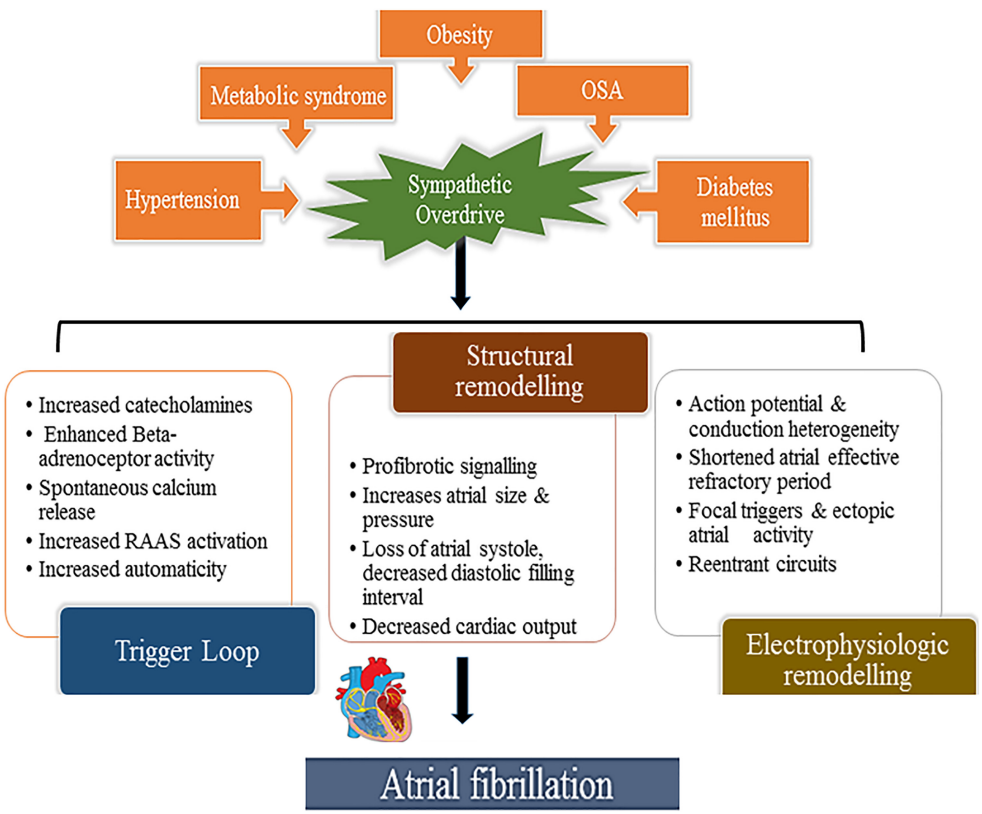

FIGURE 2 | Aberrant sympathetic activation in conditions such as obesity (and particularly increased epicardial fat), hypertension, obstructive sleep apnea, diabetes mellitus and metabolic syndrome plays a fundamental role in the development of AF. Sympathetic activation through excess catecholamines in the circulation which increases calcium entry and the spontaneous release from the myocardial sarcoplasmic reticulum leading to enhanced automaticity (trigger loop) and enhanced renin-angiotensin-aldosterone provokes pro-fibrotic signaling in the myocardium altering atrial size, pressure and consequent structural remodeling thereby inducing focal triggers and atrial ectopies. This occurs hand in hand with atrial electrical remodeling with shortened action potential duration, conduction disturbances, also facilitating re-entry circuits, promoting and sustaining AF.

(Báez-Escudero et al., 2014). On the other hand, AF triggers are not restrained to densely innervated tissue alone. A study reported that in ∼30% of patients who required a repeat PV isolation ectopic firing from the left atrial appendage was detected (Di Biase et al., 2010).

Intense atrial fibrosis formation and cardiomyocyte hypertrophy are common features of structural remodeling. Atrial tissue fibrosis damages electrophysiological cell-to-cell coupling and conduction (Allessie et al., 2001; Nattel, 2002; Iwasaki et al., 2011; Schotten et al., 2011; Wakili et al., 2011). Long-term AF induces myocyte hypertrophy and increases endomysial fibrosis. This is accompanied by dissociated conduction and electrical dissociation between the epicardial layer and the endocardial bundle connections frequently promoting permanent forms of AF (Eckstein et al., 2011; Schotten et al., 2011). Conditions other than AF can also lead to atrial structural remodeling including chronic arterial hypertension which has been shown to cause electro-structural changes characterized by conduction abnormalities, atrial inflammation and fibrosis thereby increasing the risk of AF induction (Lau et al., 2010). Congestive heart failure induces structural remodeling characterized by increased fibrosis and changes in gap junctions, provoking conduction heterogeneity which promotes formation of micro-re-entry and macro-re-entry circuit pathways (Li et al., 1999). Long-term obstructive sleep apnoea is linked to significant atrial remodeling characterized by atrial enlargement, site-specific and extensive conduction abnormalities, as well as delayed sinus node recovery time in humans (Witkowski et al., 2011; Dimitri et al., 2012). The described alterations may have a crucial role in the generation of AF substrates.

Sympathetic activation also plays a major role in atrial arrhythmias following cardiac surgeries and post-operative (post-op) AF is associated with reduced long term survival with cardiac surgeries such as the coronary bypass and valvular surgeries especially the aortic valve replacement (Girerd et al., 2011). Often finding suggestive of enhanced sympathetic activation such as elevated nor-epinephrine levels (Kalman et al., 1995), increased sinus rate, atrial ectopy and time- and frequency-domain parameters of heart rate variability are associated with the onset of AF following cardiac surgeries (Dimmer et al., 1998; Amar et al., 2003). Ventral cardiac denervation significantly reduced the incidence and severity of AF in patients undergoing low-risk coronary bypass surgery (Melo et al., 2004). Post-operative AF is also common in patients who have undergone lung transplantation rather than cardiac transplantation, an effect attenuated by cardiac autonomic denervation that occurs in heart transplant patients (Dizon et al., 2009). Moreover, in a large series of patients following orthotopic cardiac transplant, macro re-entrant tachycardias (flutter and scar re-entry) seem to be the most common supraventricular arrhythmias in stable patients which are often supressed by catheter ablation. The blockade of β-receptors in patients presenting with acute post-operative AF has been effective in preventing recurrence of this arrhythmia after successful cardioversion (Kühlkamp et al., 2000; Nergårdh et al., 2007). Though post-op AF is of multifactorial etiology, sympathetic activation appears to be the most relevant predisposing mechanism of post-op AF and in line with this, the 2010 European Society of Cardiology guidelines recommend β-blocker treatment as first-line therapy in preventing post-op AF following cardiac surgeries (Camm et al., 2010).

SYMPATHOLYTIC THERAPY – A POSSIBLE STRATEGY IN THE MANAGEMENT OF AF?

Pharmacological Sympathetic Inhibition

Given the contribution of sympathetic overdrive in the development of AF, sympathetic inhibition represents a logical therapeutic approach in the management of AF and the frequently coexisting hypertension, thereby alleviating the associated cardiovascular mortality and morbidity. Autonomic dysfunction characterized by sympathetic overdrive in scenarios of organic heart disease exhibits both electrical and structural remodeling of atrial myocardium in AF. Pharmacological sympatholysis can be achieved by using drugs such as clonidine and moxonidine. Clonidine is a centrally acting α2-adrenergic agonist that supresses the sympathetic outflow in the lower brainstem (Flacke et al., 1987), the preganglionic splanchnic nerve fibers and in postganglionic cardiac nerves fibers (Langer et al., 1980). In addition, clonidine prolongs atrioventricular node refractoriness by stimulation of parasympathetic outflow with beneficial effects on the control of ventricular response in patients with new-onset rapid AF (Roth et al., 1992). Moxonidine is an imidazoline I1-receptor agonist that inhibits sympathetic outflow at the level of the rostral ventrolateral medulla. In addition to effective blood pressure (BP) lowering and metabolic benefits (Haenni and Lithell, 1999; Chazova et al., 2006), moxonidine has been demonstrated to suppress atrial arrhythmogenesis (Lepran and Papp, 1994; Edwards et al., 2012; Cagnoni et al., 2016). In a subsequent study, moxonidine significantly increased the threshold dose of ouabain-induced cardiac arrhythmia by decreasing sympathetic tone (Mest et al., 1995). Moreover, moxonidine induced sympathetic inhibition decreased the AF burden in hypertensive patients with paroxysmal AF without any side effects (Deftereos et al., 2013). Furthermore, moxonidine reduced post-ablation recurrence of AF in hypertensive patients who underwent pulmonary vein isolation for drug-refractory paroxysmal AF (Giannopoulos et al., 2014).

Moxonidine seems specifically useful in obesity related hypertension where the sympathetic overdrive sustains both obesity and BP elevation. With the well-established relationship between abdominal obesity, the metabolic syndrome, and the development of AF, obese hypertensives are at a greater risk for AF. Studies have identified that autonomic dysfunction occurs early in the pathophysiology of AF and precedes the development of metabolic abnormalities such as insulin-resistance and obesity (Huggett et al., 2006; Julius and Jamerson, 1994; Palatini et al., 1999) which in turn maintain sympathetic activation via release of adipokines and other bioactive cytokines from visceral fat depots (Grassi et al., 1995; Alvarez et al., 2002; Huggett et al., 2004; Lambert et al., 2007, 2010). Alterations

in norepinephrine transport and central sympathetic outflow have also been implicated in postural tachycardia syndrome (Lambert et al., 2008), anxiety and cardiovascular disease (Esler et al., 2006b), as well as panic disorder (Lambert et al., 2002). Furthermore, studies have shown that epi-/peri-cardial adipose tissue is an independent risk factor for AF (Al Chekakie et al., 2010) and adipocytes from the epicardial fat directly infiltrate into the myocardial wall resulting in enlargement of the ventricular myocardium and atrial septum thereby increasing the risk of AF (Iacobellis et al., 2003; Sarin et al., 2008; Mahabadi et al., 2009). Another highly relevant link in the current context is the noradrenaline-mediated increase in sodium glucose co-transporter- 2 (SGLT-2) expression (Matthews et al., 2017). This is important given that SGLT-2 inhibitors such as canagliflozin effectively reduce epicardial fat (Yagi et al., 2017) and empagliflozin improved glucose control and has been demonstrated to reduce cardiovascular events in T2DM (Zinman et al., 2015).

Sympathetic blockade at the periphery can also be achieved by beta-adrenergic blockers. Though beta-blockers are not generally regarded as membrane stabilizing agents, they delay atrial repolarization and protect against AF. It was speculated that beta-blockers suppress the pulmonary vein ectopy that triggers AF (Chen et al., 1999) as well as protect against adrenergically mediated shortening of the action potential duration (APD) which precipitates and maintains AF (Kühlkamp et al., 2000). Beta-blockers are a good first choice for the control of the ventricular response in AF and are widely used in the prevention of AF in patients following cardiothoracic surgery, in which AF occurs in approximately 30% of patients (Prystowsky et al., 1996).

Device-Based Therapeutic Approaches for Sympathetic Inhibition

Other interventions include device-based therapeutic approaches to modulate ANS to lower central sympathetic nerve activity such as renal denervation (RDN) and carotid body ablation. These approaches are primarily aimed at reducing sympathetic activity and BP in resistant hypertensive patients but are now investigated as potential treatment strategies in the context of AF.

RENAL DENERVATION AND GANGLIONATED PLEXI ABLATION

Recently, the AFFORD study, a single-arm pilot study including 20 patients with symptomatic paroxysmal or persistent AF, suggested that RDN alone was safe and able to decrease AF burden in min/day as measured using an implantable cardiac monitor (ICM) at 12-month follow-up accompanied by an improvement in quality of life (Feyz et al., 2018). A clinical study that assessed the antiarrhythmic effect of RDN in addition to pulmonary vein isolation (PVI) in HTN patients with symptomatic AF demonstrated that a mean BP reduction of 5–10 mmHg led to a 7% decrease in AF burden as measured with an ICM (Romanov et al., 2017). Pokushalov et al. (2012) showed that RDN on top of PVI in patients with symptomatic AF and resistant HTN reduced the incidence of AF recurrence significantly. At 1 year 69% of the patients in the PVI + RDN group were free of AF episodes, while in the PVI only group, only 29% of the patients remained free of AF episodes (Pokushalov et al., 2012).

Mechanistic studies demonstrated that modulation of the SNS via RDN improved AF control (Hou et al., 2013). Linz et al. (2013a,b) demonstrated the effect of RDN on heart rate (RR-interval, 708 ± 12 ms (∼85 bpm) vs. 577 ± 19 ms (∼104 bpm), post- and pre-procedure respectively; $P = 0.0021$) and ventricular rate response in pigs with permanent AF. The authors described a reduction of 24% in ventricular rate response in the treated pigs vs. sham, as well shorter AF episodes post-RDN compared with sham (12 ± 3 vs. 34 ± 4 s; $P = 0.0091$) (Linz et al., 2013a,b). Effects of RDN on cardiac electrophysiology have already been extensively studied and found to be effective in animal models and humans (Okin et al., 2006; Symplicity HTN-2 Investigators et al., 2010; Brandt et al., 2012b). RDN predominantly impacts sympathetic tone and results in a reduction in heart rate and atrioventricular-conduction velocity in resistant hypertension population (Krum et al., 2009; Schlaich et al., 2010; Ukena et al., 2013). Recently, the SPYRAL HTN-OFF MED trial reported that the higher baseline heart rate was associated with higher BP decrease, which may indicate that RDN works better in patients with high sympathetic drive (assessed in the absence of interfering drugs) (Bohm et al., 2018).

In a prospective, longitudinal study of patients with controlled hypertension, paroxysmal AF and either normal renal function or chronic kidney disease (CKD), Kiuchi et al., applying an extensive ablation technique reported the incidence of AF recurrence. It was higher in CKD patients treated with PVI alone (61.5%) than in CKD patients treated with PVI + RDN (38.5%, $P = 0.0251$) or non- CKD patients who underwent PVI (35.6%, $P < 0.0001$) over 22.4 ± 12.1 months following intervention. In addition, they found an improvement in echocardiographic parameters such as indexed left atrial volume, left ventricular end-diastolic diameter, and left ventricular mass index in patients who underwent RDN compared to baseline and to other groups. Another important finding was that patients with CKD stage 4 who underwent only PVI (64.41%) demonstrated a higher rate of AF recurrence than those subjected to PVI + RDN (33.33%, $P = 0.0409$) (Kiuchi et al., 2017).

Chronic kidney disease and AF share risk factors and putative mechanisms suggesting that common pathophysiologic processes may drive both pathologies. One possible common link between AF and CKD is activation of the renin–angiotensin–aldosterone system (RAAS) (Goette et al., 2000; Tsai et al., 2004; Wachtell et al., 2005; Baber et al., 2011; Tsai et al., 2017). Angiotensin II can increase atrial pressure, promote atrial fibrosis, and modulate ion channels, all of which are involved in structural and electrical remodeling of the atria resulting in AF (Goette et al., 2000). In addition, gene polymorphisms in encoding components of this pathway have been linked to the development of AF (Tsai et al., 2004; Lubitz et al., 2014). Supporting these results are data demonstrating that BP reduction after RDN is associated with improvements in regional and global atrial conduction with reduction in ventricular mass and fibrosis (McLellan et al., 2015). Though the antiarrhythmic effects of RDN could be due

to a synergistic effect of better BP control, withdrawing this important risk factor for AF recurrence, improves AF control by electrophysiological modification such as the prolongation of the atrial effective refractory period (Manolis et al., 2012; Wang et al., 2015).

Tsai et al. (2017) demonstrated that bilateral RDN, possibly via interrupting afferent renal innervation, led to substantial brain stem and bilateral stellate ganglion remodeling at 8 weeks' post-procedure in ambulatory canines (Tsai et al., 2017). These changes were associated with reduced ^{18}FDG (fluorodeoxyglucose) – uptake in the brainstem, left stellate ganglion nerve activity and atrial tachyarrhythmic events. It was proposed that neural remodeling in the brain stem and stellate ganglion may partially explain the described antiarrhythmic effects of RDN (Tsai et al., 2017). *Trans*-synaptic degeneration is a phenomenon in the central and peripheral nervous system that may remain active both at the level of the insult and in remote brain structures for as long as 1 year following trauma (Bramlett and Dietrich, 2007) resulting in long-term functional consequences following RDN as shown in **Figure 3**. Meckler and Weaver (1984) showed that approximately 10% of bilateral renal sympathetic neurons in cats originated from the thoracic chain ganglia (stellate through T13). Because of the connections between these two structures, RDN may directly result in retrograde cell death of the stellate ganglion. Furthermore, the application of fluorescent dyes in the renal nerves results in fluorescent labeling of the sympathetic cell bodies in paravertebral and prevertebral ganglia (Ferguson et al., 1986; Gattone et al., 1986; Sripairojthikoon and Wyss, 1987).

Since the sympathetic preganglionic neurons that project to the stellate ganglion are dispersed in spinal cord segments sections T1–T10 (Pilowsky et al., 1992), they have ample chances to interrelate with the preganglionic cells that link indirectly with sympathetic nerve fibers surrounding the renal arteries. However, some other pathways might contribute to the *trans*-synaptic degeneration (Tsai et al., 2017), as the ganglion cells of renal afferent nerves in thoracic and lumbar spine dorsal root ganglia link to the posterior and lateral hypothalamic nuclei as well as the locus ceruleus in the brain stem (Campese and Kogosov, 1995; Jansen et al., 1995). RDN may affect the described connections and result in remodeling of the critical brainstem areas and the stellate ganglia. Because transneuronal degeneration may remain active for prolonged periods of time, the effects of RDN on arrhythmia control may persist for months after the procedure (Tsai et al., 2017).

PV ISOLATION

Pulmonary vein isolation with ganglionated plexi ablation has been used in autonomic modulation of interactions between the systemic and intrinsic cardiac ANS. PVI combined with autonomic ganglia modification significantly improved success rates after PVI compared to PVI alone (Katritsis et al., 2011). In animal models of vagal induced AF, the effectiveness of pulmonary vein isolation was due to the ablation of the autonomic ganglia at the base of the pulmonary veins which eliminated rapid pulmonary vein firing in response to

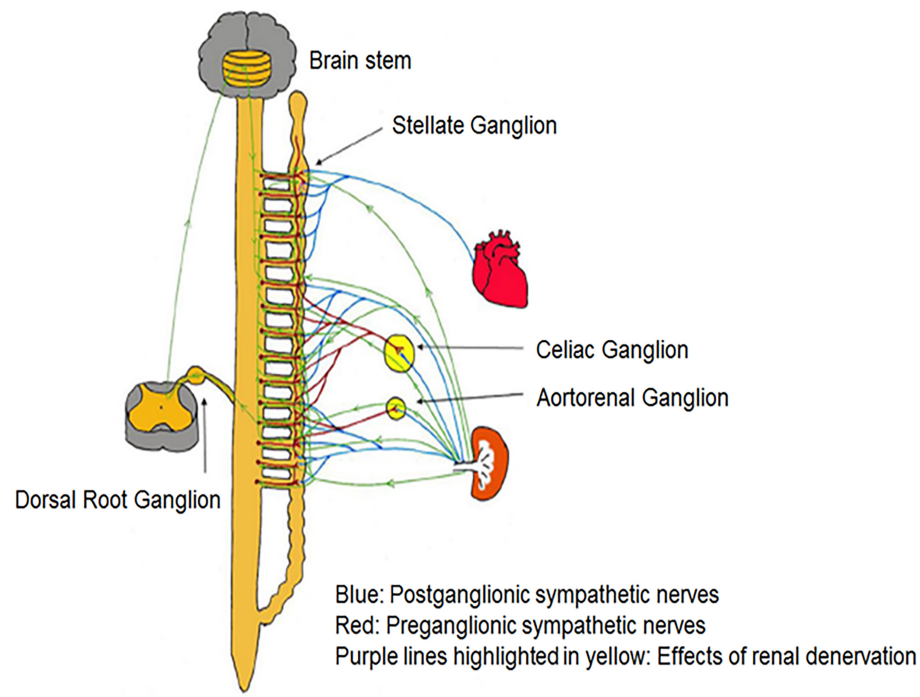

FIGURE 3 | There are multiple pathways connecting renal sympathetic nerves with the stellate ganglion. Both preganglionic and postganglionic sympathetic fibers may innervate the renal artery.

high-frequency stimulation of the ganglionated plexi (Lu et al., 2009). GP ablation inhibited AF inducibility in sleep apnea animal models (Ghias et al., 2009) and has been used in patients with both paroxysmal and persistent AF alone or combined with pulmonary vein isolation with better success rate in patients with paroxysmal AF (Pokushalov et al., 2009; Katritsis et al., 2011; Mikhaylov et al., 2011). However, though ganglionated plexi ablation appears to be a safe and efficacious adjunctive technique to improve outcomes of pulmonary vein isolation in patients with paroxysmal AF, GP ablation in animal models after acute myocardial ischemia exhibited ventricular arrhythmogenic effects compared with GP ablation of the normal heart (He et al., 2013). Hence further studies are warranted to investigate the application of these procedures in various cardiac conditions.

BOTULINUM TOXIN INJECTION

Recent studies have reported that an abundance of epicardial fat is associated with direct adipocyte infiltration into the underlying atrial myocardium (Hatem and Sanders, 2014; Mahajan et al., 2015). Moreover, increased overall adiposity has been shown to be associated with shortened effective refractory periods in the pulmonary veins, leading to the speculation that adiposity can predispose to AF initiation (Munger et al., 2012). Indeed, there is some evidence that areas of epicardial fat accumulation correlate with sites of high dominant frequency, suggesting that epicardial fat may influence AF triggers (Nagashima et al., 2012; Nakahara et al., 2014). Also, it may be possible that encasing epicardial fat influences ganglionated plexi and thus contributes to arrhythmogenesis. Recently, in a prospective, double-blind randomized controlled clinical trial (Pokushalov et al., 2015) reported that injections of botulinum toxin into epicardial fat pads in patients undergoing coronary artery bypass grafting (CABG) resulted in a substantial reduction in the incidence of atrial tachyarrhythmia (most pronounced in the first 14 months postoperatively) and AF burden throughout the 3-year follow-up period, accompanied by reduction in need for hospitalization (Pokushalov et al., 2015; Romanov et al., 2018).

STELLATE GANGLION BLOCKADE

Studies demonstrate that stimulation of the stellate ganglion increased sinus rate and predisposes to atrial arrhythmias (Mohan et al., 2001; Tan et al., 2008a,b). Increased extrinsic cardiac nerve activity in the left stellate ganglion often preceded paroxysmal atrial tachycardia or AF in animal models (Choi et al., 2010). Unilateral electrical stimulation of the stellate ganglion aggravated atrial electrical remodeling facilitating induction of AF in animal models, an effect attenuated by unilateral ganglionectomy (Zhou et al., 2013). In animal models of pacing-induced congestive heart failure, cryoablation of bilateral stellate and T2–T4 thoracic ganglia reduced sympathetic activation-induced paroxysmal AF (Ogawa et al., 2009). Bilateral ANS remodeling resulting from the increased synaptic density of stellate ganglia following myocardial infarction was associated with increased ganglion activity (Han et al., 2012). Surgical excision of stellate ganglion (left cardiac sympathetic denervation) together with T2 and T3 thoracic ganglia reduced arrhythmia in high-risk patients and animal models following myocardial infarction (Schwartz et al., 1976, 1992) and in patients with catecholaminergic polymorphic ventricular tachycardia and long-QT syndrome (Collura et al., 2009).

HIGH THORACIC EPIDURAL ANESTHESIA

In patients undergoing cardiac surgery and cardiopulmonary bypass, high thoracic epidural anesthesia was found to markedly reduce sympathetic tone (Scott et al., 2001; Liu et al., 2004) and the risk of post-operative supraventricular arrhythmias (Svircevic et al., 2011). Initiation of high thoracic epidural anesthesia decreased the arrhythmia burden in patients with refractory electrical storm (Bourke et al., 2010) and in animal models of rapid atrial pacing was found to be associated with inhibition of atrial autonomic nerve sprouting (Yang et al., 2011). However variable results have been obtained pertaining to the decreased incidence of post-operative sustained AF despite a marked reduction in sympathetic activity (Groban et al., 2000; Jidéus et al., 2001) and warrants further detailed studies to explore the definitive effect of high thoracic epidural anesthesia on atrial electrophysiology and arrhythmogenesis.

CAROTID BODY ABLATION

Hypersensitive chemoreceptors result in sympathetic excitation. Enhanced chemoreflex sensitivity potentially increasing central sympathetic drive was observed in animal models of pacing-induced congestive heart failure (Schultz and Li, 2007). Surgical denervation of peripheral chemoreceptors prevented sympathetic activation- mediated hypertensive response to hypoxic stimuli in rats with intermittent hypoxia (Lesske et al., 1997). Bilateral denervation of the carotid body and the carotid sinus baroreceptors prevented the development of hypertension in young pre-hypertensive animals and significantly decreased arterial pressure in the adult population of spontaneously hypertensive rats (Tan et al., 2010) and hypertensive humans (Nakayama, 1961). Though carotid ablation appears as a logical approach to attenuate sympathetic overdrive, hypertension and arrhythmogenic atrial autonomic signaling in AF, there are currently no studies characterizing its effects on atrial electrophysiology and atrial arrhythmogenesis.

CONCLUSION AND PERSPECTIVES

Enhanced sympathetic activation increases circulating catecholamines and causes hypertension and associated complication such as AF and congestive heart failure. Hypertension often coexists with comorbidities like obesity,

metabolic syndrome, and obstructive sleep apnea that further exaggerate and sustain the sympathetic overdrive. Substantial evidence indicates that targeting sympathetic overactivity either by pharmacotherapy or device-based interventions seems to be a logical and useful approach for the management of AF. Sympathetic ablation by RDN appears to be a promising strategy to achieve atrial antiarrhythmic effects in animal models and humans. While carotid body ablation is a proven strategy to attenuate sympathetic overdrive, the potential anti-arrhythmic effects are yet to be investigated in future studies. Other techniques employed to reduce sympathetic activity are applied in specific conditions such as stellate blockade in high-risk patients and following myocardial infarction, ganglionic plexus ablation to lower AF recurrence in patients following circumferential pulmonary vein isolation, and high thoracic epidural anesthesia in post-surgical AF management. However further clinical studies are needed to substantiate the role of various sympatholytic approaches in the management of AF.

AUTHOR CONTRIBUTIONS

RC and MS have drafted the manuscript. MK, JH, and VM have researched data, contributed to inidvidual sections, and critically reviewed the manuscript.

REFERENCES

Abed, H. S., Wittert, G. A., Leong, D. P., Shirazi, M. G., Bahrami, B., Middeldorp, M. E., et al. (2013). Effect of weight reduction and cardiometabolic risk factor management on symptom burden and severity in patients with atrial fibrillation: a randomized clinical trial. *JAMA* 310, 2050–2060. doi: 10.1001/jama.2013.280521

Aizer, A., Gaziano, J. M., Cook, N. R., Manson, J. E., Buring, J. E., and Albert, C. M. (2009). Relation of vigorous exercise to risk of atrial fibrillation. *Am. J. Cardiol.* 103, 1572–1577. doi: 10.1016/j.amjcard.2009.01.374

Al Chekakie, M. O., Welles, C. C., Metoyer, R., Ibrahim, A., Shapira, A. R., Cytron, J., et al. (2010). Pericardial fat is independently associated with human atrial fibrillation. *J. Am. Coll. Cardiol.* 56, 784–788. doi: 10.1016/j.jacc.2010.03.071

Allessie, M., and de Groot, N. (2014). Crosstalk opposing view: rotors have not been demonstrated to be the drivers of atrial fibrillation. *J. Physiol.* 592, 3167–3170. doi: 10.1113/jphysiol.2014.271809

Allessie, M. A., Boyden, P. A., Camm, A. J., Kleber, A. G., Lab, M. J., Legato, M. J., et al. (2001). Pathophysiology and prevention of atrial fibrillation. *Circulation* 103, 769–777. doi: 10.1161/01.CIR.103.5.769

Allessie, M. A., de Groot, N. M., Houben, R. P., Schotten, U., Boersma, E., Smeets, J. L., et al. (2010). Electropathological substrate of long-standing persistent atrial fibrillation in patients with structural heart disease: longitudinal dissociation. *Circ. Arrhythm. Electrophysiol.* 3, 606–615. doi: 10.1161/CIRCEP.109.910125

Alvarez, G. E., Beske, S. D., Ballard, T. P., and Davy, K. P. (2002). Sympathetic neural activation in visceral obesity. *Circulation* 106, 2533–2536. doi: 10.1161/01.CIR.0000041244.79165.25

Amar, D., Zhang, H., Miodownik, S., and Kadish, A. H. (2003). Competing autonomic mechanisms precede the onset of postoperative atrial fibrillation. *J. Am. Coll. Cardiol.* 42, 1262–1268. doi: 10.1016/S0735-1097(03)00955-0

Andersson, T., Magnuson, A., Bryngelsson, I. L., Frobert, O., Henriksson, K. M., Edvardsson, N., et al. (2013). All-cause mortality in 272,186 patients hospitalized with incident atrial fibrillation 1995-2008: a Swedish nationwide long-term case-control study. *Eur. Heart J.* 34, 1061–1067. doi: 10.1093/eurheartj/ehs469

Armour, J. A., Murphy, D. A., Yuan, B. X., Macdonald, S., and Hopkins, D. A. (1997). Gross and microscopic anatomy of the human intrinsic cardiac nervous system. *Anat. Rec.* 247, 289–298. doi: 10.1002/(SICI)1097-0185(199702)247:2<289::AID-AR15>3.0.CO;2-L

Atienza, F., Almendral, J., Moreno, J., Vaidyanathan, R., Talkachou, A., Kalifa, J., et al. (2006). Activation of inward rectifier potassium channels accelerates atrial fibrillation in humans: evidence for a reentrant mechanism. *Circulation* 114, 2434–2442. doi: 10.1161/CIRCULATIONAHA.106.633735

Baber, U., Howard, V. J., Halperin, J. L., Soliman, E. Z., Zhang, X., McClellan, W., et al. (2011). Association of chronic kidney disease with atrial fibrillation among adults in the United States: REasons for Geographic and Racial Differences in Stroke (REGARDS) Study. *Circ. Arrhythm. Electrophysiol.* 4, 26–32. doi: 10.1161/CIRCEP.110.957100

Báez-Escudero, J. L., Keida, T., Dave, A. S., Okishige, K., and Valderrabano, M. (2014). Ethanol infusion in the vein of Marshall leads to parasympathetic denervation of the human left atrium: implications for atrial fibrillation. *J. Am. Coll. Cardiol.* 63, 1892–1901. doi: 10.1016/j.jacc.2014.01.032

Beukema, W. P., Sie, H. T., Misier, A. R., Delnoy, P. P., Wellens, H. J., and Elvan, A. (2008). Predictive factors of sustained sinus rhythm and recurrent atrial fibrillation after a radiofrequency modified Maze procedure. *Eur. J. Cardiothorac. Surg.* 34, 771–775. doi: 10.1016/j.ejcts.2008.07.026

Bohm, M., Kandzari, D., Townsend, R., Mahfoud, F., Weber, M., Fahy, M., et al. (2018). Spyral Htn-off med trial: changes in office and ambulatory heart rate. *J. Hypertens.* 36, e23–e24. doi: 10.1097/01.hjh.0000539024.31308.8d

Bourke, T., Vaseghi, M., Michowitz, Y., Sankhla, V., Shah, M., Swapna, N., et al. (2010). Neuraxial modulation for refractory ventricular arrhythmias: value of thoracic epidural anesthesia and surgical left cardiac sympathetic denervation. *Circulation* 121, 2255–2262. doi: 10.1161/CIRCULATIONAHA.109.929703

Bramlett, H. M., and Dietrich, W. D. (2007). Progressive damage after brain and spinal cord injury: pathomechanisms and treatment strategies. *Prog. Brain Res.* 161, 125–141. doi: 10.1016/S0079-6123(06)61009-1

Brandt, M. C., Mahfoud, F., Reda, S., Schirmer, S. H., Erdmann, E., Bohm, M., et al. (2012a). Renal sympathetic denervation reduces left ventricular hypertrophy and improves cardiac function in patients with resistant hypertension. *J. Am. Coll. Cardiol.* 59, 901–909. doi: 10.1016/j.jacc.2011.11.034

Brandt, M. C., Reda, S., Mahfoud, F., Lenski, M., Bohm, M., and Hoppe, U. C. (2012b). Effects of renal sympathetic denervation on arterial stiffness and central hemodynamics in patients with resistant hypertension. *J. Am. Coll. Cardiol.* 60, 1956–1965. doi: 10.1016/j.jacc.2012.08.959

Brignole, M., Gianfranchi, L., Menozzi, C., Raviele, A., Oddone, D., Lolli, G., et al. (1993). Role of autonomic reflexes in syncope associated with paroxysmal atrial fibrillation. *J. Am. Coll. Cardiol.* 22, 1123–1129. doi: 10.1016/0735-1097(93)90426-2

Buch, P., Friberg, J., Scharling, H., Lange, P., and Prescott, E. (2003). Reduced lung function and risk of atrial fibrillation in the Copenhagen city heart study. *Eur. Respir. J.* 21, 1012–1016. doi: 10.1183/09031936.03.00051502

Cagnoni, F., Destro, M., Bontempelli, E., Locatelli, G., Hering, D., and Schlaich, M. P. (2016). Central sympathetic inhibition: a neglected approach for treatment of cardiac arrhythmias? *Curr. Hypertens. Rep.* 18:13. doi: 10.1007/s11906-015-0619-0

Calkins, H., Kuck, K. H., Cappato, R., Brugada, J., Camm, A. J., Chen, S. A., et al. (2012). 2012 HRS/EHRA/ECAS expert consensus statement on catheter and surgical ablation of atrial fibrillation: recommendations for patient selection, procedural techniques, patient management and follow-up, definitions, endpoints, and research trial design. *J. Interv. Card. Electrophysiol.* 33, 171–257. doi: 10.1007/s10840-012-9672-7

Camm, A. J., Kirchhof, P., Lip, G. Y., Schotten, U., Savelieva, I., Ernst, S., et al. (2010). Guidelines for the management of atrial fibrillation: the task force for the management of Atrial Fibrillation of the European Society of Cardiology (ESC). *Europace* 12, 1360–1420. doi: 10.1093/europace/euq350

Campese, V. M., and Kogosov, E. (1995). Renal afferent denervation prevents hypertension in rats with chronic renal failure. *Hypertension* 25(4 Pt 2), 878–882. doi: 10.1161/01.HYP.25.4.878

Chamberlain, A. M., Agarwal, S. K., Folsom, A. R., Duval, S., Soliman, E. Z., Ambrose, M., et al. (2011). Smoking and incidence of atrial fibrillation: results from the Atherosclerosis Risk in Communities (ARIC) study. *Heart Rhythm* 8, 1160–1166. doi: 10.1016/j.hrthm.2011.03.038

Chazova, I., Almazov, V. A., and Shlyakhto, E. (2006). Moxonidine improves glycaemic control in mildly hypertensive, overweight patients: a comparison with metformin. *Diabetes Obes. Metab.* 8, 456–465. doi: 10.1111/j.1463-1326.2006.00606.x

Chen, P. S., and Tan, A. Y. (2007). Autonomic nerve activity and atrial fibrillation. *Heart Rhythm* 4(3 Suppl.), S61–S64. doi: 10.1016/j.hrthm.2006.12.006

Chen, S. A., Hsieh, M. H., Tai, C. T., Tsai, C. F., Prakash, V. S., Yu, W. C., et al. (1999). Initiation of atrial fibrillation by ectopic beats originating from the pulmonary veins: electrophysiological characteristics, pharmacological responses, and effects of radiofrequency ablation. *Circulation* 100, 1879–1886. doi: 10.1161/01.CIR.100.18.1879

Chen, J., Mandapati, R., Berenfeld, O., Skanes, A. C., Gray, R. A., and Jalife, J. (2000). Dynamics of wavelets and their role in atrial fibrillation in the isolated sheep heart. *Cardiovasc. Res.* 48, 220–232.

Chevalier, P., Tabib, A., Meyronnet, D., Chalabreysse, L., Restier, L., Ludman, V., et al. (2005). Quantitative study of nerves of the human left atrium. *Heart Rhythm* 2, 518–522. doi: 10.1016/j.hrthm.2005.01.022

Choi, E. K., Shen, M. J., Han, S., Kim, D., Hwang, S., Sayfo, S., et al. (2010). Intrinsic cardiac nerve activity and paroxysmal atrial tachyarrhythmia in ambulatory dogs. *Circulation* 121, 2615–2623. doi: 10.1161/CIRCULATIONAHA.109.919829

Christ, T., Rozmaritsa, N., Engel, A., Berk, E., Knaut, M., Metzner, K., et al. (2014). Arrhythmias, elicited by catecholamines and serotonin, vanish in human chronic atrial fibrillation. *Proc. Natl. Acad. Sci. U.S.A.* 111, 11193–11198. doi: 10.1073/pnas.1324132111

Collura, C. A., Johnson, J. N., Moir, C., and Ackerman, M. J. (2009). Left cardiac sympathetic denervation for the treatment of long QT syndrome and catecholaminergic polymorphic ventricular tachycardia using video-assisted thoracic surgery. *Heart Rhythm* 6, 752–759. doi: 10.1016/j.hrthm.2009.03.024

Coumel, P. (1996). Autonomic influences in atrial tachyarrhythmias. *J. Cardiovasc. Electrophysiol.* 7, 999–1007. doi: 10.1111/j.1540-8167.1996.tb00474.x

Cox, J. L., Canavan, T. E., Schuessler, R. B., Cain, M. E., Lindsay, B. D., Stone, C., et al. (1991). The surgical treatment of atrial fibrillation. II. Intraoperative electrophysiologic mapping and description of the electrophysiologic basis of atrial flutter and atrial fibrillation. *J. Thorac. Cardiovasc. Surg.* 101, 406–426.

de Groot, N. M., Houben, R. P., Smeets, J. L., Boersma, E., Schotten, U., Schalij, M. J., et al. (2010). Electropathological substrate of longstanding persistent atrial fibrillation in patients with structural heart disease: epicardial breakthrough. *Circulation* 122, 1674–1682. doi: 10.1161/CIRCULATIONAHA.109.910901

Deftereos, S., Giannopoulos, G., Kossyvakis, C., Efremidis, M., Panagopoulou, V., Raisakis, K., et al. (2013). Effectiveness of moxonidine to reduce atrial fibrillation burden in hypertensive patients. *Am. J. Cardiol.* 112, 684–687. doi: 10.1016/j.amjcard.2013.04.049

Deneke, T., Chaar, H., de Groot, J. R., Wilde, A. A., Lawo, T., Mundig, J., et al. (2011). Shift in the pattern of autonomic atrial innervation in subjects with persistent atrial fibrillation. *Heart Rhythm* 8, 1357–1363. doi: 10.1016/j.hrthm.2011.04.013

Di Biase, L., Burkhardt, J. D., Mohanty, P., Sanchez, J., Mohanty, S., Horton, R., et al. (2010). Left atrial appendage: an underrecognized trigger site of atrial fibrillation. *Circulation* 122, 109–118. doi: 10.1161/CIRCULATIONAHA.109.928903

Dimitri, H., Ng, M., Brooks, A. G., Kuklik, P., Stiles, M. K., Lau, D. H., et al. (2012). Atrial remodeling in obstructive sleep apnea: implications for atrial fibrillation. *Heart Rhythm* 9, 321–327. doi: 10.1016/j.hrthm.2011.10.017

Dimmer, C., Tavernier, R., Gjorgov, N., Van Nooten, G., Clement, D. L., and Jordaens, L. (1998). Variations of autonomic tone preceding onset of atrial fibrillation after coronary artery bypass grafting. *Am. J. Cardiol.* 82, 22–25. doi: 10.1016/S0002-9149(98)00231-8

Dizon, J. M., Chen, K., Bacchetta, M., Argenziano, M., Mancini, D., Biviano, A., et al. (2009). A comparison of atrial arrhythmias after heart or double-lung transplantation at a single center: insights into the mechanism of post-operative atrial fibrillation. *J. Am. Coll. Cardiol.* 54, 2043–2048. doi: 10.1016/j.jacc.2009.08.029

Dobrev, D., Friedrich, A., Voigt, N., Jost, N., Wettwer, E., Christ, T., et al. (2005). The G protein-gated potassium current I(K,ACh) is constitutively active in patients with chronic atrial fibrillation. *Circulation* 112, 3697–3706. doi: 10.1161/CIRCULATIONAHA.105.575332

Eckstein, J., Maesen, B., Linz, D., Zeemering, S., van Hunnik, A., Verheule, S., et al. (2011). Time course and mechanisms of endo-epicardial electrical dissociation during atrial fibrillation in the goat. *Cardiovasc. Res.* 89, 816–824. doi: 10.1093/cvr/cvq336

Edwards, L. P., Brown-Bryan, T. A., McLean, L., and Ernsberger, P. (2012). Pharmacological properties of the central antihypertensive agent, moxonidine. *Cardiovasc. Ther.* 30, 199–208. doi: 10.1111/j.1755-5922.2011.00268.x

Ehrlich, J. R., Hohnloser, S. H., and Nattel, S. (2006). Role of angiotensin system and effects of its inhibition in atrial fibrillation: clinical and experimental evidence. *Eur. Heart J.* 27, 512–518. doi: 10.1093/eurheartj/ehi668

Esler, M. (2004). Looking at the sympathetic nervous system as a primary source. *Handb. Hypertens.* 22, 81–102.

Esler, M., Alvarenga, M., Pier, C., Richards, J., El-Osta, A., Barton, D., et al. (2006a). The neuronal noradrenaline transporter, anxiety and cardiovascular disease. *J. Psychopharmacol.* 20(4 Suppl.), 60–66. doi: 10.1177/1359786806066055

Esler, M., Straznicky, N., Eikelis, N., Masuo, K., Lambert, G., and Lambert, E. (2006b). Mechanisms of sympathetic activation in obesity-related hypertension. *Hypertension* 48, 787–796. doi: 10.1161/01.HYP.0000242642.42177.49

Ferguson, M., Ryan, G. B., and Bell, C. (1986). Localization of sympathetic and sensory neurons innervating the rat kidney. *J. Auton Nerv. Syst.* 16, 279–288. doi: 10.1016/0165-1838(86)90034-2

Feyz, L., Theuns, D. A., Bhagwandien, R., Strachinaru, M., Kardys, I., Van Mieghem, N. M., et al. (2018). Atrial fibrillation reduction by renal sympathetic denervation: 12 months' results of the AFFORD study. *Clin. Res. Cardiol.* doi: 10.1007/s00392-018-1391-3 [Epub ahead of print].,

Flacke, J. W., Bloor, B. C., Flacke, W. E., Wong, D., Dazza, S., Stead, S. W., et al. (1987). Reduced narcotic requirement by clonidine with improved hemodynamic and adrenergic stability in patients undergoing coronary bypass surgery. *Anesthesiology* 67, 11–19. doi: 10.1097/00000542-198707000-00003

Furukawa, T., Hirao, K., Horikawa-Tanami, T., Hachiya, H., and Isobe, M. (2009). Influence of autonomic stimulation on the genesis of atrial fibrillation in remodeled canine atria not the same as in normal atria. *Circ. J.* 73, 468–475. doi: 10.1253/circj.CJ-08-0869

Gami, A. S., Hodge, D. O., Herges, R. M., Olson, E. J., Nykodym, J., Kara, T., et al. (2007). Obstructive sleep apnea, obesity, and the risk of incident atrial fibrillation. *J. Am. Coll. Cardiol.* 49, 565–571. doi: 10.1016/j.jacc.2006.08.060

Gattone, V. H. II, Marfurt, C. F., and Dallie, S. (1986). Extrinsic innervation of the rat kidney: a retrograde tracing study. *Am. J. Physiol.* 250(2 Pt 2), F189–F196. doi: 10.1152/ajprenal.1986.250.2.F189

Ghias, M., Scherlag, B. J., Lu, Z., Niu, G., Moers, A., Jackman, W. M., et al. (2009). The role of ganglionated plexi in apnea-related atrial fibrillation. *J. Am. Coll. Cardiol.* 54, 2075–2083. doi: 10.1016/j.jacc.2009.09.014

Giannopoulos, G., Kossyvakis, C., Efremidis, M., Katsivas, A., Panagopoulou, V., Doudoumis, K., et al. (2014). Central sympathetic inhibition to reduce postablation atrial fibrillation recurrences in hypertensive patients: a randomized, controlled study. *Circulation* 130, 1346–1352. doi: 10.1161/CIRCULATIONAHA.114.010999

Girerd, N., Magne, J., Pibarot, P., Voisine, P., Dagenais, F., and Mathieu, P. (2011). Postoperative atrial fibrillation predicts long-term survival after aortic-valve surgery but not after mitral-valve surgery: a retrospective study. *BMJ Open* 1:e000385. doi: 10.1136/bmjopen-2011-000385

Goette, A., Staack, T., Rocken, C., Arndt, M., Geller, J. C., Huth, C., et al. (2000). Increased expression of extracellular signal-regulated kinase and angiotensin-converting enzyme in human atria during atrial fibrillation. *J. Am. Coll. Cardiol.* 35, 1669–1677. doi: 10.1016/S0735-1097(00)00611-2

Gould, P. A., Yii, M., McLean, C., Finch, S., Marshall, T., Lambert, G. W., et al. (2006). Evidence for increased atrial sympathetic innervation in persistent human atrial fibrillation. *Pacing Clin. Electrophysiol.* 29, 821–829. doi: 10.1111/j.1540-8159.2006.00447.x

Grassi, G., Seravalle, G., Cattaneo, B. M., Bolla, G. B., Lanfranchi, A., Colombo, M., et al. (1995). Sympathetic activation in obese normotensive subjects. *Hypertension* 25(4 Pt 1), 560–563. doi: 10.1161/01.HYP.25.4.560

Greiser, M., Kerfant, B. G., Williams, G. S., Voigt, N., Harks, E., Dibb, K. M., et al. (2014). Tachycardia-induced silencing of subcellular Ca2+ signaling in atrial myocytes. *J. Clin. Invest.* 124, 4759–4772. doi: 10.1172/JCI70102

Groban, L., Dolinski, S. Y., Zvara, D. A., and Oaks, T. (2000). Thoracic epidural analgesia: its role in postthoracotomy atrial arrhythmias. *J. Cardiothorac. Vasc. Anesth.* 14, 662–665. doi: 10.1053/jcan.2000.18318

Haenni, A., and Lithell, H. (1999). Moxonidine improves insulin sensitivity in insulin-resistant hypertensives. *J. Hypertens.* 17, S29–S35.

Haissaguerre, M., Hocini, M., Denis, A., Shah, A. J., Komatsu, Y., Yamashita, S., et al. (2014). Driver domains in persistent atrial fibrillation. *Circulation* 130, 530–538. doi: 10.1161/CIRCULATIONAHA.113.005421

Haissaguerre, M., Jais, P., Shah, D. C., Takahashi, A., Hocini, M., Quiniou, G., et al. (1998). Spontaneous initiation of atrial fibrillation by ectopic beats originating in the pulmonary veins. *N. Engl. J. Med.* 339, 659–666. doi: 10.1056/NEJM199809033391003

Haissaguerre, M., Sanders, P., Hocini, M., Takahashi, Y., Rotter, M., Sacher, F., et al. (2005). Catheter ablation of long-lasting persistent atrial fibrillation: critical structures for termination. *J. Cardiovasc. Electrophysiol.* 16, 1125–1137. doi: 10.1111/j.1540-8167.2005.00307.x

Han, S., Kobayashi, K., Joung, B., Piccirillo, G., Maruyama, M., Vinters, H. V., et al. (2012). Electroanatomic remodeling of the left stellate ganglion after myocardial infarction. *J. Am. Coll. Cardiol.* 59, 954–961. doi: 10.1016/j.jacc.2011.11.030

Hatem, S. N., and Sanders, P. (2014). Epicardial adipose tissue and atrial fibrillation. *Cardiovasc. Res.* 102, 205–213. doi: 10.1093/cvr/cvu045

He, B., Lu, Z., He, W., Wu, L., Cui, B., Hu, X., et al. (2013). Effects of ganglionated plexi ablation on ventricular electrophysiological properties in normal hearts and after acute myocardial ischemia. *Int. J. Cardiol.* 168, 86–93. doi: 10.1016/j.ijcard.2012.09.067

Hou, Y., Hu, J., Po, S. S., Wang, H., Zhang, L., Zhang, F., et al. (2013). Catheter-based renal sympathetic denervation significantly inhibits atrial fibrillation induced by electrical stimulation of the left stellate ganglion and rapid atrial pacing. *PLoS One* 8:e78218. doi: 10.1371/journal.pone.0078218

Hou, Y., Scherlag, B. J., Lin, J., Zhou, J., Song, J., Zhang, Y., et al. (2007). Interactive atrial neural network: determining the connections between Ganglionated plexi. *Heart Rhythm* 4, 56–63. doi: 10.1016/j.hrthm.2006.09.020

Huggett, R. J., Burns, J., Mackintosh, A. F., and Mary, D. A. (2004). Sympathetic neural activation in nondiabetic metabolic syndrome and its further augmentation by hypertension. *Hypertension* 44, 847–852. doi: 10.1161/01.HYP.0000147893.08533.d8

Huggett, R. J., Hogarth, A. J., Mackintosh, A. F., and Mary, D. A. (2006). Sympathetic nerve hyperactivity in non-diabetic offspring of patients with type 2 diabetes mellitus. *Diabetologia* 49, 2741–2744. doi: 10.1007/s00125-006-0399-9

Iacobellis, G., Ribaudo, M. C., Assael, F., Vecci, E., Tiberti, C., Zappaterreno, A., et al. (2003). Echocardiographic epicardial adipose tissue is related to anthropometric and clinical parameters of metabolic syndrome: a new indicator of cardiovascular risk. *J. Clin. Endocrinol. Metab.* 88, 5163–5168. doi: 10.1210/jc.2003-030698

Iwasaki, Y. K., Nishida, K., Kato, T., and Nattel, S. (2011). Atrial fibrillation pathophysiology: implications for management. *Circulation* 124, 2264–2274. doi: 10.1161/CIRCULATIONAHA.111.019893

Jalife, J., Berenfeld, O., and Mansour, M. (2002). Mother rotors and fibrillatory conduction: a mechanism of atrial fibrillation. *Cardiovasc. Res.* 54, 204–216. doi: 10.1016/S0008-6363(02)00223-7

Jansen, A. S., Wessendorf, M. W., and Loewy, A. D. (1995). Transneuronal labeling of CNS neuropeptide and monoamine neurons after pseudorabies virus injections into the stellate ganglion. *Brain Res.* 683, 1–24. doi: 10.1016/0006-8993(95)00276-V

Jayachandran, J. V., Sih, H. J., Winkle, W., Zipes, D. P., Hutchins, G. D., and Olgin, J. E. (2000). Atrial fibrillation produced by prolonged rapid atrial pacing is associated with heterogeneous changes in atrial sympathetic innervation. *Circulation* 101, 1185–1191. doi: 10.1161/01.CIR.101.10.1185

Jideus, L., Joachimsson, P. O., Stridsberg, M., Ericson, M., Tyden, H., Nilsson, L., et al. (2001). Thoracic epidural anesthesia does not influence the occurrence of postoperative sustained atrial fibrillation. *Ann. Thorac. Surg.* 72, 65–71. doi: 10.1016/S0003-4975(01)02631-5

Julius, S., and Jamerson, K. (1994). Sympathetics, insulin resistance and coronary risk in hypertension: the 'chicken-and-egg' question. *J. Hypertens.* 12, 495–502. doi: 10.1097/00004872-199405000-00001

Kalman, J. M., Munawar, M., Howes, L. G., Louis, W. J., Buxton, B. F., Gutteridge, G., et al. (1995). Atrial fibrillation after coronary artery bypass grafting is associated with sympathetic activation. *Ann. Thorac. Surg.* 60, 1709–1715. doi: 10.1016/0003-4975(95)00718-0

Katritsis, D. G., Giazitzoglou, E., Zografos, T., Pokushalov, E., Po, S. S., and Camm, A. J. (2011). Rapid pulmonary vein isolation combined with autonomic ganglia modification: a randomized study. *Heart Rhythm* 8, 672–678. doi: 10.1016/j.hrthm.2010.12.047

Kawano, H., Okada, R., and Yano, K. (2003). Histological study on the distribution of autonomic nerves in the human heart. *Heart Vessel* 18, 32–39. doi: 10.1007/s003800300005

Kawashima, T. (2005). The autonomic nervous system of the human heart with special reference to its origin, course, and peripheral distribution. *Anat. Embryol.* 209, 425–438. doi: 10.1007/s00429-005-0462-1

Kim, D. T., Lai, A. C., Hwang, C., Fan, L. T., Karagueuzian, H. S., Chen, P. S., et al. (2000). The ligament of Marshall: a structural analysis in human hearts with implications for atrial arrhythmias. *J. Am. Coll. Cardiol.* 36, 1324–1327. doi: 10.1016/S0735-1097(00)00819-6

Kim, E. J., Lyass, A., Wang, N., Massaro, J. M., Fox, C. S., Benjamin, E. J., et al. (2014). Relation of hypothyroidism and incident atrial fibrillation (from the Framingham Heart Study). *Am. Heart. J.* 167, 123–126. doi: 10.1016/j.ahj.2013.10.012

Kimura, K., Ieda, M., and Fukuda, K. (2012). Development, maturation, and transdifferentiation of cardiac sympathetic nerves. *Circ. Res.* 110, 325–336. doi: 10.1161/CIRCRESAHA.111.257253

Kirchhof, P., Benussi, S., Kotecha, D., Ahlsson, A., Atar, D., Casadei, B., et al. (2016). 2016 ESC guidelines for the management of atrial fibrillation developed in collaboration with EACTS. *Eur. Heart J.* 37, 2893–2962. doi: 10.1093/eurheartj/ehw210

Kiuchi, M. G., Chen, S., E Silver, G. R., Rodrigues Paz, L. M., Kiuchi, T., de Paula Filho, A. G., et al. (2017). The addition of renal sympathetic denervation to pulmonary vein isolation reduces recurrence of paroxysmal atrial fibrillation in chronic kidney disease patients. *J. Interv. Card. Electrophysiol.* 48, 215–222. doi: 10.1007/s10840-016-0186-6

Krum, H., Schlaich, M., Whitbourn, R., Sobotka, P. A., Sadowski, J., Bartus, K., et al. (2009). Catheter-based renal sympathetic denervation for resistant hypertension: a multicentre safety and proof-of-principle cohort study. *Lancet* 373, 1275–1281. doi: 10.1016/S0140-6736(09)60566-3

Kühlkamp, V., Schirdewan, A., Stangl, K., Homberg, M., Ploch, M., and Beck, O. A. (2000). Use of metoprolol CR/XL to maintain sinus rhythm after conversion from persistent atrial fibrillation: a randomized, double-blind, placebo-controlled study. *J. Am. Coll. Cardiol.* 36, 139–146. doi: 10.1016/S0735-1097(00)00693-8

Kumagai, K., Nakashima, H., Urata, H., Gondo, N., Arakawa, K., and Saku, K. (2003). Effects of angiotensin II type 1 receptor antagonist on electrical and structural remodeling in atrial fibrillation. *J. Am. Coll. Cardiol.* 41, 2197–2204. doi: 10.1016/S0735-1097(03)00464-9

Lambert, E., Eikelis, N., Esler, M., Dawood, T., Schlaich, M., Bayles, R., et al. (2008). Altered sympathetic nervous reactivity and norepinephrine transporter expression in patients with postural tachycardia syndrome. *Circ. Arrhythm Electrophysiol.* 1, 103–109. doi: 10.1161/CIRCEP.107.750471

Lambert, E., Sari, C. I., Dawood, T., Nguyen, J., McGrane, M., Eikelis, N., et al. (2010). Sympathetic nervous system activity is associated with obesity-induced subclinical organ damage in young adults. *Hypertension* 56, 351–358. doi: 10.1161/HYPERTENSIONAHA.110.155663

Lambert, E., Straznicky, N., Eikelis, N., Esler, M., Dawood, T., Masuo, K., et al. (2007). Gender differences in sympathetic nervous activity: influence of body mass and blood pressure. *J. Hypertens.* 25, 1411–1419. doi: 10.1097/HJH.0b013e3281053af4

Lambert, E. A., Thompson, J., Schlaich, M., Laude, D., Elghozi, J. L., Esler, M. D., et al. (2002). Sympathetic and cardiac baroreflex function in panic disorder. *J. Hypertens.* 20, 2445–2451. doi: 10.1097/01.hjh.0000042882.24999.27

Langer, S. Z., Cavero, I., and Massingham, R. (1980). Recent developments in noradrenergic neurotransmission and its relevance to the mechanism of action of certain antihypertensive agents. *Hypertension* 2, 372–382. doi: 10.1161/01.HYP.2.4.372

Larsson, S. C., Drca, N., and Wolk, A. (2014). Alcohol consumption and risk of atrial fibrillation: a prospective study and dose-response meta-analysis. *J. Am. Coll. Cardiol.* 64, 281–289. doi: 10.1016/j.jacc.2014.03.048

Lau, D. H., Mackenzie, L., Kelly, D. J., Psaltis, P. J., Brooks, A. G., Worthington, M., et al. (2010). Hypertension and atrial fibrillation: evidence of progressive atrial remodeling with electrostructural correlate in a conscious chronically instrumented ovine model. *Heart Rhythm* 7, 1282–1290. doi: 10.1016/j.hrthm.2010.05.010

Lepran, I., and Papp, J. G. (1994). Effect of moxonidine on arrhythmias induced by coronary artery occlusion and reperfusion. *J. Cardiovasc. Pharmacol.* 24(Suppl. 1), S9–S15. doi: 10.1097/00005344-199424001-00003

Lesske, J., Fletcher, E. C., Bao, G., and Unger, T. (1997). Hypertension caused by chronic intermittent hypoxia–influence of chemoreceptors and sympathetic nervous system. *J. Hypertens.* 15(12 Pt 2), 1593–1603.

Li, D., Fareh, S., Leung, T. K., and Nattel, S. (1999). Promotion of atrial fibrillation by heart failure in dogs: atrial remodeling of a different sort. *Circulation* 100, 87–95. doi: 10.1161/01.CIR.100.1.87

Lim, P. B., Malcolme-Lawes, L. C., Stuber, T., Wright, I., Francis, D. P., Davies, D. W., et al. (2011). Intrinsic cardiac autonomic stimulation induces pulmonary vein ectopy and triggers atrial fibrillation in humans. *J. Cardiovasc. Electrophysiol.* 22, 638–646. doi: 10.1111/j.1540-8167.2010.01992.x

Linz, D., Hohl, M., Nickel, A., Mahfoud, F., Wagner, M., Ewen, S., et al. (2013a). Effect of renal denervation on neurohumoral activation triggering atrial fibrillation in obstructive sleep apnea. *Hypertension* 62, 767–774. doi: 10.1161/HYPERTENSIONAHA.113.01728

Linz, D., Mahfoud, F., Schotten, U., Ukena, C., Hohl, M., Neuberger, H. R., et al. (2013b). Renal sympathetic denervation provides ventricular rate control but does not prevent atrial electrical remodeling during atrial fibrillation. *Hypertension* 61, 225–231. doi: 10.1161/HYPERTENSIONAHA.111.00182

Linz, D., Mahfoud, F., Schotten, U., Ukena, C., Neuberger, H. R., Wirth, K., et al. (2012). Renal sympathetic denervation suppresses postapneic blood pressure rises and atrial fibrillation in a model for sleep apnea. *Hypertension* 60, 172–178. doi: 10.1161/HYPERTENSIONAHA.112.191965

Liu, S. S., Block, B. M., and Wu, C. L. (2004). Effects of perioperative central neuraxial analgesia on outcome after coronary artery bypass surgery: a meta-analysis. *Anesthesiology* 101, 153–161. doi: 10.1097/00000542-200407000-00024

Lu, Z., Scherlag, B. J., Lin, J., Niu, G., Ghias, M., Jackman, W. M., et al. (2008). Autonomic mechanism for complex fractionated atrial electrograms: evidence by fast fourier transform analysis. *J. Cardiovasc. Electrophysiol.* 19, 835–842. doi: 10.1111/j.1540-8167.2008.01131.x

Lu, Z., Scherlag, B. J., Lin, J., Yu, L., Guo, J. H., Niu, G., et al. (2009). Autonomic mechanism for initiation of rapid firing from atria and pulmonary veins: evidence by ablation of ganglionated plexi. *Cardiovasc. Res.* 84, 245–252. doi: 10.1093/cvr/cvp194

Lubitz, S. A., Lunetta, K. L., Lin, H., Arking, D. E., Trompet, S., Li, G., et al. (2014). Novel genetic markers associate with atrial fibrillation risk in Europeans and Japanese. *J. Am. Coll. Cardiol.* 63, 1200–1210. doi: 10.1016/j.jacc.2013.12.015

Mahabadi, A. A., Massaro, J. M., Rosito, G. A., Levy, D., Murabito, J. M., Wolf, P. A., et al. (2009). Association of pericardial fat, intrathoracic fat, and visceral abdominal fat with cardiovascular disease burden: the Framingham Heart Study. *Eur. Heart J.* 30, 850–856. doi: 10.1093/eurheartj/ehn573

Mahajan, R., Lau, D. H., Brooks, A. G., Shipp, N. J., Manavis, J., Wood, J. P., et al. (2015). Electrophysiological, electroanatomical, and structural remodeling of the Atria as consequences of sustained obesity. *J. Am. Coll. Cardiol.* 66, 1–11. doi: 10.1016/j.jacc.2015.04.058

Mahfoud, F., Schlaich, M., Kindermann, I., Ukena, C., Cremers, B., Brandt, M. C., et al. (2011). Effect of renal sympathetic denervation on glucose metabolism in patients with resistant hypertension: a pilot study. *Circulation* 123, 1940–1946. doi: 10.1161/CIRCULATIONAHA.110.991869

Malcolme-Lawes, L. C., Lim, P. B., Wright, I., Kojodjojo, P., Koa-Wing, M., Jamil-Copley, S., et al. (2013). Characterization of the left atrial neural network and its impact on autonomic modification procedures. *Circ. Arrhythm Electrophysiol.* 6, 632–640. doi: 10.1161/CIRCEP.113.000193

Mandapati, R., Skanes, A., Chen, J., Berenfeld, O., and Jalife, J. (2000). Stable microreentrant sources as a mechanism of atrial fibrillation in the isolated sheep heart. *Circulation* 101, 194–199. doi: 10.1161/01.CIR.101.2.194

Manolis, A. J., Rosei, E. A., Coca, A., Cifkova, R., Erdine, S. E., Kjeldsen, S., et al. (2012). Hypertension and atrial fibrillation: diagnostic approach, prevention and treatment. Position paper of the Working Group 'Hypertension Arrhythmias and Thrombosis' of the European Society of Hypertension. *J. Hypertens.* 30, 239–252. doi: 10.1097/HJH.0b013e32834f03bf

Marron, K., Wharton, J., Sheppard, M. N., Fagan, D., Royston, D., Kuhn, D. M., et al. (1995). Distribution, morphology, and neurochemistry of endocardial and epicardial nerve terminal arborizations in the human heart. *Circulation* 92, 2343–2351. doi: 10.1161/01.CIR.92.8.2343

Marron, K., Wharton, J., Sheppard, M. N., Gulbenkian, S., Royston, D., Yacoub, M. H., et al. (1994). Human endocardial innervation and its relationship to the endothelium: an immunohistochemical, histochemical, and quantitative study. *Cardiovasc. Res.* 28, 1490–1499. doi: 10.1093/cvr/28.10.1490

Matthews, V. B., Elliot, R. H., Rudnicka, C., Hricova, J., Herat, L., and Schlaich, M. P. (2017). Role of the sympathetic nervous system in regulation of the sodium glucose cotransporter 2. *J. Hypertens.* 35, 2059–2068. doi: 10.1097/HJH.0000000000001434

McLellan, A. J., Schlaich, M. P., Taylor, A. J., Prabhu, S., Hering, D., Hammond, L., et al. (2015). Reverse cardiac remodeling after renal denervation: atrial electrophysiologic and structural changes associated with blood pressure lowering. *Heart Rhythm* 12, 982–990. doi: 10.1016/j.hrthm.2015.01.039

Meckler, R. L., and Weaver, L. C. (1984). Comparison of the distributions of renal and splenic neurons in sympathetic ganglia. *J. Auton Nerv. Syst.* 11, 189–200. doi: 10.1016/0165-1838(84)90076-6

Melo, J., Voigt, P., Sonmez, B., Ferreira, M., Abecasis, M., Rebocho, M., et al. (2004). Ventral cardiac denervation reduces the incidence of atrial fibrillation after coronary artery bypass grafting. *J. Thorac. Cardiovasc. Surg.* 127, 511–516. doi: 10.1016/S0022

Mest, H. J., Thomsen, P., and Raap, A. (1995). Antiarrhythmic effect of the selective I1-imidazoline receptor modulator moxonidine on ouabain-induced cardiac arrhythmia in guinea pigs. *Ann. N. Y. Acad. Sci.* 763, 620–633. doi: 10.1111/j.1749-6632.1995.tb32457.x

Mikhaylov, E., Kanidieva, A., Sviridova, N., Abramov, M., Gureev, S., Szili-Torok, T., et al. (2011). Outcome of anatomic ganglionated plexi ablation to treat paroxysmal atrial fibrillation: a 3-year follow-up study. *Europace* 13, 362–370. doi: 10.1093/europace/euq416

Moe, G. K., and Abildskov, J. A. (1959). Atrial fibrillation as a self-sustaining arrhythmia independent of focal discharge. *Am. Heart. J.* 58, 59–70. doi: 10.1016/0002-8703(59)90274-1

Moe, G. K., Rheinboldt, W. C., and Abildskov, J. A. (1964). A computer model of atrial fibrillation. *Am. Heart J.* 67, 200–220. doi: 10.1016/0002-8703(64)90371-0

Mohan, R. M., Golding, S., and Paterson, D. J. (2001). Intermittent hypoxia modulates nNOS expression and heart rate response to sympathetic nerve stimulation. *Am. J. Physiol. Heart Circ. Physiol.* 281, H132–H138. doi: 10.1152/ajpheart.2001.281.1.H132

Munger, T. M., Dong, Y. X., Masaki, M., Oh, J. K., Mankad, S. V., Borlaug, B. A., et al. (2012). Electrophysiological and hemodynamic characteristics associated with obesity in patients with atrial fibrillation. *J. Am. Coll. Cardiol.* 60, 851–860. doi: 10.1016/j.jacc.2012.03.042

Nagashima, K., Okumura, Y., Watanabe, I., Nakai, T., Ohkubo, K., Kofune, M., et al. (2012). Does location of epicardial adipose tissue correspond to endocardial high dominant frequency or complex fractionated atrial electrogram sites during atrial fibrillation? *Circ. Arrhythm Electrophysiol.* 5, 676–683. doi: 10.1161/CIRCEP.112.971200

Nakahara, S., Hori, Y., Kobayashi, S., Sakai, Y., Taguchi, I., Takayanagi, K., et al. (2014). Epicardial adipose tissue-based defragmentation approach to persistent atrial fibrillation: its impact on complex fractionated electrograms and ablation outcome. *Heart Rhythm* 11, 1343–1351. doi: 10.1016/j.hrthm.2014.04.040

Nakayama, K. (1961). Surgical removal of the carotid body for bronchial asthma. *Dis. Chest* 40, 595–604. doi: 10.1378/chest.40.6.595

Narayan, S. M., Krummen, D. E., Shivkumar, K., Clopton, P., Rappel, W. J., and Miller, J. M. (2012). Treatment of atrial fibrillation by the ablation of localized sources: CONFIRM (Conventional Ablation for Atrial Fibrillation With or Without Focal Impulse and Rotor Modulation) trial. *J. Am. Coll. Cardiol.* 60, 628–636. doi: 10.1016/j.jacc.2012.05.022

Nattel, S. (2002). New ideas about atrial fibrillation 50 years on. *Nature* 415, 219–226. doi: 10.1038/415219a

Nergårdh, A. K., Rosenqvist, M., Nordlander, R., and Frick, M. (2007). Maintenance of sinus rhythm with metoprolol CR initiated before cardioversion and repeated cardioversion of atrial fibrillation: a randomized double-blind placebo-controlled study. *Eur. Heart J.* 28, 1351–1357. doi: 10.1093/eurheartj/ehl544

Ng, J., Villuendas, R., Cokic, I., Schliamser, J. E., Gordon, D., Koduri, H., et al. (2011). Autonomic remodeling in the left atrium and pulmonary veins in heart failure: creation of a dynamic substrate for atrial fibrillation. *Circ. Arrhythm Electrophysiol.* 4, 388–396. doi: 10.1161/CIRCEP.110.959650

Nguyen, B. L., Fishbein, M. C., Chen, L. S., Chen, P. S., and Masroor, S. (2009). Histopathological substrate for chronic atrial fibrillation in humans. *Heart Rhythm* 6, 454–460. doi: 10.1016/j.hrthm.2009.01.010

Ogawa, M., Tan, A. Y., Song, J., Kobayashi, K., Fishbein, M. C., Lin, S. F., et al. (2009). Cryoablation of stellate ganglia and atrial arrhythmia in ambulatory dogs with pacing-induced heart failure. *Heart Rhythm* 6, 1772–1779. doi: 10.1016/j.hrthm.2009.08.011

Ogawa, M., Zhou, S., Tan, A. Y., Song, J., Gholmieh, G., Fishbein, M. C., et al. (2007). Left stellate ganglion and vagal nerve activity and cardiac arrhythmias in ambulatory dogs with pacing-induced congestive heart failure. *J. Am. Coll. Cardiol.* 50, 335–343. doi: 10.1016/j.jacc.2007.03.045

Okin, P. M., Wachtell, K., Devereux, R. B., Harris, K. E., Jern, S., Kjeldsen, S. E., et al. (2006). Regression of electrocardiographic left ventricular hypertrophy and decreased incidence of new-onset atrial fibrillation in patients with hypertension. *JAMA* 296, 1242–1248. doi: 10.1001/jama.296.10.1242

Palatini, P., Vriz, O., Nesbitt, S., Amerena, J., Majahalme, S., Valentini, M., et al. (1999). Parental hyperdynamic circulation predicts insulin resistance in offspring: the Tecumseh Offspring Study. *Hypertension* 33, 769–774. doi: 10.1161/01.HYP.33.3.769

Pathak, R. K., Middeldorp, M. E., Lau, D. H., Mehta, A. B., Mahajan, R., Twomey, D., et al. (2014). Aggressive risk factor reduction study for atrial fibrillation and implications for the outcome of ablation: the ARREST-AF cohort study. *J. Am. Coll. Cardiol.* 64, 2222–2231. doi: 10.1016/j.jacc.2014.09.028

Patterson, E., Jackman, W. M., Beckman, K. J., Lazzara, R., Lockwood, D., Scherlag, B. J., et al. (2007). Spontaneous pulmonary vein firing in man: relationship to tachycardia-pause early afterdepolarizations and triggered arrhythmia in canine pulmonary veins in vitro. *J. Cardiovasc. Electrophysiol.* 18, 1067–1075. doi: 10.1111/j.1540-8167.2007.00909.x

Patterson, E., Po, S. S., Scherlag, B. J., and Lazzara, R. (2005). Triggered firing in pulmonary veins initiated by in vitro autonomic nerve stimulation. *Heart Rhythm* 2, 624–631. doi: 10.1016/j.hrthm.2005.02.012

Pauza, D. H., Skripka, V., Pauziene, N., and Stropus, R. (2000). Morphology, distribution, and variability of the epicardiac neural ganglionated subplexuses in the human heart. *Anat. Rec.* 259, 353–382. doi: 10.1002/1097-0185(20000801)259:4<353::AID-AR10>3.0.CO;2-R

Petraitiene, V., Pauza, D. H., and Benetis, R. (2014). Distribution of adrenergic and cholinergic nerve fibres within intrinsic nerves at the level of the human heart hilum. *Eur. J. Cardiothorac. Surg.* 45, 1097–1105. doi: 10.1093/ejcts/ezt575

Pilowsky, P., Llewellyn-Smith, I. J., Minson, J., and Chalmers, J. (1992). Sympathetic preganglionic neurons in rabbit spinal cord that project to the stellate or the superior cervical ganglion. *Brain Res.* 577, 181–188. doi: 10.1016/0006-8993(92)90272-B

Pokushalov, E., Kozlov, B., Romanov, A., Strelnikov, A., Bayramova, S., Sergeevichev, D., et al. (2015). Long-term suppression of atrial fibrillation by botulinum toxin injection into epicardial fat pads in patients undergoing cardiac surgery: One-year follow-up of a randomized pilot study. *Circ. Arrhythm. Electrophysiol.* 8, 1334–1341. doi: 10.1161/CIRCEP.115.003199

Pokushalov, E., Romanov, A., Corbucci, G., Artyomenko, S., Baranova, V., Turov, A., et al. (2012). A randomized comparison of pulmonary vein isolation with versus without concomitant renal artery denervation in patients with refractory symptomatic atrial fibrillation and resistant hypertension. *J. Am. Coll. Cardiol.* 60, 1163–1170. doi: 10.1016/j.jacc.2012.05.036

Pokushalov, E., Romanov, A., Shugayev, P., Artyomenko, S., Shirokova, N., Turov, A., et al. (2009). Selective ganglionated plexi ablation for paroxysmal atrial fibrillation. *Heart Rhythm* 6, 1257–1264. doi: 10.1016/j.hrthm.2009.05.018

Prystowsky, E. N., Benson, D. W. Jr., Fuster, V., Hart, R. G., Kay, G. N., and Myerburg, R. J. (1996). Management of patients with atrial fibrillation. A statement for healthcare professionals. From the subcommittee on electrocardiography and electrophysiology, American Heart Association. *Circulation* 93, 1262–1277. doi: 10.1161/01.CIR.93.6.1262

Psaty, B. M., Manolio, T. A., Kuller, L. H., Kronmal, R. A., Cushman, M., Fried, L. P., et al. (1997). Incidence of and risk factors for atrial fibrillation in older adults. *Circulation* 96, 2455–2461. doi: 10.1161/01.CIR.96.7.2455

Ravelli, F., and Mase, M. (2014). Computational mapping in atrial fibrillation: how the integration of signal-derived maps may guide the localization of critical sources. *Europace* 16, 714–723. doi: 10.1093/europace/eut376

Reil, J. C., Hohl, M., Selejan, S., Lipp, P., Drautz, F., Kazakow, A., et al. (2012). Aldosterone promotes atrial fibrillation. *Eur. Heart J.* 33, 2098–2108. doi: 10.1093/eurheartj/ehr266

Romanov, A., Pokushalov, E., Ponomarev, D., Bayramova, S., Shabanov, V., Losik, D., et al. (2018). Long-term suppression of atrial fibrillation by botulinum toxin injection into epicardial fat pads in patients undergoing cardiac surgery: three-year follow-up of a randomized study. *Heart Rhythm* doi: 10.1016/j.hrthm.2018.08.019 [Epub ahead of print].

Romanov, A., Pokushalov, E., Ponomarev, D., Strelnikov, A., Shabanov, V., Losik, D., et al. (2017). Pulmonary vein isolation with concomitant renal artery denervation is associated with reduction in both arterial blood pressure and atrial fibrillation burden: data from implantable cardiac monitor. *Cardiovasc. Ther.* 35:e12264. doi: 10.1111/1755-5922.12264

Roth, A., Kaluski, E., Felner, S., Heller, K., and Laniado, S. (1992). Clonidine for patients with rapid atrial fibrillation. *Ann. Intern. Med.* 116, 388–390. doi: 10.7326/0003-4819-116-5-388

Sahadevan, J., Ryu, K., Peltz, L., Khrestian, C. M., Stewart, R. W., Markowitz, A. H., et al. (2004). Epicardial mapping of chronic atrial fibrillation in patients: preliminary observations. *Circulation* 110, 3293–3299. doi: 10.1161/01.CIR.0000147781.02738.13

Sanders, P., Nalliah, C. J., Dubois, R., Takahashi, Y., Hocini, M., Rotter, M., et al. (2006). Frequency mapping of the pulmonary veins in paroxysmal versus permanent atrial fibrillation. *J. Cardiovasc. Electrophysiol.* 17, 965–972. doi: 10.1111/j.1540-8167.2006.00546.x

Sankaranarayanan, R., Kirkwood, G., Dibb, K., and Garratt, C. J. (2013). Comparison of Atrial Fibrillation in the young versus that in the elderly: a review. *Cardiol. Res. Pract.* 2013:976976. doi: 10.1155/2013/976976

Sarin, S., Wenger, C., Marwaha, A., Qureshi, A., Go, B. D., Woomert, C. A., et al. (2008). Clinical significance of epicardial fat measured using cardiac multislice computed tomography. *Am. J. Cardiol.* 102, 767–771. doi: 10.1016/j.amjcard.2008.04.058

Scherlag, B. J., Yamanashi, W., Patel, U., Lazzara, R., and Jackman, W. M. (2005). Autonomically induced conversion of pulmonary vein focal firing into atrial fibrillation. *J. Am. Coll. Cardiol.* 45, 1878–1886. doi: 10.1016/j.jacc.2005.01.057

Schlaich, M. P., Krum, H., and Sobotka, P. A. (2010). Renal sympathetic nerve ablation: the new frontier in the treatment of hypertension. *Curr. Hypertens. Rep.* 12, 39–46. doi: 10.1007/s11906-009-0078-6

Schnabel, R. B., Yin, X., Gona, P., Larson, M. G., Beiser, A. S., McManus, D. D., et al. (2015). 50 year trends in atrial fibrillation prevalence, incidence, risk factors, and mortality in the Framingham Heart Study: a cohort study. *Lancet* 386, 154–162. doi: 10.1016/S0140-6736(14)61774-8

Schoonderwoerd, B. A., Smit, M. D., Pen, L., and Van Gelder, I. C. (2008). New risk factors for atrial fibrillation: causes of 'not-so-lone atrial fibrillation'. *Europace* 10, 668–673. doi: 10.1093/europace/eun124

Schotten, U., Verheule, S., Kirchhof, P., and Goette, A. (2011). Pathophysiological mechanisms of atrial fibrillation: a translational appraisal. *Physiol. Rev.* 91, 265–325. doi: 10.1152/physrev.00031.2009

Schuessler, R. B., Grayson, T. M., Bromberg, B. I., Cox, J. L., and Boineau, J. P. (1992). Cholinergically mediated tachyarrhythmias induced by a single extrastimulus in the isolated canine right atrium. *Circ. Res.* 71, 1254–1267. doi: 10.1161/01.RES.71.5.1254

Schultz, H. D., and Li, Y. L. (2007). Carotid body function in heart failure. *Respir. Physiol. Neurobiol.* 157, 171–185. doi: 10.1016/j.resp.2007.02.011

Schwartz, P. J., Motolese, M., Pollavini, G., Lotto, A., Ruberti, U. G. O., Trazzi, R., et al. (1992). Prevention of sudden cardiac death after a first myocardial infarction by pharmacologic or surgical antiadrenergic interventions. *J. Cardiovasc. Electrophysiol.* 3, 2–16. doi: 10.1111/j.1540-8167.1992.tb01090.x

Schwartz, P. J., Snebold, N. G., and Brown, A. M. (1976). Effects of unilateral cardiac sympathetic denervation on the ventricular fibrillation threshold. *Am. J. Cardiol.* 37, 1034–1040. doi: 10.1016/0002-9149(76)90420-3

Scott, N. B., Turfrey, D. J., Ray, D. A., Nzewi, O., Sutcliffe, N. P., Lal, A. B., et al. (2001). A prospective randomized study of the potential benefits of thoracic epidural anesthesia and analgesia in patients undergoing coronary artery bypass grafting. *Anesth. Analg.* 93, 528–535. doi: 10.1097/00000539-200109000-00003

Seki, A., Green, H. R., Lee, T. D., Hong, L., Tan, J., Vinters, H. V., et al. (2014). Sympathetic nerve fibers in human cervical and thoracic vagus nerves. *Heart Rhythm* 11, 1411–1417. doi: 10.1016/j.hrthm.2014.04.032

Selmer, C., Olesen, J. B., Hansen, M. L., Lindhardsen, J., Olsen, A. M., Madsen, J. C., et al. (2012). The spectrum of thyroid disease and risk of new onset atrial fibrillation: a large population cohort study. *BMJ* 345:e7895. doi: 10.1136/bmj.e7895

Sharifov, O. F., Fedorov, V. V., Beloshapko, G. G., Glukhov, A. V., Yushmanova, A. V., and Rosenshtraukh, L. V. (2004). Roles of adrenergic and cholinergic stimulation in spontaneous atrial fibrillation in dogs. *J. Am. Coll. Cardiol.* 43, 483–490. doi: 10.1016/j.jacc.2003.09.030

Shen, M. J., Choi, E. K., Tan, A. Y., Lin, S. F., Fishbein, M. C., Chen, L. S., et al. (2011). Neural mechanisms of atrial arrhythmias. *Nat. Rev. Cardiol.* 9, 30–39. doi: 10.1038/nrcardio.2011.139

Shen, M. J., and Zipes, D. P. (2014). Role of the autonomic nervous system in modulating cardiac arrhythmias. *Circ. Res.* 114, 1004–1021. doi: 10.1161/CIRCRESAHA.113.302549

Skanes, A. C., Mandapati, R., Berenfeld, O., Davidenko, J. M., and Jalife, J. (1998). Spatiotemporal periodicity during atrial fibrillation in the isolated sheep heart. *Circulation* 98, 1236–1248. doi: 10.1161/01.CIR.98.12.1236

Sripairojthikoon, W., and Wyss, J. M. (1987). Cells of origin of the sympathetic renal innervation in rat. *Am. J. Physiol.* 252(6 Pt 2), F957–F963. doi: 10.1152/ajprenal.1987.252.6.F957

Svircevic, V., van Dijk, D., Nierich, A. P., Passier, M. P., Kalkman, C. J., van der Heijden, G. J., et al. (2011). Meta-analysis of thoracic epidural anesthesia versus general anesthesia for cardiac surgery. *Anesthesiology* 114, 271–282. doi: 10.1097/ALN.0b013e318201d300

Symplicity HTN-2 Investigators, Esler, M. D., Krum, H., Sobotka, P. A., Schlaich, M. P., Schmieder, R. E., et al. (2010). Renal sympathetic denervation in patients with treatment-resistant hypertension (The Symplicity HTN-2 Trial): a randomised controlled trial. *Lancet* 376, 1903–1909. doi: 10.1016/S0140-6736(10)62039-9

Tan, A. Y., Li, H., Wachsmann-Hogiu, S., Chen, L. S., Chen, P. S., and Fishbein, M. C. (2006). Autonomic innervation and segmental muscular disconnections at the human pulmonary vein-atrial junction: implications for catheter ablation of atrial-pulmonary vein junction. *J. Am. Coll. Cardiol.* 48, 132–143. doi: 10.1016/j.jacc.2006.02.054

Tan, A. Y., Zhou, S., Jung, B. C., Ogawa, M., Chen, L. S., Fishbein, M. C., et al. (2008a). Ectopic atrial arrhythmias arising from canine thoracic veins during in vivo stellate ganglia stimulation. *Am. J. Physiol. Heart Circ. Physiol.* 295, H691–H698. doi: 10.1152/ajpheart.01321.2007

Tan, A. Y., Zhou, S., Ogawa, M., Song, J., Chu, M., Li, H., et al. (2008b). Neural mechanisms of paroxysmal atrial fibrillation and paroxysmal atrial tachycardia in ambulatory canines. *Circulation* 118, 916–925. doi: 10.1161/CIRCULATIONAHA.108.776203

Tan, Z. Y., Lu, Y., Whiteis, C. A., Simms, A. E., Paton, J. F., Chapleau, M. W., et al. (2010). Chemoreceptor hypersensitivity, sympathetic excitation, and overexpression of ASIC and TASK channels before the onset of hypertension in SHR. *Circ. Res.* 106, 536–545. doi: 10.1161/CIRCRESAHA.109.206946

Tsai, C. T., Lai, L. P., Lin, J. L., Chiang, F. T., Hwang, J. J., Ritchie, M. D., et al. (2004). Renin-angiotensin system gene polymorphisms and atrial fibrillation. *Circulation* 109, 1640–1646. doi: 10.1161/01.CIR.0000124487.36586.26

Tsai, W. C., Chan, Y. H., Chinda, K., Chen, Z., Patel, J., Shen, C., et al. (2017). Effects of renal sympathetic denervation on the stellate ganglion and brain stem in dogs. *Heart Rhythm* 14, 255–262. doi: 10.1016/j.hrthm.2016.10.003

Ukena, C., Mahfoud, F., Spies, A., Kindermann, I., Linz, D., Cremers, B., et al. (2013). Effects of renal sympathetic denervation on heart rate and atrioventricular conduction in patients with resistant hypertension. *Int. J. Cardiol.* 167, 2846–2851. doi: 10.1016/j.ijcard.2012.07.027

Ulphani, J. S., Arora, R., Cain, J. H., Villuendas, R., Shen, S., Gordon, D., et al. (2007). The ligament of marshall as a parasympathetic conduit. *Am. J. Physiol. Heart Circ. Physiol.* 293, H1629–H1635. doi: 10.1152/ajpheart.00139.2007

Van Wagoner, D. R., Pond, A. L., Lamorgese, M., Rossie, S. S., McCarthy, P. M., and Nerbonne, J. M. (1999). Atrial L-type Ca2+ currents and human atrial fibrillation. *Circ. Res.* 85, 428–436. doi: 10.1161/01.RES.85.5.428

Vaquero, M., Calvo, D., and Jalife, J. (2008). Cardiac fibrillation: from ion channels to rotors in the human heart. *Heart Rhythm* 5, 872–879. doi: 10.1016/j.hrthm.2008.02.034

Verheule, S., Tuyls, E., van Hunnik, A., Kuiper, M., Schotten, U., and Allessie, M. (2010). Fibrillatory conduction in the atrial free walls of goats in persistent and permanent atrial fibrillation. *Circ. Arrhythm Electrophysiol.* 3, 590–599. doi: 10.1161/CIRCEP.109.931634

Vermond, R. A., Geelhoed, B., Verweij, N., Tieleman, R. G., Van der Harst, P., Hillege, H. L., et al. (2015). Incidence of Atrial Fibrillation and relationship with cardiovascular events, heart failure, and mortality: a community-based study from the Netherlands. *J. Am. Coll. Cardiol.* 66, 1000–1007. doi: 10.1016/j.jacc.2015.06.1314

Voigt, N., Heijman, J., Wang, Q., Chiang, D. Y., Li, N., Karck, M., et al. (2014). Cellular and molecular mechanisms of atrial arrhythmogenesis in patients with paroxysmal atrial fibrillation. *Circulation* 129, 145–156. doi: 10.1161/CIRCULATIONAHA.113.006641

Voigt, N., Li, N., Wang, Q., Wang, W., Trafford, A. W., Abu-Taha, I., et al. (2012). Enhanced sarcoplasmic reticulum Ca2+ leak and increased Na+-Ca2+ exchanger function underlie delayed afterdepolarizations in patients with chronic atrial fibrillation. *Circulation* 125, 2059–2070. doi: 10.1161/CIRCULATIONAHA.111.067306

Vollmann, D., Sossalla, S., Schroeter, M. R., and Zabel, M. (2013). Renal artery ablation instead of pulmonary vein ablation in a hypertensive patient with symptomatic, drug-resistant, persistent atrial fibrillation. *Clin. Res. Cardiol.* 102, 315–318. doi: 10.1007/s00392-012-0529-y

Wachtell, K., Lehto, M., Gerdts, E., Olsen, M. H., Hornestam, B., Dahlof, B., et al. (2005). Angiotensin II receptor blockade reduces new-onset atrial fibrillation and subsequent stroke compared to atenolol: the Losartan Intervention For End Point Reduction in Hypertension (LIFE) study. *J. Am. Coll. Cardiol.* 45, 712–719. doi: 10.1016/j.jacc.2004.10.068

Wakili, R., Voigt, N., Kaab, S., Dobrev, D., and Nattel, S. (2011). Recent advances in the molecular pathophysiology of atrial fibrillation. *J. Clin. Invest.* 121, 2955–2968. doi: 10.1172/JCI46315

Wang, X., Huang, C., Zhao, Q., Huang, H., Tang, Y., Dai, Z., et al. (2015). Effect of renal sympathetic denervation on the progression of paroxysmal atrial fibrillation in canines with long-term intermittent atrial pacing. *Europace* 17, 647–654. doi: 10.1093/europace/euu212

Witkowski, A., Prejbisz, A., Florczak, E., Kadziela, J., Sliwinski, P., Bielen, P., et al. (2011). Effects of renal sympathetic denervation on blood pressure, sleep apnea course, and glycemic control in patients with resistant hypertension and sleep apnea. *Hypertension* 58, 559–565. doi: 10.1161/HYPERTENSIONAHA.111.173799

Yagi, S., Hirata, Y., Ise, T., Kusunose, K., Yamada, H., Fukuda, D., et al. (2017). Canagliflozin reduces epicardial fat in patients with type 2 diabetes mellitus. *Diabetol. Metab. Syndr.* 9:78. doi: 10.1186/s13098-017-0275-4

Yang, S. S., Han, W., Cao, Y., Dong, G., Zhou, G., Li, W. M., et al. (2011). Effects of high thoracic epidural anesthesia on atrial electrophysiological characteristics and sympathetic nerve sprouting in a canine model of atrial fibrillation. *Basic Res. Cardiol.* 106, 495–506. doi: 10.1007/s00395-011-0154-3

Zhou, Q., Hu, J., Guo, Y., Zhang, F., Yang, X., Zhang, L., et al. (2013). Effect of the stellate ganglion on atrial fibrillation and atrial electrophysiological properties and its left-right asymmetry in a canine model. *Exp. Clin. Cardiol.* 18, 38–42.

Zinman, B., Wanner, C., Lachin, J. M., Fitchett, D., Bluhmki, E., Hantel, S., et al. (2015). Empagliflozin, cardiovascular outcomes, and mortality in type 2 diabetes. *N. Engl. J. Med.* 373, 2117–2128. doi: 10.1056/NEJMoa1504720

Zlochiver, S., Yamazaki, M., Kalifa, J., and Berenfeld, O. (2008). Rotor meandering contributes to irregularity in electrograms during atrial fibrillation. *Heart Rhythm* 5, 846–854. doi: 10.1016/j.hrthm.2008.03.010

Conflict of Interest Statement: MS is supported by an NHMRC Research Fellowship and has received consulting fees, and/or travel and research support from Medtronic, Abbott, Novartis, Servier, Pfizer, and Boehringer-Ingelheim.

The remaining authors declare that the research was conducted in the absence of any commercial or financial relationships that could be construed as a potential conflict of interest.

frontiers in Neuroscience

BRIEF RESEARCH REPORT
published: 31 January 2019
doi: 10.3389/fnins.2019.00033

Central Effects of Beta-Blockers May Be Due to Nitric Oxide and Hydrogen Peroxide Release Independently of Their Ability to Cross the Blood-Brain Barrier

Claire Laurens[1†], Anne Abot[2], Alain Delarue[1] and Claude Knauf[3]*

[1] Pierre Fabre Dermatologie, Lavaur, France, [2] Enterosys SAS, Prologue Biotech, Toulouse, France, [3] INSERM U1220 Institut de Recherche en Santé Digestive, CHU Purpan, Université Toulouse III Paul Sabatier, Toulouse, France

Propranolol is the first-line treatment for infants suffering from infantile hemangioma. Recently, some authors raised the question of potential neurologic side effects of propranolol due to its lipophilic nature and thus its ability to passively cross the blood-brain barrier (BBB) and accumulate into the brain. Hydrophilic beta-blockers, such as atenolol and nadolol, where therefore introduced in clinical practice. In addition to their classical mode of action in the brain, circulating factors may modulate the release of reactive oxygen/nitrogen species (ROS/RNS) from endothelial cells that compose the BBB without entering the brain. Due to their high capacity to diffuse across membranes, ROS/RNS can reach neurons and modify their activity. The aim of this study was to investigate other mechanisms of actions in which these molecules may display a central effect without actually crossing the BBB. We first performed an oral treatment in mice to measure the accumulation of propranolol, atenolol and nadolol in different brain regions *in vivo*. We then evaluated the ability of these molecules to induce the release of nitric oxide (NO) and hydrogen peroxide (H_2O_2) *ex vivo* in the hypothalamus. As expected, propranolol is able to cross the BBB and is found in brain tissue in higher amounts than atenolol and nadolol. However, all of these beta-blockers are able to induce the secretion of signaling molecules (i.e., NO and/or H_2O_2) in the hypothalamus, independently of their ability to cross the BBB, deciphering a new potential deleterious impact of hydrophilic beta-blockers in the brain.

Keywords: beta-blockers, propranolol, blood-brain barrier, infantile hemangioma, reactive oxygen species

OPEN ACCESS

Edited by:
Bernhard Schaller, University of Zurich, Switzerland

Reviewed by:
Stephen B. G. Abbott, University of Virginia, United States
Lionel Carneiro, Johns Hopkins University, United States

****Correspondence:***
Claude Knauf
claude.knauf@inserm.fr

†Present address:
Claire Laurens, CNRS, IPHC UMR 7178, Université de Strasbourg, Strasbourg, France

Specialty section:
This article was submitted to Autonomic Neuroscience, a section of the journal Frontiers in Neuroscience

Received: *07 November 2018*
Accepted: *15 January 2019*
Published: *31 January 2019*

Citation:
Laurens C, Abot A, Delarue A and Knauf C (2019) Central Effects of Beta-Blockers May Be Due to Nitric Oxide and Hydrogen Peroxide Release Independently of Their Ability to Cross the Blood-Brain Barrier. Front. Neurosci. 13:33. doi: 10.3389/fnins.2019.00033

INTRODUCTION

Since its discovery in 1960 by J. W. Black, the non-selective beta-blocker propranolol has been widely used in the treatment of hypertension, tachycardia and other cardiac disorders. More recently, propranolol has been introduced as first-line therapy for infantile hemangiomas, the most common soft-tissue tumors of childhood (Leaute-Labreze et al., 2015).

As propranolol is a lipophilic molecule, its use in infants raised the question of its ability to passively cross the blood-brain barrier (BBB) and directly activate adrenoreceptors on neuronal cells, and to subsequently impact the neurologic development of the child. Even if many reports have documented that propranolol treatment during infancy does not alter further brain development when compared to child and adolescents from

the general population examined several years after cessation of treatment (Moyakine et al., 2016, 2017; Gonzalez-Llorente et al., 2017; Mahon et al., 2018), other beta-blockers with hydrophilic properties have been here or there introduced in the treatment of infantile hemangiomas. The most commonly used molecules are nadolol and atenolol, which display hydrophilic properties and are therefore suggested to be unable to cross the BBB (Neil-Dwyer et al., 1981; Dahlof and Dimenas, 1990) and thus potentially decrease the risk to induce deleterious central effects (de Graaf et al., 2013; Pope et al., 2013; Tasani et al., 2017; Alexopoulos et al., 2018). However, these assumptions are based on biophysical characteristics of these molecules, and data regarding long-term safety are clearly lacking.

Alternative mechanisms in which some molecules are able to induce signaling pathways in the brain without crossing the blood-brain barrier have been described. One mechanism, that requires diffusible factors between two partners, implies central neurons and endothelial cells located in vascular wall. Indeed, brain endothelial cells have the capacity to produce second messengers such as nitric oxide (NO) to control the release of neurotransmitters (Knauf et al., 2001). This is especially the case in the mediobasal hypothalamus that includes the median eminence, a circumventricular organ where the BBB is physiologically absent (Rodriguez et al., 2005, 2010; Horsburgh and Massoud, 2013). For example, circulating hormones like estrogen (Prevot et al., 1999) or apelin (Duparc et al., 2011) induce endothelial NO release, with consequences on physiological functions, such as ovulation and glucose homeostasis, respectively. Hydrogen peroxide (H_2O_2) is another way to induce a signaling pathway in this brain region. As previously described for NO signaling, high dose of apelin can modify the release of hypothalamic H_2O_2 that could participate to an over-activation of the sympathetic system leading to the development of a type 2 diabetic state (Drougard et al., 2014). Thus, some molecules can modulate the activity of neuronal cells despite the absence of passage through the BBB and of direct activation of specific receptors on these cells.

The aim of the present study was to investigate whether propranolol, atenolol and nadolol induce the secretion of signaling molecules (i.e., NO and H_2O_2) in the hypothalamus, independently of their ability to directly stimulate adrenoreceptors on neuronal cells.

METHODS

Animals and Mass Spectrometry Analyses

All procedures are performed in accordance with the Directive 2010/63/UE recommendations and with French Veterinary Authorities agreement. *Ex vivo* design and procedures were approved by Ethical Committee (under protocol CEEA-122 2014-53). Eight weeks-old C57BL/6J male mice (n = 10/group, mean body weight = 25 g) were orally treated with either propranolol (3 mg/kg/day), atenolol (2 mg/kg/day) or nadolol (1 mg/kg/day) during 7 days, once a day for vehicle, nadolol and atenolol groups (at 8.00 am) and twice a day for propranolol group (at 8.00 am and 6.00 pm). Dose and administration scheme were selected to mimic therapeutic use of these molecules in infants suffering from infantile hemangioma. Mice were euthanized 1 h after the last gavage. Cortex, hypothalamus, cerebellum and brainstem were collected and immediately frozen in liquid nitrogen.

The concentrations of propranolol, atenolol and nadolol were determined after solid phase extraction followed by LC/ESI-MS/MS detection. Tissues were diluted in 9 ml of ultrapure water for 1 g of brain and homogenized by sonication over crushed ice. Atenolol-D7 and propranolol-D7 were used as internal standards. Dynamic concentration range was comprised between 1 and 8000 ng/ml for each compound. The chromatographic peaks for tested compound and internal standards were identified according to their retention times and MRM ion transitions and integrated by analytical software (MassLynx version 4.1, Waters).

Nitric Oxide and Hydrogen Peroxyde *ex vivo* Amperometric Measurements

Calibration of the electrochemical sensor was performed as previously published (Duparc et al., 2011; Drougard et al., 2014; Fournel et al., 2017; Abot et al., 2018). After dissection, hypothalamus was washed in Krebs-Ringer bicarbonate/glucose buffer (pH 7.4) in an atmosphere of 95%O_2–5%CO_2 and then immersed in Eppendorf tubes containing the same medium. Spontaneous NO or H_2O_2 release was measured at 37°C for 10 min by using either a NO-specific (ISO-NOPF, World Precision Instruments) or a H_2O_2-specific (ISO-HPO, World Precision Instruments) amperometric probe implanted in the hypothalamus. Ten micro liter saline solution (vehicle) was injected directly in the survival medium. After 10 min of record, 10 µl beta-blocker solution at increasing concentration was injected (final concentrations: 50 and 250 ng/ml). These concentrations were chosen to mimic plasma concentration of these molecules after an oral therapeutic dose in humans (i.e., approximately 50 ng/ml for propranolol and nadolol, and 250 ng/ml for atenolol). The concentration of NO or H_2O_2 gas in solution was measured in real-time (TBR1025, World Precision Instruments). DataTrax2 software (World Precision Instruments) performed data acquisition. Data are expressed as delta variation of NO or H_2O_2 release from basal.

Statistical Analyses

All statistical analyses were performed using GraphPad Prism 5.0 for Windows (GraphPad Software Inc., San Diego, CA, United States). Two-way ANOVA and Bonferroni's *post hoc* tests when used when appropriate. All values are presented as mean ± SEM. Statistical significance was set at $p < 0.05$.

RESULTS

Propranolol, Atenolol, and Nadolol Concentration in the Brain

We have first evaluated the capacity of the three beta-blockers to reach brain tissues (**Figure 1**). As previously described,

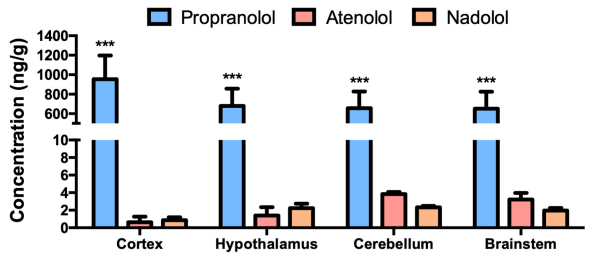

FIGURE 1 | Accumulation of propranolol, atenolol, and nadolol in different brain regions after a chronic oral treatment in mice. Concentration of propranolol, atenolol, and nadolol measured in the cortex, hypothalamus, brainstem, and cerebellum after 1 week of daily oral treatment in mice; n = 10/group; ***p < 0,001 vs. atenolol and nadolol.

propranolol is found at a high concentration in the brain after an oral treatment. In the same experimental conditions, the concentrations of nadolol and atenolol are lower in all brain regions, including a neurohemal structure such as the hypothalamus. This last result suggests that hydrophilic molecules cannot massively penetrate into the brain whether or not the BBB is leaky.

Hypothalamic NO Release in Response to Beta-Blockers

At the dose of 50 ng/ml, propranolol rapidly increased NO release from hypothalamus from 5 to 10 min (**Figure 2A**). Interestingly, atenolol was, at the same dose, also able to increase NO secretion from 6 to 10 min (**Figure 2B**), while delta variation of NO release in response to nadolol treatment was significantly induced after 9 min (**Figure 2C**). Taken together, these results show that, at a low dose, all three tested beta-blockers are able to induce NO release from hypothalamus.

When hypothalamus was treated with propranolol at a higher dose (i.e., 250 ng/ml), no significant variation in NO release was observed (**Figure 2D**). Surprisingly, atenolol displayed an opposite effect at the high dose compared to low dose treatment by significantly decreasing NO release after 6 min of treatment (**Figure 2E**). As observed for propranolol, nadolol treatment at this same dose did not induce any significant variation of NO release by the hypothalamus (**Figure 2F**).

These data indicate that lipophilic propranolol and hydrophilic atenolol and nadolol are all able to induce NO release from the hypothalamus at a low dose. Contrasting results observed at a higher dose suggest that alternative mechanisms may be activated to counterbalance the effects of massive NO release in the brain.

Hypothalamic H_2O_2 Release in Response to Beta-Blockers

Treatment with a low dose of propranolol (i.e., 50 ng/ml) did not induce any significant variation of H_2O_2 release from the hypothalamus (**Figure 2G**). Similar results have been observed upon atenolol treatment (**Figure 2H**). However, in response to nadolol at a low dose, delta variation of H_2O_2 release from basal significantly increased from 5 min (**Figure 2I**).

At a higher dose of 250 ng/ml, no significant changes of H_2O_2 production were observed in response to propranolol treatment (**Figure 2J**), while both atenolol (**Figure 2K**) and nadolol (**Figure 2L**) treatment rapidly increased H_2O_2 release.

Altogether, these results clearly show that, while propranolol treatment does not induce H_2O_2 release from the hypothalamic explants at any dose, a high dose of atenolol or nadolol rapidly induce H_2O_2 release from the hypothalamus. The amplitude of H_2O_2 production is particularly high in response to nadolol treatment, either at a low or high dose.

DISCUSSION

We have shown that, despite the inability of hydrophilic beta-blockers to cross the BBB and thus to accumulate into the brain, all three beta-blockers tested in this study, either lipophilic or hydrophilic, were able to modulate the release of NO and/or H_2O_2 in the hypothalamus. As these small molecules can passively diffuse in brain tissue, they could have an impact on neuronal activity of central neurons. This could explain some of the potential deleterious effects of these molecules in the brain such as sleep disorders (de Graaf et al., 2013; Pope et al., 2013; Labreze et al., 2015; Leaute-Labreze et al., 2015; Randhawa et al., 2015; Ji et al., 2016) and in periphery such as hypoglycemia (Holland et al., 2010; Poterucha et al., 2015).

Despite its ability to accumulate into the brain, propranolol failed to increase the release of hypothalamic H_2O_2 that is usually associated with oxidative stress (Fisher-Wellman and Neufer, 2012; Angelova and Abramov, 2018). Little is known in the literature to explain the mode of action of propranolol to avoid H_2O_2 release. It has been shown that, in the skin of frog, propranolol is able to decrease water permeability induced by arginine vasotocin (AVT) (Ogushi et al., 2010; Saitoh et al., 2014). In this model, aquaporins are translocated at the membrane in response to AVT. We can speculate that propranolol, by acting on aquaporins translocation, could decrease the negative impact of H_2O_2, which is known to use aquaporins to cross cell membrane (Tamma et al., 2018).

The effect of atenolol on hypothalamic NO/H_2O_2 release is also unexpected. At low dose, atenolol induces NO release from hypothalamic explants, but at higher dose of 250 ng/ml, corresponding to plasma concentration measured after an oral administration at the therapeutic dose, it decreases NO release and increases H_2O_2 secretion. Even if this dual effect seems surprising, our group has previously demonstrated the existence of such physiological phenomenon in another physiological context. Indeed, apelin, an adipokine released by the adipose tissue, stimulates the release of hypothalamic NO at a low dose (Duparc et al., 2011), but inhibits NO release and stimulates H_2O_2 release at a high dose (Duparc et al., 2011; Drougard et al., 2014). In our experimental model, this dual effect can be explained by pharmacological and physiological hypotheses. For instance, the decrease of NO release could be due to its interaction with H_2O_2 to generate hydroxyl radical (Nappi and Vass, 1998).

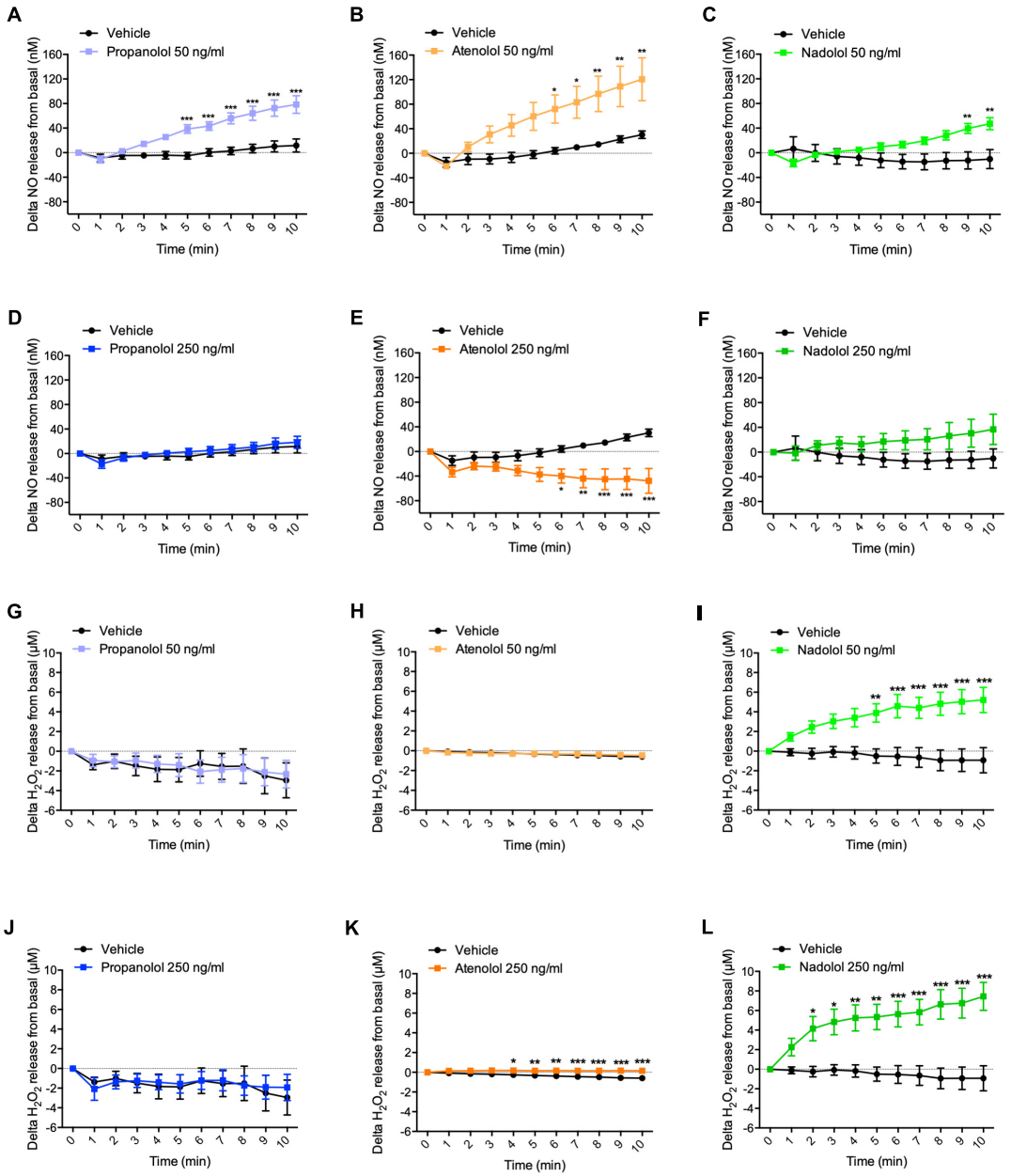

FIGURE 2 | Hypothalamic NO and H_2O_2 release in response to propranolol, atenolol, and nadolol treatment. *Ex vivo* NO **(A–F)** and H_2O_2 **(G–L)** release from hypothalamus in response to propranolol **(A,D,G,J)**, atenolol **(B,E,H,K)**, or nadolol **(C,F,I,L)** at either low dose 50 ng/mL **(A–C,G–I)** or high dose 250 ng/mL **(D–F,J–L)**; n = 10/group; *$p < 0{,}05$, **$p < 0{,}01$, and ***$p < 0{,}001$ vs. vehicle.

In addition, we observed that nadolol induces both NO and H_2O_2 secretion either at a low or high dose. The low dose reproduces plasma concentration measured after an oral therapeutic dose of nadolol. This result demonstrates that the ability to cross the BBB is not mandatory to induce signaling in the brain, and thus further activation/inactivation of specific neuronal populations.

Finally, the magnitude of NO/H_2O_2 release in response to the different treatments also needs to be considered. Indeed, while a release in the range of pM to nM induces physiological effects such as signal transduction and neurotransmission (either beneficial or detrimental depending on targeted neurons), a release in the range of nM to µM induces deleterious effects such as oxidative stress and DNA damage leading to cellular dysfunction (Bredt, 1999; Mustafa et al., 2009). In this study we show that, at a concentration mimicking plasma concentration of the three beta-blockers after a therapeutic dose, propranolol induced a release of 80 nM of NO and no change in H_2O_2 production. In contrast, atenolol decreased NO release but

increased H2O2 production in the range of μM. Nadolol was responsible of the release of 50 nM of NO and, more importantly, induced a 5 μM release of H_2O_2, which is probably leading to oxidative stress and cellular toxicity. Altogether, these data indicate that, even if they do not cross the BBB and do not accumulate in brain tissues, both atenolol and nadolol are able to induce central toxicity.

Of course, our study is limited by the use of murine *ex vivo* models which do not reflect the exact physiological conditions observed *in vivo*. A similar approach (i.e., NO/H_2O_2 real-time measurements) could be performed *in vivo* in different brain regions in mice in response to an oral load of beta-blockers (Fournel et al., 2017).

To conclude, our study brings new elements to decipher the mode of action (and the potential related side effects) of beta-blockers in the brain. The mode of communication through endothelial cells and production of NO/H_2O_2 that does not require the entry of a beta-blocker molecule into the brain has to be considered when using such molecule.

AUTHOR CONTRIBUTIONS

All authors have designed the experiments and wrote the manuscript. AA had performed the experiments.

FUNDING

This study was funded by Pierre Fabre Dermatologie. AD is employed by Pierre Fabre. CK is co-founder of *Enterosys* SAS (Labège, France).

REFERENCES

Abot, A., Lucas, A., Bautzova, T., Bessac, A., Fournel, A., Le-Gonidec, S., et al. (2018). Galanin enhances systemic glucose metabolism through enteric nitric oxide synthase-expressed neurons. *Mol. Metab.* 10, 100–108. doi: 10.1016/j.molmet.2018.01.020

Alexopoulos, A., Thanopoulou, I., Dakoutrou, M., Georgiadou, E., Chrousos, G. P., and Kakourou, T. (2018). Atenolol treatment for severe infantile hemangiomas: a single-centre prospective study. *J. Eur. Acad. Dermatol. Venereol.* 32, e117–e119. doi: 10.1111/jdv.14590

Angelova, P. R., and Abramov, A. Y. (2018). Role of mitochondrial ROS in the brain: from physiology to neurodegeneration. *FEBS Lett.* 592, 692–702. doi: 10.1002/1873-3468.12964

Bredt, D. S. (1999). Endogenous nitric oxide synthesis: biological functions and pathophysiology. *Free Radic Res.* 31, 577–596. doi: 10.1080/10715769900301161

Dahlof, C., and Dimenas, E. (1990). Side effects of beta-blocker treatments as related to the central nervous system. *Am. J. Med. Sci.* 299, 236–244. doi: 10.1097/00000441-199004000-00004

de Graaf, M., Raphael, M. F., Breugem, C. C., Knol, M. J., Bruijnzeel-Koomen, C. A., Kon, M., et al. (2013). Treatment of infantile haemangiomas with atenolol: comparison with a historical propranolol group. *J. Plast Reconstr. Aesthet. Surg.* 66, 1732–1740. doi: 10.1016/j.bjps.2013.07.035

Drougard, A., Duparc, T., Brenachot, X., Carneiro, L., Gouaze, A., Fournel, A., et al. (2014). Hypothalamic apelin/reactive oxygen species signaling controls hepatic glucose metabolism in the onset of diabetes. *Antioxid. Redox Signal.* 20, 557–573. doi: 10.1089/ars.2013.5182

Duparc, T., Colom, A., Cani, P. D., Massaly, N., Rastrelli, S., Drougard, A., et al. (2011). Central apelin controls glucose homeostasis via a nitric oxide-dependent pathway in mice. *Antioxid. Redox Signal.* 15, 1477–1496. doi: 10.1089/ars.2010.3454

Fisher-Wellman, K. H., and Neufer, P. D. (2012). Linking mitochondrial bioenergetics to insulin resistance via redox biology. *Trends Endocrinol. Metab.* 23, 142–153. doi: 10.1016/j.tem.2011.12.008

Fournel, A., Drougard, A., Duparc, T., Marlin, A., Brierley, S. M., Castro, J., et al. (2017). Apelin targets gut contraction to control glucose metabolism via the brain. *Gut* 66, 258–269. doi: 10.1136/gutjnl-2015-310230

Gonzalez-Llorente, N., Del Olmo-Benito, I., Munoz-Ollero, N., Descalzo, M. A., Garcia-Doval, I., and Torrelo, A. (2017). Study of cognitive function in children treated with propranolol for infantile hemangioma. *Pediatr. Dermatol.* 34, 554–558. doi: 10.1111/pde.13229

Holland, K. E., Frieden, I. J., Frommelt, P. C., Mancini, A. J., Wyatt, D., and Drolet, B. A. (2010). Hypoglycemia in children taking propranolol for the treatment of infantile hemangioma. *Arch. Dermatol.* 146, 775–778. doi: 10.1001/archdermatol.2010.158

Horsburgh, A., and Massoud, T. F. (2013). The circumventricular organs of the brain: conspicuity on clinical 3T MRI and a review of functional anatomy. *Surg. Radiol. Anat.* 35, 343–349. doi: 10.1007/s00276-012-1048-2

Ji, Y., Wang, Q., Chen, S., Xiang, B., Xu, Z., Li, Y., et al. (2016). Oral atenolol therapy for proliferating infantile hemangioma: a prospective study. *Medicine* 95:e3908. doi: 10.1097/MD.0000000000003908

Knauf, C., Ferreira, S., Hamdane, M., Mailliot, C., Prevot, V., Beauvillain, J. C., et al. (2001). Variation of endothelial nitric oxide synthase synthesis in the median eminence during the rat estrous cycle: an additional argument for the implication of vascular blood vessel in the control of GnRH release. *Endocrinology.* 142, 4288–4294. doi: 10.1210/endo.142.10.8443

Labreze, C., Voisard, J. J., Delarue, A., and Moore, N. (2015). Risk of neurodevelopmental abnormalities in children treated with propranolol. *Br. J. Dermatol.* 173, 1562–1564. doi: 10.1111/bjd.14000

Leaute-Labreze, C., Hoeger, P., Mazereeuw-Hautier, J., Guibaud, L., Baselga, E., Posiunas, G., et al. (2015). A randomized, controlled trial of oral propranolol in infantile hemangioma. *N. Engl. J. Med.* 372, 735–746. doi: 10.1056/NEJMoa1404710

Mahon, C., Heron, G., Perkins, D., Drage, A., and Wargon, O. (2018). Oral propranolol for infantile haemangioma may be associated with transient gross motor delay. *Br. J. Dermatol.* 178, 1443–1444. doi: 10.1111/bjd.16334

Moyakine, A. V., Kerstjens, J. M., Spillekom-van Koulil, S., and van der Vleuten, C. J. (2016). Propranolol treatment of infantile hemangioma (IH) is not associated with developmental risk or growth impairment at age 4 years. *J. Am. Acad. Dermatol.* 75, 59.e1–63.e1. doi: 10.1016/j.jaad.2016.02.1218

Moyakine, A. V., Spillekom-van Koulil, S., and van der Vleuten, C. J. M. (2017). Propranolol treatment of infantile hemangioma is not associated with psychological problems at 7 years of age. *J. Am. Acad. Dermatol.* 77, 105–108. doi: 10.1016/j.jaad.2017.01.025

Mustafa, A. K., Gadalla, M. M., and Snyder, S. H. (2009). Signaling by gasotransmitters. *Sci. Signal.* 2, re2. doi: 10.1126/scisignal.268re2

Nappi, A. J., and Vass, E. (1998). Hydroxyl radical formation resulting from the interaction of nitric oxide and hydrogen peroxide. *Biochim. Biophys. Acta.* 1380, 55–63. doi: 10.1016/S0304-4165(97)00125-6

Neil-Dwyer, G., Bartlett, J., McAinsh, J., and Cruickshank, J. M. (1981). Beta-adrenoceptor blockers and the blood-brian barrier. *Br. J. Clin. Pharmacol.* 11, 549–553. doi: 10.1111/j.1365-2125.1981.tb01169.x

Ogushi, Y., Kitagawa, D., Hasegawa, T., Suzuki, M., and Tanaka, S. (2010). Correlation between aquaporin and water permeability in response to vasotocin, hydrin and {beta}-adrenergic effectors in the ventral pelvic skin of the tree frog Hyla japonica. *J. Exp. Biol.* 213, 288–294. doi: 10.1242/jeb.036871

Pope, E., Chakkittakandiyil, A., Lara-Corrales, I., Maki, E., and Weinstein, M. (2013). Expanding the therapeutic repertoire of infantile haemangiomas: cohort-blinded study of oral nadolol compared with propranolol. *Br. J. Dermatol.* 168, 222–224. doi: 10.1111/j.1365-2133.2012.11131.x

Poterucha, J. T., Bos, J. M., Cannon, B. C., and Ackerman, M. J. (2015). Frequency and severity of hypoglycemia in children with beta-blocker-treated long QT syndrome. *Heart Rhythm.* 12, 1815–1819. doi: 10.1016/j.hrthm.2015.04.034

Prevot, V., Croix, D., Rialas, C. M., Poulain, P., Fricchione, G. L., Stefano, G. B., et al. (1999). Estradiol coupling to endothelial nitric oxide stimulates

gonadotropin-releasing hormone release from rat median eminence via a membrane receptor. *Endocrinology.* 140, 652–659. doi: 10.1210/endo.140.2.6484

Randhawa, H. K., Sibbald, C., Garcia Romero, M. T., and Pope, E. (2015). Oral Nadolol for the Treatment of Infantile Hemangiomas: a Single-Institution Retrospective Cohort Study. *Pediatr. Dermatol.* 32, 690–695. doi: 10.1111/pde.12655

Rodriguez, E. M., Blazquez, J. L., and Guerra, M. (2010). The design of barriers in the hypothalamus allows the median eminence and the arcuate nucleus to enjoy private milieus: the former opens to the portal blood and the latter to the cerebrospinal fluid. *Peptides.* 31, 757–776. doi: 10.1016/j.peptides.2010.01.003

Rodriguez, E. M., Blazquez, J. L., Pastor, F. E., Pelaez, B., Pena, P., Peruzzo, B., et al. (2005). Hypothalamic tanycytes: a key component of brain-endocrine interaction. *Int. Rev. Cytol.* 247, 89–164. doi: 10.1016/S0074-7696(05)47003-5

Saitoh, Y., Ogushi, Y., Shibata, Y., Okada, R., Tanaka, S., and Suzuki, M. (2014). Novel vasotocin-regulated aquaporins expressed in the ventral skin of semiaquatic anuran amphibians: evolution of cutaneous water-absorbing mechanisms. *Endocrinology.* 155, 2166–2177. doi: 10.1210/en.2013-1928

Tamma, G., Valenti, G., Grossini, E., Donnini, S., Marino, A., Marinelli, R. A., et al. (2018). Aquaporin membrane channels in oxidative stress, cell signaling, and aging: recent advances and research trends. *Oxid. Med. Cell Longev.* 2018:1501847. doi: 10.1155/2018/1501847

Tasani, M., Glover, M., Martinez, A. E., and Shaw, L. (2017). Atenolol treatment for infantile haemangioma. *Br. J. Dermatol.* 176, 1400–1402. doi: 10.1111/bjd.15317

Conflict of Interest Statement: The authors declare that the research was conducted in the absence of any commercial or financial relationships that could be construed as a potential conflict of interest.

frontiers in Neuroscience

ORIGINAL RESEARCH
published: 29 March 2019
doi: 10.3389/fnins.2019.00301

Proconvertase Furin Is Downregulated in Postural Orthostatic Tachycardia Syndrome

*Jasmina Medic Spahic[1,2], Fabrizio Ricci[1,3], Nay Aung[4], Jonas Axelsson[1,5], Olle Melander[1,2], Richard Sutton[6], Viktor Hamrefors[1,2] and Artur Fedorowski[1,7]**

[1] Department of Clinical Sciences, Faculty of Medicine, Clinical Research Center, Lund University, Malmö, Sweden, [2] Department of Internal Medicine, Skåne University Hospital, Malmö, Sweden, [3] Institute for Advanced Biomedical Technologies, Department of Neuroscience, Imaging and Clinical Sciences, Università degli Studi "G. d'Annunzio" Chieti-Pescara, Chieti, Italy, [4] The William Harvey Research Institute, NIHR Cardiovascular Biomedical Research Unit at Barts, Queen Mary University of London, London, United Kingdom, [5] Department of Clinical Immunology and Transfusion Medicine, Karolinska University Hospital, Stockholm, Sweden, [6] National Heart and Lung Institute, Imperial College London, London, United Kingdom, [7] Department of Cardiology, Skåne University Hospital, Malmö, Sweden

Background: Postural Orthostatic Tachycardia Syndrome (POTS) is a cardiovascular autonomic disorder characterized by orthostatic intolerance and high prevalence among young women. The etiology of POTS is uncertain, though autoimmunity and inflammation may play an important role. We aimed to identify novel inflammatory biomarkers associated with POTS.

Methods and Results: In the Syncope Study of Unselected Population in Malmö (SYSTEMA) cohort, we identified 396 patients (age range, 15–50 years) with either POTS (n = 113) or normal haemodynamic response during passive head-up-tilt test (n = 283). Blood samples were analyzed using antibody-based Proximity Extension Assay technique simultaneously measuring 57 inflammatory protein biomarkers. The discovery algorithm was a sequential two-step process of biomarker signature identification by supervised, multivariate, principal component analysis and verification by univariate ANOVA with Bonferroni correction. POTS patients were younger (26 vs. 31 years; $p < 0.001$) and there was no significant difference in sex distribution (74% vs. 67% females, $p = 0.24$). PCA and Bonferroni-adjusted ANOVA identified proconvertase furin as the most robust biomarker signature for POTS. Plasma level of proconvertase furin was lower (6.38 vs. 6.58 of normalized protein expression units (NPX); $p < 0.001$ in POTS, compared with the reference group. Proconvertase furin met Bonferroni-adjusted significance criteria in both uni- and multivariable regression analyses.

Conclusion: Patients with POTS have lower plasma level of proconvertase furin compared with individuals with normal postural hemodynamic response. This finding suggests the presence of a specific autoimmune trait with disruption of immune peripheral tolerance in this hitherto unexplained condition. Further studies are needed for external validation of our results.

Keywords: postural orthostatic tachycardia syndrome, inflammation, biomarkers, proteomics, proconvertase furin

OPEN ACCESS

Edited by:
Erwin Lemche, King's College London, United Kingdom

Reviewed by:
Chamini Perera, University of New South Wales, Australia
Satish R. Raj, University of Calgary, Canada

***Correspondence:**
Artur Fedorowski
artur.fedorowski@med.lu.se

Specialty section:
This article was submitted to Autonomic Neuroscience, a section of the journal Frontiers in Neuroscience

Received: *07 January 2019*
Accepted: *15 March 2019*
Published: *29 March 2019*

Citation:
Spahic JM, Ricci F, Aung N, Axelsson J, Melander O, Sutton R, Hamrefors V and Fedorowski A (2019) Proconvertase Furin Is Downregulated in Postural Orthostatic Tachycardia Syndrome. Front. Neurosci. 13:301. doi: 10.3389/fnins.2019.00301

INTRODUCTION

Postural orthostatic tachycardia syndrome (POTS) is a complex condition featuring signs of autonomic dysfunction with both cardiovascular and non-cardiovascular symptoms (Benarroch, 2012). Although typically multi-symptomatic, POTS is by definition characterized by an abnormally increased heart rate upon standing and symptoms of orthostatic intolerance without significant blood pressure decrease (Sheldon et al., 2015). The syndrome affects predominantly young women (70–80%) with increasing incidence in developed countries, but its etiology has not been established (Sheldon et al., 2015; Brinth et al., 2018). Aside from orthostatic intolerance, patient frequently report headache, palpitations, brain fog and fatigue, which is believed to be a consequence of both hyperadrenergic state and decreased blood flow to the brain (Benarroch, 2012; Li et al., 2014; Arnold et al., 2018).

As etiology of POTS is still unknown, effective treatment for this syndrome is yet to be developed. Therapeutic options available today have modest efficacy and focus only on alleviating symptoms, thus, further research is mandatory. It has been observed that some patients develop POTS after experiencing a febrile illness, presumably viral (Grubb, 2008; Li et al., 2014). This has led to the hypothesis of an autoimmune-mediated etiology of POTS, and recent case series of POTS following immune triggers like infection or vaccination (Blitshteyn, 2015; Brinth et al., 2015; Watari et al., 2018) support this hypothesis. It has already been established that activating autoantibodies (AAb) to the α1-adrenergic (α1AR), β1/2-adrenergic receptors (β1/2AR), and angiotensin-receptor type 1 can be found in serum from POTS patients but not in controls (Fedorowski et al., 2017; Yu et al., 2018). In current knowledge of the presence of autoantibodies and possible immunological triggers, exploration of expression of inflammatory mediators in POTS is required, both as a potential diagnostic tool and therapeutic target in this ill-understood condition for which there is no effective treatment.

In this study, we sought to discover inflammatory biomarkers associated with POTS in order to identify a signature, which could potentially be useful to understand the pathophysiology underlying the syndrome. We applied a new method of multiple-protein screening using oligonucleotide-labeled antibodies against selected serum proteins.

MATERIALS AND METHODS

Study Population

The study was performed between September 2008 and May 2014 on a series of 545 consecutive patients aged 15–50 years enrolled in the ongoing Syncope Study of Unselected Population in Malmö (SYSTEMA) (Fedorowski et al., 2010). The age range was based on previous epidemiological studies on POTS incidence (Goodman, 2018). The recruited patients were referred to the tertiary syncope investigation unit at Skåne University Hospital in Malmö from primary and outpatient care clinics as well as hospitals in the southern region of Sweden due to unexplained syncope and/or symptoms of orthostatic intolerance. The referred patient underwent an initial diagnostic workup, typically including clinical history, resting, exercise and ambulatory prolonged electrocardiogram (Holter-ECG), transthoracic echocardiography, coronary and pulmonary angiography, brain imaging and encephalography, if requested by the referring physician. In the Syncope Unit, the patients were investigated by cardiovascular autonomic tests including head-up tilt testing (HUT), according to the European syncope guidelines available during this period (Moya et al., 2009). Blood samples were collected during the examination. The final study population included 113 POTS individuals and 283 controls with normal hemodynamic response during HUT as well as without prevalent cardiovascular disease (ischemic heart disease, heart failure, and stroke) or hypertension.

The study protocol conformed to the ethical guidelines of the 1975 Declaration of Helsinki and was approved by The Regional Ethical Review Board of Lund University (No 82/2008). All patients gave their written informed consent.

The PICO model was as follows: patients with unexplained syncope or orthostatic intolerance (Population), blood samples and HUT (Intervention), POTS patients versus controls (Comparison), and targeted protein biomarker discovery and haemodynamic response (Outcome).

Examination Protocol

Patients discontinued cardiovascular drugs 48 h before the test, fasted for 2 h prior to examination and were allowed to drink water at will. The past medical history was explored using a standard study questionnaire. The patients were placed on a tilt table and a venous cannula was inserted in the forearm after which a rest period for at least 10 min was allowed before blood samples were collected through the cannula. As soon as the haemodynamic parameters were stable, a standard 70°HUT was carried out according to the Italian protocol recommended by ESC (Bartoletti et al., 2000; Moya et al., 2009). Beat-to-beat blood pressure and ECG were monitored continuously by a validated non-invasive photoplethysmographic method (Nexfin monitor; BMEYE, Amsterdam, Netherlands) with a wrist unit and finger cuff of appropriate size (Eeftinck Schattenkerk et al., 2009). POTS was defined as reproduction of symptoms of orthostatic intolerance (lightheadedness, dizziness, or discomfort) along with heart rate increase >30 beats/min or sinus tachycardia >120 beats/min during first 10 min of HUT; or increase >40 beats/min for those under 18 years of age, with a history of orthostatic intolerance for at least 6 months (Sheldon et al., 2015).

Multiplex Protein Analysis

Plasma biomarkers were measured from supine blood samples (total volume: 30 ml) that had been first centrifuged, then stored as 16 × 250 μL aliquots of EDTA plasma in plastic thermotubes, and frozen at −80°C. For biomarker analysis, the samples were thawed and examined by the Proximity Extension Assay technique using the Olink Proteomics Proseek Multiplex Oncology I v1 96 × 96 reagents kit, which simultaneously measures 57 inflammatory and cancer-related human protein biomarkers in plasma (**Supplementary Table S1**). Briefly, a pair of oligonucleotide-labeled antibodies, Proseek probes, binds to

the target protein in the plasma sample. When the two Proseek probes are in close proximity, a new polymerase-chain reaction (PCR) target sequence is formed by a proximity-dependent DNA polymerization event. This complex is subsequently detected and quantified using standard real-time PCR. The generated Normalised Protein Expression (NPX) unit is on a log2 scale, which means that a larger number represents a higher protein level in the sample. Additional information concerning limit of detection, reproducibility and validation is available at the Olink Proteomics website[1].

Statistical Analysis

For the statistical analyses, patients with available proteomics data and definitive diagnosis of POTS (n = 113) or normal hemodynamic response during HUT (n = 283), i.e., without orthostatic hypotension (Moya et al., 2009; Freeman et al., 2011) and abnormal postural tachycardia, as well as without prevalent cardiovascular disease (ischemic heart disease, heart failure, and stroke) or hypertension were selected. Missing data was imputed with multiple imputations by chained equations (MICE) approach to create 10 complete datasets. We used predictive mean matching for continuous variables, logistic regression for binary variables, and polytomous regression for categorical variables. All covariates were included in the imputation models. The maximum iteration was set at 20 and convergence was confirmed by visual examination of trace plots. The main characteristics of study population were calculated as mean and standard deviation for continuous variables and as percentages for categorical variables, both for the total study population, and separately for POTS-positive and -negative patients.

The discovery algorithm for the identification of potentially relevant biomarkers associated with the presence of POTS was a sequential two-step process of (i) biomarker signature identification by a supervised, multivariate, principal component analysis, and (ii) verification by univariate ANOVA with Bonferroni correction. This method has been previously validated in our hands (Johansson et al., 2018a,b).

After defining a minimal call rate <75%, we screened the biomarker panel through supervised principal component analysis, according to the algorithm first described by Hastie et al. (2013), which includes the following steps:

(1) For each biomarker, compute the standardized univariate logistic regression coefficient which represents the effect size for the outcome (presence or absence of POTS).
(2) Using an arbitrary effect size threshold θ from the list $0 \leq \theta_1 < \theta_2 < \cdots < \theta_K$.
    (a) Form a reduced data matrix consisting of only those biomarkers whose univariate coefficient exceeds θ in absolute value, and compute the principal components of this matrix.
    (b) Use these principal components in a multivariate logistic regression model to predict POTS status.
(3) Select the threshold θ which gives the best predictive accuracy by 10-fold cross-validation.

[1]http://www.olink.com/products/document-download-center

Thereafter, for the verification of the selected biomarkers we applied a conservative univariate ANOVA approach, using a Bonferroni-adjusted significance level of $p < 0.05$/number of PCA-selected biomarkers. Box plots were generated to display the distribution of biomarker levels between groups.

Furthermore, we performed both univariate and multivariate ordinary least square linear regression and logistic regression models for bivariate correlation between plasma level of selected biomarkers and maximum orthostatic heart rate change (ΔHR) or POTS status, respectively. In multivariate regression models we adjusted for age and sex. Finally, we performed a quantile-regression analysis in order to identify differing relationships at different quartiles of HR changes during HUT. The mean estimates and standard errors of the beta-coefficients for the imputed datasets were combined with Rubin's rules (Rubin, 1987). Statistical analyses were carried out using IBM SPSS Statistics version 25 (SPSS Inc., Chicago, IL, United States) and R Statistical Software (version 3.4.4; R Foundation for Statistical Computing, Vienna, Austria).

RESULTS

Biomarker Signature Discovery

The dataset consisted of 396 patients (113 POTS and 283 controls). Baseline characteristics of the study population by POTS status are shown in **Table 1**. There was no significant difference in characteristics between the whole cohort and complete cases without missing data (**Supplementary Table S2**). Since the principal component analysis requires pairwise complete data, we did not include markers with high missingness, i.e., above 35%. This filter resulted in removal of 9 biomarkers: erythropoietin, interleukin-2, interferon-gamma, tumor necrosis factor, carcinoembryonic antigen, vascular endothelial statin, lipopolysaccharide-induced tumor necrosis factor (TNF)-alpha factor, myeloid differentiation primary response protein, MHC class I polypeptide-related sequence A. Univariate logistic

TABLE 1 | Baseline characteristics of the study population.

Characteristic	POTS− (n = 283)	POTS+ (n = 113)	P-value
Age	31.47 (9.85)	26.27 (8.41)	<0.001
Female sex, *n* (%)	189 (66.8)	83 (73.5)	0.241
BMI, Kg/m^2	24.33 (4.14)	22.69 (3.50)	<0.001
SBP supine, mmHg	120.07 (14.16)	120.41 (14.20)	0.833
DBP supine, mmHg	69.98 (8.21)	70.22 (8.22)	0.788
HR supine, bpm	68.86 (11.87)	71.13 (11.57)	0.084
SBP HUT min, mmHg	112.34 (13.35)	107.58 (16.24)	0.003
DBP HUT min, mmHg	71.83 (9.11)	72.46 (10.58)	0.552
HR HUT max, bpm	84.77 (13.77)	112.41 (15.63)	<0.001
Smoking, *n* (%)	58 (20.5)	16 (14.2)	0.188

P-values for differences between the groups are shown as mean and SD for continuous variables and as percentages for categorical variables; DBP, diastolic blood pressure; HR, heart rate; HUT min/max, lowest/highest value during passive head-up tilt test; IHD, ischemic heart disease; POTS, postural orthostatic tachycardia syndrome; SBP, systolic blood pressure.

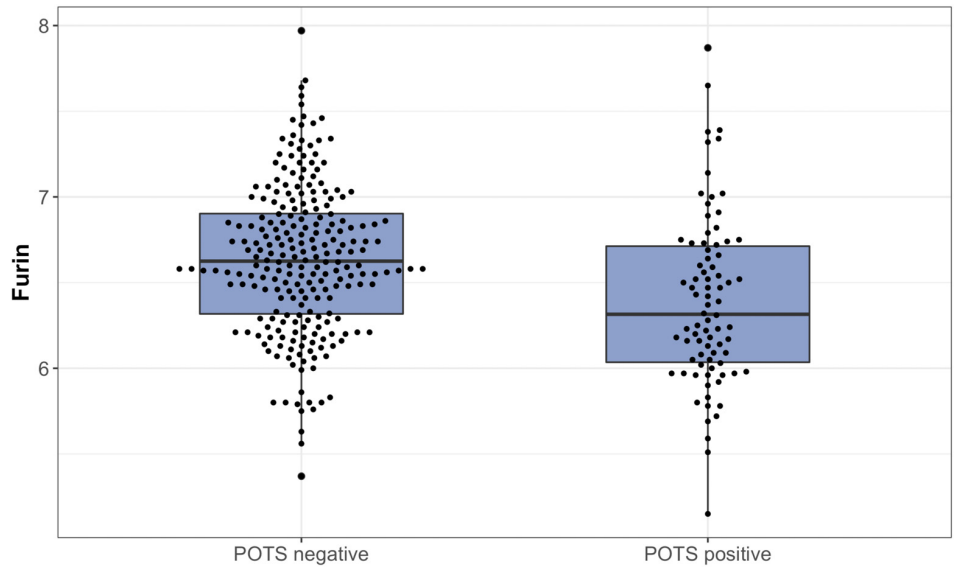

FIGURE 1 | The plasma levels of proconvertase furin, expressed on a log2 scale, presented in relation to POTS status. Data are shown as a box and whisker plot with median in the box and the whiskers representing the 5th and 95th percentiles in relation to plasmatic biomarker levels.

regression was performed for each of the 48 biomarkers. Heatmap representation of the data showing the hierarchical clustering of the 48 biomarkers by POTS status is shown in **Supplementary Figure S2**.

The regression coefficients were then standardized by dividing the coefficient with its standard error. All possible thresholds (Standardized coefficient (θ) ranging from minimum to maximum with 0.05 increments) were used to select groups of biomarkers and construct principal components (PCs). The outcome variable (POTS status) was then regressed onto the 1st two PCs from each group of biomarkers using the binomial link function. This step identified the group of biomarkers which gave the best classification accuracy. The threshold that gave the best classification accuracy (POTS+ vs. controls) was selected by ten-fold cross-validation. The following four biomarkers reached this threshold: carbonic anhydrase IX; receptor tyrosine-protein kinase erbB-2; Fms-related tyrosine kinase 3 ligand; and proconvertase furin.

Biomarker Verification

All PCA-selected biomarkers except carbonic anhydrase IX differed significantly in pairwise comparison, but only proconvertase furin attained significance after Bonferroni correction (**Figure 1** and **Table 2**). In multivariate regression analysis both POTS status and maximum orthostatic ΔHR were significantly associated with proconvertase furin (**Tables 3**, **4**). Quantile regression analyses investigating the relationships between proconvertase furin and the quartiles of ΔHR did not reveal any obvious threshold effect or step function (**Supplementary Figure S1**). Finally, tertiles of proconvertase furin were inversely proportional to duration of symptoms (ANOVA, *p*-value for multiple comparisons = 0.021), defined as the time elapsed from the first symptom manifestation (presyncope or syncope) in patient's history and the time of diagnostic examination (HUT).

DISCUSSION

In this study, we explored the inflammatory proteomic signature of POTS in order to elucidate pathophysiological mechanisms underlying this particular phenotype of cardiovascular autonomic dysfunction. We demonstrated that POTS is

TABLE 2 | High throughput multiplex analysis biomarkers selected by supervised multivariate principal component analysis.

Biomarker	POTS+ (*n* = 113)	POTS− (*n* = 283)	*P*-value
FUR	6.38 (0.05)	6.58 (0.03)	0.000276*
CAIX	1.53 (0.09)	1.73 (0.06)	0.050109
Flt3L	7.76 (0.05)	7.89 (0.03)	0.012979
ErbB2HER2	7.79 (0.04)	7.92 (0.03)	0.026045

*Plasma concentrations of the assessed proteins are expressed on a log2-scale. Inter-group differences were assessed using analysis of variance method. *Bonferroni-corrected significant values ($p < 0.012$). CAIX, Carbonic anhydrase IX; ErbB2HER2, Receptor tyrosine-protein kinase erbB-2; Flt3L, Fms-related tyrosine kinase 3 ligand; FUR, furin.*

TABLE 3 | Relationship between POTS status and selected biomarker in univariate and multivariate regression.

Biomarker	Univariate			Multivariate*		
	OR	95% CI	*P*-value	*OR*	95% CI	*P*-value
FUR	0.81	0.73–0.92	<0.001	0.86	0.77–0.96	0.009

**Adjusted for age, sex.*

TABLE 4 | Relationship between changes in heart rate during head-up tilt test and selected biomarker in univariate and multivariate regression.

Biomarker	Univariate			Multivariate*		
	β	95% CI	*P*-value	β	95% CI	P-value
FUR	−7.0	−10.6 to −3.38	<0.001	−4.2	−7.9 to −0.5	0.03

Adjusted for age, sex.

associated with lower circulating levels of proprotein convertases subtilisin/kexin type (PCSK)-3, i.e., proconvertase furin. Interestingly, the earlier the disease starts, the lower the proconvertase furin level.

Our findings confirm and further expand the growing body of evidence pointing to an immune dysregulation as the primary pathophysiological mechanism underlying POTS. However, it is noteworthy that pro-inflammatory cytokines and chemokines, i.e., interleukin-7, interleukin-12 and CXC motif chemokine 13, associated with systemic inflammatory diseases such as systemic lupus erythromatosus or rheumatoid arthritis were not increased among POTS-positive patients.

The Role of Immune System in POTS

The presence of immunoglobulins activating and modulating multiple G-protein coupled receptors (GPCR) linked to the autonomic nervous system has been previously demonstrated in POTS patients (Fedorowski et al., 2017; Yu et al., 2018), as well as their ability to alter dose-response to the natural ligands *in vitro*. Patients suffering from POTS are most frequently young females of childbearing age (Li et al., 2014). Its onset is occasionally preceded by or associated with a viral-like illness or post vaccination which leads to the suspicion that autoimmunity may have an important role in these patients (Li et al., 2014; Brinth et al., 2015). Studies performed recently indicate that patients with POTS have higher prevalence of autoimmune markers and co-morbid autoimmune disorders compared with the general population (Blitshteyn, 2015). Accordingly, nearly one fourth of patients with POTS have positive ANA and one in three have some type of autoimmune markers (Blitshteyn, 2015). Moreover, a high proportion of POTS patients are seropositive for circulating antiganglionic acetylcholine receptor antibodies (Watari et al., 2018).

Finally, presence of antibodies against adrenergic and cholinergic receptors were confirmed in patients suffering from POTS in a number of studies, which could explain the adrenergic-related symptoms including exaggerated heart rate during orthostatic challenge (Ruzieh et al., 2017).

Proconvertase Furin

Proconvertase furin is one of seven proprotein convertase family members that promote proteolytic maturation of proproteins (Barr et al., 1991). Ubiquitously expressed it has been reported to process a variety of secreted factors including cytokines and chemokines such as anti-inflammatory transforming growth factor (TGF)-β1 and secreted TNF-family receptors (Loetscher et al., 1990). Interestingly, previous evidence has suggested that proconvertase furin inhibition may result in a breakdown of peripheral tolerance (Pesu et al., 2008) and development of systemic autoimmune disease (Lisi et al., 2010). In experimental models of rheumatoid arthritis, exogenous proconvertase furin has been successfully used to harness autoimmunity (Lin et al., 2012). This is consistent also with recent findings reporting the association between high proconvertase furin levels and lower systemic activity disease in primary Sjögren's syndrome (Ranta et al., 2018). Considering that proconvertase furin appears to be involved in maintaining immune homeostasis, it is important to note that only one POTS patient in our series had overt autoimmune comorbidity. Consequently, we may reasonably exclude that we have tracked down the effect of parallel autoimmune disorders on proconvertase furin in POTS population.

While the exact source of circulating levels of this protein in POTS patients remains unclear, we speculate that they may reflect a so far undetected viral activity. Indeed, cleavage of the human papilloma virus capsid protein L2 by proconvertase furin is necessary for infection (Richards et al., 2006), while the HIV-1 protein *Nef* is known to bind furin in order to sequester human leukocyte antigen-family receptors in the *trans*-Golgi network (Piguet et al., 2000). Presumably as a countermeasure, proconvertase furin is down-regulated during inflammation in a suppressor of cytokine signaling (Sox)-dependent manner (Guimont et al., 2007).

Taken together, further studies are warranted to confirm these findings in independent populations before proconvertase furin can be considered as an objective serum marker of POTS.

Limitations

There is a number of important limitations that should be addressed. Firstly, inflammatory biomarkers have been sampled only at the time of POTS diagnosis; the lack of serial measurements prevent us to understand whether the alterations seen are a cause or a consequence of POTS, and whether there is any temporal correlation between proconvertase furin levels and the progression of the disease.

Secondly, this is a hypothesis-generating study aimed to discover alternative pathophysiological pathways involved in POTS, requiring external validation in another cohort.

Thirdly, data on important pro-inflammatory cytokines like IL-2, TNF-a, IFN is lacking.

Finally, in order to rule-out possible false positive signals, our findings should be verified and validated with alternative technologies enabling as much sensitive and robust detection and quantification of biomarkers; However, the use of a proximity assay with the requirement for a dual binding event which ensures minimal background signal, and the robust discovery algorithm, based on a sequential two-step process including principal component analysis and a very strict Bonferroni correction, would make a false positive result less likely.

CONCLUSION

Proteomic profiling by proximity extension technique revealed an inflammation-specific biomarker fingerprint in

POTS patients. Circulating levels of proconvertase furin are downregulated in POTS suggesting a complex and intriguing interplay between autoimmune activity and cardiovascular autonomic dysfunction.

ETHICS STATEMENT

This study was carried out in accordance with the recommendations of local ethics guidelines, the Local Ethic Committee of Lund University, with written informed consent from all subjects. All subjects gave written informed consent in accordance with the Declaration of Helsinki. The protocol was approved by The Regional Ethical Review Board of Lund University (No. 82/2008).

AUTHOR CONTRIBUTIONS

FR, AF, JS, and NA had full access to all the data in the study and took responsibility of the data and accuracy of the data analysis. OM, AF, JS, VH, and JA contributed to the study conception and design. OM and AF contributed to the acquisition of data. All authors analyzed and interpreted the data. AF was the study supervisor. NA and FR did the statistical analysis. JS, FR, AF, and VH drafted the manuscript with critical revision for important intellectual content from all authors.

FUNDING

This study was supported by grants from the Swedish Heart-Lung Foundation, the Swedish Heart and Lung Association, the Medical Faculty of Lund University, ALF funds, Skåne University Hospital Funds, Crafoord Foundation, Ernhold Lundströms Research Foundation, Region Skåne, Hulda and Conrad Mossfelt Foundation, and Anna-Lisa and Sven Eric Lundgrens Foundation for Medical Research.

ACKNOWLEDGMENTS

We thank Jackie Cooper, Senior Statistician, Queen Mary University of London, United Kingdom.

SUPPLEMENTARY MATERIAL

The Supplementary Material for this article can be found online at: https://www.frontiersin.org/articles/10.3389/fnins.2019.00301/full#supplementary-material

FIGURE S1 | Heatmap visualization of the proteomics data showing the hierarchical clustering of 48 biomarkers by POTS status.

FIGURE S2 | Quantile regression analysis. Furin regressed on 25th, 50th and 75th quantiles of delta HR max. The x axis is the quantile of delta HR max (black dots in the plots represent the regression coefficient at 0.25, 0.5 (median) and 0.75). The gray bands are the 95% CI of the quantile regression coefficient. The horizontal red and the two horizontal dotted lines are the ordinary least square (OLS) linear regression lines. What you can see here is that 95% CI of the coefficients from quantile regression overlaps widely with OLS lines indicating that Furin does not have differing effects on different quantiles of delta HR max.

TABLE S1 | Immuno-oncology panel: biomarker list.

TABLE S2 | Comparison of baseline characteristics between the whole cohort and complete cases without missing data.

REFERENCES

Arnold, A. C., Ng, J., and Raj, S. R. (2018). Postural tachycardia syndrome - diagnosis, physiology, and prognosis. *Auton. Neurosci.* 215, 3–11. doi: 10.1016/j.autneu.2018.02.005

Barr, P. J., Mason, O. B., Landsberg, K. E., Wong, P. A., Kiefer, M. C., and Brake, A. J. (1991). cDNA and gene structure for a human subtilisin-like protease with cleavage specificity for paired basic amino acid residues. *DNA Cell Biol.* 10, 319–328. doi: 10.1089/dna.1991.10.319

Bartoletti, A., Alboni, P., Ammirati, F., Brignole, M., Del Rosso, A., Foglia Manzillo, G., et al. (2000). 'The Italian Protocol': a simplified head-up tilt testing potentiated with oral nitroglycerin to assess patients with unexplained syncope. *Europace* 2, 339–342. doi: 10.1053/eupc.2000.0125

Benarroch, E. E. (2012). Postural tachycardia syndrome: a heterogeneous and multifactorial disorder. *Mayo Clin. Proc.* 87, 1214–1225. doi: 10.1016/j.mayocp.2012.08.013

Blitshteyn, S. (2015). Autoimmune markers and autoimmune disorders in patients with postural tachycardia syndrome (POTS). *Lupus* 24, 1364–1369. doi: 10.1177/0961203315587566

Brinth, L., Pors, K., Spahic, J. M., Sutton, R., Fedorowski, A., and Mehlsen, J. (2018). Postural Orthostatic Tachycardia Syndrome (POTS) in denmark: increasingly recognized or new epidemic? *Auton. Neurosci.* 213, 92–95. doi: 10.1016/j.autneu.2018.03.001

Brinth, L. S., Pors, K., Theibel, A. C., and Mehlsen, J. (2015). Orthostatic intolerance and postural tachycardia syndrome as suspected adverse effects of vaccination against human papilloma virus. *Vaccine* 33, 2602–2605. doi: 10.1016/j.vaccine.2015.03.098

Eeftinck Schattenkerk, D. W., Van Lieshout, J. J., Van Den Meiracker, A. H., Wesseling, K. R., Blanc, S., Wieling, W., et al. (2009). Nexfin noninvasive continuous blood pressure validated against Riva-Rocci/Korotkoff. *Am. J. Hypertens.* 22, 378–383. doi: 10.1038/ajh.2008.368

Fedorowski, A., Burri, P., Juul-Moller, S., and Melander, O. (2010). A dedicated investigation unit improves management of syncopal attacks (Syncope Study of Unselected Population in Malmo–SYSTEMA I). *Europace* 12, 1322–1328. doi: 10.1093/europace/euq168

Fedorowski, A., Li, H., Yu, X., Koelsch, K. A., Harris, V. M., Liles, C., et al. (2017). Antiadrenergic autoimmunity in postural tachycardia syndrome. *Europace* 19, 1211–1219. doi: 10.1093/europace/euw154

Freeman, R., Wieling, W., Axelrod, F. B., Benditt, D. G., Benarroch, E., Biaggioni, I., et al. (2011). Consensus statement on the definition of orthostatic hypotension, neurally mediated syncope and the postural tachycardia syndrome. *Auton. Neurosci.* 161, 46–48. doi: 10.1016/j.autneu.2011.02.004

Goodman, B. P. (2018). Evaluation of postural tachycardia syndrome (POTS). *Auton. Neurosci.* 215, 12–19. doi: 10.1016/j.autneu.2018.04.004

Grubb, B. P. (2008). Postural tachycardia syndrome. *Circulation* 117, 2814–2817. doi: 10.1161/CIRCULATIONAHA.107.761643

Guimont, P., Grondin, F., and Dubois, C. M. (2007). Sox9-dependent transcriptional regulation of the proprotein convertase furin. *Am. J. Physiol. Cell Physiol.* 293, C172–C183. doi: 10.1152/ajpcell.00349.2006

Hastie, T., Tibshirani, R., and Friedman, J. (2013). *The Elements of Statistical Learning: Data Mining, Inference, and Prediction.* New York, NY: Springer.

Johansson, M., Ricci, F., Aung, N., Sutton, R., Melander, O., and Fedorowski, A. (2018a). Inflammatory biomarker profiling in classical orthostatic hypotension: insights from the SYSTEMA cohort. *Int. J. Cardiol.* 259, 192–197. doi: 10.1016/j.ijcard.2017.12.020

Johansson, M., Ricci, F., Aung, N., Sutton, R., Melander, O., and Fedorowski, A. (2018b). Proteomic profiling for cardiovascular biomarker discovery in

orthostatic hypotension. *Hypertension* 71, 465–472. doi: 10.1161/HYPERTENSIONAHA.117.10365

Li, H., Yu, X., Liles, C., Khan, M., Vanderlinde-Wood, M., Galloway, A., et al. (2014). Autoimmune basis for postural tachycardia syndrome. *J. Am. Heart Assoc.* 3:e000755. doi: 10.1161/JAHA.113.000755

Lin, H., Ah Kioon, M. D., Lalou, C., Larghero, J., Launay, J. M., Khatib, A. M., et al. (2012). Protective role of systemic furin in immune response-induced arthritis. *Arthritis Rheum.* 64, 2878–2886. doi: 10.1002/art.34523

Lisi, S., Sisto, M., Lofrumento, D. D., Cucci, L., Frassanito, M. A., Mitolo, V., et al. (2010). Pro-inflammatory role of Anti-Ro/SSA autoantibodies through the activation of Furin-TACE-amphiregulin axis. *J. Autoimmun.* 35, 160–170. doi: 10.1016/j.jaut.2010.06.020

Loetscher, H., Pan, Y. C., Lahm, H. W., Gentz, R., Brockhaus, M., Tabuchi, H., et al. (1990). Molecular cloning and expression of the human 55 kd tumor necrosis factor receptor. *Cell* 61, 351–359. doi: 10.1016/0092-8674(90)90815-V

Moya, A., Sutton, R., Ammirati, F., Blanc, J. J., Brignole, M., Dahm, J. B., et al. (2009). Guidelines for the diagnosis and management of syncope (version 2009): the task force for the diagnosis and management of syncope of the european society of cardiology (ESC). *Eur. Heart J.* 30, 2631–2671. doi: 10.1093/eurheartj/ehp298

Pesu, M., Watford, W. T., Wei, L., Xu, L., Fuss, I., Strober, W., et al. (2008). T-cell-expressed proprotein convertase furin is essential for maintenance of peripheral immune tolerance. *Nature* 455, 246–250. doi: 10.1038/nature07210

Piguet, V., Wan, L., Borel, C., Mangasarian, A., Demaurex, N., Thomas, G., et al. (2000). HIV-1 Nef protein binds to the cellular protein PACS-1 to downregulate class I major histocompatibility complexes. *Nat. Cell. Biol.* 2, 163–167. doi: 10.1038/35004038

Ranta, N., Valli, A., Gronholm, A., Silvennoinen, O., Isomaki, P., Pesu, M., et al. (2018). Proprotein convertase enzyme FURIN is upregulated in primary Sjogren's syndrome. *Clin. Exp. Rheumatol.* 36(Suppl. 112), 47–50.

Richards, R. M., Lowy, D. R., Schiller, J. T., and Day, P. M. (2006). Cleavage of the papillomavirus minor capsid protein, L2, at a furin consensus site is necessary for infection. *Proc. Natl. Acad. Sci. U.S.A.* 103, 1522–1527. doi: 10.1073/pnas.0508815103

Rubin, D. B. (1987). *Multiple Imputation for Nonresponse in Surveys*. New York, NY: John Wiley & Sons. doi: 10.1002/9780470316696

Ruzieh, M., Batizy, L., Dasa, O., Oostra, C., and Grubb, B. (2017). The role of autoantibodies in the syndromes of orthostatic intolerance: a systematic review. *Scand. Cardiovasc. J.* 51, 243–247. doi: 10.1080/14017431.2017.1355068

Sheldon, R. S., Grubb, B. P. II, Olshansky, B., Shen, W. K., Calkins, H., Brignole, M., et al. (2015). 2015 heart rhythm society expert consensus statement on the diagnosis and treatment of postural tachycardia syndrome, inappropriate sinus tachycardia, and vasovagal syncope. *Heart Rhythm.* 12, e41–e63. doi: 10.1016/j.hrthm.2015.03.029

Watari, M., Nakane, S., Mukaino, A., Nakajima, M., Mori, Y., Maeda, Y., et al. (2018). Autoimmune postural orthostatic tachycardia syndrome. *Ann. Clin. Transl. Neurol.* 5, 486–492. doi: 10.1002/acn3.524

Yu, X., Li, H., Murphy, T. A., Nuss, Z., Liles, J., Liles, C., et al. (2018). Angiotensin II type 1 receptor autoantibodies in postural tachycardia syndrome. *J. Am. Heart Assoc.* 7:e008351. doi: 10.1161/JAHA.117.008351

Conflict of Interest Statement: The authors declare that the research was conducted in the absence of any commercial or financial relationships that could be construed as a potential conflict of interest.

frontiers in Neuroscience

ORIGINAL RESEARCH
published: 09 April 2019
doi: 10.3389/fnins.2019.00341

A Comparison of Muscle Sympathetic Nerve Activity to Non-contracting Muscle During Isometric Exercise in the Upper and Lower Limbs

*Daniel Boulton[1], Simon Green[1,2,3], Vaughan G. Macefield[1,3,4] and Chloe E. Taylor[1,2]**

[1] School of Medicine, Western Sydney University, Sydney, NSW, Australia, [2] School of Science and Health, Western Sydney University, Sydney, NSW, Australia, [3] Neuroscience Research Australia, Sydney, NSW, Australia, [4] Human Autonomic Neurophysiology, Baker Heart and Diabetes Institute, Melbourne, VIC, Australia

Previous research indicates that greater sympathetic vasoconstrictor drive to skeletal muscle occurs during isometric upper limb exercise compared to lower limb exercise. However, potential disparity between blood flow and metaboreflex activation in contracting upper and lower limbs could contribute to the augmented sympathetic response during upper limb exercise. Therefore, the aim of this study was to examine MSNA responses during ankle dorsiflexion and handgrip exercise under ischaemic conditions, in order to standardize the conditions in terms of perfusion and metaboreflex activation. Eight healthy male subjects performed 4-min contractions of ischaemic isometric handgrip and ankle dorsiflexion at ∼10% maximal voluntary contraction, followed by 6 min of post-exercise ischaemia. MSNA was recorded continuously by microneurography of the common peroneal nerve of the non-contracting leg and quantified from negative-going sympathetic spikes in the neurogram, synchronized with the cardiac cycle. The time-course of MSNA exhibited parallel increases during exercise of the upper and lower limbs, rising throughout the contraction to peak at 4 min. This represented an increase of 100% relative to resting levels for handgrip exercise (66 ± 24 vs. 33 ± 7 spikes/min at rest) and 103% for dorsiflexion (63 ± 25 vs. 31 ± 8 spikes/min at rest; $P < 0.01$). In both conditions MSNA remained elevated during post-exercise ischaemia and returned to pre-contraction levels during recovery. These findings demonstrate that that the MSNA response to metaboreflex activation is similar for upper and lower limb exercise when perfusion is controlled for.

Keywords: muscle contraction, metaboreflex, ischaemia, microneurography, muscle sympathetic nerve activity

OPEN ACCESS

Edited by:
David Andrew Low, Liverpool John Moores University, United Kingdom

Reviewed by:
Philip J. Millar, University of Guelph, Canada
Jonathan Patrick Moore, Bangor University, United Kingdom

***Correspondence:**
Chloe E. Taylor
C.Taylor@westernsydney.edu.au

Specialty section:
This article was submitted to Autonomic Neuroscience, a section of the journal Frontiers in Neuroscience

Received: *19 December 2018*
Accepted: *25 March 2019*
Published: *09 April 2019*

Citation:
Boulton D, Green S, Macefield VG and Taylor CE (2019) A Comparison of Muscle Sympathetic Nerve Activity to Non-contracting Muscle During Isometric Exercise in the Upper and Lower Limbs. Front. Neurosci. 13:341. doi: 10.3389/fnins.2019.00341

INTRODUCTION

Muscle metaboreflex activation during sustained isometric exercise causes a progressive decrease in muscle vascular conductance (via sympathetically mediated vasoconstriction) and an increase in arterial pressure (Mitchell et al., 1983; Andersen and Saltin, 1985). Whilst there are reports of increases in muscle sympathetic nerve activity (MSNA) to inactive skeletal muscle in the arm

(Saito et al., 1989; Seals and Enoka, 1989; Cui et al., 2001; Ichinose et al., 2004, 2006) and leg (Ray et al., 1992; Ray and Mark, 1993; Hansen et al., 1994) during exercise, the consistency of cardiovascular and sympathetic responses to exercise between different muscle groups is not clear. Ray et al. (1992) reported that MSNA is augmented during upper limb exercise compared to lower limb exercise at the same intensity. However, the isometric handgrip and knee extension exercise performed in this study involve vastly disparate muscle masses, which may account for the differential cardiovascular and sympathetic responses to exercise.

Saito (1995) compared MSNA responses to upper and lower limb exercise during isometric handgrip, dorsiflexion and plantarflexion, thus providing greater consistency with regards to muscle mass. They reported that the increases in MSNA were greatest during handgrip, followed by dorsiflexion and finally plantarflexion, which they attributed to differences in fiber type composition and the metabolic capacity associated with these fibers. The relative proportion of type II to type I fibers is greater in the forearm muscles compared with the tibialis anterior, and the proportion of type II is lower still in the soleus muscles (Johnson et al., 1973). Since type II fibers are highly glycolytic and fatiguable, muscles with greater proportions of these fibers may evoke a greater metaboreflex response and thus greater increases in MSNA. However, it should be noted that, when comparing responses between dorsiflexors and handgrip, there were no significant differences at the lowest (20% MVC) and highest (50% MVC) forces, but the MSNA response was significantly higher for handgrip at 33% MVC. These data suggest that the differences are not large and there is not a clear intensity-dependent effect. However, other influential factors, besides muscle mass and fiber type, may differ between upper and lower limbs during exercise. For instance, there is evidence to suggest that muscle blood flow during sustained contractions may be limited at different exercise intensities in the upper vs. lower limbs. During sustained contractions in the upper limb there is an increase in blood flow at intensities up to 70% MVC before blood flow is restricted (Kagaya and Homma, 1997). During sustained lower limb contractions, the increase in blood flow is limited to much lower intensities (Barcroft and Millen, 1939); Green et al. (2011) reported that hyperaemia was not present during sustained calf contractions exceeding 20% MVC. Given the lack of direct comparisons between upper and lower limb blood flow during sustained contractions, we cannot assume the blood flow is comparable even at lower exercise intensities. We therefore propose that contractions are performed whilst occluding blood flow to, firstly, standardize the conditions for the two limbs as much as possible (i.e., in terms of perfusion) and, secondly, to maximize metaboreflex activation. These conditions also provide the opportunity to use lower contraction intensities, during which a more stable MSNA recording can be maintained and contractions can be sustained for longer (4 min).

Both central command and the muscle metaboreflex have been implicated with the sympathetic and cardiovascular responses to sustained isometric exercise (Goodwin et al., 1972; Saito et al., 1989; Ray and Mark, 1993; Victor et al., 1995; Ichinose et al., 2006; Matsukawa, 2012). We have previously shown that central command is an important mechanism for mediating the sympathetic response to contracting muscle but has a negligible influence on MSNA to a non-contracting leg during exercise of the contralateral leg (Boulton et al., 2014, 2018). It is important to point out that these experiments consisted of isometric exercise; recent evidence suggests that central command may influence MSNA to non-contracting muscles during *isotonic* exercise, albeit attenuating a fall in total MSNA to non-contracting muscles through an increase in MSNA burst strength (Doherty et al., 2018). It is unclear whether metaboreflex-driven increases in MSNA to non-contracting muscles could respond differently to isometric contractions of the upper limb compared to isometric contractions of the lower limb. It is hypothesized that the MSNA response to metaboreflex activation does not differ between the upper and lower limb when contracting without perfusion. Therefore, the aim of the present study was to investigate sympathetic outflow to inactive leg muscles during ischaemic handgrip and dorsiflexion. A cuff was inflated to supra-systolic pressures around the upper arm (during handgrip) and thigh (during dorsiflexion). This expedites the build-up and turnover of metabolites stimulating group III/IV afferents, and standardizes the conditions in terms of perfusion. Sympathetic activity was measured from the negative-going sympathetic spikes in the raw neurogram (Bent et al., 2006; Fatouleh and Macefield, 2011, 2013; Hammam et al., 2011).

MATERIALS AND METHODS

Participants

Experiments were performed on 11 healthy male subjects, aged 18 to 33 years, with no cardiorespiratory, metabolic or neuromuscular disease. Participants were instructed to abstain from alcohol consumption and vigorous exercise for 24 h prior to the study, and from caffeine on the day of the study. Individuals who smoked or took regular medication were excluded from participation in the study. The study was conducted with the approval of the Human Research Ethics committee, Western Sydney University, and in accordance with the Declaration of Helsinki. Participants provided written informed consent before taking part in the study. The data for the dorsiflexion condition have previously been presented in our study comparing MSNA responses to contracting vs. non-contracting muscles (Boulton et al., 2018).

Measurements

Subjects were positioned semi-recumbent in a chair with their backs at 45°, legs supported horizontally and feet strapped in a plantarflexed position (95°) to independent footplates connected to a force transducer. Tungsten microelectrodes (Frederick Haer and Co., Bowdoinham, ME, United States) were used for microneurography to measure spontaneous MSNA from muscle fascicles of the left common peroneal nerve, located near the level of the fibular head, innervating the ankle dorsiflexor, ankle everter and toe extensor muscles; a reference microelectrode with an uninsulated tip was inserted approximately 1 cm from the active microelectrode. The common peroneal nerve was

identified by electrical stimulation through a 2 mm diameter probe delivering a 0.2 ms pulse at 1 Hz with a 2–10 mA current (Stimulus Isolator, ADInstruments, Sydney, NSW, Australia). Further stimulation was used at a much lower current (1 mA) until twitches of the innervated muscle could be detected at 20 μA. Additional manipulation of the microelectrode was performed until specific observations were made: (i) electrical stimulation produced small contractions of the innervated muscle; (ii) increases of afferent discharges occurred upon passive stretching or tapping of the innervated muscle but not light stroking of the skin; (iii) clear, spontaneous bursts of MSNA were synchronized to the cardiac cycle; and (iv) a maximal inspiratory apnoea produced a sustained increase of spontaneous cardiac-locked bursts. Neural activity was amplified (gain 2×10^4) and filtered (bandpass 0.3–5.0 kHz sampling) using an isolated amplifier and headstage (NeuroAmpEX, ADInstruments) and stored on computer (10 kHz sampling) using a computer-based data acquisition and analysis system (PowerLab 16SP hardware and LabChart, version 8; ADInstruments).

A single lead (II) electrocardiogram (0.3–1 kHz) was recorded with Ag-AgCl surface electrodes (BioAmp, PowerLab, ADInstruments) on the chest and sampled at 2 kHz. Respiration (DC – 100 Hz) was recorded using a strain gauge transducer (Pneumotrace II; UFI, Morro Bay, CA, United States) around the chest and sampled at 100 Hz. Continuous, non-invasive beat-to-beat blood pressure was measured at 400 Hz from the middle finger of the right hand using digital arterial plethysmography (Finometer Pro, Finapres Medical Systems, Enschede, Netherlands). An electromyogram (EMG) (10 Hz to 1 kHz) was recorded with Ag-AgCl surface electrodes over the tibialis anterior muscle and sampled at 2 kHz, which was normalized to the EMG during a maximal voluntary contraction (MVC). Force was measured using two load cells (Aluminum S Type EG PT) connected to two independent footplates, amplified (gain × 200, bandpass DC–10 Hz; Quad Bridge Amplifier; ADInstruments), sampled at 100 Hz and normalized to the MVC of the subject. To control blood flow to the right leg, a large (22 cm) sphygmomanometer cuff was wrapped around the right upper thigh and attached to a rapid cuff inflation system (AG101 and E20; Hokanson, Bellevue, WA, United States), which was set to a suprasystolic pressure (220 mmHg). Blood flow occlusion was verified by the absence of a pulse in the second toe, which was assessed using a piezoelectric pulse transducer (UFI, Morro Bay, CA, United States). A smaller cuff (13 cm) was wrapped around the right upper arm and attached to the rapid inflation system, with a switch to enable occlusion of blood flow to either the right arm or right leg. Again, absence of blood flow was confirmed by monitoring the pulse in a finger using the pulse transducer referred to above.

Experimental Procedures

Maximal voluntary contraction of the right ankle (dorsiflexion) and right forearm (handgrip) was determined from two three-second attempts under freely perfused conditions. The experimental protocol began once a continuous MSNA recording was achieved. An initial 5-min baseline period was recorded to obtain resting measures of cardiovascular and sympathetic variables. In a random order, subjects performed one sustained isometric ankle dorsiflexion and one period of handgrip exercise, both at 10% MVC for 4 min. Ischaemia was imposed approximately 5 s before the onset of contraction and continued for 6 min post-contraction (**Figure 1**). Ten minutes of rest separated each contraction and the protocol was concluded with a 5-min rest period. To test the effect of ischaemia alone, an additional 5-min period of ischaemic rest was recorded at the end.

MSNA Analysis

Negative spikes (half width 0.2–0.6 ms) were clearly observed in the neurogram during contractions and detected using window discriminator software (Spike Histogram, LabChart 2.5, ADInstruments). To account for the delay between the R-wave (ECG) and MSNA in the peroneal nerve (Fagius and Wallin, 1980), the neurogram was shifted back in time (∼1.15–1.30 s) relative to the R wave. As previously described (Boulton et al., 2016), autocorrelation histograms for the cardiac signal were generated in 50 ms bins. Cross-correlation and post-stimulus time histograms were generated between negative spikes and R-R intervals, ensuring that robust cardiac modulation of spike counts was apparent. Minimal changes in heart rate occurred during contraction (see section "Results"). However, to ensure that any differences in spike counts between contraction and rest could be attributed to changes in MSNA burst intensity

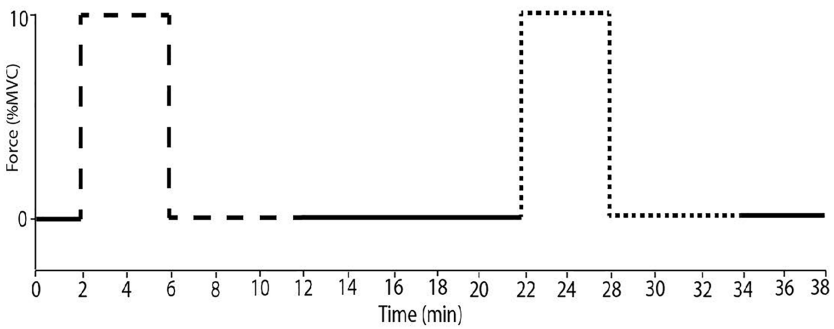

FIGURE 1 | The experimental protocol. Subjects performed sustained ischaemic handgrip (dashed line) for 4 min at 10% MVC with ischaemia imposed for 6 min after contraction. Sustained dorsiflexion (dotted line) was performed under the same conditions with a minimum of 10 min of rest.

or incidence as opposed to heart rate, an equal number of cardiac cycles were used for the analysis of contraction and rest periods for each subject (mean number of cardiac cycles used = 68 ± 12). MSNA spike counts were measured in 1-min epochs, meaning that the number of cardiac cycles for the first minute of rest were determined, and the same number of cardiac cycles were used from each subsequent 1-min epoch. MSNA spike counts included the number of spikes during 600 ms periods after each R-wave (i.e., diastole) and which centered about a peak spike count. Autocorrelation, cross-correlation and post-stimulus time histograms between the MSNA and R-R intervals of the electrocardiogram were sampled in 50 ms bins to determine the cardiac modulation and verify the sympathetic origin of the selected spikes (**Figure 2**).

Statistical Analysis

A two-way repeated measures ANOVA was performed to test for main effects and interactions between "time" and "exercising limb" (upper vs. lower limb) (Prism 5.0, GraphPad Software, United States). When a significant main effect was found by two-way ANOVA, the Sidak *post hoc* test was performed to make pairwise multiple comparisons between the last minute of rest prior to contraction and each of the subsequent minutes in the protocol. Significance was set at $P < 0.05$ and results are expressed as mean ± SD.

RESULTS

Resting MSNA

Sympathetic recordings of negative-going spikes from one subject during an ischaemic isometric dorsiflexion of the right ankle (A) and an ischaemic isometric handgrip performed on the right side (B) are shown in **Figure 3**. The total number of sympathetic spikes for each 1-min epoch was measured from the post-stimulus time histogram of successful recordings from eight subjects. A rest period of 5 min before and after the protocol demonstrated a stable sympathetic signal, with MSNA being similar in each period (31 ± 9 vs. 29 ± 10 spikes/min; $P = 0.50$). At the end of the protocol a period of ischaemia without contraction showed no effect on MSNA (29 ± 9 spikes/min; $P = 0.56$) when compared with the initial 5-min rest period. MSNA in the minute of rest immediately prior to contraction were not significantly different for upper vs. lower limb exercise, with 33 ± 7 spikes/min prior to handgrip and 31 ± 8 spikes/min prior to dorsiflexion ($P = 0.40$).

Effect of Upper Versus Lower Limb Exercise on MSNA

Experimental results for MSNA during ankle dorsiflexion and handgrip are shown in **Figure 3**. There was a significant main effect of time on MSNA ($P < 0.01$, $F = 20.33$), but no main effect of exercising limb ($P = 0.42$, $F = 0.74$) or significant interaction ($P = 0.72$, $F = 0.76$). For both handgrip and ankle dorsiflexion, MSNA increased incrementally for each minute of contraction, peaking at 63 ± 25 spikes/min for ankle dorsiflexion and 66 ± 24 spikes/min for handgrip, an increase of 103 and 100% of resting levels, respectively. In both conditions, MSNA remained elevated for the duration of post-exercise ischaemia and, upon cessation of circulatory arrest, returned toward pre-contraction levels.

Cardiovascular Responses

By design, there were no significant differences between the relative force outputs for handgrip and ankle dorsiflexion ($P = 0.11$) and no main effects of "time" or "limb" (upper vs. lower limb exercise) on respiratory rate ($P > 0.05$). Mean arterial blood pressure and heart rate responses were similar during ischaemic ankle dorsiflexion and handgrip (**Figure 3**). There was a significant effect of time ($P < 0.01$, $F = 26.24$), but not exercising limb ($P = 0.23$, $F = 1.73$) on mean arterial pressure. During both handgrip and dorsiflexion, blood pressure significantly increased during the first minute of contraction ($P < 0.03$) and continued to increase for each subsequent minute. In both conditions, the period of post-exercise ischaemia was associated with a small drop in blood pressure, but it remained elevated above pre-contraction levels ($P < 0.01$) until the cessation of ischaemia. **Figure 4** indicates a gradual increase in heart rate during dorsiflexion and handgrip exercise, but this was not significant ($P > 0.21$). Heart rate remained at resting levels for the duration of post-exercise ischaemia and recovery after dorsiflexion and handgrip.

DISCUSSION

In this study MSNA was measured to non-contracting muscles during sustained dorsiflexion of the ankle and sustained handgrip exercise, both performed in the presence of occlusion of blood flow to the contracting muscle and followed by a period of post-exercise ischaemia. The ischaemic nature of the contractions enhanced the excitation of metaboreceptors during these low intensity contractions and controlled for the potentially confounding factor of perfusion. The results revealed a similar incremental increase in MSNA during contractions of the upper and lower limbs. MSNA was elevated for the duration of post-exercise ischaemia and returned to pre-contraction levels upon cessation of ischaemia. The incremental rise in MSNA throughout the contraction indicates that the muscle metaboreflex may be the dominant mechanism involved in driving sympathetic outflow to non-contracting muscles, a conclusion we had reached in earlier studies (Boulton et al., 2014, 2016, 2018). The present findings demonstrate that sympathetic responses during isometric contractions of the upper and lower limbs are similar when controlling for potential differences in blood flow and muscle metaboreflex activation.

MSNA During Upper Versus Lower Limb Contraction

Prior to the current study the behavior of sympathetic outflow to sustained contractions of the upper and lower limbs was not clear. Ray et al. (1992) reported an increase in MSNA during moderate-intensity handgrip (2 min at 30% MVC) but a decrease in MSNA during the first minute of knee extension at the same

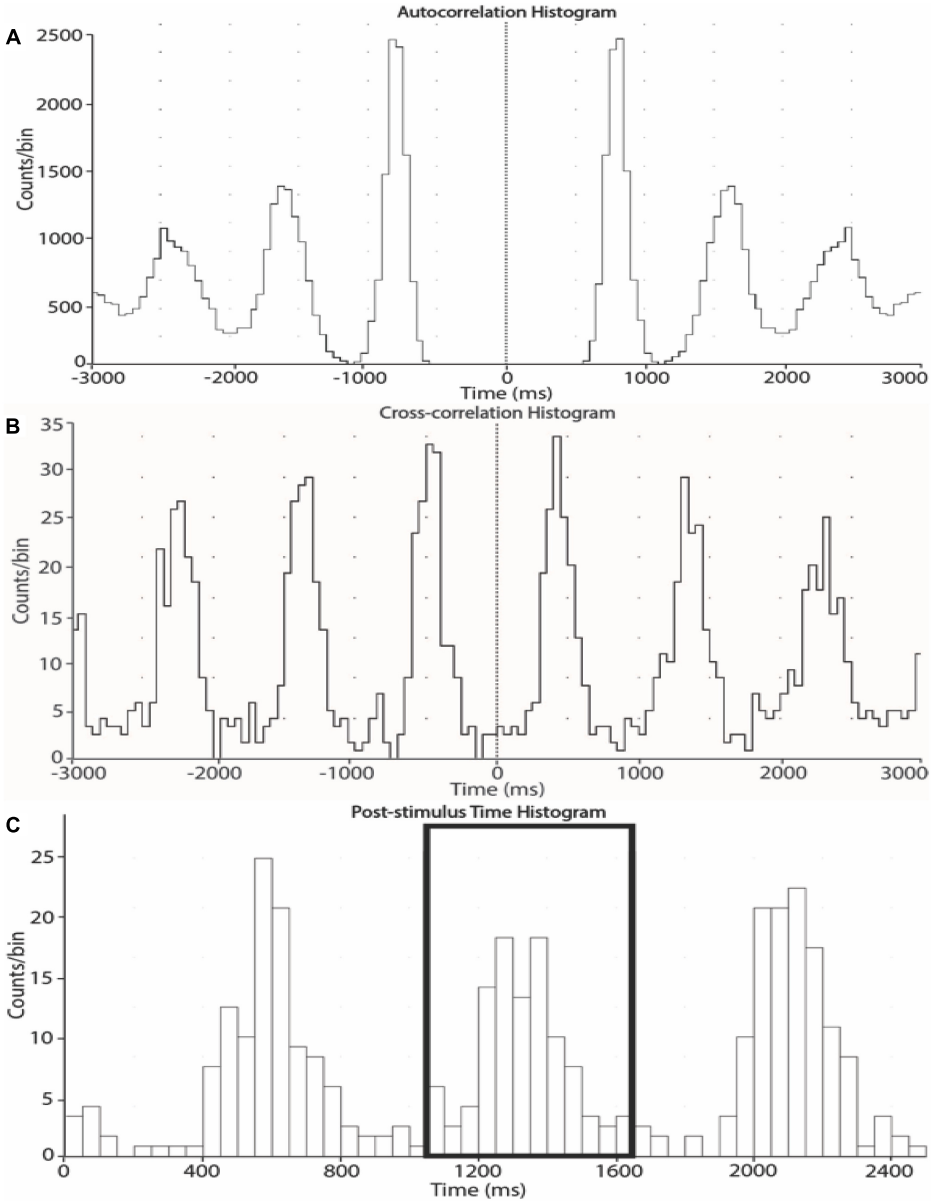

FIGURE 2 | Autocorrelation **(A)**, cross-correlation **(B)** and post-stimulus time **(C)** histograms from one subject. The histograms were generated from 1-min epochs to measure the timing of neural spikes relative to cardiac beats and count the number of sympathetic spikes during each epoch.

intensity, followed by an increase during the second minute. With such disparity in muscle mass we might expect to observe these differences in cardiovascular and sympathetic responses to exercise. For instance, Seals (1989) reported augmented sympathetic and cardiovascular responses to a larger active muscle mass during two-arm handgrip compared to single-arm handgrip. However, the observations by Seals (1989) could also be a product of increasing the number of simultaneously active limbs, both with respect to central command to, and reflex inputs from, the contracting muscles. The size of the muscle groups used in upper and lower limb exercise in the current study are more comparable, and therefore discrepancies in muscle mass are less likely to influence the results. Certainly, the parallel cardiovascular and sympathetic responses in the current study indicate that the forearm and pretibial flexor muscles produced the same level of work for each contraction.

Differential sympathetic responses to exercise of the upper and lower limbs observed in previous studies could be due to differences in intramuscular blood flow during exercise of the upper and lower limbs. Previous research suggests that blood flow through contracting muscle is restricted at significantly lower exercise intensities during lower limb exercise compared with exercise of the upper limb (Barcroft and Millen, 1939; Green et al., 2011). The metaboreflex represents a response to a

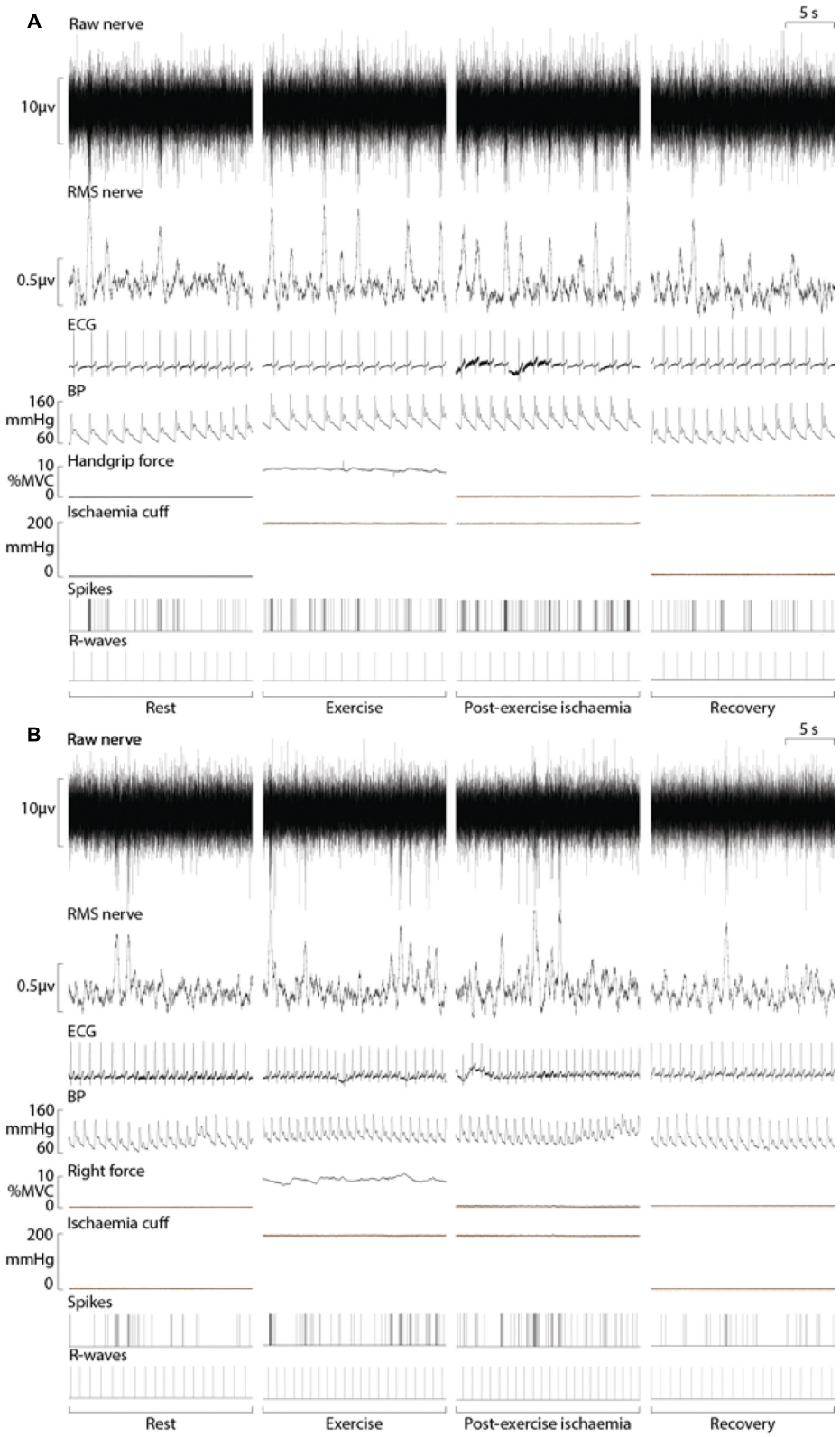

FIGURE 3 | Experimental records from one subject during ischaemic handgrip **(A)** and ankle dorsiflexion **(B)** with a period of post-exercise ischaemia. Analysis of MSNA involved measuring the negative-going sympathetic spikes of the raw nerve signal.

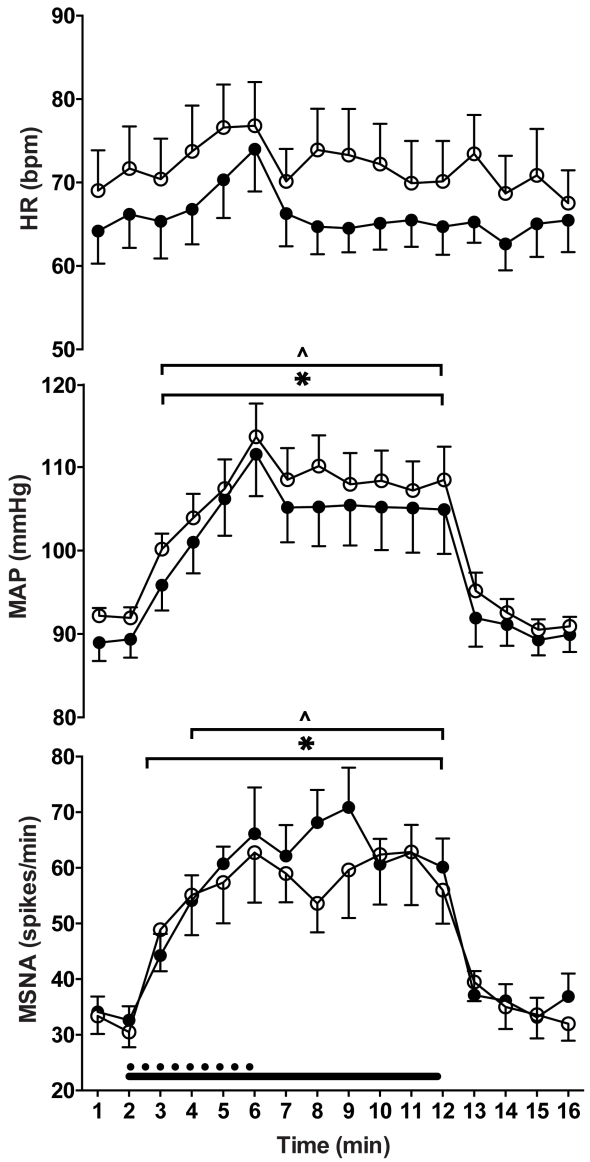

FIGURE 4 | Heart rate (HR), mean arterial pressure (MAP) and muscle sympathetic nerve activity (MSNA) responses to contraction of the upper (filled circles) and lower (empty circles) limbs. There were significant increases from rest (last min of rest period preceding contraction) during contraction of the lower (*) and upper limbs (^) ($P \leq 0.05$).

mismatch between blood flow and metabolic demand, whereby inadequate blood flow during exercise leads to the build-up of metabolites produced during contraction and a reflex increase in arterial pressure (Alam and Smirk, 1937; Rowell et al., 1976; O'Leary and Joyner, 2006). Given that the blunting of hyperaemia may occur at lower exercise intensities in the leg vs. arm, it is conceivable that this mismatch occurs more readily in the lower limbs, thereby leading to an earlier activation of metaboreceptors. Although Green et al. (2011) demonstrated that hyperaemia may be blunted in the lower limbs at intensities of 20% MVC, we cannot rule out potential limb-dependent differences in blood flow and therefore possible disparities in metaboreflex activation between upper and lower limbs. Given that previous studies have indicated that MSNA responses to upper and lower limb exercise differ when blood flow is not experimentally occluded (Saito, 1995), our findings suggest that perfusion may have a role to play in the level of metaboreflex activation between limbs. However, if hyperaemia is blunted at lower intensities in the lower limb vs. upper limb, we might expect greater metaboreflex activation and thus greater MSNA responses to have been reported for lower limb exercise. Saito (1995), however, reported greater MSNA responses to handgrip exercise compared with dorsiflexion, albeit these differences were significant only for contractions at 33% MVC and not 20 or 50%. Our data therefore suggests that the effect observed by Saito (1995) may not be related to fiber type *per se* but is related to perfusion and its effect on susceptibility to fatigue. Saito et al. (1989) showed in a separate study that the sensation of fatigue in the working muscles during contraction is correlated with the increase in MSNA. Although type II fibers are highly fatigable, and thus muscles with greater proportions of these fibers may evoke a greater MSNA response, the fatigability of different fiber types are more similar when the muscles are deprived of blood and oxygen. This may explain the lack of differences in the MSNA responses in the current study. Specifically, we demonstrate that when the level of metaboreflex activation is controlled for, the MSNA responses to that activation are similar for muscles of the upper and lower limbs.

Metaboreflex Control of MSNA

The failure of MSNA to increase during contraction in previous studies (Ray et al., 1992; Saito, 1995) could be due to an inadequate exercise stimulus (intensity and/or duration) (Ray and Mark, 1993) and metaboreflex activation. The contractions performed in the studies by Ray et al. (1992) and Saito (1995) were moderate to high-intensity (20–50% MVC) and of relatively short duration (2 min). The exercise parameters in the current study (ischaemic, low-intensity, sustained contractions) were implemented to reduce the influence of perfusion, while ensuring the metaboreflex was activated. Occlusion of blood flow to the active limb at the onset of contraction increases the concentration of metabolites, thus maximizing the stimulus for metaboreflex activation, as demonstrated by the sustained elevation in blood pressure during contraction and post-exercise ischaemia. In the present study, MSNA increased by 33% of resting levels during the first minute of ischaemic handgrip and by 58% of resting levels during the first minute of ankle dorsiflexion. These prompt increases in MSNA to contraction are quicker than observed in previous studies (Saito et al., 1986, 1989; Wallin et al., 1989; Ray et al., 1992; Ray and Mark, 1993; Saito, 1995; Cui et al., 2001; Ichinose et al., 2006) possibly because metabolic by-products were trapped from the onset of contraction, causing a more rapid increase in metabolite accumulation and a decrease in muscle acidity (pH) (Victor et al., 1988).

Numerous studies have indicated that central command does not directly contribute to the exercise-induced response of MSNA to non-active muscle (Victor et al., 1989; Wallin et al., 1992; Hansen et al., 1994), but rather exerts an influence on baroreflex resetting and vagal outflow to the heart during

exercise (Victor et al., 1987; Cui et al., 2001; Querry et al., 2001; Matsukawa et al., 2005). However, the potential influence of central command on MSNA to an inactive limb cannot be dismissed because MSNA increased within 1 min of the start of exercise. Evidence suggests it has a role to play in isotonic exercise: Doherty et al. (2018) reported that the fall observed in total MSNA to inactive limbs during one-legged cycling is partially offset by an increase in MSNA burst strength driven by central command.

Methodological Considerations

The rationale for occluding blood flow both during and after exercise was to eliminate the potentially confounding factor of limb blood flow and to control for metaboreflex activation by attempting to maximize activation in both limbs studied. Whilst this does allow us to examine the intrinsic muscle response to metaboreflex activation, it is acknowledged that the current study is limited by a lack of an exercise condition without occlusion, which would have allowed confirmation of such differences in MSNA responses between limbs. In addition, it is possible that exercise training status may influence metaboreflex activation (Sinoway et al., 1996) and, whilst we did not recruit participants based on their training history, we did collect self-reported activity levels. These reports indicate that the participants were typically involved in combinations of aerobic and resistance training of the upper and lower limbs (>2 times per week). Future research may be directed toward examining the effects of training history on metaboreflex activation through comparisons between sedentary, aerobic and resistance trained individuals.

We appreciate that presenting traditional MSNA burst analysis may have allowed for comparisons with other studies in the literature. However, we have used spike analysis for a number of reasons. Firstly, for consistency with our previous studies in which this approach was necessary due to the fact that EMG can infiltrate the MSNA signal, as can the activity of muscle spindle and Golgi tendon organ afferents and alpha motor axons when recording MSNA to the contracting limb. Secondly, the spike analysis is a more sensitive approach for capturing a greater proportion of the sympathetic nerve activity, because the negative-going spikes extracted from the neurogram are defined as sympathetic because of their strong cardiac rhythmicity. Conversely, the traditional burst analysis may suffer from a poor signal-to-noise ratio and baseline shifts due to the participant tensing leg muscles, leading to periods of EMG infiltration. This can significantly hinder the ability to reliably identify bursts and measure their amplitude.

CONCLUSION

Metabolically mediated reflex control of sympathetic outflow to non-active skeletal muscle is essentially important for the regulation of blood pressure during movement and exercise. By controlling for differences in metaboreflex activation, our results support differences in metaboreflex activation as a mechanism for differences observed between upper and lower limb exercise in previous studies. Our findings suggest that the MSNA response is similar for upper and lower limb exercise, indicating that what actually differs is the level of metaboreflex activation when these muscles are "freely perfused." Intrinsically, muscles do not differ in terms of the impact they have on MSNA; our data suggest that perfusion may be more important.

ETHICS STATEMENT

The study was conducted with the approval of the Human Research Ethics committee, Western Sydney University, and in accordance with the Declaration of Helsinki. Participants provided written informed consent before taking part in the study.

AUTHOR CONTRIBUTIONS

Experiments were performed in the School of Medicine (Western Sydney University). All authors were involved in the design of the experiments and/or data acquisition and analysis of the data, as well as the writing or editing of this manuscript, and approved the final version of this manuscript and agreed to be accountable for all aspects of the work.

FUNDING

This work was supported by the National Health and Medical Research Council of Australia (GNT1029782 and GNT11000420).

REFERENCES

Alam, M., and Smirk, F. H. (1937). Observations in man upon a blood pressure raising reflex arising from the voluntary muscles. *J. Physiol.* 89, 372–383. doi: 10.1113/jphysiol.1937.sp003485

Andersen, P., and Saltin, B. (1985). Maximal perfusion of skeletal muscle in man. *J. Physiol.* 366, 233–249. doi: 10.1113/jphysiol.1937.sp003485

Barcroft, H., and Millen, J. L. E. (1939). The blood flow through muscle during sustained contraction. *J. Physiol.* 97, 17–31. doi: 10.1113/jphysiol.1939.sp003789

Bent, L. R., Bolton, P. S., and Macefield, V. G. (2006). Modulation of muscle sympathetic bursts by sinusoidal galvanic vestibular stimulation in human subjects. *Exp. Brain Res.* 174, 701–711. doi: 10.1007/s00221-006-0515-6

Boulton, D., Taylor, C. E., Green, S., and Macefield, V. G. (2018). The metaboreflex does not contribute to the increase in muscle sympathetic nerve activity to contracting muscle during static exercise in humans. *J. Physiol.* 596, 1091–1102. doi: 10.1113/JP275526

Boulton, D., Taylor, C. E., Macefield, V. G., and Green, S. (2014). Effect of contraction intensity on sympathetic nerve activity to active human skeletal muscle. *Front. Physiol.* 5:9. doi: 10.3389/fphys.2014.00194

Boulton, D., Taylor, C. E., Macefield, V. G., and Green, S. (2016). Contributions of central command and muscle feedback to sympathetic nerve activity in

contracting human skeletal muscle. *Front. Physiol.* 7:163. doi: 10.3389/fphys.2016.00163

Cui, J., Wilson, T. E., Shibasaki, M., Hodges, N. A., and Crandall, C. G. (2001). Baroreflex modulation of muscle sympathetic nerve activity during posthandgrip muscle ischemia in humans. *J. Appl. Physiol.* 91, 1679–1686. doi: 10.1152/jappl.2001.91.4.1679

Doherty, C. J., Incognito, A. V., Notay, K., Burns, M. J., Slysz, J. T., Seed, J. D., et al. (2018). Muscle sympathetic nerve responses to passive and active one-legged cycling: insight into the contributions of central command. *Am. J. Physiol. Heart Circul. Physiol.* 314, H3–H10. doi: 10.1152/ajpheart.00494.2017

Fagius, J., and Wallin, B. G. (1980). Sympathetic reflex latencies and conduction velocities in normal man. *J. Neurol. Sci.* 47, 433–448. doi: 10.1016/0022-510X(80)90098-2

Fatouleh, R., and Macefield, V. G. (2011). Respiratory modulation of muscle sympathetic nerve activity is not increased in essential hypertension or chronic obstructive pulmonary disease. *J. Physiol.* 589, 4997–5006. doi: 10.1113/jphysiol.2011.210534

Fatouleh, R., and Macefield, V. G. (2013). Cardiorespiratory coupling of sympathetic outflow inhumans: a comparison of respiratory and cardiac modulation of sympathetic nerve activity to skin and muscle. *Exp. Physiol.* 98, 1327–1336. doi: 10.1113/expphysiol.2013.072421

Goodwin, G. M., McCloskey, D. I., and Mitchell, J. H. (1972). Cardiovascular and respiratory responses to changes in central command during isometric exercise at constant muscle tension. *J. Physiol.* 226, 173–190. doi: 10.1113/jphysiol.1972.sp009979

Green, S., Thorp, R., Reeder, E. J., Donnelly, J., and Fordy, G. (2011). Venous occlusion plethysmography versus Doppler ultrasound in the assessment of leg blood flow during calf exercise. *Eur. J. Appl. Physiol.* 111, 1889–1900. doi: 10.1007/s00421-010-1819-6

Hammam, E., James, C., Dawood, T., and Macefield, V. G. (2011). Low-frequency sinusoidal galvanic stimulation of the left and right vestibular nerves reveals two peaks of modulation in muscle sympathetic nerve activity. *Exp. Brain Res.* 213, 507–514. doi: 10.1007/s00221-011-2800-2

Hansen, J., Thomas, G. D., Jacobsen, T. N., and Victor, R. G. (1994). Muscle metaboreflex triggers parallel sympathetic activation in exercising and resting human skeletal muscle. *Am. J. Physiol. Heart Circ. Physiol.* 266, H2508–H2514. doi: 10.1152/ajpheart.1994.266.6.H2508

Ichinose, M., Saito, M., Kondo, N., and Nishiyasu, T. (2006). Time-dependent modulation of arterial baroreflex control of muscle sympathetic nerve activity during isometric exercise in humans. *Am. J. Physiol. Heart Circ. Physiol.* 290, H1419–H1426. doi: 10.1152/ajpheart.00847.2005

Ichinose, M., Saito, M., Wada, H., Kitano, A., Kondo, N., and Nishiyasu, T. (2004). Modulation of arterial baroreflex control of muscle sympathetic nerve activity by muscle metaboreflex in humans. *Am. J. Physiol. Heart Circ. Physiol.* 286, H701–H707. doi: 10.1152/ajpheart.00618.2003

Johnson, M., Polgar, J., Weightman, D., and Appleton, D. (1973). Data on the distribution of fibre types in thirty-six human muscles: an autopsy study. *J. Neurol. Sci.* 18, 111–129. doi: 10.1016/0022-510X(73)90023-3

Kagaya, A., and Homma, S. (1997). Brachial arterial blood flow during static handgrip exercise of short duration at varying intensities studied by a doppler ultrasound method. *Acta Physiol. Scand.* 160, 257–265. doi: 10.1046/j.1365-201X.1997.00158.x

Matsukawa, K. (2012). Central command: control of cardiac sympathetic and vagal efferent nerve activity and the arterial baroreflex during spontaneous motor behaviour in animals. *Exp. Physiol.* 97, 20–28. doi: 10.1113/expphysiol.2011.057661

Matsukawa, K., Komine, H., Nakamoto, T., and Murata, J. (2005). Central command blunts sensitivity of arterial baroreceptor-heart rate reflex at onset of voluntary static exercise. *Am. J. Physiol. Heart Circ. Physiol.* 290, H200–H208. doi: 10.1152/ajpheart.00013.2005

Mitchell, J. H., Kaufman, M. P., and Iwamoto, G. A. (1983). The exercise pressor reflex: its cardiovascular effects, afferent mechanisms, and central pathways. *Annu. Rev. Physiol.* 45, 229–242. doi: 10.1146/annurev.ph.45.030183.001305

O'Leary, D. S., and Joyner, M. J. (2006). Counterpoint: the muscle metaboreflex does not restore blood flow to contracting muscles. *J. Appl. Physiol.* 100, 357–361. doi: 10.1152/japplphysiol.01222.2005

Querry, R. G., Smith, S. A., Stromstad, M., Ide, K., Raven, P. B., and Secher, N. H. (2001). Neural blockade during exercise augments central command's contribution to carotid baroreflex resetting. *Am. J. Physiol. Heart Circ. Physiol.* 280, H1635–H1644. doi: 10.1152/ajpheart.2001.280.4.H1635

Ray, C. A., and Mark, A. L. (1993). Augmentation of muscle sympathetic nerve activity during fatiguing isometric leg exercise. *J. Appl. Physiol.* 75, 228–232. doi: 10.1152/jappl.1993.75.1.228

Ray, C. A., Rea, R. F., Clary, M. P., and Mark, A. L. (1992). Muscle sympathetic nerve responses to static leg exercise. *J. Appl. Physiol.* 73, 1523–1529. doi: 10.1152/jappl.1992.73.4.1523

Rowell, L. B., Hermansen, L., and Blackmon, J. R. (1976). Human cardiovascular and respiratory responses to graded muscle ischemia. *J. Appl. Physiol.* 41, 693–701. doi: 10.1152/jappl.1976.41.5.693

Saito, M. (1995). Differences in muscle sympathetic nerve response to isometric exercise in different muscle groups. *Eur. J. Appl. Physiol. Occup. Physiol.* 70, 26–35. doi: 10.1007/BF00601805

Saito, M., Mano, T., Abe, H., and Iwase, S. (1986). Responses in muscle sympathetic nerve activity to sustained hand-grips of different tensions in humans. *Eur. J. Appl. Physiol. Occup. Physiol.* 55, 493–498. doi: 10.1007/BF00421643

Saito, M., Mano, T., and Iwase, S. (1989). Sympathetic nerve activity related to local fatigue sensation during static contraction. *J. Appl. Physiol.* 67, 980–984. doi: 10.1152/jappl.1989.67.3.980

Seals, D. R. (1989). Influence of muscle mass on sympathetic neural activation during isometric exercise. *J. Appl. Physiol.* 67, 1801–1806. doi: 10.1152/jappl.1989.67.5.1801

Seals, D. R., and Enoka, R. M. (1989). Sympathetic activation is associated with increases in EMG during fatiguing exercise. *J. Appl. Physiol.* 66, 88–95. doi: 10.1152/jappl.1989.66.1.88

Sinoway, L., Shenberger, J., Leaman, G., Zelis, R., Gray, K., Baily, R., et al. (1996). Forearm training attenuates sympathetic responses to prolonged rhythmic forearm exercise. *J. Appl. Physiol.* 81, 1778–1784. doi: 10.1152/jappl.1996.81.4.1778

Victor, R. G., Bertocci, L. A., Pryor, S. L., and Nunnally, R. L. (1988). Sympathetic nerve discharge is coupled to muscle pH during exercise in humans. *J. Clin. Invest.* 82, 1301–1305. doi: 10.1172/JCI113730

Victor, R. G., Pryor, S. L., Secher, N. H., and Mitchell, J. H. (1989). Effects of partial neuromuscular blockade on sympathetic nerve responses to static exercise in humans. *J. Am. Heart Assoc.* 65, 468–476. doi: 10.1161/01.RES.65.2.468

Victor, R. G., Seals, D. R., and Mark, A. L. (1987). Differential control of heart rate and sympathetic nerve activity during dynamic exercise. Insight from intraneural recordings in humans. *J. Clin. Invest.* 79, 508–516. doi: 10.1172/JCI112841

Victor, R. G., Secher, N. H., Lyson, T., and Mitchell, J. H. (1995). Central command increases muscle sympathetic nerve activity during intense intermittent isometric exercise in humans. *Circ. Res.* 76, 127–131. doi: 10.1161/01.RES.76.1.127

Wallin, B. G., Burke, D., and Gandevia, S. C. (1992). Coherence between the sympathetic drives to relaxed and contracting muscles of different limbs of human subjects. *J. Physiol.* 455, 219–233. doi: 10.1113/jphysiol.1992.sp019298

Wallin, B. G., Victor, R. G., and Mark, A. L. (1989). Sympathetic outflow to resting muscles during static handgrip and postcontraction muscle ischemia. *Am. J. Physiol.* 256, H105–H110. doi: 10.1152/ajpheart.1989.256.1.H105

Conflict of Interest Statement: The authors declare that the research was conducted in the absence of any commercial or financial relationships that could be construed as a potential conflict of interest.

frontiers in Neuroscience

ORIGINAL RESEARCH
published: 01 May 2019
doi: 10.3389/fnins.2019.00426

Endogenous Glutamate Excites Myenteric Calbindin Neurons by Activating Group I Metabotropic Glutamate Receptors in the Mouse Colon

*Mathusi Swaminathan[1], Elisa L. Hill-Yardin[1,2], Joel C. Bornstein[1] and Jaime P. P. Foong[1]**

[1] Department of Physiology, The University of Melbourne, Parkville, VIC, Australia, [2] School of Health and Biomedical Sciences, RMIT University, Bundoora, VIC, Australia

OPEN ACCESS

Edited by:
Jack Grider, Virginia Commonwealth University, United States

Reviewed by:
Michael Schemann, Technische Universität München, Germany
Werend Boesmans, University of Hasselt, Belgium

***Correspondence:**
Jaime P. P. Foong
j.foong@unimelb.edu.au

Specialty section:
This article was submitted to Autonomic Neuroscience, a section of the journal Frontiers in Neuroscience

Received: *06 March 2019*
Accepted: *15 April 2019*
Published: *01 May 2019*

Citation:
Swaminathan M, Hill-Yardin EL, Bornstein JC and Foong JPP (2019) Endogenous Glutamate Excites Myenteric Calbindin Neurons by Activating Group I Metabotropic Glutamate Receptors in the Mouse Colon. Front. Neurosci. 13:426. doi: 10.3389/fnins.2019.00426

Glutamate is a classic excitatory neurotransmitter in the central nervous system (CNS), but despite several studies reporting the expression of glutamate together with its various receptors and transporters within the enteric nervous system (ENS), its role in the gut remains elusive. In this study, we characterized the expression of the vesicular glutamate transporter, vGluT2, and examined the function of glutamate in the myenteric plexus of the distal colon by employing calcium (Ca^{2+})-imaging on Wnt1-Cre; R26R-GCaMP3 mice which express a genetically encoded fluorescent Ca^{2+} indicator in all enteric neurons and glia. Most vGluT2 labeled varicosities contained the synaptic vesicle release protein, synaptophysin, but not vesicular acetylcholine transporter, vAChT, which labels vesicles containing acetylcholine, the primary excitatory neurotransmitter in the ENS. The somata of all calbindin (calb) immunoreactive neurons examined received close contacts from vGluT2 varicosities, which were more numerous than those contacting nitrergic neurons. Exogenous application of L-glutamic acid (L-Glu) and *N*-methyl-D-aspartate (NMDA) transiently increased the intracellular Ca^{2+} concentration $[Ca^{2+}]_i$ in about 25% of myenteric neurons. Most L-Glu responsive neurons were calb immunoreactive. Blockade of NMDA receptors with APV significantly reduced the number of neurons responsive to L-Glu and NMDA, thus showing functional expression of NMDA receptors on enteric neurons. However, APV resistant responses to L-Glu and NMDA suggest that other glutamate receptors were present. APV did not affect $[Ca^{2+}]_i$ transients evoked by electrical stimulation of interganglionic nerve fiber tracts, which suggests that NMDA receptors are not involved in synaptic transmission. The group I metabotropic glutamate receptor (mGluR) antagonist, PHCCC, significantly reduced the amplitude of $[Ca^{2+}]_i$ transients evoked by a 20 pulse (20 Hz) train of electrical stimuli in L-Glu responsive neurons. This stimulus is known to induce slow synaptic depolarizations. Further, some neurons that had PHCCC sensitive $[Ca^{2+}]_i$

transients were calb immunoreactive and received vGluT2 varicosities. Overall, we conclude that electrically evoked release of endogenous glutamate mediates slow synaptic transmission via activation of group I mGluRs expressed by myenteric neurons, particularly those immunoreactive for calb.

Keywords: glutamate, synaptic transmission, metabotropic group I glutamate receptors, vGluT2, enteric nervous system, myenteric plexus

INTRODUCTION

Glutamate is the primary excitatory transmitter in the central nervous system (CNS). But its role the enteric nervous system (ENS) of the gut has remained elusive despite several reports of possible function (Kirchgessner, 2001; Filpa et al., 2016; Seifi and Swinny, 2016).

Several ultrastructural and immunofluorescence studies in rodent models provide evidence for the expression of glutamate, its release and re-uptake transporters, and its various receptor subtypes within the ENS (Liu et al., 1997; Tong et al., 2001; Giaroni et al., 2003; Tsai, 2005; Brumovsky et al., 2011; Seifi and Swinny, 2016). Enteric neurons immunoreactive for glutamate are found in the guinea-pig ileum and are reported to co-express choline acetyltransferase (ChAT), substance P (SP) and/or calbindin (calb) (Liu et al., 1997). Vesicular glutamate transporters (vGluTs) aid in the release of glutamate at presynaptic terminals. Although three distinct isoforms of vGluTs (vGluT1, vGluT2, and vGluT3) have been identified in the CNS, vGluT2 is the predominant isoform in the ENS (Tong et al., 2001; Brumovsky et al., 2011; Seifi and Swinny, 2016). While vGluT2 is expressed in enteric varicosities (Tong et al., 2001; Seifi and Swinny, 2016), the targets of these varicosities within the ENS have not been identified. Excitatory levels of glutamate are tightly regulated via excitatory amino acid transporters (EAATs). EAAT is expressed within the ENS, particularly by enteric glia (Liu et al., 1997; Seifi and Swinny, 2016). This is similar to the CNS where EAATs are expressed by glial cells including astrocytes (Rothstein et al., 1994; Lehre et al., 1995). Furthermore, the ionotropic glutamate receptors, *N*-methyl-D-aspartate (NMDA) and α-amino-3-hydroxy-5-methyl-4-isoxazole propionic acid (AMPA), as well as subtypes of metabotropic glutamate receptors (mGluRs) are found on enteric neurons (Broussard et al., 1994; Burns et al., 1994; Liu et al., 1997; Liu and Kirchgessner, 2000; McRoberts et al., 2001; Chen and Kirchgessner, 2002; Tong and Kirchgessner, 2003; Del Valle-Pinero et al., 2007; Foong and Bornstein, 2009; Seifi and Swinny, 2016).

Despite the consensus in the literature about the expression of glutamate and its associated transporters and receptors in the ENS, its role in mediating synaptic transmission remains contentious (Liu et al., 1997; Liu and Kirchgessner, 2000; Ren et al., 2000; Foong and Bornstein, 2009; Wang et al., 2014). In the guinea-pig ENS, NMDA, and AMPA receptors were reported to mediate excitatory post synaptic potentials (EPSPs) in one study (Liu et al., 1997), while a later study found no functional role for ionotropic receptors, but instead demonstrated involvement of slower Group I mGluRs (Ren et al., 2000). Further, pharmacological studies have focused the role of NMDA and AMPA receptors in mediating gut contractility (Luzzi et al., 1988; Shannon and Sawyer, 1989; Wiley et al., 1991; Seifi and Swinny, 2016).

In this study, we examined potential roles of glutamate and its receptors in synaptic transmission within the myenteric plexus. We used calcium (Ca^{2+})-imaging to examine activity of neurons in the myenteric plexus. Connections between glutamatergic terminals and myenteric neurons were examined using high-resolution microscopy and advanced analysis methods. We found that antisera to vGluT2 stain varicosities that contact myenteric neurons. Exogenous application of glutamate excited myenteric neurons by activating glutamate receptors including NMDA receptors, while electrical stimulation evoked responses apparently mediated by group I mGluRs. Most glutamate responsive neurons were calb immunoreactive. Moreover, all calb immunoreactive neurons receive vGluT2 varicosities, thereby suggesting a role for glutamate modulating the excitation of these neurons.

MATERIALS AND METHODS

Experimental Animals

Adult mice (8–15 weeks old) were used. Wnt1-Cre; R26R-GCaMP3 mice of either sex were used in Ca^{2+} imaging experiments. They were the progeny of Wnt1-Cre mice and R2R-GCaMP3 mice (both C57BL/6 background, The Jackson Laboratory) and express the genetically encoded Ca^{2+} indicator, GCaMP3, in all neural crest derived cells including enteric neurons and glia (Danielian et al., 1998; Zariwala et al., 2012; Boesmans et al., 2013). Male C57BL/6 or female R2R-GCaMP3 mice were used for immunohistochemistry studies. All mice were killed by cervical dislocation, as approved by the University of Melbourne Animal Experimentation Ethics Committee. The colon was removed from each mouse and immediately placed in physiological saline (composition in mM: NaCl 118, $NaHCO_3$ 25, D-glucose 11, KCl 4.8, $CaCl_2$ 2.5, $MgSO_4$ 1.2, NaH_2PO_4 1.0) bubbled with carbogen gas (95% O_2, 5% CO_2) or in phosphate-buffered saline (PBS). The colon was cut along the mesenteric border, stretched and pinned flat mucosal side up in a Petri dish lined with silicon elastomer (Sylgard 184; Dow Corning, North Ryde, NSW, Australia). The distal colonic region was defined as the area of the colon (3 cm in length) that is 2 cm proximal to the anus.

Immunohistochemistry

Tissue Preparation

Pinned and stretched colonic segments were fixed overnight in 4% formaldehyde in 0.1 M phosphate buffer, pH 7.2, at 4°C, and

TABLE 1 | Primary and secondary antisera.

Primary antisera	Raised in	Dilution factor	Source
vGluT2	Guinea pig	1:1000	Synaptic Systems
vAChT	Rabbit	1:1000	Synaptic Systems
Synaptophysin	Rabbit	1:100	Abcam
calb	Rabbit	1:1600	SWANT
calr	Goat	1:1000	SWANT
nNOS	Sheep	1:1000	Gift from P. Emson
Hu	Human	1:5000	Gift from Dr. V. Lennon
Secondary antisera	**Raised in**	**Dilution factor**	**Source**
Anti-Guinea Pig 594	Donkey	1:400	Jackson Immuno Research Labs
Anti-Guinea Pig FITC	Donkey	1:100	Millipore
Anti-Guinea Pig 647	Donkey	1:200	Jackson Immuno Research Labs
Anti-Rabbit 488	Donkey	1:400	Molecular Probes
Anti-Rabbit 594	Donkey	1:400	Molecular Probes
Anti-Rabbit 647	Donkey	1:400	Molecular Probes
Anti-Sheep 488	Donkey	1:400	Molecular Probes
Anti-Sheep 647	Donkey	1:400	Molecular Probes
Anti-Hu 594	Human	1:750	Jackson Immuno Research Labs

then cleared of fixative via three washes with PBS. Longitudinal muscle-myenteric plexus (LMMP) whole mount preparations were obtained from the distal colon by microdissection to remove the overlying mucosa-submucosa-circular muscle layers. LMMP preparations were then treated with 0.1% Triton X-100 + 10% CASBLOCK (Invitrogen, Mount Waverley, VIC, Australia; ProSciTech, Thuringowa, QLD, Australia) prior to incubating with a combination of primary antibodies (**Table 1**) for 24–48 h at 4°C. Preparations were cleared of excess primary antibodies with 3 × 10 min PBS washes, and then incubated with appropriate secondary antibodies (**Table 1**) for 2.5 h at room temperature. Following another wash with PBS (3 × 10 min), preparations were mounted on a glass slide using a mounting medium (DAKO, Carpinteria, CA, United States).

Expression of vGluT2 in the myenteric plexus

Longitudinal muscle-myenteric plexus preparations double-labeled for vGluT2 and either one of two synaptic markers (vAChT or synaptophysin) were used to examine the expression pattern of vGluT2 and to determine the degree of co-expression of vGluT2 with the synaptic markers. Tissue samples were viewed using a Zeiss LSM880 Airyscan microscope (Carl Zeiss Microscopy, North Ryde, NSW, Australia). Preparations were labeled with secondary fluorophores 594 (for vGluT2) and 488 (either synaptophysin or vAChT) and were excited with VIS lasers 594 and 488 nm, respectively. Emission was detected using Airyscan filters (BP 420–480 + LP605 for 594 nm and BP 495–550 + LP 570 for 488 nm). Images (1748 pixels × 1748 pixels) were obtained using a Plan-Apochromat 63×/1.40 Oil DIC M27 objective, with a numerical aperture of 1.4, a 1.8× software zoom, z steps of 0.19 μm, 0.60 μs pixel dwell and averaging of 2 using the Zen Black software (Carl Zeiss Microscopy, North Ryde, NSW, Australia). For each combination (vGluT2 and vAChT; vGluT2 and synaptophysin), a total of 3 preparations, each from different animals were examined. In each preparation, 5 images of myenteric ganglia were chosen to be imaged based on their counterstains (vAChT or synaptophysin). The proportion of co-localization between vGluT2 with vAChT or synaptophysin in enteric varicosities was quantified using the image analysis software Imaris 9.0.0 (Bitplane).

The number of vGluT2 immunoreactive varicosities that made close contacts with the cell bodies and dendrites of neuronal nitric oxide synthase (nNOS)+ and calb+ myenteric neurons was examined. Cells positive for nNOS and calb were chosen as they both display characteristic cytoplasmic staining (Mann et al., 1997; Neal and Bornstein, 2007), which facilitates reliable 3D rendering of neuronal surfaces. Additionally, nNOS and calb neurons comprise 35 and 30% of all myenteric neurons in the mouse colon and represent distinct functional classes (Sang and Young, 1996, 1998). High-resolution confocal *z*-stacks were obtained using the Zeiss LSM880 Airyscan microscope (Carl Zeiss Microscopy, North Ryde, NSW, Australia) using parameters described above. For each combination (vGluT2 and nNOS; vGluT2 and calb) a total of 3 preparations, each from different animals were examined. Nine or ten calb or nNOS immunoreactive neurons were examined from each preparation. Imaris software was used to 3D render neuronal and varicosity labeling. We used the distance transformation extension to identify the number of vGluT2 surfaces that were in close contact with each calb and nNOS neurons. This extension creates a pseudo-colored channel, the intensity of this channel indicates the distance between vGluT2 varicosities and 3D rendered neurons of interest. High channel intensity indicates greater distance away from the 3D rendered neuron, and low channel intensity indicates proximity to the 3D rendered neuron. To filter vGluT2 varicosities that were in close contact with 3D rendered neurons of interest, we selected vGluT2 varicosities that located at sites where the pseudo channel intensity was 0 (indicating proximity to the neuron).

Proportion of calb and calr neurons in the myenteric plexus

Longitudinal muscle-myenteric plexus preparations were stained for calb, calretinin (calr) and Hu (pan neuronal marker) (**Table 1**). Immunofluorescently labeled samples were viewed using a LSM Pascal laser scanning microscope (Carl Zeiss Microscopy, North Ryde, NSW, Australia). *Z* stacks were obtained (1024 pixels × 1024 pixels) using a EC Plan-Neofluar 40×/1.30 Oil DIC M27 objective, with a 0.9× software zoom, z-steps of 0.9 μm, 1.60 μs pixel dwell and averaging of 2 using Zen 2.3 (blue edition) software (Zeiss, Australia). A total of 3 preparations were examined, each from a different animal. In each preparation, images of 10 myenteric ganglia were taken based on positive Hu labeling, and at least 250 Hu+ cell bodies were counted. Cell bodies with indistinct faint labeling, likely resulting from auto fluorescence or cross-labeling, were omitted from analysis. The mean proportions of Hu+ neurons immunoreactive for calb, calr or both were determined by calculating the averages from 3 animals.

Statistical analysis

All data are represented as mean ± SEM. Unpaired *t*-test analysis was used to compare the proportion of co-localization between vGluT2 with vAChT or synaptophysin (n = number of animals examined) and the number of vGluT2 surfaces that were in contact with myenteric neurons (n = number of neurons examined). One-way ANOVA was used to compare the mean proportions of Hu+ neurons that label for calb, calr or both (n = number of animals examined). All statistical analysis was performed using GraphPad Prism 5.0 (GraphPad Software, San Diego, CA, United States). $P < 0.05$ was considered to be statistically significant.

Calcium Imaging

Tissue Preparation

Distal colon segments were removed from each Wnt1-Cre; R26R-GCaMP mice and placed in Mg^{2+} free physiological saline (composition in mM: NaCl 134 mM, KCl: 3.4 mM, $CaCl_2$ 2.8 mM, $NaHCO_3$: 16 mM, D-glucose: 7.7 mM; modified from Shannon and Sawyer, 1989). All Ca^{2+}-imaging experiments were performed in Mg^{2+} free physiological saline as it has previously been shown in the guinea pig ileum that extracellular Mg^{2+} blocks enteric NMDA receptors so removing Mg^{2+} reveals increased effects of L-glutamate (Luzzi et al., 1988; Shannon and Sawyer, 1989; McRoberts et al., 2011). Colon segments were cut along the mesenteric borders, stretched, and pinned flat mucosal side up in a Sylgard-lined petri dish. Overlaying mucosal and submucosal layers were removed, then the tissues were flipped, and the longitudinal muscle layer was carefully stripped away using fine microdissection forceps to finally obtain preparations of myenteric plexus attached to circular muscle layer (CMMP). The CMMP preparations were stretched over a small inox ring and stabilized by a matched rubber O-ring (Vanden Berghe et al., 2002). A maximum of 3 rings were prepared from each segment of distal colon. The rings were transferred to an organ bath for imaging. The bath was continuously superfused (1 ml/min) with 95% O_2, 5% CO_2 Mg^{2+} free physiological saline at room temperature.

Imaging and Experimental Protocols

Myenteric ganglia positive for the Ca^{2+} indicator GCaMP3 were imaged (512 pixels × 512 pixels) using a Plan-Apochromat 20×/1,0 DIC (UV) VIS-IR M27 water dipping objective, with a numerical aperture of 1 and a 1× software zoom on an upright Zeiss (Axio Examiner Z.1) microscope with an Axiocam 702 camera (Carl Zeiss Microscopy, North Ryde, NSW, Australia). Images (16 bit) were acquired at 7 Hz. The responses of myenteric neurons to agonists (glutamate, NMDA, AMPA, and GABA) were examined via pressure ejection (spritz, 2 s duration) of each agonist from a micropipette placed at the edge of the imaged ganglion. Up to 5 myenteric ganglia were examined from each animal. At least 3 animals per agonist were investigated unless otherwise stated.

Effects of NMDA receptor antagonist APV on NMDA (100 mM)-evoked and L-Glu (50 mM) evoked $[Ca^{2+}]_i$ transients was investigated. In each preparation, time controls were first obtained by examining the $[Ca^{2+}]_i$ transients of myenteric neurons evoked by two spritzes of either agonists (10 min apart) onto a myenteric ganglion in control saline. After this, a different ganglion was chosen and the agonist-evoked $[Ca^{2+}]_i$ transients of myenteric neurons were examined firstly in control saline, then in the presence of an antagonist following superfusion of the drug for 10 min. Each ringed preparation was only exposed to an antagonist once and up to 4 CMMPs (each from different animals) were investigated per antagonist.

We examined the effects of glutamate receptor antagonists on neurons that displayed both L-Glu (50 mM) spritz- and electrically evoked $[Ca^{2+}]_i$ transients. Firstly, myenteric ganglia were chemically stimulated via L-Glu (50 mM) spritz as described above. As reported by others (Liu et al., 1997; Kirchgessner, 2001), prolonged and repetitive exposure to L-Glu desensitized GCaMP3+ cells, accordingly the micropipette containing L-Glu was moved away from the ganglia between applications. An interganglionic fiber tract entering the recorded ganglion was electrically stimulated with a single pulse and then a train of pulses (20 pulses, 20 Hz) using a focal stimulating electrode (tungsten wire; 50 μm). The stimuli were applied 1 min apart. Single pulses and trains of 20 pulses (20 Hz) evoke fast and fast-slow EPSPs, respectively (Nurgali et al., 2004; Gwynne and Bornstein, 2007; Foong et al., 2012; Fung et al., 2018). Time controls and antagonist experiments were performed on each preparation as described by Koussoulas et al. (2018). For time controls, the stimulation protocol was performed twice separated by 10 min on a myenteric ganglion in control saline. To test the effects of the antagonists, another ganglion was chosen from the same preparation, and the stimulation protocol was first performed in control saline, then after superfusion of the antagonist into the organ bath for 10 min. Each ringed preparation was only exposed once to an antagonist. A different stimulation protocol was used to examine the effect of the AMPA receptor antagonist CNQX, as only L-Glu-evoked $[Ca^{2+}]_i$ transients were investigated and only two preparations, each from a different animal, were examined. For all other antagonists, up to 3 CMMPs (each from different animals) were investigated.

Following live-imaging experiments, tissue preparations were fixed overnight with 4% formaldehyde at 4°C and immunostained using primary antisera to the neuron subtype markers nNOS, calb, and calr, or for calb and vGluT2 (**Table 1**). Imaged ganglia were relocated using an EC Plan-Neofluar 40×/0.75 M27 objective with a numerical aperture of 0.75 on a Zeiss Axio Imager M2 microscope by matching the micrographs with the Ca^{2+} imaging videos. Images were acquired with an Axiocam 506 mono camera using Zen 2.3 (blue edition) software (all from Zeiss, Australia). The immunoreactivity of responding GCaMP3+ neurons to calb, nNOS, or calr was identified.

Data Analysis and Statistical Analysis

Analysis was performed using custom-written directives (Li et al., 2019) in IGOR Pro (Wave Metrics, Lake Oswego, OR, United States). Regions of interest were drawn over a selected area of the cytoplasm for each neuron, excluding the nucleus because GCaMP3 is absent from the nuclei (Tian et al., 2009; Yamada and Mikoshiba, 2012). The amplitudes of $[Ca^{2+}]_i$

transients evoked chemically or electrically were calculated and expressed as the maximum increase in fluorescence from the baseline ($\Delta F_i/F_0$). $[Ca^{2+}]_i$ transients were only considered if the signal increased above baseline by at least 5 times the intrinsic noise.

For both time control and antagonist experiments, the $\Delta F_i/F_0$ of the second L-Glu spritz or the second electrical stimulation response was normalized and expressed as a fraction of the first (% $\Delta F_i/F_0$). For all L-Glu time control and antagonist experiments consisting of both chemical and electrical stimulations, $[Ca^{2+}]_i$ transients evoked by electrical stimulation were only analyzed for neurons that previously responded to L-Glu spritz.

At least 3 animals were examined for each experimental set, unless stated otherwise. Data are presented as the mean % $\Delta F_i/F_0$ of the control ± SEM where n = number of neurons examined. Statistical analyses were performed using unpaired *t*-tests with $P < 0.05$ considered statistically significant. Comparisons were performed using GraphPad Prism 5.0 (GraphPad Software, San Diego, CA, United States).

Drugs Used

Agonists used included L-Glutamic acid, GABA, *N*-Methyl-D-aspartic acid (NMDA) and Amino-3-hydroxy-5-methylisoxazole-4-propionic acid (AMPA) (all from Sigma-Aldrich, Castle Hill, NSW, Australia). Antagonists used were DL-2-Amino-5-phosphonopentanoic acid (APV) (Sigma-Aldrich), *N*-Phenyl-7-(hydroxyimino) cyclopropa[b]chromen-1a-carboxamide (PHCCC) and 6-Cyano-7-nitroquinoxaline-2,3-dione (CNQX) (from Tocris Bioscience, Avonmouth, Bristol, United Kingdom). All drugs were diluted in distilled water to make stock solutions and in Mg^{2+} free physiological saline on the day of experimentation.

RESULTS

vGluT2 Is Mainly Expressed in Non-cholinergic Terminals in the Myenteric Plexus

We found vGluT2 immunoreactivity in varicosities and terminals, but not in neuronal cell bodies, in the myenteric plexus of the mouse distal colon (**Figures 1A,B**). This is consistent with previous studies conducted in the rat and mouse oesophageal myenteric plexus (Raab and Neuhuber, 2004, 2005), mouse colorectal (Brumovsky et al., 2011), and colonic myenteric plexuses (Seifi and Swinny, 2016).

To establish the nature of vGluT2 varicosities and terminals in the myenteric plexus, we quantified the co-localization of vGluT2 with two key markers of enteric varicosities (vAChT and synaptophysin). Antisera to synaptophysin (a synaptic vesicle protein) and vAChT (marker of cholinergic varicosities) label many varicosities in the myenteric plexus (Sang and Young, 1998; Sharrad et al., 2013). Most vGluT2 containing varicosities co-expressed synaptophysin (60 ± 5% of vGluT2+ varicosities, **Figures 1A,C**), but very few synaptophysin+ varicosities contained vGluT2 (5 ± 1% of synaptophysin+ varicosities). Some vGluT2+ varicosities contained vAChT (35 ± 5% of vGluT2+ varicosities, **Figures 1B,C**), but vAChT varicosities rarely co-expressed vGluT2 (4 ± 1% of vAChT+ varicosities). Thus, only a minority of terminals that release glutamate in the myenteric plexus of the distal colon are likely to be cholinergic.

vGluT2 Varicosities Innervate Calb Immunoreactive Myenteric Neurons

Examination of close contacts between enteric varicosities and neurons can reveal potential sites of synaptic communication (Mann et al., 1997; Neal and Bornstein, 2007). The number of vGluT2+ close contacts onto two major subtypes of myenteric neurons, calb+ (**Figures 1D,E**) and nNOS+ (**Figures 1F,G**) neurons, was quantified to examine whether they receive glutamatergic innervation. Calb+ neurons have either Dogiel type I or II morphology, where type I neurons have elongated cell bodies and lamellar dendrites, while type II neurons have multiple axons and smooth cell bodies (Furness, 2006). Furthermore, Dogiel type I neurons comprise of the interneurons and motor neurons within the enteric circuitry, while type II neurons are typically intrinsic sensory neurons. In this study, most calb+ neurons examined for close contact analysis had Dogiel type I morphology (27/29), the remaining 2/29 had Dogiel type II morphology. The disparity between the two morphological groups was because the outlines of type I neurons were easily distinguishable with high-intensity staining which allowed for 3D rendering of the cell surface, while the staining of the Dogiel type II neurons was weaker and so less suitable for the analysis. All (29/29) calb+ neurons, and 28/29 nNOS+ neurons examined received vGluT2+ innervation. However, calb+ neurons received 3 times as many vGluT2 immunoreactive varicosities compared to nitrergic neurons (calb+ neurons: 41 ± 6, nNOS+ neurons: 14 ± 2 vGluT2+ varicosities; both $n = 29$ neurons, $p < 0.0001$, **Figure 1H**). Note, the two Dogiel type II calb+ neurons included in the sample had 33 and 43 vGluT2 contacts, well above the mean contacts to nNOS+ neurons. Additionally, the average volume of contacting vGluT2 varicosities was significantly larger for calb+ compared to nNOS+ neurons (calb+: 1.0 ± 0.1 μm^3, nNOS+: 0.7 ± 0.05 μm^3; both $n = 29$ neurons, $p = 0.04$, unpaired *t*-test). This suggests that neurally released glutamate plays a greater role in the excitation of calb+ neurons than of nitrergic neurons.

We found both distinct and co-expression of the two Ca^{2+} binding proteins, calb and calr, which is similar to previous studies (Sang et al., 1997; Sang and Young, 1998). Thirty ± 4% (**Figures 1I,J**) and 43 ± 1% of all Hu immunoreactive myenteric neurons in the distal colon expressed calb and calr, respectively. Of all Hu+ myenteric neurons, 26 ± 4% contain both calb and calr (**Figures 1I,J**), 17 ± 3% ($n = 3$ animals) only express calr and 4 ± 0.1% only contain calb.

Many Myenteric Neurons Have Either Glutamate or GABA Receptors or Both

Central nervous system neurons receive both glutamatergic and GABAergic synaptic inputs. In a previous study, we showed that GABA (1 mM) evokes $[Ca^{2+}]_i$ transients in over 20% of

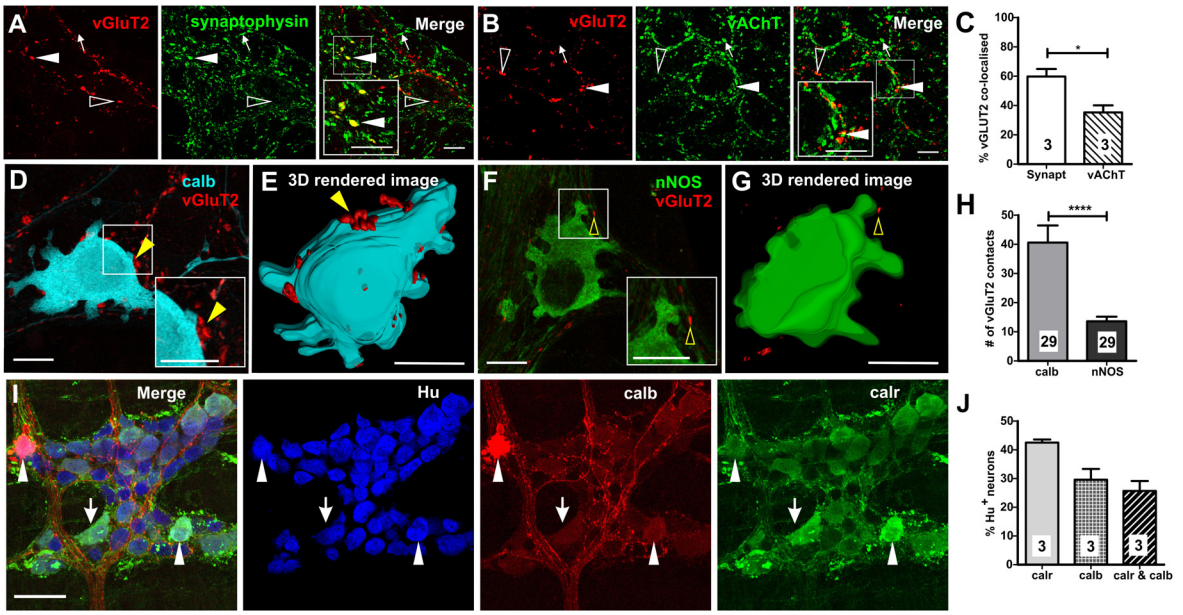

FIGURE 1 | Expression of vGluT2 in the myenteric plexus of mouse distal colon. **(A,B)** High-resolution micrographs illustrating vGluT2 (red), synaptophysin (green), and vAChT (green) immunoreactive varicosities within the myenteric plexus of mouse colon. Scale bars = 10 μm. **(A)** Several vGluT2 immunoreactive varicosities contain synaptophysin (filled arrowhead) but some lack synaptophysin (open arrowhead). Some synaptophysin varicosities lack vGluT2 (arrow). **(B)** Some vGluT2 varicosities contain vAChT (filled arrowhead), but most vGluT2 varicosities lack vAChT (open arrowhead). Likewise, many vAChT varicosities do not express vGluT2 (arrow). **(C)** Histogram showing the percentage of vGluT2 varicosities co-localized with synaptophysin and with vAChT. A significantly higher percentage of vGluT2 varicosities contain synaptophysin compared to those containing vAChT. Numbers on the bar graphs indicate numbers of animals examined. Fluorescence images **(D,F)** and 3D rendered surfaces **(E,G)** of vGluT2 varicosities (red) with a calb+ neuron **(D,E)** (pseudo colored cyan) and a nNOS+ neuron **(F,G)** (green) shows vGluT2 varicosities contacting the calb+ (yellow filled arrowheads) but not the nNOS+ neuron (yellow open arrowheads). All scale bars = 10 μm. **(H)** Histogram illustrating the number of vGluT2 varicosities contacting calb neurons and nNOS neurons. Calb neurons receive significantly more vGluT2 immunoreactive varicosities compared to nNOS neurons. Numbers on the bar graphs indicate numbers of neurons examined. **(I)** Fluorescence micrograph of the myenteric plexus from the distal colon of a C57Bl/6 mice stained for calb (red), calr (green), and pan-neuronal marker Hu (blue). Some calb neurons lack calr (open arrowheads), some calr neurons lack calb (arrows) and some Hu+ neurons contain both calb and calr (filled arrowheads). Scale bar = 50 μm. **(J)** Histogram showing the proportions of calr and/or calb+, Hu+ neurons in the myenteric plexus. Numbers on the bar graphs indicate number of animals examined. $^{*}p < 0.05$, $^{****}p$-value < 0.0001; unpaired *t*-test.

all GCaMP3+ neurons in the mouse ileum (Koussoulas et al., 2018). For comparison, in the mouse distal colon, we spritzed GABA (1 mM) onto 18 myenteric ganglia and found that this induced robust $[Ca^{2+}]_i$ transients ($\Delta F_i/F_0 = 0.60 \pm 0.02$, $n = 169$ neurons; **Figures 2A,F,G**) in 23 ± 3% of all GCaMP3+ cells. As in the ileum (Koussoulas et al., 2018), GABA-evoked $[Ca^{2+}]_i$ transients in the distal colon are most likely to be exhibited exclusively by neurons, as the cell bodies of responding cells were ∼20 μm in diameter consistent with the larger size of enteric neurons compared to glia (Gabella and Trigg, 1984). Further, GABA induced responses were immediate and it is reported that neurons respond instantaneously to stimuli with a sharp increase in $[Ca^{2+}]_i$, while glia tend to have slower increases in $[Ca^{2+}]_I$ (Boesmans et al., 2013). L-Glu (50 mM) spritz also evoked robust increases in $[Ca^{2+}]_i$ in a proportion (26 ± 3%) of all GCaMP3+ cells examined ($\Delta F_i/F_0 = 0.53 \pm 0.02$, $n = 229$ neurons, 21 ganglia; **Figures 2B–D,F,G**). In contrast to GABA, L-Glu spritz also evoked $[Ca^{2+}]_i$ transients in some GCaMP3+ cells that express the glia marker, glial fibrillary acidic protein (GFAP) (**Figures 2B–D**) but this was not further investigated in this study. We next recorded the proportion of myenteric neurons that responded to L-Glu (50 mM) and/or GABA (1 mM) (**Figure 2E**). Seven ganglia (from 2 animals) were spritzed with L-Glu followed by GABA. Of the 392 GCaMP3+ cells examined, 101 (25.8%) responded to L-Glu, 134 (34.2%) to GABA and only 57 (14.5%) had $[Ca^{2+}]_i$ transients evoked by both L-Glu and GABA. Hence, unlike the CNS, many GCaMP3+ enteric neurons responded to only one of the two amino acids.

As we previously examined GABA-induced responses in mouse enteric preparations, albeit in the distal ileum (Koussoulas et al., 2018), the rest of this study focused on characterizing L-Glu evoked $[Ca^{2+}]_i$ transients in the mouse distal colon.

L-Glu Evoked $[Ca^{2+}]_i$ Transients in Calb+ Myenteric Neurons

Most neurons (85/146, 58%) that responded to L-Glu (50 mM) were immunoreactive for calb. The amplitude of the L-Glu response was similar in neurons that either expressed or lacked calb (calb+ $\Delta F_i/F_0$: 0.5 ± 0.03, $n = 85$ neurons; calb− $\Delta F_i/F_0$: 0.5 ± 0.03; $n = 61$ neurons). Calb staining co-localized with calr in two preparations. Of the 36 L-Glu responders in these preparations, 14 were calb+/calr+, 11 were calb−/calr−, 10 were calb+ only, and 1 neuron was calr+ only (**Figures 3A,B**). Calb+ neurons that responded to L-Glu included both Dogiel types I and II neurons. The majority of calr+ neurons in the ganglia examined did not respond to L-Glu (68%). The amplitudes of

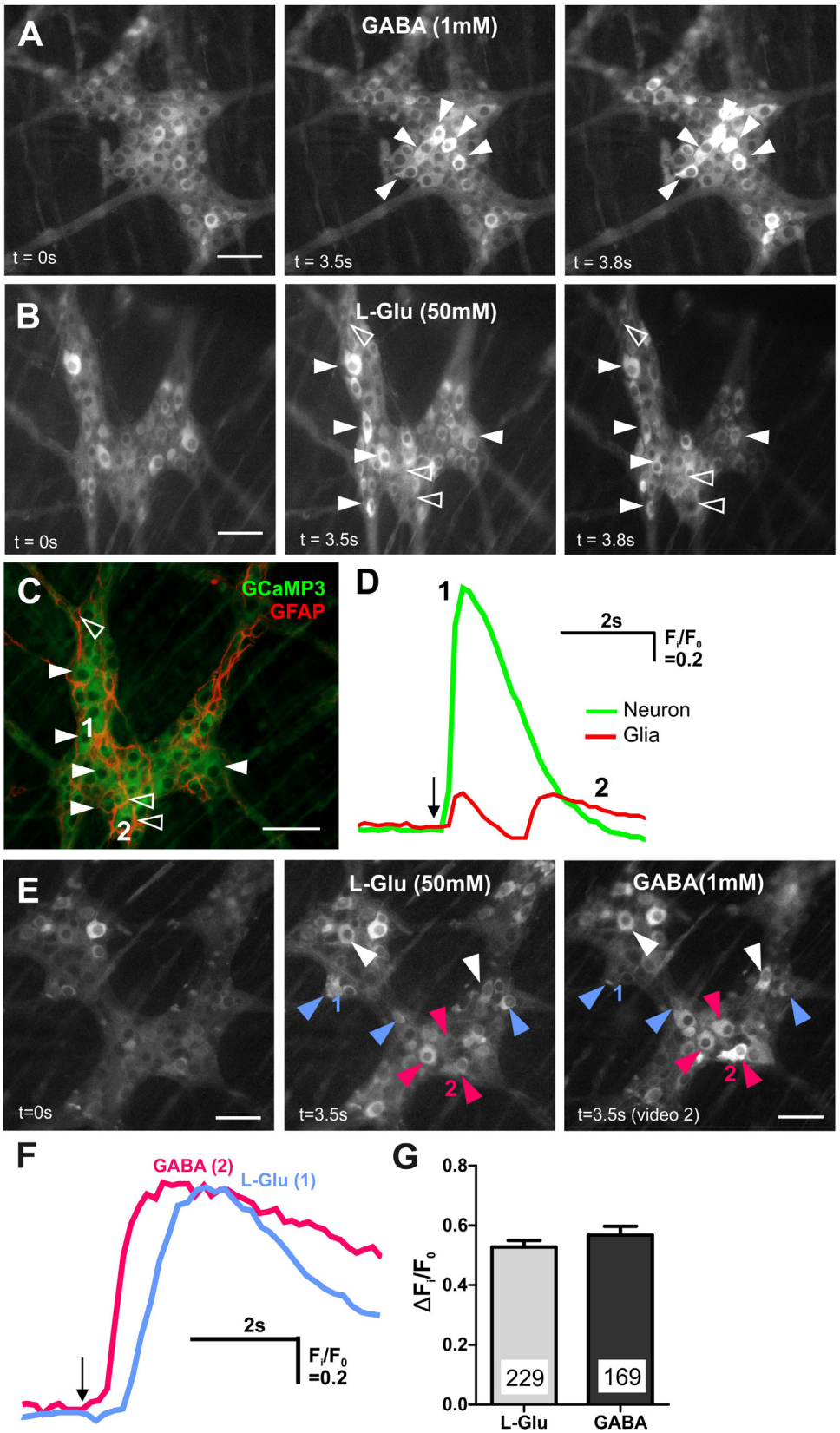

FIGURE 2 | Continued

FIGURE 2 | GABA and L-Glu evokes $[Ca^{2+}]_i$ transients predominantly in different enteric neurons. **(A)** Representative fluorescence micrographs of GABA (1 mM) evoked $[Ca^{2+}]_i$ transients in myenteric neurons (filled arrowheads) [GCaMP3 signal at rest (t = 0 s) and during GABA spritz in neurons (t = 3.5 s)]. GABA did not evoke $[Ca^{2+}]_i$ transients in glia (t = 3.8 s) **(B)** fluorescence micrograph of L-Glu evoked $[Ca^{2+}]_i$ transients in myenteric neurons (filled arrowheads) and glia (open arrowheads) [GCaMP3 signal at rest (t = 0s) and during L-Glu stimuation in neurons (t = 3.5 s) and in glia (t = 3.8 s)]. **(C)** Confocal micrograph of the imaged myenteric ganglion (in **B**) showing GCaMP3+ neurons (filled arrowheads) and GCaMP3+/GFAP+ glia (open arrowheads) that responded to L-Glu spritz. **(D)** Example traces from a neuron (1; green) and a glial cell (2; red) that responded to L-Glu (marked in **C**). The amplitude of $[Ca^{2+}]_i$ transients were larger in enteric neurons compared to glia. Arrow indicates L-Glu application. **(E)** Representative fluorescence micrographs of L-Glu (50 mM) and GABA (1 mM) evoked $[Ca^{2+}]_i$ transients in myenteric neurons [GCaMP3 signal at rest (t = 0 s) and during L-Glu (t = 3.5 s) stimulation and GABA (t = 3.5 s) stimulation, respectively]. Most neurons either responded to L-Glu (blue arrowheads) or GABA (pink arrowheads). Few neurons responded to both L-Glu and GABA (white arrowheads). **(F)** $[Ca^{2+}]_i$ transient traces obtained from neuron 1 and neuron 2 (marked in **E**). Arrow indicates drug application. **(G)** Histogram showing the average amplitude of $[Ca^{2+}]_i$ transients in response to L-Glu and GABA stimulation. All scale bars = 50 μm. Numbers on the bar graphs indicate numbers of neurons examined.

responses in neurons that expressed both calb and calr were significantly lower than in neurons that only contained calb (calb+/calr+ $\Delta F_i/F_0$: 0.19 ± 0.03, n = 14 neurons; calb+ only $\Delta F_i/F_0$: 0.53 ± 0.10, n = 10 neurons, p = 0.003, One-way ANOVA, **Figures 3C,D**). No significant differences in the amplitude of Ca^{2+} responses were observed between the other groups identified. These findings suggest that glutamate has a greater influence on the excitation of neurons that are immunoreactive for calb only and not calr.

A large proportion of L-Glu responsive neurons (61/146) did not express calb, so we examined immunoreactivity of these neurons for nNOS, which marks another major subpopulation of myenteric neurons (**Figures 3E,F**). Only 7/27 (26%) L-Glu-responding neurons were nNOS+ and the amplitude of this response was significantly lower than in neurons without nNOS (nNOS+ $\Delta F_i/F_0$: 0.2 ± 0.05, n = 7 neurons; nNOS− $\Delta F_i/F_0$: 0.4 ± 0.06, n = 20 neurons, p = 0.04, **Figures 3E–H**). This suggests that glutamate does not have a major influence in exciting nNOS+ neurons.

Although NMDA Receptors Are Expressed by L-Glu Responding Neurons, They Are Not Involved in Glutamatergic Synaptic Transmission

Ionotropic glutamate receptors and their subunits are present on guinea-pig enteric neurons, where they have been reported to mediate glutamatergic neurotransmission (Liu et al., 1997; Kirchgessner, 2001). We found that spritzed NMDA (100 mM) induced an increase in $[Ca^{2+}]_i$ in 22 ± 3% of GCaMP3+ cells examined ($\Delta F_i/F_0$ = 0.5 ± 0.04, n = 95 neurons, 10 ganglia; **Figures 4A,B**). Like L-Glu, NMDA spritz evoked delayed $[Ca^{2+}]_i$ transients in some GCaMP3+ glia (**Figures 4A,B**), but the glial responses were not investigated further. L-Glu (50 mM) was applied to 4 myenteric ganglia (from 1 animal) followed by NMDA to examine if neurons respond to both L-Glu and NMDA (**Figures 4C,D**). Of the 212 GCaMP3+ cells examined, 39 (18%) responded to L-Glu, 29 (14%) responded to NMDA, and 17 (8%) responded to both L-Glu and NMDA. Hence, most (17/29, 59%) NMDA responding GCaMP3+ cells also responded to L-Glu. Many L-Glu responding GCaMP3+ cells (22/39, 56%) did not respond to NMDA, probably because other glutamate receptors were present. Likewise, some (12/29, 41%) NMDA responding GCaMP3+ cells did not respond to L-Glu, indicating that there may be non-specific actions of NMDA on myenteric neurons.

We examined the effects of the NMDA receptor antagonist APV (100–500 μM) on $[Ca^{2+}]_i$ transients evoked by exogenous NMDA and L-Glu. APV significantly reduced the proportion of GCaMP3+ cells that responded to NMDA (100 mM) (Fisher's exact test p = 0.023, **Table 2**), but had no effect on the amplitude of NMDA-evoked $[Ca^{2+}]_i$ transients (% $\Delta F_i/F_0$ control: 59.5 ± 5.2, n = 65 neurons; APV: 53.1 ± 6.6, n = 57 neurons; **Figure 4E**). Similarly, APV significantly reduced the number of L-Glu responding neurons (Fisher's exact test p = 0.02, **Table 2**), but not the amplitude of the L-Glu- evoked $[Ca^{2+}]_i$ transients (% $\Delta F_i/F_0$ control: 73 ± 8, n = 54 neurons; APV: 54 ± 11, n = 30 neurons; p = 0.2; **Figure 4F**).

Inputs to myenteric ganglia were electrically stimulated to investigate the effects of APV on potential endogenous glutamate neurotransmission. APV (500 μM) did not affect 1 pulse- (% $\Delta F_i/F_0$ control: 65 ± 17%, n = 27 neurons; % $\Delta F_i/F_0$ APV: 72 ± 25%, n = 14 neurons; p = 0.8; **Figure 4G**) or 20 pulse-evoked (% $\Delta F_i/F_0$ control: 104 ± 18, n = 41 neurons; % $\Delta F_i/F_0$ APV: 114 ± 25%, n = 27 neurons; p = 0.8; **Figure 4H**) $[Ca^{2+}]_i$ transients in L-Glu responding neurons. Further, APV did not affect the number of neurons that exhibited electrically evoked $[Ca^{2+}]_i$ transients relative to time controls (**Table 2**).

We applied AMPA (50 and 100 μM) to some myenteric ganglia using concentrations effective in other studies (Parsons et al., 1994; Nissen et al., 1995), but it did not evoke reliable responses. Further, the AMPA receptor antagonist CNQX (20 μM) did not alter the number of neurons that exhibited L-Glu evoked $[Ca^{2+}]_i$ transients relative to time controls (**Table 2**) or their amplitude (% $\Delta F_i/F_0$ control: 69 ± 12, n = 25 neurons; CNQX: 87 ± 17, n = 38 neurons; p = 0.4). Thus, AMPA receptors were not investigated further.

Glutamatergic Synaptic Transmission Involves Group I mGlu Receptors in Myenteric Ganglia

Group I metabotropic glutamate receptors (mGluRs) are involved in enteric neurotransmission in guinea pig (Ren et al., 2000; Foong and Bornstein, 2009). We focused on neurons that expressed glutamate receptors by first identifying the neurons that responded to exogenous L-Glu (50 mM). However, it should be noted that L-Glu responsive neurons may include secondary neurons that do not express glutamate receptors themselves but receive synaptic input from other neurons that do. We examined whether the Group I mGluR antagonist PHCCC (30 μM) affects the L-Glu- and electrically evoked $[Ca^{2+}]_i$

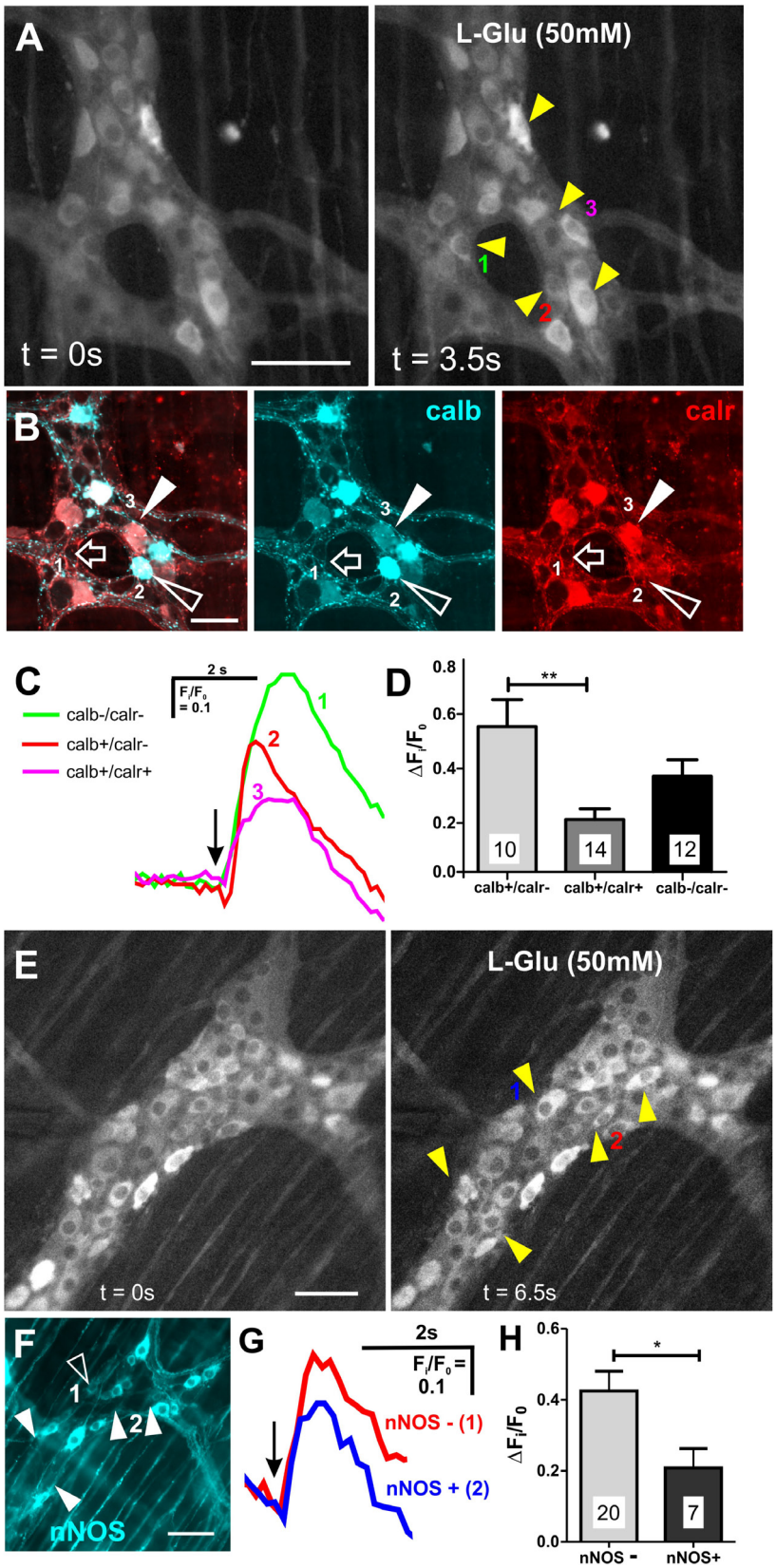

FIGURE 3 | Continued

FIGURE 3 | Neurons that expressed calb or lacked nNOS had larger L-Glu-evoked $[Ca^{2+}]_i$ transients. **(A)** Representative fluroescence micrographs of L-Glu (50 mM) evoked $[Ca^{2+}]_i$ transients in myenteric neurons [GCaMP3 signal at rest (t = 0 s) and during L-Glu stimuation (t = 3.5 s)]. **(B)** Confocal micrograph of the imaged myenteric ganglion (in **A**) shows some L-Glu responsive neurons that did not express calb or calr (open arrow, neuron 1), was only immunoreactive for calb (open arrowhead, neuron 2) or was immunoreactive for calb and calr (filled arrowhead, neuron 3). **(C)** Example traces from the 3 neurons (marked in **A,B**) that responded to L-Glu, demonstrating that the neuron that contained calb only exhibited larger L-Glu-evoked $[Ca^{2+}]_i$ transient. Arrow indicates the when L-Glu was spritzed. **(D)** Histogram showing the average amplitude of L-Glu-evoked $[Ca^{2+}]_i$ transients. Neurons only positive for calb had larger amplitudes compared to those that contained both calb and calr. **(E)** Representative fluroescence micrographs of L-Glu (50 mM) evoked $[Ca^{2+}]_i$ transients in myenteric neurons [GCaMP3 signal at rest (t = 0 s) and during L-Glu stimuation (t = 3.5 s)]. **(F)** Confocal micrograph of the imaged myenteric ganglion (in **A**) shows some L-Glu responsive neurons were nNOS+ (psuedo colored cyan; open arrowheads). Most L-Glu responding neurons lacked nNOS (filled arrowheads). **(G)** Example traces from 2 neurons (marked in **E,F**) that responded to L-Glu, demonstrating that the nNOS – neuron (2) exhibited larger L-Glu-evoked $[Ca^{2+}]_i$ transient compared to the nNOS+ neuron (1). Arrow indicates when L-Glu was spritzed. **(H)** Histogram showing the average amplitude of L-Glu-evoked $[Ca^{2+}]_i$ transients. nNOS– neurons had larger amplitudes compared to nNOS+ neurons. All scale bars 50μm. Number of neurons examined are indicated on the bar graphs; $^*p < 0.01$, $^{**}p = 0.003$; unpaired t-test.

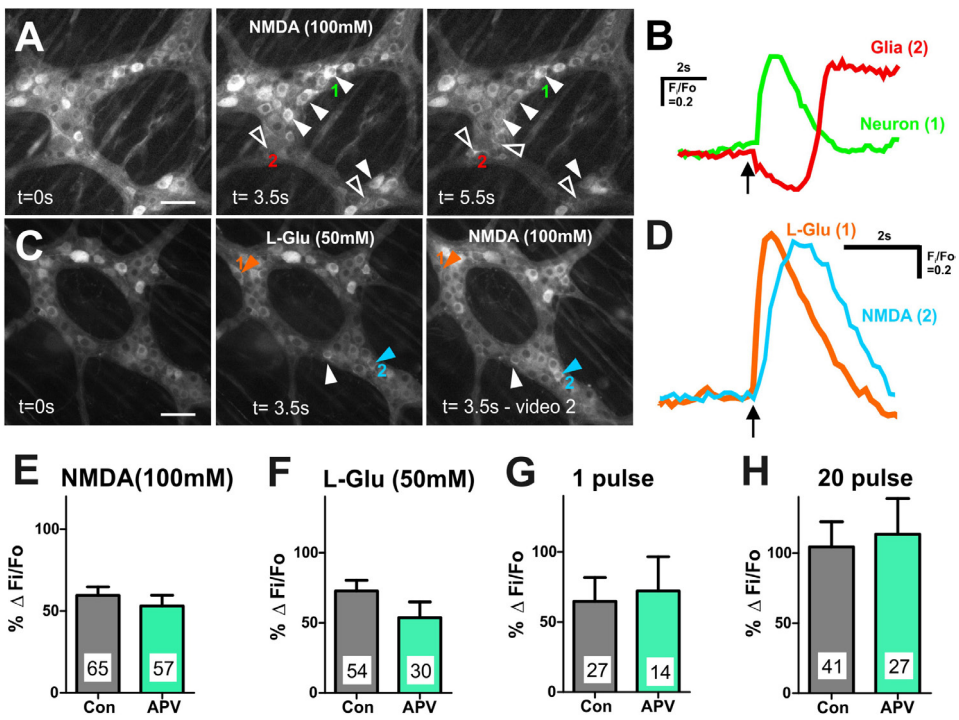

FIGURE 4 | Many myenteric neurons exhibited $[Ca^{2+}]_i$ transients in response to L-Glu and NMDA. **(A)** Representative fluorescence micrographs of NMDA (100 mM) evoked $[Ca^{2+}]_i$ transients in myenteric neurons (filled arrowheads) and glia (open arrowheads) [GCaMP3 signal at rest (t = 0 s) and during NMDA spritz in neurons (t = 3.5 s) and in glia (t = 5.5 s)]. **(B)** Example traces from a neuron (1) and a glial cell (2; marked in **A**) that responded to L-Glu. Glial cell shows delayed response to NMDA compared to the GCaMP3+ neuron. Arrow indicates NMDA application. **(C)** Representative fluorescence micrographs of L-Glu (50 mM) and NMDA (100 mM) evoked $[Ca^{2+}]_i$ transients in myenteric neurons [GCaMP3 signal at rest (t = 0 s) and during L-Glu stimulation and NMDA stimulation, respectively]. Most L-Glu responding neurons also respond to NMDA (filled arrowhead). Some neurons either respond to L-Glu (orange arrowhead) or NMDA (blue arrowhead). **(D)** $[Ca^{2+}]_i$ transient traces obtained from neuron 1 and neuron 2 (marked in **C**). Arrow indicates drug application. Histograms showing pooled $[Ca^{2+}]_i$ transient amplitudes from all neurons stimulated with NMDA **(E)** and L-Glu **(F)**, and from L-Glu responding neurons stimulated with 1 pulse **(G)** and 20 pulse **(H)** in time control (con) and in the presence of APV. Changes in amplitude after application APV are presented as a percentage of the first response in control saline (% $\Delta F_i/F_0$). APV did not alter the amplitude of agonist or electrically evoked $[Ca^{2+}]_i$ transients in myenteric neurons. All scale bars 50 μm. Number of neurons examined are indicated on the bar graphs.

transients of these neurons to determine whether they express Group I mGluRs, and if the probable release of endogenous glutamate in response to electrical stimuli can activate these receptors.

PHCCC did not alter the proportion of GCaMP3+ cells that responded to L-Glu (**Table 2**) or the amplitude of L-Glu evoked $[Ca^{2+}]_i$ transients (% $\Delta F_i/F_0$ control: 59 ± 6, n = 75 neurons; % $\Delta F_i/F_0$ PHCCC: 53 ± 8, n = 61 neurons; **Figure 5A**). PHCCC also did not affect the proportion of responsive GCaMP3+ cells (**Table 2**) or amplitude of $[Ca^{2+}]_i$ transients evoked by 1 pulse stimulation (% $\Delta F_i/F_0$ control: 68 ± 12%, n = 35 neurons; % $\Delta F_i/F_0$ PHCCC: 63 ± 17%, n = 37 neurons; p = 0.828, **Figure 5B**). However, it significantly reduced the proportion of neurons that responded to 20 pulse stimulation (p = 0.04, Fisher's exact test; **Table 2**) and the amplitude of the 20 pulse-evoked $[Ca^{2+}]_i$ transients (% $\Delta F_i/F_0$ control: 96 ± 10, n = 62 neurons; % $\Delta F_i/F_0$ PHCCC: 58 ± 6, n = 50; p = 0.003, **Figure 5C**).

TABLE 2 | Number of responding neurons during time controls and in the presence antagonists.

Stimulation/antagonist	Time control (1)	Time control (2)	Control	Antagonist
NMDA (100 mM) spritz/APV (100 μM)	65	54/65	57	37/57*
L-Glu (50 mM) spritz/APV (500 μM)	54	47/54	30	19/30*
1 pulse/APV (500 μM)	27	14/27	21	14/21
20 pulse/APV (500 μM)	41	29/41	27	17/27
L-Glu (50 mM) spritz/CNQX (20 μM)	25	18/25	38	30/38
L-Glu (50 mM) spritz/PHCCC (30 μM)	75	60/75	61	41/61
1 pulse/PHCCC (30 μM)	35	24/35	37	15/37
20/PHCCC (30μM)	62	56/62	50	37/50*

*$P < 0.05$ Fisher's Exact Test.

Post hoc immunohistochemistry was conducted to identify the neurochemistry of the responding neurons. Of the 49 neurons that exhibited 1 pulse-evoked $[Ca^{2+}]_i$ transients, 24 (49%) were immunoreactive for calb+, while 39/73 (53%) of the neurons that exhibited 20 pulse-evoked $[Ca^{2+}]_i$ transients were immunoreactive for calb. In a particular ganglion examined, 6 of the 17 neurons that responded to 20 pulse stimulation were calb+ and of these 5 had vGluT2+ varicosities contacting their somata (**Figures 5D–G**). Moreover, the 20 pulse responses in the calb+ neurons in this ganglion were depressed by the group I mGluR antagonist. Thus, calb+ myenteric neurons receive glutamatergic innervation and receive slow synaptic inputs mediated by endogenous release of glutamate activating group I mGluRs.

PHCCC was dissolved in DMSO, so vehicle control experiments were conducted to eliminate the possibility of DMSO effects on $[Ca^{2+}]_i$ transients. DMSO did not affect the proportion of L-Glu responders (Fisher's exact test $p = 0.6$, **Table 2**) or the amplitude of L-Glu-evoked $[Ca^{2+}]_i$ transients (% $\Delta F_i/F_0$ control: 94 ± 12%, $n = 20$ neurons; % $\Delta F_i/F_0$; DMSO: 79 ± 7%, $n = 35$ neurons; $p = 0.3$). DMSO also did not affect the numbers of responsive neurons that responded to 1 pulse or 20 pulse stimulation (both $p > 0.3$ Fisher exact test, **Table 2**) or the amplitude of electrically evoked $[Ca^{2+}]_i$ transients (% $\Delta F_i/F_0$ 1 pulse control: 158 ± 36%, $n = 15$ neurons; % $\Delta F_i/F_0$ DMSO: 124 ± 35%, $n = 20$ neurons; $p = 0.5$; 20 pulse % $\Delta F_i/F_0$ control: 104 ± 14%, $n = 17$ neurons; % $\Delta F_i/F_0$ DMSO: 114 ± 17%, $n = 30$ neurons; $p = 0.7$).

DISCUSSION

How glutamate mediates synaptic transmission in the ENS has been difficult to decipher even though several studies implicate glutamate in the regulation of gastrointestinal function (Kirchgessner, 2001; Filpa et al., 2016). This may be due to its role as an auxiliary neurotransmitter compared to the dominant neurotransmitter acetylcholine, and to the vast

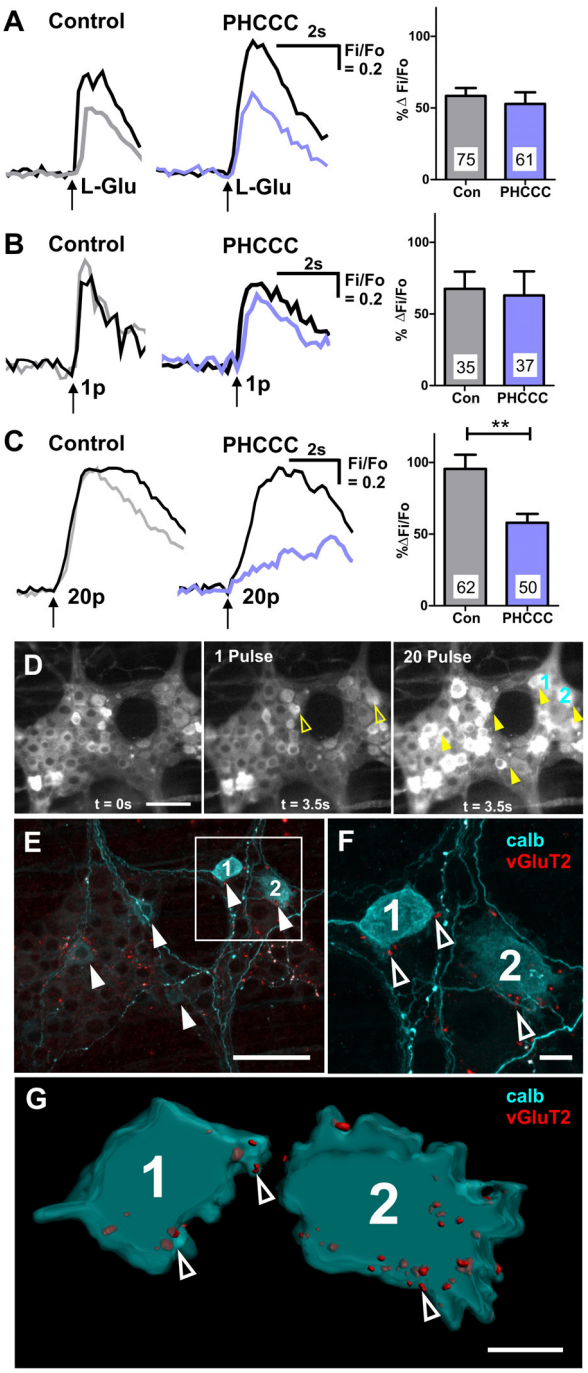

FIGURE 5 | Calbindin+ myenteric neurons receive vGluT2+ varicosities, and exhibit 20 pulse-evoked $[Ca^{2+}]_i$ transients that are mediated by Group I mGluRs. Representative traces of $[Ca^{2+}]_i$ transients evoked by L-Glu (50 mM) spritz **(A)**, 1 pulse **(B)**, and 20 pulse **(C)** electrical stimulation during time controls (1st stimulation: black trace; 2nd stimulation: gray trace) and PHCCC treatment (control: black trace; PHCCC: purple). Histograms showing pooled $[Ca^{2+}]_i$ transient amplitudes from all neurons stimulated with L-Glu **(A)**, 1 pulse **(B)**, and 20 pulse **(C)** in time control (con) and in the presence of PHCCC. Changes in amplitude after application PHCCC are presented as a percentage of the first response in control saline (% $\Delta F_i/F_0$). Numbers on bar graphs indicate the number of neurons examined. PHCCC significantly

(Continued)

FIGURE 5 | Continued
reduced the amplitude of 20 pulse-evoked $[Ca^{2+}]_i$ transients in L-Glu responding neurons (**$p < 0.01$; unpaired *t*-test). **(D)** Representative fluroescence micrographs of 1 pulse and 20 pulse electrical stimulation-evoked $[Ca^{2+}]_i$ transients in myenteric neurons [GCaMP3 signal at rest ($t = 0$ s) and during 1 pulse and 20 pulse electrical stimulation stimuation ($t = 3.5$ s), respectively]. **(E)** Confocal micrograph of the imaged myenteric ganglion (in **D**) stained for calb. Some neurons calb+ neurons responded to 1 pulse (yellow open arrows in **D**), most calb+ neurons identified responded to 20 pulse stimulations (yellow filled arrows in **D**). Scale bars 50 μm. Enlarged confocal micrograph **(F)** and 3D rendered surfaces **(G)** of a section in **(E)**, illustrate close contacts of vGluT2 varicosities (open arrowheads) onto two calb+ neurons (marked 1 and 2) that responded to 20 pulse stimulation. Scale bar 10 μm.

diversity of glutamatergic receptors expressed in this system (Liu et al., 1997; Ren et al., 2000; Kirchgessner, 2001; Seifi and Swinny, 2016). Here, we provide several lines of evidence for glutamatergic excitation of a proportion of calb immunoreactive neurons via activation of Group I mGluRs. Firstly, we show that most vGluT2+ varicosities are non-cholinergic and many express synaptophysin. We also show that vGluT2+ varicosities preferentially surround calb+ neurons rather than nitrergic neurons. Likewise, we found that calb+ neurons are excited by glutamate receptors. Further, we showed that electrically evoked release of putative endogenous glutamate contributes to slow synaptic transmission in myenteric neurons, especially those immunoreactive for calb, via the activation of Group I mGluRs.

vGluT2+ Varicosities Are Often Non-cholinergic and Contain the Synaptic Vesicle Protein Synaptophysin

Although vGluT2 expression is observed in varicosities within the myenteric plexus of several rodent models, the neurochemistry of glutamate containing varicosities and their innervation patterns have not been examined in detail (Liu et al., 1997; Tong et al., 2001; Brumovsky et al., 2011; Seifi and Swinny, 2016). Our observation of vGluT2 expression in myenteric varicosities of mouse is consistent with previous studies (Tong et al., 2001; Brumovsky et al., 2011; Seifi and Swinny, 2016). Varicosities are putative neurotransmitter release sites in the enteric neural circuitry. Using advanced imaging and quantification methods adapted for enteric preparations, we found that most vGluT2+ varicosities (∼65%) are non-cholinergic as they lacked vAChT, confirming previous qualitative descriptions (Tong et al., 2001; Seifi and Swinny, 2016). We found that only a small proportion of few vGluT2+ varicosities contain vAChT. These varicosities are likely to originate from intrinsic glutamatergic enteric neurons or from dorsal root ganglion neurons (Liu et al., 1997; Tong et al., 2001). The non-cholinergic vGluT2+ varicosities may also originate from extrinsic neurons, as previous studies have reported the expression of vGluT2+ neurons in the nodose and dorsal root ganglia, which innervate the mouse stomach (Tong et al., 2001). In addition, we found that most vGluT2+ varicosities (60%) co-express the synaptic vesicle protein synaptophysin, a protein involved in exo- and endocytosis of synaptic vesicles in the CNS (Edelmann et al., 1995; Takamori et al., 2006; Kwon and Chapman, 2011). Thus, potential glutamate release sites are present within the myenteric plexus, and synaptophysin, a major constituent of glutamatergic synaptic vesicles in the CNS (Takamori et al., 2006), is most likely involved in regulating glutamate release in the ENS. However, given that some vGluT2+ varicosities lack synaptophysin, other families of synaptic vesicles are probably involved in endo- and exocytosis of glutamate within the ENS.

Glutamate Excites Calb+ Myenteric Neurons by Activating Glutamate Receptors Including NMDA and Group I mGluRs

Exogenous application of L-Glu evoked $[Ca^{2+}]_i$ transients in some myenteric neurons, these neurons were largely distinct from those that responded to the other prominent CNS neurotransmitter, GABA. Most L-Glu responders were calb+, some of which co-express calr, but fewer L-Glu responders were nNOS+, indicating that functional glutamatergic receptors are predominantly localized to calb+ myenteric neurons. These findings align with our anatomical observations that all calb+ neurons examined received vGlu2+ varicosities and are contacted by substantially more vGluT2+ varicosities than nNOS+ neurons. L-Glu responding calb+ neurons exhibit either Dogiel types I and II morphology. In combination with our finding that all Dogiel type I calb+ neurons examined receive vGluT2 innervation, we provide strong evidence that glutamate excites calb+ interneurons. Though under-represented, our data also suggests that Dogiel type II, calb+ neurons which are typical intrinsic sensory neurons also receive functional glutamatergic inputs. Moreover, the L-Glu responsive neurons that co-express calb and calr are probably either intrinsic sensory and interneurons, as calb+ varicosities do not innervate the smooth muscle layers (Sang and Young, 1998). Most calr+ only and nNOS+ neurons were unresponsive to L-Glu, suggesting that glutamate does not influence the excitation of motor neurons, interneurons and some intrinsic sensory neurons identified by these markers. Therefore, these observations indicate that glutamate is likely to play a significant role in modulating the activity of neural pathways involving calb+ interneurons and intrinsic sensory neurons.

Thus far, electrophysiological studies have resulted in conflicting findings in relation to the involvement of NMDA receptors in mediating glutamate-evoked depolarizations within the ENS (Liu et al., 1997; Ren et al., 2000). Liu et al. (1997) observed that the NMDA receptor antagonist AP5 inhibited glutamate-elicited slow depolarizations in enteric neurons. However, Ren et al. (2000) reported that glutamate induced excitation was unaffected by the NMDA receptor antagonists MK-801 and D-APV. In this study, we found that the amplitudes of NMDA- and L-Glu-evoked $[Ca^{2+}]_i$ transients were unaffected by APV, but that APV reduced the number of neurons that respond to NMDA and L-Glu.

Although our findings align with previous reports that identify expression of NMDA receptors in enteric neurons (Broussard et al., 1994; Burns et al., 1994; Liu et al., 1997;

McRoberts et al., 2001; Del Valle-Pinero et al., 2007), the lack of effect of NMDA receptor blockade could be due to the presence of other glutamate receptors such as Kainate receptors, which have also been shown to be expressed on myenteric neurons (Carpanese et al., 2014). Likewise, $[Ca^{2+}]_i$ transients are dominated by Ca^{2+} entry due to action potentials (Vanden Berghe et al., 2000), therefore it is likely that the amount of Ca^{2+} into these neurons was insufficient to evoke depolarizations. It is also possible that the lack of response observed in some neurons during NMDA blockade could be due to the high-density of NMDA receptors on those particular neurons. Indicating potential heterogeneity in the expression of NMDA receptors on myenteric neurons. Therefore, further clarification into the expression of NMDA receptor subunits within the myenteric plexus is required. Additionally, it should be noted that the concentration (100 mM) of NMDA in the spritz pipette required to evoke $[Ca^{2+}]_i$ transients in this study is higher than the concentration (10 mM) used in a previous study which examined membrane potentials of neurons with intracellular recording (Liu et al., 1997), thus, we cannot exclude the possibility of potential non-specific effects of the agonist in this study.

Calb+ Myenteric Neurons Receive Slow Synaptic Transmission Mediated by Group I mGluRs

Activation of NMDA, AMPA, and Group I mGlu receptors depolarizes enteric neurons in guinea pig tissues (Liu et al., 1997; Liu and Kirchgessner, 2000; Ren et al., 2000; Foong and Bornstein, 2009), but the precise involvement of these receptors in synaptic transmission is unclear. We used a single pulse and a train of electrical pulses as stimuli, which evoke fast, and fast-slow EPSPs in mouse myenteric neurons (Shuttleworth and Smith, 1999; Nurgali et al., 2004; Gwynne and Bornstein, 2007; Foong et al., 2012, 2015; Koussoulas et al., 2018) to ascertain the effects of potential endogenous glutamate release on L-Glu–responsive neurons. The amplitudes of both electrically evoked $[Ca^{2+}]_i$ transients, and the number of neurons responding to electrical stimuli were unaffected by the competitive NMDA receptor antagonist, APV. Thus, NMDA receptors are unlikely to mediate fast and slow EPSPs in mouse myenteric neurons, as previously reported for guinea pig (Liu et al., 1997; Ren et al., 2000). Nevertheless, Liu et al. (1997) found that APV reduced the amplitude of glutamate-evoked slow depolarizations in guinea pig enteric neurons but suggested that these slow responses are unlikely to represent slow EPSPs and that NMDA receptors play a modulatory role in the enteric neural circuitry. NMDA receptors are non-specific cation channels (Hansen et al., 2018), and increase underlying membrane conductance, but slow EPSPs in the ENS are associated with decreases in membrane conductance (Gwynne and Bornstein, 2007). Indeed activation of NMDA receptors would produce $[Ca^{2+}]_i$ transients in the absence of action potentials. Thus, even a subthreshold NMDA response might mimic an action potential driven $[Ca^{2+}]_i$ transient. The antagonist used in this study acts on all four GluN2 subunits of the NMDA receptor, so the lack of effect observed in this study is unlikely due to antagonist specificity and efficiency issues (Ogden and Traynelis, 2011). However, the involvement of NMDA receptors in mediating synaptic transmission within the ENS cannot yet be ruled out.

Despite considerable evidence for the expression of AMPA receptor subunits in rodents (Liu et al., 1997; Seifi and Swinny, 2016), we did not find robust effect of exogenous AMPA on myenteric neurons, or any effect of AMPA blockade on L-Glu evoked responses. However, the role of AMPA receptors in the ENS warrants future investigation.

The Group I mGluR antagonist (PHCCC), which targets both mGlu1 and mGlu5 receptor subtypes, did not alter $[Ca^{2+}]_i$ transients or the number of neurons responsive to exogenous L-Glu. It could be that the effect of exogenous glutamate is dominated by receptors other than group I mGluRs, and hence the antagonist was ineffective. However, 20 pulse train-evoked $[Ca^{2+}]_i$ transients were significantly reduced by PHCCC. This indicates that endogenous release of glutamate activates Group I mGluRs to regulate slow synaptic potentials. Moreover, it is likely that glutamate mediates slow transmission to calb+ myenteric neurons, as calb+ neurons receive substantial numbers of vGluT2+ varicosities and constitute the majority of L-Glu and 20 pulse responsive neurons. These observations are consistent with several electrophysiological studies that implicate Group I mGluRs in slow excitatory synaptic events in enteric neural circuitry (Liu and Kirchgessner, 2000; Ren et al., 2000; Foong and Bornstein, 2009). This suggests a role for both glutamate in mediating transmission within enteric circuits and for Group I mGluRs in the regulation of gastrointestinal function.

CONCLUSION

We used anatomical and functional assays to demonstrate that glutamate excites calb+ neurons via the activation of Group I mGluRs. Further investigation of the group I mGluR subtypes involved could be fruitful in identifying the mechanism behind glutamatergic action on calb+ neurons, and the reflex circuitry underlying colonic motility.

DATA AVAILABILITY

All datasets generated for this study are included in the manuscript and/or the supplementary files.

ETHICS STATEMENT

This study was carried out in accordance with the recommendations of the 'University of Melbourne Animal Experimentation Ethics Committee'. The protocol was approved by the 'University of Melbourne Animal Experimentation Ethics Committee'.

AUTHOR CONTRIBUTIONS

MS, JB, and JF conceived and designed the experiments. MS and JF performed the experiments. MS analyzed the data. JB and JF contributed reagents, materials, and analysis tools. MS, EH-Y,

and JF wrote the manuscript. All authors contributed to editing and revising the manuscript. All authors read and approved the final manuscript.

FUNDING

This research was supported by National Health and Medical Research Council of Australia Project grants #1099016 (JF and JB), and Australian Research Council grant #DP130101596 (JB).

ACKNOWLEDGMENTS

We thank H. Young for kindly providing the transgenic mice (Wnt1-Cre; R26R-GCaMP3), Annette Bergner for excellent technical assistance. The Biological Optical Microscopy Platform in the University of Melbourne for the use of their facilities and Dr. Hyun-Jung Cho for consultation services. We would also like to thank Dr. Pieter Vanden Berghe (Katholieke Universiteit Leuven, Belgium) for kindly providing us with the source code for conducting Ca^{2+} imaging analysis.

REFERENCES

Boesmans, W., Martens, M., Weltens, N., Hao, M., Tack, J., Cirillo, C., et al. (2013). Imaging neuron-glia interactions in the enteric nervous system. *Front. Cell. Neurosci.* 7:183. doi: 10.3389/fncel.2013.00183

Broussard, D. L., Li, X., Pritchett, D. B., Lynch, D., Bannermann, P. G., and Pleasure, D. (1994). The expression of a NMDA receptor gene in guinea-pig myenteric plexus. *NeuroReport* 5, 973–976.

Brumovsky, P., Robinson, D., La, J.-H., Seroogy, K., Lundgren, K., Albers, K., et al. (2011). Expression of vesicular glutamate transporters type 1 and 2 in sensory and autonomic neurons innervating the mouse colorectum. *J. Comp. Neurol.* 519, 3346–3366. doi: 10.1002/cne.22730

Burns, G. A., Stephens, K. E., and Benson, J. A. (1994). Expression of mRNA for the N-methyl-D-aspartate (NMDAR1) receptor by the enteric neurons of the rat. *Neurosci. Lett.* 170, 87–90.

Carpanese, E., Moretto, P., Filpa, V., Marchet, S., Moro, E., Crema, F., et al. (2014). Antagonism of ionotropic glutamate receptors attenuates chemical ischemia-induced injury in rat primary cultured myenteric ganglia. *PLoS One* 9:e113613. doi: 10.1371/journal.pone.0113613

Chen, W.-P., and Kirchgessner, A. (2002). Activation of group II mGlu receptors inhibits voltage-gated Ca2+ currents in myenteric neurons. *AJP Gastrointest. Liver Physiol.* 283, G1282–G1289.

Danielian, P. S., Muccino, D., Rowitch, D. H., Michael, S. K., and Mcmahon, A. P. (1998). Modification of gene activity in mouse embryos in utero by a tamoxifen-inducible form of Cre recombinase. *Curr. Biol.* 8, 1323–1326.

Del Valle-Pinero, A. Y., Suckow, S. K., Zhou, Q., Perez, F. M., Verne, G. N., and Caudle, R. M. (2007). Expression of the N-methyl-D-aspartate receptor NR1 splice variants and NR2 subunit subtypes in the rat colon. *Neuroscience* 147, 164–173.

Edelmann, L., Hanson, P. I., Chapman, E. R., and Jahn, R. (1995). Synaptobrevin binding to synaptophysin: a potential mechanism for controlling the exocytotic fusion machine. *EMBO J.* 14, 224–231.

Filpa, V., Moro, E., Protasoni, M., Crema, F., Frigo, G., and Giaroni, C. (2016). Role of glutamatergic neurotransmission in the enteric nervous system and brain-gut axis in health and disease. *Neuropharmacology* 111, 14–33. doi: 10.1016/j.neuropharm.2016.08.024

Foong, J. P., and Bornstein, J. C. (2009). mGluR(1) receptors contribute to non-purinergic slow excitatory transmission to submucosal VIP neurons of guinea-pig Ileum. *Front. Neurosci.* 3:46. doi: 10.3389/neuro.21.001.2009

Foong, J. P. P., Hirst, C., Hao, M., Mckeown, S., Boesmans, W., Young, H., et al. (2015). Changes in nicotinic neurotransmission during enteric nervous system development. *J. Neurosci.* 35, 7106–7115.

Foong, J. P. P., Nguyen, T., Furness, J., Bornstein, J., and Young, H. (2012). Myenteric neurons of the mouse small intestine undergo significant electrophysiological and morphological changes during postnatal development. *J. Physiol.* 590, 2375–2390. doi: 10.1113/jphysiol.2011.225938

Fung, C., Koussoulas, K., Unterweger, P., Allen, A., Bornstein, J., and Foong, J. P. P. (2018). Cholinergic submucosal neurons display increased excitability following in vivo cholera toxin exposure in mouse ileum. *Front. Physiol.* 9:260. doi: 10.3389/fphys.2018.00260

Furness, J. B. (2006). *The Enteric Nervous System*. Boston, MA: Blackwell Publishing.

Gabella, G., and Trigg, P. (1984). Size of neurons and glial cells in the enteric ganglia of mice, guinea-pigs, rabbits and sheep. *J. Neurocytol.* 13, 49–71.

Giaroni, C., Zanetti, E., Chiaravalli, A., Albarello, L., Dominioni, L., Capella, C., et al. (2003). Evidence for a glutamatergic modulation of the cholinergic function in the human enteric nervous system via NMDA receptors. *Eur. J. Pharmacol.* 476, 63–69.

Gwynne, R. M., and Bornstein, J. C. (2007). Synaptic transmission at functionally identified synapses in the enteric nervous system: roles for both ionotropic and metabotropic receptors. *Curr. Neuropharmacol.* 5, 1–17.

Hansen, K., Yi, F., Perszyk, R., Furukawa, H., Wollmuth, L., Gibb, A., et al. (2018). Structure, function, and allosteric modulation of NMDA receptors. *J. Gen. Physiol.* 150, 1081–1105. doi: 10.1085/jgp.201812032

Kirchgessner, A. L. (2001). Glutamate in the enteric nervous system. *Curr. Opin. Pharmacol.* 1, 591–596.

Koussoulas, K., Swaminathan, M., Fung, C., Bornstein, J. C., and Foong, J. P. P. (2018). Neurally released GABA Acts via GABAC receptors to modulate Ca(2+) transients evoked by trains of synaptic inputs, but not responses evoked by single stimuli, in myenteric neurons of mouse ileum. *Front. Physiol.* 9:97.

Kwon, S. E., and Chapman, E. R. (2011). Synaptophysin regulates the kinetics of synaptic vesicle endocytosis in central neurons. *Neuron* 70, 847–854. doi: 10.1016/j.neuron.2011.04.001

Lehre, K. P., Levy, L. M., Ottersen, O. P., Storm-Mathisen, J., and Danbolt, N. C. (1995). Differential expression of two glial glutamate transporters in the rat brain: quantitative and immunocytochemical observations. *J. Neurosci.* 15, 1835–1853. doi: 10.1523/JNEUROSCI.15-03-01835.1995

Li, Z., Hao, M., Van den Haute, C., Baekelandt, V., Boesmans, W., and Vanden Berghe, P. (2019). Regional complexity in enteric neuron wiring reflects diversity of motility patterns in the mouse large intestine. *eLife* 8:e42914. doi: 10.7554/eLife.42914

Liu, M., and Kirchgessner, A. L. (2000). Agonist- and reflex-evoked internalization of metabotropic glutamate receptor 5 in enteric neurons. *J. Neurosci.* 20, 3200–3205.

Liu, M. T., Rothstein, J. D., Gershon, M. D., and Kirchgessner, A. L. (1997). Glutamatergic enteric neurons. *J. Neurosci.* 17, 4764–4784.

Luzzi, S., Zilletti, L., Franchi Micheli, S., Gori, A. M., and Moroni, F. (1988). Agonists, antagonists and modulators of excitatory amino acid receptors in the guinea-pig myenteric plexus. *Br. J. Pharmacol.* 95, 1271–1277.

Mann, P. T., Southwell, B. R., Young, H. M., and Furness, J. B. (1997). Appositions made by axons of descending interneurons in the guinea-pig small intestine, investigated by confocal microscopy. *J. Chem. Neuroanat.* 12, 151–164.

McRoberts, J. A., Coutinho, S. V., Marvizón, J. C. G., Grady, E. F., Tognetto, M., Sengupta, J. N., et al. (2001). Role of peripheral N-methyl-D-aspartate (n.d.) receptors in visceral nociception in rats. *Gastroenterology* 120, 1737–1748.

McRoberts, J. A., Ennes, H. S., Marvizon, J. C., Fanselow, M. S., Mayer, E. A., and Vissel, B. (2011). Selective knockdown of NMDA receptors in primary afferent neurons decreases pain during phase 2 of the formalin test. *Neuroscience* 172, 474–482. doi: 10.1016/j.neuroscience.2010.10.045

Neal, K. B., and Bornstein, J. C. (2007). Mapping 5-HT inputs to enteric neurons of the guinea-pig small intestine. *Neuroscience* 145, 556–567.

Nissen, R., Hu, B., and Renaud, L. P. (1995). Regulation of spontaneous phasic firing of rat supraoptic vasopressin neurones in vivo by glutamate receptors. *J. Physiol.* 484, 415–424.

Nurgali, K., Stebbing, M., and Furness, J. (2004). Correlation of electrophysiological and morphological characteristics of enteric neurons in the mouse colon. *J. Comp. Neurol.* 468, 112–124.

Ogden, K., and Traynelis, S. (2011). New advances in NMDA receptor pharmacology. *Trends Pharmacol. Sci.* 32, 726–733. doi: 10.1016/j.tips.2011.08.003

Parsons, C. G., Gruner, R., and Rozental, J. (1994). Comparative patch clamp studies on the kinetics and selectivity of glutamate receptor antagonism by 2,3-dihydroxy-6-nitro-7-sulfamoyl-benzo(F)quinoxaline (NBQX) and 1-(4-amino-phenyl)-4-methyl-7,8-methyl-endioxyl-5H-2,3-benzodiaze pine (GYKI 52466). *Neuropharmacology* 33, 589–604.

Raab, M., and Neuhuber, W. L. (2004). Intraganglionic laminar endings and their relationships with neuronal and glial structures of myenteric ganglia in the esophagus of rat and mouse. *Histochem. Cell Biol.* 122, 445–459.

Raab, M., and Neuhuber, W. L. (2005). Number and distribution of intraganglionic laminar endings in the mouse esophagus as demonstrated with two different immunohistochemical markers. *J. Histochem. Cytochem.* 53, 1023–1031.

Ren, J., Hu, H. Z., Liu, S., Xia, Y., and Wood, J. D. (2000). Glutamate receptors in the enteric nervous system: ionotropic or metabotropic? *Neurogastroenterol. Motil.* 12, 257–264.

Rothstein, J. D., Martin, L., Levey, A. I., Dykes-Hoberg, M., Jin, L., Wu, D., et al. (1994). Localization of neuronal and glial glutamate transporters. *Neuron* 13, 713–725. doi: 10.1016/0896-6273(94)90038-8

Sang, Q., Williamson, S., and Young, H. M. (1997). Projections of chemically identified myenteric neurons of the small and large intestine of the mouse. *J. Anat.* 190, 209–222.

Sang, Q., and Young, H. M. (1996). Chemical coding of neurons in the myenteric plexus and external muscle of the small and large intestine of the mouse. *Cell Tissue Res.* 284, 39–53.

Sang, Q., and Young, H. M. (1998). The identification and chemical coding of cholinergic neurons in the small and large intestine of the mouse. *Anatom. Rec.* 251, 185–199.

Seifi, M., and Swinny, J. D. (2016). Immunolocalization of AMPA receptor subunits within the enteric nervous system of the mouse colon and the effect of their activation on spontaneous colonic contractions. *Neurogastroenterol. Motil.* 28, 705–720. doi: 10.1111/nmo.12768

Shannon, H. E., and Sawyer, B. D. (1989). Glutamate receptors of the N-methyl-D-aspartate subtype in the myenteric plexus of the guinea pig ileum. *J. Pharmacol. Exp. Ther.* 251, 518–523.

Sharrad, D., Gai, W.-P., and Brookes, S. J. H. (2013). Selective coexpression of synaptic proteins, α-synuclein, cysteine string protein-α, synaptophysin, synaptotagmin-1, and synaptobrevin-2 in vesicular acetylcholine transporter-immunoreactive axons in the guinea pig ileum. *J. Comp. Neurol.* 521, 2523–2537. doi: 10.1002/cne.23296

Shuttleworth, C. W., and Smith, T. K. (1999). Action potential-dependent calcium transients in myenteric S neurons of the guinea-pig ileum. *Neuroscience* 92, 751–762.

Takamori, S., Holt, M., Stenius, K., Lemke, E. A., Gronborg, M., Riedel, D., et al. (2006). Molecular anatomy of a trafficking organelle. *Cell* 127, 831–846.

Tian, L., Hires, S. A., Mao, T., Huber, D., Chiappe, M. E., Chalasani, S., et al. (2009). Imaging neural activity in worms, flies and mice with improved GCaMP calcium indicators. *Nat. Methods* 6, 875–881. doi: 10.1038/nmeth.1398

Tong, Q., and Kirchgessner, A. (2003). Localization and function of metabotropic glutamate receptor 8 in the enteric nervous system. *AJP-Gastrointest. Liver Physiol.* 285, G992–G1003.

Tong, Q., Ma, J., and Kirchgessner, A. L. (2001). Vesicular glutamate transporter 2 in the brain-gut axis. *NeuroReport* 12, 3929–3934.

Tsai, L. H. (2005). Function of GABAergic and glutamatergic neurons in the stomach. *J. Biomed. Sci.* 12, 255–266.

Vanden Berghe, P., Kenyon, J., and Smith, T. (2002). Mitochondrial Ca2+ uptake regulates the excitability of myenteric neurons. *J. Neurosci.* 22, 6962–6971.

Vanden Berghe, P., Tack, J., Coulie, B., Andrioli, A., Bellon, E., and Janssens, J. (2000). Synaptic transmission induces transient Ca2+ concentration changes in cultured myenteric neurones. *Neurogastroenterol. Motil.* 12, 117–124.

Wang, G. D., Wang, X. Y., Xia, Y., and Wood, J. D. (2014). Dietary glutamate: interactions with the enteric nervous system. *J. Neurogastroenterol. Motil.* 20, 41–53. doi: 10.5056/jnm.2014.20.1.41

Wiley, J. W., Lu, Y. X., and Owyang, C. (1991). Evidence for a glutamatergic neural pathway in the myenteric plexus. *Am. J. Physiol.* 261, G693–G700.

Yamada, Y., and Mikoshiba, K. (2012). Quantitative comparison of novel GCaMP-type genetically encoded Ca(2+) indicators in mammalian neurons. *Front. Cell. Neurosci.* 6:41. doi: 10.3389/fncel.2012.00041

Zariwala, H., Borghuis, B., Hoogland, T., Madisen, L., Tian, L., De Zeeuw, C., et al. (2012). A Cre-dependent GCaMP3 reporter mouse for neuronal imaging in vivo. *J. Neurosci.* 32, 3131–3141. doi: 10.1523/JNEUROSCI.4469-11.2012

Conflict of Interest Statement: The authors declare that the research was conducted in the absence of any commercial or financial relationships that could be construed as a potential conflict of interest.

frontiers in Neuroscience

ORIGINAL RESEARCH
published: 08 May 2019
doi: 10.3389/fnins.2019.00406

Autonomic Nervous System Activity During a Speech Task

Naomi Dodo[1] and Ryusaku Hashimoto[2]*

[1] *Department of Clinical Psychology, School of Psychological Science, Health Sciences University of Hokkaido, Tōbetsu, Japan,* [2] *Department of Communication Disorders, School of Rehabilitation Sciences, Health Sciences, University of Hokkaido, Tōbetsu, Japan*

Previous research has reported that different coping types (active or passive) are required depending on the stress-inducing task. The aim of this study was to examine the autonomic nervous response during speech tasks that require active coping, by using Lorenz plot analysis. Thirty-one university students participated in this study (M = 21.03 years, SD = 2.27). This study included 3 phases: (1) resting phase, (2) silent reading phase, and (3) reading aloud phase. Autonomic nervous system responses were recorded in each phase. We asked participants to evaluate their subjective states (arousal, valence, and mood) after the silent reading phase and the reading aloud phase. We observed that the cardiac sympathetic index (CSI) for the sympathetic nervous response was significantly higher during the reading aloud phase than during the silent reading phase. In contrast, the cardiac vagal index (CVI) for the parasympathetic nervous response was significantly higher during the reading aloud phase than during the resting phase. There were no significant differences between the resting phase and the silent reading phase in both cardiac sympathetic and CVIs. We also observed that the degree of arousal was significantly higher after the reading aloud phase than after the silent reading phase. Our findings indicate that the psychological load during silent reading is ineffective for activating the sympathetic nervous system. The sympathetic nervous response was activated in the reading aloud phase. Also, the parasympathetic nervous response in the reading aloud phase was activated compared with the resting phase. Reading aloud is necessary to adequately activate the parasympathetic nervous system by requiring participants to respire (i.e., expiration) more than during resting and silent reading tasks. The increase in the CVI likely stems from activating the parasympathetic nervous system during expiration. Although the speech task required participants to perform active coping, it was designed to activate both the sympathetic and parasympathetic nervous systems during expiration.

Keywords: autonomic nervous system responses, speech, active coping, cardiac sympathetic index, cardiac vagal index, stress

OPEN ACCESS

Edited by:
Bernhard Schaller, University of Zurich, Switzerland

Reviewed by:
Olga Dergacheva, George Washington University, United States
Alessandro Tonacci, Institute of Clinical Physiology (IFC), Italy

****Correspondence:***
Naomi Dodo
ndodo@hoku-iryo-u.ac.jp

Specialty section:
This article was submitted to Autonomic Neuroscience, a section of the journal Frontiers in Neuroscience

Received: *12 February 2019*
Accepted: *09 April 2019*
Published: *08 May 2019*

Citation:
Dodo N and Hashimoto R (2019) Autonomic Nervous System Activity During a Speech Task. Front. Neurosci. 13:406. doi: 10.3389/fnins.2019.00406

Abbreviations: CSI, cardiac sympathetic index; CVI, cardiac vagal index; HF, high frequency (0.15–0.40 Hz); LF, low frequency (0.04–0.15 Hz); R phase, resting phase; RA phase, reading aloud phase; SR phase, silent reading phase; VLF, very low frequency (0–0.04 Hz).

INTRODUCTION

Both time-domain analysis and frequency-domain analysis are used as methods of analyzing autonomic nervous response. Billeci et al. (2018) and Dodo and Hashimoto (2015) recently used both methods of analysis. Frequency-domain analysis (spectral analysis) of short (≤5 min) interbeat interval (IBIs, or R–R intervals) time series typically yields 3 peaks: 0–0.04 Hz, very low frequency (VLF); 0.04–0.15 Hz, low frequency (LF); and 0.15–0.40 Hz, high frequency (HF). The HF component represents parasympathetic nervous system activity and is strongly influenced by respiratory sinus arrhythmia. VLF and LF are used as indicators of sympathetic nervous system activity. However, as noted by Sawada (1999) and Lahiri et al. (2008), the LF and VLF components are affected by both sympathetic and parasympathetic nervous system activities. Therefore, it is difficult to use spectrum analysis to independently measure sympathetic nervous system activity. Lorenz plot analysis is a type of time-domain analysis. Notably, Lorenz plot analysis allows parasympathetic and sympathetic nervous system activities to be measured separately (Toichi et al., 1997). Lorentz plot analysis uses the cardiac sympathetic index (CSI) as an indicator of sympathetic nervous system activity; it uses the cardiac vagal index (CVI) as an indicator of parasympathetic nervous system activity. Dodo and Hashimoto (2015) found that time-domain analysis (Lorenz plot analysis) is a useful method for examining autonomic nervous system activity during a cold presser test (CPT), whereas frequency-domain analysis (spectral analysis) of heart rate variability (HRV) is not.

Obrist (1981) suggested that different coping types (active or passive) are required depending on the stress-inducing task. With active coping, sympathetic nervous system activity increases and parasympathetic nervous system activity decreases from baseline. During passive coping, sympathetic nervous system activity decreases and parasympathetic nervous system increases from baseline. Allen et al. (2007) reported results of a mental arithmetic task that requires active coping using Lorenz plot analysis. In the mental arithmetic task, the CSI increased and the CVI did not change, compared to baseline. Dodo and Hashimoto (2015, 2017) conducted CPT studies that required passive coping. In CPT, the CSI did not change and the CVI increased, compared to baseline. Indexes activated during tasks that required active or passive coping were consistent with those identified by Obrist; active coping activated CSI, whereas passive coping activated CVI.

Other tasks that require active coping include speech and mental arithmetic tasks. Most studies of HRV during speech tasks use frequency-domain analysis (spectral analysis; for review, see Bernardi et al., 2001). However, respiratory patterns change with utterance during speech. When analyzing HRV using spectral analysis, Sawada (1999) noted that, with changes in respiratory patterns, the values of both HF and LF components increase. Beda et al. (2007) compared tasks with and without utterance. They suggested that the use of spectral analysis to assess autonomic function during tasks with utterance was problematic.

Therefore, our study aimed to use Lorentz plot analysis (i.e., independent analysis of the sympathetic and parasympathetic nervous systems) to examine influence on the autonomic nervous system during tasks with utterance.

MATERIALS AND METHODS

Participants

We selected 40 university students to participate in this study. For participating in the experiment, we paid approximately 9 US dollars (1,000 Japanese yen) to each participant, and we provided all students with written informed consent forms before participation. We asked them to refrain from eating or drinking anything other than water for at least 2 h before arriving at the laboratory. We excluded four volunteers because they were smokers or were taking medications. Because smoking and medications affect the autonomic nervous system, these were not permitted. We also excluded five volunteers due to electrocardiogram (ECG) artifacts. Thus, we included 31 participants (10 male and 21 female; age range: 19–29 years; mean age: 21.03 years; SD age: 2.17).

Procedure

Stimuli

We prepared several stories that cited the famous classical essay "Tsurezuregusa" ("Essays in Idleness") by Yoshida Kenkō (1330–1332). Words and expressions used in classical literature are rarely used in modern literature. Therefore, participants could not easily read the stories, as they were difficult to comprehend. We selected four of the less familiar stories from the essay. We divided each story into 12 texts. We presented the 12 texts on a display at a constant pace. Each text was presented every 13 s. The intertext interval was 2 s.

Experiment

The study was composed of three phases: (1) resting phase (R phase), (2) silent reading phase (SR phase), and (3) reading aloud phase (RA phase). Each phase lasted 3 min. Participants were seated and maintained their posture throughout the experiment. In the R phase, they watched a silent movie. In the SR phase, they were shown text on the display and read it in silence. During the RA phase, we asked them to read the text presented on the screen with clear enunciation. Based on the findings of Piferi et al. (2000), we streamed a monochrome silent movie in the R phase. The content of the movie was summer flower scenery that did not change the psychological state of participants. We gave the following instructions to participants prior to the movie: "Please sit back in the chair. Please watch the movie in a relaxed posture without moving."

To prevent the autonomic nervous system from being affected by the content of the presented story, we randomly showed one of the four stories in each phase. We monitored participants' faces using a video camera placed in front of them and observed their commitment to the task. Furthermore, we recorded any comments they made with their consent.

We asked participants to evaluate their subjective states (degrees of arousal and valence) and mood after the silent reading and reading aloud phases. After the RA phase, all participants evaluated their performance on the reading aloud task (self-evaluation).

Psychological Estimation

Subjective state

We queried participants' degree of arousal and valence according to the dimensions of affect proposed by Russell et al. (1989). We asked participants to assess their subjective states (degrees of arousal and valence), using a seven-point Likert scale. For the degree of arousal, the median score (4) was neutral. The highest score represented low arousal (7), while the lowest score denoted high arousal (1). Regarding valence, the highest score denoted more positive affect (7), the lowest score denoted more negative affect (1), and the scale midpoint (4) represented neutral affect.

Mood

We asked participants to judge their subjective moods (happy, melancholy, feeling pleasure, sad, lonely, or satisfied) using a seven-point Likert scale (Sakaki, 2006). Each descriptor was scored from 1 (not applicable) to 7 (perfectly applicable). We applied reverse scoring for three descriptors (melancholy, sad, and lonely). We recorded the total score of the six descriptors as the mood score.

Self-evaluation

We directed participants to rate their performance (fluency) on the reading aloud task, using a seven-point Likert scale that ranged from poor (1) to excellent (7), while the midpoint (4) denoted average performance.

Autonomic Nervous Response

We recorded heart rate in all three phases. To assess HRV, we administered an ECG with three Ag–AgCl disposable electrodes (PSC-SC43m, Senstec Co., Ltd., Tokyo, Japan) arranged in a similar manner to that of a lead II configuration (i.e., two electrodes on the breastbone and one on the left lower abdomen). We digitized the ECG data using a 12 bit A/D converter at a sampling rate of 1 kHz (MaP222A, NIHONSANTEKU Co., Ltd., Osaka, Japan) and recorded data to a notebook computer (T60, IBM Japan, Ltd., Tokyo, Japan).

We evaluated HRV using Lorenz plot analysis (MaP1060, NIHONSANTEKU Co., Ltd., Osaka, Japan). We observed fluctuations of the IBI and transformed them into an ellipsoid distribution using the Lorenz plot. Following Toichi et al. (1997), a program (MaP1060) calculated the length of the longitudinal (L) and transverse (T) axes within the ellipsoid distribution. The CVI was calculated as a log10 (L × T) transformation, and the CSI was calculated as L/T (Toichi et al., 1997).

Statistical Analyses

The data were analyzed using IBM SPSS, Version 25. The Shapiro–Wilk test was applied to evaluate whether the variables considered were normally distributed. If the data had normal distribution, we performed a paired *t*-test for psychological measures or a one-way repeated-measure analysis of variance (ANOVA) for autonomic nervous response with phases. If the data had a non-normal distribution, we performed the Wilcoxon signed-rank test for psychological measures or the Friedman test for autonomic nervous response among phases. We carried out *post hoc* analyses with Bonferroni correction.

RESULTS

The Shapiro–Wilk test was applied to evaluate whether the variables considered were normally distributed. The data were analyzed using IBM SPSS, Version 25.

Psychological Measures

Subjective State

According to the results of the Shapiro–Wilk test, state had a non-normal distribution in the R, SR, and RA phases. Thus, we used the Wilcoxon signed-rank test for comparison of subjective state. Arousal scores were significantly higher after the SR phase (M = 4.26, SD = 1.26) than after the RA phase (M = 3.03, SD = 1.17) ($p < 0.05$). This result means that the degree of arousal was higher after the RA phase. Valence scores were not significantly different after the SR phase (M = 4.48, SD = 0.89), relative to those of the RA phase (M = 4.23, SD = 0.99; **Table 1**).

Mood

According to the results of the Shapiro–Wilk test, mood had a non-normal distribution in the R, SR, and RA phases. Thus, we used the Wilcoxon signed-rank test for comparison of mood; notably, it did not significantly differ between the SR phase (M = 27.74, SD = 4.88) and the RA phase (**Table 1**).

Self-Evaluation

The mean self-evaluation score was 3.26 (SD = 1.41).

Autonomic Nervous Response

According to the results of the Shapiro–Wilk test, CSI and CVI had normal distributions in the R, SR, and RA phases. Thus, we conducted a one-way repeated-measures ANOVA of CSI and CVI values with phase (resting, silent reading, and reading aloud) as the factor. We observed a significant main effect of the phase on CSI [$F(2, 60) = 3.95$, $p < 0.05$, $\eta_p^2 = 0.12$]. CSI values during the R phase (M = 2.96, SD = 0.91) were significantly lower than in the RA phase (M = 3.33, SD = 0.95; d = 0.40; **Figure 1**). We observed a significant main effect of phase on CVI [$F(2, 60) = 7.40$, $p < 0.05$, $\eta_p^2 = 0.20$]. CVI values in the R phase (M = 4.35, SD = 0.33) and the SR phase (M = 4.29, SD = 0.36) were significantly lower than those in the RA phase (M = 4.44, SD = 0.26; R versus RA: d = 0.30, SR versus RA: d = 0.48; **Figure 2**).

TABLE 1 | Psychological estimation.

	After SR phase		After RA phase	
Subjective State				
Arousal	4.26	(1.26)	3.03	(1.17)
Valence	4.48	(0.89)	4.23	(0.99)
Mood	27.74	(4.88)	28.35	(5.90)

Values for subjective state and mood scores are expressed as mean (SDs).

DISCUSSION

We observed that the degree of arousal was significantly higher after the RA phase than after the SR phase. Moreover, the sympathetic nervous response was significantly higher during the RA phase than during the SR phase, and the parasympathetic nervous response was significantly higher during the RA phase than during the R phase.

Psychological Response

The degree of arousal was greater after the RA phase than after the SR phase. However, there was no difference in valence after the SR phase, nor after the RA phase. In contrast, because there is no significant difference between valence and moods, the emotional influence on the autonomic nervous system caused by the tasks is considered equivalent for the silent reading and reading aloud conditions. The self-evaluation scores were slightly lower than the midpoint ("average") of the seven-category scale. Thus, participants evaluated their reading quality as below average. This signifies that the chosen text was challenging. According to the results of the psychological ratings, reading aloud produces greater psychological loading.

Autonomic Nervous System

There was no significant difference between CSI values, which is an index sympathetic nervous system activity, during the resting and silent reading phases. However, it was found that CSI values significantly increase during the RA phase rather than in the SR phase. The CSI findings during the RA phase are consistent with an increase in the sympathetic nervous system due to tasks requiring active coping, as noted by Obrist (1981). The CSI did not increase more in the SR phase than during the R phase; this finding suggests that psychological loading in the SR phase is ineffective as an active coping task.

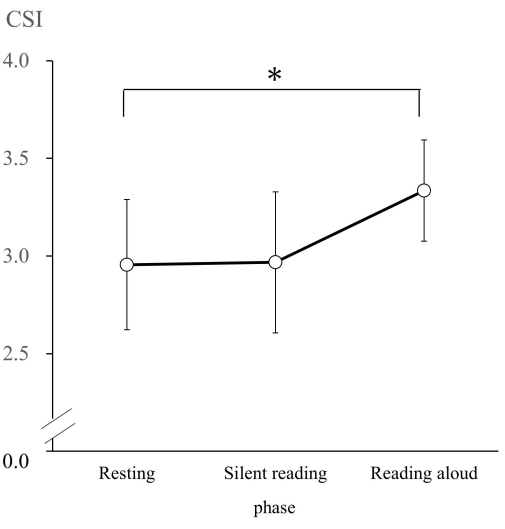

FIGURE 1 | Cardiac sympathetic index (CSI) changes during the resting, silent reading, and reading aloud phases. Values are expressed as means and SDs. *$p < 0.05$.

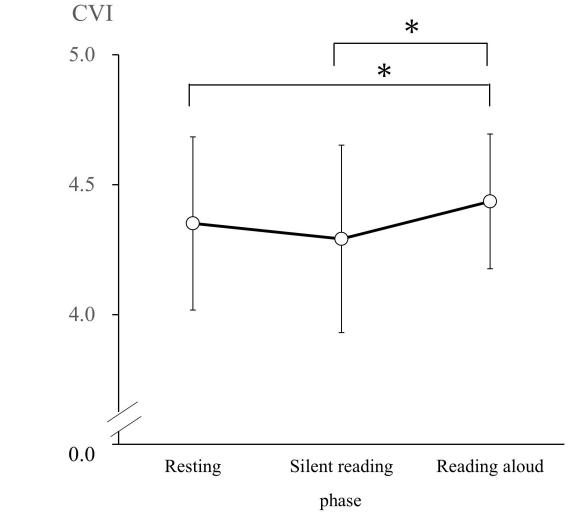

FIGURE 2 | Cardiac vagal index (CVI) changes during the resting, silent reading, and reading aloud phases. Values are expressed as means and SDs. *$p < 0.05$.

Obrist (1981) indicated that the parasympathetic nervous system activity decreases below baseline during tasks that require active coping. However, our data show that the CVI, a measure of the parasympathetic nervous system, rises significantly more during the RA phase than in the R phase. The reading aloud task requires vocalization and causes participants to respire (expirate) more than in the resting and silent reading tasks. Increases in the CVI are considered to result from activating the parasympathetic nervous system by said expiration. Although the speech task required participants to perform active coping, it also activated both the sympathetic and parasympathetic nervous systems during expiration.

Allen et al. (2007) utilized Lorenz plot analysis with a mental arithmetic task that required active coping; they found that the CSI increased during the arithmetic task, which was consistent with our findings in CSI during the RA phase. We speculate that the increase in CSI (i.e., the sympathetic nervous system index) arose from active engagement in the task among participants. Allen et al. (2007) also reported that the CVI did not change during the mental arithmetic task. However, we found that the CVI increased during the RA phase. In the RA phase, respiratory pattern changed with utterance, but not with the mental arithmetic task. The difference in respiratory pattern may have led to the difference in CVI between RA and mental arithmetic tasks. We considered that the increase in CVI (i.e., the parasympathetic nervous system index) during the RA phase resulted from changes in respiratory pattern during speech.

Limitations

The main purpose of this study was to examine influence on the autonomic nervous system during a reading task with utterance. However, we did not confirm if the participants were reading with effort or not reading at all during the SR phase. For example, a memory task is a method for confirming the engagement of the participants in reading. Adding a memory task to the reading tasks would change this to a dual task, which is a higher psychological load. Thus, we would not be able to clearly discern the effect of utterance alone. In the present study, we did not add a memory task during silent reading or reading aloud. We monitored participants' faces using a video camera placed in front of them; thus, we observed their commitment to the task. No participants closed their eyes except to blink during the SR phase.

We did not perform the SR and RA phases in random order. The outcome of the RA phase may have been contaminated by habituation. However, arousal during the RA phase was significantly higher than in the SR phase. This suggests that habituation to the reading task did not affect the outcomes of the RA phase.

CONCLUSION

For speech tasks requiring active coping, we separately analyzed sympathetic and parasympathetic nervous system activity, using Lorenz plot analysis. Our results suggest that each effect on the autonomic nervous system is evoked by two different behaviors: one behavior was the action of reading aloud, which required active coping and led to the activation of the sympathetic nerve system. The other behavior was the action of speech with utterance; respiratory pattern changed during speech, and this change led to the activation of the parasympathetic nervous system. When evaluating the activity of the autonomic nervous system in tasks associated with utterance, Lorenz plot analysis is recommended.

DATA AVAILABILITY

The datasets generated for this study are available on request to the corresponding author.

ETHICS STATEMENT

This study was carried out in accordance with the recommendations of the Psychological Science Ethics Review Committee guidelines, the Ethics Committee of Health Sciences University of Hokkaido. The protocol was approved by the Ethics Committee of Health Sciences University of Hokkaido. All subjects gave written informed consent, in accordance with the Declaration of Helsinki.

AUTHOR CONTRIBUTIONS

ND contributed to the design of the experiment, performance of the experiment, data analysis, and writing of the manuscript. RH contributed to the design of the experiment, performance of the experiment, and writing of the manuscript.

FUNDING

This work was supported by the JSPS (Japan Society for the Promotion of Science) KAKENHI Grant No. 26380939 (ND) and the Research Institute of Personalized Health Sciences (RH).

REFERENCES

Allen, J. J. B., Chambers, A. S., and Towers, D. N. (2007). The many metrics of cardiac chronotropy: a pragmatic primer and a brief comparison of metrics. *Biol. Psychol.* 74, 243–262. doi: 10.1016/j.biopsycho.2006.08.005

Beda, A., Jandre, F. C., Phillips, D. I., Giannella-Neto, A., and Simpson, D. M. (2007). Heart-rate and blood-pressure variability during psychophysiological tasks involving speech: influence of respiration. *Psychophysiology* 44, 767–778. doi: 10.1111/j.1469-8986.2007.00542.x

Bernardi, L., Porta, C., Gabutti, A., Spicuzza, L., and Sleight, P. (2001). Modulatory effects of respiration. *Auton. Neurosci.* 90, 47–56. doi: 10.1016/S1566-0702(01)00267-3

Billeci, L., Tonacci, A., Narzisi, A., Manigrasso, Z., Varanini, M., Fulceri, F., et al. (2018). Heart rate variability during a joint attention task in toddlers with autism spectrum disorders. *Front. Psychol.* 9:4679. doi: 10.3389/fphys.2018.00467

Dodo, N., and Hashimoto, R. (2015). The effect of anxiety sensitivity on the autonomic nervous reaction during the cold pressor test: a pilot study. *Int. J. Psychol. Behav. Sci.* 5, 179–183. doi: 10.5923/j.ijpbs.20150505.01

Dodo, N., and Hashimoto, R. (2017). The effect of anxiety sensitivity on psychological and biological variables during the cold pressor test. *Auton. Neurosci.* 205, 72–76. doi: 10.1016/j.autneu.2017.05.006

Lahiri, M. K., Kannankeril, P. J., and Goldberger, J. J. (2008). Assessment of autonomic function in cardiovascular disease: physiological basis and prognostic implications. *J. Am. Coll. Cardiol.* 51, 1725–1733. doi: 10.1016/j.jacc.2008.01.038

Obrist, P. A. (1981). *Cardiovascular Psychophysiology: a Perspective*. New York: Plenum Press.

Piferi, R. L., Kline, K. A., Younger, J., and Lawler, K. A. (2000). An alternative approach for achieving cardiovascular baseline: viewing an aquatic video. *Int. J. Psychophysiol.* 37, 207–217. doi: 10.1016/s0167-8760(00)00102-1

Russell, J. A., Weiss, A., and Mendelsohn, G. A. (1989). Affect grid: a single-item scale of pleasure and arousal. *J. Pers. Soc. Psychol.* 57, 493–502. doi: 10.1037//0022-3514.57.3.493

Sakaki, M. (2006). Effects of structure of self-knowledge on mood-incongruent effect. *Shinrigaku. Kenkyu.* 77, 217–226. doi: 10.4992/jjpsy.77.217

Sawada, Y. (1999). Heart rate variability: is it available in psychophysiological research? *Jpn. J. Biofeedback Res.* 26, 8–13. doi: 10.20595/jjbf.26.0_8

Toichi, M., Sugiura, T., Murai, T., and Sengoku, A. (1997). A new method of assessing cardiac autonomic function and its comparison with spectral analysis and coefficient of variation of R–R interval. *J. Autonom. Nerv. Syst.* 62, 79–84. doi: 10.1016/s0165-1838(96)00112-9

Conflict of Interest Statement: The authors declare that the research was conducted in the absence of any commercial or financial relationships that could be construed as a potential conflict of interest.

frontiers in Neuroscience

ORIGINAL RESEARCH
published: 14 May 2019
doi: 10.3389/fnins.2019.00458

HbA1C Variability Is Strongly Associated With the Severity of Cardiovascular Autonomic Neuropathy in Patients With Type 2 Diabetes After Longer Diabetes Duration

*Yun-Ru Lai[1,2], Chih-Cheng Huang[2], Wen-Chan Chiu[3], Rue-Tsuan Liu[3], Nai-Wen Tsai[2], Hung-Chen Wang[4], Wei-Che Lin[5], Ben-Chung Cheng[1,3], Yu-Jih Su[3], Chih-Min Su[6], Sheng-Yuan Hsiao[1,6], Pei-Wen Wang[3], Jung-Fu Chen[3] and Cheng-Hsien Lu[1,2,7,8]**

[1] Department of Biological Science, National Sun Yat-sen University, Kaohsiung, Taiwan, [2] Department of Neurology, Kaohsiung Chang Gung Memorial Hospital, Chang Gung University College of Medicine, Kaohsiung, Taiwan, [3] Department of Internal Medicine, Kaohsiung Chang Gung Memorial Hospital, Chang Gung University College of Medicine, Kaohsiung, Taiwan, [4] Department of Neurosurgery, Kaohsiung Chang Gung Memorial Hospital, Chang Gung University College of Medicine, Kaohsiung, Taiwan, [5] Department of Radiology, Kaohsiung Chang Gung Memorial Hospital, Chang Gung University College of Medicine, Kaohsiung, Taiwan, [6] Emergency Medicine, Kaohsiung Chang Gung Memorial Hospital, Chang Gung University College of Medicine, Kaohsiung, Taiwan, [7] Center for Shockwave Medicine and Tissue Engineering, Kaohsiung Chang Gung Memorial Hospital, Chang Gung University College of Medicine, Kaohsiung, Taiwan, [8] Department of Neurology, Xiamen Chang Gung Memorial Hospital, Xiamen, China

OPEN ACCESS

Edited by:
Maurizio Acampa, Azienda Ospedaliera Universitaria Senese, Italy

Reviewed by:
Antonio Roberto Zamunér, Catholic University of Maule, Chile
Giuseppe Raffaele Micieli, Fondazione Istituto Neurologico Nazionale Casimiro Mondino (IRCCS), Italy

***Correspondence:**
Cheng-Hsien Lu
chlu99@ms44.url.com.tw;
chlu99@adm.cgmh.org.tw

Specialty section:
This article was submitted to Autonomic Neuroscience, a section of the journal Frontiers in Neuroscience

Received: *14 February 2019*
Accepted: *24 April 2019*
Published: *14 May 2019*

Citation:
Lai Y-R, Huang C-C, Chiu W-C, Liu R-T, Tsai N-W, Wang H-C, Lin W-C, Cheng B-C, Su Y-J, Su C-M, Hsiao S-Y, Wang P-W, Chen J-F and Lu C-H (2019) HbA1C Variability Is Strongly Associated With the Severity of Cardiovascular Autonomic Neuropathy in Patients With Type 2 Diabetes After Longer Diabetes Duration. Front. Neurosci. 13:458. doi: 10.3389/fnins.2019.00458

Background: Variability in the glycated hemoglobin (HbA1c) level is associated with a higher risk of microvascular complications in patients with type 2 diabetes. We tested the hypothesis that HbA1c variability is not only strongly associated with the presence but also the degree of severity of cardiovascular autonomic neuropathy (CAN) in patients with long diabetes durations (more than 10 years).

Methods: For each patient, the intrapersonal mean, standard deviation (SD), and coefficient of variation (CV) for HbA1c were calculated using all measurements obtained 3 years before the study. We constructed the composite autonomic scoring scale (CASS) as a measure of the severity of cardiovascular autonomic functions. Stepwise logistic regression and linear regression analyses were performed to evaluate the presence of CAN and the influence of independent variables on the mean CASS, respectively.

Results: Those with CAN had a higher mean age, a higher low-density lipoprotein cholesterol (LDL-C), HbA1c-SD, HbA1c-CV, mean HbA1c, and index HbA1c, higher prevalence of retinopathy as the underlying disease, and lower high-density lipoprotein (HDL) levels. Stepwise logistic regression showed that HbA1c-SD and retinopathy were risk factors that were independently associated with the presence of CAN. Mean HbA1c, HbA1c-CV, HbA1c-SD, and index HbA1c were positively correlated with mean CASS,

and a multiple linear regression analysis revealed that HbA1c-SD was independently associated with the mean CASS.

Conclusion: HbA1c variability is strongly associated with not only the presence but also the degree of severity of CAN. A longitudinal study is required to confirm whether controlling blood glucose level is effective in reducing CAN progression.

Keywords: cardiovascular autonomic neuropathy, composite autonomic scoring scale, HbA1c variability, long diabetes duration, type 2 diabetes

BACKGROUND

Diabetic cardiovascular autonomic neuropathy (CAN) is common but is one of the most overlooked complications of diabetes (Ewing et al., 1980). Autonomic nervous systems, including parasympathetic and sympathetic nervous systems, innervate various organ systems and modulate their function. CAN indicates a length-dependent pattern of the disease (Papanas and Ziegler, 2015). The vagus nerve, responsible for approximately 75% of the parasympathetic activity in humans, can be damaged in the early phase of CAN (Ewing et al., 1985), resulting in decreased parasympathetic activity and contributing to sympathetic predominance. As the disease progresses, sympathetic denervation occurs in the late stage of CAN. Therefore, it has a wide spectrum of clinical presentation.

There is a wide variation in the prevalence of CAN, depending on the definition and criteria used for diagnosis. Estimating the severity of CAN is also a formidable challenge for clinicians. Although there are no uniform criteria for diagnosing or staging CAN (Tesfaye et al., 2010; Rolim et al., 2013), the recent Toronto Consensus recommends the use of four cardiovascular reflex tests [deep breathing, Valsalva maneuver (VM), orthostatic (30:15) and orthostatic hypotension] and frequency-domain tests as the most sensitive and specific method of assessing the presence of CAN in patients with diabetes (Spallone et al., 2011). Further, Phillip Low constructed the composite autonomic scoring scales (CASS) for laboratory quantification of generalized autonomic failure (Low, 1993) and the CASS have been proven useful for estimating the severity of CAN (Huang et al., 2016).

There are several well-known risk factors associated with CAN development, including age, diabetes duration, glycemic control, hypertension, and dyslipidemia, body mass index (BMI), and development of other microvascular complications (e.g., retinopathy, proteinuria) (Dafaalla et al., 2016). Glycemic variability (GV) is a term used to describe the impairment of glycemic control. Multiple measures of GV have been suggested as potential predictors for CAN, and long-term GV assessment using HbA1c variability is significantly associated with the presence of CAN (Fleischer, 2012; Jun et al., 2015; Yang et al., 2018).

Cardiovascular autonomic neuropathy has a strong influence on various cardiovascular diseases and leads to severe morbidity and mortality in patients with diabetes (Vinik et al., 2003; Vinik and Ziegler, 2007). To date, there is paucity of information on the estimation of the overall severity of CAN using the CASS and its relationship between chronic glycemic impairment and different cardio-metabolic parameters in patients with long-duration type 2 diabetes. Scientists have been exploring the role of chronic GV in the subsequent severity of CAN and developing therapeutic strategies that may be beneficial in patients with diabetes. Therefore, potential risk factors need to be delineated to determine patients who are most appropriate for aggressive treatment. In this study, we tested the hypothesis that chronic GV is not only a risk factor for the presence of CAN but is also associated with the severity of CAN in patients with type 2 diabetes. The successful translation of these approaches offers the promise of reducing microvascular complications and improving the quality of life of patients with type 2 diabetes.

Abbreviations: BMI, body mass index; BRS, Baroreflex sensitivity; CAN, cardiac autonomic neuropathy; DBP, diastolic blood pressure; HbA1c, glycohemoglobin; HDL-C, high-density lipoprotein cholesterol; HR_DB, heart rate response to deep breathing; LDL-C, low-density lipoprotein cholesterol; SBP, systolic blood pressure; SD, standard deviation; VR, Valsalva ratio.

PATIENTS AND METHODS

Patients

A total of 238 patients (≥20 years old) with type 2 diabetes who visited the outpatient diabetic clinic at Kaohsiung Chang Gung Memorial Hospital in Taiwan were identified from our previous cross-sectional prospective study (IRB 96-1361B, 99-2276C) (Huang et al., 2016). The exclusion criteria included (1) number of HbA1c measurements less than four, (2) diabetes duration less than 10 years; (3) moderate-to-severe heart failure [New York Heart Association (NYHA) class III and IV]; and (4) any type of arrhythmia that prevents the analysis of heart rate variability, or pacemaker implantation due to any cause. Thus, only 110 participants were enrolled in the study (**Figure 1**). The study was approved by the Ethics Committee of Chang Gung Memorial Hospital Institutional Review Board (201701243B0 and 201800388B0C501).

Baseline Clinical and Laboratory Measurements

All patients underwent complete neurological and physical examinations upon enrollment and at their subsequent follow-ups at the outpatient clinic. A detailed medical history regarding prior use of medications was obtained from the patients and their families through standardized questions. Demographic data, including age, sex, duration of diabetes (years), BMI, systolic, and diastolic blood pressure

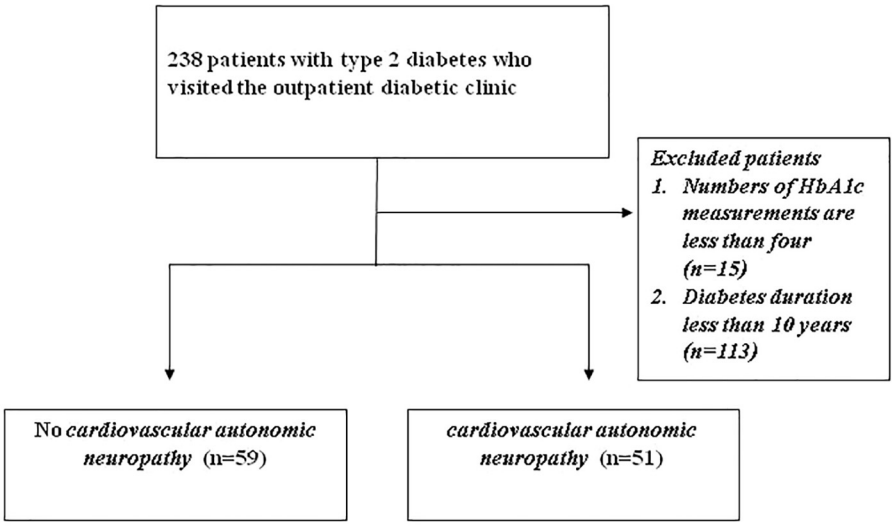

FIGURE 1 | Enrollment of patients.

(BP) during autonomic function testing, underlying diseases [hypertension, coronary artery disease (CAD), ischemic stroke, and diabetic retinopathy (DR)], and laboratory parameters were obtained at baseline.

Assessment of Glycemic Variability

For each patient, the intrapersonal mean, SD, and coefficient of variation [CV = HbA1c-SD/(0.1 × mean HbA1c)] of HbA1c was calculated using all measurements obtained 3 years before the study. The HbA1c-SD was considered a measure of GV and the CV, a normalized measure of GV. Because the number of individual visits could influence the HbA1c-SD (with fewer visits likely to artificially inflate SD), we defined the adjusted SD of HbA1c as the SD of HbA1c divided by $[n/(n-1)]^{0.5}$ (where n is the number of HbA1c measurements), to minimize any effect of different values of HbA1c on the ones calculated (Kilpatrick et al., 2008). Our study was repeated using adjusted HbA1c-SD instead of HbA1c-SD.

Assessment and Scoring of Cardiovascular Autonomic Functions

All subjects underwent a standardized evaluation of the cardiovascular autonomic function, as described by Low (2003). The test battery consisted of the heart rate response to deep breathing (HR_DB), Valsalva ratio (VR), and baroreflex sensitivity (BRS). The heart rate was derived using a continuously recorded standard three-lead electrocardiography (Model 3000; Ivy Biomedical, Branford, CT, United States). Arterial BP was continuously measured at the finger, using beat-to-beat photoplethysmographic recordings (Finameter Pro; Ohmeda, Englewood, OH, United States). The tests were done between 9:00 am to noon for all patients. No coffee, food, alcohol, or nicotine was permitted 4 h before the tests. Patients on medications known to cause orthostatic hypotension or otherwise affecting autonomic testing were asked to stop taking the drug for five half-lives, provided that it was not harmful to the patient's well-being. For patients on β-blockers for BP control, the drug was omitted on the day of the study and resumed after the test. The detailed computing of HR_DB and VR were as described by Low (2003). To quantify BRS, a linear regression analysis was performed between systolic BP and RR interval (RRI) changes during the early phase II of VM. In this phase, there was a progressive decrease in systolic BP due to reduced preload (venous return) and stroke volume with associated tachycardia (gradual shortening of RRI).

To improve the assessment of laboratory grading of CAN, we constructed a CASS for laboratory quantification of CAN according to our previous diabetic study (Huang et al., 2016). The severity of CAN was assessed using the cardiovagal and adrenergic sub-scores of the CASS. In this study, the scale was modified in the adrenergic sub-score since the 5-min head-up tilt test (HUTT) was not done in the current study. Thus, the CASS version used here allotted 3 points instead of 4 for the adrenergic domain. Further, patients with a CASS score $\geq$2 were defined as having CAN (Huang et al., 2016).

Statistical Analysis

Data are expressed as means ± standard derivations (SDs) or medians (interquartile ranges). Categorical variables were compared using Chi-square or Fisher's exact tests. Continuous variables that were not normally distributed in the Kolmogorov–Smirnov test were logarithmically transformed to improve normality and compared. Four separate statistical analyses were performed. Firstly, patients were stratified into two groups according to the presence or absence of CAN. One-way analysis of covariance (ANCOVA) was used to compare parameters of cardiovascular autonomic study with age as the added covariate. Secondly, the risk factors for the presence of CAN including sex and baseline characteristics, underlying diseases, and parameters of laboratory testing were analyzed using stepwise logistic

regression. Thirdly, correlation analysis was used to evaluate the relationship between the CASS and variables that included age, diabetes duration, BMI, waist circumference, systolic and diastolic BP, and peripheral blood studies for vascular risks. Fourthly, stepwise models of multiple linear regression analysis were used to evaluate the influence of independent variables on the mean CASS. All statistical analyses were conducted using the SAS software package, version 9.1 (2002, SAS Statistical Institute, Cary, North Carolina).

RESULTS

General Characteristics of the Patients With Diabetes

The 110 patients with diabetes included 45 women and 65 men. Patient characteristics, baseline underlying diseases and laboratory data at assessment are presented in **Table 1**, stratified into two groups according to the presence or absence of CAN. Those with CAN had higher mean age (P = 0.002), higher low-density lipoprotein cholesterol (LDL-C), HbA1c-SD, HbA1c-CV, mean HbA1c and index HbA1c (P = 0.04, P = 0.003, P = 0.009, P = 0.009, and P = 0.01, respectively), higher prevalence of retinopathy as the underlying disease (P < 0.0001) and lower high-density lipoprotein (HDL) levels (P = 0.02). Significant variables used in the stepwise logistic regression model included mean age, baseline LDL-C, HbA1c-SD, CV HbA1c, mean HbA1c, index HbA1c, and HDL level and the presence of retinopathy as the underlying disease. After analysis of all the aforementioned variables, only HbA1c-SD (P = 0.007, OR = 10.1, 95% CI = 1.90–54.4) and presence of retinopathy (P < 0.0001, OR = 731.1, 95% CI = 67.9–7869.3) were independently associated with the presence of CAN.

TABLE 1 | Baseline characteristics of patients with Type 2 diabetes.

	No CAN (n = 59)	CAN (n = 51)	Crude P-value	Adjusted OR (95% CI)	Adjusted P-value
Characteristics					
Age (year)	62.2 ± 8.8	67.2 ± 7.6	0.002**		
Sex (male/female)	34/25	31/20	0.74		
Diabetes duration (year)	17.4 ± 5.8	17.4 ± 6.3	1.0		
Body mass index	25.6 ± 3.3	26.2 ± 3.7	0.35		
SBP (mmHg)	140.5 ± 19.7	144.4 ± 19.1	0.29		
DBP (mmHg)	74.5 ± 11.4	75.5 ± 11.2	0.65		
Baseline underlying disease					
Retinopathy, n (%)	2 (3%)	43 (84%)	<0.0001***	731.1 (67.9–7869.3)	<0.0001***
Proteinuria, n (%)	38 (64%)	37 (73%)	0.21		
Coronary heart disease (%)	10 (17%)	11 (22%)	0.54		
Ischemic stroke (%)	13 (22%)	12 (24%)	0.85		
Laboratory test findings					
Total cholesterol (mmol/L)	152.9 ± 27.8	157.1 ± 27.4	0.43		
Triglyceride (mmol/L)	133.1 ± 75.4	142.0 ± 73.9	0.54		
HDL-C (mmol/L)	55.7 ± 14.9	49.2 ± 13.0	0.02*		
LDL-C (mmol L)	70.9 ± 24.8	80.7 ± 25.4	0.04*		
Index HbA1c (%) 6.9 ± 0.9 7.4 ± 0.9 7.3 ± 1.1 7.4 ± 1.3 0.171	7.0 ± 1.0	7.5 ± 1.0	0.01*		
Mean HbA1c (%)	7.4 ± 1.0	7.9 ± 1.1	0.009**		
HbA1c-SD (%)	0.6 ± 0.4	0.9 ± 0.5	0.003**	10.1 (1.90–54.4)	0.007**
HbA1c-CV	9.0 ± 4.8	12.1 ± 7.4	0.009**		
Type of diabetes treatment					
OHA only	37	28	0.71		
Insulin only	14	26			
No treatment	2	4			
Other concomitant medications					
ACE inhibitor or ARB	40	41	0.57		
Beta-blocker	16	16	0.76		
Calcium channel blocker	21	18	0.31		
Diuretics	27	23	0.23		
Lipid-lowering medications	40	40	0.45		

*Data are presented as means ± standard deviations or n (%). *P < 0.05; **P < 0.01; ***P < 0.001. CAN, cardiac autonomic neuropathy; n, number of cases; SBP, systolic blood pressure; DBP, diastolic blood pressure; HDL-C, high-density lipoprotein cholesterol; LDL-C, low-density lipoprotein cholesterol; HbA1c, glycohemoglobin; CV, coefficient of variation; SD: standard deviations; OHA, oral hypoglycemic agent; ACE, angiotensin-converting enzyme; ARB, angiotensin II receptor blocker.*

Parameters of Cardiovascular Autonomic Study Between Patients With or Without CAN

Cardiovascular autonomic study in patients with type 2 diabetes stratified into two groups according to the presence or absence of CAN is presented in **Table 2**. The parameters of cardiovascular autonomic study were compared by ANCOVA after controlling for age. Those with CAN had higher CASS ($P < 0.0001$) and lower HR_DB ($P < 0.0001$), VR $P < 0.0001$, and BRS $P < 0.0001$.

Effect of Glycemic Variability and Other Vascular Risk Factors on Composite Autonomic Scoring

Correlation analysis parameters used to test the influence of GV and other vascular risk factors on CASS are listed in **Table 3**. The significant statistical results (correlation coefficient, *P*-value) were as follows: mean HbA1c (%) ($r = 0.220$, $P = 0.028$), HbA1c-CV ($r = 0.197$, $P = 0.05$), HbA1c-SD ($r = 0.232$, $P = 0.02$), index HbA1c (%) ($r = 0.207$, $P = 0.039$). All the correlation coefficients in mean HbA1c (%), HbA1c-CV, HbA1c-SD, and index HbA1c (%) indicate a weak positive linear relationship ($r < 0.4$).

Clinical Factors Are Significantly Associated With Composite Autonomic Scoring

Effects of the variables on the CASS in patients with type 2 diabetes according to correlation analysis are listed in **Table 4**. Statistical analysis was subsequently carried out to decipher the relationship between the augmented CASS in patients with diabetes and GV. Based on correlation analysis, our results revealed that mean HbA1c, HbA1c-SD, and index HbA1c were significantly correlated with CASS (**Table 3**). We further employed multiple linear regression analysis on the aforementioned variables to identify the crucial determinant that underlies the augmented CASS in patients with diabetes. Results from the model analysis (**Table 4**) revealed that only HbA1c-SD were significantly associated with the CASS.

TABLE 2 | Baseline cardiovascular autonomic study with Type 2 diabetes.

	No CAN ($n = 59$)	CAN ($n = 51$)	$F^{\dagger}$	P-value†
Composite Autonomic Scoring Scale	0.7 ± 0.4	2.9 ± 1.3	119.3	<0.0001***
HR_DB (beats/min)	8.3 ± 4.7	4.3 ± 2.6	46.2	<0.0001***
Valsalva ratio	1.3 ± 0.1	1.2 ± 0.1	22.5	<0.0001***
Baroreflex sensitivity	1.6 ± 0.9	0.9 ± 0.8	13.9	<0.0001***

*Data are presented as means ± standard deviations or n (%). *P < 0.05; **P < 0.01; ***P < 0.001. Parameters of cardiovascular autonomic study were compared by ANCOVA after controlling for age. F† and P† represent the comparison between CAN vs.no CAN group. n, number of cases; HR_DB, heart rate response to deep breathing; CAN, cardiac autonomic neuropathy.*

TABLE 3 | Correlation analysis of composite autonomic scoring scale in patients with type 2 diabetes.

Variables	Composite Autonomic Scoring Scale ($n = 110$)	
	r	P-value
Age (year)	−0.123	0.089
Diabetes duration (year)	0.036	0.725
Body mass index	0.042	0.675
SBP (mmHg)	0.121	0.230
DBP (mmHg)	0.021	0.839
Total cholesterol (mmol/L)	0.149	0.140
Triglyceride (mmol/L)	0.024	0.816
HDL-C (mmol/L)	−0.101	0.315
LDL-C (mmol/L)	0.194	0.053
Index HbA1c (%)	0.207	0.039*
Mean HbA1c (%)	0.220	0.028*
HbA1c-CV	0.197	0.05*
HbA1c-SD	0.232	0.02*

**P < 0.05. r, correlation coefficient. n, number of cases; SBP, systolic blood pressure; DBP, diastolic blood pressure; HDL-C, high-density lipoprotein cholesterol; LDL-C, low-density lipoprotein cholesterol; HbA1c, glycohemoglobin; CV, coefficient of variation.*

TABLE 4 | Effects of the variables on composite autonomic scoring scale in patients with type 2 diabetes according to correlation analysis.

	Regression coefficient	Standard error	P-value
Constant	1.148	0.299	<0.0001
HbA1c-SD	0.784	0.327	0.018*
Mean HbA1c	0.07	0.222	0.753
Index HbA1c	0.209	0.222	0.348

*Regression coefficient for each individual variable. *P < 0.05. HbA1c, glycohemoglobin; CV, coefficient of variation; SD, standard deviations.*

DISCUSSION

Major Findings of Our Study

To our knowledge, this is the first study to confirm the hypothesis that HbA1c variability is not only strongly associated with the presence but also the degree of severity of CAN, in patients with long-duration type 2 diabetes. We examined the role of HbA1c variability on the presence and severity of CAN to obtain three major findings.

First, those with CAN had higher mean age, higher LDL-C, HbA1c-SD, HbA1c-CV, mean HbA1c, and index HbA1c, higher prevalence of retinopathy as the underlying disease, and lower HDL levels. Second, HbA1c-SD and the presence of retinopathy were independently associated with the presence of CAN. Finally, although mean HbA1c (%), HbA1c-CV, HbA1c-SD, and index HbA1c were positively correlated with the CASS score in correlation analysis, the correlation coefficient indicates a weak positive linear relationship ($r < 0.4$). Multiple linear regression analysis revealed that HbA1c-SD was independently associated with the mean CASS.

The Role of Persistent Poor Glucose Control and Glycemic Variability in Diabetic Complications

Aggressive control of blood glucose is pivotal for patients with type 2 diabetes, and can prevent microvascular and macrovascular complications (Brownlee and Hirsch, 2006; Siegelaar et al., 2010). Short-term GV indicated that patients with similar mean glucose or HbA1c values can show markedly different daily glucose profiles (Brownlee and Hirsch, 2006; Siegelaar et al., 2010). Either fluctuating or persisting high glucose levels can induce oxidative stress, contribute to endothelial dysfunction, and finally result in diabetic complications (Brownlee and Hirsch, 2006; Siegelaar et al., 2010). Recently, clinical evidence also demonstrated that long term GV might be related to microvascular complications in type 2 diabetes (Fleischer, 2012; Jun et al., 2015; Wei et al., 2016; Yang et al., 2018).

Glycemic Variability and Other Potential Risk Factors Associated With the Development of CAN

The pathophysiological mechanism of CAN development is multifactorial, and several studies reported the important role of cardiovascular risk factors, such as systolic BP, triglyceride levels, BMI, and smoking, in the development of CAN (Rolim et al., 2008; Dafaalla et al., 2016). Even more important, however, were the results of one clinical study that concluded that intensified multifactorial intervention (hyperglycemia, hypertension, dyslipidemia, and microalbuminuria) in patients with type 2 diabetes reduced the risk of CAN progression by 68% (Gæde et al., 1999). Another study also enhanced the role of intensive control in preventing and slowing the progression of CAN in patients with type 1 diabetes (The Diabetes Control and Complications Trial Research Group, 1998).

Glycemic Variability and the Severity of CAN

The risk factors for CAN that were identified may provide important clues to etiologies, or merely reflect chance associations. Only when the same risk factor is found to be associated with the severity of CAN consistently, can it be concluded that there is a plausible mechanistic link between the risk factor and the disease progression or prevention. To the best of our knowledge, only limited studies have investigated the impact of GV on the severity of CAN in type 2 diabetes (Jun et al., 2015; Yang et al., 2018). One study of 110 patients with type 2 diabetes who underwent both short term and long term GV (HbA1c variability) demonstrated that only long term GV (HbA1c variability) was significantly associated with the presence of CAN by logistic regression analysis, and higher long term GV (HbA1c variability) had an increased risk of advanced CAN (Jun et al., 2015). In this study, the authors only investigate the role of both short term and long term GV without other vascular risk factors in the severity of CAN which was graded using ordinal logistic regression analysis. Another study enrolled 681 subjects (294 normal, 318 early, and 69 severe CAN) and the severity of CAN was categorized as normal, early, or severe according to the cardiac autonomic reflex tests (CARTs) score. The study was repeated using HbA1c-CV or adj-HbA1c-SD instead of HbA1c-SD as a measure of HbA1c variability and performed to test the association between the CAN and HbA1c variability indices by multivariable logistic regression analysis (Yang et al., 2018). In comparison to the patients described in the previous two studies, our patients were older and had longer diabetes durations and HbA1c variability was not only strongly associated with the presence but also the degree of severity of CAN. The discrepancy between these studies and our study may be attributed to different enrollment criteria (e.g., age and diabetes duration of patients, the time period before the study for measurement of HbA1c variability was obtained, the minimum number of HbA1c measurements), diagnostic criteria for CAN, and statistical methods used for assessing the severity of CAN (ordinal logistic regression, multiple logistic regression and linear regression).

TABLE 5 | Comparison of composite autonomic scoring Scale (CASS) and Modified CASS (sub-scores in cardiovagal and adrenergic domains).

CASS		**Modified CASS**	
Cardio-vagal		**Cardio-vagal**	
0	Normal	0	The same with CASS
1	HR_DB mildly reduced but >50% of minimum	1	
2	HR_DB reduced to <50% of minimum or HR_DB + VR reduced	2	
3	Both HR_DB and VR reduced to <50% of minimum	3	
Adrenergic		**Adrenergic**	
0	Normal	0	Normal
1	Early phase II reduction > 20 but <40 mmHg MBP (30–40 if >50 years). Late phase II does not return to baseline Pulse pressure reduction to ≤50% of baseline.	1	Early phase II reduction > 20 but <40 mmHg MBP (30–40 if >50 years) Late phase II does not return to baseline. Pulse pressure reduction to ≤50% of baseline.
2	Early phase II reduction >40 mmHg MBP.	2	Early phase II reduction >40 mmHg MBP.
3	Early phase II reduction >40 mmHg + absent late phase II and phase IV.	3	Early phase II reduction >40 mmHg + absent late phase II and phase IV.
4	Criteria for 3 + orthostatic hypotension (SBP decrease ≥30 mmHg or MBP ≥ 20 mmHg).		

Modified CASS allots 3 points instead of 4 for the adrenergic domain. HR_DB, heart rate response to deep breathing; VR, Valsalva ratio; SBP, systolic blood pressure; MBP, mean blood pressure.

Study Limitations

This study has several limitations. Firstly, although the measurement of HbA1c variability was obtained 3 years before the study and there was a relationship between HbA1c variability and the degree of severity of CAN in patients with diabetes in this observational study, our study does not allow inferring causality or whether controlling blood glucose can improve CAN, even though it can be a starting point for future studies. A prospective longitudinal study is necessary to evaluate the efficiency of CASS as a scale of severity in clinical follow-up. Secondly, we excluded patients whose disease duration for diabetes was less than 10 years and the number of HbA1c measurements were less than four. Thus, there is uncertainty in assessing the role of chronic glycemic impairment and other cardio-metabolic parameters in the patients with type 2 diabetes who were omitted. Thirdly, the severity of CAN was assessed using the modified CASS rather than the original version because the 5-min HUTT was not done in this study. We aimed to set up a highly effective autonomic screening service at the out-patient clinic. The tests of deep breathing and VM can be conducted only by one technician within 10–15 min. One may argue about the validity of the modified CASS. **Table 5** lists the comparison between the modified and the original versions of CASS. The only difference is in the three points versus four points in the adrenergic sub-score. If the 5-min HUTT is done, the adrenergic sub-score may reach to four points in a patient with extremely severe autonomic failure. In other words, the limitation of modified CASS is mainly in its resolution in differentiating severe from extremely severe patients. However, it is uncommon for patients with diabetes to have severe autonomic failure. It was reported as occurring in about 1–5% of the diabetic population (Low, 1996). In the current study, only four patients had severe adrenergic failure (three points in adrenergic sub-score). The four patients are those who may have different scores between the two versions of CASS. In other words, it is certain that the other 106 patients (96%) would have the same scores even if the original version of CASS was used. Therefore, we suppose that the impact of alteration in CASS is trivial to this study. The final limitation is that only cardiovagal and adrenergic domains were assessed, and the sympathetic sudomotor function was not included in this study. Thus, all the variability in severity found in CAN may not have been accounted for and this may produce statistical bias. Other quantitative approaches to assess the sudomotor function, such as quantitative sudomotor axon reflex test or sudoscan, should be taken into account for future studies.

CONCLUSION

Based on our results, HbA1c variability is not only strongly associated with the presence but also the degree of severity of CAN. As HbA1c variability is considered a prognostic factor, a longitudinal study is required in order to state that controlling blood glucose is effective in reduce CAN progression.

DATA AVAILABILITY

The data from this study can be acquired from the corresponding author upon reasonable request.

ETHICS STATEMENT

This study conformed to the guidelines of the Declaration of Helsinki, and the study has been approved by the Institutional Review Board of Chang Gung Memorial Hospital (201701243B0 and 201800388B0C501).

AUTHOR CONTRIBUTIONS

Y-RL participated in the design of the study and drafted the manuscript. W-CC, C-CH, R-TL, N-WT, H-CW, W-CL, B-CC, Y-JS, C-MS, S-YH, P-WW, and J-FC participated in the sequence alignment and clinical evaluation of patients. C-CH performed the statistical analysis. C-HL conceived the idea for the study, and participated in its design and coordination, and helped to draft the manuscript. All authors read and approved the final manuscript.

FUNDING

This work was supported by grants from Chang Gung Memorial Hospital (Chang Gung Medical Research Project CMRPG8H0501).

ACKNOWLEDGMENTS

The authors thank all the subjects who participated in this study.

REFERENCES

Brownlee, M., and Hirsch, I. B. (2006). Glycemic variability: a hemoglobin A1c–independent risk factor for diabetic complications. *JAMA* 295, 1707–1708. doi: 10.1001/jama.295.14.1707

Dafaalla, M. D., Nimir, M. N., Mohammed, M. I., Ali, O. A., and Hussein, A. (2016). Risk factors of diabetic cardiac autonomic neuropathy in patients with type 1 diabetes mellitus: a meta-analysis. *Open Heart* 3:e000336. doi: 10.1136/openhrt-2015-000336

Ewing, D., Campbell, I., and Clarke, B. (1980). Assessment of cardiovascular effects in diabetic autonomic neuropathy and prognostic implications. *Ann. Intern. Med.* 92, 308–311. doi: 10.7326/0003-4819-92-2-308

Ewing, D. J., Martyn, C. N., Young, R. J., and Clarke, B. F. (1985). The value of cardiovascular autonomic function tests: 10 years experience in diabetes. *Diabetes Care* 8, 491–498. doi: 10.2337/diacare.8.5.491

Fleischer, J. (2012). Diabetic autonomic imbalance and glycemic variability. *J. Diabetes Sci. Technol.* 6, 1207–1215. doi: 10.1177/193229681200600526

Gæde, P., Vedel, P., Parving, H.-H., and Pedersen, O. (1999). Intensified multifactorial intervention in patients with type 2 diabetes mellitus and microalbuminuria: the Steno type 2 randomised study. *Lancet* 353, 617–622. doi: 10.1016/S0140-6736(98)07368-1

Huang, C.-C., Lee, J.-J., Lin, T.-K., Tsai, N.-W., Huang, C.-R., Chen, S.-F., et al. (2016). Diabetic retinopathy is strongly predictive of cardiovascular autonomic

neuropathy in type 2 diabetes. *J. Diabetes Res.* 2016:6090749. doi: 10.1155/2016/6090749

Jun, J. E., Jin, S.-M., Baek, J., Oh, S., Hur, K. Y., Lee, M.-S., et al. (2015). The association between glycemic variability and diabetic cardiovascular autonomic neuropathy in patients with type 2 diabetes. *Cardiovasc. Diabetol.* 14:70. doi: 10.1186/s12933-015-0233-0

Kilpatrick, E. S., Rigby, A. S., and Atkin, S. L. (2008). HbA1c variability and the risk of microvascular complications in type 1 diabetes: data from the DCCT. *Diabetes Care* 31, 2198–2202. doi: 10.2337/dc08-0864

Low, P. A. (1993). Composite autonomic scoring scale for laboratory quantification of generalized autonomic failure. Mayo. *Clin. Proc.* 68, 748–752. doi: 10.1016/S0025-6196(12)60631-4

Low, P. A. (1996). Diabetic autonomic neuropathy. *Semin. Neurol.* 16, 143–151. doi: 10.1055/s-2008-1040970

Low, P. A. (2003). Testing the autonomic nervous system. *Semin. Neurol.* 23, 407–421. doi: 10.1055/s-2004-817725

Papanas, N., and Ziegler, D. (2015). Risk factors and comorbidities in diabetic neuropathy: an update 2015. *Rev. Diabet. Stud.* 12, 48–62. doi: 10.1900/RDS.2015.12.48

Rolim, L. C., Sá, J. R., Chacra, A. R., and Dib, S. A. (2008). Diabetic cardiovascular autonomic neuropathy: risk factors, clinical impact and early diagnosis. *Arq. Bras. Cardiol.* 90, e24–e31. doi: 10.1590/S0066-782X2008000400014

Rolim, L. C., Souza, J. S. T., and Dib, S. (2013). Tests for early diagnosis of cardiovascular autonomic neuropathy: critical analysis and relevance. *Front. Endocrinol.* 4:173. doi: 10.3389/fendo.2013.00173

Siegelaar, S. E., Holleman, F., Hoekstra, J. B., and Devries, J. H. (2010). Glucose variability; does it matter? *Endocr. Rev.* 31, 171–182. doi: 10.1210/er.2009-0021

Spallone, V., Bellavere, F., Scionti, L., Maule, S., Quadri, R., Bax, G., et al. (2011). Recommendations for the use of cardiovascular tests in diagnosing diabetic autonomic neuropathy. *Nutr. Metab. Cardiovasc. Dis.* 21, 69–78. doi: 10.1016/j.numecd.2010.07.005

Tesfaye, S., Boulton, A. J., Dyck, P. J., Freeman, R., Horowitz, M., Kempler, P., et al. (2010). Diabetic neuropathies: update on definitions, diagnostic criteria, estimation of severity, and treatments. *Diabetes Care* 33, 2285–2293. doi: 10.2337/dc10-1303

The Diabetes Control and Complications Trial Research Group. (1998). The effect of intensive diabetes therapy on measures of autonomic nervous system function in the Diabetes Control and Complications Trial (DCCT). *Diabetologia* 41, 416–423. doi: 10.1007/s001250050924

Vinik, A. I., Maser, R. E., Mitchell, B. D., and Freeman, R. (2003). Diabetic autonomic neuropathy. *Diabetes Care* 26, 1553–1579. doi: 10.2337/dc10-1303

Vinik, A. I., and Ziegler, D. (2007). Diabetic cardiovascular autonomic neuropathy. *Circulation* 115, 387–397. doi: 10.1161/CIRCULATIONAHA.106.634949

Wei, F., Sun, X., Zhao, Y., Zhang, H., Diao, Y., and Liu, Z. (2016). Excessive visit-to-visit glycemic variability independently deteriorates the progression of endothelial and renal dysfunction in patients with type 2 diabetes mellitus. *BMC Nephrol.* 17:67. doi: 10.1186/s12882-016-0300-0

Yang, Y., Lee, E.-Y., Cho, J.-H., Park, Y.-M., Ko, S.-H., Yoon, K.-H., et al. (2018). Cardiovascular autonomic neuropathy predicts higher HbA1c variability in subjects with type 2 diabetes mellitus. *Diabetes Metab. J.* 42, 496–512. doi: 10.4093/dmj.2018.0026

Conflict of Interest Statement: The authors declare that the research was conducted in the absence of any commercial or financial relationships that could be construed as a potential conflict of interest.

frontiers in Neuroscience

ORIGINAL RESEARCH
published: 24 May 2019
doi: 10.3389/fnins.2019.00500

Respiratory Sinus Arrhythmia Acts as a Moderator of the Relationship Between Parental Marital Conflict and Adolescents' Internalizing Problems

Sumaira Khurshid[1,2†], *Yuan Peng*[1,2*†] *and Zhenhong Wang*[1,2*]

[1] School of Psychology, Shaanxi Normal University, Xi'an, China, [2] Shaanxi Province Key Research Centre of Child Mental and Behavioral Health, Xi'an, China

OPEN ACCESS

Edited by:
Erwin Lemche,
King's College London,
United Kingdom

Reviewed by:
Karen J. Mathewson,
McMaster University, Canada
Alessandro Tonacci,
Institute of Clinical Physiology (IFC),
Italy
David A. Smith,
University of Notre Dame,
United States
Briana Robustelli,
VA Puget Sound Health Care System,
United States

***Correspondence:**
Yuan Peng
pengyuan1866@163.com
Zhenhong Wang
wangzhenhong@snnu.edu.cn

[†]These authors have contributed equally to this work

Specialty section:
This article was submitted to Autonomic Neuroscience, a section of the journal Frontiers in Neuroscience

Received: 05 February 2019
Accepted: 30 April 2019
Published: 24 May 2019

Citation:
Khurshid S, Peng Y and Wang Z (2019) Respiratory Sinus Arrhythmia Acts as a Moderator of the Relationship Between Parental Marital Conflict and Adolescents' Internalizing Problems. Front. Neurosci. 13:500. doi: 10.3389/fnins.2019.00500

The present study examined the potential moderating role respiratory sinus arrhythmia (RSA) plays in the relationship between parental marital conflict and adolescents' internalizing problems. To examine this issue, data were collected from 330 adolescents (13–14 years, 182 boys). The Chinese version of the Achenbach Youth Self-Report-2001 and the Chinese version of the Children's Perception of Interparental Conflict were used to assess the adolescents' internalizing problems and their perceptions of parental marital conflict. To obtain RSA data, electrocardiogram monitoring was performed on the adolescents at baseline and during a series of stress tasks (watching a film clip depicting marital conflict, a mental arithmetic task, and a speech task). The results indicated that baseline RSA and RSA reactivity to the film clip moderated the relationship between parental marital conflict and internalizing problems in early adolescents. The moderating effect of baseline RSA supported the BSCT hypothesis. Specifically, adolescents with low baseline RSA have both the highest and lowest levels of internalizing problems, depending on the level of marital conflict. In contrast, adolescents with high levels of baseline RSA have moderate levels in internalizing problems, regardless of the level of marital conflict they experience. Similarly, high marital conflict was related to internalizing problems for adolescents with less RSA suppression or RSA augmentation but not for those with greater RSA suppression. This effect was specific to stress related to marital conflict, as RSA reactivity to the mental arithmetic task and speech task did not moderate the relationship between marital conflict and internalizing problems. These findings suggest that certain profile of parasympathetic nervous activity is a risk factor for internalizing problems particularly for those who experience high-conflict environments.

Keywords: marital conflict, internalizing problems, respiratory sinus arrhythmia, adolescent, interaction

INTRODUCTION

Internalizing problems (e.g., anxiety, depression) are common in adolescents and predict pervasive impairment in relation to social adaptation and academic achievement (e.g., Forns et al., 2012; Scalco et al., 2014). Thus, from a prevention viewpoint, it is critical to investigate and identify related vulnerabilities and protective factors regarding such problems. The developmental

psychopathology framework suggests that multiple environmental and individual risk factors contribute to the development of internalizing problems (Cummings and Davies, 2002; Saxbe et al., 2012; Barroso et al., 2018) and, among such environmental risk factors, marital conflict has begun to be regarded as an important adverse family factor related to internalizing problems in adolescents (Cummings and Davies, 2010; El-Sheikh et al., 2013). Similarly, parasympathetic nervous system (PNS) function, indexed by respiratory sinus arrhythmia (RSA) activity, has been regarded as a physiological protective or risk factor that decreases or increases internalizing problems (Dietrich et al., 2007; Porges, 2007; Gentzler et al., 2009; El-Sheikh et al., 2013). Several studies have explored RSA activity, including baseline RSA and RSA reactivity interact with marital conflict, through the Person × Environment perspective (Cicchetti, 2006), mainly in attempts to predict internalizing problems among children and adolescents (Katz and Gottman, 1997; Whitson and El-Sheikh, 2003; El-Sheikh and Whitson, 2006); however, the findings have been inconclusive. As a result, the present study was conducted to examine how baseline RSA and RSA reactivity to stress interact with marital conflict to predict adolescents' internalizing problems. In particular, this study sought to clarify whether high or low baseline RSA is an indicator of high physiological reactivity to marital-conflict environments, and whether the interacting role of marital conflict and RSA reactivity in predicting adolescents' internalizing problems is influenced by RSA reactivity measured during different tasks.

Marital conflict is defined as any difference, disagreement, or argument regarding an issue of family life, and this includes all kinds of psychological and physical conflicts (Cummings and Davies, 2002). Marital conflict is widely regarded as a core indicator of family solidarity and the key element in determining the quality of family life (Erel and Burman, 1995; Cummings and Davies, 2002). The emotional security theory (Davies and Cummings, 1994; Davies et al., 2002) proposes that marital conflict disrupts children's and adolescents' emotional security and increases their negative emotional and behavioral responses, thereby increasing their psychological maladjustment, including their risk of developing internalizing problems (Tu et al., 2016). Moreover, a large number of studies have demonstrated that marital conflict is associated with a broad array of adjustment problems in adolescents, such as academic difficulties, externalizing problems, and internalizing problems (for reviews, see Grych and Fincham, 2001; Davies and Lindsay, 2004; Cummings and Davies, 2010; Tu et al., 2016).

According to recent conceptual and empirical work, individual factors, such as certain profiles of PNS activity, may play a role in influencing the vulnerability of psychopathology including internalizing problems (Beauchaine, 2001; Porges, 2007). PNS activity can be assessed using a cardiac measure of RSA, which reflects rhythmic fluctuations in heart rate in relation to phases of the respiratory cycle (e.g., Porges, 1995; Gentzler et al., 2009). Baseline RSA (i.e., RSA level when in a resting state) and RSA reactivity (i.e., estimated by RSA change from baseline to a challenging state) are two commonly used RSA indices. Research has proposed that baseline RSA reflects a person's ability to maintain organism homeostasis, focus attention in normal situations, and conduct social engagement (Porges, 1995, 2007), while RSA reactivity reveals the extent to which a person can respond flexibly to internal stimuli and external environmental changes (Porges, 1995, 2007; Thayer and Lane, 2000). RSA reactivity can be quantified as RSA suppression (decreased RSA when performing tasks as compared to that at baseline) or RSA augmentation (increased RSA when performing tasks as compared to that at baseline). Specifically, during a challenging task, RSA suppression is generally considered an index of individuals' ability to adapt flexibly to environmental demands, which in turn reflects the physiological processes that help the individuals address the challenge and self-regulate their emotions and/or behaviors (Beauchaine, 2001; Calkins and Keane, 2004; Gentzler et al., 2009). RSA augmentation represents a heightened parasympathetic response, which is associated with hypervigilance and predicts problem behaviors such as internalizing problems (Katz, 2007; Graziano and Derefinko, 2013).

Many studies have found that lower baseline RSA is linked to internalizing problems (Forbes et al., 2006; Dietrich et al., 2007; Wei et al., 2017), while in contrast, other studies have found that lower baseline RSA is not linked to internalizing problems in children and adolescents (El-Sheikh et al., 2011; Hinnant and El-Sheikh, 2013). One possible explanation for these conflicting findings is that the association between baseline RSA and internalizing problems might partly be affected by environmental variables. Similarly, mixed findings have been found in regard to the association between RSA reactivity and internalizing problems. Some studies have found that greater RSA suppression is associated with less internalizing problems (Pearson et al., 2005; Gentzler et al., 2009), some other studies have observed contradictory results (Boyce et al., 2001; Hinnant and El-Sheikh, 2009), and another set of studies has found no direct link between RSA reactivity and internalizing problems such as depression in non-clinical samples (Hinnant and El-Sheikh, 2013; Koenig et al., 2016). One potential explanation for such mixed findings is that the association between RSA reactivity and adjustment outcomes largely depends on the characteristics of the environmental challenge in question (Porges, 2007; Obradović et al., 2011; Overbeek et al., 2014; Cui et al., 2015).

The diathesis-stress model and the biological sensitivity to context theory (BSCT; Boyce and Ellis, 2005) propose that individual temperament, genetics, or autonomic nervous system responses interact with the environment to exacerbate or attenuate an individual's maladaptation (Belsky and Pluess, 2009; Obradoviæ et al., 2010). Considering that baseline RSA is associated with self-regulatory capacity, and that RSA reactivity during a task is associated with self-regulatory effort (Segerstrom and Nes, 2007; Thayer et al., 2009; Balzarotti et al., 2017), RSA activity has recently been considered a moderator between environment and an individual's adaptation (e.g., El-Sheikh et al., 2001; Obradović et al., 2011). In contrast to the diathesis-stress model, which conceptualizes high reactivity as a vulnerability factor for maladjustment (Monroe and Simons, 1991), the BSCT proposes that high physiological stress reactivity reflects high biological sensitivity to context (Boyce and Ellis, 2005). It also posits that children with high physiological reactivity

are more sensitive to both negative and positive environments. In other words, in an adverse environment, high physiological reactivity might intensify the risk of maladjustment, whereas in supportive and nurturing environments, it might result in positive adjustment. In contrast, low biological stress reactivity is less affected by the environment (Boyce and Ellis, 2005).

In this regard, whether high or low baseline RSA represents high physiological reactivity still remains an open question. Some researchers have suggested that high baseline RSA reflects greater physiological reactivity, as it facilitates flexible responses to stress, and the ability to adapt to environmental challenges (Thayer and Lane, 2000; Porges, 2007). However, some other researchers have proposed that low baseline RSA reflects high physiological reactivity (Eisenberg et al., 2012), as it is related to higher negative emotional reactivity and motor/affective reactivity, which have been viewed as indicators of susceptibility to the environment (Fabes and Eisenberg, 1997; Beauchaine, 2001; Kagan and Fox, 2007; Eisenberg et al., 2012). Therefore, whether high or low baseline RSA represents high physiological reactivity in response to marital-conflict environment is needed to be clarified further.

Several studies have identified the moderating effect of RSA reactivity on the relationship between marital conflict and internalizing problems (Katz and Gottman, 1997; El-Sheikh et al., 2001; Whitson and El-Sheikh, 2003; El-Sheikh and Whitson, 2006). In contrast to the BSCT, these studies have found that children and adolescents who showed greater RSA suppression while watching a mock adult argument were less affected by the negative effects of adverse family environments, whereas children and adolescents who showed less RSA suppression or RSA augmentation while watching the mock adult argument were more vulnerable to adverse family environments (Katz and Gottman, 1997; El-Sheikh et al., 2001; Whitson and El-Sheikh, 2003; El-Sheikh and Whitson, 2006). However, other studies have failed to find a moderating effect of RSA reactivity in the connection between marital conflict and internalizing problems, using both cognitive tasks and watching peer-bullying film clips as stressors (Obradović et al., 2011). This indicates, and previous studies have suggested, that the moderating effect of RSA reactivity on the relationship between family factors (including marital conflict) and individuals' adjustment may largely depend on the characteristics of the laboratory challenge tasks used to elicit RSA reactivity (Obradović et al., 2011; Overbeek et al., 2014; Cui et al., 2015). Therefore, it is important to examine whether the characteristics of the stress tasks used to evoke RSA reactivity affect the relationship between family environment and psychological adaptation in children and adolescents. Considering this, in the present study, watching a film clip depicting marital conflict, a mental arithmetic task, and a speech task were used to explore interaction effects between RSA reactivity and marital conflict in regard to predicting internalizing problems. These tasks were chosen because they are common stress-induction stimuli used in reactivity protocols (Dickerson and Kemeny, 2004; Lü et al., 2017).

The present study was performed on a sample of early adolescents. Early adolescence has been regarded as a critical period during which individuals' biological and psychological states undergo marked developmental changes and they face a series of challenges, such as more complicated school tasks (Cicchetti and Rogosch, 2002). Previous studies have suggested that there is also a marked increase in internalizing problems during this crucial developmental stage (Angold et al., 2002); therefore, the present study focused on internalizing problems in early adolescents.

In addition, there is mixed evidence for gender difference in the moderating effect of RSA on the relationship between marital conflict and internalizing problems (El-Sheikh and Erath, 2011). Therefore, the present study also examined whether the moderating effect of RSA activity on the relationship between parental marital conflict and adolescents' internalizing problems differed by sex.

Overall, the present study was conducted to examine whether high or low baseline RSA represents high biological susceptibility to marital-conflict environment. This study also examined whether greater RSA suppression might function as a protective factor and moderate the association between marital conflict and adolescent's internalizing problems, and whether the moderating effect of RSA suppression on the relationship between marital conflict and adolescents' internalizing problems might depend on RSA reactivity measured during different challenge tasks.

MATERIALS AND METHODS

Participants

Three hundred and forty-six junior high school students aged 13–14 years, all from two-parent families, were recruited from a city in northwest China. Their parents were married and were the students' biological parents. Almost all participants (97%) were of Chinese Han ethnicity, and all were Mandarin Chinese speaking students. Of these, the data of six participants were excluded from the analysis because they did not complete the questionnaires, and the physiological data of 10 participants were not usable as a result of acquisition issues (e.g., equipment malfunction or electrode misplacement). Therefore, data from 330 participants [182 boys, mean age = 13.7 years, standard deviation (*SD*) = 0.8] were valid. They completed questionnaires that assessed internalizing problems and parental marital conflict, and then participated in a laboratory-based physiological experiment. All of the participants reported no history of cardiovascular disease and that they were not taking any medications that could interfere with the research results. All of the participants reported normal or corrected-to-normal vision.

The participants were asked to report their parents' monthly income using a 4-point scale (1 = less than ¥3000, 2 = ¥3000-¥7000, 3 = ¥7000-¥10000, and 4 = more than ¥10000) and their parents' education level using a 7-point scale (1 = lower than elementary school, 2 = elementary school, 3 = junior high school, 4 = high school, 5 = college or university, 6 = master's degree, 7 = doctoral degree). The participants' socioeconomic status (SES) was obtained by summing the standard scores (M = 0, SD = 1) of the following three variables according to previous studies (Schulting et al., 2005; Cohen et al., 2006): (a) the father's education level (M = 2.64, SD = 0.92); (b) the mother's education level (M = 2.60, SD = 0.94); and (c) household income (M = 2.88,

SD = 0.39). Among the participants' parents, 59% of mothers and 71% of fathers had an educational attainment ranging from vocational school to a college or university degree. Most of their parents worked outside the home in occupations ranging from blue collar to professional. The mean monthly combined family income was between about ¥7000 and ¥10000. The sample was well representative of school adolescents in urban China. All participants were compensated ¥60 (approximately $10) for their participation.

Procedure

This study was approved by the Institutional Review Board of the Psychology School of Shaanxi Normal University. Written informed consent was obtained from the parents of all participants prior to data collection, and the participants were informed of the nature of the study and were told that there was no penalty for not participating. The experiment was conducted from 2:00 pm to 5:00 pm every day for 4 weeks, with each participant attending for a single day. The participants were invited into a brightly lit, quiet room, which was equipped with computers. Before the formal test, detailed instructions were provided to ensure that the participants clearly understood the experimental procedures. All participants were instructed to refrain from performing physical exercise or consuming any caffeine or alcohol for 2 h before the commencement of the experiment, which was in order to eliminate the risk of any exogenous effects on the physiological measures. After completing the questionnaires, electrocardiogram (ECG) recording electrodes (SOMNOtouch^{TM} device) were attached to the participants. The participants were then given 10 min to acclimate to the laboratory and to relax. After this, the formal physiological experiment began, with all instructions for the experimental procedure being simultaneously presented on a monitor screen.

The entire experiment included seven phases (see **Figure 1**), and after each phase, the participants were asked to rate their subjective emotional experience (SEE), including nervousness and anxiety, on two 5-point scales from 0 ("relaxed") to 4 ("nervous" or "anxious"). First, the participants were shown a neutral picture on the computer screen (a picture of a cup, selected from the International Affective Picture System, IAPS; Lang et al., 2005), which was designed to keep them relaxing while ECG and respiration signals were recorded; this enabled the measurement of the participants' 5-min baseline RSA values. Second, the participants were instructed to watch a film clip depicting marital conflict, which served to induce a stress response. Third, the participants were given 5 min for rest (recovery period 1), during which they were instructed to sit, relax, and view neutral pictures (e.g., a picture of a cup or an umbrella also selected from the IAPS; Lang et al., 2005). Fourth, the participants were requested to complete a mental arithmetic task (Diamond et al., 2012). Fifth, the participants rested again (recovery period 2). Sixth, the participants were instructed to give a speech. Seventh, the participants rested again (recovery period 3).

In order to reduce the impact of order effects, the sequences of the three stress tasks were balanced across the entire experiment. Specifically, one third of the participants watched the marital-conflict film clip first, then performed the mental arithmetic task second, and performed the speech task third; one third performed the mental arithmetic task first, the speech task second, and watched the marital-conflict film clip third; and the other third performed the speech task first, watched the marital-conflict film clip second, and performed the mental arithmetic task third.

Stress Tasks

Watching a Marital-Conflict Film Clip Task

The participants were instructed to watch a 5-min film clip featuring marital conflict. The suitability of the conflict film, featuring verbal and physical conflict between a couple, was previously assessed through a preliminary experiment. Pre-experimental testing showed that the watching the film clip task induced higher subjective and physiological responses[1].

Mental Arithmetic Task

The participants were informed that their mathematical skills would be evaluated based on their performance in the task, in which they were asked to subtract 13 from a series of four-digit numbers as fast and accurately as possible. Every 4.5 s, the correct number would be displayed on the monitor, accompanied by a beep sound. The participants were requested to state the result of their calculation before the correct answer was displayed on the monitor after the beep. For avoiding social-evaluative threat, the two research assistants who were present with them left the experiment room when the participants performed the mental arithmetic task.

[1]Pre-experimental testing with a sample of 32 participants (boys = 16, mean age = 12.8 years) showed that the film clip depicting marital conflict elicited greater subjective nervousness [$t(30) = 2.34$, $p = 0.031$, $d = 1.08$], subjective anxiety [$t(30) = 2.34$, $p = 0.031$, $d = 1.08$], and RSA stress reactivity [$t(30) = 2.23$, $p = 0.039$, $d = 1.04$] compared to the scores before watching the film clip.

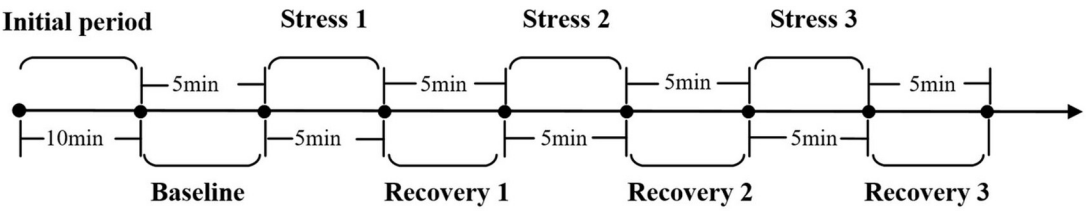

FIGURE 1 | Time-line of experimental session.

Speech Task

The participants were told to give a speech for a mock class-leader election. Two research assistants served as live interviewers for each speech. The participants were provided with the following instruction (originally given in Chinese): "You will deliver a speech for a class-leader election, for which you have 120 s to prepare; then, you will have 5 min to state the type of position you are running for, as well as the reasons you qualify for this position. Your performance will be evaluated by the research assistants in terms of overall content, clarity, and delivery." After the 120-s preparation phase, the participants delivered their 5-min speech to the two assistants. During the speech period, whenever the participants paused for more than 10 s, they were prompted to continue. The validity of the social stress task has been verified in a previous study (Lü et al., 2016).

Measures

Marital Conflict

The conflict characteristics subscale of the Chinese version of the Children's Perception of Interparental Conflict (the original instrument was developed by Grych and Fincham, 1990, and the Chinese version was revised by Chi and Xin, 2003) was used to measure parental marital conflict. This subscale includes three dimensions: conflict frequency (six items; e.g., "I often see my parents arguing"), conflict intensity (seven items; e.g., "when my parents have an argument, they yell a lot"), and conflict resolution (six items; e.g., "even after my parents stop arguing, they stay mad at each other"). The three dimensions are summed to create a single overall measure of parental marital conflict, with higher scores indicating greater parental marital conflict. Responses are given using a 5-point scale ranging from 1 ("never") to 5 ("always"). For the present study, the Cronbach's α for this subscale was 0.86.

Internalizing Problems

Internalizing problems were assessed using the Chinese Version of the Achenbach Youth Self-Report-2001 (Achenbach and Rescorla, 2001; Wang et al., 2016). The internalizing problem subscale contains 30 items that measure withdrawal/depressed, anxious/depressed, and somatic complaints, which are then summed to create a single overall measure of internalizing problems; higher scores indicate more internalizing problems. Sample items include "I worry a lot" and "I am unhappy, sad, or depressed." Responses are provided using a 3-point scale ranging from 0 ("not true") to 2 ("very true or often true"). For the present study, the Cronbach's α for the internalizing subscale was 0.88.

Physiological Data

The ECG data were continuously recorded using SOMNOtouch^{TM} RESP (SOMNOmedics, Germany), with a sampling rate of 256 Hz. Disposable Ag-AgCl electrodes were attached to each participant's lower left rib and right and left clavicle. The ECG sensors were subsequently connected to the SOMNOtouch^{TM} RESP.

The ECG data were then transferred into DOMINO light software 1.4.0 (SOMNOmedics, Germany) for automatic detection of artifacts (which were to be discarded from the analysis). In data preparation, the R-R intervals were resampled at 4 Hz and detrended based on the smoothness prior approach (Tarvainen et al., 2002). RSA was quantified via a high-frequency interbeat-interval power spectrum (0.22–0.40 Hz for adolescents aged 13 years and 0.20–0.40 Hz for adolescents aged 14; Shader et al., 2018) corresponding to the respiratory cycle, and the values were natural log transformed (ln) to fit the assumption of linear analyses, yielding ln units (ms^2). RSA during each study phase was averaged to compute mean level for each experimental period (i.e., baseline RSA and RSA reactivity). Additionally, a standardized residual score was computed to remove overlap between baseline RSA and RSA reactivity scores (Calkins and Keane, 2004). RSA reactivity was computed as the standardized residual of the RSA value that was predicted for each stress task based on the RSA value during the baseline period (Hastings et al., 2008; Burt and Obradoviæ, 2013). A positive standardized residual score would indicate a significant increase from baseline (RSA augmentation), while a negative standardized residual score would indicate a significant decrease from baseline (RSA suppression; Hastings et al., 2008).

Analytic Strategy

Outliers, $+/-3$ *SD* from the mean, were identified for the study variables. One adolescent had very low baseline RSA, three had a very strong RSA suppression response to speech task, and two had a very strong RSA augmentation response to the speech task. All of the outlier data points were replaced with the next value present in the data (Wilcox, 2012), and the main findings were not changed by using this approach.

First, to test whether the challenging tasks successfully induced participants' stress reactivity, within-subject comparisons of subjective nervousness, subjective anxiety and RSA data obtained during baseline, the watching the film clip task, the mental arithmetic task, the speech task, and the recovery periods were performed with separate repeated measures analyses of variance (ANOVAs). Pairwise comparisons were conducted using Bonferroni correction. Greenhouse-Geisser corrections would be applied if the assumption of sphericity was violated.

All statistical tests were conducted using SPSS 22 (IBM, United States). First, difference scores (the absolute change between baseline and RSA response to each challenge) analysis was conducted to report the general variation trends in RSA from baseline to the stress task periods. Second, Pearson correlations were computed to examine the associations among the study variables. Third, separate multiple regression analyses were used to examine the main effects of marital conflict and RSA variables (baseline RSA and RSA reactivity) and the interaction effects on adolescents' internalizing problems; all the predictor variables were mean-centered prior to conducting regression analyses (Aiken and West, 1991). In each regression, the main effects of sex, marital conflict, and baseline RSA (or RSA reactivity) were entered in the first step, and the two-way interaction terms (i.e., marital conflict × baseline RSA) were entered in the second step. The three-way interaction of sex × marital conflict × baseline RSA (or RSA suppression) was entered in the third step. A power analysis indicated that to detect a three-way interaction with a medium effect size

(i.e., 0.15), a sample size of at least 89 is needed. Thus, our sample size is comparably large and can be used to reliably detect a three-way interaction. To evaluate the significant interaction, the procedures outlined by Aiken and West (1991) were used to plot the predicted outcome variable for levels of the independent variable (ranging from −1 *SD* to +1 *SD*) at both high and low levels of the moderator (ranging from −1 *SD* to +1 *SD*).

RESULTS

Descriptive Statistics

The means and standard deviations of the variables are provided in **Table 1**. Compared to boys (M = 10.33, SD = 7.70), girls had greater internalizing problems (M = 14.50, SD = 9.14). No other difference was observed between boys and girls.

During the watching the film clip task, 156 (47%) children displayed RSA augmentation, and 174 (53%) displayed RSA suppression. During the mental arithmetic task, 128 (39%) children displayed RSA augmentation, and 202 (61%) displayed RSA suppression. During the speech task, 125 (38%) children displayed RSA augmentation, and 205 (62%) displayed RSA suppression.

Analyses of Variance (ANOVAs) by Task

Regarding the watching the marital-conflict film clip task, the repeated measures ANOVAs showed significant main effects for subjective nervousness [$F(1.99, 640.92) = 74.34$, $p < 0.001$, $\eta^2_p = 0.19$], subjective anxiety [$F(1.98, 638.48) = 45.75$, $p < 0.001$, $\eta^2_p = 0.12$], and RSA [$F(1.79, 585.64) = 23.31$, $p < 0.001$, $\eta^2_p = 0.10$]. *Post hoc* tests indicated that the levels of subjective nervousness and anxiety were greater during the challenge task than during the baseline period [$t(329) = 7.96$, $p < 0.001$; $t(329) = 8.51$, $p < 0.001$] and the recovery period [$t(329) = 10.18$, $p < 0.001$; $t(329) = 8.00$, $p < 0.001$]. Similarly, *post hoc* tests also showed that RSA decreased significantly from baseline to the challenge task period [$t(329) = 5.62$, $p < 0.001$], and then increased significantly during the recovery period [$t(329) = 3.72$, $p < 0.01$]. These results showed that using the watching the marital-conflict film clip task was effective in inducing changes in individuals' subjective and physiological reactivity.

TABLE 1 | Descriptive statistics among variables.

	Mean	*SD*
Marital conflict	13.39	3.64
Baseline RSA	6.32	1.15
RSAR[a] (mental arithmetic)	−0.002	0.58
RSAR[a] (speech)	−0.008	0.61
RSAR[a] (film clip)	−0.01	0.66
Internalizing problems	12.13	8.56

*RSAR = RSA reactivity. Sex was coded 0 for males and 1 for females. [a]Standardized residual score (with baseline RSA partialed out), *p < 0.05, **p < 0.01, ***p < 0.001.*

Regarding the mental arithmetic task, the repeated measures ANOVAs significant main effects for subjective nervousness [$F(1.96, 640.14) = 166.04$, $p < 0.001$, $\eta^2_p = 0.34$], subjective anxiety [$F(1.98, 642.22) = 161.96$, $p < 0.001$, $\eta^2_p = 0.55$], and RSA [$F(1.92, 619.04) = 49.71$, $p < 0.001$, $\eta^2_p = 0.13$]. *Post hoc* tests indicated that the levels of subjective nervousness and anxiety were greater during the challenge task than during the baseline period [$t(329) = 11.03$, $p < 0.001$; $t(325) = 10.18$, $p < 0.001$] and the recovery period [$t(329) = 12.12$, $p < 0.001$; $t(329) = 13.08$, $p < 0.001$]. Similarly, *post hoc* tests also showed that RSA decreased significantly from baseline to the challenge task period [$t(329) = 4.11$, $p < 0.001$], and then increased significantly during the recovery period [$t(329) = 2.87$, $p < 0.01$]. These results showed that using a mathematical challenge task was also effective in inducing changes in individuals' subjective and physiological reactivity.

Finally, with regard to the speech task, the repeated measures ANOVA showed significant main effects for subjective nervousness [$F(1.84, 157.98) = 179.13$, $p < 0.001$, $\eta^2_p = 0.36$], subjective anxiety [$F(1.94, 629.59) = 93.50$, $p < 0.001$, $\eta^2_p = 0.22$], and RSA [$F(1.74, 589.61) = 50.63$, $p < 0.001$, $\eta^2_p = 0.14$]. *Post hoc* tests indicated that the levels of subjective nervousness and anxiety were greater during the challenge task than during the baseline period [$t(329) = 9.80$, $p < 0.001$; $t(329) = 8.80$, $p < 0.001$] and the recovery period [$t(329) = 10.23$, $p < 0.001$; $t(329) = 9.21$, $p < 0.001$]. Similarly, *post hoc* tests also showed that RSA decreased significantly from baseline to the challenge task period [$t(329) = 4.24$, $p < 0.001$], and then increased significantly during the recovery period [$t(329) = 2.05$, $p < 0.05$]. These findings showed that using a speech task was also effective in inducing changes in individuals' subjective and physiological reactivity.

Correlations Analyses

Correlations among study variables were presented in **Table 2**. As hypothesized, exposure to marital conflict was related to a high level of internalizing problems. Moreover, baseline RSA and RSA reactivity to the three challenge tasks were not related to internalizing problems as main effects.

Predictions for Internalizing Problems Based on Marital Conflict and Baseline RSA

The results of the regression analyses were presented in **Tables 3**, **4**. As shown in **Table 3**, the moderating effect of baseline RSA (t = -2.26, $p < 0.05$) on the relationship between marital conflict and internalizing problems was significant (see **Figures 2**, **3**). The simple slope test found that for adolescents with low baseline RSA, marital conflict significantly predicted internalizing problems [simple slope = 2.50, SE = 0.06, $t(329) = 0.62$, $p < 0.001$], but for adolescents with high baseline RSA, marital conflict did not have significant effect on internalizing problems [simple slope = 0.62, SE = 0.05, $t(329) = 3.85$, $p > 0.05$]. The three-way

TABLE 2 | Correlation among variables.

	1	2	3	4	5	6	7	8
1 Sex	1							
2 SES	−0.04	1						
3 Marital conflict	0.09	−0.13*	1					
4 Baseline RSA	0.02	−0.08	0.02	1				
5 RSAR[a] (mental arithmetic)	0.001	0.04	0.05	−0.06	1			
6 RSAR[a] (speech)	0.10	0.05	0.02	−0.08	0.52**	1		
7 RSAR[a] (film clip)	0.002	0.04	0.08	−0.12	0.50**	0.42**	1	
8 Internalizing problems	0.25**	0.03	0.19**	0.06	−0.06	0.03	−0.04	1

TABLE 3 | Main effect and interactive effect of marital conflict and baseline RSA.

	Internalizing problems					
	B	*SE*	β	*t*	95% CI for *B*	ΔR^2
Step 1						0.07
Marital conflict	1.30	0.48	0.15	2.71**	[0.36, 2.24]	
Baseline RSA	0.25	0.47	0.03	0.53	[−0.68, 1.18]	
Sex	1.91	0.46	0.22	4.17***	[1.01, 2.81]	
Step 2						0.09
Marital conflict × Baseline RSA	−1.20	0.47	−0.14	−2.56*	[−2.12, −0.28]	
Marital conflict × Sex	0.04	0.47	0.005	0.09	[−0.87, 0.95]	
Baseline RSA × Sex	0.83	0.43	0.10	1.75	[−0.10, 1.76]	
Step 3						0.09
Marital conflict × Baseline RSA × Sex	0.24	0.44	0.03	0.51	[−0.68, 1.15]	
Total R^2 = 0.11, $F(7, 322)$ = 5.38***						

interaction role of sex × marital conflict × baseline RSA was not significant ($p > 0.05$).

Predictions for Internalizing Problems Based on Marital Conflict and RSA Reactivity

As shown in **Table 4**, RSA reactivity to the marital-conflict film clip (t = -2.34, $p < 0.05$) had a significant moderating effect on the relationship between marital conflict and internalizing problems (see **Figures 4**, **5**). The simple slope test found that for adolescents with RSA augmentation, marital conflict significantly predicted internalizing problems [simple slope = 2.55, SE = 0.06, $t(329)$ = 3.76, $p < 0.001$], but for adolescents with greater RSA suppression, marital conflict did not have significant effect on internalizing problems [simple slope = 0.61, SE = 0.06, $t(329)$ = 0.92, $p > 0.05$]. The three-way interaction role of sex × marital conflict × RSA reactivity (watching film clip) was not significant ($p > 0.05$). Meanwhile, as shown in **Tables 5**, **6**, RSA reactivity to the mental arithmetic and speech tasks ($ps > 0.05$) did not have significant moderating effects on the relationship between marital conflict and internalizing problems. The three-way interaction roles of sex × marital conflict × RSA reactivity (mental arithmetic and speech tasks) were not significant ($ps > 0.05$).

TABLE 4 | Main effect and interactive effect of marital conflict and RSAR (watching film clip).

	Internalizing problems					
	B	*SE*	β	*t*	95% CI for *B*	ΔR^2
Step 1						0.08
Marital conflict	1.36	0.48	0.16	2.84**	[0.42, 2.30]	
RSAR	−0.43	0.46	−0.05	0.53	[−0.68, 1.18]	
Sex	2.05	0.46	0.24	4.48***	[1.15, 2.95]	
Step 2						0.11
Marital conflict ×RSAR	−1.05	0.48	−0.12	−2.17*	[−2.00, −0.10]	
Marital conflict × Sex	0.21	0.47	0.03	0.46	[−0.70, 1.13]	
RSAR × Sex	0.75	0.45	0.08	1.62	[−0.16, 1.67]	
Step 3						0.11
Marital conflict × RSAR × Sex	−0.71	0.47	−0.09	−1.52	[−1.64, 0.21]	
Total R^2 = 0.11, $F(7, 322)$ = 5.86***						

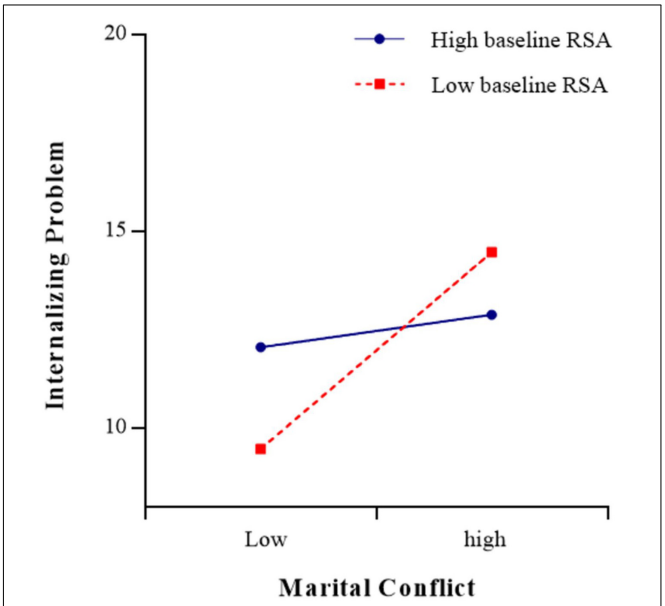

FIGURE 2 | The association between marital conflict and adolescents' internalizing problems at low (–1 *SD*) and high (+1 *SD*) levels of baseline RSA.

DISCUSSION

The present study examined the associations among parental marital conflict, adolescents' RSA variables (baseline RSA and RSA reactivity), and adolescents' internalizing problems. The results showed that the adolescents' baseline RSA and RSA reactivity in response to a film clip depicting marital conflict moderated the relationship between parental marital conflict and adolescents' internalizing problems.

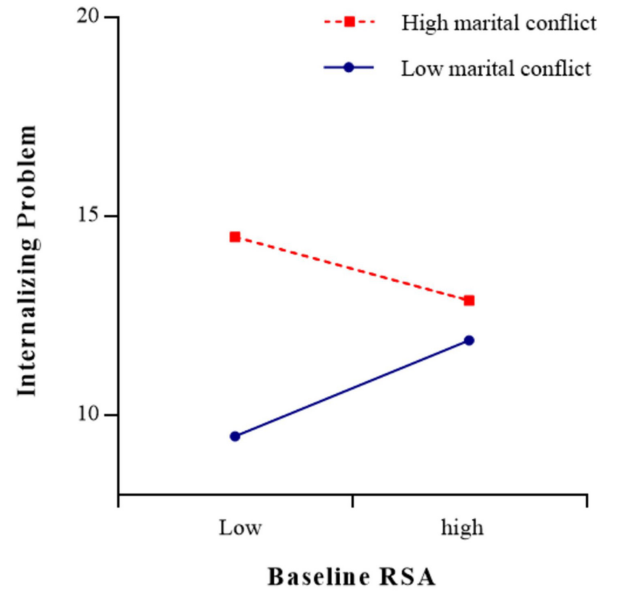

FIGURE 3 | The association between baseline RSA and adolescents' internalizing problems at low (–1 *SD*) and high (+1 *SD*) levels of marital conflict.

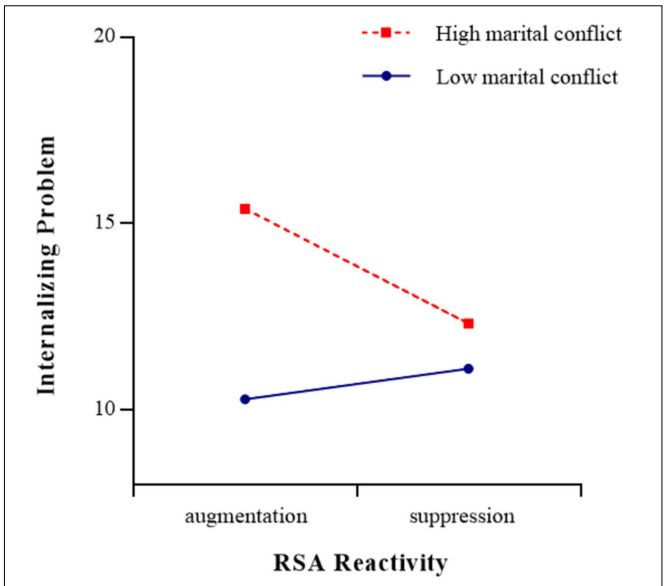

FIGURE 5 | The association between RSA reactivity (watching film clip task) and adolescents' internalizing problems at low (–1 *SD*) and high (+1 *SD*) levels of marital conflict.

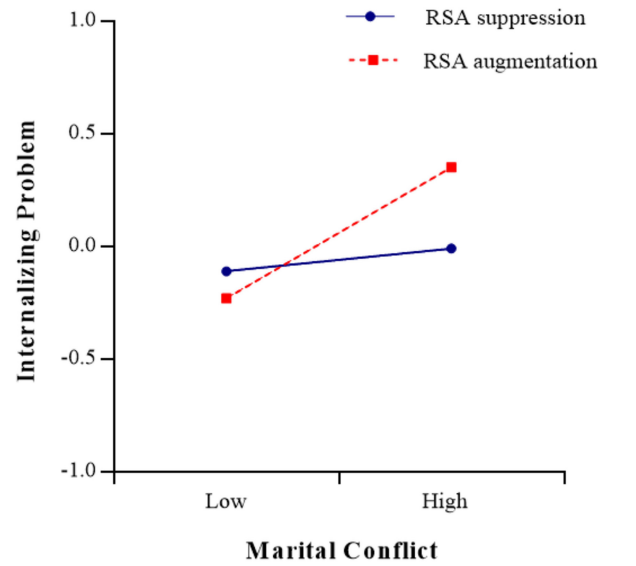

FIGURE 4 | The association between marital conflict and adolescents' internalizing problems at low (–1 *SD*) and high (+1 *SD*) levels of RSA reactivity under watching film clip task.

Consistent with previous studies (Cummings and Davies, 2010; El-Sheikh et al., 2013), the present study found that marital conflict is positively related to adolescents' internalizing problems, that is, high marital conflict is related to more internalizing problems in adolescents. According to the emotional security theory (Davies and Cummings, 1994; Davies et al., 2002), marital conflict disrupts adolescents' emotional security, causes negative emotional responses, undermines their psychological adjustment, and increases the likelihood of internalizing problems (Tu et al., 2016). The present study together with previous studies (Cummings and Davies, 2010; El-Sheikh et al., 2013) demonstrate that high parental marital conflict has a negative association with children's psychological functioning and may elevate the risk of adolescents' internalizing problems.

Similar to some previous studies (El-Sheikh and Erath, 2011; Hinnant and El-Sheikh, 2013; Koenig et al., 2016), the present study did not find any direct association between baseline RSA or RSA reactivity and adolescents' internalizing problems. However, consistent with previous studies (Katz and Gottman, 1997; El-Sheikh and Erath, 2011), the present study found that baseline RSA has a significant moderating effect on the relationship between marital conflict and adolescents' internalizing problems. The moderating effect of baseline RSA supported the BSCT hypothesis. The moderating effect indicated that adolescents with low baseline RSA have low levels of internalizing problems only if they lived in low-conflict environments. Low baseline RSA reflected a low threshold for autonomic nervous system arousal, which may facilitate adolescents' sensitivity to the support and resources from positive family environments. However, in a high-conflict family, such adolescents were also biological vulnerable to the negative effect of their parents' psychological and physical conflicts and had little protection from the risk of internalizing problems. In contrast, adolescents with high levels of baseline RSA have moderate levels in internalizing problems, regardless of the level of marital conflict they experience. Adolescents with high baseline RSA were more likely to maintain calm and to have the ability to adaptively regulate their emotions and behavior and were better able to cope with marital conflict, and may be at less risk of internalizing problems in high-conflict environments.

TABLE 5 | Main effect and interactive effect of marital conflict and RSAR (mental arithmetic task).

	Internalizing problems					
	B	***SE***	**β**	***t***	**95% CI for *B***	**ΔR^2**
Step 1						0.09
Marital conflict	1.46	0.47	0.17	3.12**	[0.54, 2.38]	
RSAR	−0.43	0.46	−0.05	0.53	[−0.68, 1.18]	
Sex	2.05	0.46	0.24	4.48***	[1.15, 2.95]	
Step 2						0.01
Marital conflict × RSAR	−0.76	0.46	−0.09	−1.64	[−1.67, 0.15]	
Marital conflict × Sex	−0.18	0.46	−0.02	−0.40	[−1.11, 0.73]	
RSAR × Sex	0.81	0.47	0.09	1.72	[−0.12, 1.75]	
Step 3						0.00
Marital conflict × RSAR × Sex	0.06	0.46	0.008	0.14	[−0.84, 0.97]	
	Total R^2 = 0.11, $F(7, 322)$ = 5.86***					

TABLE 6 | Main effect and interactive effect of marital conflict and RSAR (speech task).

	Internalizing problems					
	B	***SE***	**β**	***t***	**95% CI for *B***	**ΔR^2**
Step 1						0.09
Marital conflict	1.51	0.47	0.17	3.22**	[0.58, 2.44]	
RSAR	0.04	0.46	0.005	0.098	[−0.87, 0.96]	
Sex	1.94	0.46	0.22	4.22***	[1.03, 2.84]	
Step 2						0.008
Marital conflict ×RSAR	−0.16	0.46	−0.02	−0.34	[−1.06, 0.74]	
Marital conflict × Sex	−0.11	0.47	−0.01	−0.24	[−1.03, 0.81]	
RSAR × Sex	0.77	0.46	0.09	1.63	[−0.15, 1.69]	
Step 3						0.004
Marital conflict × RSAR × Sex	0.58	0.45	0.06	1.25	[−0.32, 1.47]	
	Total R^2 = 0.10, $F(7, 322)$ = 5.21***					

Moreover, consistent with previous studies (Whitson and El-Sheikh, 2003; El-Sheikh and Whitson, 2006), the present study found that RSA reactivity in response to a film clip depicting marital conflict moderated the relationship between marital conflict and adolescents' internalizing problems and the moderating effect didn't support the BSCT hypothesis. In other words, adolescents who showed appropriate RSA responses (greater RSA suppression) during marital conflict appear to be protected from internalizing problems, even when marital conflict was high, whereas adolescents who showed inappropriate RSA responses (either RSA augmentation or less RSA suppression) to marital conflict film clip were only protected from internalizing problems if they lived in a low-conflict environment (a more peaceful family). In the context of marital conflict, adolescents with greater RSA suppression might be able to better regulate their physiological arousal and emotional response and may be at less risk of internalizing problems (e.g., Whitson and El-Sheikh, 2003; El-Sheikh and Whitson, 2006). In contrast, adolescents with either RSA augmentation or less RSA suppression tended to be hypervigilant to negative emotional environments and might exhibit poor emotional regulation (Katz, 2007; Graziano and Derefinko, 2013), and such adolescents were more likely to develop internalizing problems in high-conflict environments.

In addition, considering that moderating effects are symmetrical, the results also suggested that marital conflict has significant moderating effects on the relationship between RSA activity (baseline RSA and RSA reactivity in response to marital-conflict film clip) and adolescents' internalizing problems. The moderating effects indicated that in a high marital-conflict environment, adolescents with lower baseline RSA or RSA augmentation exhibited the most internalizing problems, and in a low marital-conflict environment, adolescents with lower baseline RSA exhibited the least internalizing problems; however, adolescents with higher baseline RSA or greater RSA suppression exhibited less internalizing problems even lived in a high marital-conflict environment. Therefore, in families with parental conflict, more attention should be paid to signs of internalizing problems in adolescents with more limited physical resources.

Despite the above, the present study did not find RSA reactivity to the mental arithmetic and speech tasks have significant moderating effects on the relationship between marital conflict and adolescents' internalizing problems. These findings indicated that, as previous researchers have suggested, the moderating effects of RSA reactivity on the relationship between adverse family environments and adolescents' maladaptive outcomes might vary with the characteristics of the laboratory stress tasks applied (Porges, 2007; Obradović et al., 2011; Overbeek et al., 2014; Cui et al., 2015). Previous studies have suggested that the mental arithmetic and speech tasks can be categorized as motivated performance tasks, while watching a film clip can be categorized as a passive task (Blascovich and Mendes, 2000), and that these stressors activate different cognitive and affective processes and have different central nervous system underpinnings (Dickerson and Kemeny, 2004). Moreover, it is plausible that the moderating effects depend on a match between RSA reactivity to the particular task and the task-related predictor. Watching a marital-conflict film clip closely resembles a parental marital-conflict situation that many adolescents witness in their daily lives, RSA reactivity to a marital-conflict film clip might be consistent with the RSA reactivity they usually experience during their parent's conflict, and this might partly cause explain the present study observation that RSA reactivity to the marital-conflict film clip had a significant moderating effect on the relationship between marital conflict and adolescents' internalizing problems.

The present study also examined whether the interactions between marital conflict and RSA activity in the prediction of adolescents' internalizing problems differed by sex. Consistent with previous studies, the present study found that girls had greater internalizing problems than boys (Nolen-Hoeksema and Girgus, 1994), while no other difference was noted between boys and girls. These results suggested that higher baseline RSA and greater RSA suppression might protect both boys

and girls against internalizing problems associated with marital conflict, and low baseline RSA among boys and girls might reflect their biological susceptibility to both negative and positive family environments.

Several limitations to the present study should be considered. First, although the findings indicated that baseline RSA and RSA reactivity interact with marital conflict to predict internalizing problems, as a result of the cross-sectional nature of the present study, no conclusion regarding causality or the direction of the effect can be drawn. Thus, future longitudinal research must explore the temporal relations among these variables. Second, marital conflict scores were obtained through adolescents' self-reports. Although previous studies have noted that children's and adolescents' self-reports of marital conflict are more consistent predictors of adjustment than are parents' reports of marital conflict (Grych et al., 2000), future research should include parents' reports of marital conflict to fully evaluate the effect of family environments on adolescents. Third, the present study did not measure interpersonal violence at home. Future research should measure this factor as it is known to make adolescents feel less safe at home and lead to the development of more internalizing problems. Fourth, a low level of marital conflict does not necessarily indicate a supportive and nurturing environment; further studies should explore the issues that exist in positive family environments. Finally, the present study examined the moderating roles of RSA activity on the relationship between marital conflict and early adolescents' internalizing problems. Future researchers should extend the findings to samples with a broader age range such as elementary and high school students to improve the generalizability of the results.

CONCLUSION

In conclusion, the present study identified the moderating effects of PNS activity (baseline RSA and RSA reactivity) on the relationship between parental marital conflict and internalizing problems in early adolescents. It provided evidence indicating that poor parasympathetic regulation (low baseline RSA and inappropriate augmentation to a stressor) is a risk factor for internalizing problems particularly for those who experience high-conflict environments. It also provided preliminary evidence suggesting that the moderating effect of baseline RSA supported the BSCT hypothesis. Moreover, it indicated that the moderating effect of RSA reactivity on the relationship between parental marital conflict and early adolescents' internalizing problems partly depend on the RSA reactivity measured during different challenge tasks.

ETHICS STATEMENT

The authors assert that all procedures contributing to this work comply with the ethical standards of the relevant national and institutional committees on human experimentation and with the Helsinki Declaration of 1975, as revised in 2008. This study was approved by the Institutional Review Board of the Psychology School of Shaanxi Normal University.

AUTHOR CONTRIBUTIONS

All authors listed have made a substantial, direct and intellectual contribution to this work, and approved it for publication.

FUNDING

This research was supported by the National Science Foundation Grant (31671152) of China, and the Research Program Funds of the Collaborative Innovation Center of Assessment toward Basic Education Quality at Beijing Normal University (2016-05-004-BZK01), awarded to ZW, and the Fundamental Research Funds for the Central Universities (2018TS085) awarded to YP.

ACKNOWLEDGMENTS

We wish to express our gratitude to the adolescents who consented to participate in this study.

REFERENCES

Achenbach, T. M., and Rescorla, L. A. (2001). *Manual for the ASEBA School-Age Forms and Profiles*. Burlington, VT: University of Vermont.

Aiken, L. S., and West, S. G. (1991). *Multiple regression: Testing and interpreting interactions*. Thousand Oaks, CA: Sage Publications Inc.

Angold, A., Erkanli, A., Silberg, J., Eaves, L., and Costello, E. J. (2002). Depression scale scores in 8-17-year-olds: effects of age and gender. *J. Child Psychol. Psychiatry* 43, 1052–1063. doi: 10.1111/1469-7610.00232

Balzarotti, S., Biassoni, F., Colombo, B., and Ciceri, M. R. (2017). Cardiac vagal control as a marker of emotion regulation in healthy adults: a review. *Biol. Psychol.* 130, 54–66. doi: 10.1016/j.biopsycho.2017.10.008

Barroso, N. E., Mendez, L., Graziano, P. A., and Bagner, D. M. (2018). Parenting stress through the lens of different clinical groups: a systematic review and meta-analysis. *J. Abnorm. Child Psychol.* 46, 449–461. doi: 10.1007/s10802-017-0313-6

Beauchaine, T. (2001). Vagal tone, development, and gray's motivational theory: toward an integrated model of autonomic nervous system functioning in psychopathology. *Dev. Psychopathol.* 13, 183–214. doi: 10.1017/S0954579401002012

Belsky, J., and Pluess, M. (2009). Beyond diathesis-stress: differential susceptibility to environmental influences. *Psychol. Bull.* 135, 885–908. doi: 10.1037/a0017376

Blascovich, J., and Mendes, W. B. (2000). "Challenge and threat appraisals: the role of affective cues," in *Feeling and Thinking: the Role of Affect in Social Cognition*, ed. J. Forgas (Cambridge: Cambridge University Press), 59–82.

Boyce, W. T., and Ellis, B. J. (2005). Biological sensitivity to context: I. An evolutionary-developmental theory of the origins and functions of stress reactivity. *Dev. Psychopathol.* 17, 271–301. doi: 10.1017/S0954579405050145

Boyce, W. T., Quas, J., Alkon, A., Smider, N. A., Essex, M. J., and Kupfer, D. J. (2001). Autonomic reactivity and psychopathology in middle childhood. *Brit. J. Psychiatry* 179, 144–150. doi: 10.1192/bjp.179.2.144

Burt, K. B., and Obradoviæ, J. (2013). The construct of psychophysiological reactivity: statistical and psychometric issues. *Dev.Rev.* 33, 29–57. doi: 10.1016/j.dr.2012.10.002

Calkins, S. D., and Keane, S. P. (2004). Cardiac vagal regulation across the preschool period: STABILITY, continuity, and implications for childhood adjustment. *Dev. Psychobiol.* 45, 101–112. doi: 10.1002/dev.20020

Chi, L. P., and Xin, Z. Q. (2003). The revision of children's perception of marital conflict scale. *Chin. Men. Health* 17, 554–556.

Cicchetti, D. (2006). "Development and Psychopathology," in *Developmental Psychopathology: Vol. 1. Theory and methods*, 2nd Edn, eds D. Cicchetti and D. J. Cohen (New York, NY: Wiley), 1–23.

Cicchetti, D., and Rogosch, F. A. (2002). A developmental psychopathology perspective on adolescence. *J. Consult. Clin. Psychol.* 70, 6–20. doi: 10.1037/0022-006X.70.1.6

Cohen, S., Doyle, W. J., and Baum, A. (2006). Socioeconomic status is associated with stress hormones. *Psychosom. Med.* 68, 414–420. doi: 10.1097/01.psy.0000221236.37158.b9

Cui, L., Morris, A. S., Harrist, A. W., Larzelere, R. E., Criss, M. M., and Houltberg, B. J. (2015). Adolescent RSA responses during an anger discussion task: relations to emotion regulation and adjustment. *Emotion* 15, 360–372. doi: 10.1037/emo0000040

Cummings, E. M., and Davies, P. T. (2002). Effects of marital conflict on children: recent advances and emerging themes in process-oriented research. *J. Child Psychol. Psychiatry* 43, 31–63. doi: 10.1111/1469-7610.00003

Cummings, E. M., and Davies, P. T. (2010). *Marital Conflict and Children: an Emotional Security Perspective*. New York, NY: Guilford Press.

Davies, P. T., and Cummings, E. M. (1994). Marital conflict and child adjustment: an emotional security hypothesis. *Psychol. Bull.* 116, 387–411. doi: 10.1037/0033-2909.116.3.387

Davies, P. T., Harold, G. T., Goeke-Morey, M. C., Cummings, E. M., Shelton, K., Rasi, J. A., et al. (2002). Child emotional security and interparental conflict. *Monogr. Soc. Res. Child Dev.* 67, 121–127. doi: 10.1111/1540-5834.00205

Davies, P. T., and Lindsay, L. L. (2004). Interparental conflict and adolescent adjustment: why does gender moderate early adolescent vulnerability? *J. Fam. Psycho.* 18, 160–170. doi: 10.1037/0893-3200.18.1.160

Diamond, L. M., Fagundes, C. P., and Cribbet, M. R. (2012). Individual differences in adolescents' sympathetic and parasympathetic functioning moderate associations between family environment and psychosocial adjustment. *Dev. Psychol.* 48, 918–931. doi: 10.1037/a0026901

Dickerson, S. S., and Kemeny, M. E. (2004). Acute stressors and cortisol responses: a theoretical integration and synthesis of laboratory research. *Psychol. Bull.* 130, 355–391. doi: 10.1037/0033-2909.130.3.355

Dietrich, A., Riese, H., Sondeijker, F. E., Greaves-Lord, K., Ormel, J., Neeleman, J., et al. (2007). Externalizing and internalizing problems in relation to autonomic function: a population-based study in preadolescents. *J. Am. Acad. Child Adolesc. Psychiatry* 6, 378–386. doi: 10.1097/CHI.0b013e31802b91ea

Eisenberg, N., Sulik, M. J., Spinrad, T. L., Edwards, A., Eggum, N. D., Liew, J., et al. (2012). Differential susceptibility and the early development of aggression: interactive effects of respiratory sinus arrhythmia and environmental quality. *Dev. Psycho.* 48, 755–768. doi: 10.1037/a0026518

El-Sheikh, M., Arsiwalla, D. D., Hinnant, J. B., and Erath, S. A. (2011). Children's internalizing symptoms: the role of interactions between cortisol and respiratory sinus arrhythmia. *Physiol. Behav.* 103, 225–232. doi: 10.1016/j.physbeh.2011.02.004

El-Sheikh, M., and Erath, S. A. (2011). Family conflict, autonomic nervous system functioning, and child adaptation: state of the science and future directions. *Dev. Psychopathol.* 23, 703–721. doi: 10.1017/S0954579411000034

El-Sheikh, M., Harger, J., and Whitson, S. (2001). Exposure to parental conflict and children's adjustment and physical health: the moderating role of vagal tone. *Child Dev.* 72, 1617–1636. doi: 10.1111/1467-8624.00369

El-Sheikh, M., Keiley, M., Erath, S., and Dyer, W. J. (2013). Marital conflict and growth in children's internalizing symptoms: the role of autonomic nervous system activity. *Dev. Psychol.* 49, 92–108. doi: 10.1037/a0027703

El-Sheikh, M., and Whitson, S. A. (2006). Longitudinal relations between marital conflict and child adjustment: vagal regulation as a protective factor. *J. Fam. Psychol.* 20, 30–39. doi: 10.1037/0893-3200.20.1.30

Erel, O., and Burman, B. (1995). Interrelatedness of marital relations and parent-child relations: a meta-analytic review. *Psychol. Bull.* 118, 108–132. doi: 10.1037//0033-2909.118.1.108

Fabes, R. A., and Eisenberg, N. (1997). Regulatory control and adults'stress-related responses to daily life events. *J. Pers. Soc. Psycho.* 73, 1107–1117. doi: 10.1037/0022-3514.73.5.1107

Forbes, E. E., Fox, N. A., Cohn, J. F., Galles, S. F., and Kovacs, M. (2006). Children's affect regulation during a disappointment: psychophysiological responses and relation to parent history of depression. *Biol. Psychol.* 71, 264–277. doi: 10.1016/j.biopsycho.2005.05.004

Forns, M., Abad, J., and Kirchner, T. (2012). "Internalizing problems," in *Encyclopedia of Adolescence*, eds J. R. Roger and J. D. Levesque (Berlin: Springer), 1464–1469.

Gentzler, A. L., Santucci, A. K., Kovacs, M., and Fox, N. A. (2009). Respiratory sinus arrhythmia reactivity predicts emotion regulation and depressive symptoms in at-risk and control children. *Biol. Psychol.* 82, 156–163. doi: 10.1016/j.biopsycho.2009.07.002

Graziano, P., and Derefinko, K. (2013). Cardiac vagal control and children's adaptive functioning: a meta-analysis. *Biol. Psychol.* 94, 22–37. doi: 10.1016/j.biopsycho.2013.04.011

Grych, J. H., and Fincham, F. D. (1990). Marital conflict and children's adjustment: a cognitive-contextual framework. *Psychol. Bull.* 108, 267–290. doi: 10.1037/0033-2909.108.2.267

Grych, J. H., and Fincham, F. D. (2001). *Interparental Conflict and Child Development: Theory, Research, and Applications*. New York, NY: Cambridge University Press.

Grych, J. H., Jouriles, E. N., Swank, P. R., McDonald, R., and Norwood, W. D. (2000). Patterns of adjustment among children of battered women. *J. Consult. Clin. Psychol.* 68, 84–94. doi: 10.1037//0022-006x.68.1.84

Hastings, P. D., Sullivan, C., McShane, K. E., Coplan, R. J., Utendale, W. T., and Vyncke, J. D. (2008). Parental socialization, vagal regulation, and preschoolers' anxious difficulties: direct mothers and moderated fathers. *Child Dev.* 79, 45–64. doi: 10.1111/j.1467-8624.2007.01110.x

Hinnant, J. B., and El-Sheikh, M. (2009). Children's externalizing and internalizing symptoms over time: the role of individual differences in patterns of RSA responding. *J. Abnorm. Child Psychol.* 37, 1049–1061. doi: 10.1007/s10802-009-9341-1

Hinnant, J. B., and El-Sheikh, M. (2013). Codevelopment of externalizing and internalizing symptoms in middle to late childhood: sex, baseline respiratory sinus arrhythmia, and respiratory sinus arrhythmia reactivity as predictors. *Dev. Psychopathol.* 25, 419–436. doi: 10.1017/S0954579412001150

Kagan, J., and Fox, N. A. (2007). "Biology, Culture, and Temperamental Biases," in *Handbook of Child Psychology: Vol. 3: Social, Emotional, and Personality Development*, eds N. Eisenberg, W. Damon, and R. L. Lerner (New York, NY: Wiley), 167–225.

Katz, L. F. (2007). Domestic violence and vagal reactivity to peer provocation. *Biol. Psychol.* 74, 154–164. doi: 10.1016/j.biopsycho.2005.10.010

Katz, L. F., and Gottman, J. M. (1997). Buffering children from marital conflict and dissolution. *J. Clin. Child Psychol.* 26, 157–171. doi: 10.1207/s15374424jccp2602_4

Koenig, J., Kemp, A. H., Beauchaine, T. P., Thayer, J. F., and Kaess, M. (2016). Depression and resting state heart rate variability in children and adolescents - a systematic review and meta-analysis. *Clin. Psychol. Rev.* 46, 136–150. doi: 10.1016/j.cpr.2016.04.013

Lang, P. J., Bradley, M. M., and Cuthbert, B. N. (2005). *International Affective Picture System (IAPS): Affective Rating of Pictures and Instruction Manual*. Gainesville, FL: University of Florida Center for Research in Psychophysiology.

Lü, W., Wang, Z. H., and Hughes, B. M. (2016). Openness and physiological responses to recurrent social stress. *Int. J. Psychophysiol.* 106, 135–140. doi: 10.1016/j.ijpsycho.2016.05.004

Lü, W., Xing, W., Hughes, B. M., and Wang, Z. H. (2017). Extraversion and cardiovascular responses to recurrent social stress: effect of stress intensity. *Int. J. Psychophysiol.* 131, 144–151. doi: 10.1016/j.ijpsycho.2017.10.008

Monroe, S. M., and Simons, A. D. (1991). Diathesis-stress theories in the context of life stress research: implication for the depressive disorders. *Psychol. Bull.* 110, 406–425. doi: 10.1037/0033-2909.110.3.406

Nolen-Hoeksema, S., and Girgus, J. S. (1994). The emergence of gender differences in depression during adolescence. *Psychol. Bull.* 115, 424–443. doi: 10.1037/0033-2909.115.3.424

Obradović, J., Bush, N. R., and Boyce, W. T. (2011). The interactive effect of marital conflict and stress reactivity on externalizing and internalizing symptoms: the role of laboratory stressors. *Dev. Psychopathol.* 23, 101–114. doi: 10.1017/S0954579410000672

Obradoviæ, J., Bush, N. R., Stamperdahl, J., Adler, N. E., and Boyce, W. T. (2010). Biological sensitivity to context: the interactive effects of stress reactivity and family adversity on socio-emotional behavior and school readiness. *Child Dev.* 81, 270–289. doi: 10.1111/j.1467-8624.2009.01394.x

Overbeek, T. J. M., van Boxtel, A., and Westerink, J. H. D. M. (2014). Respiratory sinus arrhythmia responses to cognitive tasks: effects of task factors and RSA indices. *Biol. Psychol.* 99, 1–14. doi: 10.1016/j.biopsycho.2014.02.006

Pearson, S. R., Alkon, A., Treadwell, M., Wolff, B., Quirolo, K., and Boyce, W. T. (2005). Autonomic reactivity and clinical severity in children with sickle cell disease. *Clin. Auton. Res.* 15, 400–407. doi: 10.1007/s10286-005-0300-9

Porges, S. W. (1995). Orienting in a defensive world: mammalian modifications of our evolutionary heritage. A polyvagal theory. *Psychophysiology* 32, 301–318. doi: 10.1111/j.1469-8986.1995.tb01213.x

Porges, S. W. (2007). The polyvagal perspective. *Biol. Psychol.* 74, 116–143. doi: 10.1016/j.biopsycho.2006.06.009

Saxbe, D. E., Margolin, G., Spies Shapiro, L. A., and Baucom, B. R. (2012). Does dampened physiological reactivity protect youth in aggressive family environments? *Child Dev.* 83, 821–830. doi: 10.1111/j.1467-8624.2012.01752.x

Scalco, M. D., Colder, C. R., Hawk, L. W., Read, J. P., Wieczorek, W. F., and Lengua, L. J. (2014). Internalizing and externalizing problem behavior and early adolescent substance use: a test of a latent variable interaction and conditional indirect effects. *Psychol. Addict. Behav.* 28, 828–840. doi: 10.1037/a0035805

Schulting, A. B., Malone, P. S., and Dodge, K. A. (2005). The effect of school-based kindergarten transition policies and practices on child academic outcomes. *Dev. Psychol.* 41, 860–871. doi: 10.1037/0012-1649.41.6.860

Segerstrom, S. C., and Nes, L. S. (2007). Heart rate variability reflects self-regulatory strength, effort, and fatigue. *Psycho. Sci.* 18, 275–281. doi: 10.1111/j.1467-9280.2007.01888.x

Shader, T. M., Gatzkekopp, L. M., Crowell, S. E., Jamila, R. M., Thayer, J. F., Vasey, M. W., et al. (2018). Quantifying respiratory sinus arrhythmia: effects of misspecifying breathing frequencies across development. *Dev. Psychopathol.* 30, 351–366. doi: 10.1017/S0954579417000669

Tarvainen, M. P., Ranta-aho, P. O., and Karjalainen, P. A. (2002). An advanced detrending method with application to HRV analysis. *IEEE.Bio-med. Eng.* 49, 172–175. doi: 10.1109/10.979357

Thayer, J. F., Hansen, A. L., Saus-Rose, E., and Johnsen, B. H. (2009). Heart rate variability, prefrontal neural function, and cognitive performance: the neurovisceral integration perspective on self-regulation, adaptation, and health. *Ann. Behav. Med.* 37, 141–153. doi: 10.1007/s12160-009-9101-z

Thayer, J. F., and Lane, R. D. (2000). A model of neurovisceral integration in emotion regulation and dysregulation. *J. Affect. Disord.* 61, 201–216. doi: 10.1016/S0165-0327(00)00338-4

Tu, K. M., Erath, S. A., and El-Sheikh, M. (2016). Coping responses moderate prospective associations between marital conflict and youth adjustment. *J. Fam. Psychol.* 30, 523–532. doi: 10.1037/fam0000169

Wang, R. C., Wang, M. C., Gao, Y. D., Jiang, Y. L., Zhang, X. C., and Yao, S. Q. (2016). Reliability and validity of the Chinese version of achenbach youth self-report (2001 version). *Chin. J. Clin. Psychol* 21, 977–980. doi: 10.16128/j.cnki.1005-3611.2013.06.036

Wei, Z., Fagan, S. E., and Yu, G. (2017). Respiratory sinus arrhythmia activity predicts internalizing and externalizing behaviors in non-referred boys. *Front. Psychol.* 8:1496. doi: 10.3389/fpsyg.2017.01496

Whitson, S. M., and El-Sheikh, M. (2003). Moderators of family conflict and children's adjustment and health. *J. Emot. Abus.* 3, 47–73. doi: 10.1300/J135v03n01_03

Wilcox, R. R. (2012). *Introduction to Robust Estimation and Hypothesis Testing*, 3rd Edn. Cambridge, MA: Academic Press.

Conflict of Interest Statement: The authors declare that the research was conducted in the absence of any commercial or financial relationships that could be construed as a potential conflict of interest.

frontiers in Neuroscience

METHODS
published: 12 June 2019
doi: 10.3389/fnins.2019.00566

A Protocol to Evaluate Retinal Vascular Response Using Optical Coherence Tomography Angiography

David Cordeiro Sousa[1,2,3], Inês Leal[1,2], Susana Moreira[4], Sónia do Vale[5,6], Ana S. Silva-Herdade[7], Patrício Aguiar[8,9], Patrícia Dionísio[4], Luís Abegão Pinto[1,2], Miguel A. R. B. Castanho[7] and Carlos Marques-Neves[1,2]*

[1] Ophthalmology Department, Hospital de Santa Maria, Centro Hospitalar Universitário Lisboa Norte, Lisbon, Portugal, [2] Vision Sciences Study Center, CECV, Faculdade de Medicina, Universidade de Lisboa, Lisbon, Portugal, [3] Manchester Royal Eye Hospital, Manchester University Hospitals NHS Foundation Trust, Manchester, United Kingdom, [4] Respiratory Medicine Department, Hospital de Santa Maria, Centro Hospitalar Universitário Lisboa Norte, Lisbon, Portugal, [5] Endocrinology Department, Hospital de Santa Maria, Centro Hospitalar Universitário Lisboa Norte, Lisbon, Portugal, [6] Endocrinology Department, Faculdade de Medicina, Universidade de Lisboa, Lisbon, Portugal, [7] Instituto de Bioquímica, Instituto de Medicina Molecular, Faculdade de Medicina, Universidade de Lisboa, Lisbon, Portugal, [8] Medicine I Department, Centro Hospitalar Universitário Lisboa Norte, Lisbon, Portugal, [9] Clinica Universitária de Medicina I, Faculdade de Medicina, Universidade de Lisboa, Lisbon, Portugal

OPEN ACCESS

Edited by:
Eugene Golanov, Houston Methodist Hospital, United States

Reviewed by:
Can Ozan Tan, Harvard Medical School, United States
Luiz Roisman, Federal University of São Paulo, Brazil

***Correspondence:**
David Cordeiro Sousa
davidsousa@medicina.ulisboa.pt

Specialty section:
This article was submitted to Autonomic Neuroscience, a section of the journal Frontiers in Neuroscience

Received: *20 March 2019*
Accepted: *17 May 2019*
Published: *12 June 2019*

Citation:
Sousa DC, Leal I, Moreira S, do Vale S, Silva-Herdade AS, Aguiar P, Dionísio P, Abegão Pinto L, Castanho MARB and Marques-Neves C (2019) A Protocol to Evaluate Retinal Vascular Response Using Optical Coherence Tomography Angiography. Front. Neurosci. 13:566. doi: 10.3389/fnins.2019.00566

Introduction: Optical coherence tomography angiography (OCT-A) is a novel diagnostic tool with increasing applications in ophthalmology clinics that provides non-invasive high-resolution imaging of the retinal microvasculature. Our aim is to report in detail an experimental protocol for analyzing both vasodilatory and vasoconstriction retinal vascular responses with the available OCT-A technology.

Methods: A commercial OCT-A device was used (AngioVue®, Optovue, CA, United States), and all examinations were performed by an experienced technician using the standard protocol for macular examination. Two standardized tests were applied: (i) the hypoxia challenge test (HCT) and (ii) the handgrip test, in order to induce a vasodilatory and vasoconstriction response, respectively. OCT-A was performed at baseline conditions and during the stress test. Macular parafoveal vessel density of the superficial and deep plexuses was assessed from the *en face* angiograms. Statistical analysis was performed using STATA v14.1 and $p < 0.05$ was considered for statistical significance.

Results: Twenty-four eyes of 24 healthy subjects (10 male) were studied. Mean age was 31.8 ± 8.2 years (range, 18–57 years). Mean parafoveal vessel density in the superficial plexus increased from 54.7 ± 2.6 in baseline conditions to 56.0 ± 2.0 in hypoxia ($p < 0.01$). Mean parafoveal vessel density in the deep plexuses also increased, from 60.4 ± 2.2 at baseline to 61.5 ± 2.1 during hypoxia ($p < 0.01$). The OCT-A during the handgrip test revealed a decrease in vessel density in both superficial (55.5 ± 2.6 to 53.7 ± 2.9, $p < 0.001$) and deep (60.2 ± 1.8 to 56.7 ± 2.8, $p < 0.001$) parafoveal plexuses.

Discussion: In this work, we detail a simple, non-invasive, safe, and non-costly protocol to assess a central nervous system vascular response (i.e., the retinal circulation)

using OCT-A technology. A vasodilatory response and a vasoconstriction response were observed in two physiologic conditions—mild hypoxia and isometric exercise, respectively. This protocol constitutes a new way of studying retinal vascular changes that may be applied in health and disease of multiple medical fields.

Keywords: optical coherence tomography angiography, retinal vascular response, retinal superficial plexus, retinal deep plexus, hypoxia challenge test, handgrip test, autonomic nervous system

INTRODUCTION

In the central nervous system, the possibility of direct visualization of the vascular system is unique to the retina vessels, which derive from the ophthalmic artery, the first branch of the internal carotid artery. (Riva et al., 2016). As one of the most metabolically active tissues in the body, the retina requires an effective blood flow regulation for its normal functioning (Wei et al., 2018). It has the ability for local autoregulation, which is important to keep blood flow relatively constant despite the variations in perfusion pressure (Arjamaa and Nikinmaa, 2006).

The impairment of the normal retinal vascular response is reported in the early stages of a number of ocular diseases, such as diabetic retinopathy (Nguyen et al., 2009; Pemp et al., 2009; Yau et al., 2012; Ramm et al., 2016), age-related macular degeneration, and glaucoma (Garhöfer et al., 2004; Gugleta et al., 2013). Therefore, the study of retinal vessel behavior and blood flow regulatory function is crucial to increase our knowledge about the mechanisms behind several ocular vascular diseases.

A number of non-invasive methods have been used to for retinal vessels' assessment, including laser Doppler velocimetry (Riva et al., 1985), laser Doppler flowmetry (Riva, 2001; Riva et al., 2010), laser speckle flowgraphy (Tamaki et al., 1994), blue-field entoptoscopy (Riva and Petrig, 1980; Fallon et al., 1985), and color Doppler imaging (Stalmans et al., 2011; Abegao Pinto et al., 2012). However, these devices and techniques are not widely available in clinic, being mostly limited to research purposes (Wang and Luo, 2017; Wei et al., 2018).

Optical coherence tomography angiography (OCT-A) is a novel diagnostic tool with increasing applications in ophthalmology clinics. OCT-A technology uses infrared wavelengths to provide non-invasive, high-contrast, high-resolution imaging of the retinal microvasculature (Koustenis et al., 2017; Spaide et al., 2017; Wei et al., 2018). This technology is an extension of the widely used optical coherence tomography (OCT) and generates images of unprecedented detail by interferometrically measuring the amplitude and delay of reflected or backscattered light from moving erythrocytes. It does so by detecting motion contrast produced by moving blood cells in retinal vessels. Retinal blood flow induces a change between sequential B-scans, while no-flow areas produce no variation. Since no motion in the retina other than blood flow is expected, stationary objects will not produce a significant change in sequential images, while moving objects produce a detectable change. By comparing changes over time, the generated final image clearly defines retinal microvasculature. Recent advances in projection artifact removal allowed researchers to accurately define the deep retinal vascular layers and not only the superficial plexus, overcoming one of its main limitations (Garrity et al., 2017). Its potential for clinical use is tremendous; not only does it allow clinical evaluation of vascular pathologies without the need for invasive procedures, but it can also allow quantitative assessment of the retinal vascular bed. Furthermore, it unlocks new possibilities in detecting functional changes subjects with no visible structural defects.

Our research group has previously reported the potential of OCT-A to detect changes in retinal vessels, having recently published a proof of concept in healthy volunteers to characterize the physiologic retinal vascular response under hypoxic conditions. This work confirmed the ability of this technology to non-invasively detect a significant retinal vasodilatory response to a mild hypoxic stress, in a healthy cohort (Sousa et al., 2017).

Given the reported ability of OCT-A to assess dynamic retinal vascular changes, this manuscript aims to report in detail a protocol for analyzing both vasodilatory and vasoconstriction retinal vascular responses to a standard stimulus with the widely used clinically available OCT-A technology.

MATERIALS AND METHODS

Ethics and Informed Consent

This research protocol follows the tenets of the Declaration of Helsinki (Carlson et al., 2004) and was submitted and approved by the Ethics Committee of Lisbon Academic Medical Center in March 2018. Written informed consent was obtained from all the participants before enrolment, after detailed explanation of the objectives, procedures, and risks of the study. Two standardized tests were applied: i) the hypoxia challenge test (HCT; Vohra and Klocke, 1993) and ii) the handgrip test (Ewing et al., 1985).

As recommended by the Ethics Committee, in order to minimize ethical concerns regarding the HCT, patients and volunteers recruited must had the intention to fly in the future. All the safety recommendations regarding the handgrip test were also followed and the test was stopped if necessary (Ewing et al., 1985). Only the physicians had access to each subject's electronic health records. Medical confidentiality was assured. By agreeing to be part of this study, all the participants had access to a comprehensive ophthalmological exam. At any time, enrolled subjects could anonymously withdraw from the study.

Participants

Twenty-four healthy volunteers were recruited. An anonymous questionnaire was carried out, including the following questions: age, gender, smoking-pack years, known diseases and current chronic medication, previous intraocular surgery or trauma,

symptoms during previous flights, and intention to fly in the future. Subjects were also asked to abstain from alcohol and caffeine for at least 6 h before the study to reduce the possible autonomic effects and measurement bias (Vinader-Caerols et al., 2012) and were instructed to rest for 10 min in a sitting position before the protocol start.

Exclusion ophthalmological criteria were as follows: the presence of significant lens opacities (Lens Opacities Classification System III equal to or higher than stage 2), high refractive error (spherical equivalent below −6.50 or above +4.00 diopters), history of glaucoma or ocular hypertension, neuro-ophthalmic disease, and previous intraocular surgery. Exclusion systemic criteria included the following: hypertension (defined as systolic blood pressure higher than 140 mmHg and diastolic blood pressure higher than 90 mmHg or use of anti-hypertensive drugs), nephropathy or other documented microvascular complication, diabetes mellitus, local or systemic inflammatory diseases, those taking vasoactive drugs, and smokers of more than 20 cigarettes a day. Pregnant women were excluded.

Protocol

Firstly, the study protocol was explained individually to every subject, a written consent was given, and the questionnaire was filled. Then, a complete ophthalmological examination was conducted to all subjects, including best-corrected visual acuity, slit-lamp biomicroscopy with fundoscopy, auto-refractometer (RK-5®, Canon Europe®, The Netherlands), fundus photography (CR-2®, Canon, United States), intraocular pressure, and eye biometry (Lenstar®, Haag-Streit, Switzerland). Other baseline measurements performed included arterial pressure (Carescape®V100, GE Healthcare, Portugal) and pulse oximetry. Room temperature was kept at 22°C, and similar mesopic conditions were adopted throughout the study.

Optical Coherence Tomography Angiography

A commercial OCT-A device was used (AngioVue®, Optovue, CA, United States), which has an A-scan rate of 70,000 A-Scan/s with 5-μm axial resolution and uses the split-spectrum amplitude-decorrelation angiography (SSADA) algorithm, thus enhancing signal-to-noise ratio of flow detection. The device used also included the latest projection artifact removal algorithm, allowing for a more precise deep plexus analysis.

All examinations were performed by an experienced technician at the required timepoints using the standard protocol for macular examination. Two repeated scans were performed at baseline and during the stress test, respectively. Vessel density of the superficial and deep plexuses was assessed from the *en face* angiograms, by analyzing a predefined annulus with an outer diameter of 3 mm and an inner diameter of 1 mm, corresponding to the parafoveal region. This variable was automatically gathered using AngioAnalytics®, the built-in software of the OCT-A device, as a ratio of the white pixels to the total number of pixels (i.e., the proportion of the image occupied by retinal vessels; Yu et al., 2015). Only high-quality images (high signal strength, focused, and without movement artifacts) were considered.

Vasodilatory Response—Hypoxia Challenge Test

The vasodilatory response with retinal blood flow increase in response to a decreased arterial oxygen value has already been reported as a physiologic response, mainly associated with the local release of hypoxia-related metabolites, such as retinal relaxing factor, prostacyclin, and lactate (Pournaras et al., 2008; Cheng et al., 2016).

The following protocol was designed in order to comparatively characterize with OCT-A the retinal vessel density changes induced under hypoxia conditions using HCT as a hypoxic stress test. The HCT is performed at sea level in order to create a normobaric hypoxic environment by reducing FiO_2 and making it equivalent to the flight cabin values. The British Thoracic Society (BTS) proposes a practical and inexpensive protocol to perform HCT (Vohra and Klocke, 1993). Briefly, participants had to breathe FiO_2 of 15% by using a gas mixture with a supply of 99.993% nitrogen (Linde Healthcare®, Portugal) through a 40% flow Venturi mask (Intersurgical®, United Kingdom) at 10 L/min. Cardiorespiratory monitoring during HCT was performed using a polygraph and an oximeter in a hand finger (Alice PDX, Philips-Respironics®, United States). The parameters monitored during HCT were oxygen peripheral saturation, arterial pressure, and continuous electrocardiography.

As established by the BTS, the recommended HCT duration to obtain stable conditions is 20 min. Accordingly, OCT-A was performed at baseline and then, again, 30 min after HCT start, under the described hypoxic conditions. Then, the Venturi mask and cardiorespiratory monitoring devices were withdrawn. All symptoms were recorded, and the test was stopped if medically necessary.

Vasoconstrictive Response—Handgrip Test

The handgrip test, as an isometric exercise, is a sympatheticomimetic test causing steady and safe increases in heart rate and arterial pressure. The associated physiologic retinal vascular response consists in a vasoconstriction response (Ewing et al., 1985; Blum et al., 1999; Zhang et al., 2012).

The following protocol was conducted after having been previously explained in detail to all participants. Subjects sat in a chair in front of the OCT-A device, with the forearm in neutral position, the elbow flexed at 90°, and the wrist with the thumb facing upward. The participants were asked to hold a Jamar hydraulic dynamometer, and maximal grip force (MGF) was calculated with the dominant arm. Systemic blood pressure was monitored in the contralateral arm. The participants were then instructed to relax and place the chin in the OCT-A chinstrap and be prepared for examination. When ready, a voice signal requested the participant to keep a steady contraction of at least one-third of the maximal calculated force (monitored by an investigator). After 90 s, the OCT-A acquisition started, completed for both eyes within the 3- to 5-min handgrip test. The arterial pressure in the contralateral arm was measured every minute and registered. According to the handgrip test recommendations (Ewing et al., 1985), if a diastolic blood pressure higher than 120 mmHg and/or any adverse symptom was registered, the test was interrupted. The procedure was

repeated after a 15-min resting time if any reliability-limiting situation occurred.

Statistics

Statistical analysis was performed using STATA v14.1. A repeated-measures ANOVA model was used to assess differences between the baseline and stress measurements. The Shapiro–Wilk and skewness/kurtosis test suggested the normal distribution of the variables considered, and the inexistence of significant outlier values was also confirmed. Equality of variances was investigated, and the results were reported accordingly, applying the Greenhouse–Geisser correction when variables' variances were not equal. $p < 0.05$ was considered for statistical significance. To guarantee independence of observations, only the right eye of each patient was considered for analysis.

RESULTS

Demographics and Baseline Data

Twenty-four eyes of 24 healthy subjects (10 male) were studied. Mean age was 31.8 ± 8.2 years (range, 18–57 years). Mean best-corrected visual acuity was 0.0 LogMar, mean intraocular pressure was 13.3 ± 2.1 mmHg (range, 10–18 mmHg), with a mean spherical equivalent of −1.3 ± 1.8 D (range, −5 to 2 D) and mean axial length of 24.12 ± 0.9 mm (range, 22.5–25.9 mm). Mean body mass index was 22.6 ± 3.0 kg/m^2 (range, 18.6–28.7 kg/m^2).

Vasodilatory Response—Hypoxia Challenge Test

The peripheral oxygen saturation decreased from 98 ± 1% to stable minimum values of 87 ± 2% during HCT (**Table 1**). The mean parafoveal vessel density in the superficial plexus increased from 54.7 ± 2.6 in baseline conditions to 56.0 ± 2.0 in hypoxia ($F_{1,23} = 15.69$, $p < 0.001$). The mean parafoveal vessel density in the deep plexuses also increased, from 60.4 ± 2.2 at baseline to 61.5 ± 2.1 during hypoxia ($F_{1,23} = 16.26$, $p < 0.001$) (**Table 1**). The increase in vessel density was observed in 22 (92%) of the 24 eyes in both plexuses.

TABLE 1 | Systemic variables and retinal vascular response to the hypoxia challenge test.

		Baseline	Hypoxia	*p*-value
SAP (mmHg)		118 ± 11	114 ± 10	0.15
DAP (mmHg)		75 ± 9	75 ± 10	0.29
MAP (mmHg)		89 ± 9	88 ± 9	0.97
Heart rate (bpm)		64 ± 8	76 ± 12	0.03
O_2 Hb saturation (%)		98 ± 1	87 ± 2	<0.0001
Parafoveal vessel density	Superficial plexus	54.7 ± 2.6	56.0 ± 2.0	<0.001
	Deep plexus	60.4 ± 2.2	61.5 ± 2.1	<0.001

Mean values and standard deviations are presented. bpm, beats per minute; DAP, diastolic arterial pressure; Hb, hemoglobin; MAP, mean arterial pressure; SAP, systolic arterial pressure.

Vasoconstrictive Response—Handgrip Test

As depicted in **Table 2**, the handgrip test was associated with an expected heart rate and systolic and diastolic blood pressure increase compared to baseline (all $p < 0.001$).

The OCT-A during the handgrip test revealed that isometric exercise elicited a decrease in vessel density in both superficial (55.5 ± 2.6 to 53.7 ± 2.9, $F_{1,23} = 27.37$, $p < 0.0001$) and deep (60.2 ± 1.8 to 56.7 ± 2.8, $F_{1,23} = 27.90$, $p < 0.0001$) parafoveal plexuses (**Table 2**). The decrease in vessel density was observed in 22 (92%) and 23 (96%) of the 24 eyes in the superficial and deep plexuses, respectively.

Regarding the systemic response, the mean percent increase in mean arterial pressure and heart rate was 32 ± 1.7% and 23 ± 1.7%, respectively. **Table 2** summarizes both OCT-A and cardiovascular response findings to the handgrip test.

DISCUSSION

As an energy-demanding tissue, the retina blood flow autoregulatory mechanisms are crucial to keep blood flow relatively constant despite the variations in perfusion pressure (Arjamaa and Nikinmaa, 2006; Wei et al., 2018). In this study with OCT-A, we report a standardized, reliable, and non-invasive way of studying retinal vascular vasodilatory and vasoconstrictive responses to hypoxia and isometric exercise, respectively.

Despite the constant blood flow thought to be provided by the choroidal circulation, retinal vessels are believed to present a large reserve for vasodilation and vasoconstriction in order to balance changes in the arterial pressure of oxygen (Geiser et al., 2000; Cheng et al., 2016). The encountered vasodilatory response under mild hypoxic conditions is consistent with the findings of previous studies using different technologies, such as blue-field entoptic phenomenon and scanning laser Doppler flowmetry (Fallon et al., 1985; Strenn et al., 1997). The stress test used

TABLE 2 | Systemic variables and retinal vascular response to the handgrip test.

		Baseline	Handgrip	*p*-value
SAP (mmHg)		117 ± 12	150 ± 18	<0.0001
DAP (mmHg)		78 ± 10	102 ± 14	<0.0001
MAP (mmHg)		91 ± 10	118 ± 15	<0.0001
Heart rate (bpm)		64 ± 8	78 ± 10	<0.0001
Parafoveal vessel density	Superficial plexus	55.5 ± 2.6	53.7 ± 2.9	<0.0001
	Deep plexus	60.2 ± 1.8	56.7 ± 2.8	< 0.0001

Mean values and standard deviations are presented. Bpm, beats per minute; DAP, diastolic arterial pressure; MAP, mean arterial pressure; SAP, systolic arterial pressure.

in our study, HCT, consistently induced the expected systemic responses, with an increase in heart rate accompanying the hypoxemia. A few OCT-A studies have been published reporting the vasoconstrictive response to hyperoxia (Xu et al., 2016; Hagag et al., 2018). However, to the best of our knowledge, our group was the first to report the vasodilatory response to hypoxia, using the standardized HCT as the hypoxic stimulus.

Although it is believed that autonomic innervation of retinal vasculature is not significant (Pournaras et al., 2008; McDougal and Gamlin, 2015), the vasoconstrictive response to isometric exercise was clearly observed in our study. This response was associated with the expected sympathetic nervous system induced increase in arterial blood pressure and heart rate. As previously described, this regulation should be, at least partially, induced by the local response to the increase in arterial pressure—the Bayliss effect in retinal autoregulation (Robinson et al., 1986; Blum et al., 1999). This observed vasoconstrictive response in retinal vessels is similar to the one described in peripheral arteries' behavior (Ewing et al., 1985). However, with still so much to unveil about mechanisms behind the retinal autoregulation, we are not able to definitely attribute this retinal vascular response to a specific factor.

For both retinal vascular responses, the differences observed in our sample were striking and quite homogeneous, with more than 90% of the subjects presenting a similar vessel density change in both plexuses. This reinforces the potential of the above-described protocol as a repeatable method for the evaluation of retinal vascular function, in a healthy retina and possibly in a pathologic vascular setting as well. Although the clinical significance of the statistically significant findings encountered should be discussed, the magnitude of change we encountered is comparable to other OCT-A studies. For example (Simonett et al., 2017) were able to distinguish a healthy cohort from patients with no or mild diabetic retinopathy with changes in vessel density similar in magnitude to the ones reported in our study.

In a recent study, Hagag et al. have demonstrated a reduction on the flow index and vessel density (−7.8%) of the deep capillary plexus only and in the flow index of the all-plexus slab measured by OCT-A with hyperoxia. These authors describe an approach to induce hyperoxia that consists in fitting a simple face mask and giving supplemental oxygen for 10 min at a flow rate of 15 L/min, which delivers 60–90% oxygen in the inspired oxygen, therefore creating a systemic hyperoxic condition (Hagag et al., 2018). In contrast, in our work, in order to induce vasoconstriction, we used the handgrip test. We found a significant decrease in the vessel density of both superficial and deep plexus, although with a lower magnitude of change, as detailed in **Table 2**. The small sample in the work of Hagag et al. and the fact that another vasoconstrictor stimulus (with a different physiologic mechanism) was chosen may have contributed to this difference. These results should be validated by performing both tests (induced hyperoxia and handgrip tests) and comparing the retinal vascular response with OCT-A technology.

Regarding the vasodilatory response, an alternative method that could be considered to induce retinal vessel dilation is the hypercapnia test, as described elsewhere (Raurich et al., 2008, 2009). However, compared to our choice to induce a safe level of hypoxia, this test involves re-inhalation of expired air by inserting a length of corrugated tube between the Y-piece and the endotracheal tube, which increases the deadspace by a volume similar to the tidal volume (V_T) obtained with a pressure support of 7 cmH_2O (Raurich et al., 2009). Comparatively, we believe that our work presents a simpler, safer, and reproducible methodology to induce a detectable vasodilation in the retina using OCT-A.

After establishing a protocol to evaluate retinal vascular response with OCT-A, it will be possible to study not only the healthy eye but also responses in a compromised vascular setting, such as in diabetic retinopathy, age-related macular degeneration, and glaucoma. We hypothesize that local factors may play a crucial role when it comes to the retinal vascular regulation and responses in metabolic diseases. In fact, a recent thesis (Eliasdottir, 2018) has suggested that retinal autoregulation is mostly due to myogenic and metabolic factors in order to accommodate local blood flow to differences in perfusion pressure and metabolic needs. In this context, we think that this protocol, once established, could be used to assess functional changes in the retinal vascular physiology before clinically detectable diseases, taking the paradigmatic example of DR.

In summary, this work details a simple, non-invasive, safe, and non-costly method to assess vascular changes in healthy subjects that can be the stepping stone for several experiments. It has gone some way toward enhancing our understanding of possible and reproducible methods to induce and detect vasoconstriction and vasodilation in retinal vessels. Because OCT-A technology and devices are increasingly used in ophthalmology, we hope that our research will serve as an encouragement for the development of technology capable of dynamically assessing the vascular response in opposition to static images only. In fact, and contrary to other devices with mainly research purposes, OCT-A technology is easy to use and increasingly available in ophthalmology clinical practice worldwide (Sadda, 2017) and therefore we think that establishing a protocol with an available tool will have an impact in the neurosciences community.

Limitations

As a first limitation of our study, we should mention the relatively small sample size, which limits association analysis with demographic and ophthalmic features of the participants. Secondly, the current OCT-A technology is still evolving and one should be careful in the interpretation of the findings and their magnitude. As an example, with the current device, we are not able to estimate absolute blood flow values, but only *perfused vessel densities*. Thirdly, in both protocols, there is an autonomic nervous system activation and, therefore, we are not able to isolate the factor inducing the retinal vascular response from the autonomic-related vascular consequences. Moreover, despite reporting statistical significance in the parafoveal vessel density means in response to both the hypoxic and handgrip tests, we are unsure of the clinical significance of these differences. In fact, there are no current data in literature to indicate what would normal inter-exam variation be when calculating parafoveal vessel density. To be able to comment more accurately about the obtained results, it is essential to know the error associated with the built-in software and then be able to distinguish

clinical change from measurement variability. Assessing the reproducibility of these measurements would then be a next step to overcome this caveat (Bland and Altman, 1996). With this study, we expect to promote the development of the technology in order to allow for larger studies to confirm our results with a dynamic (and continuous, ideally) analysis of retinal vascular responses in health and disease, with potentially relevant diagnostic and therapeutic implications.

CONCLUSION

This study on human volunteers constitutes a proof of concept on how to evaluate a central nervous system response (i.e., the retinal circulation) in two physiologic conditions—hypoxia and isometric exercise. The importance of identifying such a response with a rapid, non-invasive, and reliable technology used in clinical practice—OCT-A—may be a stepping stone for new lines of research not only in ophthalmology, but also in physiology and neuroscience.

DATA AVAILABILITY

The datasets generated for this study are available on request to the corresponding author.

ETHICS STATEMENT

This research protocol follows the tenets of the Declaration of Helsinki (Carlson et al., 2004) and was submitted and approved by the Ethics Committee of Lisbon Academic Medical Center in March 2018. Written informed consent was obtained from all the participants before enrolment, after detailed explanation of the objectives, procedures and risks of the study. Two standardized tests were applied: (i) the hypoxia challenge test (HCT; Vohra and Klocke, 1993), and (ii) the handgrip test (Ewing et al., 1985).

AUTHOR CONTRIBUTIONS

All authors were involved in the design of the study, contributed to the manuscript writing, and approved the submitted version. DS, IL, SM, SdV, PD, LP, and CM-N were specifically involved in participants' recruitment, coordination of the study logistics, and preparation and conduction of the protocol. SM and PD were responsible for the hypoxia challenge test protocol. PA provided the equipment and gave support and know-how regarding the handgrip test. DS and CM-N applied the test.

FUNDING

This study was supported by the Faculty of Medicine of the University of Lisbon, AstraZeneca Foundation – 14th Grant.

ACKNOWLEDGMENTS

The authors would like to thank Faculty of Medicine of the University of Lisbon, AstraZeneca Foundation for funding, as well as the technicians involved in the study: Diana Francisco, Sofia Silva, and Telma Gala. The authors would also like to thank Professor J. L. Ducla-Soares and the Autonomic Nervous System Department of Lisbon Academic Medical Center for all the support, as well as José Cotta for providing the necessary equipment and logistic backing for the study.

REFERENCES

Abegao Pinto, L., Vandewalle, E., De Clerck, E., Marques-Neves, C., and Stalmans, I. (2012). Ophthalmic artery Doppler waveform changes associated with increased damage in glaucoma patients. *Invest. Ophthalmol. Vis. Sci.* 53, 2448–2453. doi: 10.1167/iovs.11-9388

Arjamaa, O., and Nikinmaa, M. (2006). Oxygen-dependent diseases in the retina: role of hypoxia-inducible factors. *Exp. Eye Res.* 83, 473–483. doi: 10.1016/j.exer.2006.01.016

Bland, J. M., and Altman, D. G. (1996). Measurement error. *BMJ* 312:1654.

Blum, M., Bachmann, K., Wintzer, D., Riemer, T., Vilser, W., and Strobel, J. (1999). Noninvasive measurement of the Bayliss effect in retinal autoregulation. *Graefe's Arch. Clin. Exp. Ophthalmol.* 237, 296–300. doi: 10.1007/s004170050236

Carlson, R. V., Boyd, K. M., and Webb, D. J. (2004). The revision of the declaration of Helsinki: past, present and future. *Br. J. Clin. Pharmacol.* 57, 695–713. doi: 10.1111/j.1365-2125.2004.02103.x

Cheng, R. W., Yusof, F., Tsui, E., Jong, M., Duffin, J., Flanagan, J. G., et al. (2016). Relationship between retinal blood flow and arterial oxygen. *J. Physiol.* 594, 625–640. doi: 10.1113/JP271182

Eliasdottir, T. S. (2018). Retinal oximetry and systemic arterial oxygen levels. *Acta Ophthalmol.* 96(Suppl. A113), 1–44. doi: 10.1111/aos.13932

Ewing, D. J., Martyn, C. N., Young, R. J., and Clarke, B. F. (1985). The value of cardiovascular autonomic function tests: 10 years experience in diabetes. *Diabetes Care* 8, 491–498. doi: 10.2337/diacare.8.5.491

Fallon, T. J., Maxwell, D., and Kohner, E. M. (1985). Retinal vascular autoregulation in conditions of hyperoxia and hypoxia using the blue field entoptic phenomenon. *Ophthalmology* 92, 701–705. doi: 10.1016/s0161-6420(85)33978-7

Garhöfer, G., Zawinka, C., Resch, H., Kothy, P., Schmetterer, L., and Dorner, G. T. (2004). Reduced response of retinal vessel diameters to flicker stimulation in patients with diabetes. *Br. J. Ophthalmol.* 88, 887–890.

Garrity, S. T., Iafe, N. A., Phasukkijwatana, N., Chen, X., and Sarraf, D. (2017). Quantitative analysis of three distinct retinal capillary plexuses in healthy eyes using optical coherence tomography angiography. *Invest. Ophthalmol. Vis. Sci.* 58, 5548–5555. doi: 10.1167/iovs.17-22036

Geiser, M. H., Riva, C. E., Dorner, G. T., Diermann, U., Luksch, A., and Schmetterer, L. (2000). Response of choroidal blood flow in the foveal region to hyperoxia and hyperoxia-hypercapnia. *Curr. Eye Res.* 21, 669–676. doi: 10.1076/0271-3683(200008)21:2;1-v;ft669

Gugleta, K., Waldmann, N., Polunina, A., Kochkorov, A., Katamay, R., Flammer, J., et al. (2013). Retinal neurovascular coupling in patients with glaucoma, and ocular hypertension, and its association with the level of glaucomatous damage. *Graefe's Arch. Clin. Exp. Ophthalmol.* 251, 1577–1585. doi: 10.1007/s00417-013-2276-9

Hagag, A. M., Pechauer, A. D., Liu, L., Wang, J., Zhang, M., Jia, Y., et al. (2018). OCT angiography changes in the 3 parafoveal retinal plexuses in response to hyperoxia. *Ophthalmol. Retina* 2, 329–336. doi: 10.1016/j.oret.2017.07.022

Koustenis, A., Harris, A., Gross, J., Januleviciene, I., Shah, A., and Siesky, B. (2017). Optical coherence tomography angiography: an overview of the technology

and an assessment of applications for clinical research. *Br. J. Ophthalmol.* 101, 16–20. doi: 10.1136/bjophthalmol-2016-309389

McDougal, D. H., and Gamlin, P. D. (2015). Autonomic control of the eye. *Compr. Physiol.* 5, 439–473. doi: 10.1002/cphy.c140014

Nguyen, T. T., Kawasaki, R., Jie, J. W., Kreis, A. J., Shaw, J., Vilser, W., et al. (2009). Flicker light-induced retinal vasodilation in diabetes and diabetic retinopathy. *Diabetes Care* 32, 2075–2080. doi: 10.2337/dc09-0075

Pemp, B., Garhofer, G., Weigert, G., Karl, K., Resch, H., Wolzt, M., et al. (2009). Reduced retinal vessel response to flicker stimulation but not to exogenous nitric oxide in type 1 diabetes. *Invest. Ophthalmol. Vis. Sci.* 50, 4029–4032.

Pournaras, C. J., Rungger-Brändle, E., Riva, C. E., Hardarson, S. H., and Stefansson, E. (2008). Regulation of retinal blood flow in health and disease. *Prog. Retin. Eye Res.* 27, 284–330. doi: 10.1016/j.preteyeres.2008.02.002

Ramm, L., Jentsch, S., Peters, S., Sauer, L., Augsten, R., and Hammer, M. (2016). Dependence of diameters and oxygen saturation of retinal vessels on visual field damage and age in primary open-angle glaucoma. *Acta Ophthalmol.* 94, 276–281. doi: 10.1111/aos.12727

Raurich, J. M., Rialp, G., Ibáñez, J., Ayestarán, I., Llompart-Pou, J. A., and Togores, B. (2009). Hypercapnia test and weaning outcome from mechanical ventilation in COPD patients. *Anaesth. Intensive Care* 37, 726–732. doi: 10.1177/0310057x0903700507

Raurich, J. M., Rialp, G., Ibáñez, J., Campillo, C., Ayestarán, I., and Blanco, C. (2008). Hypercapnia test as a predictor of success in spontaneous breathing trials and extubation. *Respir. Care* 53, 1012–1018.

Riva, C. E. (2001). Basic principles of laser Doppler flowmetry and application to the ocular circulation. *Int. Ophthalmol.* 23, 183–189.

Riva, C. E., Alm, A., and Pournaras, C. J. (2016). "Ocular circulation," in *Adler's Physiology of the Eye*. 11th Edn, eds L. A. Levin, S. F. E. Nilsson, J. Ver Hoeve, and S. M. Wu (Philadelphia: Saunders/Elsevier), 243–273.

Riva, C. E., Geiser, M., and Petrig, B. L. (2010). Ocular blood flow assessment using continuous laser Doppler flowmetry. *Acta Ophthalmol.* 88, 622–629. doi: 10.1111/j.1755-3768.2009.01621.x

Riva, C. E., Grunwald, J. E., Sinclair, S. H., and Petrig, B. L. (1985). Blood velocity and volumetric flow rate in human retinal vessels. *Invest. Ophthalmol. Vis. Sci.* 26, 1124–1132.

Riva, C. E., and Petrig, B. (1980). Blue field entoptic phenomenon and blood velocity in the retinal capillaries. *J. Opt. Soc. Am.* 70, 1234–1238.

Robinson, F., Riva, C. E., Grunwald, J. E., Petrig, B. L., and Sinclair, S. H. (1986). Retinal blood flow autoregulation in response to an acute increase in blood pressure. *Invest. Ophthalmol. Vis. Sci.* 27, 722–726.

Sadda, S. V. R. (2017). Defining the role of OCT angiography in clinical practice. *Ophthalmol. Retin.* 1, 261–262. doi: 10.1016/j.oret.2017.05.001

Simonett, J. M., Scarinci, F., Picconi, F., Giorno, P., De Geronimo, D., Di Renzo, A., et al. (2017). Early microvascular retinal changes in optical coherence tomography angiography in patients with type 1 diabetes mellitus. *Acta Ophthalmol.* 95, e751–e755. doi: 10.1111/aos.13404

Sousa, D. C., Leal, I., Moreira, S., Dionísio, P., Abegão Pinto, L., and Marques-Neves, C. (2017). Hypoxia challenge test and retinal circulation changes - a study using ocular coherence tomography angiography. *Acta Ophthalmol.* 96, e315–e319. doi: 10.1111/aos.13622

Spaide, R. F., Fujimoto, J. G., Waheed, N. K., Sadda, S. R., and Staurenghi, G. (2017). Optical coherence tomography angiography. *Prog. Retin. Eye Res.* 64, 1–55. doi: 10.1016/j.preteyeres.2017.11.003

Stalmans, I., Vandewalle, E., Anderson, D. R., Costa, V. P., Frenkel, R. E. P., Garhofer, G., et al. (2011). Use of colour Doppler imaging in ocular blood flow research. *Acta Ophthalmol.* 89, e609–e630. doi: 10.1111/j.1755-3768.2011.02178.x

Strenn, K., Menapace, R., Rainer, G., Findl, O., Wolzt, M., and Schmetterer, L. (1997). Reproducibility and sensitivity of scanning laser Doppler flowmetry during graded changes in Po2. *Br. J. Ophthalmol.* 81, 360–364. doi: 10.1136/bjo.81.5.360

Tamaki, Y., Araie, M., Kawamoto, E., Eguchi, S., and Fujii, H. (1994). Noncontact, two-dimensional measurement of retinal microcirculation using laser speckle phenomenon. *Invest. Ophthalmol. Vis. Sci.* 35, 3825–3834.

Vinader-Caerols, C., Monleón, S., Carrasco, C., and Parra, A. (2012). Effects of alcohol, coffee, and tobacco, alone or in combination, on physiological parameters and anxiety in a young population. *J. Caffeine Res.* 2, 70–76. doi: 10.1089/jcr.2012.0018

Vohra, K. P., and Klocke, R. A. (1993). Detection and correction of hypoxemia associated with air travel. *Am. Rev. Respir. Dis.* 148, 1215–1219. doi: 10.1164/ajrccm/148.5.1215

Wang, Y., and Luo, Y. (2017). The applications of optical coherence tomography angiography in diabetic retinopathy. *Ann. Eye Sci.* 2:52. doi: 10.21037/aes.2017.06.08

Wei, X., Balne, P. K., Meissner, K. E., Barathi, V. A., Schmetterer, L., and Agrawal, R. (2018). Assessment of flow dynamics in retinal and choroidal microcirculation. *Surv. Ophthalmol.* 63, 646–664. doi: 10.1016/j.survophthal.2018.03.003

Xu, H., Deng, G., Jiang, C., Kong, X., Yu, J., and Sun, X. (2016). Microcirculatory responses to hyperoxia in macular and peripapillary regions. *Invest. Ophthalmol. Vis. Sci.* 57, 4464–4468. doi: 10.1167/iovs.16-19603

Yau, J. W. Y., Rogers, S. L., Kawasaki, R., Lamoureux, E. L., Kowalski, J. W., Bek, T., et al. (2012). Global prevalence and major risk factors of diabetic retinopathy. *Diabetes Care* 35, 556–564. doi: 10.2337/dc11-1909

Yu, J., Jiang, C., Wang, X., Zhu, L., Gu, R., Xu, H., et al. (2015). Macular perfusion in healthy chinese: an optical coherence tomography angiogram study. *Invest. Ophthalmol. Vis. Sci.* 56, 3212–3217.

Zhang, Y., Emeterio Nateras, O. S., Peng, Q., Rosende, C. A., and Duong, T. Q. (2012). Blood flow MRI of the human retina/choroid during rest and isometric exercise. *Invest. Ophthalmol. Vis. Sci.* 53, 4299–4305. doi: 10.1167/iovs.11-9384

Conflict of Interest Statement: The authors declare that the research was conducted in the absence of any commercial or financial relationships that could be construed as a potential conflict of interest.

frontiers in Neuroscience

REVIEW
published: 13 June 2019
doi: 10.3389/fnins.2019.00535

The Central Autonomic Network and Regulation of Bladder Function

Holly Ann Roy[1] *and Alexander L. Green*[2]*

[1] Department of Neurosurgery, Plymouth Hospitals NHS Trust, Plymouth, United Kingdom, [2] Nuffield Department of Surgical Sciences, Medical Sciences Division, University of Oxford, Oxford, United Kingdom

The autonomic nervous system (ANS) is involved in the regulation of physiologic and homeostatic parameters relating particularly to the visceral organs and the co-ordination of physiological responses to threat. Blood pressure and heart rate, respiration, pupillomotor reactivity, sexual function, gastrointestinal secretions and motility, and urine storage and micturition are all under a degree of ANS control. Furthermore, there is close integration between the ANS and other neural functions such as emotion and cognition, and thus brain regions that are known to be important for autonomic control are also implicated in emotional functions. In this review we explore the role of the central ANS in the control of the bladder, and the implications of this for bladder dysfunction in diseases of the ANS.

Keywords: bladder, autonomic, periaquecductal gray, multiple system atrophy, Parkinson's disease

OPEN ACCESS

Edited by:
Janet R. Keast,
The University of Melbourne, Australia

Reviewed by:
Naoki Yoshimura,
University of Pittsburgh, United States
Stephen A. Zderic,
Children's Hospital of Philadelphia, United States
Jonathan M. Beckel,
University of Pittsburgh, United States

***Correspondence:**
Alexander L. Green
alex.green@nds.ox.ac.uk

Specialty section:
This article was submitted to Autonomic Neuroscience, a section of the journal Frontiers in Neuroscience

Received: *07 January 2019*
Accepted: *08 May 2019*
Published: *13 June 2019*

Citation:
Roy HA and Green AL (2019) The Central Autonomic Network and Regulation of Bladder Function. Front. Neurosci. 13:535. doi: 10.3389/fnins.2019.00535

INTRODUCTION

Normal bladder function in the mature human relies on integration between the autonomic and somatic nervous systems. In disease, and during development, the balance may be altered so that the autonomic nervous system (ANS) plays an increased or altered role in bladder control. However, most studies highlight the role of the ANS in bladder control at the level of peripheral nerve and spinal networks, neglecting the role of supraspinal autonomic nuclei. In this review we describe the anatomic distribution of the central autonomic network (CAN), and then discuss what is known about the supraspinal control of the bladder, and consider the overlap between the CAN and central bladder network. Finally, we consider the implications of central autonomic bladder centers for our understanding of diseases affecting the bladder.

SUPRASPINAL NEURAL ORGANIZATION OF AUTONOMIC CONTROL

Collectively, the network of brain areas involved in maintaining and regulating the ANS is known as the 'central autonomic network' (CAN). Important progress in our understanding of the anatomy and function of the CAN in the human has been made in recent years, including its role in other neural functions such as emotion and cognition (Critchley and Garfinkel, 2015). Much of this progress is due to developments in neuroimaging techniques (Hyam et al., 2012; Macey et al., 2016). Furthermore, modulation of activity within the CAN at specifically selected anatomic targets, using deep brain stimulation (DBS), offers a possible means of altering or modifying autonomic functions in human patients, and carefully observed studies of autonomic side effects arising from

DBS for other indications, have made it possible to experimentally test the effects of DBS on the ANS (Lovick, 2014).

Regulation of autonomic function occurs via the interaction of various brain structures, which contribute to the CAN. Functions of the CAN include regulating the balance of sympathetic and parasympathetic activity at any one time. This regulation can occur as part of feedback loops that are specific to selected organ systems, or secondary to central command mechanisms which are generated by higher cortical areas, for example, as occurs in preparation for exercise (Basnayake et al., 2012). Brainstem sites that are important for autonomic outflow include the locus coeruleus, the parabrachial nucleus of the pons (Loewy, 1991; Napadow et al., 2008), and various nuclei within the medulla including sympathetic outflow pathways in the ventral medulla, the caudal and rostroventral medulla (Loewy, 1982; Gianaros et al., 2012) and parasympathetic outflow nuclei including the nucleus ambiguus and the dorsal motor nucleus (Gianaros et al., 2012). Important subcortical autonomic input nuclei include the nucleus of the solitary tract (NTS) in the medulla, which receives afferent input from the sympathetic and parasympathetic systems, and from baroreceptors and chemoreceptors. The interaction between midbrain, diencephalic and forebrain structures and the brainstem autonomic nuclei are extensive. The role of these regions has been extensively studied in animal recording and lesion studies as well as human cases of stroke and other lesions. Now, autonomic challenges can be applied during functional magnetic resonance imaging (fMRI) to study neural changes associated with autonomic activation in the human. Autonomic challenges include the Valsalva maneuver and handgrip challenges (Saito et al., 1986), forehead, foot or hand cold pressor tests (Macey et al., 2014) and end-expiratory breath hold challenges, which produce sympathetic excitation (Zubin Maslov et al., 2014). These tasks typically induce global changes in blood oxygenation and blood flow in addition to local changes related to increased or decreased neural activation, thus, the global changes are typically excluded from analyses as confounding factors (Macey et al., 2016). fMRI has been particularly useful for investigating the role of cortical structures in autonomic control.

One important cortical region in higher response to autonomic challenges is the insula (Napadow et al., 2008; Al-Otaibi et al., 2010; Critchley et al., 2015; Macey et al., 2016). The insular cortex is buried within the lateral sulcus, and is overlain by and intimately related to, the parietal opercula, whose gyri and sulci interdigitate with those of the insula (Ture et al., 1999). Its activity may affect autonomic outflow via connections to thalamic, limbic and brainstem regions, including the hypothalamus (Allen et al., 1991). Certain fMRI paradigms, using a foot cold pressor challenge, handgrip task (both with predominantly sympathetic components) and Valsalva maneuvre (activating both sympathetic and parasympathetic pathways) have demonstrated a topographical organization of autonomic response within the insula, with an anteroposterior and lateralized differentiation of responses over the 5 gyri of the insula and the two brain hemispheres (Macey et al., 2012) and a unique pattern of activation associated with each task.

The cingulate cortex has also been established as a key region for autonomic response with anterior, mid and posterior cingulate cortex showing differential involvement. For example, posterior cingulate cortex activity has been associated with a withdrawal or reduction in parasympathetic activity (O'Connor et al., 2007; Wong et al., 2007), while anterior cingulate cortex activity has been correlated with sympathetic nervous system activity using pupillary dilatation and skin conductance to infer sympathetic activation (Nagai et al., 2004; Critchley et al., 2005). Stressor-evoked suppression of baroreflex sensitivity was found to co-vary with signal in the perigenual anterior cingulate cortex, dorsal anterior cingulate cortex and posterior cingulate cortex (Gianaros et al., 2012), as well as producing increased functional connectivity between the perigenual ACC and the amygdala, periaqueductal gray area (PAG), and pons.

The hippocampus and amygdala both respond to changes related to activation of the sympathetic nervous system, such as blood pressure challenges (Harper et al., 2000) and tasks evoking effortful stress (Critchley et al., 2000). Their activity has also been shown to correlate with changes in a heart rate variability derived high frequency regressor, which is thought to provide an indication of parasympathetic output to the heart (Napadow et al., 2008). Both amygdala and hippocampus are activated in tasks involving the Valsalva maneuver (Harper et al., 1998; Henderson et al., 2002); the amygdala during hypoxic breathing challenge (Critchley et al., 2015), and the hippocampus in tasks involving inspiratory resistance (Faull et al., 2016). Interestingly, feedback from the ANS modulates activation of these regions in response to an emotional fear task: both amygdala and hippocampus demonstrated a significant main effect of cardiac cycle (systole/diastole) in their response to fearful stimuli (Garfinkel et al., 2014).

Other cortical regions that have been implicated in autonomic function include the ventromedial prefrontal cortex (Verberne et al., 1997), and sensorimotor cortices (pre- and post- central gyrus). Autonomic activation of sensorimotor cortex is difficult to dissociate from task based motor and sensory activation, however, Nowak et al. (1999) demonstrated increased activation of post-central gyrus with a hand grip exercise that persisted after the application of local anesthesia, supposedly ruling out a direct sensory input to the region, and activation of the post-central gyrus has also been described during heart rate changes in a task designed to elicit baroreceptor activation alone independent of motor or cognitive effort by inducing baroreflex responses using lower body negative pressure (Kimmerly et al., 2005). Ventromedial prefrontal activity has been show to vary with skin conductance level (Nagai et al., 2004) and stimulation of muscle sensory afferents (Goswami et al., 2011) and it has been suggested that its activity is related to hippocampal activation.

Finally, the cerebellum appears to have an important role in autonomic control. The cerebellum responds to blood pressure changes that occur in a variety of tasks including Valsalva (Harper et al., 1998; Henderson et al., 2002), ventilatory challenges of 5 and 10% CO_2 (Harper et al., 1998), changes in minute ventilation (Critchley et al., 2015), heart rate changes (Gray et al., 2007) forehead and hand cold pressor tasks (Harper et al., 1998), a moderate intensity handgrip task (Wong et al., 2007), and

emotional arousal (O'Connor et al., 2007). Activation of the cerebellar vermis specifically has been reported during effortful tasks designed to elicit a stress response (Critchley et al., 2000) as well as emotional arousal (O'Connor et al., 2007), moderate intensity handgrip (Wong et al., 2007) and blood pressure increases (Critchley et al., 2015).

SUPRASPINAL ORGANIZATION OF BLADDER CONROL AND OVERLAP WITH THE CENTRAL AUTONOMIC NETWORK

The central nervous system plays a critical role in the regulation of the urinary bladder. Bladder control involves various autonomic, cognitive and sensorimotor operations, and establishing an understanding about the functional role of different brain regions in bladder circuitry, and how these regions interact with each other and with the peripheral nervous system, has been a key goal of neuro-urological research. The bladder is somewhat unique, in that while it is regulated by autonomic networks at the level of the spinal cord (and in the human infant is entirely under autonomic control) there is conscious awareness of bladder filling and voluntary control over the process of micturition. Moreover, in many non-human animals, there are major social functions of urination besides expulsion of waste products from the body (Hou et al., 2016). By default, the lower urinary tract remains in "storage" mode during bladder filling- in this state, the external urethral sphincter must remain contracted and the detrusor muscle relaxed to facilitate urine collection. It is thought that a set of brain areas are active in the storage state to maintain these properties of the detrusor and sphincter, but also to monitor the progression of bladder filling, whether in a conscious or subconscious fashion. When the bladder becomes full, there is a "switch" (requiring another set of neural events) to "voiding" mode. The "voiding" mode is the state in which the bladder sphincters relax and the detrusor muscle contracts, permitting micturition, and calls into play a third distinct pattern of brain activity. The mechanistic control of the bladder detrusor muscle and sphincters occurs through the activity of autonomic and somatic networks in the spinal cord, which communicate reciprocally with supraspinal centers, although a direct connection between the pontine micturition center (PMC) and sympathetic preganglionic neurons has there has not currently been demonstrated. There are two separate circuits for bladder control; bladder storage pathways which exist entirely within the spinal cord itself, and the supraspinal pathway which is thought to maintain continence when the bladder is significantly full, and which in non-human animal species may also be important for the social functions of micturition. Parasympathetic nerves (otherwise known as pelvic splanchnic nerves) are derived from the S2-4 nerve roots, which pass via the pelvic plexus and trigger bladder contraction during voiding. Sympathetic neurons have the effect of maintaining bladder relaxation, and travel along the iliohypogastric nerve (derived from T10-L2 roots, formed in the lumbar plexus). Somatic cholinergic nerves arising in Onuf's nucleus (located at S2-4 spinal level) travel in the pudendal nerve (formed from ventral rami of S2-4 and the coccygeal nerve in the sacral plexus) to innervate the external urethral sphincter; Onuf's nucleus is likely to be innervated by the pontine L region or pontine continence center, which is separate to the PMC and important for maintaining continence during times of urgency (Griffiths et al., 1990). Sensory information about bladder fullness is carried along the pelvic (S2-4) and iliohypogastric nerves (T12-L1), while sensory information from the bladder neck and urethra is transmitted by the pudendal nerve and iliohypogastric nerve (Fowler et al., 2008) (see **Figure 1** for afferent and efferent nerves involved in bladder control). In the spinal cord, animal studies suggest that bladder afferents travel in Lissauer's tract before projecting in lamina I, V–VII, and X of the dorsal horn (de Groat and Yoshimura, 2010). Parasympathetic preganglionic neurons, responsible for detrusor contraction, receive projections from the lateral and dorsolateral funiculus, the dorsal gray commissure, and lamina I of the dorsal horn (likely transmitting primary afferent bladder information) (de Groat and Wickens, 2013).

To understand the supraspinal control of the lower urinary tract, various experimental approaches have been used. Animal studies, using tract tracing, electrical stimulation, lesioning, and neural recording techniques were instrumental in identifying key subcortical regions important for bladder control, including the PMC which represents the major outflow tract to initiate micturition (Loewy et al., 1979; Holstege et al., 1986; Blok and Holstege, 1997), the pontine continence center (Holstege et al., 1986; Griffiths et al., 1990), the PAG, which receives afferent information about bladder filling and may be significant in switching from storage to voiding mode (Noto et al., 1991; Blok et al., 1995; Liu et al., 2004), and the globus pallidus (Lewin and Porter, 1965; Porter et al., 1971), amongst many others. Of particular relevance to the ANS, the role of the locus coeruleus (LC) in bladder control has been demonstrated (Valentino et al., 1996); the LC is activated along with the PMC, by PAG stimulation (Meriaux et al., 2018) and displays neuronal activity that temporally correlates with the initiation of micturition (Manohar et al., 2017). More recently, newer techniques such as optogenetics and fiber photometry have built on earlier studies to deepen insights into the supraspinal pathways involved in bladder control. For example, Hou et al. (2016) used optogenetic techniques to identify a population of corticotrophin-releasing hormone (Crh) positive neurons within the mouse PMC whose activity correlated with bladder contractions. These neurons were found to send glutamatergic projections to the spinal cord, consistent with an excitatory role, and, using rabies-based retrograde trans-synaptic labeling, the group identified widespread connections from higher brain centers potentially capable of modulating activity of the Crh-positive neuronal population. These connecting regions included areas regarded as important for autonomic control, such as the anterior cingulate cortex, hypothalamus, central amygdalar nucleus, and PAG; as well as other regions such as the motor and somatosensory cortex. Similarly, Keller et al. (2018) used optogenetics to identify a subset of neurons within Barrington's

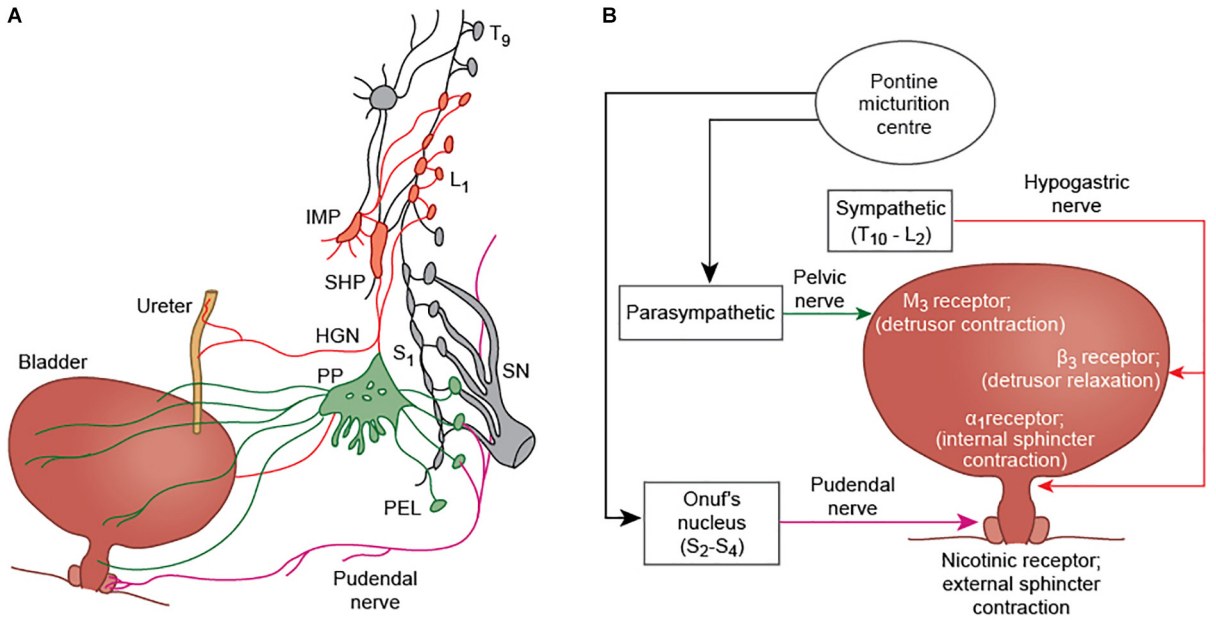

FIGURE 1 | (A) Efferent innervation of the bladder, ureter, and external urethral sphincter (modified from Fowler et al., 2008). Parasympathetic fibers (green) arise from S2-4 nerve roots. They travel in the pelvic nerve and pass via the pelvic plexus to innervate the bladder detrusor muscle of the bladder. Sympathetic fibers (red) arising from T11-L2 segments, pass via the inferior mesenteric plexus (IMP) and travel in the hypogastric nerve (HGN) to innervate the ureter and the detrusor smooth muscle. Somatic innervation of the external urethral sphincter is via the pudendal nerve, and arises from Onuf's nucleus at S2-S4. **(B)** A simplified schematic showing the major nerves and neurotransmitters involved in bladder control. The pudendal nerve causes contraction of the external urethral sphincter via nicotinic receptors (+N); parasympathetic fibers produce contraction of the detrusor muscle by acting at M3 receptors; and sympathetic innervation inhibits detrusor contraction through β3 receptors, and contraction of the internal urethral sphincter by α1 receptor activation.

nucleus expressing estrogen receptor 1 which may be involved in relaxing the external urethral sphincter.

Despite a good understanding of bladder control networks in animal models, confirming similar networks in the human have traditionally been challenging. Early insights into bladder control networks in humans were inferred through studies of patients with brain lesions that impaired urinary function (Andrew and Nathan, 1964). Important areas identified by this approach included the frontal lobes in general (Maurice-Williams, 1974), and brainstem regions including the PAG (Yaguchi et al., 2004). More recently, alterations in bladder function have been reported following implantation of DBS electrodes within the thalamus (Kessler et al., 2008), subthalamic nucleus (STN; Seif et al., 2004; Herzog et al., 2006, 2008), internal globus pallidus (GPi) (Mordasini et al., 2014), PAG (Green et al., 2012) and pedunculopontine nucleus (PPN; Aviles-Olmos et al., 2011; Roy et al., 2018b), implicating all of these regions in some aspect of human urinary control. Finally, developments in functional brain imaging have facilitated a controlled, systematic, experimental whole-brain approach to investigate the neural control of the bladder in both healthy human subjects and those with bladder disorders. Functional imaging experiments are able to identify patterns of neural activation that occur in response to specific bladder-related tasks or states, including urinary voiding, bladder filling or the subjective experience of certain bladder-related sensations, such as urinary urgency. Although a range of functional imaging methodologies have been used including positron emission tomography (PET; e.g., Blok and Holstege, 1997; Nour et al., 2000), fMRI (fMRI; e.g., Griffiths et al., 2005; Mehnert et al., 2008) and near infrared spectroscopy (Matsumoto et al., 2009), fMRI, as a relatively safe and non-invasive technique, with good spatiotemporal resolution, is rapidly becoming the dominant modality.

The most common type of paradigm used for brain-bladder fMRI is an "infusion withdrawal" paradigm (see Griffiths et al., 2005), whereby many repetitions of infusion and withdrawal of small volumes of fluid into the bladder are carried out, usually at a relatively empty bladder and a relatively full bladder (in many cases, the bladder is filled to provoke the sensation of urgency). The contrast (infusion-withdrawal) is averaged over multiple trials, due to the inherently low signal-to-noise of fMRI, and is thought to reveal brain activations associated with bladder filling or the experience of urinary urgency (depending on the exact details of the trial). Other approaches using fMRI to study brain-bladder activity include measuring the BOLD signal during or immediately preceding urinary voiding (Krhut et al., 2012; Shy et al., 2014) and, more recently, the use of resting state fMRI (Nardos et al., 2014) in the full and empty bladder state.

fMRI studies designed to elicit brain activations relating to the "storage" mode have demonstrated activations in regions including frontal cortex, anterior cingulate cortex, insula, parahippocampal gyrus and cerebellum, as well as activations in the thalamus and brainstem (Mehnert et al., 2008; Tadic et al., 2010, 2013; Krhut et al., 2014). Voiding-related

fMRI activity occurs predominantly within the bilateral cingulate cortex and bilateral medial frontal cortex (i.e., SMA), occipito-parietal regions, insula, parahippocampal gyrus, and pons (Krhut et al., 2012; Shy et al., 2014) (see **Figures 2**, **3**).

A current integrative model for the neural control of the bladder summarizes bladder control in terms of three separate 'circuits' of brain areas, which converge on a central hub (Griffiths, 2015). Circuit 1 involves the thalamus, insula, and lateral prefrontal cortex (connecting to the medial prefrontal cortex which regulates voiding) and is modeled as the normal circuitry for handling bladder sensation. Circuit 2 involves the dorsal anterior cingulate cortex (dACC) and supplementary motor area (SMA), important in creating a sensation of urgency and controlling pelvic floor muscles to prevent accidental urinary leakage in patients with urge urinary incontinence. Circuit 3 is thought to involve the parahippocampal gyrus although its precise functional role is not described in detail.

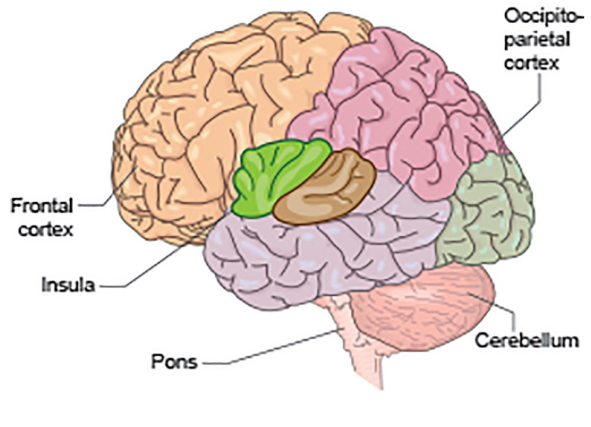

FIGURE 2 | Schematic to illustrate some of the key anatomical regions significant for bladder control, including the pons, cerebellum, insula, occipito-parietal cortex, and frontal cortex.

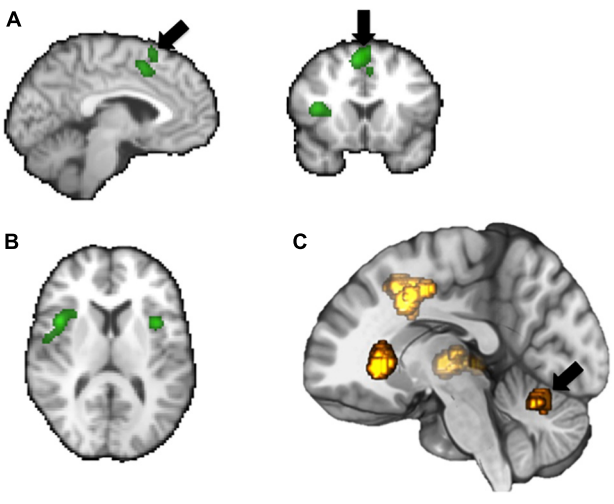

FIGURE 3 | Summary of some key brain areas demonstrated to be involved in bladder related tasks based on fMRI: supplementary motor area (SMA), mid-cingulate gyrus **(A)**, frontal operculum **(B)**, insula **(C)**, cerebellum.

Despite our growing knowledge of brain activity associated with urine storage and voiding, few frameworks have been created to help conceptualize which parts of these bladder functional networks relate to autonomic control. Indeed, most thinking about autonomic control of the bladder relates to the peripheral bladder storage pathways which exist at the level of the spinal cord. However, considering our present understanding of the central bladder network, and incorporating separate research on central autonomic control, brain areas common to both include the insula, cerebellum, and cingulate cortex. The insula is thought to be the primary cortical area for the representation of visceral interoception, receiving afferent information from Aδ and C fibers and creating a subjective awareness of an individual's homeostatic state (Craig, 2003), including with regard to bladder filling, and from an autonomic perspective, is thought of as an autonomic sensorimotor region (Hyam et al., 2012), playing a key role in autonomic challenges including blood pressure challenges (Macey et al., 2016). The cingulate cortex is activated during both storage and voiding, and in the model above may also be linked to the experience of urinary urgency. This fits with the view that the ACC is the brain's homeostatic motor area (Craig, 2003), regulating motor and autonomic responses to maintain internal balance (Critchley et al., 2003), including, perhaps, regulating urinary voiding when necessary. Cerebellar activation is frequently reported during bladder filling in PET and fMRI (e.g., Nour et al., 2000; Athwal et al., 2001; Matsuura et al., 2002) as well as in various autonomic challenges such as Valsalva (Harper et al., 2000) and static hand grip testing (Macefield and Henderson, 2015). Interestingly, without deliberate reference to autonomic control, it has been proposed that the cerebellum, anterior insula, and cingulate cortex are functionally part of a common network, which may have an attentional role (Jarrahi et al., 2015). Studies that combine autonomic function tests with bladder filling or urinary voiding paradigms in the fMRI scanner are the next step in defining more completely to what extent these brain regions are playing an "autonomic" role in bladder control.

It may also be that brainstem regions important for bladder control but difficult to resolve with current fMRI techniques due to technical challenges of brainstem imaging, provide the critical link between somatic and autonomic systems regulating the bladder. For example, the raphe nuclei, the noradrenergic cell population in the locus coeruleus and the A11 dopaminergic cell group connect with autonomic and somatic motorneurons and also project to bladder motorneurons and Onuf's nucleus (Holstege, 2005). Similarly, the paraventricular nucleus of the hypothalamus (also difficult to resolve using neuroimaging) has projections both to autonomic motoneurons and to Onuf's nucleus (Holstege, 1987), while the PAG has major effects on autonomic control (Lovick, 1992; Green et al., 2010) and fight or flight responses (These regions may be pivotal in understanding the supraspinal control of the bladder and integration of somatic and autonomic control mechanisms.). However, although newer studies are providing insights into the activity of specific sub-populations of cells within brain areas and bladder function in animal models, this level of specificity is yet to be achieved in

human studies although newer technologies such as 7T MRI scanning and local field potential recordings from implanted depth electrodes (Roy et al., 2018a) may help to isolate smaller neuronal populations.

AUTONOMIC DISORDERS AND EFFECTS ON BLADDER CONTROL

A number of neurodegenerative diseases with a clear autonomic component are associated with lower urinary tract symptoms. Research is needed to clarify the exact mechanism giving rise to bladder dysfunction in these conditions, and to determine whether the symptoms are a direct consequence of damage to autonomic bladder circuits or associated parts of the brain-bladder network.

Parkinson's Disease

Parkinson's disease is a neurodegenerative disease characterized by loss of dopaminergic neurons within the substantia nigra, and aggregation of alpha-synuclein deposits as Lewy bodies in neurons. The result is a prominent motor disorder accompanied by autonomic and cognitive symptoms. Common autonomic symptoms in Parkinson's disease include orthostatic hypotension, swallowing difficulties, sweating, constipation, diarrhea, and urinary storage symptoms including frequency, urgency, and nocturia (Sakakibara et al., 2001; Chaudhuri et al., 2006; Jain, 2011). Bladder symptoms are experienced by 38–71% of patients with PD (Sakakibara et al., 2018). Peripheral nerve and peripheral organ involvement appears to contribute to autonomic symptom development in PD; most convincingly, cardiac sympathetic denervation has been associated with orthostatic hypotension (Goldstein et al., 2002; Goldstein et al., 2007), while links have also been made with peripheral Lewy body pathology and associated autonomic symptomatology in other organ systems, particularly the enteric nervous system (Lebouvier et al., 2010; Cersosimo and Benarroch, 2012). However, despite the demonstration of peripheral nervous system involvement in the onset of autonomic symptoms, central nervous system abnormalities are also likely to be implicated. Brain structural abnormalities that underlie these common autonomic symptoms in Parkinson's disease have not been conclusively investigated, although hypothetically, it might be expected that structural alterations within the CAN, such as the ventromedial medulla, hippocampus, insula, cingulate cortex, ventromedial prefrontal cortex, and cerebellum (Macey et al., 2016) could be implicated. Chen et al. (2016) described reduced baroreflex sensitivity and reduced gray matter in the left hippocampus, right amygdala, bilateral insula, bilateral cerebellum, bilateral caudate, right fusiform, and left middle frontal gyrus in patients with Parkinson's disease (Chen et al., 2016).

Bladder symptoms in Parkinson's disease are predominantly storage-related, producing a clinical picture of overactive bladder (Sakakibara et al., 2018). Urodynamic features include reduced bladder capacity, detrusor overactivity (Sakakibara et al., 2001), uninhibited sphincter relaxation and reduced detrusor contractility during voiding (Terayama et al., 2012). It is thought that overactive bladder symptoms might relate to the primary loss of dopaminergic neurons in the substantia nigra and the reduction in the inhibitory influence of dopamine acting at D1 receptors and interacting with bladder circuitry (Kitta et al., 2008), however altered function of CAN centers as a result of Lewy body pathology may also be significant. However, there are limited functional or structural MRI studies which investigate bladder symptoms in PD, and although urinary symptoms are often classified as an autonomic feature of PD, the specific neuroanatomical correlates for this classification have not yet been confirmed.

Multiple System Atrophy

Like PD, multiple system atrophy (MSA) is characterized by alpha-synuclein aggregates. However, in MSA, these develop within the oligodendrocytes rather than neurons and are known as glial cytoplasmic inclusions. The alpha-synuclein pathology tends to be more widespread than in PD and includes involvement of the spinal cord. Bladder dysfunction in MSA occurs at an earlier stage in disease than in PD, and tends to be more severe. Over 90% of patients with MSA have some form of lower urinary tract symptoms (Yamamoto et al., 2009, 2011). Moreover, prominent voiding symptoms, characterized by urinary retention, are observed in addition to symptoms of overactive bladder (Sakakibara et al., 2018). Detrusor underactivity, which significantly contributes to voiding difficulties in MSA, may result from degeneration in the PMC, whereas overactive bladder symptoms are more likely to result from degenerative changes in the locus coeruleus, pontomedullary raphe (Ito et al., 2006), and cerebellar vermis (Sakakibara et al., 2004), all of which have been identified as brain regions important for autonomic control. Alongside changes within the brain, spinal, and peripheral neurodegeneration also occurs which may contribute to symptoms. In particular, Onuf's nucleus in the anterior horn of the sacral spinal cord, which contains the somatic motor supply to the external urethral sphincter, undergoes neuronal cell loss in MSA, and although there is not always a clear correlation between symptoms and neurogenic changes on EMG, weakness of the sphincter can result in incontinence in female MSA patients. There is also thought to be loss of sympathetic innervation of the bladder neck due to degeneration at the intermediolateral nucleus, resulting in a high incidence of open bladder neck.

Other Central Autonomic Disorders

Various other autonomic disorders such as postural tachycardia syndrome (POTS) (Kaufman et al., 2017) and pure autonomic failure (PAF) (Singer et al., 2017) also have associated bladder dysfunction. This reflects the intimate relationship between the lower urinary tract system and the ANS.

Emotional and Affective Disorders

Given the overlap between "limbic" neurocircuitry and both autonomic and bladder control regions, we were interested to identify whether there is evidence for bladder dysfunction in emotional or affective disorders. Research from the animal literature demonstrates a link between social stress in rats

(Wood et al., 2009) and mice (Chang et al., 2009; Mingin et al., 2014) and changes in bladder physiology. For example, Wood et al. (2009) found that in rats subjected to social defeat, there was a significant increase in bladder to body weight ratio, which correlated inversely with the latency to adopt the defeat posture during social stress. Rats in the social defeat group also demonstrated changes in the pattern of micturition including reduced frequency of voiding and altered voiding pattern (voiding in the corner of the cage) compared with control animals, which maintained the same number of voiding spots as at the start of the experiment and also continued to void throughout the cage. Increased expression of corticotropin releasing factor in neurons of Barrington's nucleus in the social stress group was proposed as a possible mechanism mediating the changes in bladder function.

From human clinical studies, however, there is surprisingly little research to investigate the relationship between bladder control and stress, trauma or emotional/affective disorders. This is likely to be in part due to the challenges associated with developing an appropriate and ethical experimental paradigm in humans. Nevertheless, it appears that trauma may have a profound impact on bladder control, particularly childhood trauma. For example, Durkin et al. (1993) carried out a population-based neurodevelopmental study of children in a rural community in Bangladesh. 6 months later, there was a devastating flood, the most severe ever recorded at that point in Bangladesh. Following this, a subset of the surviving children were re-evaluted. The group found that lack of sphincter control (bowel/bladder) had increased from 16.8% at baseline to 40.4% following the flood, a change which was statistically significant (Durkin et al., 1993). There was also a significant increase in aggressive behavior. Similarly, in a study comparing adult patients with interstitial cystitis/bladder pain syndrome with healthy controls presenting with acute cystitis, Chiu et al. (2017) identified higher rates of physical abuse in childhood or adulthood, and higher rates of childhood trauma by close others, in the IC/BPS group (Chiu et al., 2017). In a prospective study of female veterans who had returned from active service, Bradley et al. (2017) identified baseline anxiety, post-traumatic stress disorder and lifetime history of sexual assault as predisposing factors associated with the development of new overactive bladder syndrome at 1 year follow up. Clearly, the link between emotional/affective disorders, particularly PTSD and bladder dysfunction, needs further investigation with neuroimaging involvement to understand the link between these conditions more deeply, however, it is likely that common substrates to autonomic and bladder control such as the anterior cingulate cortex (Rinne-Albers et al., 2017), insula (Perez et al., 2017), and PAG (Johansen et al., 2010; Nicholson et al., 2017) may be involved.

CONCLUSION

Research into the central organization of autonomic control and bladder control have until now progressed relatively independently. However, there is clear overlap between supraspinal networks regulating autonomic and bladder function, with implications for the development of lower urinary tract symptoms in disease. Further research to explore the specific autonomic role of known areas in the bladder control network is needed, as is detailed investigation of the structural and functional brain changes associated with urinary symptoms in autonomic and emotional/affective disorders.

AUTHOR CONTRIBUTIONS

All authors listed have made a substantial, direct and intellectual contribution to the work, and approved it for publication.

FUNDING

The research was supported by the National Institute for Health Research (NIHR) Oxford Biomedical Research Centre based at Oxford University Hospitals NHS Trust and University of Oxford.

ACKNOWLEDGMENTS

We would like to thank Jonathan Owen for his excellent assistance in creating the illustrations.

REFERENCES

Allen, G. V., Saper, C. B., Hurley, K. M., and Cechetto, D. F. (1991). Organization of visceral and limbic connections in the insular cortex of the rat. *J. Comp. Neurol.* 311, 1–16. doi: 10.1002/cne.903110102

Al-Otaibi, F., Wong, S. W., Shoemaker, J. K., Parrent, A. G., and Mirsattari, S. M. (2010). The cardioinhibitory responses of the right posterior insular cortex in an epileptic patient. *Stereotact. Funct. Neurosurg.* 88, 390–397. doi: 10.1159/000321182

Andrew, J., and Nathan, P. W. (1964). Lesions on the anterior frontal lobes and disturbances of micturition and defaecation. *Brain* 87, 233–262. doi: 10.1093/brain/87.2.233

Athwal, B. S., Berkley, K. J., Hussain, I., Brennan, A., Craggs, M., Sakakibara, R., et al. (2001). Brain responses to changes in bladder volume and urge to void in healthy men. *Brain* 124(Pt. 2), 369–377. doi: 10.1093/brain/124.2.369

Aviles-Olmos, I., Foltynie, T., Panicker, J., Cowie, D., Limousin, P., Hariz, M., et al. (2011). Urinary incontinence following deep brain stimulation of the pedunculopontine nucleus. *Acta Neurochirur.* 153, 2357–2360. doi: 10.1007/s00701-011-1155-6

Basnayake, S. D., Green, A. L., and Paterson, D. J. (2012). Mapping the central neurocircuitry that integrates the cardiovascular response to exercise in humans. *Exp. Physiol.* 97, 29–38. doi: 10.1113/expphysiol.2011.060848

Blok, B. F., De Weerd, H., and Holstege, G. (1995). Ultrastructural evidence for a paucity of projections from the lumbosacral cord to the pontine micturition center or M-region in the cat: a new concept for the organization of the micturition reflex with the periaqueductal gray as central relay. *J. Comp. Neurol.* 359, 300–309. doi: 10.1002/cne.903590208

Blok, B. F., and Holstege, G. (1997). Ultrastructural evidence for a direct pathway from the pontine micturition center to the parasympathetic preganglionic

motoneurons of the bladder of the cat. *Neurosci. Lett.* 222, 195–198. doi: 10.1016/s0304-3940(97)13384-5

Bradley, C. S., Nygaard, I. E., Hillis, S. L., Torner, J. C., and Sadler, A. G. (2017). Longitudinal associations between mental health conditions and overactive bladder in women veterans. *Am. J. Obstet. Gynecol.* 217, 430.e1–430.e8. doi: 10.1016/j.ajog.2017.06.016

Cersosimo, M. G., and Benarroch, E. E. (2012). Pathological correlates of gastrointestinal dysfunction in Parkinson's disease. *Neurobiol. Dis.* 46, 559–564. doi: 10.1016/j.nbd.2011.10.014

Chang, A., Butler, S., Sliwoski, J., Valentino, R., Canning, D., and Zderic, S. (2009). Social stress in mice induces voiding dysfunction and bladder wall remodeling. *Am. J. Physiol. Renal Physiol.* 297, F1101–F1108. doi: 10.1152/ajprenal.90749.2008

Chaudhuri, K. R., Healy, D. G., and Schapira, A. H. (2006). Non-motor symptoms of Parkinson's disease: diagnosis and management. *Lancet Neurol.* 5, 235–245.

Chen, M. H., Lu, C. H., Chen, P. C., Tsai, N. W., Huang, C. C., Chen, H. L., et al. (2016). Association between autonomic impairment and structural deficit in Parkinson disease. *Medicine* 95:e3086. doi: 10.1097/MD.0000000000003086

Chiu, C. D., Lee, M. H., Chen, W. C., Ho, H. L., and Wu, H. C. (2017). Childhood trauma perpetrated by close others, psychiatric dysfunction, and urological symptoms in patients with interstitial cystitis/bladder pain syndrome. *J. Psychosom. Res.* 93, 90–95. doi: 10.1016/j.jpsychores.2016.12.014

Craig, A. D. (2003). Interoception: the sense of the physiological condition of the body. *Curr. Opin. Neurobiol.* 13, 500–505. doi: 10.1016/s0959-4388(03)00090-4

Critchley, H. D., Corfield, D. R., Chandler, M. P., Mathias, C. J., and Dolan, R. J. (2000). Cerebral correlates of autonomic cardiovascular arousal: a functional neuroimaging investigation in humans. *J. Physiol.* 523(Pt. 1), 259–270. doi: 10.1111/j.1469-7793.2000.t01-1-00259.x

Critchley, H. D., and Garfinkel, S. N. (2015). Interactions between visceral afferent signaling and stimulus processing. *Front. Neurosci.* 9:286. doi: 10.3389/fnins.2015.00286

Critchley, H. D., Mathias, C. J., Josephs, O., O'Doherty, J., Zanini, S., Dewar, B. K., et al. (2003). Human cingulate cortex and autonomic control: converging neuroimaging and clinical evidence. *Brain* 126(Pt. 10), 2139–2152. doi: 10.1093/brain/awg216

Critchley, H. D., Nicotra, A., Chiesa, P. A., Nagai, Y., Gray, M. A., Minati, L., et al. (2015). Slow breathing and hypoxic challenge: cardiorespiratory consequences and their central neural substrates. *PLoS One* 10:e0127082. doi: 10.1371/journal.pone.0127082

Critchley, H. D., Tang, J., Glaser, D., Butterworth, B., and Dolan, R. J. (2005). Anterior cingulate activity during error and autonomic response. *Neuroimage* 27, 885–895. doi: 10.1016/j.neuroimage.2005.05.047

de Groat, W. C., and Wickens, C. (2013). Organization of the neural switching circuitry underlying reflex micturition. *Acta Physiol.* 207, 66–84. doi: 10.1111/apha.12014

de Groat, W. C., and Yoshimura, N. (2010). Changes in afferent activity after spinal cord injury. *Neurourol. Urodyn.* 29, 63–76. doi: 10.1002/nau.20761

Durkin, M. S., Khan, N., Davidson, L. L., Zaman, S. S., and Stein, Z. A. (1993). The effects of a natural disaster on child behavior: evidence for posttraumatic stress. *Am. J. Public Health* 83, 1549–1553. doi: 10.2105/ajph.83.11.1549

Faull, O. K., Jenkinson, M., Ezra, M., and Pattinson, K. (2016). Conditioned respiratory threat in the subdivisions of the human periaqueductal gray. *eLife* 5:e12047. doi: 10.7554/eLife.12047

Fowler, C. J., Griffiths, D., and de Groat, W. C. (2008). The neural control of micturition. *Nat. Rev. Neurosci.* 9, 453–466. doi: 10.1038/nrn2401

Garfinkel, S. N., Minati, L., Gray, M. A., Seth, A. K., Dolan, R. J., and Critchley, H. D. (2014). Fear from the heart: sensitivity to fear stimuli depends on individual heartbeats. *J. Neurosci.* 34, 6573–6582. doi: 10.1523/JNEUROSCI.3507-13.2014

Gianaros, P. J., Onyewuenyi, I. C., Sheu, L. K., Christie, I. C., and Critchley, H. D. (2012). Brain systems for baroreflex suppression during stress in humans. *Hum. Brain Mapp.* 33, 1700–1716. doi: 10.1002/hbm.21315

Goldstein, D. S., Holmes, C. S., Dendi, R., Bruce, S. R., and Li, S. T. (2002). Orthostatic hypotension from sympathetic denervation in Parkinson's disease. *Neurology* 58, 1247–1255. doi: 10.1212/wnl.58.8.1247

Goldstein, D. S., Sharabi, Y., Karp, B. I., Bentho, O., Saleem, A., Pacak, K., et al. (2007). Cardiac sympathetic denervation preceding motor signs in Parkinson disease. *Clin. Auton. Res.* 17, 118–121. doi: 10.1007/s10286-007-0396-1

Goswami, R., Frances, M. F., and Shoemaker, J. K. (2011). Representation of somatosensory inputs within the cortical autonomic network. *Neuroimage* 54, 1211–1220. doi: 10.1016/j.neuroimage.2010.09.050

Gray, M. A., Harrison, N. A., Wiens, S., and Critchley, H. D. (2007). Modulation of emotional appraisal by false physiological feedback during fMRI. *PLoS One* 2:e546. doi: 10.1371/journal.pone.0000546

Green, A. L., Hyam, J. A., Williams, C., Wang, S., Shlugman, D., Stein, J. F., et al. (2010). Intra-operative deep brain stimulation of the periaqueductal grey matter modulates blood pressure and heart rate variability in humans. *Neuromodulation* 13, 174–181. doi: 10.1111/j.1525-1403.2010.00274.x

Green, A. L., Stone, E., Sitsapesan, H., Turney, B. W., Coote, J. H., Aziz, T. Z., et al. (2012). Switching off micturition using deep brain stimulation at midbrain sites. *Ann. Neurol.* 72, 144–147. doi: 10.1002/ana.23571

Griffiths, D., Derbyshire, S., Stenger, A., and Resnick, N. (2005). Brain control of normal and overactive bladder. *J. Urol.* 174, 1862–1867. doi: 10.1097/01.ju.0000177450.34451.97

Griffiths, D., Holstege, G., Dalm, E., and de Wall, H. (1990). Control and coordination of bladder and urethral function in the brainstem of the cat. *Neurourol. Urodyn.* 9, 63–82. doi: 10.1002/nau.1930090108

Griffiths, D. J. (2015). Neural control of micturition in humans: a working model. *Nat. Rev. Urol.* 12, 695–705. doi: 10.1038/nrurol.2015.266

Harper, R. M., Bandler, R., Spriggs, D., and Alger, J. R. (2000). Lateralized and widespread brain activation during transient blood pressure elevation revealed by magnetic resonance imaging. *J. Comp. Neurol.* 417, 195–204. doi: 10.1002/(sici)1096-9861(20000207)417:2<195::aid-cne5>3.0.co;2-v

Harper, R. M., Gozal, D., Bandler, R., Spriggs, D., Lee, J., and Alger, J. V. (1998). Regional brain activation in humans during respiratory and blood pressure challenges. *Clin. Exp. Pharmacol. Physiol.* 25, 483–486. doi: 10.1111/j.1440-1681.1998.tb02240.x

Henderson, L. A., Macey, P. M., Macey, K. E., Frysinger, R. C., Woo, M. A., Harper, R. K., et al. (2002). Brain responses associated with the Valsalva maneuver revealed by functional magnetic resonance imaging. *J. Neurophysiol.* 88, 3477–3486. doi: 10.1152/jn.00107.2002

Herzog, J., Weiss, P. H., Assmus, A., Wefer, B., Seif, C., Braun, P. M., et al. (2006). Subthalamic stimulation modulates cortical control of urinary bladder in Parkinson's disease. *Brain* 129(Pt. 12), 3366–3375. doi: 10.1093/brain/awl302

Herzog, J., Weiss, P. H., Assmus, A., Wefer, B., Seif, C., Braun, P. M., et al. (2008). Improved sensory gating of urinary bladder afferents in Parkinson's disease following subthalamic stimulation. *Brain* 131(Pt. 1), 132–145. doi: 10.1093/brain/awm254

Holstege, G. (1987). Some anatomical observations on the projections from the hypothalamus to brainstem and spinal cord: an HRP and autoradiographic tracing study in the cat. *J. Comp. Neurol.* 260, 98–126. doi: 10.1002/cne.902600109

Holstege, G. (2005). Micturition and the soul. *J. Comp. Neurol.* 493, 15–20. doi: 10.1002/cne.20785

Holstege, G., Griffiths, D., de Wall, H., and Dalm, E. (1986). Anatomical and physiological observations on supraspinal control of bladder and urethral sphincter muscles in the cat. *J. Comp. Neurol.* 250, 449–461. doi: 10.1002/cne.902500404

Hou, X. H., Hyun, M., Taranda, J., Huang, K. W., Todd, E., Feng, D., et al. (2016). Central control circuit for context-dependent micturition. *Cell* 167, 73–86. doi: 10.1016/j.cell.2016.08.073

Hyam, J. A., Kringelbach, M. L., Silburn, P. A., Aziz, T. Z., and Green, A. L. (2012). The autonomic effects of deep brain stimulation–a therapeutic opportunity. *Nat. Rev. Neurol.* 8, 391–400. doi: 10.1038/nrneurol.2012.100

Ito, T., Sakakibara, R., Nakazawa, K., Uchiyama, T., Yamamoto, T., Liu, Z., et al. (2006). Effects of electrical stimulation of the raphe area on the micturition reflex in cats. *Neuroscience* 142, 1273–1280. doi: 10.1016/j.neuroscience.2006.06.044

Jain, S. (2011). Multi-organ autonomic dysfunction in Parkinson disease. *Parkinsonism Relat. Disord.* 17, 77–83. doi: 10.1016/j.parkreldis.2010.08.022

Jarrahi, B., Mantini, D., Balsters, J. H., Michels, L., Kessler, T. M., Mehnert, U., et al. (2015). Differential functional brain network connectivity during visceral interoception as revealed by independent component analysis of fMRI TIME-series. *Hum. Brain Mapp.* 36, 4438–4468. doi: 10.1002/hbm.22929

Johansen, J. P., Tarpley, J. W., LeDoux, J. E., and Blair, H. T. (2010). Neural substrates for expectation-modulated fear learning in the amygdala and periaqueductal gray. *Nat. Neurosci.* 13, 979–986. doi: 10.1038/nn.2594

Kaufman, M. R., Chang-Kit, L., Raj, S. R., Black, B. K., Milam, D. F., Reynolds, W. S., et al. (2017). Overactive bladder and autonomic dysfunction: lower urinary tract symptoms in females with postural tachycardia syndrome. *Neurourol. Urodyn.* 36, 610–613. doi: 10.1002/nau.22971

Keller, J., Chen, J., Simpson, S., Wang, E. H. J., Lilascharoen, V., George, O., et al. (2018). Voluntary urination control by brainstem neurons that relax the urethral sphincter. *Nat. Neurosci.* 21, 1229–1238. doi: 10.1038/s41593-018-0204-3

Kessler, T. M., Burkhard, F. C., Z'Brun, S., Stibal, A., Studer, U. E., Hess, C. W., et al. (2008). Effect of thalamic deep brain stimulation on lower urinary tract function. *Eur. Urol.* 53, 607–612. doi: 10.1016/j.eururo.2007.07.015

Kimmerly, D. S., O'Leary, D. D., Menon, R. S., Gati, J. S., and Shoemaker, J. K. (2005). Cortical regions associated with autonomic cardiovascular regulation during lower body negative pressure in humans. *J. Physiol.* 569, 331–345. doi: 10.1113/jphysiol.2005.091637

Kitta, T., Matsumoto, M., Tanaka, H., Mitsui, T., Yoshioka, M., and Nonomura, K. (2008). GABAergic mechanism mediated via D receptors in the rat periaqueductal gray participates in the micturition reflex: an *in vivo* microdialysis study. *Eur. J. Neurosci.* 27, 3216–3225. doi: 10.1111/j.1460-9568.2008.06276.x

Krhut, J., Holy, P., Tintera, J., Zachoval, R., and Zvara, P. (2014). Brain activity during bladder filling and pelvic floor muscle contractions: a study using functional magnetic resonance imaging and synchronous urodynamics. *Int. J. Urol.* 21, 169–174. doi: 10.1111/iju.12211

Krhut, J., Tintera, J., Holy, P., Zachoval, R., and Zvara, P. (2012). A preliminary report on the use of functional magnetic resonance imaging with simultaneous urodynamics to record brain activity during micturition. *J. Urol.* 188, 474–479. doi: 10.1016/j.juro.2012.04.004

Lebouvier, T., Neunlist, M., Bruley des Varannes, S., Coron, E., Drouard, A., N'Guyen, J. M., et al. (2010). Colonic biopsies to assess the neuropathology of Parkinson's disease and its relationship with symptoms. *PLoS One* 5:e12728. doi: 10.1371/journal.pone.0012728

Lewin, R. J., and Porter, R. W. (1965). Inhibition of spontaneous bladder activity by stimulation of the globus pallidus. *Neurology* 15, 1049–1052.

Liu, Z., Sakakibara, R., Nakazawa, K., Uchiyama, T., Yamamoto, T., Ito, T., et al. (2004). Micturition-related neuronal firing in the periaqueductal gray area in cats. *Neuroscience* 126, 1075–1082. doi: 10.1016/j.neuroscience.2004.04.033

Loewy, A. D. (1982). Descending pathways to the sympathetic preganglionic neurons. *Prog. Brain Res.* 57, 267–277. doi: 10.1016/s0079-6123(08)64133-3

Loewy, A. D. (1991). Forebrain nuclei involved in autonomic control. *Prog. Brain Res.* 87, 253–268. doi: 10.1016/s0079-6123(08)63055-1

Loewy, A. D., Saper, C. B., and Baker, R. P. (1979). Descending projections from the pontine micturition center. *Brain Res.* 172, 533–538. doi: 10.1016/0006-8993(79)90584-5

Lovick, T. (2014). Deep brain stimulation and autonomic control. *Exp. Physiol.* 99, 320–325. doi: 10.1113/expphysiol.2013.072694

Lovick, T. A. (1992). Inhibitory modulation of the cardiovascular defence response by the ventrolateral periaqueductal grey matter in rats. *Exp. Brain Res.* 89, 133–139.

Macefield, V. G., and Henderson, L. A. (2015). Autonomic responses to exercise: cortical and subcortical responses during post-exercise ischaemia and muscle pain. *Auton. Neurosci.* 188, 10–18. doi: 10.1016/j.autneu.2014.10.021

Macey, P. M., Kumar, R., Ogren, J. A., Woo, M. A., and Harper, R. M. (2014). Global brain blood-oxygen level responses to autonomic challenges in obstructive sleep apnea. *PLoS One* 9:e105261. doi: 10.1371/journal.pone.0105261

Macey, P. M., Ogren, J. A., Kumar, R., and Harper, R. M. (2016). Functional imaging of autonomic regulation: methods and key findings. *Front. Neurosci.* 9:513. doi: 10.3389/fnins.2015.00513

Macey, P. M., Wu, P., Kumar, R., Ogren, J. A., Richardson, H. L., Woo, M. A., et al. (2012). Differential responses of the insular cortex gyri to autonomic challenges. *Auton. Neurosci.* 168, 72–81. doi: 10.1016/j.autneu.2012.01.009

Manohar, A., Curtis, A. L., Zderic, S. A., and Valentino, R. J. (2017). Brainstem network dynamics underlying the encoding of bladder information. *Elife* 6:e29917. doi: 10.7554/eLife.29917

Matsumoto, S., Ishikawa, A., Kume, H., Takeuchi, T., and Homma, Y. (2009). Near infrared spectroscopy study of the central nervous activity during artificial changes in bladder sensation in men. *Int. J. Urol.* 16, 760–764. doi: 10.1111/j.1442-2042.2009.02358.x

Matsuura, S., Kakizaki, H., Mitsui, T., Shiga, T., Tamaki, N., and Koyanagi, T. (2002). Human brain region response to distention or cold stimulation of the bladder: a positron emission tomography study. *J. Urol.* 168, 2035–2039. doi: 10.1097/00005392-200211000-00033

Maurice-Williams, R. S. (1974). Micturition symptoms in frontal tumours. *J. Neurol. Neurosurg. Psychiatry* 37, 431–436. doi: 10.1136/jnnp.37.4.431

Mehnert, U., Boy, S., Svensson, J., Michels, L., Reitz, A., Candia, V., et al. (2008). Brain activation in response to bladder filling and simultaneous stimulation of the dorsal clitoral nerve–an fMRI study in healthy women. *Neuroimage* 41, 682–689. doi: 10.1016/j.neuroimage.2008.03.006

Meriaux, C., Hohnen, R., Schipper, S., Zare, A., Jahanshahi, A., Birder, L. A., et al. (2018). Neuronal activation in the periaqueductal gray matter upon electrical stimulation of the bladder. *Front. Cell. Neurosci.* 12:133. doi: 10.3389/fncel.2018.00133

Mingin, G. C., Peterson, A., Erickson, C. S., Nelson, M. T., and Vizzard, M. A. (2014). Social stress induces changes in urinary bladder function, bladder NGF content and generalized bladder inflammation in mice. *Am. J. Physiol. Regul. Integr. Comp. Physiol.* 307, R893–R900. doi: 10.1152/ajpregu.00500.2013

Mordasini, L., Kessler, T. M., Kiss, B., Schupbach, M., Pollo, C., and Kaelin-Lang, A. (2014). Bladder function in patients with dystonia undergoing deep brain stimulation. *Parkinsonism Relat. Disord.* 20, 1015–1017. doi: 10.1016/j.parkreldis.2014.05.016

Nagai, Y., Critchley, H. D., Featherstone, E., Trimble, M. R., and Dolan, R. J. (2004). Activity in ventromedial prefrontal cortex covaries with sympathetic skin conductance level: a physiological account of a "default mode" of brain function. *Neuroimage* 22, 243–251. doi: 10.1016/j.neuroimage.2004.01.019

Napadow, V., Dhond, R., Conti, G., Makris, N., Brown, E. N., and Barbieri, R. (2008). Brain correlates of autonomic modulation: combining heart rate variability with fMRI. *Neuroimage* 42, 169–177. doi: 10.1016/j.neuroimage.2008.04.238

Nardos, R., Gregory, W. T., Krisky, C., Newell, A., Nardos, B., Schlaggar, B., et al. (2014). Examining mechanisms of brain control of bladder function with resting state functional connectivity MRI. *Neurourol. Urodyn.* 33, 493–501. doi: 10.1002/nau.22458

Nicholson, A. A., Friston, K. J., Zeidman, P., Harricharan, S., McKinnon, M. C., Densmore, M., et al. (2017). Dynamic causal modeling in PTSD and its dissociative subtype: bottom-up versus top-down processing within fear and emotion regulation circuitry. *Hum. Brain Mapp.* 38, 5551–5561. doi: 10.1002/hbm.23748

Noto, H., Roppolo, J. R., Steers, W. D., and de Groat, W. C. (1991). Electrophysiological analysis of the ascending and descending components of the micturition reflex pathway in the rat. *Brain Res.* 549, 95–105. doi: 10.1016/0006-8993(91)90604-t

Nour, S., Svarer, C., Kristensen, J. K., Paulson, O. B., and Law, I. (2000). Cerebral activation during micturition in normal men. *Brain* 123(Pt. 4), 781–789. doi: 10.1093/brain/123.4.781

Nowak, M., Olsen, K. S., Law, I., Holm, S., Paulson, O. B., and Secher, N. H. (1999). Command-related distribution of regional cerebral blood flow during attempted handgrip. *J. Appl. Physiol.* 86, 819–824. doi: 10.1152/jappl.1999.86.3.819

O'Connor, M. F., Gundel, H., McRae, K., and Lane, R. D. (2007). Baseline vagal tone predicts BOLD response during elicitation of grief. *Neuropsychopharmacology* 32, 2184–2189. doi: 10.1038/sj.npp.1301342

Perez, D. L., Matin, N., Barsky, A., Costumero-Ramos, V., Makaretz, S. J., Young, S. S., et al. (2017). Cingulo-insular structural alterations associated with psychogenic symptoms, childhood abuse and PTSD in functional neurological disorders. *J. Neurol. Neurosurg. Psychiatry* 88, 491–497. doi: 10.1136/jnnp-2016-314998

Porter, R. W., Pazo, J. H., and Dillard, G. V. (1971). Triphasic brain stem response to detrusor contraction. *Brain Res.* 35, 119–126. doi: 10.1016/0006-8993(71)90598-1

Rinne-Albers, M. A., Pannekoek, J. N., van Hoof, M. J., van Lang, N. D., Lamers-Winkelman, F., Rombouts, S. A., et al. (2017). Anterior cingulate cortex grey matter volume abnormalities in adolescents with PTSD after childhood sexual abuse. *Eur. Neuropsychopharmacol.* 27, 1163–1171. doi: 10.1016/j.euroneuro.2017.08.432

Roy, H. A., Aziz, T. Z., FitzGerald, J. J., and Green, A. L. (2018a). Beta oscillations and urinary voiding in Parkinson's disease. *Neurology* 90, e1530–e1534. doi: 10.1212/WNL.0000000000005355

Roy, H. A., Pond, D., Roy, C., Forrow, B., Foltynie, T., Zrinzo, L., et al. (2018b). Effects of pedunculopontine nucleus stimulation on human bladder function. *Neurourol. Urodyn.* 37, 726–734. doi: 10.1002/nau.23321

Saito, M., Mano, T., Abe, H., and Iwase, S. (1986). Responses in muscle sympathetic nerve activity to sustained hand-grips of different tensions in humans. *Eur. J. Appl. Physiol. Occup. Physiol.* 55, 493–498. doi: 10.1007/bf00421643

Sakakibara, R., Shinotoh, H., Uchiyama, T., Sakuma, M., Kashiwado, M., Yoshiyama, M., et al. (2001). Questionnaire-based assessment of pelvic organ dysfunction in Parkinson's disease. *Auton. Neurosci.* 92, 76–85. doi: 10.1016/s1566-0702(01)00295-8

Sakakibara, R., Tateno, F., Yamamoto, T., Uchiyama, T., and Yamanishi, T. (2018). Urological dysfunction in synucleinopathies: epidemiology, pathophysiology and management. *Clin. Auton. Res.* 28, 83–101. doi: 10.1007/s10286-017-0480-0

Sakakibara, R., Uchida, Y., Uchiyama, T., Yamanishi, T., and Hattori, T. (2004). Reduced cerebellar vermis activation during urinary storage and micturition in multiple system atrophy: 99mTc-labelled ECD SPECT study. *Eur. J. Neurol.* 11, 705–708. doi: 10.1111/j.1468-1331.2004.00872.x

Seif, C., Herzog, J., van der Horst, C., Schrader, B., Volkmann, J., Deuschl, G., et al. (2004). Effect of subthalamic deep brain stimulation on the function of the urinary bladder. *Ann. Neurol.* 55, 118–120. doi: 10.1002/ana.10806

Shy, M., Fung, S., Boone, T. B., Karmonik, C., Fletcher, S. G., and Khavari, R. (2014). Functional magnetic resonance imaging during urodynamic testing identifies brain structures initiating micturition. *J. Urol.* 192, 1149–1154. doi: 10.1016/j.juro.2014.04.090

Singer, W., Berini, S. E., Sandroni, P., Fealey, R. D., Coon, E. A., Suarez, M. D., et al. (2017). Pure autonomic failure: predictors of conversion to clinical CNS involvement. *Neurology* 88, 1129–1136. doi: 10.1212/WNL.0000000000003737

Tadic, S. D., Griffiths, D., Murrin, A., Schaefer, W., Aizenstein, H. J., and Resnick, N. M. (2010). Brain activity during bladder filling is related to white matter structural changes in older women with urinary incontinence. *Neuroimage* 51, 1294–1302. doi: 10.1016/j.neuroimage.2010.03.016

Tadic, S. D., Tannenbaum, C., Resnick, N. M., and Griffiths, D. (2013). Brain responses to bladder filling in older women without urgency incontinence. *Neurourol. Urodyn.* 32, 435–440. doi: 10.1002/nau.22320

Terayama, K., Sakakibara, R., Ogawa, A., Haruta, H., Akiba, T., Nagao, T., et al. (2012). Weak detrusor contractility correlates with motor disorders in Parkinson's disease. *Mov. Disord.* 27, 1775–1780. doi: 10.1002/mds.25225

Ture, U., Yasargil, D. C., Al-Mefty, O., and Yasargil, M. G. (1999). Topographic anatomy of the insular region. *J. Neurosurg.* 90, 720–733. doi: 10.3171/jns.1999.90.4.0720

Valentino, R. J., Chen, S., Zhu, Y., and Aston-Jones, G. (1996). Evidence for divergent projections to the brain noradrenergic system and the spinal parasympathetic system from Barrington's nucleus. *Brain Res.* 732, 1–15. doi: 10.1016/0006-8993(96)00482-9

Verberne, A. J., Lam, W., Owens, N. C., and Sartor, D. (1997). Supramedullary modulation of sympathetic vasomotor function. *Clin. Exp. Pharmacol. Physiol.* 24, 748–754. doi: 10.1111/j.1440-1681.1997.tb02126.x

Wong, S. W., Masse, N., Kimmerly, D. S., Menon, R. S., and Shoemaker, J. K. (2007). Ventral medial prefrontal cortex and cardiovagal control in conscious humans. *Neuroimage* 35, 698–708. doi: 10.1016/j.neuroimage.2006.12.027

Wood, S. K., Baez, M. A., Bhatnagar, S., and Valentino, R. J. (2009). Social stress-induced bladder dysfunction: potential role of corticotropin-releasing factor. *Am. J. Physiol. Regul. Integr. Comp. Physiol.* 296, R1671–R1678. doi: 10.1152/ajpregu.91013.2008

Yaguchi, H., Soma, H., Miyazaki, Y., Tashiro, J., Yabe, I., Kikuchi, S., et al. (2004). A case of acute urinary retention caused by periaqueductal grey lesion. *J. Neurol. Neurosurg. Psychiatry* 75, 1202–1203. doi: 10.1136/jnnp.2003.027516

Yamamoto, T., Sakakibara, R., Uchiyama, T., Liu, Z., Ito, T., Awa, Y., et al. (2009). Questionnaire-based assessment of pelvic organ dysfunction in multiple system atrophy. *Mov. Disord.* 24, 972–978. doi: 10.1002/mds.22332

Yamamoto, T., Sakakibara, R., Uchiyama, T., Yamaguchi, C., Nomura, F., Ito, T., et al. (2011). Pelvic organ dysfunction is more prevalent and severe in MSA-P compared to Parkinson's disease. *Neurourol. Urodyn.* 30, 102–107. doi: 10.1002/nau.20948

Zubin Maslov, P., Shoemaker, J. K., and Dujic, Z. (2014). Firing patterns of muscle sympathetic neurons during apnea in chronic heart failure patients and healthy controls. *Auton. Neurosci.* 180, 66–69. doi: 10.1016/j.autneu.2013.09.016

Conflict of Interest Statement: The authors declare that the research was conducted in the absence of any commercial or financial relationships that could be construed as a potential conflict of interest.

frontiers in Neuroscience

ORIGINAL RESEARCH
published: 18 June 2019
doi: 10.3389/fnins.2019.00615

Overexpression of a Neuronal Type Adenylyl Cyclase (Type 8) in Sinoatrial Node Markedly Impacts Heart Rate and Rhythm

*Jack M. Moen[1,2†], Michael G. Matt[1,3†], Christopher Ramirez[1], Kirill V. Tarasov[1], Khalid Chakir[1], Yelena S. Tarasova[1], Yevgeniya Lukyanenko[1], Kenta Tsutsui[1], Oliver Monfredi[1,4], Christopher H. Morrell[1,5], Syevda Tagirova[1], Yael Yaniv[6], Thanh Huynh[7], Karel Pacak[7], Ismayil Ahmet[1] and Edward G. Lakatta[1]**

[1] Intramural Research Program, Laboratory of Cardiovascular Science, National Institute on Aging, National Institutes of Health, Baltimore, MD, United States, [2] Cellular and Molecular Physiology, Yale University, New Haven, CT, United States, [3] School of Medicine, University of Pittsburgh, Pittsburgh, PA, United States, [4] Department of Cardiovascular and Electrophysiology, The Johns Hopkins Hospital, Baltimore, MD, United States, [5] Department of Mathematics, Loyola University Maryland, Baltimore, MD, United States, [6] Faculty of Biomedical Engineering, Technion Israel Institute of Technology, Haifa, Israel, [7] Section on Medical Neuroendocrinology, Eunice Kennedy Shriver National Institute of Child Health and Human Development, National Institutes of Health, Bethesda, MD, United States

OPEN ACCESS

Edited by:
Alberto Porta,
University of Milan, Italy

Reviewed by:
Mirko Baruscotti,
University of Milan, Italy
Antonio Roberto Zamunér,
Catholic University of the Maule, Chile

***Correspondence:**
Edward G. Lakatta
lakattae@grc.nia.nih.gov

† These authors have contributed equally to this work

Specialty section:
This article was submitted to Autonomic Neuroscience, a section of the journal Frontiers in Neuroscience

Received: *22 February 2019*
Accepted: *29 May 2019*
Published: *18 June 2019*

Citation:
Moen JM, Matt MG, Ramirez C, Tarasov KV, Chakir K, Tarasova YS, Lukyanenko Y, Tsutsui K, Monfredi O, Morrell CH, Tagirova S, Yaniv Y, Huynh T, Pacak K, Ahmet I and Lakatta EG (2019) Overexpression of a Neuronal Type Adenylyl Cyclase (Type 8) in Sinoatrial Node Markedly Impacts Heart Rate and Rhythm. Front. Neurosci. 13:615. doi: 10.3389/fnins.2019.00615

Heart rate (HR) and HR variability (HRV), predictors of over-all organism health, are widely believed to be driven by autonomic input to the sinoatrial node (SAN), with sympathetic input increasing HR and reducing HRV. However, variability in spontaneous beating intervals in isolated SAN tissue and single SAN cells, devoid of autonomic neural input, suggests that clocks intrinsic to SAN cells may also contribute to HR and HRV *in vivo*. We assessed contributions of both intrinsic and autonomic neuronal input mechanisms of SAN cell function on HR and HRV via *in vivo*, telemetric EKG recordings. This was done in both wild type (WT) mice, and those in which adenylyl cyclase type 8 (ADCY8), a main driver of intrinsic cAMP-PKA-Ca^{2+} mediated pacemaker function, was overexpressed exclusively in the heart (TG^{AC8}). We hypothesized that TG^{AC8} mice would: (1) manifest a more coherent pattern of HRV *in vivo*, i.e., a reduced HRV driven by mechanisms intrinsic to SAN cells, and less so to modulation by autonomic input and (2) utilize unique adaptations to limit sympathetic input to a heart with high levels of intrinsic cAMP-Ca^{2+} signaling. Increased adenylyl cyclase (AC) activity in TG^{AC8} SAN tissue was accompanied by a marked increase in HR and a concurrent marked reduction in HRV, both in the absence or presence of dual autonomic blockade. The marked increase in intrinsic HR and coherence of HRV in TG^{AC8} mice occurred in the context of: (1) reduced HR and HRV responses to β-adrenergic receptor (β-AR) stimulation; (2) increased transcription of genes and expression of proteins [β-Arrestin, G Protein-Coupled Receptor Kinase 5 (GRK5) and Clathrin Adaptor Protein (Dab2)] that desensitize β-AR signaling within SAN tissue, (3) reduced transcripts or protein levels of enzymes [dopamine beta-hydorxylase (DBH) and phenylethanolamine *N*-methyltransferase (PNMT)] required for catecholamine production in intrinsic cardiac

adrenergic cells, and (4) substantially reduced plasma catecholamine levels. Thus, mechanisms driven by cAMP-PKA-Ca^{2+} signaling intrinsic to SAN cells underlie the marked coherence of TG^{AC8} mice HRV. Adaptations to limit additional activation of AC signaling, via decreased neuronal sympathetic input, are utilized to ensure the hearts survival and prevent Ca^{2+} overload.

Keywords: sinoatrial node, adenylyl cyclase, heart rate, heart rate variability, adenylyl cyclase type 8, parasympathetic activity, sympathetic activity, ivabradine

INTRODUCTION

Heart rate variability (HRV) is a series of complex rhythms buried within beat-to-beat R wave interval time series. HRV is regulated by alterations in autonomic neurotransmitter input from the brain to the sinoatrial node (SAN), and the responses of SAN cells to this input (Yaniv et al., 2014a). Neuronal input modulates an intrinsic coupled-clock system that governs SAN cells automaticity. We have discovered that an intrinsic coupled-clock system [i.e., in the absence of β-adrenergic receptor (β-AR) stimulation] within the SAN cells is crucially dependent on activation of a neuronal-type adenylyl cyclase (AC) type 8 (AC8) that drives cAMP-PKA-Ca^{2+}. This cAMP driven signaling is regulated by phosphodiesterase activity to maintain basal pacemaker function near its dynamic mid-range. β-AR stimulation of SAN cells activates intracellular AC signaling, increasing the mean spontaneous action potential (AP) firing rate and reducing inter AP cycle variability (Yaniv et al., 2014a). In contrast, blocking intrinsic AC activity, or its downstream cAMP-dependent signaling, reduces the mean SAN cell AP firing rate and increases intra-AP cycle variability (Vinogradova et al., 2006; Mangoni and Nargeot, 2008 for review; Yaniv et al., 2014a).

Complexity or coherency within the heart rhythm can be estimated from EKG RR time series. Complexity is largely driven by muscarinic cholinergic input to the SAN, while coherency results largely from sympathetic autonomic input to the SAN (Goldberger, 1991; Goldberger et al., 2002; Thayer et al., 2010). Based upon our findings that a coupled-clock system regulates the spontaneous AP firing rate of isolated SAN cells (Lakatta et al., 2010; Yaniv et al., 2014b), we hypothesized that overexpression of AC8 within the SAN cells would generate an increased mean HR in TG^{AC8} mice *in vivo*. We speculated that this would be due to mechanisms intrinsic to SAN cells and would be accompanied by a markedly coherent heart rhythm *in vivo* (McCraty and Zayas, 2014; Smith et al., 2017), rather than to an increased sympathetic input into the SAN. The coherent rhythm would manifest as a reduced variability of EKG RR intervals in the time domain, and a marked reduction in both total power and other rhythm components in the frequency domain in the presence or absence of autonomic blockade. We also reasoned that in the context of HR and HRV changes induced by AC8 overexpression, we would see unique adaptations to limit extrinsic adrenergic input to the SAN, defending against Ca^{2+} overload and ensuring heart survival (Koch et al., 2000).

To test this, we utilized a transgenic mouse (Lipskaia et al., 2000) in which AC8 was exclusively overexpressed in the heart by putting it under control of the myosin heavy chain promotor. We performed comprehensive HR and HRV analyses of EKG recordings from surgically implanted telemeters in unrestrained, untethered TG^{AC8} and their wild type (WT) littermates in the presence of single or dual autonomic receptor blockade. In order to understand how extrinsic autonomic input impacted HR and HRV in TG^{AC8}, we (1) gathered EKG recordings in the presence of single or dual sympathetic and cholinergic autonomic receptor blockades; (2) assessed the HR response to a β-adrenergic agonist; (3) measured transcripts of genes and expression of proteins that regulate β-AR sensitivity and catecholamine synthesis in SAN tissue; and (4) measured circulating plasma catecholamine levels.

MATERIALS AND METHODS

Animals

All studies were performed in accordance with the Guide for the Care and Use of Laboratory Animals published by the National Institutes of Health (NIH Publication no. 85-23, revised 1996). The experimental protocols were approved by the Animal Care and Use Committee of the National Institutes of Health (protocol #441-LCS-2016). A breeder pair of TG^{AC8} mice, generated by ligating the murine α-myosin heavy chain promoter to a cDNA coding for human AC8 (Lipskaia et al., 2000), were a gift from Nicole Defer/Jacques Hanoune, Unite de Recherches, INSERM U-99, Hôpital Henri Mondor, F-94010 Créteil, France. WT littermates, bred from the C57/BL6 background, were used as controls.

Telemetry

Telemetry sensors (ETA-F20 or HDX-11, Data Sciences International, St. Paul, MN, United States) were surgically implanted into WT and TG^{AC8} mice under 2% isoflurane anesthesia administered by nosecone. Mice were allowed to recover for 2 weeks before any recordings were performed (Thireau et al., 2008). First, 24-h EKGs were recorded during a normal light–dark cycle using RPC-1 receiver plates with a sampling rate of 1000 Hz. All other data were analyzed during the mouse sleep cycle, wherein a 90-min baseline recording was obtained and then intraperitoneal injections of a saline solution containing the drug of interest were administered. This was followed by an additional 90 min of EKG recording. The injection volume was 200 μL/30 g mouse, wherein atropine (0.5 mg/kg), or propranolol (1 mg/kg) alone, or together were administered. In other mice, the β-AR agonist, dobutamine (5 mg/kg), was tested individually, followed 60 min later

by the administration of combined atropine (0.5 mg/kg) and propranolol (1 mg/kg). All recordings were performed 48 h apart. Representative EKG recordings are illustrated in **Figure 2A**.

Average Heart Rate (RR Interval) and Heart Rate Variability (RR Interval Variability) Analyses

Heart rate variability analyses were performed using a combination of LabChart 7.37 and custom python 3.5 software. EKGs were first analyzed to identify segments that fit strict selection criteria. This was mainly dependent on whether the HR was stationary and devoid of ectopic beats. Ectopic beats were defined as any interval occurring outside two standard deviations of the mean. The determination of stationarity was based on the absence of linear trends, or a stable HR. Segments that contained greater than 2048 accurate intervals, as assessed directly by hand, were then run through the in-house software developed in python 3. The data were cleaned by removing outliers greater than two standard deviations, i.e., ectopic beats, for time domain and non-linear analyses and replacing ectopic beats with a 0 for frequency-based analyses. For each animal, a set of 2048 RR intervals were transformed using a fast Fourier transform. The absolute values of the data were then squared and divided by the average interval length to give a usable transformed dataset. The set was then further broken down into ranges, in which high frequency power constituted values between 1.5 and 5.0, low frequency power between 0.4 and 1.5, and very low frequency between 0 and 0.4. Poincaré SD values were calculated by adding (for SD1) or subtracting (for SD2) successive RR intervals and then taking the square root of the variance of the set divided by the square root of 2. Multiscale entropy was calculated using the PhysioZoo algorithm for SampEn, modified to only output E1 in python 3 (Behar et al., 2018).

Sinoatrial Node (SAN) and SAN Cell Isolation

Mice were injected (intraperitoneally) with heparin and acutely anesthetized with pentobarbital-based euthanasia solution. The heart then was quickly removed and placed into Tyrode solution containing (mM): 140.0 NaCl, 10.0 HEPES, 10.0 glucose, 5.4 KCl, 1.2 KH_2PO_4, 1.8 $CaCl_2$, and 1.0 $MgCl_2$; pH was adjusted to 7.4 with NaOH. The SAN region was identified anatomically, under a dissecting microscope, between inferior and superior vena cava, crista terminalis, and intra-atrial septum and cut into strips perpendicular to the crista terminalis, washed (three times) for 5 min at 35°C in low Ca^{2+} Tyrode solution containing (mM): 140.0 NaCl, 10.0 HEPES, 20.0 glucose, 0.06 $CaCl_2$, 5.4 KCl, 1.2 KH_2PO_4, 50 taurine, and 1 mg/1 mL bovine serum albumin (BSA), pH 6.9 with NaOH. Next, SAN strips were incubated for 30 min in the same solution with addition of collagenase type 2, protease type XIV, and elastase at 35°C. After enzymatic digestion, tissue was washed (x3) in modified high potassium (KB) solution containing (mM): 100 potassium glutamate, 10 potassium aspartate, 10 Hepes, 20 glucose, 25 KCl, 2 $MgCl_2$, 10 KH_2PO_4, 20 taurine, 5 creatine, 0.5 EGTA, 1 mg/1 mL BSA, and 5.0 β-hydroxybutyric acid, pH 7.2 with KOH, and kept at 4°C for 1 h with 50 mg/mL polyvinylpyrrolidone (PVP). Finally, cells were dispersed by gentle pipetting in the KB solution and stored at 4°C. For immunolabeling studies, 250 μL of freshly isolated SAN cells in KB solution was added to each laminin coated glass (0 size) bottom MatTek dish (35 mm).

RNA Extraction, cDNA Synthesis, RT-qPCR, and Data Analysis

RT-qPCR of SAN tissue was performed to determine the transcript abundance of human AC8 genes that mediate neural autonomic input to SAN cells and for genes that regulate cardiac catecholamine synthesis (Wang et al., 2017). RNA was extracted from isolated mouse SAN ($n = 3$ pooled samples from TG^{AC8} and WT, each sample collected from four mice) or left ventricular myocytes (VMs) ($n = 4$ WT and 4 TG^{AC8} mice) with RNeasy Mini Kit (Qiagen, Valencia, CA, United States) and DNAse on column digestion; 2 μg of total RNA was used for cDNA synthesis with MMLV reverse transcriptase (Promega) in final 50 μL volume. Primers used for each transcript assessed are listed in **Supplementary Table S4**. RT-qPCR was performed on QuantStudio 6 Flex Real-Time PCR System (Thermo Fisher Scientific) with 384-well platform. Reaction was performed with FastStart Universal SYBR Green Master Kit with Rox (Roche) using manufacturer recommended conditions, and dissociation curve acquisition; all appropriate controls were included (no template; no RT control). Preliminary reactions were performed for determination of efficiency of amplification and primers validation. Each well contained 0.5 μL of cDNA solution and 10 μL of reaction mixture. Each sample was quadruplicated and repeated twice using *de novo* synthesized cDNA sets. RT-qPCR analysis was performed using ddCt method. Expression level of transcripts was normalized on expression of HPRT level.

Adenylyl Cyclase Activity

After isolation, mice SAN tissue was frozen in liquid nitrogen and homogenized in 1.5 mL plastic tube with Bel-Art™ SP Scienceware™ liquid nitrogen-cooled Mini Mortar. SAN tissue powder was further lysed in the lysis buffer containing: 70 mM Tris, pH 7.6, 0.5 mM DTT, 1 mM EGTA, 5 mM MgCl2, 0.2 mM IBMX, and 0.33% PIC, sonicated on ice (three pulses, 15 s each) and further rotated on ice for 15 min. Then lysate was centrifuged during 10 min at 1000 × *g* at 4°C to remove debris. Supernatant was used to measure protein content and to detect AC activity in the lysate. AC reaction composition: 70 mM Tris (pH 7.6), 0.5 mM DTT, 1 mM EGTA, 5 mM MgCl2, 0.2 mM IBMX, 0.25% PIC, 1 mM ATP, 5 mM creatine phosphate, 60 U/mL creatine phosphokinase, 0.2% DMSO, and a sample (SAN lysate supernatant, 100 μg of total protein in 100 μL of AC reaction). AC reaction lasted for 5 min at 35°C and was stopped by boiling during 5 min. Later AC reaction solution was cooled down, centrifuged for 15 min at 4°C at 20,000 × *g* and the supernatant was used for cAMP measurement; 9 μL of the supernatant was used in the LANCE assay (Lance cAMP384 kit 500 points, Perkin Elmer, AD0262) in a total volume of 24 μL. Buffer for the LANCE assay standard curve was prepared exactly as samples including boiling and centrifugation steps. All measurements were done

in triplicate. Protein concentration in samples was detected by Reducing Agent Compatible Pierce® Microplate BCA Protein Assay Kit # 23252.

Immunolabeling of Single Isolated Sinoatrial Node Cells

Immunolabeling of selected proteins expressed by genes examined by RT-qPCR was performed in freshly isolated mouse SAN cells. Cells were plated on laminin coated MatTek dishes for 1 h. For immunofluorescence staining, cells were fixed with 4% paraformaldehyde for 15 min at room temperature, washed three times with PBS, and then permeabilized with 0.2% Triton X-100 in PBS for 10 min at room temperature. The plates were washed two more times with PBS and then incubated with 10% goat serum for 1 h to minimize non-specific staining. Afterward, samples were incubated at 4°C overnight with primary antibodies against RGS6 (EPR6342) ab128943, DAB 2 (10109-2-AP), GRK 5 (ab64943), TH (ab112), HCN4 (MBS800358), and Adcy8 (bs-3925R) all in dilution 1:100. Cells were then washed three times with PBS and incubated with fluorescence-conjugated secondary antibodies (1:1000) (Sigma, United States) for 45 min at 37°C. Cell nuclei were labeled with DAPI (Sigma, United States). Cells were visualized by LSM 710 laser-scanning confocal microscope (Carl Zeiss) and images were captured using the Carl Zeiss Zen software. Quantitative fluorescence image analysis was performed with Image J software, according to the following protocol: http://theolb.readthedocs.io/en/latest/imaging/measuring-cell-fluorescence-using-imagej.html. Images of stained cells were transferred and analyzed with ImageJ software to calculate the basic measurements of each image, including area, mean gray value, and integrated density. To calculate the corrected total cell fluorescence (CTCF)*, small areas of positively stained fluorescent cells were selected using free hand selection tool. A background reading was created by selecting a negatively stained rectangular section near the analyzed cell. From the results, total fluorescence per cell was calculated in Excel with the following formula:

*CTCF = integrated density – (area of selected cell × mean fluorescence of background readings).

Plasma Catecholamine Measurements

Plasma concentrations of catecholamines (noradrenaline, adrenaline, Dopa, and dopamine) and their degradation products: 3,4-dihydroxyphenylglycol (DHPG) and 3,4-dihydroxy-phenylacetic acid (DOPAC) were quantified by high performance liquid chromatography with electrochemical detection. Concentrations of catecholamines were determined after extraction from plasma using alumina adsorption according to previously described methods (Eisenhofer et al., 1986).

Statistical Analyses

Statistical analyses of EKG data employed RStudio (RStudio Team, 2017) and R 3.2.3 (R Core Development Team, 2017). A linear mixed effects model (lmerTest; Kuznetsova et al., 2016) was used to compare EKG data from WT littermates and TG^{AC8}, prior to and following drug administration, looking at both drug effects, genotype effects, and drug–genotype interactions, i.e., different responses to drugs in WT and TG^{AC8} mice. For each comparison, the basal for that day was used to compare the drug effect for that day, i.e., there was a separate analysis done for each pre- and post-drug data gathered. For individual comparisons, the differences of least squares means were calculated with Satterthwaite approximation for degrees of freedom (lmerTest; Kuznetsova et al., 2016). Drug responses of HR and HRV were compared to pre-drug controls in each mouse. For the comparison of average HR over 24 h, a one-way ANOVA was used to detect a genotypic difference. RT-qPCR, immunolabeling, and plasma catecholamine data were analyzed by Student's *t*-test (p-value < 0.05 was taken as statistically significant).

RESULTS

AC8 Transcripts and Protein Expression Are Increased in TG^{AC8} SAN

We first showed that AC8 transcripts are expressed in SAN. **Figure 1A** demonstrates that a high level of human AC8 transcript was expressed in TG^{AC8} SAN tissue (**Figure 1A**, amplification plots of RT q-PCR are provided in **Supplementary Figure S1**). The expression of mouse AC8 transcripts in TG^{AC8} was markedly decreased compared to human. AC8 protein expression, assessed by immunostaining of single isolated SAN cells, was also increased in TG^{AC8} vs. WT (**Figure 1C** and **Supplementary Table S1**). Further, SAN tissue AC activity was markedly increased in TG^{AC8} vs. WT (**Figure 1B**).

Basal HR

Figure 2A illustrates representative telemetric EKG recordings from a TG^{AC8} and WT mouse. Analysis of 60-min averages of 24-h EKG telemetric recordings demonstrates that the average HR of TG^{AC8} mice is higher than that in WT over the entire 24-h period (**Figure 2B**), providing evidence to support the idea that AC activity intrinsic to SAN cells is a determinant of HR *in vivo*.

RR Interval Variability Are Markedly Reduced in TG^{AC8}

The constitutively increased HR (**Figure 2B**) is accompanied by a marked reduction in both the mean RR and the range of RR intervals measured in the basal state (**Figures 3A,B**). Selected RR variability measures are illustrated in **Figures 3B–J**. A comprehensive statistical analysis of all measured RR interval variability parameters is provided in **Supplementary Table S2**. Basal RR variability in the time domain, i.e., standard deviation of RR intervals (SDRR) is two- to threefold lower in TG^{AC8} than WT (**Figure 3C**). Rhythms that range over frequencies less than half of the mean HR are detected in the frequency domain, i.e., within the power spectrum derived fast Fourier transforms. A representative power spectrum for WT and TG^{AC8} is shown in **Supplementary Figure S2**. Basal RR interval total power and power in very low, low, and high (frequency

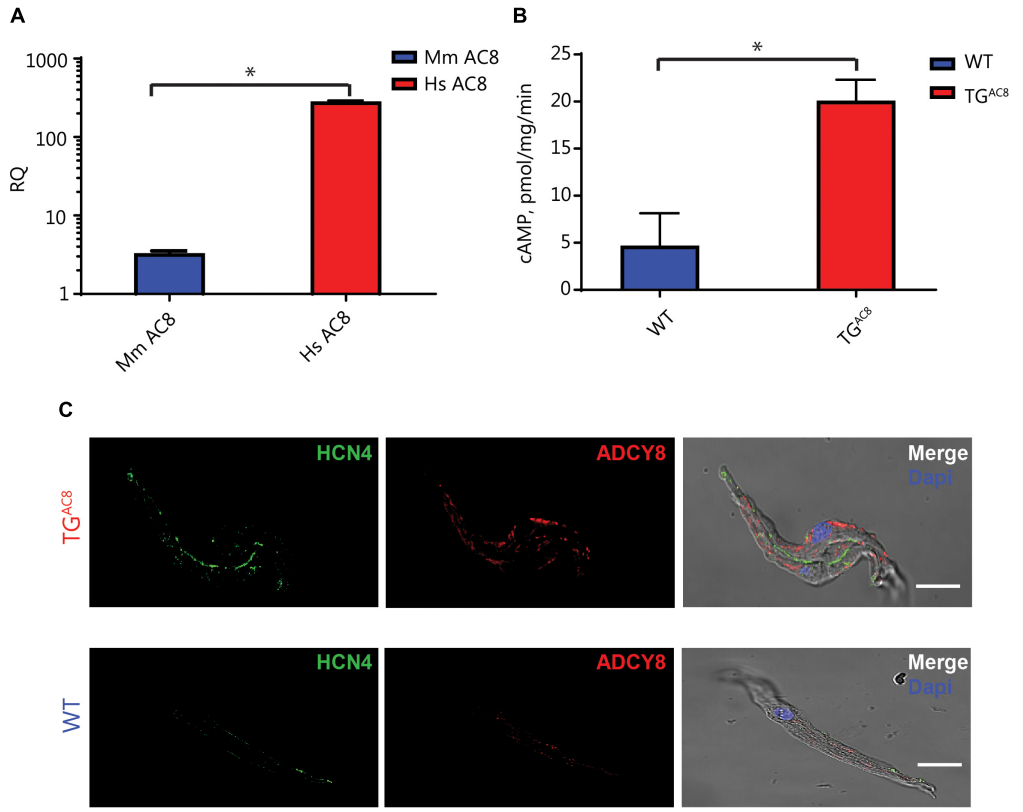

FIGURE 1 | Transcript abundance and immunolabeling of ADCY8 and AC activity in SAN tissue. **(A)** Relative quantification (RQ) transcript abundance of mouse (Mm) vs. human (Hs) AC8 in TG^{AC8} SAN tissue ($n = 3$, $^*p < 0.0001$). **(B)** AC activity of SAN tissue lysates is increased in TG^{AC8} vs. WT mice ($n = 4$, $^*p < 0.01$). **(C)** AC protein expression detected by immunolabeling for ADCY8 is increased in TG^{AC8} vs. WT mice. Left panels: HCN4 immunolabeling; middle panel: selected antibody immunolabeling; right panel: overlay of left and center panels. Scale bar, 20 μm.

domains) are also two- to threefold lower in TG^{AC8} than WT (**Figures 3D–G**). Non-linearity of rhythms buried within an EKG time series, reflected by SD1, SD2, and multiscale entropy of RR intervals, was also markedly decreased in TG^{AC8} vs. those in WT (**Figures 3H–J**). Taken together, the results in **Figure 3** demonstrate a low mean basal RR interval (high basal HR) in TG^{AC8} is accompanied by a markedly coherent heart rhythm that underlies reduced RR variability in both time and frequency domains.

Average RR Intervals and RR Interval Variability in the Presence of Double Autonomic Blockade

We repeated the HR and HRV in measurements in the presence of dual autonomic blockade (atropine and propranolol) in order to gauge the relative effects of autonomic input on intrinsic HR and HRV in both genotypes. Dual autonomic blockade had substantially larger effects on many HRV descriptors in WT than TG^{AC8} (**Figures 3A–J**), providing an initial inference for genotype differences in neurotransmitter input. Importantly, the reduction in mean basal RR and the concomitant coherent pattern of RR variability persisted in the presence of dual autonomic blockade for multiple HRV parameters (**Figures 3A,B,D,E**). This suggests that HR and coherent HRV patterns of TG^{AC8} are dominated by mechanisms intrinsic to AC8 overexpressed SAN cells.

Response to Single Autonomic Receptor Blockade

Because the marked reduction in mean RR and RR variability was not only present in the intrinsic state, but also in the basal resting state, we assessed the effects of single autonomic blockade on HR and HRV in TG^{AC8} and WT (**Figure 4** and **Supplementary Table S2**).

The cholinergic receptor blocker, atropine, reduced the mean basal RR interval in WT to a far greater extent than in TG^{AC8} (**Figure 4A**). Atropine also reduced time domain basal RR interval range in both genotypes (**Figure 4B**). Atropine reduced both the basal SDRR (**Figure 4C**) and total power frequency domain RR variability (**Figures 4D,F,G**) in both genotypes. Atropine significantly reduced non-linear basal RR interval variability parameters to a greater extent in WT than in TG^{AC8} (**Figures 4H,J**). Taken together these results indicate that blockade of basal state parasympathetic receptor signaling reduces the genotype differences in a "para-sympathetic" like neuronal input.

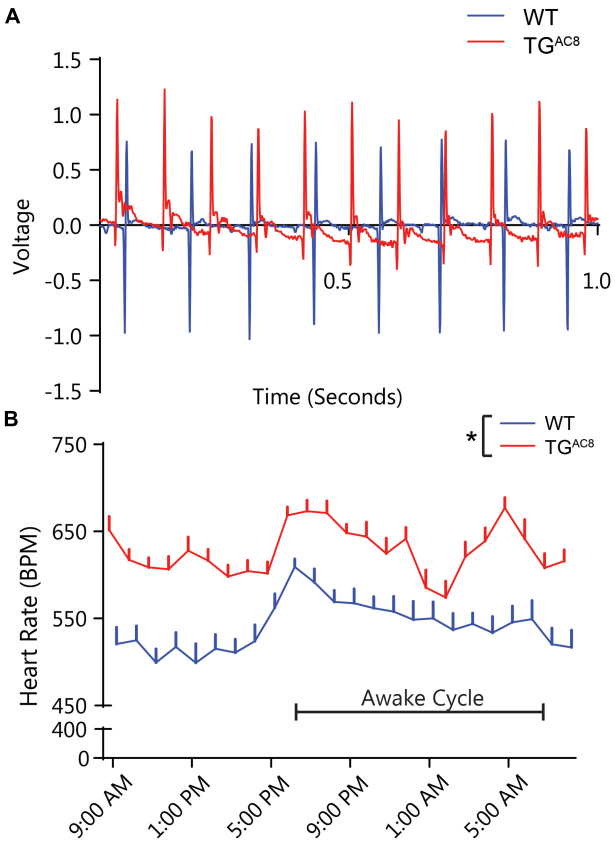

FIGURE 2 | *In vivo* telemetric EKG recordings in awake, unrestrained TG^{AC8}, and WT mice over a 24-h period. **(A)** Representative tracings of TG^{AC8} and WT mice EKG in the basal state. **(B)** Sixty-minute averages of basal HR were elevated in TG^{AC8} compared to WT throughout the 24-h period. $N = 6$ for WT and $N = 7$ for TG^{AC8}. $^*p < 0.05$ for differences determined by a one-way ANOVA.

This suggests that in the absence of atropine, responses of SAN to parasympathetic input are substantially reduced in TG^{AC8} vs. WT.

There were some genotypic differences in HR and HRV in response to propranolol, a sympathetic receptor blocker (**Supplementary Table S2**). Time domain and non-linear measures of RR intervals, i.e., SDRR, CV, MSE, etc., show a difference following sympathetic blockade, but measures of frequency domain failed to display altered genotypic effects. This may indicate that the autonomic sympathetic signaling to the SAN or the response to activation of sympathetic autonomic receptors is altered in the TG^{AC8} mice to accommodate the increased intrinsic sympathetic-like signaling.

Reduced Effectiveness of Extrinsic Adrenergic Input Into SAN

Because the increased HR and coherence within TG^{AC8} results from high levels of intrinsic cAMP-PKA-Ca^{2+} signaling, we reasoned that adaptive mechanisms within TG^{AC8} are likely utilized to limit the additional activation of cAMP-PKA-Ca^{2+} dependent catecholamine signaling. In order to test this hypothesis, we sought to utilize a dominant external adrenergic input to SAN cells via activation of β-ARs by adrenergic neurotransmitters. We stimulated β-ARs via infusion of dobutamine, a β_1-AR agonist, in TG^{AC8} and WT mice. The administration of dobutamine produced a potent effect to reduce the mean RR interval in WT mice, but its effect to reduce the mean RR in TG^{AC8} mice was markedly reduced (**Figure 5A**). Dobutamine produced a reduction in RR interval in TG^{AC8} and WT mice, with the magnitude of the effect being larger in WT mice (**Figure 5B**). Because β-AR stimulation increases intracellular cAMP-PKA-Ca^{2+} signaling in SAN cells (Vinogradova et al., 2006), the effects of dobutamine infusion should mimic overexpression of AC8 in the SAN cells of WT animals. In other terms, in the presence of β-AR stimulation, mean HR in WT mice resembles the mean HR patterns prior to dobutamine in TG^{AC8} mice.

One plausible mechanism for the reduced responsiveness of the TG^{AC8} heart to β-adrenergic neurotransmitters is through desensitization of β-Ars (Koch et al., 2000). We assessed the expression of selected markers of β-AR desensitization in TG^{AC8} and WT SAN tissue and single SAN cells. Transcripts for β-Arrestin ($Arrb_2$), G Protein-Coupled Receptor Kinase 5 (GRK5) (BARK), and Dab2 were elevated in TG^{AC8} vs. WT (**Supplementary Table S3**). This was further confirmed by immunolabeling of single, isolated, HCN4 positive SAN (**Figure 6** and **Supplementary Table S1**). HCN immunolabeling did not differ in TG_{AC8} vs. WT SAN cells (**Supplementary Table S3**). Neither transcripts of genes coding for β-ARs (ADRB1, ADRB2, ADRB3), nor for selected G proteins [Guanin Nucleotide binding protein, alpha stimulating (GNAS), G Protein Subunit Alpha I2 (GNAI2), G Protein Subunit Alpha I3 (GNAI3)] differed in TG^{AC8} compared to WT (**Supplementary Table S3**). Interestingly, transcript abundance of RGS2, which inhibits Gi signaling, leading to an inactivation of AC in SAN cells (Yang et al., 2012), was also reduced. There also was a trend toward a reduction in Regulator of G Protein Signaling 2 (RGS2) and Regulator of G Protein Signaling 6 (RGS6) (Yang et al., 2010) in TG^{AC8} vs. WT (**Supplementary Table S3**), and a significant reduction in RGS6 protein (**Supplementary Table S1**).

Enzymes Involved in Cardiac Catecholamine Production Are Altered in TG^{AC8} SAN Tissue and Cells

We postulated that, in addition to desensitization of β-AR stimulation to catecholamines, the production of catecholamines that stimulates these receptors may also be reduced in TG^{AC8} as part of a strategy to block external adrenergic input. Catecholamines that stimulate SAN cells β-ARs can arise from multiple sources, including autonomic nerve endings within the heart, from circulating plasma or from intrinsic cardiac adrenergic cells. Intrinsic cardiac adrenergic cells are populated in different locations within the murine heart including the SAN, which express enzymes that

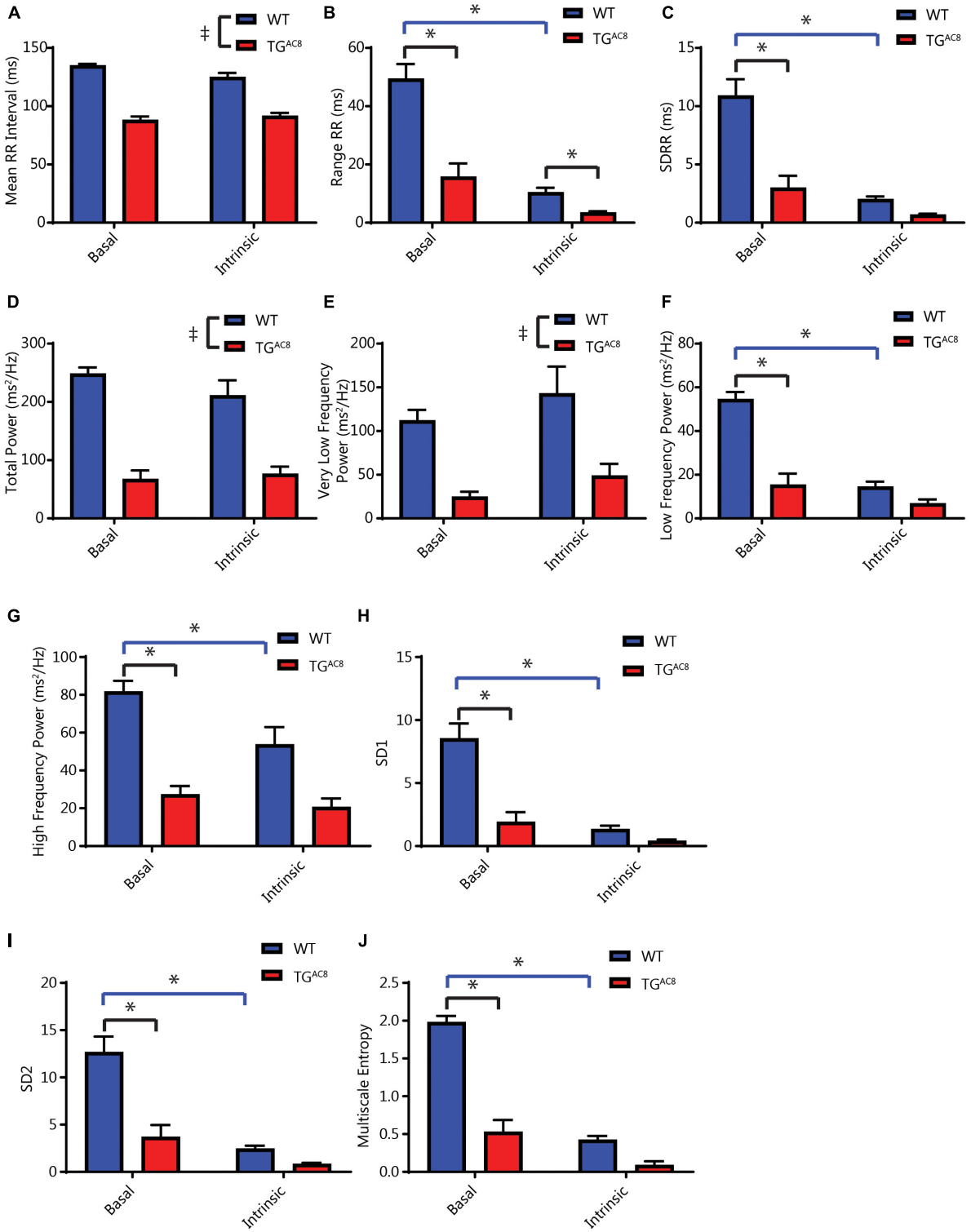

FIGURE 3 | Analyses of average basal and intrinsic (dual autonomic blockade) HR and selected HRV parameters of *in vivo* EKG time series. **(A)** Average RR interval length. **(B)** Range of RR intervals, interaction *F*-value of 30.223, *p*-value of 0.0002. **(C)** Standard deviation of RR intervals, interaction *F*-value of 20.541, *p*-value of 0.001. **(D)** Total power. **(E)** Very low frequency power. **(F)** Low frequency power, interaction *F*-value of 14.415, *p*-value of 0.003. **(G)** High frequency power, interaction *F*-value of 5.184, *p*-value of 0.046. **(H)** Poincare plot SD1, interaction *F*-value of 24.921, *p*-value of 0.0005. **(I)** Poincare plot SD2, interaction *F*-value of 17.884, *p*-value of 0.001. **(J)** Multiscale entropy, interaction *F*-value of 119.116, *p*-value of 7.09E-07. $^{\ddagger}p < 0.05$ for main effects of drug differences. $^{*}p < 0.05$ for significant pairwise differences, if a significant interaction effect was found, as determined by a linear mixed effects model. *F*-value and *p*-value provided for significant interactions. $N = 6$ for WT and $N = 6$ for TG^{AC8}.

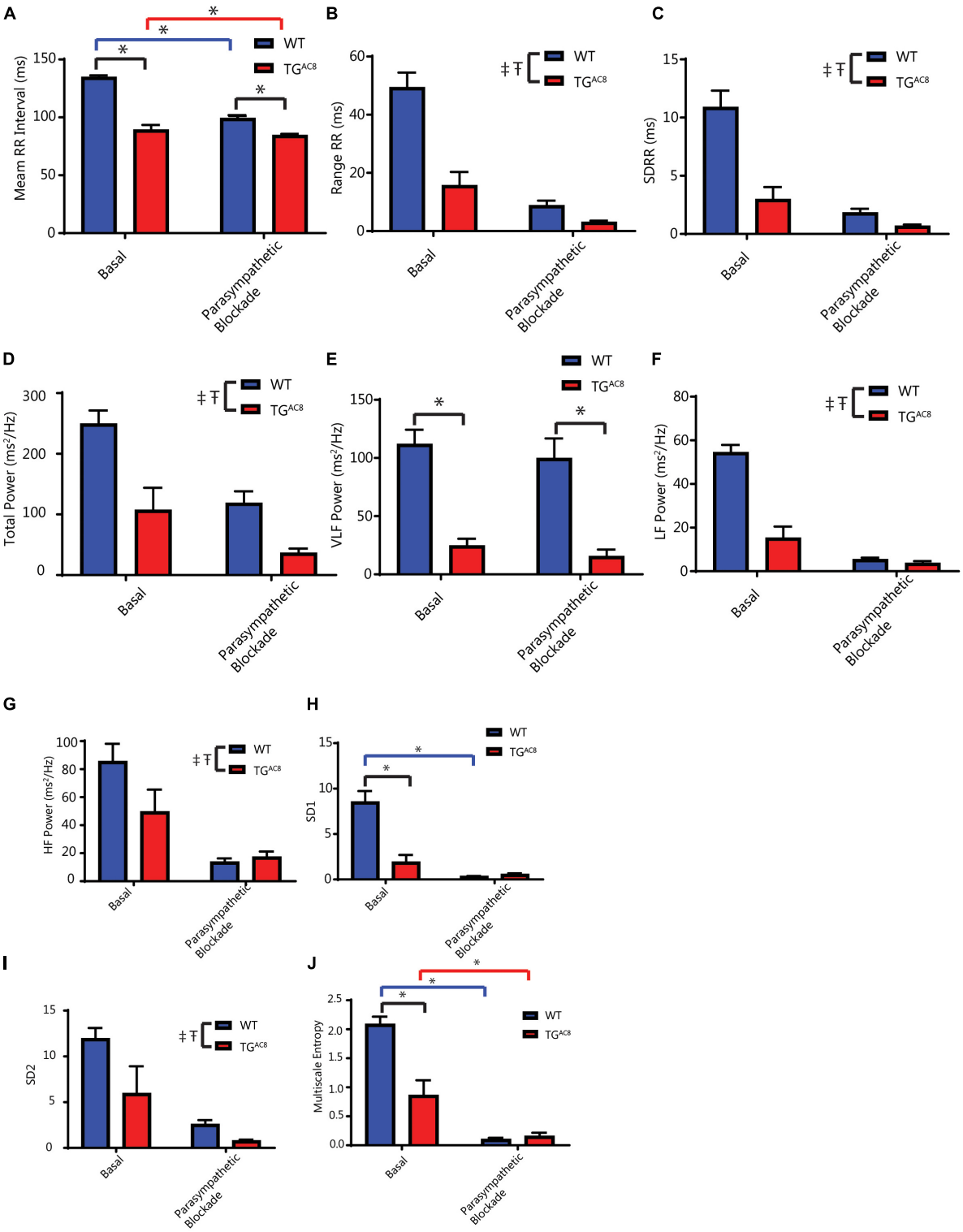

FIGURE 4 | Effects of parasympathetic blockade (atropine) on mean *in vivo* RR intervals and selected HRV parameters. **(A)** Average RR interval, interaction *F*-value of 10.883, *p*-value of 0.009. **(B)** Range of RR intervals. **(C)** Standard deviation of RR intervals. **(D)** Total power. **(E)** Very low frequency power. **(F)** Low frequency power. **(G)** High frequency power. **(H)** Poincare plot SD1, interaction *F*-value of 7.367, *p*-value of 0.023. **(I)** Poincare plot SD2. **(J)** Multiscale entropy (E1), interaction *F*-value of 26.180, *p*-value of 0.0006. ‡$p < 0.05$ for main effects of genotype differences. T$p < 0.05$ for main effects of drug differences. *$p < 0.05$ for significant pairwise differences, if a significant interaction effect was found, as determined by a linear mixed effects model. *F*-value and *p*-value provided for significant interactions. $N = 6$ for WT basal and $N = 5$ for TG^{AC8}.

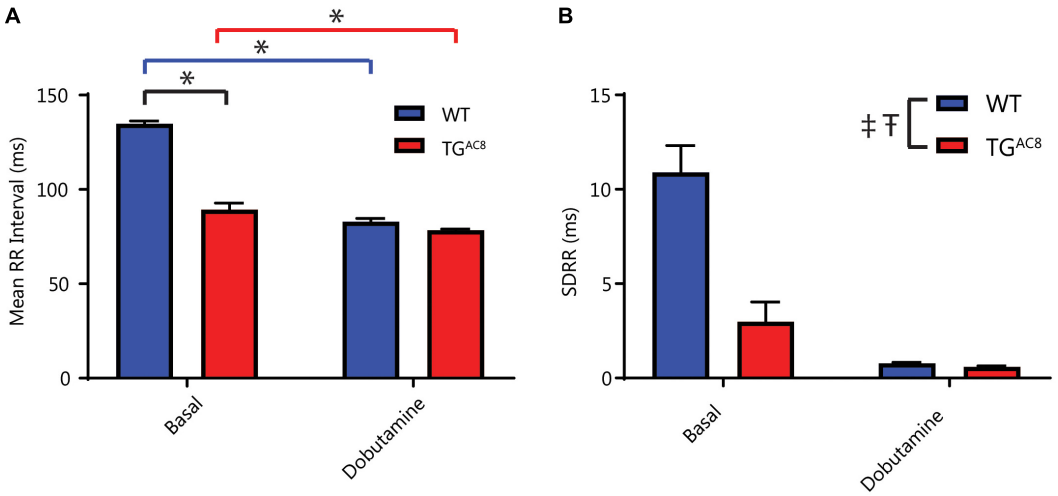

FIGURE 5 | The effects of β-AR stimulation *in vivo*. **(A)** Effect of the β1-AR agonist, dobutamine on mean RR, interaction *F*-value of 14.156, *p*-value of 0.003. **(B)** The SDRR in response to dobutamine. $^{‡}p < 0.05$ for main effects of genotype differences. $^{⊤}p < 0.05$ for main effects of drug differences. $^{*}p < 0.05$ for significant pairwise differences, if a significant interaction effect was found, as determined by a linear mixed effects model. *F*-value and *p*-value provided for significant interactions. $N = 6$ for WT basal and $N = 6$ for TG^{AC8}.

synthesize catecholamines from tyrosine (Huang et al., 1996; Wang et al., 2017).

We measured mRNA transcripts in SAN tissue (**Supplementary Table S3**) and protein expression in single isolated SAN cells (**Supplementary Table S1**) for enzymes that effect the conversion of tyrosine to L-DOPA (tyrosine hydroxylase, TH); L-DOPA to dopamine (DOPA decarboxylase); dopamine to norepinephrine [dopamine beta-hydorxylase (DBH)]; and norepinephrine to epinephrine [phenylethanolamine *N*-methyltransferase (PNMT)]. Compared to WT, protein levels for TH were increased in TG^{AC8} HCN4 positive SAN cells, while DBH protein was reduced (**Figure 6** and **Supplementary Table S1**). PNMT transcripts were also reduced in TG^{AC8} vs. WT SAN tissue (**Supplementary Table S3**).

Circulating Plasma Catecholamine Levels Are Altered in TG^{AC8}

Although AC8 overexpression in TG^{AC8} mice is cardiac specific (Lipskaia et al., 2000), afferent neuronal signals arising from within the heart can influence autonomic balance (Armour, 2008). As such, we gathered to test plasma catecholamines differences in TG^{AC8} and WT in the context of a confined pathway (**Figure 7A**). We found that circulating plasma epinephrine was significantly lower in TG^{AC8} vs. WT, and plasma norepinephrine tended to be lower in the TG^{AC8} vs. WT (**Figures 7B,C**). DOPAC, which is derived from dopamine, and DPHG, which is derived from norepinephrine, were also reduced in TG^{AC8} plasma (**Figures 7D,E**). In contrast, both DOPA and dopamine levels are increased in TG^{AC8} vs. WT (**Figures 7F,G**). The altered pattern of circulating plasma catecholamines in TG^{AC8} (**Figures 7B–G**) mirrors patterns of enzyme expression that regulate catecholamine production in TG^{AC8} SAN tissue (**Figure 7A**).

DISCUSSION

Mechanisms Intrinsic to SAN Cells Rather Than Extrinsic Autonomic Input to the SAN Drive Heart Rate Variability of the TG^{AC8}

The rate and beat to beat variability of spontaneous AP generation by the SAN, the central pacemaker of the heart, are highly dependent on characteristics of neurotransmitter signals. This includes the quantity of autonomic neurotransmitter released from nerve endings, its binding to autonomic receptors on SAN cell, transmembrane and intracellular transduction of the signals in response to neurotransmitter activation of β-adrenergic and muscarinic cholinergic receptors to various cellular secondary messengers (such as cAMP, Ca^{2+}, and protein phosphorylation). The culmination of neurotransmitter signaling, however, modulation of critical intrinsic SAN cell protein effectors that regulate their automaticity, even in the absence of autonomic input, i.e., the intrinsic automaticity of these cells, which persists in the absence of autonomic neuronal input when these cells are isolated from the SAN (Vinogradova et al., 2006, 2008; Younes et al., 2008; Lakatta et al., 2010).

It has been argued in many previous studies that changes in HRV largely result from alterations in autonomic neural input signals to the SAN (Lahiri et al., 2008; Thayer et al., 2010; Billman, 2011; Malik et al., 2019). There is, however, substantial support for the idea that like HR, regulation of HRV *in vivo* is not solely attributable to autonomic input, but also to mechanisms intrinsic to SAN cells (Boyett et al., 2019) is present *in vivo* during autonomic blockade. Significant beating rate variability has been described via *ex vivo* cardiac preparations. In the absence of external autonomic input, i.e., in isolated, adult hearts, isolated SAN tissue and isolated SAN cells

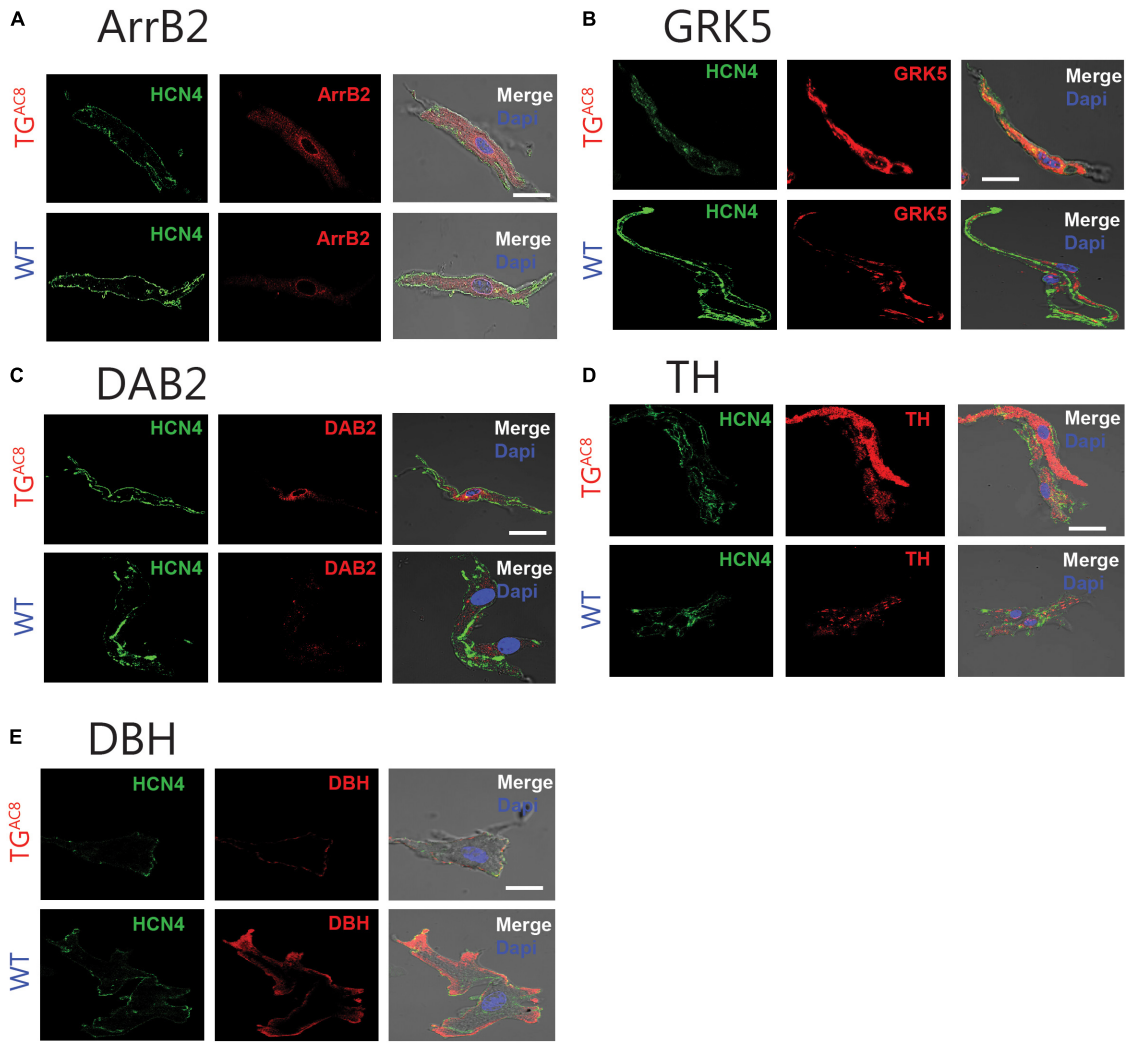

FIGURE 6 | Representative example of immunostaining of single, isolated SAN cells for proteins involved in β-AR desensitization and catecholamine synthesis in WT and TG^{AC8} for **(A)** Arrb2 and **(B)** GRK5. **(C)** DAB2. **(D)** Protein levels of TH and **(E)** DBH, enzymes involved in catecholamine synthesis in intrinsic cardiac adrenergic cells. Left panels: HCN4 immunolabeling; middle panel: selected antibody immunolabeling; right panel: overlay of left and center panels. Scale bar, 20 μm.

(Rocchetti et al., 2000; Zaza and Lombardi, 2001; Zahanich et al., 2011; Monfredi et al., 2013, 2014; Yaniv et al., 2014a,b; Tsutsui et al., 2018), as well as in human embryonic cells (Mandel et al., 2012), and induced pluripotent stem cell-derived cardiomyocytes (Ben-Ari et al., 2014).

Intrinsic mechanisms that drive the spontaneous beating rate and rhythm in isolated SAN cells are embodied within a coupled-clock system driven by Ca^{2+} calmodulin activated AC type 8 (AC8). Stimulation of autonomic receptors of single SAN cells in isolation not only alters their beating rate but also their beat to beat variability (Yaniv et al., 2013, 2014a) via modulation of the same intrinsic pacemaker cell mechanisms that link autonomic neurotransmitter signaling to its effects *in vivo*.

Although *in vivo* autonomic neural input to the SAN must modulate HR and HRV *via* signaling its effects to effector mechanisms intrinsic to the SANC coupled-clock system, whether or not the AC-driven coupled clock system intrinsic to SANC has a role in regulation of HR and HRV *in vivo* had never been clearly established. To address this conundrum, we utilized a transgenic mouse in which a critical component of the human coupled clock system, the human AC8 gene, was genetically overexpressed (TG^{AC8}) in a cardiac specific manner (Georget et al., 2002; Lipskaia et al., 2000). We hypothesized that a potent coherent intrinsic "sympathetic-like" state of TG^{AC8} might largely override autonomic input to the SAN, partially uncoupling the SAN from autonomic neural surveillance, thereby unmasking a potent intrinsic SANC component of HR and HRV regulation *in vivo*. In other terms, we hypothesized that the TG^{AC8} heart will manifest an intrinsically coherent HR and HRV that are largely independent of whole body and neurovisceral integration (McCraty and Zayas, 2014; Smith et al., 2017). To this end, we

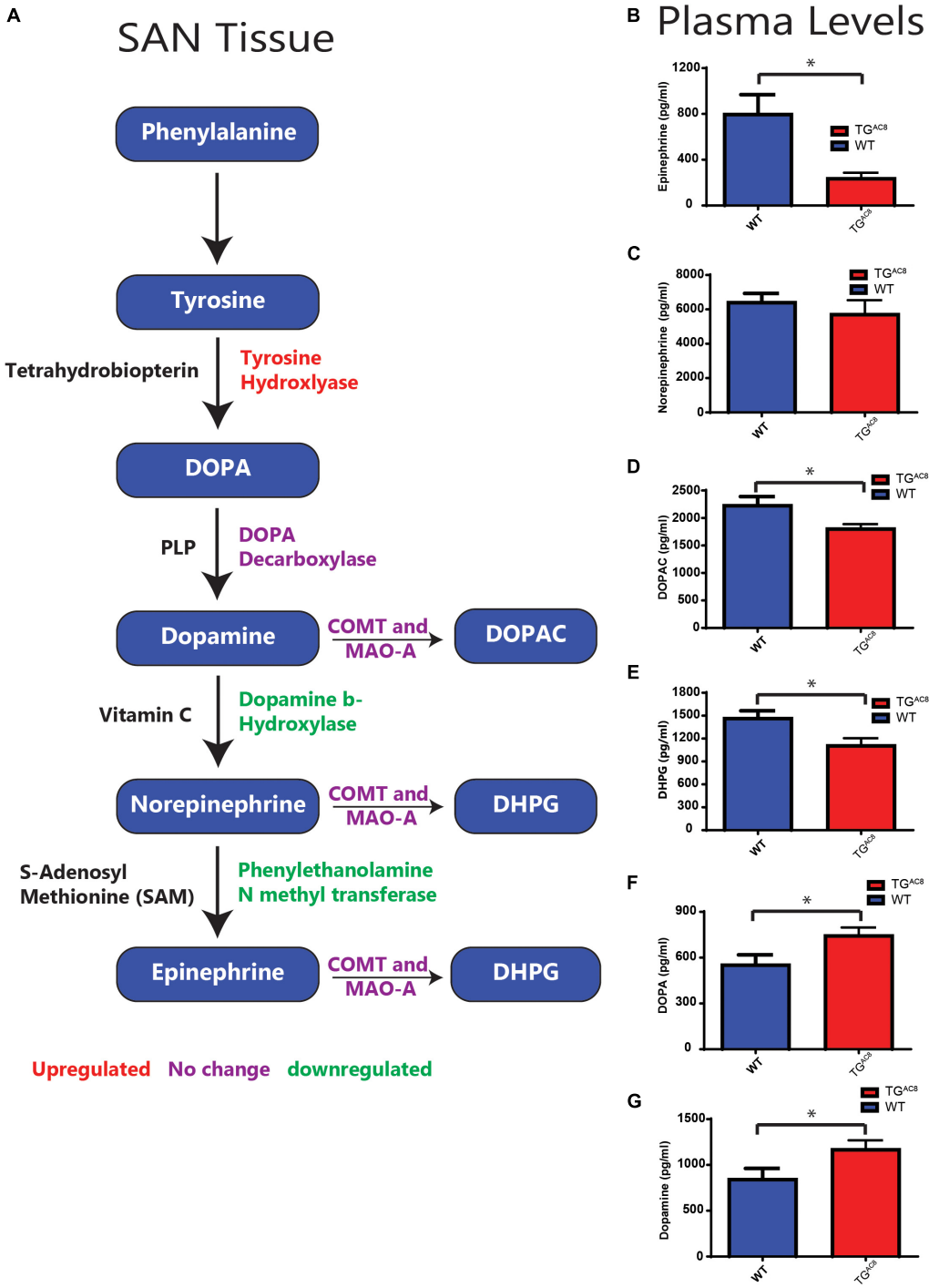

FIGURE 7 | A schematic of enzymes involving catecholamine synthesis and degradation in SAN tissue (cf. **Supplementary Tables S1**, **S3** for quantitative analysis) and circulating plasma catecholamines in TG^{AC8} and WT mice. **(A)** Red indicates genes upregulated, purple no change, and green downregulated in transcript abundance or protein expression in TG^{AC8} vs. WT SAN tissue or isolated SAN cells (cf. **Supplementary Tables S1**, **S3**). **(B–G)** Quantification of plasma catecholamine concentrations in TG^{AC8} and WT mice. **(B)** Epinephrine. **(C)** Norepinephrine. **(D)** DOPAC. **(E)** DHPG. **(F)** DOPA. **(G)** Dopamine (N = 10 WT and N = 10 TG^{AC8}). *$p < 0.05$ for concentration differences determined by Student's t-test.

performed comprehensive HR and HRV studies in unrestrained, unanesthetized mice in the absence and presence of single or dual autonomic receptor blockade (atropine and propranolol), and measured plasma catecholamine levels and transcription of genes and expression of proteins that regulate the responses to autonomic receptor input.

Our results show, for the first time, that markedly increased AC8 transcription and translation in TG^{AC8} SAN cells (**Figure 1** and **Supplementary Table S1**) produces marked increases in the mean HR *in vivo* in awake, untethered TG^{AC8} mice (**Supplementary Figure S2**), and that the *in vivo* HRV shifts to a markedly coherent pattern (**Figure 3**). Not only was mean basal *in vivo* HR considerably elevated and basal HRV markedly reduced in TG^{AC8} compared to WT, but the mean intrinsic HR (i.e., HR in the presence of dual autonomic blockade) was also elevated in TG^{AC8}, while intrinsic HRV was reduced (**Figure 3**). The *in vivo* HRV pattern exhibited by TG^{AC8} is largely attributable to coupled-clock mechanisms intrinsic to SAN cells that are driven by AC8. In other terms, mechanisms intrinsic to the TG^{AC8} SAN regulate mean HR and HRV. Likewise, the TG^{AC8} heart evades autonomic surveillance to a substantial degree. In this regard, mechanisms within TG^{AC8} SAN cells appear to function as autonomic ganglia. Because mechanisms intrinsic to SAN cells dominate TG^{AC8} HR and HRV *in vivo*, this experimental model provides proof of principle that cAMP-directed signaling intrinsic to SAN cells can markedly impact not only on mean HR but also HRV.

Significant cAMP-mediated beating rate variability, i.e., HRV in the absence of external autonomic input, is attributable to intrinsic coupled-clock mechanisms has already been described via *ex vivo* cardiac preparations. Specifically, beat-to-beat variability occurs in isolated, adult hearts, isolated SAN tissue and isolated SAN cells (Monfredi et al., 2013; Yaniv et al., 2014a), as well as in human embryonic cells (Mandel et al., 2012), and induced pluripotent stem cell-derived cardiomyocytes (Ben-Ari et al., 2014).

Adaptive Strategies of TG^{AC8} to Blunt Adrenergic Autonomic Input

We discovered that in the context of high cAMP-PKA-Ca^{2+} signaling intrinsic to SAN cells, TG^{AC8} applies adaptive strategies in order to blunt additional external sympathetic input. Adaptations that partially disengage the heart from external adrenergic input are important to prevent arrhythmias, cell necrosis, and apoptosis, thus preventing cardiomyopathy and death of the organism (Koch et al., 2000). Adaptive strategies in TG^{AC8} include (1) downregulation of mechanisms involved in catecholamine synthesis of intrinsic cardiac adrenergic cells within SAN tissue (Huang et al., 1996), (2) reductions in circulating plasma catecholamines, and (3) upregulation of pathways that desensitize β-AR receptor signaling.

Catecholamine Production in the Heart

Prior studies have demonstrated that intrinsic cardiac adrenergic cells within left ventricular myocardium contribute about 15% of total heart epinephrine, norepinephrine, or dopamine levels (Huang et al., 1996). We provide further evidence that enzymes involved in catecholamine synthesis are expressed in cells that reside within the adult SAN. Protein levels of TH, the initial enzymatic step involved in catecholamine production, was increased in TG^{AC8} vs. WT HCN4-immunolabeled SAN cells (**Supplementary Table S1** and **Figures 6**, **7**), suggesting that some pacemaker cells in adult SAN may also be intrinsic cardiac adrenergic cells. These intrinsic cardiac adrenergic cell-derived transmitters stimulate G protein coupled receptors in an autocrine/paracrine manner (Peoples et al., 2018). We assessed protein expression and transcript abundance of DBH and transcripts coding for PNMT, enzymes that catalyze the conversion of dopamine to norepinephrine or norepinephrine to epinephrine. Of note, both DBH and PNMT were reduced in TG^{AC8} vs. WT SAN tissue and cells (**Supplementary Table S1** and **Figure 7A**). Downregulation of DBH and PNMT in TG^{AC8} (**Figure 7A**) may indicate that intrinsic norepinephrine and epinephrine production by intrinsic cardiac adrenergic in TG^{AC8} SAN cells is less than that of WT. Normal fetal heart development requires DBH expression, as embryonic heart failure and death ensue when the protein coding gene is knocked out (Thomas et al., 1995). The pattern of upregulation of TH in SAN cells coupled to a reduction of DBH may indicate that, as in circulating plasma (**Figure 7G**), the concentration of dopamine is also increased in SAN tissue. Of note, dopamine can limit cell AC activity via activation of G_I coupled muscarinic receptor signaling (Missale et al., 1998). A reduction in norepinephrine and epinephrine synthesis and increased dopamine could be construed to be adaptive mechanisms employed to reduce intrinsic cardiac adrenergic signaling in TG^{AC8} SAN cells, not only to limit the HR in TG^{AC8} from going beyond the elevated values observed, but also to ensure survival of the TG^{AC8} heart (Koch et al., 2000). Unfortunately, the small volume of mouse SAN precluded any possible measurements of SAN tissue catecholamines. Whether norepinephrine and epinephrine levels are reduced in TG^{AC8} SAN tissue, or dopamine receptor signaling is increased in TG^{AC8} SAN cells merits future study.

Plasma Catecholamines

Because AC8 overexpression in TG^{AC8} mice is limited to the heart, at first glance, it was surprising to find that circulating catecholamine levels differed between WT and TG^{AC8}. The pattern of altered plasma catecholamine levels in TG^{AC8} (**Figures 7B–G**) mirrors experimental changes from the expression pattern of enzymes involved in catecholamine synthesis within TG^{AC8} SAN tissue or cells (**Supplementary Table S1** and **Figure 7A**). Circulating plasma levels of DOPAC, DPHG, and epinephrine were significantly reduced. Norepinephrine trended toward a significant reduction, and the plasma concentration of dopamine, was significantly increased. In this coherent pacemaker context, cells within the TG^{AC8} SAN would appear to act as an autonomic ganglion (**Figures 6**, **7**), generating signals to modulate catecholamine metabolism in these tissues via signaling directly to brain or indirectly to adrenal medulla (in addition to signaling to other parts of the heart). The altered pattern of circulatory catecholamines in TG^{AC8} is consistent with the idea that the TG^{AC8} heart communicates to/with other organs throughout the body via hemodynamic mechanisms, hormonal signaling, or direct afferent signaling from heat to the spinal cord or brain (Armour, 2008). Alternatively, because catecholamine production by the heart may contribute to plasma catecholamine levels (Huang et al., 1996), the reduction in circulatory plasma catecholamines of the

TG^{AC8} may also reflect, in part, reduced cardiac catecholamine synthesis within the TG^{AC8} heart.

Desensitization of β-Adrenergic Receptor Signaling

The blunted *in vivo* response to dobutamine in TG^{AC8} mice (**Figure 5**) reflects reduced effectiveness of external adrenergic input to the heart and resembles the blunted effect of isoproterenol to increase HR in the TG^{AC8} heart *ex vivo* (Georget et al., 2002). Our results demonstrate that, although neither the abundance of transcripts coding for β-AR subtype proteins, nor Gαs, Gαi1, Gαi2, or Gαi3 proteins differ from those of WT, the abundance transcripts for genes that desensitize and internalize β-ARs (Koch et al., 2000) are increased (**Supplementary Table S3**). Protein levels of Arrb2, GRK5, and Dab_2 also significantly exceed those in WT (**Supplementary Table S1**). The altered patterns of gene and protein expression in the TG^{AC8} SAN suggest that β-AR desensitization accounts, at least in part, for the reduced HR and contractility in response to β-AR stimulation. β-AR desensitization complements the reduction in catecholamines within TG^{AC8} mice, limiting the extent to which external adrenergic influences increase the high level of intracellular cAMP-PKA-Ca^{2+} signaling that result from overexpression of AC8 in the TG^{AC8} heart.

Blunted Effectiveness of Vagal Input Into the TG^{AC8} SAN

Our results demonstrate that in addition to blunted adrenergic receptor signaling, parasympathetic inhibition has a minimal effect on the TG^{AC8}. Although the reduction of basal high frequency power in TG^{AC8} might be interpreted to reflect reduced cholinergic receptor stimulation, it may be that muscarinic receptor signaling is exaggerated, but cannot overcome the extremely high AC8 induced cAMP-PKA-Ca^{2+} dependent signaling. Reductions in RGS signaling manifest as reduced transcription or overexpression of RGS2 and RGS6 in TG^{AC8} (**Supplementary Tables S1**, **S3**), are consistent with adaptations that promote receptor initiated Gi signaling, in an attempt to limit the markedly increased AC-cAMP signaling intrinsic to TG^{AC8} SAN cells.

In summary, our results provide evidence that the marked reduction to HRV in TG^{AC8} mice is minimally influenced by fluctuations in autonomic neuronal input to the SAN, and is instead driven by potent AC8 driven coupled clock mechanisms intrinsic to SAN cells. Because the overall pattern of marked coherency or loss of complexity within the TG^{AC8} heart rhythm is similar to that associated with aging or cardiac pathology (Iyengar et al., 1996; Fauchier et al., 1997; Huikuri and Stein, 2013; Yaniv et al., 2016), it will be crucial, in future studies, to determine whether TG^{AC8} will manifest a form of accelerated cardiac aging or heart failure.

Significance and Opportunities for Further Scientific Advances

Our results show that in the context of high cAMP-PKA-Ca^{2+} signaling driven by mechanisms intrinsic to SAN cells, the TG^{AC8} mouse heart applies adaptive strategies in order to blunt additional external sympathetic input. These findings provide a segway to more detailed studies of these and other adaptations that partially disengage the heart from external adrenergic input with respect to prevention of arrhythmias, cell necrosis, apoptosis, and prevention of cardiomyopathy in response to chronically increased sympathetic stress. Such studies may provide novel bases for therapeutic intervention for arrythmias and heart failure.

The TG^{AC8} mouse, in which AC8 is overexpressed only in the heart, would appear to be a specifically valuable model to the emerging field of neurocardiology. One such adaptation utilized by TG^{AC8} to reduce sympathetic input to its heart is a reduction in circulating altered plasma catecholamines. In addition to altered hemodynamic signaling to the nervous system, afferent signals from heart, spinal cord to brain are thought to emerge via a network of autonomic ganglia embedded within heart epicardial tissue to alter catecholamines (Armour, 2008). Such retrograde neuronal signaling from heart to nervous system may be a crucial adaptation, in addition to altered hemodynamic or hormonal signals, generated from within the TG^{AC8} heart to repress production of brain catecholamines or reducing brain to heart, or brain to adrenal medulla signaling. This merits further study.

DATA AVAILABILITY

All datasets generated for this study are included in the manuscript and/or the **Supplementary Files**.

ETHICS STATEMENT

All studies were performed in accordance with the Guide for the Care and Use of Laboratory Animals published by the National Institutes of Health (NIH Publication no. 85-23, revised 1996). The experimental protocols were approved by the Animal Care and Use Committee of the National Institutes of Health (protocol #441-LCS-2016).

AUTHOR CONTRIBUTIONS

JM and MM performed all of the *in vivo* studies, aided in the collection and isolation of SAN, analyzed the data, and wrote the manuscript. CR aided in the collection analysis of *in vivo* data. KC performed the sample collection for RT-qPCR and catecholamine data analysis. YL performed the AC activity assays. YT performed all RT-qPCR tissue preparation and experiments and was responsible for all immunostaining of SAN tissue. KiT did the analysis. ST isolated and prepped SAN cells for staining and analysis. KT participated in analyses of mice ECGs *in vivo*. OM guided the initial *in vivo* HRV studies and design. CM designed the LME statistical method used for *in vivo* analysis. YY helped to develop the HRV analysis methods. TH and KP analyzed the blood catecholamine levels. IA designed the initial

the study and oversaw the use and handling of animals involved. EL designed the research project, provided the materials and reagents, as well as aided in the writing of the manuscript.

FUNDING

All research was funded by the Intramural Research Program, National Institute on Aging (NIA). OM was supported by a clinical lectureship from the National Institute of Health Research, United Kingdom. KT was supported by Japan Society for the Promotion of Science Research Fellowship for Japanese Biomedical and Behavioral Researchers at the National Institutes of Health.

ACKNOWLEDGMENTS

We thank Melissa Krawczyk, Shannon Marshall, and Bruce Ziman for training and guidance on the handling of mice and telemetry sensors, overseeing breeding, and maintenance of TG^{AC8} and WT mouse lines, or for the isolation of mouse sinoatrial nodes.

SUPPLEMENTARY MATERIAL

The Supplementary Material for this article can be found online at: https://www.frontiersin.org/articles/10.3389/fnins.2019.00615/full#supplementary-material

REFERENCES

Armour, J. A. (2008). Potential clinical relevance of the 'little brain' on the mammalian heart. *Exp. Physiol.* 93, 165–176. doi: 10.1113/expphysiol.2007.041178

Behar, J. A., Rosenberg, A. A., Weiser-Bitoun, I., Shemla, O., Alexandrovich, A., Konyukhov, E., et al. (2018). PhysioZoo: a novel open access platform for heart rate variability analysis of mammalian electrocardiographic data. *Front. Physiol.* 9:1390. doi: 10.3389/fphys.2018.01390

Ben-Ari, M., Schick, R., Barad, L., Novak, A., Ben-Ari, E., Lorber, A., et al. (2014). From beat rate variability in induced pluripotent stem cell-derived pacemaker cells to heart rate variability in human subjects. *Heart Rhythm* 11, 1808–1818. doi: 10.1016/j.hrthm.2014.05.037

Billman, G. E. (2011). Heart rate variability - a historical perspective. *Front. Physiol.* 2:86. doi: 10.3389/fphys.2011.00086

Boyett, M., Wang, Y., and D'Souza, A. (2019). CrossTalk opposing view: heart rate variability as a measure of cardiac autonomic responsiveness is fundamentally flawed. *J. Physiol.* 597, 2599–2601. doi: 10.1113/JP277501

Eisenhofer, G., Goldstein, D. S., Stull, R., Keiser, H. R., Sunderland, T., Murphy, D. L., et al. (1986). Simultaneous liquid-chromatographic determination of 3,4-dihydroxyphenylglycol, catecholamines, and 3,4-dihydroxyphenylalanine in plasma, and their responses to inhibition of monoamine oxidase. *Clin. Chem.* 32, 2030–2033.

Fauchier, L., Babuty, D., Cosnay, P., Autret, M. L., and Fauchier, J. P. (1997). Heart rate variability in idiopathic dilated cardiomyopathy: characteristics and prognostic value. *J. Am. Coll. Cardiol.* 30, 1009–1014. doi: 10.1016/s0735-1097(97)00265-9

Georget, M., Mateo, P., Vandecasteele, G., Jurevicius, J., Lipskaia, L., Defer, N., et al. (2002). Augmentation of cardiac contractility with no change in L-type Ca2+ current in transgenic mice with a cardiac-directed expression of the human adenylyl cyclase type 8 (AC8). *FASEB J.* 16, 1636–1638. doi: 10.1096/fj.02-0292fje

Goldberger, A. L. (1991). Is the normal heartbeat chaotic or homeostatic? *News Physiol. Sci.* 6, 87–91. doi: 10.1152/physiologyonline.1991.6.2.87

Goldberger, A. L., Amaral, L. A., Hausdorff, J. M., Ivanov, P., Peng, C. K., and Stanley, H. E. (2002). Fractal dynamics in physiology: alterations with disease and aging. *Proc. Natl. Acad. Sci. U.S.A.* 99 (Suppl. 1), 2466–2472. doi: 10.1073/pnas.012579499

Huang, M. H., Friend, D. S., Sunday, M. E., Singh, K., Haley, K., Austen, K. F., et al. (1996). An intrinsic adrenergic system in mammalian heart. *J. Clin. Invest.* 98, 1298–1303. doi: 10.1172/JCI118916

Huikuri, H. V., and Stein, P. K. (2013). Heart rate variability in risk stratification of cardiac patients. *Prog. Cardiovasc. Dis.* 56, 153–159. doi: 10.1016/j.pcad.2013.07.003

Iyengar, N., Peng, C. K., Morin, R., Goldberger, A. L., and Lipsitz, L. A. (1996). Age-related alterations in the fractal scaling of cardiac interbeat interval dynamics. *Am. J. Physiol.* 271(4 Pt 2), R1078–R1084. doi: 10.1152/ajpregu.1996.271.4.R1078

Koch, W. J., Lefkowitz, R. J., and Rockman, H. A. (2000). Functional consequences of altering myocardial adrenergic receptor signaling. *Annu. Rev. Physiol.* 62, 237–260. doi: 10.1146/annurev.physiol.62.1.237

Kuznetsova, A., Brockhoff, P. B., and Christensen, R. H. B. (2016). *lmerTest: Tests in Linear Mixed Effects Models. R package version* 2.0-33. Available at: https://CRAN.R-project.org/package=lmerTest (accessed February 11, 2019).

Lahiri, M. K., Kannankeril, P. J., and Goldberger, J. J. (2008). Assessment of autonomic function in cardiovascular disease: physiological basis and prognostic implications. *J. Am. Coll. Cardiol.* 51, 1725–1733. doi: 10.1016/j.jacc.2008.01.038

Lakatta, E. G., Maltsev, V. A., and Vinogradova, T. M. (2010). A coupled SYSTEM of intracellular Ca2+ clocks and surface membrane voltage clocks controls the timekeeping mechanism of the heart's pacemaker. *Circ. Res.* 106, 659–673. doi: 10.1161/CIRCRESAHA.109.206078

Lipskaia, L., Defer, N., Esposito, G., Hajar, I., Garel, M. C., Rockman, H. A., et al. (2000). Enhanced cardiac function in transgenic mice expressing a Ca(2+)-stimulated adenylyl cyclase. *Circ. Res.* 86, 795–801. doi: 10.1161/01.res.86.7.795

Malik, M., Hnatkova, K., Huikuri, H. V., Lombardi, F., Schmidt, G., and Zabel, M. (2019). Cross talk proposal: heart rate variability is a valid measure of cardiac autonomic responsiveness. *J. Physiol.* 597, 2595–2598. doi: 10.1113/JP277500

Mandel, Y., Weissman, A., Schick, R., Barad, L., Novak, A., Meiry, G., et al. (2012). Human embryonic and induced pluripotent stem cell-derived cardiomyocytes exhibit beat rate variability and power-law behavior. *Circulation* 125, 883–893. doi: 10.1161/CIRCULATIONAHA.111.045146

Mangoni, M. E., and Nargeot, J. (2008). Genesis and regulation of the heart automaticity. *Physiol. Rev.* 88, 919–982. doi: 10.1152/physrev.00018.2007

McCraty, R., and Zayas, M. A. (2014). Cardiac coherence, self-regulation, autonomic stability, and psychosocial well-being. *Front. Psychol.* 5:1090. doi: 10.3389/fpsyg.2014.01090

Missale, C., Nash, S. R., Robinson, S. W., Jaber, M., and Caron, M. G. (1998). Dopamine receptors: from structure to function. *Physiol. Rev.* 78, 189–225. doi: 10.1152/physrev.1998.78.1.189

Monfredi, O., Lyashkov, A. E., Johnsen, A. B., Inada, S., Schneider, H., Wang, R., et al. (2014). Biophysical characterization of the underappreciated and important relationship between heart rate variability and heart rate. *Hypertension* 64, 1334–1343. doi: 10.1161/HYPERTENSIONAHA.114.03782

Monfredi, O., Maltseva, L. A., Spurgeon, H. A., Boyett, M. R., Lakatta, E. G., and Maltsev, V. A. (2013). Beat-to-Beat variation in periodicity of local calcium releases contributes to intrinsic variations of spontaneous cycle length in isolated single sinoatrial node cells. *PLoS One* 8:e67247. doi: 10.1371/journal.pone.0067247

Peoples, J., Maxmillan, T., Le, Q., Nadochiy, S., Brookes, P., Porter, G., et al. (2018). Metabolomics reveals critical adrenergic regulatory checkpoints in glycolysis and pentose-phosphate pathways in embryonic heart. *J. Biol. Chem.* 293, 6925–6941. doi: 10.1074/jbc.RA118.002566

R Core Development Team (2017). *R: A Language and Environment for Statistical Computing*. Vienna: R Foundation for Statistical Computing.

Rocchetti, M., Malfatto, G., Lombardi, F., and Zaza, A. (2000). Role of the input/output relation of sinoatrrial myocytes in cholinergic modulation of heart rate variability. *J. Cardiovasc. Electrophysiol.* 11, 522–530. doi: 10.1111/j.1540-8167.2000.tb00005.x

RStudio Team (2017). *RStudio: Integrated Development for R*. Boston, MA: RStudio, Inc.

Smith, R., Thayer, J. F., Khalsa, S. S., and Lane, R. D. (2017). The hierarchical basis of neurovisceral integration. *Neurosci. Biobehav. Rev.* 75, 274–296. doi: 10.1016/j.neubiorev.2017.02.003

Thayer, J. F., Yamamoto, S. S., and Brosschot, J. F. (2010). The relationship of autonomic imbalance, heart rate variability and cardiovascular disease risk factors. *Int. J. Cardiol.* 141, 122–131. doi: 10.1016/j.ijcard.2009.09.543

Thireau, J., Zhang, B. L., Poisson, D., and Babuty, D. (2008). Heart rate variability in mice: a theoretical and practical guide. *Exp. Physiol.* 93, 83–94. doi: 10.1113/expphysiol.2007.040733

Thomas, S. A., Matsumoto, A. M., and Palmiter, R. D. (1995). Noradrenaline is essential for mouse fetal development. *Nature* 374, 643–646. doi: 10.1038/374643a0

Tsutsui, K., Monfredi, O. J., Sirenko-Tagirova, S. G., Maltseva, L. A., Bychkov, R., Kim, M. S., et al. (2018). A coupled-clock system drives the automaticity of human sinoatrial nodal pacemaker cells. *Sci. Signal* 11:eaa7608. doi: 10.1126/scisignal.aap7608

Vinogradova, T. M., Lyashkov, A. E., Zhu, W., Ruknudin, A. M., Sirenko, S., Yang, D., et al. (2006). High basal protein kinase A-dependent phosphorylation drives rhythmic internal Ca2+ store oscillations and spontaneous beating of cardiac pacemaker cells. *Circ. Res.* 98, 505–514. doi: 10.1161/01.RES.0000204575.94040.d1

Vinogradova, T. M., Sirenko, S., Lyashkov, A. E., Younes, A., Li, Y., Zhu, W., et al. (2008). Constitutive phosphodiesterase activity restricts spontaneous beating rate of cardiac pacemaker cells by suppressing local Ca2+ releases. *Circ. Res.* 102, 761–769. doi: 10.1161/CIRCRESAHA.107.161679

Wang, Y., Lin, W. K., Crawford, W., Ni, H., Bolton, E. L., Khan, H., et al. (2017). Optogenetic control of heart rhythm by selective stimulation of cardiomyocytes derived from Pnmt+ cells in murine heart. *Sci. Rep.* 7:40687. doi: 10.1038/srep40687

Yang, D., Lyashkov, A. E., Li, Y., Ziman, B. D., and Lakatta, E. G. (2012). RGS2 overexpression or G(i) inhibition rescues the impaired PKA signaling and slow AP firing of cultured adult rabbit pacemaker cells. *J. Mol. Cell. Cardiol.* 53, 687–694. doi: 10.1016/j.yjmcc.2012.08.007

Yang, J., Huang, J., Maity, B., Gao, Z., Lorca, R. A., Gudmundsson, H., et al. (2010). RGS6, a modulator of parasympathetic activation in heart. *Circ. Res.* 107, 1345–1349. doi: 10.1161/CIRCRESAHA.110.224220

Yaniv, Y., Ahmet, I., Liu, J., Lyashkov, A. E., Guiriba, T. R., Okamoto, Y., et al. (2014a). Synchronization of sinoatrial node pacemaker cell clocks and its autonomic modulation impart complexity to heart beating intervals. *Heart Rhythm* 11, 1210–1219. doi: 10.1016/j.hrthm.2014.03.049

Yaniv, Y., Lyashkov, A. E., Sirenko, S., Okamoto, Y., Guiriba, T. R., Ziman, B. D., et al. (2014b). Stochasticity intrinsic to coupled-clock mechanisms underlies beat-to-beat variability of spontaneous action potential firing in sinoatrial node pacemaker cells. *J. Mol. Cell. Cardiol.* 77, 1–10. doi: 10.1016/j.yjmcc.2014.09.008

Yaniv, Y., Ahmet, I., Tsutsui, K., Behar, J., Moen, J. M., Okamoto, Y., et al. (2016). Deterioration of autonomic neuronal receptor signaling and mechanisms intrinsic to heart pacemaker cells contribute to age-associated alterations in heart rate variability in vivo. *Aging Cell* 15, 716–724. doi: 10.1111/acel.12483

Yaniv, Y., Sirenko, S., Ziman, B. D., Spurgeon, H. A., Maltsev, V. A., and Lakatta, E. G. (2013). New evidence for coupled clock regulation of the normal automaticity of sinoatrial nodal pacemaker cells: bradycardic effects of ivabradine are linked to suppression of intracellular Ca(2)(+) cycling. *J. Mol. Cell. Cardiol.* 62, 80–89. doi: 10.1016/j.yjmcc.2013.04.026

Younes, A., Lyashkov, A. E., Graham, D., Sheydina, A., Volkova, M. V., Mitsak, M., et al. (2008). Ca(2+) -stimulated basal adenylyl cyclase activity localization in membrane lipid microdomains of cardiac sinoatrial nodal pacemaker cells. *J. Biol. Chem.* 283, 14461–14468. doi: 10.1074/jbc.M707540200

Zahanich, I., Sirenko, S. G., Maltseva, L. A., Tarasova, Y. S., Spurgeon, H. A., Boheler, K. R., et al. (2011). Rhythmic beating of stem cell-derived cardiac cells requires dynamic coupling of electrophysiology and Ca cycling. *J. Mol. Cell. Cardiol.* 50, 66–76. doi: 10.1016/j.yjmcc.2010.09.018

Zaza, A., and Lombardi, F. (2001). Autonomic indexes based on the analysis of heart rate variability: a view from the sinus node. *Cardiovasc. Res.* 50, 434–442. doi: 10.1016/s0008-6363(01)00240-1

Conflict of Interest Statement: The authors declare that the research was conducted in the absence of any commercial or financial relationships that could be construed as a potential conflict of interest.

frontiers in Neuroscience

MINI REVIEW
published: 21 June 2019
doi: 10.3389/fnins.2019.00530

Measures of CNS-Autonomic Interaction and Responsiveness in Disorder of Consciousness

Francesco Riganello[1,2], Stephen Karl Larroque[1], Carol Di Perri[1,3], Valeria Prada[4], Walter G. Sannita[4] and Steven Laureys[1]*

[1] Coma Science Group, GIGA-Consciousness, GIGA Institute, University Hospital of Liège, Liège, Belgium, [2] S. Anna Institute, Research in Advanced Neurorehabilitation, Crotone, Italy, [3] Centre for Clinical Brain Sciences, The University of Edinburgh, Edinburgh, United Kingdom, [4] Department of Neuroscience, Rehabilitation, Ophthalmology, Genetics, and Maternal/Child Sciences, Polyclinic Hospital San Martino IRCCS, University of Genoa, Genoa, Italy

Neuroimaging studies have demonstrated functional interactions between autonomic (ANS) and brain (CNS) structures involved in higher brain functions, including attention and conscious processes. These interactions have been described by the Central Autonomic Network (CAN), a concept model based on the brain-heart two-way integrated interaction. Heart rate variability (HRV) measures proved reliable as non-invasive descriptors of the ANS-CNS function setup and are thought to reflect higher brain functions. Autonomic function, ANS-mediated responsiveness and the ANS-CNS interaction qualify as possible independent indicators for clinical functional assessment and prognosis in Disorders of Consciousness (DoC). HRV has proved helpful to investigate residual responsiveness in DoC and predict clinical recovery. Variability due to internal (e.g., homeostatic and circadian processes) and environmental factors remains a key independent variable and systematic research with this regard is warranted. The interest in bidirectional ANS-CNS interactions in a variety of physiopathological conditions is growing, however, these interactions have not been extensively investigated in DoC. In this brief review we illustrate the potentiality of brain-heart investigation by means of HRV analysis in assessing patients with DoC. The authors' opinion is that this easy, inexpensive and non-invasive approach may provide useful information in the clinical assessment of this challenging patient population.

Keywords: central autonomic network, autonomic nervous system, disorders of consciousness, unresponsive wakefulness syndrome, heart rate variability

OPEN ACCESS

Edited by:
Yoko Nagai,
University of Sussex, United Kingdom

Reviewed by:
Cristina Ottaviani,
Sapienza University of Rome, Italy
Herbert Jelinek,
Charles Sturt University, Australia

****Correspondence:***
Francesco Riganello
f.riganello@istitutosantanna.it

Specialty section:
This article was submitted to Autonomic Neuroscience, a section of the journal Frontiers in Neuroscience

Received: *24 December 2018*
Accepted: *08 May 2019*
Published: *21 June 2019*

Citation:
Riganello F, Larroque SK, Di Perri C, Prada V, Sannita WG and Laureys S (2019) Measures of CNS-Autonomic Interaction and Responsiveness in Disorder of Consciousness. Front. Neurosci. 13:530. doi: 10.3389/fnins.2019.00530

INTRODUCTION

Clinical evidence and neuroimaging research have documented retained modular brain activation and responsiveness in patients with Disorder of Consciousness (DoC) following brain injury even in the absence of integrated large-network processes known to sustain consciousness (Laureys et al., 2002; Bekinschtein et al., 2004, 2011; Owen et al., 2006; Monti, 2012; Naro et al., 2015; **Box 1**). In this respect, residual responsiveness in DoC appears to be mediated by varying network interactions (Riganello et al., 2013, 2015c; Crone et al., 2017; Duclos et al., 2017). Activation restricted to lower-level primary sensory cortices without involvement of higher-order associative

BOX 1 | Brain injury can result in a vegetative state/unresponsive wakefulness syndrome (VS/UWS) characterized by arousal and spontaneous eye-opening in the absence of any sign of awareness, finalized action or communication. Levels of residual responsiveness define the Minimally Conscious State (MCS) (Giacino et al., 2004). A 2006 provocative report presented the case of a VS/UWS subject able to engage in mental tasks as indicated by her fMRI patterns of brain activations (Owen et al., 2006). Levels of responsiveness involving higher brain functions have been observed in subjects otherwise classified as VS/UWS according to clinical criteria (Laureys et al., 2007; Boly et al., 2008; Bruno et al., 2010; Owen, 2014; Pistoia et al., 2016; Riganello et al., 2018b). These observations were mostly based on regional brain activation in response to stimulus conditions in controlled setups; stimulus-related functional changes in the autonomic nervous system (ANS) function have also been described. Still highly debated, e.g., in subjects in a VS/UWS, these observations challenge the current definitions and our understanding of both responsiveness and consciousness, with an impact on the clinical decision-making process (Laureys et al., 2010; Riganello et al., 2016, 2018a,b). The extent to which regional brain activations can be considered equivalent to, or compatible with behavioral responses in indicating (residual or covert) consciousness remains controversial and the current standards by which patients surviving severe brain injury should be regarded as being conscious or unconscious have been questioned (Celesia, 2013; Celesia and Sannita, 2013). In this respect, scientific research has introduced novel criteria of evaluation not yet fully integrated in the current nosography of disorders of consciousness (DoC), which is now undergoing a tacit, but not uncontroversial, revision (Monti and Sannita, 2016).

cortices has been described in vegetative state/unresponsive wakefulness syndrome (VS/UWS) (Soddu et al., 2015; Marino et al., 2017). Partially preserved activation in higher-order associative cortices has been demonstrated in Minimally Conscious State (MCS) (Di Perri et al., 2013, 2016; Demertzi et al., 2015), whereas restoration of thalamocortical connectivity has shown to relate to consciousness recovery (Laureys et al., 2000; Monti et al., 2014). A large amount of research by means of neuroimaging techniques has revealed that several aspects of relatively high-level functions, including sensory and linguistic processing and learning dynamics, can survive and remain operative in DoC (Aubinet C- HBM 2018, Laureys et al., 2007; Boly et al., 2008; Majerus et al., 2009; Bruno et al., 2010).

Neuroimaging studies have further shown functional interaction between autonomic nervous structures [i.e., the parasympathetic and sympathetic branch of the Autonomic Nervous System (ANS)] and the neuronal networks involved in higher brain functions, including attention and conscious processes (Napadow et al., 2008; Thayer et al., 2012; Ruiz Vargas et al., 2016; Valenza et al., 2017). Heart Rate Variability (HRV), that is the physiological phenomenon of variation in the time interval between consecutive heartbeats, is thought to reflect the complex interaction between brain and cardiovascular system (Thayer and Lane, 2009; Ernst, 2017). HRV entropy, a measure of the complexity of HRV, has shown to discriminate VS/UWS and MCS patients and was found to correlate with the ANS functional status (Riganello et al., 2018b).

In agreement with this line of observation, indices of ANS functions have proved reliable in detecting responsiveness and predicting recovery following neuro-rehabilitation in VS/UWS (Wijnen et al., 2006; Riganello et al., 2015a). There is growing evidence that ANS function can be monitored non-invasively and neuroimaging studies have provided evidence of the two-way interplay between heart and brain. As a result, interest in the bidirectional ANS-CNS interaction in a variety of physiopathological conditions is growing (de Morree et al., 2013; Riganello et al., 2014; Bassi and Bozzali, 2015; Chen et al., 2017; Doehner et al., 2018), however, the ANS-CNS interaction in DoC has so far not been extensively investigated.

ANS-CNS INTERACTION IN DOC

A concept model Central Autonomic Network (CAN) (Benarroch, 2007b) has been proposed to describe the ANS-CNS two-way interaction and the continuous modulation of homeostatic processes and allostatic adaptation to internal or external requirements (Friedman, 2007; Thayer et al., 2012; Riganello, 2016). Its functional organization involves the forebrain (anterior cingulate, nucleus accumbens, insula, ventromedial prefrontal cortex, amygdala, and hypothalamus with bidirectional interactions between rostral and caudal systems), brainstem (periaqueductal gray, parabrachial nucleus, nucleus of the solitary tract, and the reticular formation of ventrolateral medulla). At spinal level it operates via neuronal projections of segmental reflexive ANS control (**Figure 1**). These structures receive converging visceral and nociceptive inputs (including those from thermo- and muscle receptors) and generate stimulus-specific patterns of autonomic response via projections to preganglionic sympathetic and parasympathetic neurons (Saper, 2002; Benarroch, 2007a). The forebrain and brainstem are involved in the modulation of autonomic output in response to pain and to emotional, behavioral, or "cognitive" stimuli (Hagemann et al., 2003; Berntson and Cacioppo, 2004; Thayer and Sternberg, 2006; Friedman, 2007; Thayer and Lane, 2009; Riganello et al., 2012a).

HEART RATE VARIABILITY AND HEART/BRAIN INTERPLAY

HRV measures (i.e., variables analyzed in time domain, frequency domain and non-linear measurements) describe the ANS functional setup, and are thought to reflect higher brain functions - at least to some extent - and to qualify as independent indicators of CNS-ANS interaction (Napadow et al., 2008; Thayer and Lane, 2009; Thayer et al., 2012; Tonhajzerova et al., 2012) (**Box 2** and **Table 1**). HRV measures reflect the activity of physiological factors modulating the heart rhythm and its adaptation to changing conditions (Carney et al., 2005; Garan, 2009; Shaffer et al., 2014). The vagus nerve is the major channel involved in the afferent neurological signals relayed from the heart and other visceral organs to the brain, including the baroreflex signals (de Lartigue, 2014). Brain morphological variants in the right striatal and limbic structures involved in the ANS functional organization were found to associate with differences in cardiac vagal function (Thayer and Lane, 2000; Napadow et al., 2008; Critchley, 2009; Lane et al., 2009) and to significantly contribute in the information flow in all frequency

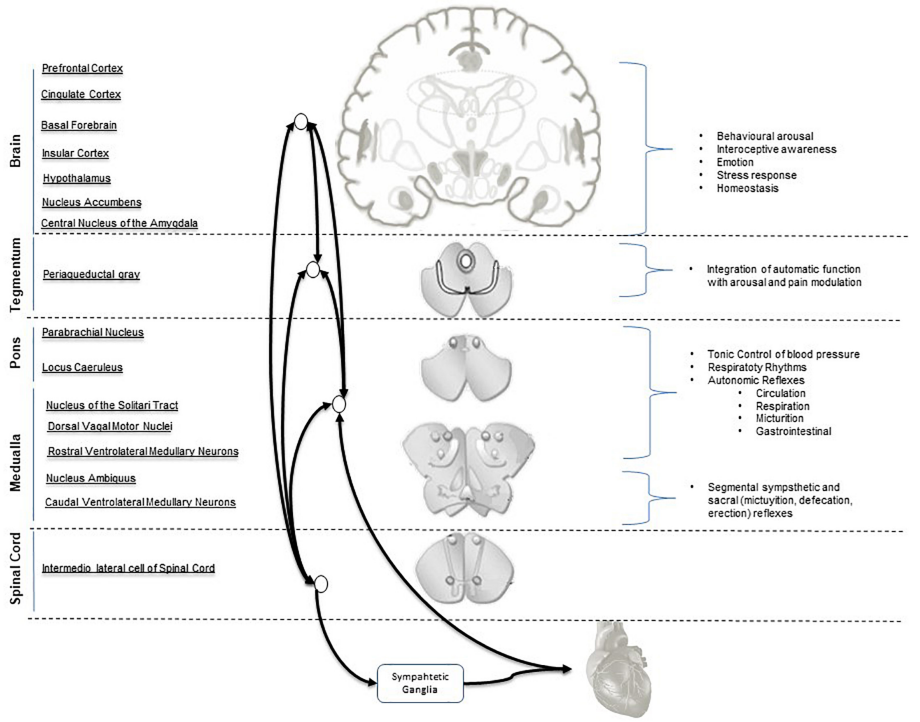

FIGURE 1 | Central Autonomic Network (CAN) hierarchical organization and interconnections. Parasympathetic output is mediated mainly by the nucleus of the vagus and nucleus ambiguous. Sympathetic output is mainly mediated by the intermediolateral column cell.

bands during sleep (Faes et al., 2014). In the absence of cardiac disorders, stimulus- or condition-related HRV changes are in the range of physiological variability and require processing in the time and frequency domains or by geometrical or non-linear methods to be identified (Task Force of the European Society of Cardiology and the North American Society of Pacing and Electrophysiology, 1996; Rajendra Acharya et al., 2006). HRV methodologies benefit from being easy to record, inexpensive and non-invasive as compared to neuroimaging techniques. HRV measures are obtained from a signal (the heart tachogram) with excellent signal-to-noise ratio; procedures for sophisticated data analyses are usable without substantial loss in information (Nait-Ali, 2009). HRV is easier to apply than alternative techniques for ANS investigation (cardiac norepinephrine spillover, microneurographic techniques, or direct recording from skeletal muscle) (Berne et al., 1992; Esler, 1993; Wallin and Charkoudian, 2007). It is particularly applicable in studies on large subject samples or under experimental conditions where accurate laboratory procedures are not possible, such as in case of limited/null collaboration (e.g., in intensive/semi-intensive care units or in DoC) (Mowery et al., 2008; Norris et al., 2008a,b; Ryan et al., 2011).

HRV AND DOC

HRV is a possible index of consciousness attention (Babo-Rebelo et al., 2016; Cobos et al., 2019) and emotional states (Shi et al., 2017) in healthy subjects. The interaction between consciousness, attention and HRV has been documented in patients with DoC. VS/UWS and MCS subjects were more likely to respond to standard visual and auditory stimuli when the HRV normalized unit of LF (nuLF) ranged between 10–70 and LF peaked around 0.1 Hz (Riganello et al., 2013), thus suggesting a functional relationship between responsiveness and the sympatho-vagal balance; a correlation between HRV parameters and improvement of consciousness has been documented, and higher value of nuLF associated to a better outcome in VS/UWS patients (Riganello et al., 2015a; Wijnen et al., 2006).

In frequency domain, HRV total power (TP) as well as LF and HF power were found significantly decreased in patients with Glasgow Coma Outcome Extended (GOSE) (Weir et al., 2012) score <5 (Hendén et al., 2014).

A correlation between HRV entropy (index of the brain-heart interaction complexity) and brain activation has been also described. Approximate Entropy (ApEn) values were lower in VS/UWS patients than in healthy control whereas no differences were found for all linear parameters [Root Mean Square of Successive Differences between normal heartbeats (RMSSD), Standard Deviation of RR peak (SDRR)] (Sarà et al., 2008). We have recently found lower Multiscale Entropy (MSE) values in VS/UWS than in MCS, which correlated with the Coma Recovery Scale (CSR-R) total score. A functional connectivity pattern involving the CAN system has been documented, thus proposing HRV entropy as an indirect tool to measure and monitor connectivity changes in this neural

BOX 2 | HRV – Heart rate variability is defined as the R-R interval fluctuation of normal sinus beats around its average value. HRV is analyzed in time domain, frequency domain and by non-linear methods both in short (usually 5 min) and long-time recordings (Task Force of the European Society of Cardiology and the North American Society of Pacing and Electrophysiology, 1996). ANS functional contributions can be differentiated by analyses in the frequency domain, usually in three frequency band: High Frequency (HF) (0.15–0.5 Hz), Low Frequency (LF) (0.04–0.15 HZ), and (VLF) Very Low Frequency band (0.0033–0.04). The power, relative power and peak of each frequency band, the normalized value of HF (nuHF) and LF (nuLF) and the ratio between HF and LF (LF/HF) are the parameters usually considered. HF reflects parasympathetic activity as the HR variations related to the respiratory cycle. LF (0.04–0.15 Hz) mainly reflects baroreceptor activity during resting conditions and is known also as "baroreceptor range" (Malliani, 1995); it reflects contributions from both the parasympathetic and sympathetic systems and blood pressure regulation via baroreceptors and the baroreceptor activity in resting conditions (Malliani, 1995; Task Force of the European Society of Cardiology and the North American Society of Pacing and Electrophysiology, 1996; Berntson et al., 2007; Lehrer, 2007). The parasympathetic system affects heart rhythms down to 0.05 Hz, while the sympathetic system does not seem to generate rhythms above ∼0.1 Hz. In humans, the delay in the feedback loops of baroreflex system have distinctive high-amplitude peak in the HRV power spectrum around 0.1 Hz (Vaschillo et al., 2011; Lehrer and Eddie, 2013) due to the feedback loops between heart and brain (deBoer et al., 1987; Baselli et al., 1994). There is some evidence for an association between VLF band (0.0033–0.04 Hz) and all-cause mortality (Shaffer et al., 2014), however, the physiological mechanisms responsible for activity within this band are not clear although probably related to thermoregulation, the renin-angiotensin system, and other hormonal factors (Akselrod et al., 1981; Cerutti, 1995; Claydon and Krassioukov, 2008). The LF/HF ratio has controversial interpretations, with the LF power possibly generated by the sympathetic, the HF power by the parasympathetic system and their ratio indicating both parasympathetic or sympathetic dominance (Pagani et al., 1984; Montano et al., 1994). HRV descriptors are also derivable by non-linear methods. Development in the non-linear theories provides new instruments to analyse the entropy domain [such as the simple or approximate entropy (ApEn)], better describe the complexity, irregularity or randomness of HRV and its changes, the non-linear temporal relationships with other metrics such as functional connectivity, and extract information about the complexity of the two way brain-heart interaction (Norris et al., 2006; Ryan et al., 2011; Shaffer et al., 2014; Riganello et al., 2018b).

system (Riganello et al., 2018b). In a Evoked Response Potential (ERP) study based on nociceptive repeated laser stimulation MCS showed partially preserved cortical activations, higher ERP γ-power magnitude and Standard Deviation of Normal-to-Normal intervals (SDNN) compared to VS/UWS patients (Calabrò et al., 2017). Other studies on nociceptive stimulation documented a correlation between the level of consciousness and HRV-entropy (Riganello et al., 2018a; Tobaldini et al., 2018), with lower values of entropy detected in VS/UWS than in MCS patients or in healthy subjects, and correlated to the CRS-R total scores (Riganello et al., 2018a). The above results indicate a decrease of complexity in the modulation of the response to noxious stimuli in VS/UWS subjects and a less complex ANS modulation in the two way brain-heart interaction compared to MCS.

Similar results have been observed in response to complex (musical) stimuli. Music interventions were associated with favorable behavioral and physiological responses in several studies, however, methodological quality and outcomes were heterogeneous (Grimm and Kreutz, 2018). After 14-day of music stimulation SDNN and RMSSD of VS/UWS patients increased, indicating the activity of the cardiovascular system was enhanced (Lee et al., 2011). Contrasting observations were found in the direction of the RMSSD values in a work on MCS and VS/UWS patient, who were presented live preferred music and live improvised music (O'Kelly and Magee, 2013). A significant decrease in entropy was observed in VS/UWS subjects listening to four musical pieces of different structural complexity, whereas no differences between the same selected musical pieces were observed in healthy controls under comparable experimental conditions (Riganello et al., 2015b). The quality (positive or negative) of the emotional responses was correlated to extreme (low or high) nuLF values (Riganello et al., 2010). Higher values in both time and frequency domain were observed during affective than during non-affective auditory stimulation in VS/UWS patients suggesting the possibility to discriminate between different stimuli (Machado et al., 2007; Gutiérrez et al., 2010).

The clinical and scientific evidence suggests a diagnostic and prognostic relevance of HRV parameters in DoC of different aetiologies (e.g., traumatic brain injury (TBI), haemorrhagic, and anoxic) (Keren et al., 2005; King et al., 2009; Ryan et al., 2011; Almeida et al., 2017). Decreased values in the different domains of HRV analysis has been associated with worsened heath condition. HRV parameters extracted in the time domain (SDNN, SDNN index, and RMSSD) were also found decreased after TBI in the absence of major DoC (Rapenne et al., 2001; DeGiorgio et al., 2010; Kim et al., 2017) and associated to clinical worsening and to mortality in the acute phase (Morris et al., 2006; Norris et al., 2006; Mowery et al., 2008; King et al., 2009). In children, suppression of LF and HF bands of the power spectrum were associated with brain death and poor outcome (Goldstein et al., 1993, 1998) and decreases in LF/HF was correlated with increases in intracranial pressure and mortality (Biswas et al., 2000). In TBI adults, decreased LF, HF, LF/HF, and TP were associated with brain death, increased mortality, increased intracranial pressure, and poor outcome (Winchell and Hoyt, 1997; Rapenne et al., 2001; Papaioannou et al., 2006). Reduced HRV complexity has proved to be an independent predictor of mortality (Batchinsky et al., 2007). Decreased ApEn values have been associated to increased mortality in acute TBI (Papaioannou et al., 2008; Gao et al., 2016) and the MSE was found to identify trauma patients at risk of in-hospital death, and predicts mortality independent of probability of survival based on location and mechanism of injury (Norris et al., 2008a,b).

COMMENT AND PERSPECTIVES

The CAN model of ANS-CNS functional interaction is helpful to describe the phenomena underlying residual responsiveness in DoC within the framework of homeostatic and allostatic organization, at least in part and to a degree of pathophysiological approximation (Friedman, 2007; Shen et al., 2016; Thome et al., 2017). The suitability of HRV analysis in detecting residual (covert) brain function in DoC has been documented (Wijnen et al., 2006; Gutiérrez et al., 2010; Riganello, 2016;

TABLE 1 | Most common measures used in HRV analysis.

	Parameter	Unit	Description	
Time domain	SDNN/SDRR	ms	Standard deviation of NN/RR intervals	In the time domain both sympathetic and parasympathetic nervous systems contribute to SDNN. Differently from "RR," "NN" means that abnormal beats, like ectopic beats, have been removed. RMSSD is used to estimate the vagally mediated changes reflected in HRV. It is strongly correlated with pNN50
	SDANN		Standard deviation of the average normal-to-normal (NN) intervals for each of the 5 min segments during a 24 h recording	
	SDNN index		Mean of the standard deviations of all the NN intervals for each 5 min segment of a 24-h HRV recording	
	pNN50	%	Percentage of adjacent NN intervals that differ from each other by more than 50 ms (pNN50) (Task Force of the European Society of Cardiology and the North American Society of Pacing and Electrophysiology, 1996)	
	RMSSD	ms	Root mean square of successive differences between normal heartbeats	
Frequency Domain	VLF,LF, and HF power HF power	ms^2	Absolute power of total or of the single band of frequency calculated by FFT or Auto Regressive model	HF, LF and VLF bands of frequency are associated with several aspects of the ANS. The HF band reflects parasympathetic activity and corresponds to the HR variations related to the respiratory cycle. The LF band reflects contributions from both the parasympathetic and sympathetic systems. It mainly reflects baroreceptor activity during resting conditions. The sympathetic system is below 0.1 Hz. The VLF band is associated to thermoregulation, the renin-angiotensin system, and other hormonal factors, but also to the intrinsic heart activity. The normalized values (nuLF and nuHF) express the quantities on a more easily understood proportion (0–1) or percentage (0–100%) scale basis. The LF/HF ratio is generally used to represents the ratio of sympathetic to parasympathetic nerve activity, also if the LF is contaminated by the vagal system. nuLF, nuHF, as well as LF/HF ratio should be considered equivalent carriers of information with regard to sympathovagal balance (Burr, 2007)
	nuLF	nu	Relative power of the low-frequency band in normal unit	
	nuHF		Relative power of the high-frequency band in normal unit	
	LF/HF		Ratio LF-to-HF power	
	Peak VLF, LF, and HF	Hz	Peak of frequency of VLF, LF, or HF band	
Non-linear methods	Approximate entropy		Measures the regularity and complexity of a time series	The entropy reflects of the amount of irregularity in the R-to-R interval. Lower or higher values are index of higher or lower complex activity of the ANS. Further higher values were associated to a higher brain-heart two way interaction. The SampEn was introduced to counteract some shortcomings of the ApEn. The SampEn does not count a self-match of vectors, eliminating the bias toward regularity, and has been suggested to be independent of data length (Yentes et al., 2013)
	Sample entropy		Measures the regularity and complexity of a time series. Sample entropy can be calculated from a much shorter time series of fewer than 200 values	
	Multiscale entropy		Quantify the degree of irregularity over a range of time scales. The time series are constructed by averaging the IBI/tachogram's data points within non-overlapping windows of increasing length	

Garbarino and Sannita, 2015). Autonomic function, ANS-mediated responsiveness and the ANS-CNS interaction qualify as possible independent indicators for clinical functional assessment, diagnosis and prognosis in DoC (King et al., 2009; Ryan et al., 2011; Sannita, 2015; Riganello, 2016). In a reversed perspective, research on the residual modular functions in DoC can provide unique information about brain mechanisms/functions and ANS-CNS interplay that can be investigated in these patients under experimental conditions that are rigorously controlled (Monti, 2012; Riganello et al., 2012b; Sannita, 2014; Shen et al., 2016; Chennu et al., 2017; Kiryachkov et al., 2017).

Brain function is modulated by complex neural networks and non-neuronal factors which interact with each other, individually or collectively account for inter/intra-individual variability, and reflect/depend on the circadian rhythms and the wakefulness/sleep alternation (Bullock, 1970; Sannita, 2006; Garbarino et al., 2014, 2019; Soddu and Bassetti, 2017). The HRV concomitants of the major shift toward sympathetic activation associated to peak cortisol levels at the morning sleep-to-wake transition are an example in this regard (Bilan et al., 2005; Boudreau et al., 2011, 2012). HRV proved reliable in investigating the ANS-CNS functional interaction underlying residual responsiveness in VS/UWS or MCS subjects (Wijnen et al., 2006; Gutiérrez et al., 2010; Candelieri et al., 2011; Sannita, 2015; Riganello, 2016). CNS and ANS setups, however, change over time spontaneously or due to homeostatic or allostatic requirements with different timing and latencies. HRV measures at rest and in response to stimulus conditions have higher time resolution and reflect rapid changes better than clinical or neuroimaging markers of damage, with greater variability during the day (Bekinschtein et al., 2009; Candelieri et al., 2011; Riganello et al., 2013, 2015c; Abbate et al., 2014; Sannita, 2015; Blume et al., 2017). Time appears to be a source of variability adding to the variety of environmental factors (light and noise in hospital settings, timing of medication or non-pharmacologic interventions, co-morbidities, etc.) also needing consideration, both as co-determinants of the circadian rhythms (Soddu and Bassetti, 2017) and in view of the ANS major role in internal environment constancy and adaptation that are fundamental to homeostasis. Systematic investigation is still lacking and appears advisable.

AUTHOR CONTRIBUTIONS

FR, SKL, CDP, VP, WS, and SL have equally collaborate to this work with substantial, direct and intellectual contribute, and approved it for publication.

FUNDING

This work was supported by the University Hospital of Liège, the French Speaking Community Concerted Research Action (ARC 12-17/01), the Belgian National Fund for Scientific Research (FRS-FNRS), the German Research Society (DFG), Human Brain Project (EU-H2020-fetflagship-hbp-sga1-ga720270), Luminous project (EU-H2020-fetopen-ga686764), the James McDonnell Foundation, Mind Science Foundation, IAP research network P7/06 of the Belgian Government (Belgian Science Policy), the European Commission, the Public Utility Foundation "Université Européenne du Travail," and "Fondazione Europea di Ricerca Biomedica". SKL is a FRS-FNRS research fellow. SL is research director at FRS-FNRS.

REFERENCES

Abbate, C., Trimarchi, P. D., Basile, I., Mazzucchi, A., and Devalle, G. (2014). Sensory stimulation for patients with disorders of consciousness: from stimulation to rehabilitation. *Front. Hum. Neurosci.* 8:616. doi: 10.3389/fnhum.2014.00616

Akselrod, S., Gordon, D., Ubel, F. A., Shannon, D. C., Berger, A. C., and Cohen, R. J. (1981). Power spectrum analysis of heart rate fluctuation: a quantitative probe of beat-to-beat cardiovascular control. *Science* 213, 220–222. doi: 10.1126/science.6166045

Almeida, R., Dias, C., Silva, M. E., and Rocha, A. P. (2017). "ARFIMA-GARCH modeling of HRV: clinical application in acute brain injury," in *Complexity and Nonlinearity in Cardiovascular Signals*, eds R. Barbieri, E. P. Scilingo, and G. Valenza (Cham: Springer), 451–468. doi: 10.1007/978-3-319-58709-7_17

Babo-Rebelo, M., Richter, C. G., and Tallon-Baudry, C. (2016). Neural responses to heartbeats in the default network encode the self in spontaneous thoughts. *J. Neurosci.* 36, 7829–7840. doi: 10.1523/JNEUROSCI.0262-16.2016

Baselli, G., Cerutti, S., Badilini, F., Biancardi, L., Porta, A., Pagani, M., et al. (1994). Model for the assessment of heart period and arterial pressure variability interactions and of respiration influences. *Med. Biol. Eng. Comput.* 32, 143–152. doi: 10.1007/bf02518911

Bassi, A., and Bozzali, M. (2015). Potential interactions between the autonomic nervous system and higher level functions in neurological and neuropsychiatric conditions. *Front. Neurol.* 6:182. doi: 10.3389/fneur.2015.00182

Batchinsky, A. I., Cancio, L. C., Salinas, J., Kuusela, T., Cooke, W. H., Wang, J. J., et al. (2007). Prehospital loss of R-to-R interval complexity is associated with mortality in trauma patients. *J. Trauma* 63, 512–518. doi: 10.1097/TA.0b013e318142d2f0

Bekinschtein, T., Niklison, J., Sigman, L., Manes, F., Leiguarda, R., Armony, J., et al. (2004). Emotion processing in the minimally conscious state. *J. Neurol. Neurosurg. Psychiatry* 75, 788–788. doi: 10.1136/jnnp.2003.034876

Bekinschtein, T. A., Golombek, D. A., Simonetta, S. H., Coleman, M. R., and Manes, F. F. (2009). Circadian rhythms in the vegetative state. *Brain Inj.* 23, 915–919. doi: 10.1080/02699050903283197

Bekinschtein, T. A., Manes, F. F., Villarreal, M., Owen, A. M., and Della Maggiore, V. (2011). Functional imaging reveals movement preparatory activity in the vegetative state. *Front. Hum. Neurosci.* 5:5. doi: 10.3389/fnhum.2011.00005

Benarroch, E. E. (2007a). Enteric nervous system Functional organization and neurologic implications. *Neurology* 69, 1953–1957. doi: 10.1212/01.wnl.0000281999.56102.b5

Benarroch, E. E. (2007b). The autonomic nervous system: basic anatomy and physiology. *Contin. Lifelong Learn. Neurol.* 13, 13–32. doi: 10.1212/01.CON.0000299964.20642.9a

Berne, C., Fagius, J., Pollare, T., and Hjemdahl, P. (1992). The sympathetic response to euglycaemic hyperinsulinaemia. *Diabetologia* 35, 873–879. doi: 10.1007/BF00399935

Berntson, G. G., and Cacioppo, J. T. (2004). "Heart rate variability: stress and psychiatric conditions," in *Dynamic Electrocardiography*, eds M. Malik and A. J. Camm (New York, NY: Blackwell/Futura), 57–64.

Berntson, G. G., Cacioppo, J. T., and Grossman, P. (2007). Whither vagal tone. *Biol. Psychol.* 74, 295–300. doi: 10.1016/j.biopsycho.2006.08.006

Bilan, A., Witczak, A., Palusiński, R., Myśliński, W., and Hanzlik, J. (2005). Circadian rhythm of spectral indices of heart rate variability in healthy subjects. *J. Electrocardiol.* 38, 239–243. doi: 10.1016/j.jelectrocard.2005.01.012

Biswas, A. K., Scott, W. A., Sommerauer, J. F., and Luckett, P. M. (2000). Heart rate variability after acute traumatic brain injury in children. *Crit. Care Med.* 28, 3907–3912. doi: 10.1097/00003246-200012000-00030

Blume, C., Lechinger, J., Santhi, N., del, Giudice R, Gnjezda, M. T., Pichler, G., et al. (2017). Significance of circadian rhythms in severely brain-injured patients: A clue to consciousness? *Neurology* 88, 1933–1941. doi: 10.1212/WNL.0000000000003942

Boly, M., Faymonville, M.-E., Schnakers, C., Peigneux, P., Lambermont, B., Phillips, C., et al. (2008). Perception of pain in the minimally conscious state with PET activation: an observational study. *Lancet Neurol.* 7, 1013–1020. doi: 10.1016/S1474-4422(08)70219-9

Boudreau, P., Dumont, G., Kin, N. M., Walker, C.-D., and Boivin, D. B. (2011). Correlation of heart rate variability and circadian markers in humans. *Conf. Proc. IEEE Eng. Med. Biol. Soc.* 2011, 681–682.

Boudreau, P., Yeh, W. H., Dumont, G. A., and Boivin, D. B. (2012). A circadian rhythm in heart rate variability contributes to the increased cardiac sympathovagal response to awakening in the morning. *Chronobiol. Int.* 29, 757–768. doi: 10.3109/07420528.2012.674592

Bruno, M.-A., Vanhaudenhuyse, A., Schnakers, C., Boly, M., Gosseries, O., Demertzi, A., et al. (2010). Visual fixation in the vegetative state: an observational case series PET study. *BMC Neurol.* 10:35. doi: 10.1186/1471-2377-10-35

Bullock, T. H. (1970). The reliability of neurons. *J. Gen. Physiol.* 55, 565–584. doi: 10.1085/jgp.55.5.565

Burr, R. L. (2007). Interpretation of normalized spectral heart rate variability indices in sleep research: a critical review. *Sleep* 30, 913–919. doi: 10.1093/sleep/30.7.913

Calabrò, R. S., Naro, A., Manuli, A., Leo, A., Luca, R. D., Buono, V. L., et al. (2017). Pain perception in patients with chronic disorders of consciousness: What can limbic system tell us? *Clin. Neurophysiol.* 128, 454–462. doi: 10.1016/j.clinph.2016.12.011

Candelieri, A., Cortese, M. D., Dolce, G., Riganello, F., and Sannita, W. G. (2011). Visual pursuit: within-day variability in the severe disorder of consciousness. *J. Neurotrauma* 28, 2013–2017. doi: 10.1089/neu.2011.1885

Carney, R. M., Blumenthal, J. A., Freedland, K. E., Stein, P. K., Howells, W. B., Berkman, L. F., et al. (2005). Low heart rate variability and the effect of depression on post–myocardial infarction mortality. *Arch. Intern. Med.* 165, 1486–1491. doi: 10.1001/archinte.165.13.1486

Celesia, G. G. (2013). Conscious awareness in patients in vegetative states: myth or reality? *Curr. Neurol. Neurosci. Rep.* 13:395. doi: 10.1007/s11910-013-0395-7

Celesia, G. G., and Sannita, W. G. (2013). Can patients in vegetative state experience pain and have conscious awareness? *Neurology* 80, 328–329. doi: 10.1212/WNL.0b013e31827f0928

Cerutti, S. (1995). *Spectral Analysis of the Heart Rate Variability Signal*. Available at: https://ci.nii.ac.jp/naid/10014992161/ (accessed November 25, 2018).

Chen, Z., Venkat, P., Seyfried, D., Chopp, M., Yan, T., and Chen, J. (2017). Brain–Heart Interaction. *Circ. Res.* 121, 451–468. doi: 10.1161/CIRCRESAHA.117.311170

Chennu, S., Annen, J., Wannez, S., Thibaut, A., Chatelle, C., Cassol, H., et al. (2017). Brain networks predict metabolism, diagnosis and prognosis at the bedside in disorders of consciousness. *Brain* 140, 2120–2132. doi: 10.1093/brain/awx163

Claydon, V. E., and Krassioukov, A. V. (2008). Clinical correlates of frequency analyses of cardiovascular control after spinal cord injury. *Am. J. Physiol. Heart Circ. Physiol.* 294, H668–H678. doi: 10.1152/ajpheart.00869.2007

Cobos, M. I., Guerra, P. M., Vila, J., and Chica, A. B. (2019). Heart-rate modulations reveal attention and consciousness interactions: COBOS ET AL. *Psychophysiology* 56, e13295. doi: 10.1111/psyp.13295

Critchley, H. D. (2009). Psychophysiology of neural, cognitive and affective integration: fMRI and autonomic indicants. *Int. J. Psychophysiol.* 73, 88–94. doi: 10.1016/j.ijpsycho.2009.01.012

Crone, J. S., Bio, B. J., Vespa, P. M., Lutkenhoff, E. S., and Monti, M. M. (2017). Restoration of thalamo-cortical connectivity after brain injury: recovery of consciousness, complex behavior, or passage of time? *J. Neurosci. Res.* 96, 671–687. doi: 10.1002/jnr.24115

de Lartigue, G. (2014). Putative roles of neuropeptides in vagal afferent signaling. *Physiol. Behav.* 0, 155–169. doi: 10.1016/j.physbeh.2014.03.011

de Morree, H. M., Szabó, B. M., Rutten, G.-J., and Kop, W. J. (2013). Central nervous system involvement in the autonomic responses to psychological distress. *Neth. Heart J.* 21, 64–69. doi: 10.1007/s12471-012-0351-1

deBoer, R. W., Karemaker, J. M., and Strackee, J. (1987). Hemodynamic fluctuations and baroreflex sensitivity in humans: a beat-to-beat model. *Am. J. Physiol.* 253, H680–H689. doi: 10.1152/ajpheart.1987.253.3.H680

DeGiorgio, C. M., Miller, P., Meymandi, S., Chin, A., Epps, J., Gordon, S., et al. (2010). RMSSD, a measure of heart rate variability, is associated with risk factors for sudep: the SUDEP-7 inventory. *Epilepsy Behav.* 19, 78–81. doi: 10.1016/j.yebeh.2010.06.011

Demertzi, A., Antonopoulos, G., Heine, L., Voss, H. U., Crone, J. S., de Los Angeles, C., et al. (2015). Intrinsic functional connectivity differentiates minimally conscious from unresponsive patients. *Brain* 138, 2619–2631. doi: 10.1093/brain/awv169

Di Perri, C., Bahri, M. A., Amico, E., Thibaut, A., Heine, L., Antonopoulos, G., et al. (2016). Neural correlates of consciousness in patients who have emerged from a minimally conscious state: a cross-sectional multimodal imaging study. *Lancet Neurol.* 15, 830–842. doi: 10.1016/S1474-4422(16)00111-3

Di Perri, C., Bastianello, S., Bartsch, A. J., Pistarini, C., Maggioni, G., Magrassi, L., et al. (2013). Limbic hyperconnectivity in the vegetative state. *Neurology* 81, 1417–1424. doi: 10.1212/WNL.0b013e3182a43b78

Doehner, W., Ural, D., Haeusler, K. G., Čelutkienė, J., Bestetti, R., Cavusoglu, Y., et al. (2018). Heart and brain interaction in patients with heart failure: overview and proposal for a taxonomy. A position paper from the Study Group on Heart and Brain Interaction of the Heart Failure Association. *Eur. J. Heart Fail.* 20, 199–215. doi: 10.1002/ejhf.1100

Duclos, C., Dumont, M., Arbour, C., Paquet, J., Blais, H., Menon, D. K., et al. (2017). Parallel recovery of consciousness and sleep in acute traumatic brain injury. *Neurology* 88, 268–275. doi: 10.1212/WNL.0000000000003508

Ernst, G. (2017). Heart-rate variability—more than heart beats? *Front. Public Health* 5:240. doi: 10.3389/fpubh.2017.00240

Esler, M. (1993). Clinical application of noradrenaline spillover methodology: delineation of regional human sympathetic nervous responses. *Pharmacol. Toxicol.* 73, 243–253. doi: 10.1111/j.1600-0773.1993.tb00579.x

Faes, L., Nollo, G., Jurysta, F., and Marinazzo, D. (2014). Information dynamics of brain–heart physiological networks during sleep. *New J. Phys.* 16:105005. doi: 10.1088/1367-2630/16/10/105005

Friedman, B. H. (2007). An autonomic flexibility–neurovisceral integration model of anxiety and cardiac vagal tone. *Biol. Psychol.* 74, 185–199. doi: 10.1016/j.biopsycho.2005.08.009

Gao, L., Smielewski, P., Czosnyka, M., and Ercole, A. (2016). Cerebrovascular signal complexity six hours after intensive care unit admission correlates with outcome after severe traumatic brain injury. *J. Neurotrauma* 33, 2011–2018. doi: 10.1089/neu.2015.4228

Garan, H. (2009). Heart rate variability in acute myocardial infarction. *Cardiology* 114, 273–274. doi: 10.1159/000235567

Garbarino, S., Lanteri, P., Feeling, N. R., Jarczok, M. N., Quintana, D. S., Koenig, J., et al. (2019). Circadian rhythms, sleep, and the autonomic nervous system: a position paper. *J. Psychophysiol.* doi: 10.1027/0269-8803/a000236

Garbarino, S., Nobili, L., and Costa, G. (eds). (2014). *Sleepiness and Human Impact Assessment*. Basel: Springer.

Garbarino, S., and Sannita, W. G. (2015). DoC: a pathophysiological continuum with high variabiity? *Neurology*. doi: 10.13140/RG.2.1.1541.0006

Giacino, J. T., Kalmar, K., and Whyte, J. (2004). The JFK coma recovery scale-revised: measurement characteristics and diagnostic utility. *Arch. Phys. Med. Rehabil.* 85, 2020–2029. doi: 10.1016/j.apmr.2004.02.033

Goldstein, B., DeKing, D., DeLong, D. J., Kempski, M. H., Cox, C., Kelly, M. M., et al. (1993). Autonomic cardiovascular state after severe brain injury and brain death in children. *Crit. Care Med.* 21, 228–233.

Goldstein, B., Fiser, D. H., Kelly, M. M., Mickelsen, D., Ruttimann, U., and Pollack, M. M. (1998). Decomplexification in critical illness and injury: relationship between heart rate variability, severity of illness, and outcome. *Crit. Care Med.* 26, 352–357. doi: 10.1097/00003246-199802000-00040

Grimm, T., and Kreutz, G. (2018). Music interventions in disorders of consciousness (DOC) – a systematic review. *Brain Inj.* 32, 704–714. doi: 10.1080/02699052.2018.1451657

Gutiérrez, J., Machado, C., Estévez, M., Olivares, A., Hernández, H., Perez, J., et al. (2010). Heart rate variability changes induced by auditory stimulation in persistent vegetative state. *Int. J. Disabil. Hum. Dev.* 9, 357–362. doi: 10.1515/IJDHD.2010.041

Hagemann, D., Waldstein, S. R., and Thayer, J. F. (2003). Central and autonomic nervous system integration in emotion. *Brain Cogn.* 52, 79–87. doi: 10.1016/S0278-2626(03)00011-3

Hendén, P. L., Söndergaard, S., Rydenhag, B., Reinsfelt, B., Ricksten, S.-E., and Aneman, A. (2014). Can baroreflex sensitivity and heart rate variability predict late neurological outcome in patients with traumatic brain injury? *J. Neurosurg. Anesthesiol.* 26, 50–59. doi: 10.1097/ANA.0b013e3182a47b62

Keren, O., Yupatov, S., Radai, M. M., Elad-Yarum, R., Faraggi, D., Abboud, S., et al. (2005). Heart rate variability (HRV) of patients with traumatic brain injury (TBI) during the post-insult sub-acute period. *Brain Inj.* 19, 605–611. doi: 10.1080/02699050400024946

Kim, S. W., Jeon, H. R., Kim, J. Y., and Kim, Y. (2017). Heart rate variability among children with acquired brain injury. *Ann. Rehabil. Med.* 41, 951–960. doi: 10.5535/arm.2017.41.6.951

King, D. R., Ogilvie, M. P., Pereira, B. M., Chang, Y., Manning, R. J., Conner, J. A., et al. (2009). Heart rate variability as a triage tool in patients with trauma during prehospital helicopter transport. *J. Trauma* 67, 436–440. doi: 10.1097/TA.0b013e3181ad67de

Kiryachkov, Y., Shelkunova, I., Shelkunova, I. G., Kolesov, D. L., and Danilec, V. V. (2017). MON-P025: association between heart rate variability measures and energy homeostasis in patients with vegetative status: a prospective clinical cohort pilot study. *Clin. Nutr.* 36:S188.

Lane, R., Mcrae, K., Reiman, E., Chen, K., Ahern, G., and Thayer, J. (2009). Neural correlates of heart rate variability during emotion. *Neuroimage* 44, 213–222. doi: 10.1016/j.neuroimage.2008.07.056

Laureys, S., Celesia, G. G., Cohadon, F., Lavrijsen, J., León-Carrión, J., Sannita, W. G., et al. (2010). Unresponsive wakefulness syndrome: a new name for the vegetative state or apallic syndrome. *BMC Med.* 8:68. doi: 10.1186/1741-7015-8-68

Laureys, S., Faymonville, M.-E., Luxen, A., Lamy, M., Franck, G., and Maquet, P. (2000). Restoration of thalamocortical connectivity after recovery from persistent vegetative state. *Lancet* 355, 1790–1791. doi: 10.1016/s0140-6736(00)02271-6

Laureys, S., Faymonville, M. E., Peigneux, P., Damas, P., Lambermont, B., Del Fiore, G., et al. (2002). Cortical processing of noxious somatosensory stimuli in the persistent vegetative state. *Neuroimage* 17, 732–741. doi: 10.1006/nimg.2002.1236

Laureys, S., Perrin, F., and Brédart, S. (2007). Self-consciousness in non-communicative patients. *Conscious. Cogn.* 16, 722–741. doi: 10.1016/j.concog.2007.04.004

Lee, Y.-C., Lei, C.-Y., Shih, Y.-S., Zhang, W.-C., Wang, H.-M., Tseng, C.-L., et al. (2011). "HRV response of vegetative state patient with music therapy," in *Proceedings of the Annual International Conference of the IEEE Engineering in Medicine and Biology Society,* Boston, MA, 1701–1704. doi: 10.1109/IEMBS.2011.6090488

Lehrer, P., and Eddie, D. (2013). Dynamic processes in regulation and some implications for biofeedback and biobehavioral interventions. *Appl. Psychophysiol. Biofeedback* 38, 143–155. doi: 10.1007/s10484-013-9217-6

Lehrer, P. M. (2007). Biofeedback training to increase heart rate variability. *Princ. Pract. Stress Manag.* 3, 227–248.

Machado, C., Korein, J., Aubert, E., Bosch, J., Alvarez, M. A., Rodríguez, R., et al. (2007). Recognizing a Mother's voice in the persistent vegetative state. *Clin. EEG Neurosci.* 38, 124–126. doi: 10.1177/155005940703800306

Majerus, S., Bruno, M.-A., Schnakers, C., Giacino, J. T., and Laureys, S. (2009). "The problem of aphasia in the assessment of consciousness in brain-damaged patients," in *Progress in Brain Research*, ed. S. Laureys, N. D. Schiff, and A. M. Owen (Amsterdam: Elsevier), 49–61. doi: 10.1016/s0079-6123(09)17705-1

Malliani, A. (1995). Association of heart rate variability components with physiological regulatory mechanisms. *Heart Rate Var.* 8, 202–242.

Marino, S., Bonanno, L., Ciurleo, R., Baglieri, A., Morabito, R., Guerrera, S., et al. (2017). Functional evaluation of awareness in vegetative and minimally conscious state. *Open Neuroimaging J.* 11, 17–25. doi: 10.2174/1874440001711010017

Montano, N., Ruscone, T. G., Porta, A., Lombardi, F., Pagani, M., and Malliani, A. (1994). Power spectrum analysis of heart rate variability to assess the changes in sympathovagal balance during graded orthostatic tilt. *Circulation* 90, 1826–1831. doi: 10.1161/01.cir.90.4.1826

Monti, M. M. (2012). Cognition in the vegetative state. *Annu. Rev. Clin. Psychol* 8, 431–454. doi: 10.1146/annurev-clinpsy-032511-143050

Monti, M. M., Rosenberg, M., Finoia, P., Kamau, E., Pickard, J. D., and Owen, A. M. (2014). Thalamo-frontal connectivity mediates top-down cognitive functions in disorders of consciousness. *Neurology* 84, 167–173. doi: 10.1212/WNL.0000000000001123

Monti, M. M., and Sannita, W. G. (eds). (2016). *Brain Function and Responsiveness in Disorders of Consciousness*. Berlin: Springer.

Morris, J. A., Norris, P. R., Ozdas, A., Waitman, L. R., Harrell, F. E., Williams, A. E., et al. (2006). Reduced heart rate variability: an indicator of cardiac uncoupling and diminished physiologic reserve in 1,425 trauma patients. *J. Trauma* 60, 1165–1173. doi: 10.1097/01.ta.0000220384.04978.3b

Mowery, N. T., Norris, P. R., Riordan, W., Jenkins, J. M., Williams, A. E., and Morris, J. A. (2008). Cardiac uncoupling and heart rate variability are associated with intracranial hypertension and mortality: a study of 145 trauma patients with continuous monitoring. *J. Trauma* 65, 621–627. doi: 10.1097/TA.0b013e3181837980

Nait-Ali, A. (2009). *Advanced Biosignal Processing*. Berlin: Springer.

Napadow, V., Dhond, R., Conti, G., Makris, N., Brown, E. N., and Barbieri, R. (2008). Brain correlates of autonomic modulation: combining heart rate variability with fMRI. *Neuroimage* 42, 169–177. doi: 10.1016/j.neuroimage.2008.04.238

Naro, A., Leo, A., Bramanti, P., and Calabrò, R. S. (2015). Moving toward conscious pain processing detection in chronic disorders of consciousness: anterior cingulate cortex neuromodulation. *J. Pain* 16, 1022–1031. doi: 10.1016/j.jpain.2015.06.014

Norris, P. R., Anderson, S. M., Jenkins, J. M., Williams, A. E., and Morris, J. A. (2008a). Heart rate multiscale entropy at three hours predicts hospital mortality in 3,154 trauma patients. *Shock* 30, 17–22. doi: 10.1097/SHK.0b013e318164e4d0

Norris, P. R., Stein, P. K., and Morris, J. A. (2008b). Reduced heart rate multiscale entropy predicts death in critical illness: a study of physiologic complexity in 285 trauma patients. *J. Crit. Care* 23, 399–405. doi: 10.1016/j.jcrc.2007.08.001

Norris, P. R., Ozdas, A., Cao, H., Williams, A. E., Harrell, F. E., Jenkins, J. M., et al. (2006). Cardiac uncoupling and heart rate variability stratify ICU patients by mortality: a study of 2088 trauma patients. *Ann. Surg.* 243, 804–812.

O'Kelly, J., and Magee, W. L. (2013). Music therapy with disorders of consciousness and neuroscience: the need for dialogue. *Nord. J. Music Ther.* 22, 93–106. doi: 10.1080/08098131.2012.709269

Owen, A. M. (2014). Disorders of consciousness: diagnostic accuracy of brain imaging in the vegetative state. *Nat. Rev. Neurol.* 10, 370–371. doi: 10.1038/nrneurol.2014.102

Owen, A. M., Coleman, M. R., Boly, M., Davis, M. H., Laureys, S., and Pickard, J. D. (2006). Detecting awareness in the vegetative state. *Science* 313, 1402–1402. doi: 10.1126/science.1130197

Pagani, M., Lombardi, F., Guzzetti, S., Sandrone, G., Rimoldi, O., Malfatto, G., et al. (1984). Power spectral density of heart rate variability as an index of sympatho-vagal interaction in normal and hypertensive subjects. *J. Hypertens. Suppl.* 2, S383–S385.

Papaioannou, V., Giannakou, M., Maglaveras, N., Sofianos, E., and Giala, M. (2008). Investigation of heart rate and blood pressure variability, baroreflex sensitivity, and approximate entropy in acute brain injury patients. *J. Crit. Care* 23, 380–386. doi: 10.1016/j.jcrc.2007.04.006

Papaioannou, V. E., Maglaveras, N., Houvarda, I., Antoniadou, E., and Vretzakis, G. (2006). Investigation of altered heart rate variability, nonlinear properties of heart rate signals, and organ dysfunction longitudinally over time in intensive care unit patients. *J. Crit. Care* 21, 95–103. doi: 10.1016/j.jcrc.2005.12.007

Pistoia, F., Sacco, S., Stewart, J., Sarà, M., Carolei, A., Pistoia, F., et al. (2016). Disorders of consciousness: painless or painful conditions?—Evidence

from neuroimaging studies. *Brain Sci.* 6:E47. doi: 10.3390/brainsci6040047

Rajendra Acharya, U., Paul Joseph, K., Kannathal, N., Lim, C. M., and Suri, J. S. (2006). Heart rate variability: a review. *Med. Biol. Eng. Comput.* 44, 1031–1051. doi: 10.1007/s11517-006-0119-0

Rapenne, T., Moreau, D., Lenfant, F., Vernet, M., Boggio, V., Cottin, Y., et al. (2001). Could heart rate variability predict outcome in patients with severe head injury? A pilot study. *J. Neurosurg. Anesthesiol.* 13, 260–268. doi: 10.1097/00008506-200107000-00016

Riganello, F. (2016). "Responsiveness and the autonomic control–CNS two-way interaction in disorders of consciousness," in *Brain Function and Responsiveness in Disorders of Consciousness*, eds M. M. Monti and W. G. Sannita (Cham: Springer), 145–155. doi: 10.1007/978-3-319-21425-2_11

Riganello, F., Candelieri, A., Quintieri, M., Conforti, D., and Dolce, G. (2010). Heart rate variability: an index of brain processing in vegetative state? An artificial intelligence, data mining study. *Clin. Neurophysiol.* 121, 2024–2034. doi: 10.1016/j.clinph.2010.05.010

Riganello, F., Chatelle, C., Schnakers, C., and Laureys, S. (2018a). Heart Rate Variability as an indicator of nociceptive pain in disorders of consciousness? *J. Pain Symptom Manage.* 57, 47–56. doi: 10.1016/j.jpainsymman.2018.09.016

Riganello, F., Cortese, M. D., Arcuri, F., Dolce, G., Lucca, L. F., and Sannita, W. G. (2015a). Autonomic nervous system functional state, neurorehabiliation, and outcome in disorders of consciousness. *J. Neurotrauma* 32, 1071–1077.

Riganello, F., Cortese, M. D., Arcuri, F., Quintieri, M., and Dolce, G. (2015b). How Can music influence the autonomic nervous system response in patients with severe disorder of consciousness? *Front. Neurosci.* 9:461. doi: 10.3389/fnins.2015.00461

Riganello, F., Cortese, M. D., Dolce, G., Lucca, L. F., and Sannita, W. G. (2015c). The autonomic system functional state predicts responsiveness in DOC. *J. Neurotrauma* 32, 1071–1077. doi: 10.1089/neu.2014.3539

Riganello, F., Cortese, M. D., Dolce, G., and Sannita, W. G. (2013). Visual pursuit response in the severe disorder of consciousness: modulation by the central autonomic system and a predictive model. *BMC Neurol.* 13:164. doi: 10.1186/1471-2377-13-164

Riganello, F., Dolce, G., and Sannita, W. (2012a). Heart rate variability and the central autonomic network in the severe disorder of consciousness. *J. Rehabil. Med.* 44, 495–501. doi: 10.2340/16501977-0975

Riganello, F., Garbarino, S., and Sannita, W. G. (2012b). Heart rate variability, homeostasis, and brain function: a tutorial and review of application. *J. Psychophysiol.* 26, 178–203. doi: 10.1027/0269-8803/a000080

Riganello, F., Garbarino, S., and Sannita, W. G. (2014). Heart rate variability and the two-way interaction between CNS and the central autonomic network. *J. Exp. Clin. Cardiol.* 20, 5584–5595.

Riganello, F., Larroque, S. K., Bahri, M. A., Heine, L., Martial, C., Carrière, M., et al. (2018b). A heartbeat away from consciousness: heart rate variability entropy can discriminate disorders of consciousness and is correlated with resting-state fMRI brain connectivity of the central autonomic network. *Front. Neurol* 9:769. doi: 10.3389/fneur.2018.00769

Riganello, F., Macri, S., Alleva, E., Petrini, C., Soddu, A., Leòn-Carriòn, J., et al. (2016). Pain perception in unresponsive wakefulness syndrome may challenge the interruption of artificial nutrition and hydration: neuroethics in action. *Front. Neurol.* 7:202. doi: 10.3389/fneur.2016.00202

Ruiz Vargas, E., Sörös, P., Shoemaker, J. K., and Hachinski, V. (2016). Human cerebral circuitry related to cardiac control: a neuroimaging meta-analysis: cardiac control. *Ann. Neurol.* 79, 709–716. doi: 10.1002/ana.24642

Ryan, M. L., Thorson, C. M., Otero, C. A., Vu, T., and Proctor, K. G. (2011). Clinical applications of heart rate variability in the triage and assessment of traumatically injured patients. *Anesthesiol. Res. Pract.* 2011:e416590. doi: 10.1155/2011/416590

Sannita, W. G. (2006). Individual variability, end-point effects and possible biases in electrophysiological research. *Clin. Neurophysiol.* 117, 2569–2583. doi: 10.1016/j.clinph.2006.04.026

Sannita, W. G. (2014). Human brain physiology investigated in the disorder of consciousness. *Front. Neurol.* 5:211. doi: 10.3389/fneur.2014.00211

Sannita, W. G. (2015). Responsiveness in DoC and individual variability. *Front. Hum. Neurosci.* 9:270. doi: 10.3389/fnhum.2015.00270

Saper, C. B. (2002). The central autonomic nervous system: conscious visceral perception and autonomic pattern generation. *Annu. Rev. Neurosci.* 25, 433–469. doi: 10.1146/annurev.neuro.25.032502.111311

Sarà, M., Sebastiano, F., Sacco, S., Pistoia, F., Onorati, P., Albertini, G., et al. (2008). Heart rate non linear dynamics in patients with persistent vegetative state: a preliminary report. *Brain Inj.* 22, 33–37. doi: 10.1080/02699050701810670

Shaffer, F., McCraty, R., and Zerr, C. L. (2014). A healthy heart is not a metronome: an integrative review of the heart's anatomy and heart rate variability. *Front Psychol.* 5:1040. doi: 10.3389/fpsyg.2014.01040

Shen, D., Cui, L., Shen, Z., Garbarino, S., Sannita, W. G., and Stevens, R. D. (2016). Resting brain activity in disorders of consciousness: a systematic review and meta-analysis. *Neurology* 84, 1272–1280.

Shi, H., Yang, L., Zhao, L., Su, Z., Mao, X., Zhang, L., et al. (2017). Differences of heart rate variability between happiness and sadness emotion states: a pilot study. *J. Med. Biol. Eng.* 37, 527–539. doi: 10.1007/s40846-017-0238-0

Soddu, A., and Bassetti, C. L. (2017). A good sleep for a fresh mind in patients with acute traumatic brain injury. *Neurology* 88, 226–227. doi: 10.1212/WNL.0000000000003529

Soddu, A., Gómez, F., Heine, L., Di Perri, C., Bahri, M. A., Voss, H. U., et al. (2015). Correlation between resting state fMRI total neuronal activity and PET metabolism in healthy controls and patients with disorders of consciousness. *Brain Behav.* 6:e00424. doi: 10.1002/brb3.424

Task Force of the European Society of Cardiology and the North American Society of Pacing and Electrophysiology (1996). Heart rate variability: standards of measurement, physiological interpretation and clinical use. *Circulation* 93, 1043–1065. doi: 10.1161/01.cir.93.5.1043

Thayer, J. F., Åhs, F., Fredrikson, M., Sollers, J. J., and Wager, T. D. (2012). A meta-analysis of heart rate variability and neuroimaging studies: implications for heart rate variability as a marker of stress and health. *Neurosci. Biobehav. Rev.* 36, 747–756. doi: 10.1016/j.neubiorev.2011.11.009

Thayer, J. F., and Lane, R. D. (2000). A model of neurovisceral integration in emotion regulation and dysregulation. *J. Affect. Disord.* 61, 201–216. doi: 10.1016/s0165-0327(00)00338-4

Thayer, J. F., and Lane, R. D. (2009). Claude Bernard and the heart–brain connection: further elaboration of a model of neurovisceral integration. *Neurosci. Biobehav. Rev.* 33, 81–88. doi: 10.1016/j.neubiorev.2008.08.004

Thayer, J. F., and Sternberg, E. (2006). Beyond heart rate variability. *Ann. N. Y. Acad. Sci.* 1088, 361–372. doi: 10.1196/annals.1366.014

Thome, J., Densmore, M., Frewen, P. A., McKinnon, M. C., Théberge, J., Nicholson, A. A., et al. (2017). Desynchronization of autonomic response and central autonomic network connectivity in posttraumatic stress disorder: CAN Connectivity and HRV in PTSD. *Hum. Brain Mapp.* 38, 27–40. doi: 10.1002/hbm.23340

Tobaldini, E., Toschi-Dias, E., Trimarchi, P. D., Brena, N., Comanducci, A., Casarotto, S., et al. (2018). Cardiac autonomic responses to nociceptive stimuli in patients with chronic disorders of consciousness. *Clin. Neurophysiol.* 129, 1083–1089. doi: 10.1016/j.clinph.2018.01.068

Tonhajzerova, I., Ondrejka, I., Turianikova, Z., Javorka, K., Calkovska, A., and Javorka, M. (2012). "Heart rate variability: an index of the brain–heart interaction," in *Tachycardia*, ed. T. Yamad (Rijeka: Intech), 185–202.

Valenza, G., Duggento, A., Passamonti, L., Diciotti, S., Tessa, C., Barbieri, R., et al. (2017). "Resting-state brain correlates of instantaneous autonomic outflow," in *Proceedings of the 39th Annual International Conference of the IEEE Engineering in Medicine and Biology Society (EMBC)*, (Seogwipo: IEEE), 3325–3328.

Vaschillo, E. G., Vaschillo, B., Pandina, R. J., and Bates, M. E. (2011). Resonances in the cardiovascular system caused by rhythmical muscle tension: rhythmical muscle tension and resonance. *Psychophysiology* 48, 927–936. doi: 10.1111/j.1469-8986.2010.01156.x

Wallin, B. G., and Charkoudian, N. (2007). Sympathetic neural control of integrated cardiovascular function: insights from measurement of human sympathetic nerve activity. *Muscle Nerve* 36, 595–614. doi: 10.1002/mus.20831

Weir, J., Steyerberg, E. W., Butcher, I., Lu, J., Lingsma, H. F., McHugh, G. S., et al. (2012). Does the extended glasgow outcome scale add value to the conventional Glasgow outcome scale? *J. Neurotrauma* 29, 53–58. doi: 10.1089/neu.2011.2137

Wijnen, V. J., Heutink, M., van Boxtel, G. J., Eilander, H. J., and de Gelder, B. (2006). Autonomic reactivity to sensory stimulation is related to consciousness level after severe traumatic brain injury. *Clin. Neurophysiol.* 117, 1794–1807. doi: 10.1016/j.clinph.2006.03.006

Winchell, R. J., and Hoyt, D. B. (1997). Analysis of heart-rate variability: a noninvasive predictor of death and poor outcome in patients with severe head injury. *J. Trauma Acute Care Surg.* 43, 927–933. doi: 10.1097/00005373-199712000-00010

Yentes, J. M., Hunt, N., Schmid, K. K., Kaipust, J. P., McGrath, D., and Stergiou, N. (2013). The appropriate use of approximate entropy and sample entropy with short data sets. *Ann. Biomed. Eng.* 41, 349–365. doi: 10.1007/s10439-012-0668-3

Conflict of Interest Statement: The authors declare that the research was conducted in the absence of any commercial or financial relationships that could be construed as a potential conflict of interest.

frontiers in Neuroscience

METHODS
published: 25 June 2019
doi: 10.3389/fnins.2019.00663

Simultaneous Measurement of Neuronal Activity in the Pontine Micturition Center and Cystometry in Freely Moving Mice

Jiwei Yao[1], Qianwei Li[1], Xianping Li[2], Han Qin[2], Shanshan Liang[2], Xiang Liao[2], Xiaowei Chen[2], Weibing Li[1,3]* and Junan Yan[1]**

[1] Department of Urology, Southwest Hospital, Third Military Medical University, Chongqing, China, [2] Brain Research Center and State Key Laboratory of Trauma, Burns, and Combined Injury, Third Military Medical University, Chongqing, China, [3] Department of Urology and Nephrology, The Third Affiliated Hospital, Chongqing Medical University, Chongqing, China

Understanding the complex neural mechanisms controlling urinary bladder activity is an extremely important topic in both neuroscience and urology. Simultaneously recording of the bladder activity and neural activity in related brain regions will largely advance this field. However, such recording approach has long been restricted to anesthetized animals, whose bladder function and urodynamic properties are largely affected by anesthetics. In our recent report, we found that it is feasible to record bladder pressure (cystometry) and the related cortical neuron activity simultaneously in freely moving mice. Here, we aimed to demonstrate the use of this combined method in freely moving mice for recording the activity of the pontine micturition center (PMC), a more difficultly approachable small region deeply located in the brainstem and a more popularly studied hub for controlling bladder function. Interestingly, we found that the duration of urination events linearly correlated to the time course of neuronal activity in the PMC. We observed that the activities of PMC neurons highly correlated with spike-like increases in bladder pressure, reflecting bladder contractions. We also found that anesthesia evoked prominent changes in the dynamics of the Ca^{2+} signals in the PMC during the bladder contraction and even induced the dripping overflow incontinence due to suppression of the neural activity in the PMC. In addition, we described in details both the system for cystometry in freely moving mice and the protocols for how to perform this combined method. Therefore, this work provides a powerful approach that enables the simultaneous measurement of neuronal activity of the PMC or any other brain sites and bladder function in freely behaving mice. This approach offers a promising possibility to examine the neural mechanisms underlying neurogenic bladder dysfunction.

Keywords: the optical fiber-based Ca^{2+} recording, cystometry, pontine micturition center, urination, freely moving mice

OPEN ACCESS

Edited by:
Stuart M. Brierley, Flinders University, Australia

Reviewed by:
Russ Chess-Williams, Bond University, Australia
Thelma Anderson Lovick, University of Bristol, United Kingdom

***Correspondence:**
Xiaowei Chen
xiaowei_chen@tmmu.edu.cn
Weibing Li
liweibing63@hospital.cqmu.edu.cn
Junan Yan
junan_yan@aliyun.com

Specialty section:
This article was submitted to Autonomic Neuroscience, a section of the journal Frontiers in Neuroscience

Received: *23 January 2019*
Accepted: *11 June 2019*
Published: *25 June 2019*

Citation:
Yao J, Li Q, Li X, Qin H, Liang S, Liao X, Chen X, Li W and Yan J (2019) Simultaneous Measurement of Neuronal Activity in the Pontine Micturition Center and Cystometry in Freely Moving Mice. Front. Neurosci. 13:663. doi: 10.3389/fnins.2019.00663

INTRODUCTION

Neural circuits integrated at different levels of the central and peripheral nervous systems tightly control normal bladder function (Fowler et al., 2008; Benarroch, 2010; de Groat et al., 2015). Injuries or diseases of the nervous system may lead to neurogenic bladder (NGB) dysfunction (Fowler et al., 2008; Harris and Lemack, 2016). NGB is generally found in patients with neurological

disorders, and affects their quality of life (Ginsberg, 2013). However, our current insights into NGB are very limited. A better understanding of the neural mechanisms controlling bladder would provide new strategies for the treatment of NGB.

The pontine micturition center (PMC) is a small brainstem nucleus located in the caudal pontine tegmentum near the locus coeruleus (LC) (Verstegen et al., 2017). The PMC is suggested to be necessary for urination in animals and humans (Valentino et al., 2011). Inhibition or lesion of the PMC causes urinary retention and prevents urination, and electrical or optogenetic stimulation in this region drives bladder contraction and triggers urination (Sugaya et al., 1987; Sugaya, 1988; Hou et al., 2016; Yao et al., 2018). Projections of PMC neurons directly go to the sacral spinal cord preganglionic bladder motor neurons (Blok and Holstege, 1998; Verstegen et al., 2017). PMC neurons integrate the pro- or anti-urination signals (Drake et al., 2010; de Groat and Wickens, 2013; Hou et al., 2016) and receive converging inputs from multiple upstream brain regions (Hou et al., 2016). Therefore, PMC neurons are an important entry point for investigations of the larger-scale brain network of bladder control.

Simultaneous measurement of neural activity and cystometry is a potentially useful approach to examine the neural mechanisms that control bladder functions (Manohar et al., 2017). Many classic studies used electrodes to record correlating neuronal responses in the PMC together with bladder pressure measurement in anesthetized or restrained animals (Willette et al., 1988; Tanaka et al., 2003). Data from traditional electrophysiology are limited by the low stability of long-lasting recordings and the lack of cell-type specificity (Guo et al., 2015). Anesthesia suppresses bladder function and affects the urodynamic results (Aizawa et al., 2015; Schneider et al., 2015). However, an efficient approach to combine the monitoring of neuronal activity with cystometry in freely moving animals has long been lacking. In our recent report, we demonstrated the feasibility of the method for recording both bladder pressure and neuronal activity of motor cortex in freely moving mice (Yao et al., 2018), but whether this method can be extended to a more difficultly reachable region, the PMC, is unclear. This is an important attempt, as the PMC plays important yet many remaining unknown functions in controlling bladder and urination, as mentioned above.

The development of genetically encoded Ca^{2+} indicators (GECIs) (Grienberger and Konnerth, 2012) and genetically targeted techniques has simplified the use of optical fiber-based Ca^{2+} recording (also known as fiber photometry). Fiber photometry is currently a popular choice for the monitoring of cell type-specific neuronal activities of any brain areas in freely behaving animals (Stroh et al., 2013; Gunaydin et al., 2014). This approach is suitable for the detection of the average spiking activity of a cluster of neurons (Adelsberger et al., 2005) or of their axon terminals (Qin et al., 2018), and the general consensus is that neuronal Ca^{2+} transients reflect neuronal action potential firing (Kerr et al., 2005). Fiber photometry costs less, and data acquisition and analyses are much simpler than electrophysiology (Cui et al., 2014). Therefore, we developed a simple method using fiber photometry to monitor the neuronal activity of PMC neurons together with cystometry in freely moving mice.

MATERIALS AND METHODS

Animals

Wild-type adult C57/BL6J mice (both sexes, aged 3–4 months old) were used in all experiments and purchased from the Laboratory Animal Center at the Third Military Medical University. Mice were socially housed under a 12-h light/dark cycle and provided with *ad libitum* food and water. Each mouse implanted with a PE10 catheter insertion into the bladder or an optic fiber into the brain was individually housed and habituated to the experimental device prior to recording. The Third Military Medical University Animal Care and Use Committee approved all experimental procedures, which were performed in accordance with institutional animal welfare guidelines.

Trans-Synaptic Tracing

Mice were anesthetized via an intraperitoneal injection (i.p.) of 1% sodium pentobarbital (10 ml/kg). Their bladders were exposed and exteriorized through the middle abdominal incision. Two injections approximately 0.5 mm deep were performed across the bladder wall by use of a small glass micropipette attached to a microsyringe (10 μl). PRV-EGFP (1.71×10^8 PFU/ml in 1 μl) was injected at each site at a speed of 200 nl/min via a syringe pump. The micropipette was held in each injection site for 5 min. Each bladder was returned to the mouse abdominal cavity, and finally the abdominal wound was closed. Mouse brains were removed at 4.5 to 5 days after PRV-EGFP injection and stored in fixative solution prior to sectioning.

Viral Injection

Mice were placed in a stereotaxic frame (RWD Technology Co., Ltd., China) with a heated pad and anesthetized with 1–1.5% isoflurane in oxygen. A scalp incision was performed using eye scissors. A craniotomy (1 mm × 1 mm) was performed using a dental drill above the PMC (AP: −5.45 mm; ML: 0.70 mm; DV: −3.15 mm). AAV-hSyn-GCaMP6f (AAV2/9, titer: 2.59×10^{12} viral particles/ml, Obio Biotechnology Co., Ltd., China) or AAV-hSyn-EGFP (AAV2/8, titer: 1.63×10^{13} viral particles/ml, Obio Biotechnology Co., Ltd., China) was delivered using a small glass micropipette with a tip diameter of ∼20 μm. The micropipette was slowly inserted to a depth of 3.15 mm (from the brain surface), and a total volume of 80–100 nl AAV-hSyn-GCaMP6f or AAV-hSyn-EGFP was injected into the PMC. The micropipette was held in each injection site for 10 min after injection and retracted. The scalp incision was closed. Each mouse was returned to the home cage and allowed to recover for at least 3 weeks.

Fiber Photometry Setup

A custom-built fiber photometry setup (**Figure 2A**) was used in this research to record population neuronal Ca^{2+} signals (Adelsberger et al., 2005; Li et al., 2017; Zhang et al., 2017; Qin et al., 2018; Yao et al., 2018). For excitation of the fluorescent

genetically encoded Ca^{2+} indicator (GCaMP6f), the excitation light (the wavelength of 450–490 nm) was delivered by a light-emitting diode (LED). The accurate adjustment of the beam intensity of LED was driven by the current. Then the beam was deflected by a dichroic mirror (Di02-R488, Semrock, United States) and focused into the end of an optic fiber (200 μm diameter, NA 0.48, Doric lenses, Quebec City, QC, Canada) through a collimator. The beam intensity at the tip of the optic fiber was about 0.22 mW/mm^2. The emitted GCaMP6f fluorescence (green) was guided back through the same fiber and then was separated from excitation blue light using the same dichroic mirror with a bandpass emission filter (FF01-535/22, Semrock, United States). Finally, the GCaMP6f fluorescence emission was monitored using an avalanche photodiode (Si APD, S2382, Hamamatsu Photonics K.K., Japan). The collected GCaMP6f fluorescence signals were digitized with a sampling frequency of 2000 Hz by the use of a multifunction I/O device (USB-6002, National Instruments, United States). Data acquisition was implemented by customized software written in the LabVIEW platform (National Instrument, United States).

Optical Fiber Recording *in vivo*

Optical fiber recordings in the PMC were performed similarly as described previously (Adelsberger et al., 2005). Mice were anesthetized with 1–1.5% isoflurane and put on a stereotactic head frame. A scalp incision was performed using eye scissors. The craniotomy (1 mm × 1 mm) was performed using a dental drill above the PMC. An optic fiber (200 μm diameter, NA 0.48, Doric lenses, Quebec City, QC, Canada) was glued into a short cannula (ID. 0.51 mm, OD. 0.82 mm), inserted through the craniotomy and advanced slowly to 3.05 mm below the brain surface. The optic fiber was secured to the mouse skull using dental cement. Mice implanted with an optic fiber were allowed to recover for 3–5 days prior to urination behavior testing. To avoid breakage of the optic fiber in freely moving mouse, the changes in the curvature of the fiber were checked every 6 h by the experimenters and the fiber was held loosely above each mouse head at a distance of 50–80 cm. During the recordings, the optic fiber was connected to the fiber photometry system directly without using the commutator. For awake freely moving recordings, each mouse was put in a chamber with a glass bottom. Neuronal Ca^{2+} transients and behaviors were recorded simultaneously. For anesthetized simultaneous recordings, the mice were put on a heated pad under the anesthetized condition. The Ca^{2+} transients were recorded using customized acquisition software based on Labview platform (National Instrument, United States). A camera (Aigo AHD-X9, China) was used to record mouse urination events at 30 Hz under the spatial resolution of 1280 × 720 pixels. The first drop from the urethral orifice represented the onset of urination events.

Cystometric Measurement *in vivo*

Mice were placed on a heated pad and anesthetized with 1–1.5% isoflurane in oxygen. Each bladder dome was exposed and exteriorized through a middle abdominal incision. A 7 cm PE10 tube was used as the catheter and inserted into the bladder. A loose tie of monofilament suture (6-0) was used to secure the catheter in the bladder. Then the end of the catheter was pulled out through an incision at the back of mouse neck. For testing the seal and patency of the PE10 tube in the bladder, a syringe (1 ml) connected with 30-gauge needle was attached to the end of the catheter, and the bladder was slowly filled with saline until a drop appearing at the urethral orifice to indicate that the cystometry surgery was successful. The abdominal wound and neck incision were closed, and each mouse was allowed to recover for at least 5 days prior to cystometry recordings. Before cystometry recordings in an awake or anesthetized mouse, a pressure transducer (YPJ01H; Chengdu Instrument Factory, China) was attached to a multi-channel physiological recording and signal processing setup (RM6240; Chengdu Instrument Factory, China) for bladder pressure recording. A 3-way tab was used to connect an infusion pump (RWD404; RWD Technology Corp., Ltd., China), the pressure transducer and appropriate adapter. The end of the adapter was connected with a PE50 tube. The catheter in the bladder of each mouse was slid into the end of the PE50 tube. Before each cystometric measurement, the pressure transducer was calibrated. Cystometry recordings were performed in awake mice with the normal saline infusion into the bladders via the catheter at a constant speed (10–50 μl/min). For anesthetized simultaneous recordings, the mice were anesthetized with 2.5% isoflurane firstly and then these mice were administered with urethane (1.2 g/kg, i.p.). The normal saline was infused into the bladders via the catheter at a constant speed (30 μl/min) under the anesthetized condition. Continuous urodynamic curves were recorded using a commercial acquisition software (Chengdu Instrument Factory, China).

Immunohistochemistry

Coronal brain slices of 40 μm were obtained using a freezing microtome (Leica) and collected in 0.1 M phosphate-buffered saline (PBS) solution. Brain slices were washed in PBST (1% Triton in 0.1 M PBS) for 40 min. A blocking solution (10% donkey serum, 0.2% Triton in 0.1 M PBS) was applied for 2 h at room temperature. Brain sections were incubated with primary antibodies (chicken anti-GFP, 1:200, Abcam, ab13970; rabbit anti-tyrosine-hydroxylase, 1:200, Millipore, AB152) overnight at 4°C followed by secondary antibodies for 2 h at room temperature. The secondary antibodies used were donkey anti-rabbit conjugated with Alexa Fluor 568 (1:200, Invitrogen, A10042) and donkey anti-chicken CF488 (1:200, Sigma-Aldrich, SAB4600031). Brain slices for DAPI staining were incubated with DAPI (1:1000, Sigma) for 20 min. Finally, these slices were mounted on coverslips and imaged. Images were obtained by the use of a scanning confocal microscope (TCS SP5, Leica) and LAS AF software (Leica).

Data Analysis

All Ca^{2+} transients were collected at the sampling frequency of 2000 Hz and low-pass filtered using the Butterworth filter. For both awake and anesthetized recordings, the relative fluorescence changes $\Delta f/f = (f - f_{baseline})/f_{baseline}$ were calculated for Ca^{2+} transients, where $f_{baseline}$ was the baseline fluorescence level taken during the current recording period during urination behavior.

If the amplitude of a Ca^{2+} transient was larger than three times the standard deviation of the noise band, it was regard as a signal. The software for data analysis was custom-written on the MATLAB (MathWorks, United States)[1]. The Ca^{2+} signals were divided into 10 segments and we randomly assigned these segments with urination events or cystometry data, in order to shuffle the fiber photometry data. The duration of each urination event was measured from the urination onset (the first drop of urine appearing at the urethral orifice) to the urination offset (no drop of urine appearing at the urethral orifice).

Statistical Analysis

Each values in this paper is represented as the mean ± s.e.m. Statistical analyses and cross-correlation analyses were calculated in MATLAB (MathWorks, United States). *P*-values for the comparison of paired data were performed using Wilcoxon signed-rank test. *P*-values for comparison of two independent samples were performed using Wilcoxon rank-sum test. $^{***}P < 0.001$, $^{**}P < 0.01$, $^{*}P < 0.05$; ns, no significant difference.

RESULTS

Verification of PMC Location

To identify the location of the PMC, we used PRV-based retrograde trans-synaptic tracing (Smith et al., 2000; Stanley et al., 2010). Immunohistochemical analyses of brain slices 4.5 to 5 days after PRV-EGFP injection into the bladder walls of mice ($n = 5$) (**Figure 1A**) revealed PRV-infected neurons in the PMC and LC according to the mouse brain atlas (**Figure 1B**), as reported recently (Yao et al., 2018). Therefore, we used this identified location of the PMC for the following recordings.

Population Ca^{2+} Transients of PMC Neurons Highly Correlate With Urination Events in Freely Moving Mice

To investigate whether the activation of PMC neurons coincided with urination in freely moving mice, we monitored the Ca^{2+} activities of PMC neurons and urination events simultaneously. A genetically encoded Ca^{2+} indicator GCaMP6f was locally expressed in the PMC using a viral injection (AAV-hSyn-GCaMP6f). Fiber photometry was used to record population Ca^{2+} activity in the PMC. This optical fiber-based Ca^{2+} recording system (**Figure 2A**) was described in our previous work (Zhang et al., 2017; Qin et al., 2018; Yao et al., 2018). Each mouse was put in the chamber, and its behavior was visualized using a camera placed under the chamber (**Figures 2A,B**). An optical fiber with a diameter of 200 μm was implanted above GCaMP6f-positive PMC neurons 1 month after the viral injection (**Figure 2C**). PMC neurons were near the LC, which was identified using the tyrosine hydroxylase (TH) expression (**Figure 2C**). Serial sectioning also confirmed that GCaMP6f-positive neurons were largely restricted to the PMC area in all the GCaMP6f-injected mice reported here ($n = 7$) (**Figure 2C**). To increase the number of urination events, each mouse was treated with an intraperitoneal (i.p.) injection of diuretic furosemide (40 mg/kg) or 2 mL saline prior to recording. A representative example revealed that Ca^{2+} transients of PMC neurons were observed in the GCaMP6f-injected group during urination (**Figure 2D**). These urination-related transients were not observed in the EGFP-injected control group (**Figures 2D,E**; GCaMP6f-injected group, max $\Delta f/f = 36.73\% \pm 4.90\%$; EGFP-injected group, max $\Delta f/f = 2.24\% \pm 0.66\%$; $P < 0.001$). These experiments indicated that the Ca^{2+} transients of the PMC in the GCaMP6f-injected group were not movement artifacts.

A closer analysis showed that Ca^{2+} transients of PMC neurons in the GCaMP6f-injected group started 402 ± 21 ms prior to the onset of urination events (**Figure 3A**). We found that each urination event was 100% associated with Ca^{2+} transients in the GCaMP6f-injected group throughout all the recordings (**Figure 3B**; $P < 0.001$). Ca^{2+} transients of PMC GCaMP6f-positive neurons started before urination onset on average and in single urination events (heat map), and this response was absent in shuffled data (**Figures 3C,D**). Further analyses indicated that the duration of urination events linearly correlated to the full width at the half maximum of Ca^{2+} transients (**Figure 3E**). Taken together, neuronal activities in the PMC highly correlated with urination.

Simultaneous Recording of Neuronal Activity in the PMC and Cystometry in Freely Moving Mice

To determine whether Ca^{2+} transients of PMC neurons correlated to bladder detrusor contraction, we simultaneously monitored population Ca^{2+} transients of PMC GCaMP6f-positive neurons and urinary bladder pressure in freely moving mice. The experimental setup included a custom-built fiber setup and cystometry system (**Figure 4A**). Bladder pressure was measured using cystometry via a catheter inserted into the mouse bladder. Representative traces of intravesical pressures were recorded in an urethane-anesthetized mouse at different bladder filling speeds (**Figure 4B**). Each voiding contraction was represented as a spike in the intravesical pressure followed by a drop to the lowest pressure and associated with urination (indicated with asterisks in **Figure 4B**), reflecting urination and empty bladder. The intercontractile interval (ICI) was the duration between two adjacent voiding contractions. Quantitative analyses demonstrated that the ICI was tightly dependent on the level of infusion speed ($n = 6$ mice) (**Figure 4C**; 10 μl/min, 179.20 s ± 21.25 s; 30 μl/min, 74.18 s ± 10.76 s; 50 μl/min, 43.38 s ± 5.94 s; $P < 0.05$). As previously reported (Hou et al., 2016), we infused saline into the bladder slowly at a constant speed, which steadily triggered spike-like bladder voiding contractions.

We placed a catheter into the bladder of each animal in which fiber photometry was successfully recorded ($n = 8$ mice). Mice recovered for at least 5 days, and simultaneous measurement of neuronal activity and cystometry showed that spike-like increases in bladder pressure (bladder contraction) correlated with Ca^{2+} transients of PMC neurons in freely moving mice (**Figure 5A**).

[1]https://github.com/xieyangshuying/FRC

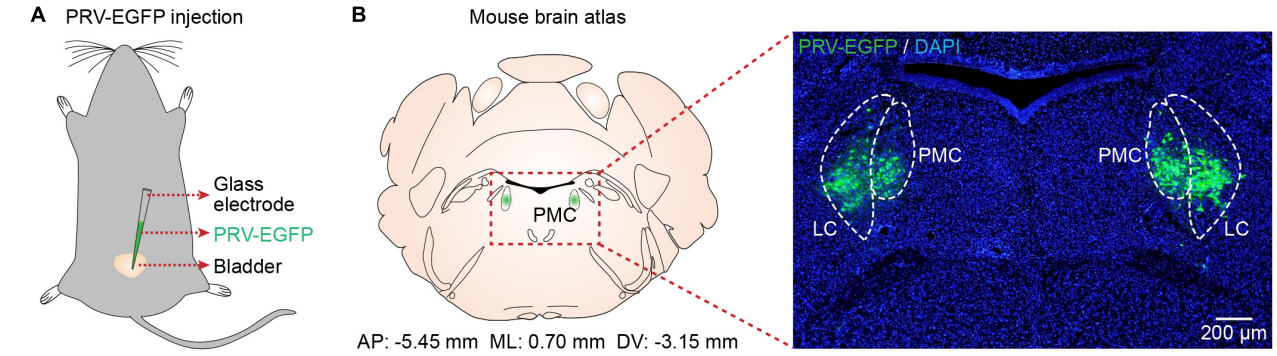

FIGURE 1 | Verification of PMC location. **(A)** Schematic of PRV-EGFP injection into the bladder walls of mice. **(B)** Left, the location of the PMC according to the mouse brain atlas. Right, confocal image showing PRV-infected neurons (green) in the PMC with DAPI (blue) staining

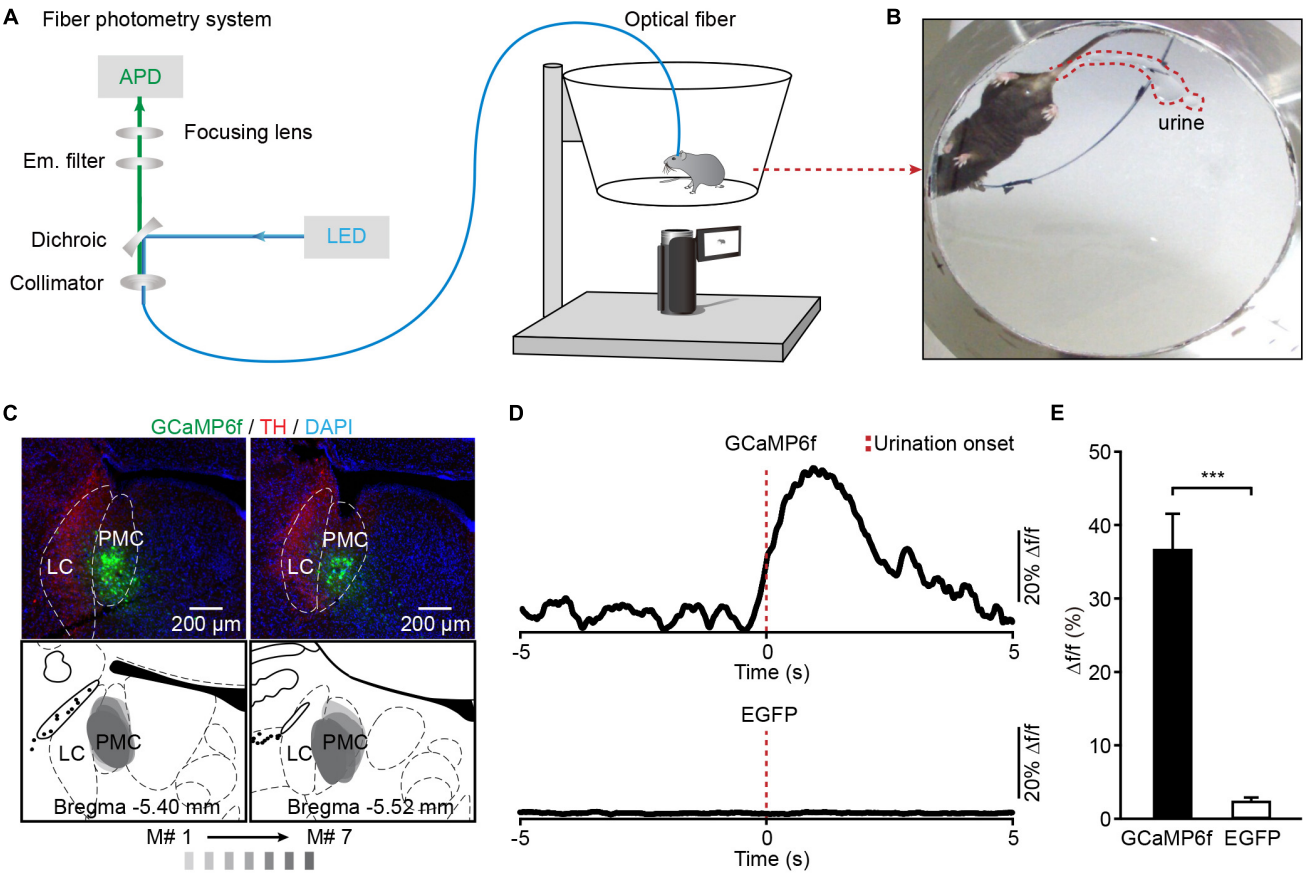

FIGURE 2 | Population Ca^{2+} transients of PMC neurons in freely moving mice during urination. **(A)** Schematic of the fiber photometry setup. **(B)** The example picture shows that the mouse behavior and urine deposition were monitored using a camera placed underneath the chamber. **(C)** The representative *post hoc* images showing AAV-hSyn-GCaMP6f-labeled neurons (green) in the PMC. LC neurons are labeled with TH (red). Serial brain sections showing overlay of viral expression areas (in gray) from 7 GCaMP6f-injected mice. **(D)** Examples of Ca^{2+} transients of PMC neurons during urination events in the GCaMP6f-injected group (upper) and the EGFP-injected group (down). The red dashed line indicates urination onset. **(E)** Quantification of amplitudes of urination-related Ca^{2+} transients in the GCaMP6f-injected group (n = 7 mice) and the EGFP-injected group (n = 7 mice). Wilcoxon rank-sum test, $^{***}P < 0.001$.

The expanded graphs in **Figure 5B** of two urination cycles indicate that the Ca^{2+} transients preceded the onset of bladder contraction. Quantitative analyses showed that the onset of Ca^{2+} transients in the PMC was ~125 ± 66 ms earlier than bladder contraction (n = 8 mice). We also found that each spike-like increase in bladder pressure was also 100% associated with Ca^{2+}

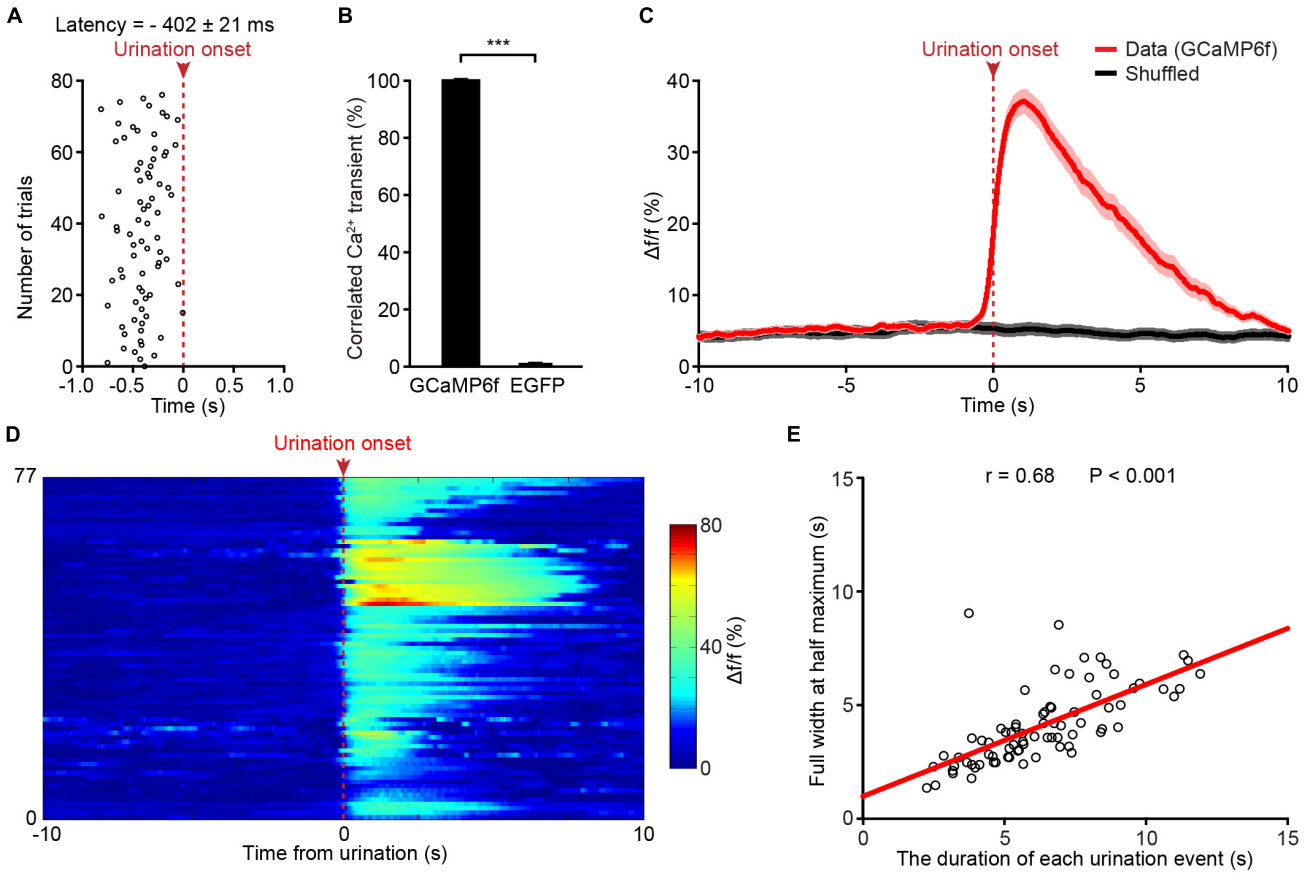

FIGURE 3 | Population Ca^{2+} transients of PMC neurons highly correlate with urination events in freely moving mice. **(A)** Onsets of PMC Ca^{2+} transients in the GCaMP6f-injected group plotted relative to the onset of urination (red dashed line). n = 77 urination events from 7 mice. **(B)** Quantification of the percentage of Ca^{2+} events that correlated with urination in the GCaMP6f-injected group and the EGFP-injected group. Wilcoxon rank-sum test, $^{***}P < 0.001$. **(C)** Averaged Ca^{2+} transients of the PMC neurons in the GCaMP6f-injected group (red, n = 77 urination events from 7 mice) aligned to the urination onset or shuffled urination onset (red dashed line). The dashed bar indicates urination onset. Shaded areas represent s.e.m. **(D)** Heatmap showing Ca^{2+} transients of the PMC neurons aligned to urination onsets in freely moving mice. n = 77 urination events from 7 mice. Warmer color indicates higher amplitude of urination-related Ca^{2+} transients. **(E)** Quantification of the full width at the half maximum of Ca^{2+} transients in D in relation to the duration of urination events. The duration of each urination event was measured from the urination onset (the first drop of urine appearing at the urethral orifice) to the urination offset (no drop of urine appearing at the urethral orifice).

transients of PMC GCaMP6f-positive neurons. Cross-correlation of Ca^{2+} transients recorded in the PMC and bladder pressure showed that the correlation coefficient of the mean peak value was higher than the shuffled data (n = 8 mice) (**Figures 5C,D**; data, 0.51 ± 0.08; shuffled, 0.09 ± 0.03; $P < 0.01$). These results demonstrate that population Ca^{2+} transients of PMC neurons correlate with bladder contraction in freely moving mice.

Anesthesia Evokes Prominent Changes in the Dynamics of Ca^{2+} Signals in the PMC During the Bladder Contraction

To assess the effect of anesthesia on the neuronal activity in the PMC, we simultaneously monitored population Ca^{2+} transients of PMC GCaMP6f-positive neurons and urinary bladder pressure in anesthetized mice (n = 4). Firstly, these catheter-implanted mice that were successfully recorded with fiber photometry were anesthetized with 2.5% isoflurane. We found that bladder contraction-related population Ca^{2+} transients of PMC neurons were completely absent under the isoflurane-anesthetized condition (**Figure 6A**). Cystometric recordings revealed that the regular urination cycles were not detected due to dripping overflow incontinence in this condition (**Figure 6A**).

Then isoflurane was withdrawn and anesthesia was maintained with urethane. Under this condition mice urinated periodically and simultaneous measurement of neuronal activity and cystometry showed that bladder contraction correlated with Ca^{2+} transients of PMC neurons (**Figure 6B**). Each spike-like increase in bladder pressure was also 100% associated with Ca^{2+} transients of PMC neurons in the urethane-anesthetized group (n = 4 mice), the same as what in the awake group (n = 8 mice) (**Figure 6C**). The dynamics of Ca^{2+} transients of PMC neurons were significantly different between awake and urethane-anesthetized mice (**Figures 5A**, **6B**). Quantitative analyses demonstrated that the full width at the half maximum of Ca^{2+} transients in the urethane-anesthetized group was smaller than

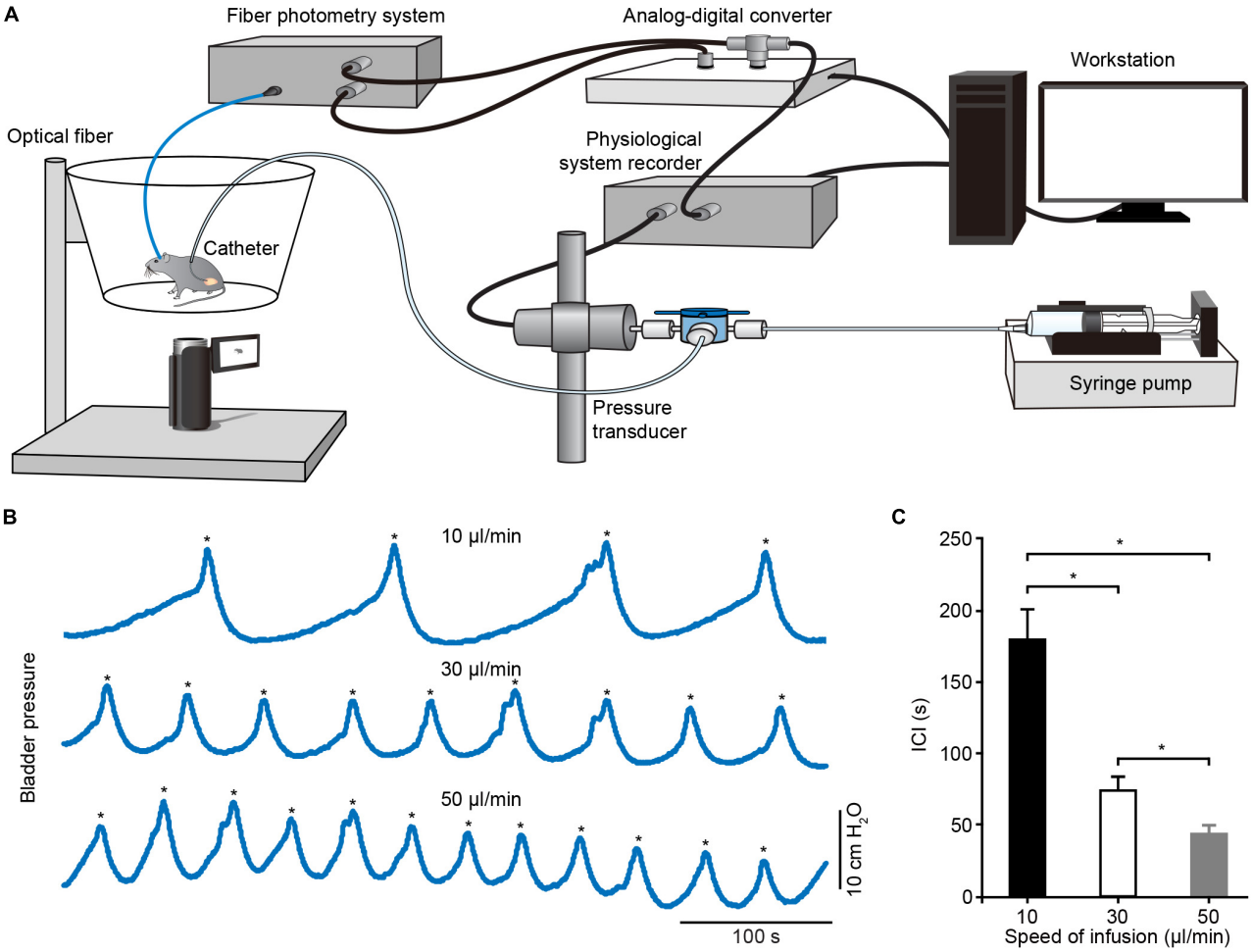

FIGURE 4 | Schematic of experimental recording setup and cystometrogram. **(A)** Schematic of the urodynamic setup incorporating the fiber photometry system in freely moving mice. **(B)** Examples showing the bladder pressures in an anesthetized mouse at different infusion speeds. The voiding contractions were pointed out with the asterisks. **(C)** Quantitative analysis of the ICI at different infusion speeds. n = 6 mice. Wilcoxon signed-rank test, $^*P < 0.05$.

that in the awake group (**Figure 6D**; the urethane-anesthetized group, 3.02 ± 0.19 s; the awake group, 6.77 ± 0.57 s; $P < 0.001$). The normal saline was infused into the mouse bladders via the catheter at 30 μl/min in each trial of the two groups (n = 40 trials from 4 awake mice; n = 44 trials from 4 urethane-anesthetized mice). Overall, these results indicate that urethane anesthesia evokes prominent changes in the dynamics of the Ca^{2+} signals in the PMC, and deep isoflurane anesthesia induces the dripping overflow incontinence which may be due, at least in part, due to suppression of the neural activity in the PMC.

DISCUSSION

The present study combined optical fiber-based Ca^{2+} recording with cystometry to examine how neural activities of PMC neurons were related to urination or bladder pressure in freely moving mice. We found that population Ca^{2+} transients of PMC neurons appeared during each bladder contraction by cystometry. We observed that the onset of Ca^{2+} transients in the PMC was ∼400 ms earlier than the onset of urination events or ∼125 ms earlier than bladder contraction. In addition, a persistent class of Ca^{2+} transients of PMC neurons was seen throughout the entire process of urination. Finally, we showed that urethane anesthesia evoked prominent changes in the dynamics of Ca^{2+} signals in the PMC and deep isoflurane anesthesia induced the dripping overflow incontinence due to suppression of the neural activity in the PMC.

Urodynamic measurements in humans are mostly collected under a fully awake state (Gammie et al., 2014). Previous studies have reported that anesthesia modifies bladder function (Matsuura and Downie, 2000; Chang and Havton, 2008; Wuethrich et al., 2013; Aizawa et al., 2015; Schneider et al., 2015). Our results also showed that anesthesia evoked prominent changes in the dynamics of the Ca^{2+} signals in the PMC during the bladder contraction and even induced the dripping overflow incontinence. Therefore, the performance of cystometry in fully awake animals would be a promising translational measurement

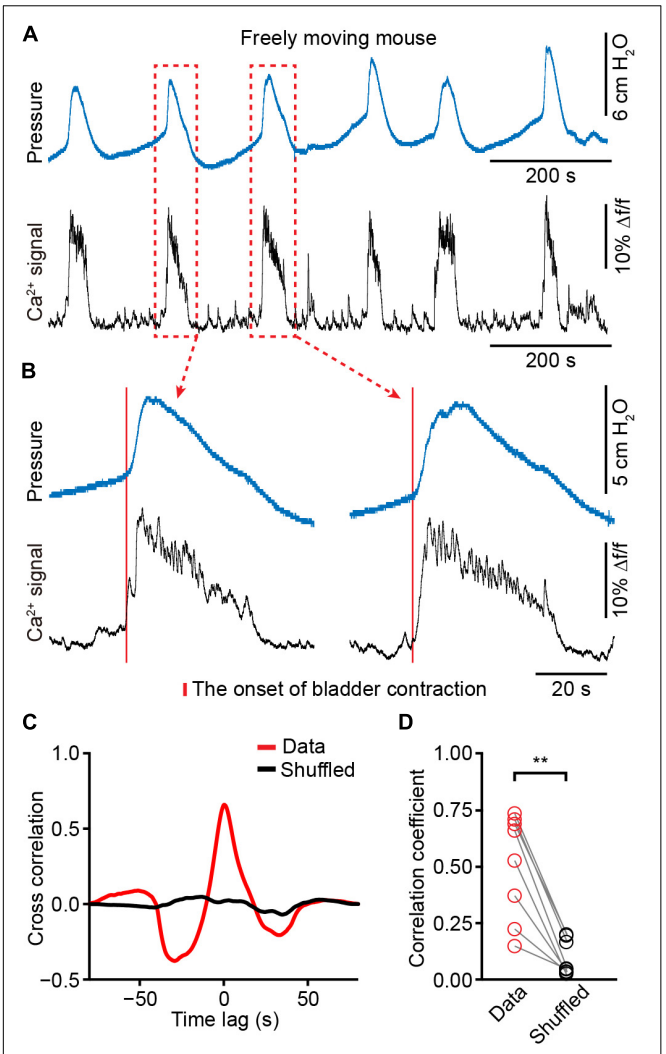

FIGURE 5 | The activities of PMC neurons highly correlate with increased bladder pressure in freely moving mice. **(A)** Example bladder pressure trace (blue) and time-locked Ca^{2+} transients of PMC neurons (black) in a freely moving mouse. **(B)** The enlarged view of the dashed line boxes from A. The red bar indicates the onset of bladder contraction. **(C)** Cross-correlation between Ca^{2+} transients of PMC neurons and bladder pressure from the awake mouse as shown in A compared to the shuffled data. **(D)** Summary of cross-correlation coefficients. n = 8 mice. Wilcoxon signed-rank test, $^{**}P < 0.01$.

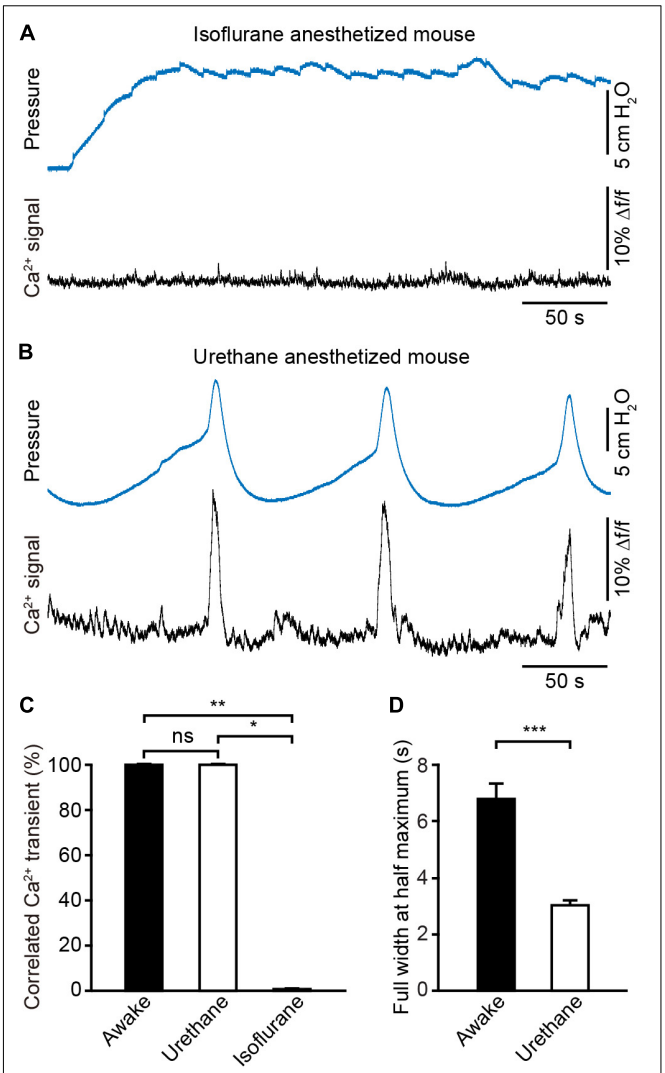

FIGURE 6 | Anesthesia evokes prominent changes in the dynamics of Ca^{2+} signals in the PMC during the bladder contraction. **(A)** Example bladder pressure trace (blue) and time-locked Ca^{2+} transients of PMC neurons (black) in an isoflurane-anesthetized mouse. **(B)** Example bladder pressure trace (blue) and time-locked Ca^{2+} transients of PMC neurons (black) in a urethane-anesthetized mouse. The mouse as shown in A and B was the same one. **(C)** Quantification of the percentage of Ca^{2+} events that correlated with the bladder contractions. n = 4 mice for anesthesia and 8 mice for wakefulness. Wilcoxon rank-sum test, $^{**}P < 0.01$ or Wilcoxon signed-rank test, $^{*}P < 0.05$. **(D)** Quantitative analysis of the full width at the half maximum of Ca^{2+} transients in each group. n = 40 trials from 4 awake mice; n = 44 trials from 4 urethane-anesthetized mice. Wilcoxon rank-sum test, $^{***}P < 0.001$.

to evaluate bladder function. However, most previous reports that recorded the neuronal activity of PMC neurons and bladder pressure simultaneously were performed in anesthetized animals (Tanaka et al., 2003; de Groat and Wickens, 2013) and no data are available for simultaneous recordings in freely moving animals. Therefore, our measurements in freely moving mice are a new and efficient approach to investigate brain functions during urination.

Cystometry is widely used to monitor the bladder pressure and micturition cycles (Griffiths, 1977; Fry et al., 2010). However, it requires chronic catheter implantation into the bladder, which causes a local bladder tissue reaction, bladder wall swelling and post-operative stress (Yaksh et al., 1986; Mann-Gow et al., 2017). Recent work compared the bladder function in the same animals before and after catheter implantation surgery and showed that the catheter implantation operation did not affect bladder function (Schneider et al., 2018). The skills of the experimenter and the amount of recovery time after catheter implantation surgery were critical for the quality and reproducibility of results. Bladder wall swelling and voiding frequency were normal at least

5 days after surgery (Mann-Gow et al., 2017). Therefore, we used a microsurgical technique that minimized bladder damage during catheter implantation surgery (Mann-Gow et al., 2017) and offered the mice at least 5 days for recovery. In addition, this measurement could not completely mimic physiological micturition cycles, which are less frequent when saline is not infused into the bladder (Manohar et al., 2017). Notably, our present findings showed that the pattern of population neuronal activities in the PMC during natural micturition cycles was similar to the micturition cycles using cystometry.

Three types of activity patterns of PMC neurons were distinguished in several reports (Tanaka et al., 2003; de Groat and Wickens, 2013; de Groat et al., 2015): (1) Some neurons fired before and during bladder contractions; (2) some neurons were suppressed during bladder contractions and activated during the storage period; and (3) other neurons only discharged at the beginning of the detrusor contractions. However, our present findings only showed that the neuronal activity of PMC neurons started prior to bladder contractions and persisted throughout the voiding in freely moving mice. This difference may be because the fiber photometry-detected Ca^{2+} transients reflected the average spiking activity of all types of PMC neurons. The rapid development of Ca^{2+} imaging techniques suggests that a micro-endoscopic approach would record population Ca^{2+} transients in any brain region of freely moving animals at single-cell resolution (Jennings et al., 2015; Resendez et al., 2016). The application of this method would further our understanding of the properties of urination-related signals of PMC neurons.

Fiber photometry is an increasingly used population method for the monitoring of population activities of specific neurons in freely moving animals, including mice and monkeys (Adelsberger et al., 2014; Gunaydin et al., 2014). Several recent studies used this method to investigate urination-related neuronal population activities in freely moving mice. Hou et al. (2016) reported urination-related activities from a cluster of neurons expressing corticotropin-releasing hormone (CRH) that modulated the bladder contraction, and Keller et al. (2018) found similar activities in a group of neurons expressing estrogen receptor 1 (ESR1), which controlled sphincter relaxation. More recently, we used fiber photometry and found voluntary urination-related activities in mouse primary motor cortex (Yao et al., 2018). These activities are required for the driving of urination through the projections to the PMC. Therefore, urodynamic measurement that incorporate the optical fiber-based Ca^{2+} recording in freely moving mice will be an efficient approach for investigating the brain circuitry that controls urination.

In summary, our results revealed that a urodynamic measurement incorporating the optical fiber-based Ca^{2+} recording was an efficient approach for the detection of population neuronal activities of any brain region during urination in freely moving mice. We provide a better insight into the neural mechanisms that control the bladder and open up a possible avenue to elucidate NGB using a translational method.

ETHICS STATEMENT

This study was approved by the Institutional Animal Care and Use Committee of Third Military Medical University. All experimental procedures were conducted in accordance with animal ethical guidelines of the Third Military Medical University Animal Care and Use Committee.

AUTHOR CONTRIBUTIONS

JiY, XC, WL, and JuY contributed to the design of the study and interpretation of the data. JiY, QL, XpL, and HQ carried out the experiments and acquired the data. JiY, XL, SL, and HQ processed and analyzed the data. JiY, XC, WL, and JuY wrote the manuscript with help from all other authors.

FUNDING

This work was supported by grants from the National Natural Science Foundation of China (No. 81671106), the National Basic Research Program of China ("973 Program": 2015CB759500), and the medical personnel military medical innovation ability promotion plan of army military medical university first affiliated hospital (SWH2018BJKJ-07).

ACKNOWLEDGMENTS

We thank Jia Lou for her assisting in the composition of the figures.

REFERENCES

Adelsberger, H., Garaschuk, O., and Konnerth, A. (2005). Cortical calcium waves in resting newborn mice. *Nat. Neurosci.* 8, 988–990. doi: 10.1038/nn1502

Adelsberger, H., Zainos, A., Alvarez, M., Romo, R., and Konnerth, A. (2014). Local domains of motor cortical activity revealed by fiber-optic calcium recordings in behaving nonhuman primates. *Proc. Natl. Acad. Sci. U.S.A.* 111, 463–468. doi: 10.1073/pnas.1321612111

Aizawa, N., Ogawa, S., Sugiyama, R., Homma, Y., and Igawa, Y. (2015). Influence of urethane-anesthesia on the effect of resiniferatoxin treatment on bladder function in rats with spinal cord injury. *Neurourol. Urodyn.* 34, 274–279. doi: 10.1002/nau.22549

Benarroch, E. E. (2010). Neural control of the bladder: recent advances and neurologic implications. *Neurology* 75, 1839–1846. doi: 10.1212/WNL.0b013e3181fdabba

Blok, B. F., and Holstege, G. (1998). The central nervous system control of micturition in cats and humans. *Behav. Brain Res.* 92, 119–125. doi: 10.1016/s0166-4328(97)00184-8

Chang, H. Y., and Havton, L. A. (2008). Differential effects of urethane and isoflurane on external urethral sphincter electromyography and cystometry in rats. *Am. J. Physiol. Renal Physiol.* 295, F1248–F1253. doi: 10.1152/ajprenal.90259.2008

Cui, G., Jun, S. B., Jin, X., Luo, G., Pham, M. D., Lovinger, D. M., et al. (2014). Deep brain optical measurements of cell type-specific neural activity in behaving mice. *Nat. Protoc.* 9, 1213–1228. doi: 10.1038/nprot.2014.080

de Groat, W. C., Griffiths, D., and Yoshimura, N. (2015). Neural control of the lower urinary tract. *Compr. Physiol.* 5, 327–396. doi: 10.1002/cphy.c130056

de Groat, W. C., and Wickens, C. (2013). Organization of the neural switching circuitry underlying reflex micturition. *Acta Physiol.* 207, 66–84. doi: 10.1111/apha.12014

Drake, M. J., Fowler, C. J., Griffiths, D., Mayer, E., Paton, J. F., and Birder, L. (2010). Neural control of the lower urinary and gastrointestinal tracts: supraspinal CNS mechanisms. *Neurourol. Urodyn.* 29, 119–127. doi: 10.1002/nau.20841

Fowler, C. J., Griffiths, D., and de Groat, W. C. (2008). The neural control of micturition. *Nat. Rev. Neurosci.* 9, 453–466. doi: 10.1038/nrn2401

Fry, C. H., Daneshgari, F., Thor, K., Drake, M., Eccles, R., Kanai, A. J., et al. (2010). Animal models and their use in understanding lower urinary tract dysfunction. *Neurourol. Urodyn.* 29, 603–608. doi: 10.1002/nau.20903

Gammie, A., Clarkson, B., Constantinou, C., Damaser, M., Drinnan, M., Geleijnse, G., et al. (2014). International continence society guidelines on urodynamic equipment performance. *Neurourol. Urodyn.* 33, 370–379. doi: 10.1002/nau.22546

Ginsberg, D. (2013). The epidemiology and pathophysiology of neurogenic bladder. *Am. J. Manag. Care* 19, s191–s196.

Grienberger, C., and Konnerth, A. (2012). Imaging calcium in neurons. *Neuron* 73, 862–885. doi: 10.1016/j.neuron.2012.02.011

Griffiths, D. J. (1977). Urodynamic assessment of bladder function. *Br. J. Urol.* 49, 29–36. doi: 10.1111/j.1464-410x.1977.tb04518.x

Gunaydin, L. A., Grosenick, L., Finkelstein, J. C., Kauvar, I. V., Fenno, L. E., Adhikari, A., et al. (2014). Natural neural projection dynamics underlying social behavior. *Cell* 157, 1535–1551. doi: 10.1016/j.cell.2014.05.017

Guo, Q., Zhou, J., Feng, Q., Lin, R., Gong, H., Luo, Q., et al. (2015). Multi-channel fiber photometry for population neuronal activity recording. *Biomed. Opt. Express* 6, 3919–3931. doi: 10.1364/BOE.6.003919

Harris, C. J., and Lemack, G. E. (2016). Neurourologic dysfunction: evaluation, surveillance and therapy. *Curr. Opin. Urol.* 26, 290–294. doi: 10.1097/MOU.0000000000000290

Hou, X. H., Hyun, M., Taranda, J., Huang, K. W., Todd, E., Feng, D., et al. (2016). Central Control Circuit for Context-Dependent Micturition. *Cell* 167:73-86.e12. doi: 10.1016/j.cell.2016.08.073

Jennings, J. H., Ung, R. L., Resendez, S. L., Stamatakis, A. M., Taylor, J. G., Huang, J., et al. (2015). Visualizing hypothalamic network dynamics for appetitive and consummatory behaviors. *Cell* 160, 516–527. doi: 10.1016/j.cell.2014.12.026

Keller, J. A., Chen, J., Simpson, S., Wang, E. H., Lilascharoen, V., George, O., et al. (2018). Voluntary urination control by brainstem neurons that relax the urethral sphincter. *Nat. Neurosci.* 21, 1229–1238. doi: 10.1038/s41593-018-0204-3

Kerr, J. N., Greenberg, D., and Helmchen, F. (2005). Imaging input and output of neocortical networks in vivo. *Proc. Natl. Acad Sci. U.S.A.* 102, 14063–14068. doi: 10.1073/pnas.0506029102

Li, J., Liao, X., Zhang, J., Wang, M., Yang, N., Zhang, J., et al. (2017). Primary auditory cortex is required for anticipatory motor response. *Cereb. Cortex* 27, 3254–3271. doi: 10.1093/cercor/bhx079

Mann-Gow, T. K., Larson, T. R., Woien, C. T., Andersen, T. M., Andersson, K. E., and Zvara, P. (2017). Evaluating the procedure for performing awake cystometry in a mouse model. *J. Vis. Exp.* e55588. doi: 10.3791/55588

Manohar, A., Curtis, A. L., Zderic, S. A., and Valentino, R. J. (2017). Brainstem network dynamics underlying the encoding of bladder information. *Elife* 6:e29917. doi: 10.7554/eLife.29917

Matsuura, S., and Downie, J. W. (2000). Effect of anesthetics on reflex micturition in the chronic cannula-implanted rat. *Neurourol. Urodyn.* 19, 87–99. doi: 10.1002/(sici)1520-6777(2000)19:1<87::aid-nau9>3.0.co;2-o

Qin, H., Fu, L., Hu, B., Liao, X., Lu, J., He, W., et al. (2018). A visual-cue-dependent memory circuit for place navigation. *Neuron* 99:47-55.e4. doi: 10.1016/j.neuron.2018.05.021

Resendez, S. L., Jennings, J. H., Ung, R. L., Namboodiri, V. M., Zhou, Z. C., Otis, J. M., et al. (2016). Visualization of cortical, subcortical and deep brain neural circuit dynamics during naturalistic mammalian behavior with head-mounted microscopes and chronically implanted lenses. *Nat. Protoc.* 11, 566–597. doi: 10.1038/nprot.2016.021

Schneider, M. P., Hughes, F. M. Jr., Engmann, A. K., Purves, J. T., Kasper, H., Tedaldi, M., et al. (2015). A novel urodynamic model for lower urinary tract assessment in awake rats. *BJU Int.* 115(Suppl. 6), 8–15. doi: 10.1111/bju.13039

Schneider, M. P., Sartori, A. M., Tampe, J., Moors, S., Engmann, A. K., Ineichen, B. V., et al. (2018). Urodynamic measurements reflect physiological bladder function in rats. *Neurourol. Urodyn.* 37, 1266–1271. doi: 10.1002/nau.23455

Smith, B. N., Banfield, B. W., Smeraski, C. A., Wilcox, C. L., Dudek, F. E., Enquist, L. W., et al. (2000). Pseudorabies virus expressing enhanced green fluorescent protein: a tool for in vitro electrophysiological analysis of transsynaptically labeled neurons in identified central nervous system circuits. *Proc. Natl. Acad Sci. U.S.A.* 97, 9264–9269. doi: 10.1073/pnas.97.16.9264

Stanley, S., Pinto, S., Segal, J., Perez, C. A., Viale, A., DeFalco, J., et al. (2010). Identification of neuronal subpopulations that project from hypothalamus to both liver and adipose tissue polysynaptically. *Proc. Natl. Acad Sci. U.S.A.* 107, 7024–7029. doi: 10.1073/pnas.1002790107

Stroh, A., Adelsberger, H., Groh, A., Ruhlmann, C., Fischer, S., Schierloh, A., et al. (2013). Making waves: initiation and propagation of corticothalamic Ca2+ waves in vivo. *Neuron* 77, 1136–1150. doi: 10.1016/j.neuron.2013.01.031

Sugaya, K. (1988). The effects of chemical stimulations of the pontine micturition center in decerebrate cats. *Nihon Hinyokika Gakkai Zasshi* 79, 1364–1371. doi: 10.5980/jpnjurol1928.79.8_1364

Sugaya, K., Matsuyama, K., Takakusaki, K., and Mori, S. (1987). Electrical and chemical stimulations of the pontine micturition center. *Neurosci. Lett.* 80, 197–201. doi: 10.1016/0304-3940(87)90653-7

Tanaka, Y., Koyama, Y., Kayama, Y., Kawauchi, A., Ukimura, O., and Miki, T. (2003). Firing of micturition center neurons in the rat mesopontine tegmentum during urinary bladder contraction. *Brain Res.* 965, 146–154. doi: 10.1016/s0006-8993(02)04154-9

Valentino, R. J., Wood, S. K., Wein, A. J., and Zderic, S. A. (2011). The bladder-brain connection: putative role of corticotropin-releasing factor. *Nat. Rev. Urol.* 8, 19–28. doi: 10.1038/nrurol.2010.203

Verstegen, A. M. J., Vanderhorst, V., Gray, P. A., Zeidel, M. L., and Geerling, J. C. (2017). Barrington's nucleus: neuroanatomic landscape of the mouse "pontine micturition center". *J. Comp. Neurol.* 525, 2287–2309. doi: 10.1002/cne.24215

Willette, R. N., Morrison, S., Sapru, H. N., and Reis, D. J. (1988). Stimulation of opiate receptors in the dorsal pontine tegmentum inhibits reflex contraction of the urinary bladder. *J. Pharmacol. Exp. Ther.* 244, 403–409.

Wuethrich, P. Y., Metzger, T., Mordasini, L., Kessler, T. M., Curatolo, M., and Burkhard, F. C. (2013). Influence of epidural mixture and surgery on bladder function after open renal surgery: a randomized clinical trial. *Anesthesiology* 118, 70–77. doi: 10.1097/ALN.0b013e318271606a

Yaksh, T. L., Durant, P. A., and Brent, C. R. (1986). Micturition in rats: a chronic model for study of bladder function and effect of anesthetics. *Am. J. Physiol.* 251, R1177–R1185. doi: 10.1152/ajpregu.1986.251.6.R1177

Yao, J., Zhang, Q., Liao, X., Li, Q., Liang, S., Li, X., et al. (2018). A corticopontine circuit for initiation of urination. *Nat. Neurosci.* 21, 1541–1550. doi: 10.1038/s41593-018-0256-4

Zhang, Q., Yao, J., Guang, Y., Liang, S., Guan, J., Qin, H., et al. (2017). Locomotion-Related Population Cortical Ca2+ Transients in Freely Behaving Mice. *Front. Neural. Circuits* 11:24. doi: 10.3389/fncir.2017.00024

Conflict of Interest Statement: The authors declare that the research was conducted in the absence of any commercial or financial relationships that could be construed as a potential conflict of interest.

frontiers in Neuroscience

ORIGINAL RESEARCH
published: 06 September 2019
doi: 10.3389/fnins.2019.00950

Association of Social Jetlag With Sleep Quality and Autonomic Cardiac Control During Sleep in Young Healthy Men

*Ágnes Réka Sűdy[1], Krisztina Ella[1], Róbert Bódizs[2,3] and Krisztina Káldi[1,4]**

[1] Department of Physiology, Semmelweis University, Budapest, Hungary, [2] Institute of Behavioural Sciences, Semmelweis University, Budapest, Hungary, [3] National Institute of Clinical Neurosciences, Budapest, Hungary, [4] Department of Laboratory Medicine, Semmelweis University, Budapest, Hungary

Social jetlag (SJL), the difference in sleep timing between work and free days is a consequence of the discrepancy between the individual's circadian rhythm and the social clock. SJL is considered a chronic stress factor and has been linked to various health problems. In this field study, we examined for the first time the association between SJL and cardiac regulation during sleep. 33 healthy young men aged 20–26 years participated in the study. The median SJL was used as a cut-off value to assign the participants into two groups with either lower or higher SJL. As a marker of autonomic control we analyzed heart rate variability (HRV) and addressed intra-individual differences between workdays and free days. In subjects with higher SJL, pNN50, an indicator of vagal activity was lower in the first 3 h of sleep on workday as compared to free day (day × sleep block × group, $p = 0.015$), indicating a more adaptable regulation on free days, when subjects slept according to their own preference. However, in subjects with lower SJL, no HRV differences were found between the two nights. SJL showed correlation with the free day-workday differences of both pNN50 and another vagal index, RMSSD in the first 2 h of sleep ($p = 0.023$ and 0.047, respectively). In subjects with higher SJL, a different HF power on workdays and free days ($p = 0.031$) also indicated that a shift in sleep timing is accompanied by an altered parasympathetic activity in the first few hours of sleep. Furthermore, subjective sleep quality on workdays was negatively associated with SJL ($p = 0.02$), and subjects with higher SJL reported worse sleep quality on workday than on free day ($p = 0.027$). Taken together, our data call attention on the potential effect of SJL on sleep quality and vagal activity during sleep.

Keywords: autonomic nervous system, heart rate variability, sleep quality, circadian misalignment, social jetlag, cardiovascular risk factor

OPEN ACCESS

Edited by:
Phyllis Kravet Stein, Washington University in St. Louis, United States

Reviewed by:
Paolo Castiglioni, Fondazione Don Carlo Gnocchi Onlus (IRCCS), Italy
Dirk Cysarz, Witten/Herdecke University, Germany

***Correspondence:**
Krisztina Káldi
kaldi.krisztina@med.semmelweis-univ.hu

Specialty section:
This article was submitted to Autonomic Neuroscience, a section of the journal Frontiers in Neuroscience

Received: *16 May 2019*
Accepted: *22 August 2019*
Published: *06 September 2019*

Citation:
Sűdy ÁR, Ella K, Bódizs R and Káldi K (2019) Association of Social Jetlag With Sleep Quality and Autonomic Cardiac Control During Sleep in Young Healthy Men. Front. Neurosci. 13:950. doi: 10.3389/fnins.2019.00950

INTRODUCTION

The circadian clock is a fundamental tool enabling organisms to track time internally and thus to adapt their physiology to daily fluctuations in the environment. Circadian time-keeping is organized at the cellular level by the action of molecular oscillators. In mammals, cellular oscillators of peripheral tissues are governed by the central clock located in the suprachiasmatic nucleus of the hypothalamus. A misalignment between the organism's internal clock and the environmental

time is often followed by desynchronization between tissue clocks. Circadian misalignment is considered as a stress factor (Wittmann et al., 2006; Puttonen et al., 2010), and has been linked to the development of various pathological states including cardiovascular diseases (Morris et al., 2017; Strohmaier et al., 2018), metabolic disturbances (Biggi et al., 2008; Vetter et al., 2015), different malignancies (Schernhammer et al., 2006; Papantoniou et al., 2018) and psychological problems (Shields, 2002).

Social jetlag (SJL) is defined as the time difference between the midpoint of sleep on workdays (MSW) and on free days, and it is a consequence of the discrepancy between an individual's own biological rhythm and the daily timing determined by social constraints (Roenneberg et al., 2003; Wittmann et al., 2006). SJL affects the majority of the adolescent and adult population worldwide. In Europe, more than 30% of the population suffer from an SJL larger than 2 h (Roenneberg et al., 2012). SJL was found to correlate with a higher risk for the development of depression (Levandovski et al., 2011), adverse metabolic changes including obesity and type 2 diabetes (Roenneberg et al., 2012; Rutters et al., 2014; Parsons et al., 2015; Wong et al., 2015; Koopman et al., 2017), and shows association with health-impairing habits such as smoking and excessive caffeine consumption (Wittmann et al., 2006). In addition, our and others' data indicate that SJL negatively impacts academic performance (Haraszti et al., 2014; Diaz-Morales and Escribano, 2015).

Both epidemiological and laboratory studies indicate that severe forms of circadian misalignment such as shift work or jetlag adversely affect the circulatory system and therefore increase the risk of the development of cardiovascular diseases (Knutsson, 2003; Grimaldi et al., 2016; Morris et al., 2016; Vetter et al., 2016; Hulsegge et al., 2018). SJL is the most frequent type of circadian misalignment, therefore its negative impact on the cardiovascular system would represent a public health concern.

The analysis of heart rate variability (HRV) is a well-established method to assess autonomic cardiac control (Malik, 1996; Laborde et al., 2017). A key advantage of this method is that well-validated programable measuring devices are available for application in field studies without causing any discomfort for the subjects. HRV represents the change in the time interval between successive heartbeats, which is modulated by the sympathetic and parasympathetic nervous system (Malik, 1996). Therefore, HRV is used as a tool to assess autonomic function at the level of the heart. Healthy cardiovascular control is signaled by higher HRV, indicating a stronger parasympathetic activity, whereas low HRV indicates reduced vagal modulation and increased sympathetic activity, which are established risk factors of cardiovascular diseases (Malik, 1996; Thayer et al., 2010). As autonomic control and sleep regulation are interconnected, HRV may be indicative for sleep quality, and efficiency as well. Falling asleep is accompanied by the shift of autonomic balance toward a parasympathetic dominance, measurable in HRV as it increases from wake to slow wave sleep (Elsenbruch et al., 1999; Trinder et al., 2001; Tobaldini et al., 2013; Chouchou and Desseilles, 2014), which is considered to be the most restorative sleep stage (Akerstedt et al., 1997).

In this study, we hypothesized that sleeping out of the endogenous phase on workdays affects cardiovascular regulation and sleep efficiency. To this end we analyzed sleep-related HRV indices and subjective sleep quality in healthy men forming a homogenous sample with respect to age, BMI, and social situation but differing in the extent of SJL, and addressed individual differences between workdays and free days.

MATERIALS AND METHODS

Participants and Protocol

Participants with regular weekly schedule were recruited via advertisements in social media (Facebook groups) and mailing list of university students. Initially 35 students participated in the study, but two of them were excluded either due to experiencing high emotional stress or for lack of appropriate cooperation. Therefore, data of 33 subjects were involved in the final analysis. The sample was homogenous with respect to age (mean ± SD of 23.2 ± 1.5 years), BMI (mean ± SD of 22.8 ± 2.5), and social situation (university students in Budapest). All subjects were healthy and none of them were taking medication. None of the subjects had a history of sleep disorder or cardiovascular problem and neither one of them experienced jetlag in the last month prior to the study. In a short interview, participants were asked about smoking habits, caffeine consumption, physical activity, blood pressure, and cholesterol levels. Answers did not indicate notable cardiovascular risk factors in any participants. Participants were asked not to undergo extreme physical activity, and to avoid drinking alcohol during the study week. Following the measurements, participants were interviewed about any unexpected events (high psychical and physical stress or any health problems). The study protocol was approved by the Semmelweis University Regional and Institutional Committee of Science and Research Ethics (Ethical approval 170/2016). Participants gave written consent prior to entering the study and were paid for their participation. The study took place in winter (2016/2017) and in the first half of spring (2017) and was paused for 2 weeks after changing to daylight saving time. The number of participants with lower and higher SJL was similar in every month. The study for each subject lasted for a week, during which the participants performed their daily activities according to their usual habit, including waking to an alarm clock on workdays but waking on their own on free days. On a workday (Wednesday) and a free day (Saturday) participants wore an ambulatory heart rate recorder (Actiheart, CamNtech Ltd., United Kingdom) during the night and filled out a sleep quality questionnaire upon waking on the next day. On the days of HRV detection, subjects collected urine samples in the evening before going to bed and in the morning directly after getting up.

Assessment of Sleep Timing

To recruit participants with different SJL and regular weekly schedule, students were asked to fill out the Hungarian version of the Munich Chronotype Questionnaire (MCTQ) (Haraszti et al., 2014). Chronotype was assessed as the midpoint of sleep on free days (MSF) corrected for oversleep on free days (MSFsc),

and SJL was calculated by subtracting the midpoint of sleep on workdays (MSW) from MSF, based on Wittmann et al. (2006). During the week of the study each participant kept a sleep diary, based on which the SJL characteristic for the study period was calculated. The mean SJL ± SD was 92.1 ± 52.9 min, which fits well with previously reported SJL values for this age group (Wittmann et al., 2006; Haraszti et al., 2014; Pilz et al., 2018). The median SJL (93 min) was used as a cut-off value to divide the participants into two groups with either lower (SJL $\leq$ 93 min) or higher SJL (SL $>$ 93 min). Using this cut-off value resulted in a 10-minutes gap between the two groups. There was no significant difference between the two groups regarding age (23.3 ± 1.9 and 23.1 ± 0.9 years mean ± SD for the lower and the higher SJL group, respectively) and BMI (22.1 ± 2.7 and 23.6 ± 2.1 years mean ± SD for the lower and the higher SJL group, respectively). Sleep onset and waking time on the days of HRV detection were estimated by the Actiheart software. These time points were controlled by comparing them with data from the sleep diary. The estimated sleep onset and waking times were used to calculate exact SJL for the days the measurements were performed. This SJL value was used to investigate correlation between SJL and HRV parameters.

Urinary Melatonin

Urine samples collected by the subjects in the evening and morning were stored at −20°C before analysis. Urinary 6-sulfatoxymelatonin, a stable melatonin metabolite, was measured by competitive ELISA according to the instructions of the manufacturer (IBL International). The creatinine concentration of the samples was determined by enzymatic assay (Diagnosticum Zrt., Budapest) to obtain a normalized 6-sulfatoxymelatonin/creatinine ratio (nmol/mmol).

HRV Analysis

The Actiheart monitor was used for the recording of heart rate. Prior to the measurements, participants came into the laboratory where a signal test was performed along with the programing of the device to start recording in the evening. On the next day participants brought the device back for data collection and recharge, before taking it again for the weekend. The Actiheart monitor collects inter-beat-interval (IBI) data, which can be further processed and used for the calculation of HRV parameters. Studies comparing Actiheart and standard ECG recordings did not find any significant difference in IBI detection (Brage et al., 2005; Barreira et al., 2009; Kristiansen et al., 2011). All HRV analyses were performed according to the standards of measurements (Malik, 1996) and the recent recommendations by Laborde et al. (2017). First, reliability of raw data was checked by visual inspection. To ensure a consistent artifact detection and correction, the ARTiiFACT software was used (Kaufmann et al., 2011). According to the international guidelines the data were decomposed into 5 min long segments for analysis of HRV parameters in both the time and frequency domains (Malik, 1996). Segments with more than 10% artifact ratio were excluded. Excluded segments and loss of electrode contact resulted in slightly varying sample sizes in the different analyses. Parameters calculated for the 5 min long segments were averaged for either 1.5- or 2-h blocks, depending on the analysis performed, as indicated in the text and legends.

In the time domain the standard deviation of the normal to normal interval (SDNN), the root mean square of successive differences (RMSSD), and the percentage of successive normal to normal intervals differing by more than 50 ms (pNN50) were calculated using the ARTiiFACT software. For the analysis of HRV in the frequency domain the DADiSP 6.7 software (DSP Development Corp., United States) was used. IBI data were first resampled to 4 Hz using cubic spline interpolation, detrended and tapered with a Hanning window. Power spectral density (PSD) was then calculated with mixed-radix Fast Fourier Transformation, yielding 600 frequency bins in the range of 0–2 Hz. From the average PSD of the successive 5 min segments very low frequency (VLF, 0.003–0.04 Hz), low frequency (LF, 0.04–0.15 Hz), and high frequency (HF, 0.15–0.4 Hz) absolute powers were calculated by numerical integration of the respective frequency ranges. Normalized units of LF (LFnu = LF/LF + HF) were also calculated. Bin-wise and band-wise PSD values were log normalized (natural base logarithm) before the statistical analyses. In our subjects respiratory rate, determined on the basis of the peak in the high frequency region of the FFT plot, was between 0.2 and 0.3 Hz (12–18/min). At this respiratory rate (resting state) HF corresponds to vagal activity, and correction of the HRV parameters for respiration is not required (Larsen et al., 2010; Bertsch et al., 2012; Laborde et al., 2017).

Assessment of Subjective Sleep Quality

For the assessment of subjective sleep quality, we used the Groningen Sleep Quality Scale (GSQS) (Meijman et al., 1988). The Hungarian version of the questionnaire translated from English was validated by Simor et al. (2009). The participants filled out the GSQS questionnaire directly upon waking following the nights with HRV measurements. The questionnaire contains 15 short, true or false questions about the previous night's sleep. The first question is not evaluated, therefore the GSQS is scored between 0 and 14, a higher score indicating lower quality of sleep.

Statistics

Normality of data (sleep times, HRV measures, questionnaire scores, and 6-sulfatoxymelatonin levels) was assessed by the Kolmogorov-Smirnov test. 6-sulfatoxymelatonin and bin-wise spectral HRV data showed non-normal distribution. For the analysis of the former the non-parametric Mann-Whitney *U* test was used. Bin-wise spectral HRV data was log normalized to achieve normality. If normal distribution was present, we used parametric statistical procedures as follows. Workday-free day differences were assessed by paired sample *t*-tests. Group differences were tested by two sample *t*-tests. For the analysis of HRV data in consecutive time blocks, repeated measures analysis of variance (ANOVA) was performed. Fisher's LSD test was used as *post hoc* test. In addition, the association of SJL with sleep quality and HRV was examined by Pearson's correlation. Log-normalized bin-wise spectral data was expressed as a difference (free day – workday) over the frequency axis (0–0.4 Hz). One-sample *t*-tests were run in order to test if the differences were significantly deviating from the null hypothesis (difference = 0).

Inflation of Type-I error in this case was handled by the procedure of descriptive data analysis (Abt, 1987). Statistical significance threshold was set at $p < 0.05$. If not otherwise indicated, data are presented as mean ± standard error of the mean (SEM). Statistical analyses were performed using Statistica software version 13.2 (StatSoft, Tulsa, OK, United States).

RESULTS

Basic Rhythm and Sleep Characteristics of the Participants

To control that the participants' actual sleep schedule during the study week was similar to their usual sleep timing, data from the sleep diary recorded during the study week were compared with data from the MCTQ filled in prior to the study. Reliable correlation for both chronotype (indicated by MSFsc) and SJL were obtained (**Supplementary Table S1**). Participants were divided into two groups based on the median SJL of the whole sample. **Table 1** shows sleep data (timing and duration) for both the workday and free day when subjective sleep quality and HRV were assessed. On workdays the two groups displayed no differences in sleep timing and duration, whereas on free days the group with higher SJL had a significantly later bedtime, sleep onset, and waking time than the other group. Both groups had longer sleep duration on free day compared to workday. As a factor of homeostatic sleep regulation we calculated the time spent awake on the days before the HRV measurements. However, neither a group nor a group x day effect was obtained (**Supplementary Table S2**).

As a marker of circadian rhythm, urinary levels of 6-sulfatoxymelatonin, the stable metabolite of melatonin, were determined in evening, and morning urinary samples. The marked difference in the levels of 6-sulfatoxymelatonin between the morning and evening samples (mean individual morning/evening ratios ± SEM, 6.75 ± 0.75) confirmed the rhythmic physiology of our participants. However, neither the evening nor the morning excretion of 6-sulfatoxymelatonin was associated with SJL (**Supplementary Table S3**).

Time-Domain Analysis of HRV

To assess how sleep timing affects autonomic cardiac control during sleep, individual HRV parameters were compared between workdays and free days. Average heart rate (HR) for the whole sleep period did not differ between the two days in either group of participants. However, in the group with higher SJL, SDNN, a basic measure of HRV, was significantly higher on the free day than on the workday (**Table 2**). To analyze HRV in the course of sleep, we calculated mean HRV parameters for consecutive 1.5-h sleep blocks from the time point of falling asleep. As the minimum sleep length on both days was 6 h, four sleep blocks were analyzed for each night and the data sets of workdays and free days were compared. **Figure 1** shows data for RMSSD and pNN50, the time-domain parameters most commonly used for the characterization of vagal control of heart function (Malik, 1996; Laborde et al., 2017). Repeated measures

TABLE 1 | Sleep characteristics of the two groups of participants on the days of the measurements.

					Comparisons	
	Workday		Free day		Workday	Free day
Time (hh:mm)	Lower SJL	Higher SJL	Lower SJL	Higher SJL	*p*	*p*
Bedtime	23:45 (00:52)	23:51 (00:49)	23:56 (00:48)	01:27 (00:52)	0.775	<0.0001
Sleep onset	23:57 (00:50)	00:03 (00:51)	00:09 (00:50)	01:36 (00:51)	0.713	<0.0001
Waking up	07:09 (00:39)	07:02 (00:28)	08:45 (01:09)	10:00 (01:40)	0.540	0.019
Sleep duration	07:13 (00:56)	06:59 (00:43)	08:35 (01:11)	08:25 (01:27)	0.433	0.706

Comparison of sleep timing and duration between groups with lower and higher SJL on workday and free day. Bedtime was indicated by entries of the sleep diary, whereas sleep onset and waking up were estimated by the Actiheart software and verified by diary data. Mean (SD), two-sample t-test, n = 17 and 16 for the group with lower and higher SJL, respectively.

TABLE 2 | HR and HRV data for the whole sleep period.

					Comparisons	
	Lower SJL		Higher SJL		Lower SJL	Higher SJL
	Workday	Free day	Workday	Free day	*p*	*p*
HR (1/min)	59.1 (2.1)	58.1 (1.3)	57.8 (1.8)	57.2 (2.1)	0.520	0.739
SDNN	86.8 (7.3)	95.1 (6.4)	91.5 (6.2)	102.2 (6.9)	0.088	0.018
RMSSD	61.1 (8.3)	64.9 (7.4)	64.1 (4.5)	72.8 (5.4)	0.422	0.092
pNN50	32.8 (5.1)	35.2 (4.3)	37.7 (3.6)	44.2 (3.9)	0.540	0.107

Mean HR and HRV data were averaged for the time period from sleep onset to waking up. Data for the workday and the free day were compared within both groups of participants. Mean (SEM), paired t-test, n = 17 and 14 for the group with lower and higher SJL, respectively.

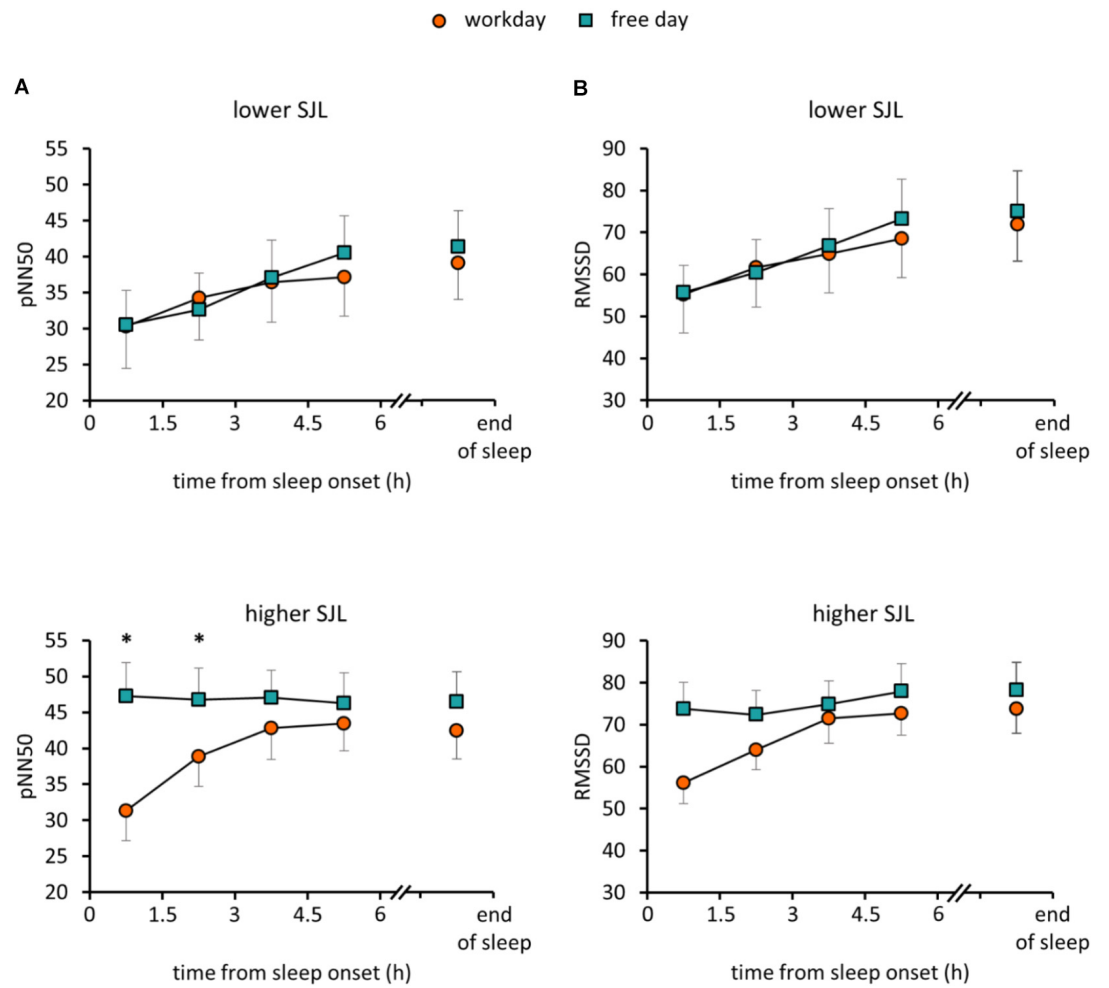

FIGURE 1 | HRV parameters in the course of sleep on workday and free day. PNN50 **(A)** and RMSSD **(B)** values were averaged for 1.5-h sleep blocks on workdays and free days for participants with lower (upper panels) and higher SJL (lower panels). The first four consecutive sleep blocks correspond to the first 6 h of sleep. The last sleep block, presented after an axis break, corresponds to the last 1.5 hour of sleep on the workday and the corresponding sleep segment (same time form sleep onset) on the free day. Analyses for the first 6 h of sleep: Repeated measures ANOVA with three levels (day, sleep block, group), *post hoc* Fisher test, $^*p < 0.05$; analyses for the last sleep block (after the axis break): paired *t*-test; $n = 15$ for the group with lower SJL and $n = 11$ for the group with higher SJL.

of ANOVA with three factors (group, day, and sleep block) revealed no significant effect of group or day, only sleep block showed significance among the main factors (**Supplementary Table S4**). Furthermore, a day × sleep block × group interaction was obtained ($p = 0.015$; $F(3,72) = 3.74$) for pNN50. While the HRV values nearly overlapped in the group with lower SJL, in the first two time blocks data of subjects with higher SJL showed intra-individual differences as their values were significantly lower on the workday than on the free day (**Figure 1A**) (higher SJL, workday, first block: 31.3 ± 4.1; second block: 38.9 ± 4.2; free day, first block: 47.3 ± 4.7, second block: 46.8 ± 4.4). *Post hoc* test did not reveal difference between the two groups in any sleep block. RMSSD showed a similar tendency, as values diverged in the first two blocks in the group with higher SJL, however, the interaction did not reach the level of significance [$p = 0.059$; $F(3,72) = 2.59$] (**Figure 1B**). To exclude that the HRV difference was counteracted by an opposite HRV difference after the sleep period previously analyzed (first 6 h), we performed a further analysis comparing the average HRV in the last 1.5 h of sleep on the workday and in the corresponding sleep segment (same time form sleep onset) on the free day (**Figures 1A,B**). However, the end-of-sleep HRV data did not display differences between workday and free day.

Next, we addressed the relationship between SJL and the HRV difference between the workday and the free day. Analyzing HRV parameters for the first 3 h, corresponding to the first two sleep blocks in **Figure 1**, a positive correlation between SJL and the free day-workday differences in pNN50 was obtained (Pearson's $r = 0.39$, $p = 0.033$, $n = 30$). When the analysis was restricted to the first 2 h, both RMSSD and pNN50 differences were positively correlated with SJL ($r = 0.365$, $p = 0.047$, $n = 30$ for RMSSD and $r = 0.4135$, $p = 0.023$, $n = 30$ for pNN50) (**Figure 2A**).

In the next analysis, we compared the beginning of sleep for a duration equal to the difference of sleep onset between the 2 days,

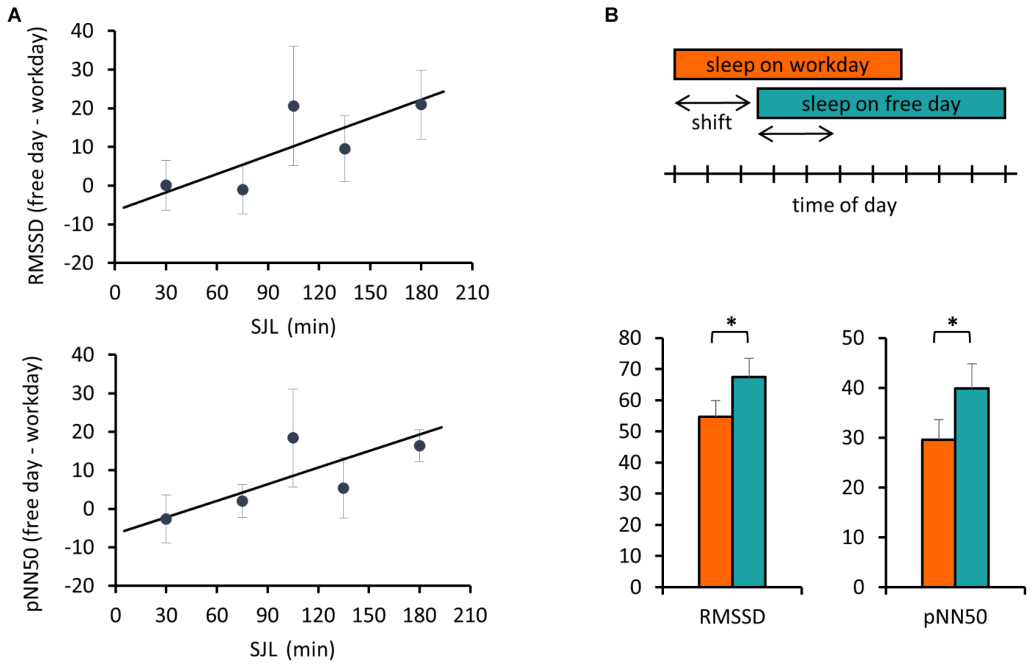

FIGURE 2 | Free day – workday differences in HRV during sleep are associated with SJL. **(A)** Correlation of SJL with the difference between free and workday values of RMSSD and pNN50. RMSSD and pNN50 values were averaged for the first 2 h of sleep. Individual free day – workday differences in RMSSD (upper panel) and pNN50 (lower panel) were calculated and correlated with SJL. For better visualization mean values for SJL intervals of either 30 or – in case of low sample number (first and last two intervals) – 60 min are shown. Trend lines for linear regression are shown (upper panel) Pearson's $r = 0.365$, $p = 0.047$, $n = 30$ and (lower panel) Pearson's $r = 0.4135$, $p = 0.023$, $n = 30$. **(B)** Advanced sleep timing on workday is related to a lower HRV. Schematic illustration of the analyzed sleep periods (indicated by the arrows) equal to the shift of sleep onset between work and free day. The boxes represent the time of day from sleep onset until waking (upper panel). RMSSD and pNN50 data were averaged for the shift periods and compared between work and free days (lower panel). Paired *t*-test, $^*p < 0.05$, $n = 18$.

referred as shift of sleep onset (**Figure 2B**). Data of all participants with more than 25 min shift were involved in this comparison. Both RMSSD and pNN50 parameters were significantly lower on the workday than on the free day (54.7 ± 5.3 and 67.5 ± 6.0, $p = 0.016$ for RMSSD, and 29.6 ± 4.1 and 39.8 ± 5.0, $p = 0.009$ for pNN50).

Frequency-Domain Analysis of HRV

To further characterize the HRV differences in the two groups of participants, frequency domain analyses were also performed. When the PSD of HRV was plotted for the first 2 h of sleep for the work and free day, the curves overlapped in the group with lower SJL, whereas they differed in the group with higher SJL (**Supplementary Figure S1**). We calculated the individual bin-wise free day – workday differences in the PSD. The difference was significant in several frequency ranges in subjects with higher SJL, but not in those with lower SJL (**Figure 3A**). The frequency band-based analysis of PSD showed that both LF [0.82 ± 0.02 and 0.85 ± 0.02 ($lnms^2$) on workday and free day, respectively, $p = 0.027$] and HF [1.45 ± 0.06 and 1.58 ± 0.06 ($lnms^2$) on workday and free day, respectively, $p = 0.031$], but not VLF [0.29 ± 0.01 and 0.30 ± 0.01 ($lnms^2$) on workday and free day, $p = 0.103$] bands were involved in the free day elevation of HRV of subjects with higher SJL (**Figure 3B**). In contrast, no differences between work and free day were found in the group with lower SJL [**Figure 3B**; VLF, 0.28 ± 0.01 and 0.29 ± 0.01; LF, 0.79 ± 0.02 and 0.81 ± 0.02; HF, 1.40 ± 0.07 and 1.43 ± 0.06 ($lnms^2$) on workday and free day, respectively]. To approach sympathetic modulation, normalized units of LF were also calculated. LFnu powers were relatively low as expected during sleep in healthy young people (Brandenberger et al., 2003; Stein and Pu, 2012). Workday and free day LFnu powers did not differ significantly in either group (**Figure 3B**).

Examination of the Association Between SJL and Subjective Sleep Quality

To assess sleep quality, we used the GSQS where a higher score indicates worse quality of sleep. We found that SJL was positively associated with the GSQS score on workday, whereas no association was obtained on the free day (**Supplementary Figure S2**). While participants in the group with lower SJL reported similar sleep quality for both days, participants with higher SJL had a significantly worse sleep quality on the workday than on the free day ($p = 0.027$) (**Figure 4**), and their workday scores were also significantly higher than those of the other group (two-sample *t*-test, $p = 0.043$).

DISCUSSION

To our knowledge, this is the first study indicating an interrelationship between SJL and the control of cardiac function.

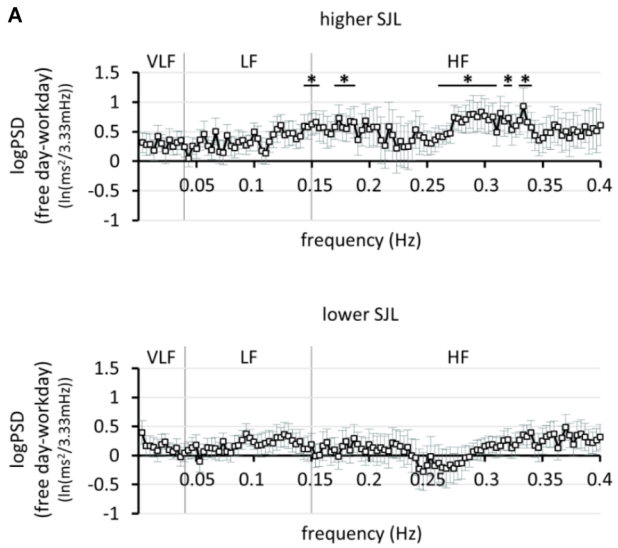

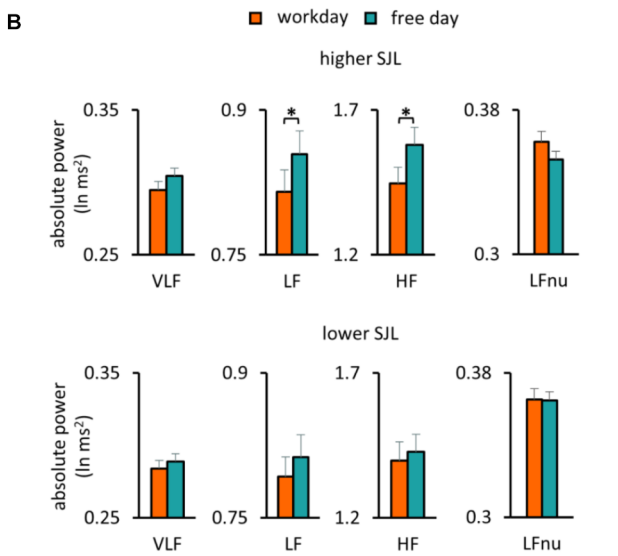

FIGURE 3 | Frequency analysis of HRV in the first 2 h of sleep. **(A)** The bin-wise differences in the power spectral density of HRV between free days and workdays in the group with higher (upper panel) and lower SJL (lower panel). One sample *t*-test, $*p < 0.05$ indicates above the chance power differences (multiple comparison corrected by the Descriptive Data Analysis protocol), $n = 13$ and 17 for the group with higher and lower SJL, respectively. **(B)** Powers of the standard frequency bands on work and free day in the group with higher (upper panel) and lower SJL (lower panel). Paired *t*-test, $*p < 0.05$, $n = 13$ and 17 for the group with higher and lower SJL, respectively.

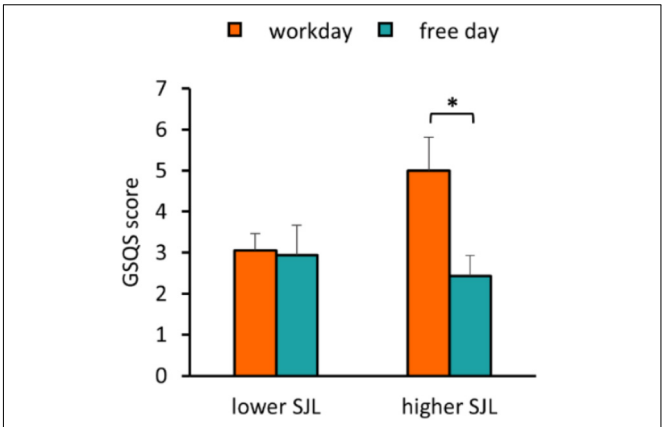

FIGURE 4 | Negative association of SJL with sleep quality. Average workday and free day GSQS scores of the participants in the groups with lower and higher SJL are shown. Paired *t*-test, $*p < 0.05$, $n = 17$ and 16 for the group with lower and higher SJL, respectively.

SJL affects most people in our society for shorter or longer periods throughout their life. As a strong and positive correlation between SJL and chronotype was found, and chronotype peaks between ages 20 and 26 years, SJL affects young adults most intensively (Wittmann et al., 2006). Therefore, for this field study we recruited male university students and addressed whether differences in sleep timing between workdays and free days show associations with sleep-related autonomic regulation and subjective sleep quality. Importantly, the measurements were performed in the participants' home environment and subjects kept their usual sleep schedules both on workdays and on free days. This was confirmed by the correlation of both chronotype (MSFsc) and SJL determined on the basis of the MCTQ (usual sleep timing) and the sleep diary (sleep timing in the study week).

We analyzed HRV, as it is a sensitive marker of the plasticity of the autonomic control of cardiac function. According to literature data, the baseline HRV can show high variations among healthy individuals and the source of these inter-individual differences is largely unclear (Goldberger et al., 2001). Beside the plasticity of autonomic control, other factors such as structural and functional properties of the brain were suggested to influence absolute HRV values (Thayer et al., 2012; Kumral et al., 2019). Therefore, intra-individual HRV changes may be more informative than inter-individual differences in absolute HRV values. Nevertheless, it is interesting to note, that in the group with higher SJL the average HRV was higher in both nights compared to the group with lower SJL. Larger sample and further investigations would be needed to analyze whether a higher HRV during sleep is characteristic for people with higher SJL and/or later chronotype.

When we examined individual changes in HRV between the workday and the free day, we found that in the first 3 h of sleep in the group with higher SJL both RMSSD and pNN50 were lower on workday than on free day. HRV parameters can display circadian variations (Hilton et al., 2000; Vandewalle et al., 2007; Scheer et al., 2009). As we had recordings from only 1/3rd of a day, we cannot assess the daily rhythm of HRV in our subjects. Nevertheless, it might be possible that in the group with higher SJL a decrease in HRV in later sleep segments leads to compensation of the high HRV observed in the first sleep blocks. However, in the end of sleep HRV showed no differences between the 2 days, suggesting that the HRV divergence in the first 3 h

of sleep was not counteracted in later sleep segments. A positive correlation between SJL and the free day-workday difference in various HRV parameters suggested that a higher SJL is associated with a larger increase of parasympathetic modulation from the workday to the free day. Results of the frequency-domain analysis were consistent with the time-domain data, as subjects with higher SJL showed different PSD of HRV on free day compared to workday, dominantly in higher frequency regions reflecting the vagal activity (Scholz et al., 1997; Montano et al., 2009; Laborde et al., 2017). Although the sleep duration of most participants was longer on free days than on workdays, this was not dependent on SJL, indicating that there were no differences in sleep deprivation during workdays between the groups of participants. Time spent awake, a main component of homeostatic sleep regulation, was also similar in the two groups. These data suggest that differences in the circadian rather than in the homeostatic sleep regulation are responsible for the workday-free day differences of HRV parameters in people with higher SJL. The apparent deviation of HRV parameters in the first two sleep blocks resulting in a different pattern of HRV in the course of sleep between workday and free day may reflect a difference in sleep structure. In this early period of workday's night, the biological clock of people with higher SJL (and later chronotype) may not promote sleep. However, the shift of sleep onset from the socially forced earlier time to the preferred later bedtime may cause a deeper sleep with greater vagal tone on free day's night compared to workday's night. A recent work showed that timing of sleep onset is associated with changes in the proportion of sleep stages (Akerstedt et al., 2018). In addition, the positive psychical effect of sleep timing without restrictions may also beneficially influence both the autonomic function and the sleep quality of participants with higher SJL.

Altogether, we suggest that SJL and the chronic changes in sleep timing cause a difference in vagal activity between work and free days' sleep and may affect the plasticity of cardiac regulation in the first few hours of sleep.

HRV parameters were found to reflect the functional properties of the cardiovascular system in both healthy populations and under pathological conditions. In young male subjects a positive correlation was obtained between vagal indices of HRV and endothelial functions (Pinter et al., 2012). Results of a recent meta-analysis based on eight studies with a total number of almost 22 000 subjects showed that low (but still normal) HRV in healthy populations, i.e., without known cardiovascular diseases, is associated with increased risk of a later cardiovascular event (Hillebrand et al., 2013). Moreover, autonomic dysregulation of the heart may contribute to hypertension (Schroeder et al., 2003), coronary artery calcification (Colhoun et al., 2001), arrhythmias, and congestive heart failure (Chen et al., 2014; Florea and Cohn, 2014; Fukuda et al., 2015).

As autonomic control and sleep regulation are interconnected, HRV can serve as an indicator of sleep quality as well. On the other hand, good subjective sleep quality *per se* is considered a marker of both healthy cardiovascular control and emotional wellbeing (Massar et al., 2017; Cespedes Feliciano et al., 2018). Our results based on the GSQS showed that SJL negatively impacts sleep quality on workdays. In a recent study using the Pittsburgh Sleep Quality Index (PSQI), Pilz et al. (2018) found that SJL mediates the effect of chronotype on the differences in sleep quality between workdays and free days. As GSQS and PSQI differ in both the items to be answered and the referred period (while the GSQS refers to the sleep quality of the previous night, the PSQI is an instrument assessing sleep quality over the last month), results of Pilz et al. (2018), and our data are complementary and together strongly indicate that SJL negatively impacts sleep quality on workdays.

Data from this study should be interpreted by considering some limitations. The sample size was relatively low. To exclude a possible effect of cycle-dependent changes in sexual hormones, only men were involved in this study. Therefore, it is possible that the interactions examined are characteristic only for men but not for women. Further studies may examine possible sex differences. In order to have a relative homogenous sample, only young adults were involved in the study. Impact of age on the associations found in our study could be the subject of future investigations.

In summary, we suggest that the chronic changes in sleep-wake patterns due to social constraints are associated with lessening of the restorative capacity of sleep on workdays. This is reflected by the differences of autonomic cardiac control between workdays and free days and the lower sleep quality during workday nights. In addition, our findings provide further support for the recent claim indicating that the cardiovascular system is particularly sensitive to circadian variation (Scheer et al., 2009; Janszky et al., 2012; Grimaldi et al., 2016).

Considering the very high prevalence of SJL in both the adolescent and the adult population, our findings together with literature data about the adverse health effects of SJL stress the requirement to develop social strategies for the reduction of SJL. Even small changes or more flexibility in school and work schedules may lessen the harmful effect of SJL. Due to shifting the phase of the circadian clock, daylight saving time (DST) also aggravates SJL and negatively affects health (Kantermann et al., 2007). Therefore, initiatives to abolish DST are currently under consideration. Individual strategies may also be important tools for the reduction of SJL. For example, increasing morning and decreasing evening light exposure can shift the biological clock to an earlier phase and thus lessen SJL. As meal acts as an effective *Zeitgeber*, appropriate meal timing could also help to adjust the body clock.

DATA AVAILABILITY

The datasets generated for this study are available on request to the corresponding author.

ETHICS STATEMENT

The studies involving human participants were reviewed and approved by the Semmelweis University Regional and Institutional Committee of Science and Research Ethics (Ethical approval 170/2016). The patients/participants provided their written informed consent to participate in this study.

AUTHOR CONTRIBUTIONS

KE and KK designed the study. ÁS and KE collected the data. ÁS, KE, and RB analyzed the data. KK, ÁS, KE, and RB wrote the manuscript and approved its final version.

FUNDING

This work was supported by the National Research, Development and Innovation Office – NKFIH (K115953) and the Higher Education Institutional Excellence Programme of the Ministry of Human Capacities in Hungary, within the framework of the FIKP programme of the Semmelweis University. KK, KE, and RB are Merit Scholars of the Semmelweis University.

ACKNOWLEDGMENTS

We thank Till Roenneberg, Norbert Gyöngyösi, and Anita Szőke for helpful comments on the manuscript. We also thank Barna Vásárhelyi for advising in 6-sulfatoxymelatonin measurements and reading of the manuscript. We are especially grateful to Bence Erdős for helping in data processing and critical reading of the manuscript and to Éva Szabó for statistical advice. We also thank Adrienn Kovács and Péter Soós for helping in subjects' recruitment.

SUPPLEMENTARY MATERIAL

The Supplementary Material for this article can be found online at: https://www.frontiersin.org/articles/10.3389/fnins.2019.00950/full#supplementary-material

REFERENCES

Abt, K. (1987). Descriptive data analysis: a concept between confirmatory and exploratory data analysis. *Methods Inf. Med.* 26, 77–88. doi: 10.1055/s-0038-1635488

Akerstedt, T., Hume, K., Minors, D., and Waterhouse, J. (1997). Good sleep–its timing and physiological sleep characteristics. *J. Sleep Res.* 6, 221–229. doi: 10.1111/j.1365-2869.1997.00221.x

Akerstedt, T., Lekander, M., Nilsonne, G., Tamm, S., D'Onofrio, P., Kecklund, G., et al. (2018). Effects of late-night short-sleep on in-home polysomnography: relation to adult age and sex. *J. Sleep Res.* 27:e12626. doi: 10.1111/jsr.12626

Barreira, T. K., Kang, M., Caputo, J. L., Farley, R. S., and Renfrow, M. S. (2009). Validation of the actiheart monitor for the measurement of physical activity. *Int. J. Exerc. Sci.* 2, 60–71.

Bertsch, K., Hagemann, D., Naumann, E., Schachinger, H., and Schulz, A. (2012). Stability of heart rate variability indices reflecting parasympathetic activity. *Psychophysiology* 49, 672–682. doi: 10.1111/j.1469-8986.2011.01341.x

Biggi, N., Consonni, D., Galluzzo, V., Sogliani, M., and Costa, G. (2008). Metabolic syndrome in permanent night workers. *Chronobiol. Int.* 25, 443–454. doi: 10.1080/07420520802114193

Brage, S., Brage, N., Franks, P. W., Ekelund, U., and Wareham, N. J. (2005). Reliability and validity of the combined heart rate and movement sensor Actiheart. *Eur. J. Clin. Nutr.* 59, 561–570. doi: 10.1038/sj.ejcn.1602118

Brandenberger, G., Viola, A. U., Ehrhart, J., Charloux, A., Geny, B., Piquard, F., et al. (2003). Age-related changes in cardiac autonomic control during sleep. *J. Sleep Res.* 12, 173–180. doi: 10.1046/j.1365-2869.2003.00353.x

Cespedes Feliciano, E. M., Quante, M., Rifas-Shiman, S. L., Redline, S., Oken, E., and Taveras, E. M. (2018). Objective sleep characteristics and cardiometabolic health in young adolescents. *Pediatrics* 142:e20174085. doi: 10.1542/peds.2017-4085

Chen, P. S., Chen, L. S., Fishbein, M. C., Lin, S. F., and Nattel, S. (2014). Role of the autonomic nervous system in atrial fibrillation: pathophysiology and therapy. *Circ. Res.* 114, 1500–1515. doi: 10.1161/CIRCRESAHA.114.303772

Chouchou, F., and Desseilles, M. (2014). Heart rate variability: a tool to explore the sleeping brain? *Front. Neurosci.* 8:402. doi: 10.3389/fnins.2014.00402

Colhoun, H. M., Francis, D. P., Rubens, M. B., Underwood, S. R., and Fuller, J. H. (2001). The association of heart-rate variability with cardiovascular risk factors and coronary artery calcification: a study in type 1 diabetic patients and the general population. *Diabetes Care* 24, 1108–1114. doi: 10.2337/diacare.24.6.1108

Diaz-Morales, J. F., and Escribano, C. (2015). Social jetlag, academic achievement and cognitive performance: understanding gender/sex differences. *Chronobiol. Int.* 32, 822–831. doi: 10.3109/07420528.2015.1041599

Elsenbruch, S., Harnish, M. J., and Orr, W. C. (1999). Heart rate variability during waking and sleep in healthy males and females. *Sleep* 22, 1067–1071. doi: 10.1093/sleep/22.8.1067

Florea, V. G., and Cohn, J. N. (2014). The autonomic nervous system and heart failure. *Circ. Res.* 114, 1815–1826. doi: 10.1161/CIRCRESAHA.114.302589

Fukuda, K., Kanazawa, H., Aizawa, Y., Ardell, J. L., and Shivkumar, K. (2015). Cardiac innervation and sudden cardiac death. *Circ. Res.* 116, 2005–2019. doi: 10.1161/CIRCRESAHA.116.304679

Goldberger, J. J., Challapalli, S., Tung, R., Parker, M. A., and Kadish, A. H. (2001). Relationship of heart rate variability to parasympathetic effect. *Circulation* 103, 1977–1983. doi: 10.1161/01.cir.103.15.1977

Grimaldi, D., Carter, J. R., Van Cauter, E., and Leproult, R. (2016). Adverse Impact of sleep restriction and circadian misalignment on autonomic function in healthy young adults. *Hypertension* 68, 243–250. doi: 10.1161/HYPERTENSIONAHA.115.06847

Haraszti, R. A., Ella, K., Gyongyosi, N., Roenneberg, T., and Kaldi, K. (2014). Social jetlag negatively correlates with academic performance in undergraduates. *Chronobiol. Int.* 31, 603–612. doi: 10.3109/07420528.2013.879164

Hillebrand, S., Gast, K. B., de Mutsert, R., Swenne, C. A., Jukema, J. W., Middeldorp, S., et al. (2013). Heart rate variability and first cardiovascular event in populations without known cardiovascular disease: meta-analysis and dose-response meta-regression. *Europace* 15, 742–749. doi: 10.1093/europace/eus341

Hilton, M. F., Umali, M. U., Czeisler, C. A., Wyatt, J. K., and Shea, S. A. (2000). Endogenous circadian control of the human autonomic nervous system. *Comput. Cardiol.* 27, 197–200.

Hulsegge, G., Gupta, N., Proper, K. I., van Lobenstein, N., IJzelenberg, W., Hallman, D. M., et al. (2018). Shift work is associated with reduced heart rate variability among men but not women. *Int. J. Cardiol.* 258, 109–114. doi: 10.1016/j.ijcard.2018.01.089

Janszky, I., Ahnve, S., Ljung, R., Mukamal, K. J., Gautam, S., Wallentin, L., et al. (2012). Daylight saving time shifts and incidence of acute myocardial infarction–swedish register of information and knowledge about swedish heart intensive care admissions (RIKS-HIA). *Sleep Med.* 13, 237–242. doi: 10.1016/j.sleep.2011.07.019

Kantermann, T., Juda, M., Merrow, M., and Roenneberg, T. (2007). The human circadian clock's seasonal adjustment is disrupted by daylight saving time. *Curr. Biol.* 17, 1996–2000. doi: 10.1016/j.cub.2007.10.025

Kaufmann, T., Sutterlin, S., Schulz, S. M., and Vogele, C. (2011). ARTiiFACT: a tool for heart rate artifact processing and heart rate variability analysis. *Behav. Res. Methods* 43, 1161–1170. doi: 10.3758/s13428-011-0107-7

Knutsson, A. (2003). Health disorders of shift workers. *Occup. Med.* 53, 103–108. doi: 10.1093/occmed/kqg048

Koopman, A. D. M., Rauh, S. P., van 't Riet, E., Groeneveld, L., van der Heijden, A. A., Elders, P. J., et al. (2017). The association between social jetlag, the metabolic syndrome, and type 2 diabetes mellitus in the general population: the new hoorn study. *J. Biol. Rhythms* 32, 359–368. doi: 10.1177/0748730417713572

Kristiansen, J., Korshoj, M., Skotte, J. H., Jespersen, T., Sogaard, K., Mortensen, O. S., et al. (2011). Comparison of two systems for long-term heart rate

variability monitoring in free-living conditions–a pilot study. *Biomed. Eng. Online* 10:27. doi: 10.1186/1475-925X-10-27

Kumral, D., Schaare, H. L., Beyer, F., Reinelt, J., Uhlig, M., Liem, F., et al. (2019). The age-dependent relationship between resting heart rate variability and functional brain connectivity. *Neuroimage* 185, 521–533. doi: 10.1016/j.neuroimage.2018.10.027

Laborde, S., Mosley, E., and Thayer, J. F. (2017). Heart rate variability and cardiac vagal tone in psychophysiological research - recommendations for experiment planning, data analysis, and data reporting. *Front. Psychol.* 8:213. doi: 10.3389/fpsyg.2017.00213

Larsen, P. D., Tzeng, Y. C., Sin, P. Y., and Galletly, D. C. (2010). Respiratory sinus arrhythmia in conscious humans during spontaneous respiration. *Respir. Physiol. Neurobiol.* 174, 111–118. doi: 10.1016/j.resp.2010.04.021

Levandovski, R., Dantas, G., Fernandes, L. C., Caumo, W., Torres, I., Roenneberg, T., et al. (2011). Depression scores associate with chronotype and social jetlag in a rural population. *Chronobiol. Int.* 28, 771–778. doi: 10.3109/07420528.2011.602445

Malik, M. (1996). Heart rate variability: standards of measurement, physiological interpretation and clinical use. Task force of the european society of cardiology and the north american society of pacing and electrophysiology. *Circulation* 93, 1043–1065. doi: 10.1161/01.cir.93.5.1043

Massar, S. A. A., Liu, J. C. J., Mohammad, N. B., and Chee, M. W. L. (2017). Poor habitual sleep efficiency is associated with increased cardiovascular and cortisol stress reactivity in men. *Psychoneuroendocrinology* 81, 151–156. doi: 10.1016/j.psyneuen.2017.04.013

Meijman, T. F., de Vries-Griever, A. H., and de Vries, G. (1988). *The evaluation of the Groningen Sleep Quality Scale*. Groningen: Heymans Bulletin (HB 88-13-EX).

Montano, N., Porta, A., Cogliati, C., Costantino, G., Tobaldini, E., Casali, K. R., et al. (2009). Heart rate variability explored in the frequency domain: a tool to investigate the link between heart and behavior. *Neurosci. Biobehav. Rev.* 33, 71–80. doi: 10.1016/j.neubiorev.2008.07.006

Morris, C. J., Purvis, T. E., Hu, K., and Scheer, F. A. (2016). Circadian misalignment increases cardiovascular disease risk factors in humans. *Proc. Natl. Acad. Sci. U.S.A.* 113, E1402–E1411. doi: 10.1073/pnas.1516953113

Morris, C. J., Purvis, T. E., Mistretta, J., Hu, K., and Scheer, F. (2017). Circadian misalignment increases C-Reactive protein and blood pressure in chronic shift workers. *J. Biol. Rhythms* 32, 154–164. doi: 10.1177/0748730417697537

Papantoniou, K., Devore, E. E., Massa, J., Strohmaier, S., Vetter, C., Yang, L., et al. (2018). Rotating night shift work and colorectal cancer risk in the nurses' health studies. *Int. J. Cancer* 143, 2709–2717. doi: 10.1002/ijc.31655

Parsons, M. J., Moffitt, T. E., Gregory, A. M., Goldman-Mellor, S., Nolan, P. M., Poulton, R., et al. (2015). Social jetlag, obesity and metabolic disorder: investigation in a cohort study. *Int. J. Obes.* 39, 842–848. doi: 10.1038/ijo.2014.201

Pilz, L. K., Keller, L. K., Lenssen, D., and Roenneberg, T. (2018). Time to rethink sleep quality: PSQI scores reflect sleep quality on workdays. *Sleep* 41:zsy029. doi: 10.1093/sleep/zsy029

Pinter, A., Horvath, T., Sarkozi, A., and Kollai, M. (2012). Relationship between heart rate variability and endothelial function in healthy subjects. *Auton. Neurosci.* 169, 107–112. doi: 10.1016/j.autneu.2012.05.005

Puttonen, S., Harma, M., and Hublin, C. (2010). Shift work and cardiovascular disease - pathways from circadian stress to morbidity. *Scand. J. Work Environ. Health* 36, 96–108. doi: 10.5271/sjweh.2894

Roenneberg, T., Allebrandt, K. V., Merrow, M., and Vetter, C. (2012). Social jetlag and obesity. *Curr. Biol.* 22, 939–943. doi: 10.1016/j.cub.2012.03.038

Roenneberg, T., Wirz-Justice, A., and Merrow, M. (2003). Life between clocks: daily temporal patterns of human chronotypes. *J. Biol. Rhythms* 18, 80–90. doi: 10.1177/0748730402239679

Rutters, F., Lemmens, S. G., Adam, T. C., Bremmer, M. A., Elders, P. J., Nijpels, G., et al. (2014). Is social jetlag associated with an adverse endocrine, behavioral, and cardiovascular risk profile? *J. Biol. Rhythms* 29, 377–383. doi: 10.1177/0748730414550199

Scheer, F. A., Hilton, M. F., Mantzoros, C. S., and Shea, S. A. (2009). Adverse metabolic and cardiovascular consequences of circadian misalignment. *Proc. Natl. Acad. Sci. U.S.A.* 106, 4453–4458. doi: 10.1073/pnas.0808180106

Schernhammer, E. S., Kroenke, C. H., Laden, F., and Hankinson, S. E. (2006). Night work and risk of breast cancer. *Epidemiology* 17, 108–111.

Scholz, U. J., Bianchi, A. M., Cerutti, S., and Kubicki, S. (1997). Vegetative background of sleep: spectral analysis of the heart rate variability. *Physiol. Behav.* 62, 1037–1043. doi: 10.1016/s0031-9384(97)00234-5

Schroeder, E. B., Liao, D., Chambless, L. E., Prineas, R. J., Evans, G. W., and Heiss, G. (2003). Hypertension, blood pressure, and heart rate variability: the atherosclerosis risk in communities (ARIC) study. *Hypertension* 42, 1106–1111. doi: 10.1161/01.HYP.0000100444.71069.73

Shields, M. (2002). Shift work and health. *Health Rep.* 13, 11–33.

Simor, P., Koteles, F., Bodizs, R., and Bardos, G. (2009). A questionnaire based study of subjective sleep quality: the psychometric evaluation of the Hungarian version of the groningen sleep quality scale. *Mentálhigiéné és Pszichoszomatika* 10, 249–261. doi: 10.1556/mental.10.2009.3.5

Stein, P. K., and Pu, Y. (2012). Heart rate variability, sleep and sleep disorders. *Sleep Med. Rev.* 16, 47–66. doi: 10.1016/j.smrv.2011.02.005

Strohmaier, S., Devore, E. E., Zhang, Y., and Schernhammer, E. S. (2018). A review of data of findings on night shift work and the development of DM and CVD events: a synthesis of the proposed molecular mechanisms. *Curr. Diab. Rep.* 18:132. doi: 10.1007/s11892-018-1102-5

Thayer, J. F., Ahs, F., Fredrikson, M., Sollers, J. J. III, and Wager, T. D. (2012). A meta-analysis of heart rate variability and neuroimaging studies: implications for heart rate variability as a marker of stress and health. *Neurosci. Biobehav. Rev.* 36, 747–756. doi: 10.1016/j.neubiorev.2011.11.009

Thayer, J. F., Yamamoto, S. S., and Brosschot, J. F. (2010). The relationship of autonomic imbalance, heart rate variability and cardiovascular disease risk factors. *Int. J. Cardiol.* 141, 122–131. doi: 10.1016/j.ijcard.2009.09.543

Tobaldini, E., Nobili, L., Strada, S., Casali, K. R., Braghiroli, A., and Montano, N. (2013). Heart rate variability in normal and pathological sleep. *Front. Physiol.* 4:294. doi: 10.3389/fphys.2013.00294

Trinder, J., Kleiman, J., Carrington, M., Smith, S., Breen, S., Tan, N., et al. (2001). Autonomic activity during human sleep as a function of time and sleep stage. *J. Sleep Res.* 10, 253–264. doi: 10.1046/j.1365-2869.2001.00263.x

Vandewalle, G., Middleton, B., Rajaratnam, S. M., Stone, B. M., Thorleifsdottir, B., Arendt, J., et al. (2007). Robust circadian rhythm in heart rate and its variability: influence of exogenous melatonin and photoperiod. *J. Sleep Res.* 16, 148–155. doi: 10.1111/j.1365-2869.2007.00581.x

Vetter, C., Devore, E. E., Ramin, C. A., Speizer, F. E., Willett, W. C., and Schernhammer, E. S. (2015). Mismatch of sleep and work timing and risk of Type 2 diabetes. *Diabetes Care* 38, 1707–1713. doi: 10.2337/dc15-0302

Vetter, C., Devore, E. E., Wegrzyn, L. R., Massa, J., Speizer, F. E., Kawachi, I., et al. (2016). Association between rotating night shift work and risk of coronary heart disease among women. *JAMA* 315, 1726–1734. doi: 10.1001/jama.2016.4454

Wittmann, M., Dinich, J., Merrow, M., and Roenneberg, T. (2006). Social jetlag: misalignment of biological and social time. *Chronobiol. Int.* 23, 497–509. doi: 10.1080/07420520500545979

Wong, P. M., Hasler, B. P., Kamarck, T. W., Muldoon, M. F., and Manuck, S. B. (2015). Social jetlag, chronotype, and cardiometabolic risk. *J. Clin. Endocrinol. Metab.* 100, 4612–4620. doi: 10.1210/jc.2015-2923

Conflict of Interest Statement: The authors declare that the research was conducted in the absence of any commercial or financial relationships that could be construed as a potential conflict of interest.

frontiers in Neuroscience

ORIGINAL RESEARCH
published: 10 September 2019
doi: 10.3389/fnins.2019.00955

Colonic Motility and Jejunal Vagal Afferent Firing Rates Are Decreased in Aged Adult Male Mice and Can Be Restored by an Aminosterol

Christine L. West[1,2], Jessica Y. Amin[1], Sohana Farhin[1], Andrew M. Stanisz[1], Yu-Kang Mao[1] and Wolfgang A. Kunze[1,2,3]*

[1] St. Joseph's Healthcare, The Brain-Body Institute, McMaster University, Hamilton, ON, Canada, [2] Department of Biology, McMaster University, Hamilton, ON, Canada, [3] Department of Psychiatry and Behavioural Neurosciences, McMaster University, Hamilton, ON, Canada

There is a general decline in gastrointestinal function in old age including decreased intestinal motility, sensory signaling, and afferent sensitivity. There is also increased prevalence of significant constipation in aged populations. We hypothesized this may be linked to reduced colonic motility and alterations in vagal-gut-brain sensory signaling. Using *in vitro* preparations from young (3 months) and old (18–24 months) male CD1 mice we report functional age-related differences in colonic motility and jejunal mesenteric afferent firing. Furthermore, we tested the effect of the aminosterol squalamine on colonic motility and jejunal vagal firing rate. Old mice had significantly reduced velocity of colonic migrating motor complexes (MMC) by 27% compared to young mice ($p = 0.0161$). Intraluminal squalamine increased colonic MMC velocity by 31% in old mice ($p = 0.0150$), which also had significantly reduced mesenteric afferent single-unit firing rates from the jejunum by 51% ($p < 0.0001$). The jejunal vagal afferent firing rate was reduced in aged mice by 62% ($p = 0.0004$). While the time to peak response to squalamine was longer in old mice compared to young mice (18.82 ± 1.37 min vs. 12.95 ± 0.99 min; $p = 0.0182$), it significantly increased vagal afferent firing rate by 36 and 56% in young and old mice, respectively ($p = 0.0006$, $p = 0.0013$). Our results show for the first time that the jejunal vagal afferent firing rate is reduced in aged-mice. They also suggest that there is translational potential for the therapeutic use of squalamine in the treatment of age-related constipation and dysmotility.

Keywords: aging, vagal afferent, motility, constipation, squalamine

OPEN ACCESS

Edited by:
Nick Spencer,
Flinders University, Australia

Reviewed by:
Jing Feng,
Washington University Medical Center, United States
Guillaume De Lartigue,
University of Florida, United States

****Correspondence:***
Christine L. West
westcl2@mcmaster.ca;
westcl294@gmail.com

Specialty section:
This article was submitted to Autonomic Neuroscience, a section of the journal Frontiers in Neuroscience

Received: *04 June 2019*
Accepted: *23 August 2019*
Published: *10 September 2019*

Citation:
West CL, Amin JY, Farhin S, Stanisz AM, Mao Y-K and Kunze WA (2019) Colonic Motility and Jejunal Vagal Afferent Firing Rates Are Decreased in Aged Adult Male Mice and Can Be Restored by an Aminosterol. Front. Neurosci. 13:955. doi: 10.3389/fnins.2019.00955

INTRODUCTION

Old age is associated with increased incidence of chronic constipation, which increases in prevalence with age (Higgins and Johanson, 2004; De Giorgio et al., 2015; Ranson and Saffrey, 2015). In addition, aging is also associated with behavioral depression (Malatynska et al., 2012). Age-related changes in the gut and gut to brain nervous signaling via the vagus nerve may underlie many of these problems in the geriatric age group, although psychosocial and economic factors may

play a role (Strawbridge et al., 1996). Old animals show delayed gastric emptying, slowed colonic transit and reduced fecal output (Smits and Lefebvre, 1996). For example, 2-year-old mice deliver fewer fecal pellets than 3-month-old ones, and when epoxy coated pellets are introduced into the colon of old mice they move with decreased velocity in the oral to anal direction (Patel et al., 2012).

Whether age-related changes in intestinal propulsion are due to alterations of smooth muscle function or cells that coordinate or pace contractions such as neurons or interstitial cells of Cajal (ICC), is unclear (Saffrey, 2014). However, while reductions in the number of ICC and enteric glial cells have been reported in the aged gut (Saffrey, 2014) the enteric nervous system (ENS) is also vulnerable to age-related damage. Generation and propagation of colonic migrating motor complexes (CMMCs) in mice are generated by activity of the ENS (Fida et al., 1997; Roberts et al., 2007; Spencer et al., 2018), recorded *in vitro* (Wang et al., 2010a,b; Wu et al., 2013) and are absent if the ENS is missing or destroyed as in Hirschsprung's or Chagas' diseases (Furness, 2006, p. 157). Indeed peristalsis, but not ICC dependent slow wave related contractions, is abolished by tetrodotoxin (Wu et al., 2013; Delungahawatta et al., 2017). In fact, neurogenic migrating motor complexes still occur in mutant mice lacking pacemaker-type ICC and slow waves in the small intestine (Spencer et al., 2003).

The myenteric plexus of the ENS is essential for normal MMCs to occur in the colon (Fida et al., 1997; Roberts et al., 2007; Wang et al., 2010b; Spencer et al., 2016, 2018). Intrinsic primary afferent neurons (IPANs) represent the class of myenteric neurons most affected by degenerative changes in old age (Wade, 2002; Wade and Cowen, 2004) and MMCs are absent if they are selectively silenced (Howe et al., 2006). However, the ENS appears to be more susceptible to age-related degeneration than other nervous systems (Saffrey, 2013). While some animal studies suggest that there may be reductions in the number of myenteric neurons in old age (El-Salhy et al., 1999; Phillips et al., 2004; Phillips and Powley, 2007; Zanesco and Souza, 2011), it is probable that myenteric neuron numbers are actually maintained, but an increasing proportion show structural degenerative changes with increasing old age (Gamage et al., 2013; Saffrey, 2013).

We are not aware of extant data on age-related functional changes in vagal nerves, but vagal afferents in aged rats have swollen varicosities in fibers innervating the myenteric plexus, smooth muscle and mucosa (Phillips and Powley, 2007). There is no information available whether there is an actual decrease in the number of vagal fiber endings supplying the myenteric plexus. However, dystrophic changes including dilations and swellings of the intraganglionic laminar endings (IGLEs) in the NIH Fisher 344 rat model of aging have been described and the extent of the terminal arbors is also reduced compared to young rats (Phillips et al., 2010). A previous study showed that aged mice had attenuated colonic and jejunal afferent mechanosensitivity and suggested that the loss or decrease of this sensory innervation or sensitivity may be linked to the reduced awareness of constipation in the elderly (Keating et al., 2015).

In the present paper we report the effects of old age on colon motility and jejunal vagal afferent firing using *in vitro* preparations from male CD1 mice. Squalamine is a prokinetic aminosterol originally synthesized by the liver of the dogfish shark (Zasloff et al., 2011), and it has previously been shown to stimulate colonic motility in a 1-year-old mouse and loperamide model (Kunze et al., 2014). Here we explore in detail the effects of old age (2-year) on colon motility and constitutive vagal afferent firing rates from the jejunum, and whether these functions might be restored to youthful levels by the aminosterol squalamine.

MATERIALS AND METHODS

Animals

Young (3 months) and old (18–24 months; retired breeder) male CD-1 mice from Charles River Laboratories (Quebec, Canada) were used for all portions of the study. Experiments were performed *in vitro* following cervical dislocation in accordance with the Animal Research Ethics Board (AREB) of McMaster University (permit 16-08-30). Mice were housed on a 12-hour light/dark cycle, food and water were provided *ad libitum*, and mice were allowed 1-week acclimatization following arrival. In view of the current debate about sex differences in mammalian nervous systems (O'Connor and Cryan, 2014), we plan to conduct future studies with female CD1 mice when these become available after an 18–24-month aging period.

Colonic Motility

The colonic motility recordings were performed as described previously (West et al., 2017). The whole colon was extracted from young (3 months) and old (18–24 months) mice, flushed with Krebs, and cannulated with silicon tubing at the oral and anal ends within a heated, Krebs-filled tissue flotation bath. Krebs was prepared with the following concentrations (mmol L^{-1}): 118 NaCl, 4.8 KCl, 25 $NaHCO_3$, 1.0 NaH_2PO_4, 1.2 $MgSO_4$, 11.1 glucose, and 2.5 $CaCl_2$, bubbled with carbogen gas (95% O_2 and 5% CO_2) and heated to 37°C (Wu et al., 2013). The inflow (oral end) and outflow (anal end) tubes were adjusted in height to create an intraluminal pressure difference of 2–3 hPa during perfusion of the lumen. Gravity-evoked contractions were recorded by a Microsoft Lifecam 3000 web camera positioned 8 cm above the tissue. The serosal compartment of the bath was constantly perfused with fresh oxygenated Krebs. Squalamine (10 μM) was applied luminally by opening and closing the stopcocks of the Mariotte tubes at the oral end [see Figure in Wu et al. (2013)].

Intestinal contractions were recorded during a 20 min Krebs control and 20 min treatment period. Spatiotemporal diameter maps were developed from the motility video recordings as described previously (Wu et al., 2013; West et al., 2017). Alternating dark and light bands indicate contraction and relaxation along the gut representing migrating motor complexes (MMCs). MMC velocity was measured as the slope of the large dark contractions. MMC frequencies were determined by measuring the number of MMCs over a given time interval and amplitude was measured as a function of the gut diameter at peak contractions.

Mesenteric Nerve Recordings

The mesenteric nerve bundle is a mixed nerve containing populations of vagal and spinal fibers (Perez-Burgos et al., 2013). Jejunal mesenteric nerve recordings were performed as described previously (Perez-Burgos et al., 2013). A 2–3 cm segment of mouse jejunum with attached mesentery was excised and mounted on an agar-coated petri dish filled with oxygenated Krebs buffer and nicardipine (3 μM) to paralyze smooth muscle. The oral and anal ends of the tissue were cannulated with silicon tubing and the luminal contents were flushed using Krebs. The remaining mesentery was pinned out and the mesenteric nerve bundle was dissected using fine-tipped forceps. The petri dish was then mounted on an inverted microscope and the nerve bundle was sucked onto with a glass micropipette attached to a microelectrode. The nerve preparation was continuously perfused with fresh oxygenated Krebs in the serosal compartment using a pump. Multi-unit electrical activity was recorded using a Multi-Clamp 700B amplifier and Digidata 1440A signal converter (Perez-Burgos et al., 2013). Control periods were recorded for 15–30 min during luminal Krebs perfusion. Intraluminal squalamine (10 μM) was perfused following the control (Krebs) for a duration of 30 min. Cholecystokinin (CCK) was applied 10 min after the cessation of treatment and Krebs washout to allow for identification of vagal fibers during *post hoc* computer analysis as vagal fibers respond potently to CCK, while spinal fibers do not (Richards et al., 1996; Hillsley and Grundy, 1998). Lastly, $5HT_3$ agonist was applied as it activates a small population of vagal afferent fibers not activated by CCK (Hillsley and Grundy, 1998) and a 37 hPa distention for 1 min tested response to painful distention or a high-threshold stimulus (Perez-Burgos et al., 2015).

Multi-unit electrical activity was analyzed for single-unit activity using principle component analysis (PCA) and spike waveform analysis in the DataView program (Heitler, 2007). Each single-unit fiber has a unique action potential spike that is distinguished from other single fibers by its shape, size and duration (Heitler, 2007; Perez-Burgos et al., 2013). Once sorted into single-units, vagal fibers were identified by response to CCK, as described previously. Single-unit vagal activity was gated for control and treatment periods and the mean interval between spike firing (the inverse of firing frequency) was measured. Decreases in the interspike interval are described as increased afferent firing rate and vice versa.

Statistics

Researchers were not blinded to experimental groups (young vs. old mice). Percent difference was calculated by (treatment-control)/control for paired before and after treatment or (old-young)/young for age comparisons. Data are presented as mean ± SEM. *N* represents number of mice. Where multiple afferent fibers are measured from one animal, *N* is represented as *N* = # of mice (# of fibers). Statistical comparisons were performed using paired or unpaired, two-tailed *t*-tests using GraphPad Prism software (Version 7.0). Any outliers were identified or removed using Grubbs' test (α = 0.05) or the ROUT Method (*Q* = 1%).

RESULTS

Colonic Contractile Motility Is Reduced in Aged Mice

Colonic contractile motility was assessed in a total of 32 male CD1 mice; 22 old mice (18–24+ months) and 10 young mice (3 months). The whole length of the colon was excised and the colonic MMCs were video recorded in our gut motility apparatus during Krebs luminal perfusion for later measurements of MMC velocity, frequency and amplitude. Means for MMC velocity in old CD-1 mice during Krebs control were significantly reduced compared to young mice controls. Mean MMC velocity in old mice controls was 0.948 ± 0.09 mm/s, 27% slower than young mice controls, 1.31 ± 0.10 mm/s (p = 0.0161) (**Figure 1A**). MMC frequency and amplitude were not significantly affected by age. Mean frequency was 7.2% smaller in old mice controls (0.007 ± 0.001 Hz) compared to young mice controls, 0.008 ± 0.001 Hz (p = 0.5639) (**Figure 1B**). Mean MMC amplitude in old mice was 0.601 ± 0.062 cm, 4.4% smaller than for young mice, 0.628 ± 0.116 cm (p = 0.8356) (**Figure 1C**). Based on these findings there was a reduction in contractility with age in the colon, with the greatest effect being a reduction in MMC velocity.

Squalamine Restores Colon Motility in Aged Mice

Squalamine (10 μM) was added *in vitro* to the lumen of colon segments taken from old mice (N = 9), following a 20-minute period of control recording with only Krebs in the lumen. Changes to MMC parameters before and after adding squalamine were measured from spatiotemporal maps. Intraluminal squalamine significantly increased mean velocity by 31% from 0.99 ± 0.06 mm/s during Krebs control to 1.3 ± 0.11 mm/s (p = 0.0150) (**Figure 2A**). Intraluminal squalamine increased frequency 26% from 0.007 ± 0.001 to 0.009 ± 0.001 Hz (p = 0.1964), but not within statistical significance (**Figure 2B**). Amplitude was significantly increased 65% from 0.50 ± 0.07 to 0.83 ± 0.15 mm (p = 0.0100) (**Figure 2C**). Spatiotemporal heat maps of MMCs demonstrate a loss of contractile motility and regularity in old (**Figure 2E**) compared to a young mouse (**Figure 2D**). Propulsive contractility was restored in the old mice following application of intraluminal squalamine (**Figure 2F**).

Single-Unit Firing From the Mesenteric Afferent Nerve Bundle Is Reduced in Aged Mice

Baseline multiunit mesenteric nerve afferent firing in old (N = 9) or young mice (N = 10) was measured to determine the effect of aging on afferent discharge, *in vitro*. Afferent firing was measured as mean interspike intervals, in which a decrease in the mean interval between spikes indicates an increase in the firing frequency of the fiber. The multiunit interspike interval of 81.9 ± 19.4 ms for old mice was 55% longer than that for young mice (52.9 ± 6.72 ms) but did not reach statistical significance

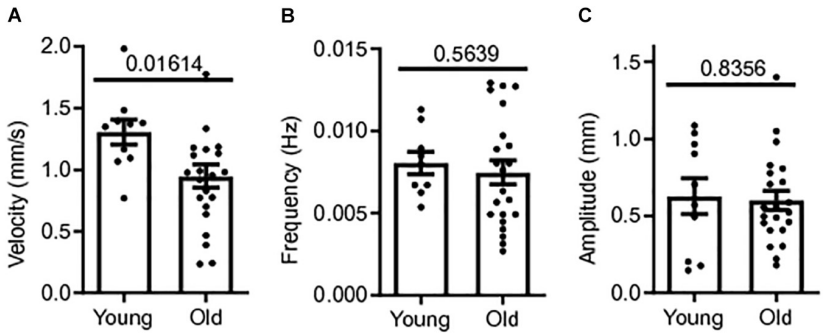

FIGURE 1 | Colonic contractile motility is reduced in aged mice. **(A)** Sample MMC velocity was decreased in old mice (N = 22) compared to young mice controls (N = 10). **(B)** Sample MMC frequency in old mice compared to young mice controls. **(C)** Sample MMC amplitude in old mice compared to young mice controls. Data represented as mean with SEM, t-test unpaired, two-tailed, with Welch's correction.

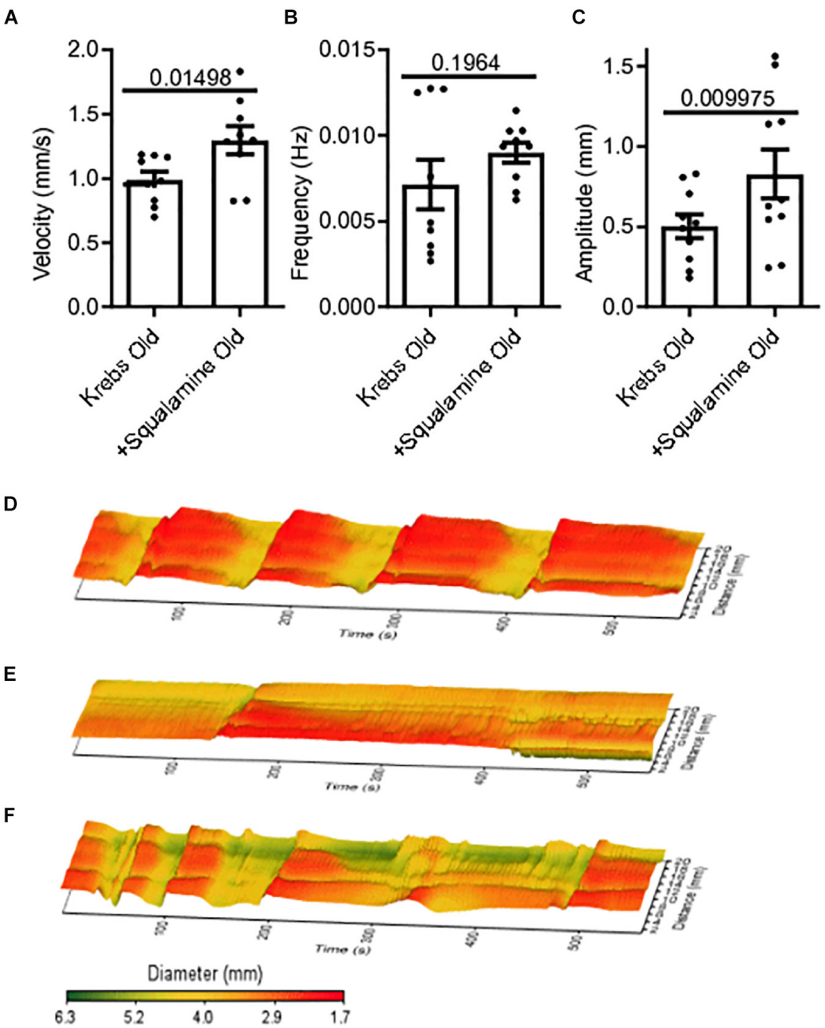

FIGURE 2 | Reduced colonic motor activity could be partially restored by intraluminal application of the aminosterol squalamine. **(A)** Intraluminal squalamine (10 μM) increased sample colonic MMC velocity in aged mice (N = 10). **(B)** Intraluminal squalamine and colonic MMC frequency in aged mice. **(C)** Intraluminal squalamine increased colonic MMC amplitude in aged mice. 3D spatiotemporal heat maps display MMC contractions over time (x-axis) and distance (y-axis). Areas of contraction or small diameter are red, while areas of relaxation or larger diameter are yellow to green for **(D)** a young mouse during Krebs control, **(E)** an old mouse during Krebs control, and **(F)** an old mouse after intraluminal treatment with squalamine. Data represented as mean with SEM, paired t-tests, two-tailed.

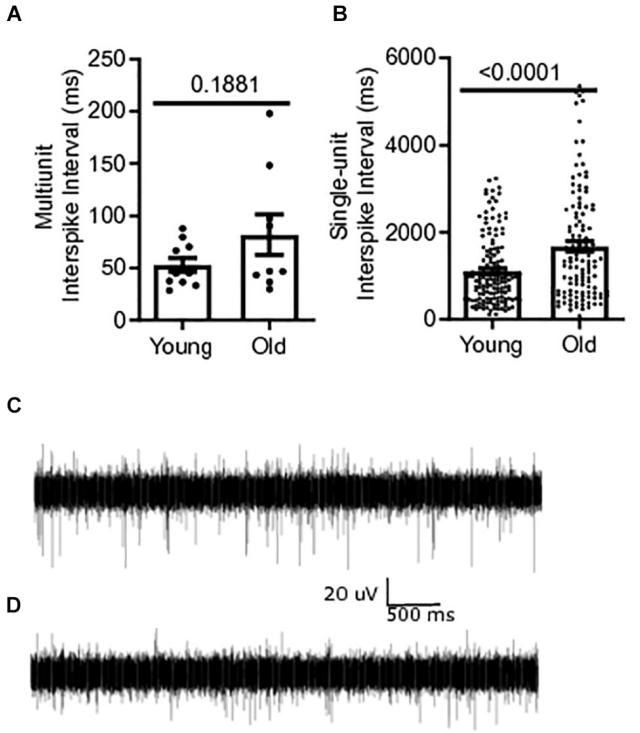

FIGURE 3 | Mesenteric single-unit afferent sensory signaling is decreased in aged mice. **(A)** Multi-unit mesenteric afferent firing from the mesenteric nerve in old mice compared to young mice (N = 10 mice). **(B)** Single-unit mesenteric afferent firing from the mesenteric nerve had longer interspike intervals, indicating decreased afferent firing in old mice (N = 121 and 149 fibers). **(C)** Representative traces of mesenteric afferent firing for young mice, and **(D)** mesenteric afferent firing for old mice. Data represented as mean with SEM, t-test unpaired, two-tailed, with Welch's correction.

(P = 0.1881) (**Figure 3A**). Single-unit firing from individual afferent fibers in the mesenteric nerve bundle was identified from multi-unit recordings using DataView as described in the section "Materials and Methods" (Heitler, 2007). The mean interspike interval from all single-unit fibers was 51% longer in old mice, 1676 ± 117.8 ms [N = 9(121)], compared to young mice, 1111 ± 63.36 ms [N = 10(149)], (P < 0.0001) (**Figure 3B**). A representative trace of multi-unit afferent firing from a young mouse is shown in **Figure 3C**. **Figure 3D** shows the same obtained using an old mouse.

Single Vagal Fiber Firing Rate Is Decreased in Aged Mice but Can Be Rescued by Squalamine

Single-unit afferents within the multiunit mesenteric nerve bundle recordings were identified as vagal afferents based on their response to CCK, which selectively stimulates vagal fibers (Grundy et al., 1998). Single unit vagal afferent firing rate was assessed from the mesenteric nerve bundle of the jejunum of young and old mice. Mean vagal single unit interspike intervals were 62% longer for old mice, 1886 ± 176.9 ms [N = 10(65)], compared to young mice, 1166 ± 86.22 ms [N = 9(83)], (p = 0.0004) (**Figure 4A**).

The ability of squalamine to stimulate vagal fibers was first tested in young mice. Squalamine (10 μM) decreased the mean intervals between vagal spikes by 36% from 1118 ± 117 ms to 718 ± 45.2 ms in young mice [N = 3(38), p = 0.0006)] (**Figure 4B**). We then tested whether squalamine could increase the vagal firing rate recorded from the *in vitro* mesenteric nerve preparation taken from old mice. For old mice intraluminal squalamine (10 μM) decreased the mean interval between vagal spikes by 56% from 2509 ± 396 ms to 1093 ± 105 ms [N = 4(22), p = 0.0013] (**Figure 4C**). Thus, the reduction in vagal afferent firing for old mice was at least partially reversed by intraluminal squalamine, and squalamine increased vagal firing rate in old mice more strongly than in young mice, 56 vs. 36% increases over the resting firing rates recorded with only Krebs in the lumen.

Onset to Peak Response of Squalamine Is Longer in Old Mice

The onset to peak response of squalamine was measured in single-unit vagal afferents of young mice [N = 3(38)] and old mice [N = 4(22)]. Onset to peak response was measured from the time of addition of squalamine to the lumen to the time that squalamine increased vagal firing rate to peak. The onset to peak response following luminal addition of squalamine was significantly longer for old mice (P = 0.0182) (**Figure 5A**). The onset to peak response in young mice was 12.95 ± 0.99 min compared to 18.82 ± 1.37 min in old mice. Representative frequency histograms over the course of the experiment demonstrate the squalamine onset to peak response to increase vagal afferent firing between young and old mice (**Figures 5B,C**). We hypothesize that vagal afferent firing is stimulated via an intramural sensory synapse between intrinsic primary afferent neurons (IPANs) of the enteric nervous system and vagal afferent endings (Perez-Burgos et al., 2014). A longer onset to peak response in aged mice would be consistent with a decrease in the excitability of these IPANs in old mice and is discussed later.

DISCUSSION

In the present study, we used *in vitro* preparations to measure male CD1 mouse colon motility and single unit vagal afferent spike firing rates from the jejunal mesenteric nerve. We showed that motility and spike firing are reduced for old compared to young mice. We also demonstrated that acute intraluminal application of squalamine could partially reverse the effects of old age on motility and constitutive vagal single unit firing rates. The stimulatory effect of squalamine on vagal firing rates had a longer onset latency to peak response in old compared to young mice.

Constipation and decreased gastrointestinal motility disproportionately affect old humans and animal models (Higgins and Johanson, 2004; De Giorgio et al., 2015; Ranson and Saffrey, 2015). For example, aged 2-year-old mice had reduced total fecal output compared to their younger 3-month-old counterparts (Patel et al., 2012); in particular, there was a

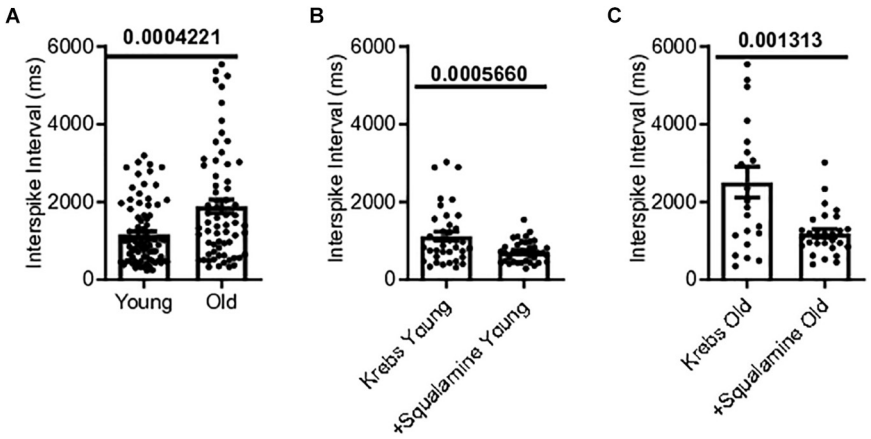

FIGURE 4 | Single vagal afferent firing was reduced in aged mice but could be rescued. **(A)** Mean interval between spikes of vagal afferents were longer in aged mice, indicating a reduction in vagal afferent firing rate in the aged mice (N = 148 fibers). **(B)** Intraluminal squalamine (10 μM) reduced the mean interval between vagal spikes in young mice (N = 38 fibers). **(C)** Intraluminal squalamine (10 μM) reduced the mean interval between vagal spikes in aged mice, increasing firing frequency toward that of the young controls (N = 22 fibers). Data represented as mean with SEM, two-tailed t-test unpaired, with Welch's correction and paired, two-tailed t-tests.

decrease in velocity of epoxy coated pellet movement in the colon and an increase in impaction (Patel et al., 2012). Despite the large range of laxatives including prokinetics and secretagogues that are available, a significant number of constipated patients are dissatisfied with treatment results (De Giorgio et al., 2015; Sbahi and Cash, 2015). The present work is the first complete report, except for a pilot data abstract in a different mouse model (Kunze et al., 2014), showing that squalamine can partially reverse the old age-related decrease in MMCs velocity in otherwise healthy mice.

Squalamine is a cationic amphipathic sterol with broad antibacterial and antiviral properties (Zasloff et al., 2011) that was first isolated from tissues of the dogfish shark *Squalus acanthias* (Moore et al., 1993). As well as having broad-spectrum antimicrobial activity, squalamine may have potential for treating a variety of diseases such as cancers, age-related macular degeneration and obesity (Brunel et al., 2005). Squalamine has also been shown to restore motility in a *C. elegans* model of Parkinson's disease (Perni et al., 2017). We have previously reported in abstract form the results of a pilot study showing that the firing rates of vagal afferent fibers are decreased in old compared to young mice and that squalamine increases this function (West et al., 2018). Our present study shows that squalamine can restore colonic motility and vagal afferent firing rates back toward young controls, following a decrease in function with age.

The vagus nerve exhibits anatomic degenerative changes in older animals displaying swollen varicosities (Phillips and Powley, 2007), yet there has so far been little evidence of a reduction in vagal firing in old age. Intestinal mesenteric nerve discharge has been reported to be decreased for old compared to young humans (Yu et al., 2016) and mice (Keating et al., 2015). However, the intestinal mesenteric nerve is a mixed nerve and it is not clear whether the reduction recorded was from vagal, spinal or other fibers. Heart rate variability indices obtained from power spectral density and time domain analysis showed a significant decrease in vagal activity in the elderly (68–85 years) compared to matched young (21–34 years) adults. There was no indication in this study whether afferent, efferent or both types of vagal fibers innervating the heart were involved (Junior and Oliveira, 2017). Of the vagal fibers innervating the gastrointestinal tract we have selected those activated by CCK. We believe our present results are the first to demonstrate reduced constitutive afferent vagal discharge for old compared to young animals. Although the *in vitro* vagal nerve recording methodology is commonly employed, a potential limitation could be that the full scope of sensory signals available *in vivo* may not be available *in vitro*.

Although the vagus can modulate small and large intestinal motility (Collman et al., 1983, 1984; Raybould and Tache, 1988; Gustafsson and Delbro, 1994; Tong et al., 2010), it is not known whether or to what extent reduced vagal firing rates contribute to a decrease in propulsive peristalsis in old mice *in vivo*. Chronic extrinsic denervation of the intestine allowing extrinsic nerve fibers to fully degenerate does not abolish or alter peristalsis reflexes (Furness et al., 1995) further emphasizing that MMCs are generated by the ENS. On the other hand, propulsive peristalsis directly reflects intrinsic primary afferent neuron (IPAN) functioning (Howe et al., 2006) and the same IPANs transmit to vagal afferent endings (Perez-Burgos et al., 2014) suggesting that compromised IPAN functioning may be an important determinant in reduced propulsion and vagal firing in old age. Therefore, it may be more likely that reduced colonic motility and reduced vagal afferent firing are not completely causally linked to each other. Because squalamine stimulates colonic motility in the absence of extrinsic innervation, it is likely that squalamine stimulated IPAN firing and that this may produce improvements in both the aged colon motility and vagal afferent firing.

The increased onset latency to peak response of squalamine on afferent vagal firing in tissue taken from old compared to young mice may be interpreted by the effects of old age on

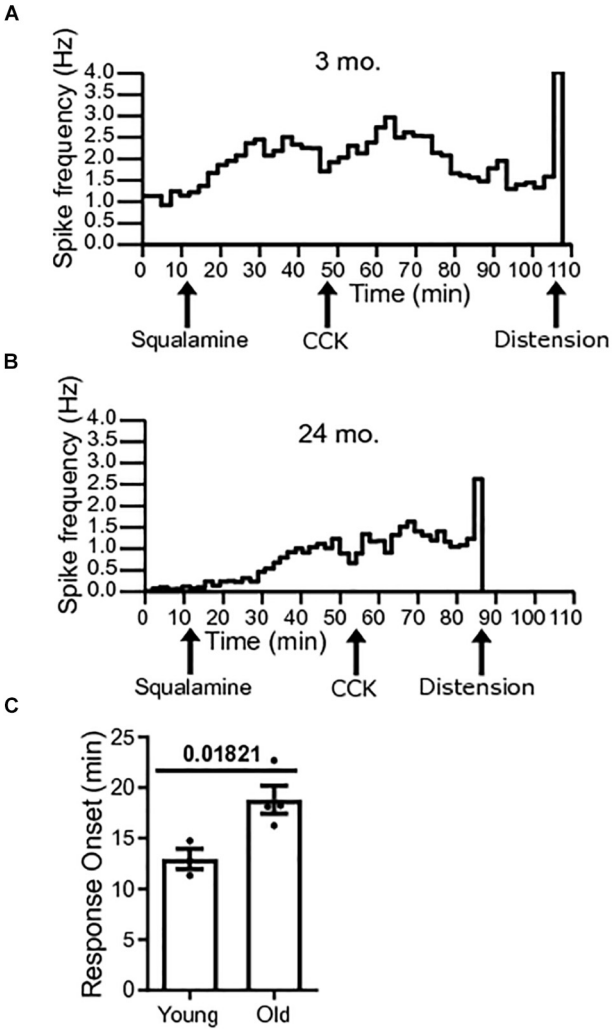

FIGURE 5 | Response onset to squalamine is longer in old mice. **(A)** Spike frequency histograms show changes in spike frequency over the course of the experiment. Onset to peak squalamine response in vagal afferent fibers in a young mouse after addition of squalamine at 12 min. **(B)** Response onset to squalamine in vagal afferent fibers in an old mouse after addition of squalamine. **(C)** Response onset to squalamine on vagal afferent firing rate was longer in old mice [N = 4(22)] compared to young mice [N = 3(38)]. Data represented as mean with SEM, t-test unpaired, with Welch's correction, two-tailed.

the enteric nervous system. Ninety to 95% of sensory neuron processes innervating the intestinal epithelium arise from the ENS, with the rest originating from neurons whose somata are located outside the intestine (Keast et al., 1984; Ekblad et al., 1987). In agreement with this anatomical data, is our recent discovery that more than two thirds of vagal afferent signals evoked by a luminal commensal bacteria is relayed to the vagus via the enteric neurons (Perez-Burgos et al., 2014). Neuroactive luminal molecules first excite juxtaepithelial neurites belonging to IPANs whose cell bodies are located within the ENS. The excited IPANs release acetylcholine and perhaps other neurotransmitters to activate vagal IGLEs which closely surround and abut the IPANs (Berthoud et al., 1997; Perez-Burgos et al., 2014). The IPAN to IGLE nicotinic sensory synapse we have described (Perez-Burgos et al., 2014), is perfectly positioned to act as a gatekeeper to regulate gut to brain signaling. Accordingly, the amount of information transmitted to the brain via the vagus would be markedly influenced by whether IPANs are refractory or readily responsive to luminal stimuli, and by the density of IPAN sensory innervation of the epithelium. Given the important role of enteric IPANs in gut to brain signaling (Perez-Burgos et al., 2014), the vulnerability of the ENS to old age in terms of numbers and degeneration could have a significant impact on the amount, quality and latency of signals reaching the brain from the gut. Thus, even if the numbers of vagal afferent fibers are not appreciably reduced in old age there could be decreased and delayed vagal afferent responses to luminal stimuli.

Functional GI disorders are often comorbid with mood and anxiety disorders (Ballou et al., 2019). In a study of 54 constipated patients with motility disorders, 22.2% showed depression using the Hospital Anxiety and Depression Scale (HADS) and 31.5% on the Mini-International Neuropsychiatric Interview (MINI) (Hosseinzadeh et al., 2011). As previously mentioned, constipation incidence and prevalence increases with age (Higgins and Johanson, 2004; De Giorgio et al., 2015; Ranson and Saffrey, 2015) and depression is common in old age (Beekman et al., 1999; Djernes, 2006; McCall and Kintziger, 2013). Clinically relevant depressive symptoms may, for example, reach a prevalence of up to 49% in institutionalized elderly Caucasians (Djernes, 2006). Indeed in a cross-sectional study between psychiatric diagnoses and constipation, inpatients older than 60 years had a significantly increased risk of constipation (odds ratios 3.38–6.52) (Jessurun et al., 2016). Increased depression in old age may be related, at least in part, to alterations in vagus nerve activity (Forsythe et al., 2014) and successful treatment of depression may also relieve the associated constipation. Vagal nerve stimulation is FDA approved, and shows promise as an essential or adjunct antidepressant treatment in humans (Carreno and Frazer, 2017; Johnson and Wilson, 2018). Indeed, a 5-year observational follow up of vagal nerve stimulation in depression has shown very promising results (Aaronson et al., 2017).

Activation of the visceral afferent vagus appears to have antidepressant behavioral and mood-altering effects in mice. Indeed, the antidepressant effects of certain neuroactive microbes, which increase discharge frequency in mesenteric vagal afferents (Perez-Burgos et al., 2013), depend on the presence of an intact vagal nerve since subdiaphragmatic vagotomy abrogated both the antidepressant effects and regional changes in GABA receptor expression in the brain (Bravo et al., 2011).

Our results show that vagal afferent firing is reduced in old age, but these changes are not permanent regardless of causation since these effects can be restored to within range of the young mouse controls. Future studies should seek to evaluate the effect of reduced vagal afferent firing in old age on depression and also GI function as a whole. Additionally, experiments should be repeated *in vivo* where possible to test for translatability of the *in vitro* results. The marked improvement induced by squalamine in the disordered motility of aged mice may have a translatable

clinical use in treating old age-related constipation and awaits clinical testing.

DATA AVAILABILITY

The datasets generated for this study are available on request to the corresponding author.

ETHICS STATEMENT

This study was approved by and conducted in accordance with the Animal Research Ethics Board (AREB) of McMaster University (permit 16-08-30). Experiments were performed *in vitro* following cervical dislocation.

AUTHOR CONTRIBUTIONS

CW, JA, and SF performed the colonic motility experiments and analyzed the data. CW performed the mesenteric nerve experiments and analyzed the data. Y-KM and AS provided the technical support for the experiments. CW and WK prepared the figures, and wrote and reviewed the manuscript. CW, AS, and WK contributed to the conception, design, facilitation, and supervision of the study. All authors read and approved the manuscript.

FUNDING

This work was supported by a grant from the Natural Sciences and Engineering Research Council of Canada Discovery Grant (2014-05517) awarded to WK.

ACKNOWLEDGMENTS

The authors would like to gratefully acknowledge Dr. Michael Zasloff, Georgetown University (Washington, DC, United States) for the donation of the squalamine used in this study and Dr. John Bienenstock, McMaster University (Hamilton, ON, Canada) for his critical review of the manuscript.

REFERENCES

Aaronson, S. T., Sears, P., Ruvuna, F., Bunker, M., Conway, C. R., Dougherty, D. D., et al. (2017). A 5-Year observational study of patients with treatment-resistant depression treated with vagus nerve stimulation or treatment as usual: comparison of response, remission, and suicidality. *Am. J. Psychiatry* 174, 640–648. doi: 10.1176/appi.ajp.2017.16010034

Ballou, S., Katon, J., Singh, P., Rangan, V., Lee, H. N., McMahon, C., et al. (2019). Chronic diarrhea and constipation are more common in depressed individuals. *Clin. Gastroenterol. Hepatol.* doi: 10.1016/j.cgh.2019.03.046 [Epub ahead of print].

Beekman, A. T. F., Copeland, J., and Prince, M. J. (1999). Review of community prevalence of depression in later life. *Br. J. Psychiatry* 174, 307–311. doi: 10.1192/bjp.174.4.307

Berthoud, H. R., Patterson, L. M., Neumann, F., and Neuhuber, W. L. (1997). Distribution and structure of vagal afferent intraganglionic laminar endings (IGLEs) in the rat gastrointestinal tract. *Anat. Embryol.* 195, 183–191. doi: 10.1007/s004290050037

Bravo, J. A., Forsythe, P., Chew, M. V., Escaravage, E., Savignac, H. M., Dinan, T. G., et al. (2011). Ingestion of *Lactobacillus* strain regulates emotional behavior and central GABA receptor expression in a mouse via the vagus nerve. *Proc. Natl. Acad. Sci. U.S.A.* 108, 16050–16055. doi: 10.1073/pnas.1102999108

Brunel, J. M., Salmi, C., Loncle, C., Vidal, N., and Letourneux, Y. (2005). Squalamine: a polyvalent drug of the future? *Curr. Cancer Drug Targets* 5, 267–272. doi: 10.2174/1568009054064642

Carreno, F. R., and Frazer, A. (2017). Vagal nerve stimulation for treatment-resistant depression. *Neurotherapeutics* 14, 716–727. doi: 10.1007/s13311-017-0537-8

Collman, P. I., Grundy, D., and Scratcherd, T. (1983). Vagal influences on the jejunal 'minute rhythm' in the anaesthetized ferret. *J. Physiol.* 345, 65–74. doi: 10.1113/jphysiol.1983.sp014965

Collman, P. I., Grundy, D., and Scratcherd, T. (1984). Vagal control of colonic motility in the anaesthetized ferret: evidence for a non-cholinergic excitatory innervation. *J. Physiol.* 348, 35–42. doi: 10.1113/jphysiol.1984.sp015097

De Giorgio, R., Ruggeri, E., Stanghellini, V., Eusebi, L. H., Bazzoli, F., and Chiarioni, G. (2015). Chronic constipation in the elderly: a primer for the gastroenterologist. *BMC Gastroenterol.* 15:130. doi: 10.1186/s12876-015-0366-3

Delungahawatta, T., Amin, J. Y., Stanisz, A. M., Bienenstock, J., Forsythe, P., and Kunze, W. A. (2017). Antibiotic driven changes in gut motility suggest direct modulation of enteric nervous system. *Front. Neurosci.* 11:588. doi: 10.3389/fnins.2017.00588

Djernes, J. K. (2006). Prevalence and predictors of depression in populations of elderly: a review. *Acta Psychiatr. Scand.* 113, 372–387. doi: 10.1111/j.1600-0447.2006.00770.x

Ekblad, E., Winther, C., Ekman, R., Hakanson, R., and Sundler, F. (1987). Projections of peptide-containing neurons in rat small intestine. *Neuroscience* 20, 169–188. doi: 10.1016/0306-4522(87)90010-8

El-Salhy, M., Sandstrom, O., and Holmlund, F. (1999). Age-induced changes in the enteric nervous system in the mouse. *Mech. Ageing Dev.* 107, 93–103. doi: 10.1016/s0047-6374(98)00142-0

Fida, R., Lyster, D. J. K., Bywater, R. A. R., and Taylor, G. S. (1997). Colonic migrating motor complexes (CMMCs) in the isolated mouse colon. *Neurogastroenterol. Motil.* 9, 99–107. doi: 10.1046/j.1365-2982.1997.d01-25.x

Forsythe, P., Bienenstock, J., and Kunze, W. (2014). Vagal pathways for microbiome-brain-gut axis communication. *Adv. Exp. Med. Biol.* 817, 115–133. doi: 10.1007/978-1-4939-0897-4_5

Furness, J. B. (2006). *The Enteric Nervous System*. Hoboken, NJ: Blackwell Publishing.

Furness, J. B., Johnson, P. J., Pompolo, S., and Bornstein, J. C. (1995). Evidence that enteric motility reflexes can be initiated through entirely intrinsic mechanisms in the guinea-pig small intestine. *Neurogastroenterol. Motil.* 7, 89–96. doi: 10.1111/j.1365-2982.1995.tb00213.x

Gamage, P. P., Ranson, R. N., Patel, B. A., Yeoman, M. S., and Saffrey, M. J. (2013). Myenteric neuron numbers are maintained in aging mouse distal colon. *Neurogastroenterol. Motil.* 25, e495–e505. doi: 10.1111/nmo.12114

Grundy, D., Hillsley, K., Kirkup, A. J., and Richards, W. (1998). Mesenteric afferent sensitivity to cholecystokinin and 5-hydroxytryptamine. *Dtsch. Tierarztl. Wochenschr.* 105, 466–468.

Gustafsson, B. I., and Delbro, D. S. (1994). Vagal influence on the motility of the feline jejunum. *J. Physiol.* 480(Pt 3), 587–595. doi: 10.1113/jphysiol.1994.sp020386

Heitler, W. J. (2007). DataView: a tutorial tool for data analysis. template-based spike sorting and frequency analysis. *J. Undergrad. Neurosci. Educ.* 6, A1–A7.

Higgins, P. D., and Johanson, J. F. (2004). Epidemiology of constipation in North America: a systematic review. *Am. J. Gastroenterol.* 99, 750–759. doi: 10.1111/j.1572-0241.2004.04114.x

Hillsley, K., and Grundy, D. (1998). Serotonin and cholecystokinin activate different populations of rat mesenteric vagal afferents. *Neurosci. Lett.* 255, 63–66. doi: 10.1016/s0304-3940(98)00690-9

Hosseinzadeh, S. T., Poorsaadati, S., Radkani, B., and Forootan, M. (2011). Psychological disorders in patients with chronic constipation. *Gastroenterol. Hepatol. Bed Bench* 4, 159–163.

Howe, D., Clarke, C., Yan, H., Willis, B., Schneider, D., McKnight, G., et al. (2006). Inhibition of protein kinase A in murine enteric neurons causes lethal intestinal pseudo-obstruction. *J. Neurobiol.* 66, 256–272. doi: 10.1002/neu.20217

Jessurun, J. G., van Harten, P. N., Egberts, T. C., Pijl, Y. J., Wilting, I., and Tenback, D. E. (2016). The relation between psychiatric diagnoses and constipation in hospitalized patients: a cross-sectional study. *Psychiatry J.* 2016:2459693. doi: 10.1155/2016/2459693

Johnson, R. L., and Wilson, C. G. (2018). A review of vagus nerve stimulation as a therapeutic intervention. *J. Inflamm. Res.* 11, 203–213. doi: 10.2147/JIR.S163248

Junior, E. C., and Oliveira, F. M. (2017). Attenuation of vagal modulation with aging: univariate and bivariate analysis of HRV. *Conf. Proc. IEEE Eng. Med. Biol. Soc.* 2017, 3178–3181. doi: 10.1109/embc.2017.8037532

Keast, J. R., Furness, J. B., and Costa, M. (1984). Origins of peptide and norepinephrine nerves in the mucosa of the guinea pig small intestine. *Gastroenterology* 86, 637–644.

Keating, C., Nocchi, L., Yu, Y., Donovan, J., and Grundy, D. (2015). Ageing and gastrointestinal sensory function: altered colonic mechanosensory and chemosensory function in the aged mouse. *J. Physiol.* 594, 4549–4564. doi: 10.1113/JP271403

Kunze, W., Yan, R. M., Min, K. K., Pasyk, M., Stanisz, A., and Zasloff, M. (2014). Squalamine reverses age and loperamide associated dysmotility in a mouse biomarker model of constipation. *Gastroenterology* 146:S356.

Malatynska, E., Steinbusch, H., Redkozubova, O., Bolkunov, A., Kubatiev, A., Yeritsyan, N., et al. (2012). Anhedonic-like traits and lack of affective deficits in 18-month-old C57BL/6 mice: implications for modeling elderly depression. *Exp. Gerontol.* 47, 552–564. doi: 10.1016/j.exger.2012.04.010

McCall, W. V., and Kintziger, K. W. (2013). Late life depression: a global problem with few resources. *Psychiatr. Clin. North. Am.* 36, 475–481. doi: 10.1016/j.psc.2013.07.001

Moore, K. S., Wehrli, S., Roder, H., Rogers, M., Forrest, JN Jr., McCrimmon, D., et al. (1993). Squalamine: an aminosterol antibiotic from the shark. *Proc. Natl. Acad. Sci. U.S.A.* 90, 1354–1358. doi: 10.1073/pnas.90.4.1354

O'Connor, R., and Cryan, J. (2014). Adolescent brain vulnerability and psychopathology through the generations: role of diet and dopamine. *Biol. Psychiatry* 75, 4–6. doi: 10.1016/j.biopsych.2013.10.022

Patel, B., Patel, N., Fidalgo, S., Ranson, R., Saffrey, J., and Yeoman, M. (2012). Age-related changes in colonic motility, faecal output and the properties of faecal pellets in the mouse. *Neurogastroenterol. Motil.* 24:129.

Perez-Burgos, A., Mao, Y., Bienenstock, J., and Kunze, W. (2014). The gut-brain axis rewired: adding a functional vagal nicotinic "sensory synapse". *FASEB J.* 28, 3064–3074. doi: 10.1096/fj.13-245282

Perez-Burgos, A., Wang, B., Mao, Y. K., Mistry, B., McVey Neufeld, K. A., Bienenstock, J., et al. (2013). Psychoactive bacteria *Lactobacillus rhamnosus* (JB-1) elicits rapid frequency facilitation in vagal afferents. *Am. J. Physiol. Gastrointest Liver Physiol.* 304, G211–G220. doi: 10.1152/ajpgi.00128.2012

Perez-Burgos, A., Wang, L., McVey Neufeld, K. A., Mao, Y. K., Ahmadzai, M., Janssen, L. J., et al. (2015). The TRPV1 channel in rodents is a major target for antinociceptive effect of the probiotic *Lactobacillus reuteri* DSM 17938. *J. Physiol.* 593, 3943–3957. doi: 10.1113/JP270229

Perni, M., Galvagnion, C., Maltsev, A., Meisl, G., Muller, M. B., Challa, P. K., et al. (2017). A natural product inhibits the initiation of alpha-synuclein aggregation and suppresses its toxicity. *Proc. Natl. Acad. Sci. U.S.A.* 114, E1009–E1017. doi: 10.1073/pnas.1610586114

Phillips, R. J., Kieffer, E. J., and Powley, T. L. (2004). Loss of glia and neurons in the myenteric plexus of the aged Fischer 344 rat. *Anat. Embryol.* 209, 19–30. doi: 10.1007/s00429-004-0426-x

Phillips, R. J., and Powley, T. L. (2007). Innervation of the gastrointestinal tract: patterns of aging. *Auton. Neurosci.* 136, 1–19. doi: 10.1016/j.autneu.2007.04.005

Phillips, R. J., Walter, G. C., and Powley, T. L. (2010). Age-related changes in vagal afferents innervating the gastrointestinal tract. *Auton. Neurosci.* 153, 90–98. doi: 10.1016/j.autneu.2009.07.009

Ranson, R. N., and Saffrey, M. J. (2015). Neurogenic mechanisms in bladder and bowel ageing. *Biogerontology* 16, 265–284. doi: 10.1007/s10522-015-9554-3

Raybould, H. E., and Tache, Y. (1988). Cholecystokinin inhibits gastric motility and emptying via a capsaicin-sensitive vagal pathway in rats. *Am. J. Physiol.* 255(2 Pt 1), G242–G246.

Richards, W., Hillsley, K., Eastwood, C., and Grundy, D. (1996). Sensitivity of vagal mucosal afferents to cholecystokinin and its role in afferent signal transduction in the rat. *J. Physiol.* 497(Pt 2), 473–481. doi: 10.1113/jphysiol.1996.sp021781

Roberts, R. R., Murphy, J. F., Young, H. M., and Bornstein, J. C. (2007). Development of colonic motility in the neonatal mouse-studies using spatiotemporal maps. *Am. J. Physiol. Gastrointest Liver Physiol.* 292, G930–G938. doi: 10.1152/ajpgi.00444.2006

Saffrey, M. J. (2013). Cellular changes in the enteric nervous system during ageing. *Dev. Biol.* 382, 344–355. doi: 10.1016/j.ydbio.2013.03.015

Saffrey, M. J. (2014). Aging of the mammalian gastrointestinal tract: a complex organ system. *Age* 36:9603. doi: 10.1007/s11357-013-9603-2

Sbahi, H., and Cash, B. D. (2015). Chronic constipation: a review of current literature. *Curr. Gastroenterol. Rep.* 17:47. doi: 10.1007/s11894-015-0471-z

Smits, G. J., and Lefebvre, R. A. (1996). Influence of aging on gastric emptying of liquids, small intestine transit, and fecal output in rats. *Exp. Gerontol.* 31, 589–596. doi: 10.1016/0531-5565(96)00029-0

Spencer, N. J., Dinning, P. G., Brookes, S. J., and Costa, M. (2016). Insights into the mechanisms underlying colonic motor patterns. *J. Physiol.* 594, 4099–4116. doi: 10.1113/JP271919

Spencer, N. J., Hibberd, T. J., Travis, L., Wiklendt, L., Costa, M., Hu, H., et al. (2018). Identification of a rhythmic firing pattern in the enteric nervous system that generates rhythmic electrical activity in smooth muscle. *J. Neurosci.* 38, 5507–5522. doi: 10.1523/JNEUROSCI.3489-17.2018

Spencer, N. J., Sanders, K. M., and Smith, T. K. (2003). Migrating motor complexes do not require electrical slow waves in the mouse small intestine. *J. Physiol.* 553(Pt 3), 881–893. doi: 10.1113/jphysiol.2003.049700

Strawbridge, W., Cohen, R., Shema, S., and Kaplan, G. (1996). Successful aging: predictors and associated activities. *Am. J. Epidemiol.* 144, 135–141. doi: 10.1093/oxfordjournals.aje.a008900

Tong, W. D., Ridolfi, T. J., Kosinski, L., Ludwig, K., and Takahashi, T. (2010). Effects of autonomic nerve stimulation on colorectal motility in rats. *Neurogastroenterol. Motil.* 22, 688–693. doi: 10.1111/j.1365-2982.2009.01461.x

Wade, P. R. (2002). I. Age-related changes in the enteric nervous system. *Am. J. Physiol. Gastrointest. Liver Physiol.* 283, G489–G495. doi: 10.1152/ajpgi.00091.2002

Wade, P. R., and Cowen, T. (2004). Neurodegeneration: a key factor in the ageing gut. *Neurogastroenterol. Motil.* 16(Suppl. 1), 19–23. doi: 10.1111/j.1743-3150.2004.00469.x

Wang, B., Mao, Y. K., Diorio, C., Pasyk, M., Wu, R. Y., Bienenstock, J., et al. (2010a). Luminal administration ex vivo of a live *Lactobacillus* species moderates mouse jejunal motility within minutes. *FASEB J.* 24, 4078–4088. doi: 10.1096/fj.09-153841

Wang, B., Mao, Y. K., Diorio, C., Wang, L., Huizinga, J. D., Bienenstock, J., et al. (2010b). *Lactobacillus reuteri* ingestion and IK(Ca) channel blockade have similar effects on rat colon motility and myenteric neurones. *Neurogastroenterol. Motil.* 22:e133. doi: 10.1111/j.1365-2982.2009.01384.x

West, C., Stanisz, A., Bienenstock, J., Barbut, D., Zasloff, M., and Kunze, W. A. (2018). A293 squalamine increases vagal afferent firing frequency in aging mice. *J. Can. Assoc. Gastroenterol.* 1(Suppl. 2):421. doi: 10.1093/jcag/gwy009.293

West, C., Wu, R. Y., Wong, A., Stanisz, A. M., Yan, R., Min, K. K., et al. (2017). *Lactobacillus rhamnosus strain JB-1 reverses restraint stress-induced gut dysmotility. Neurogastroenterol. Motil.* 29, 1–11. doi: 10.1111/nmo.12903

Wu, R. Y., Pasyk, M., Wang, B., Forsythe, P., Bienenstock, J., Mao, Y. K., et al. (2013). Spatiotemporal maps reveal regional differences in the effects on gut motility for *Lactobacillus reuteri* and *rhamnosus* strains. *Neurogastroenterol. Motil.* 25, e205–e214. doi: 10.1111/nmo.12072

Yu, Y., Daly, D., Adam, I., Kitsanta, P., Hill, C., Wild, J., et al. (2016). Interplay between mast cells, enterochromaffin cells, and sensory signaling in the aging human bowel. *Neurogastroenterol. Motil.* 28, 1465–1479. doi: 10.1111/nmo.12842

Zanesco, M., and Souza, R. (2011). Morphoquantitative study of the submucous plexus (of Meissner) of the jejunum-ileum of young and old guinea pigs. *Arq. Neuropsiquiatr* .69, 85–90. doi: 10.1590/s0004-282x20110001000017

Zasloff, M., Adams, A. P., Beckerman, B., Campbell, A., Han, Z., Luijten, E., et al. (2011). Squalamine as a broad-spectrum systemic antiviral agent with therapeutic potential. *Proc. Natl. Acad. Sci. U.S.A.* 108, 15978–15983. doi: 10.1073/pnas.1108558108

Conflict of Interest Statement: WK is member of the scientific advisory board of Enterin Inc., but has received no personal remuneration from them. Enterin Inc., was not involved in any aspect of the design or conduct of this study, including the preparation of the manuscript.

The remaining authors declare that the research was conducted in the absence of any commercial or financial relationships that could be construed as a potential conflict of interest.

frontiers in Neuroscience

ORIGINAL RESEARCH
published: 12 November 2019
doi: 10.3389/fnins.2019.01214

Heart Rate Variability Predicts Therapeutic Response to Metoprolol in Children With Postural Tachycardia Syndrome

Yuanyuan Wang[1,2†], Chunyu Zhang[1†], Selena Chen[3], Ping Liu[1], Yuli Wang[1], Chaoshu Tang[4,5], Hongfang Jin[1,2] and Junbao Du[1,5]**

[1] Department of Pediatrics, Peking University First Hospital, Beijing, China, [2] Research Unit of Clinical Diagnosis and Treatment of Pediatric Syncope and Cardiovascular Diseases, Chinese Academy of Medical Sciences, Beijing, China, [3] Division of Biological Sciences, University of California, San Diego, San Diego, CA, United States, [4] Key Laboratory of Molecular Cardiovascular Sciences, Ministry of Education, Beijing, China, [5] Department of Physiology and Pathophysiology, Health Sciences Centre, Peking University, Beijing, China

OPEN ACCESS

Edited by:
Alberto Porta,
University of Milan, Italy

Reviewed by:
Roberto Maestri,
IRCCS Scientific Clinical Institutes Maugeri (ICS Maugeri), Italy
Karina Rabello Casali,
Federal University of São Paulo, Brazil
Mathias Baumert,
The University of Adelaide, Australia

***Correspondence:**
Hongfang Jin
jinhongfang51@126.com
Junbao Du
junbaodu1@126.com

† These authors have contributed equally to this work

Specialty section:
This article was submitted to Autonomic Neuroscience, a section of the journal Frontiers in Neuroscience

Received: 28 July 2019
Accepted: 28 October 2019
Published: 12 November 2019

Citation:
Wang Y, Zhang C, Chen S, Liu P, Wang Y, Tang C, Jin H and Du J (2019) Heart Rate Variability Predicts Therapeutic Response to Metoprolol in Children With Postural Tachycardia Syndrome. Front. Neurosci. 13:1214. doi: 10.3389/fnins.2019.01214

Purpose: To improve the metoprolol therapeutic effectiveness, we aimed to explore whether baseline heart rate variability (HRV) indicators before metoprolol treatment were useful for predicting its efficacy for postural tachycardia syndrome (POTS).

Methods: We recruited 45 children with POTS who received metoprolol and 17 healthy controls. All children underwent a standing test or basic head-up tilt test and 24-h dynamic electrocardiography before treatment. After 3 months of metoprolol, therapeutic responsiveness was evaluated. The usefulness of baseline HRV parameters in predicting the effectiveness of metoprolol was studied and the long-term cumulative symptom rate was analyzed.

Results: The baseline HRV frequency domain indicators for power, ultra-low frequency, very-low frequency, low frequency (LF), high frequency (HF), and total power (TP) as well as time domain indicators were significantly lower for responders than non-responders to metoprolol; however, low-frequency normalized units and LF/HF ratio were markedly greater for responders than non-responders. On series-parallel analysis, combined baseline triangular (TR) index $\leq$ 33.7 and standard deviation of all normal-to-normal intervals (SDNN) index $\leq$ 79.0 ms as cut-off values yielded sensitivity, specificity and accuracy of 85.3, 81.8, and 84.4%, respectively, to predict therapeutic responsiveness to metoprolol. On long-term follow-up, the cumulative symptom rate was significantly higher with TR index $>$ 33.7 and SDNN index $\leq$ 79.0 ms, TR index $\leq$ 33.7 and SDNN index $>$ 79.0 ms or TR index $>$ 33.7 and SDNN index $>$ 79.0 ms than TR index $\leq$ 33.7 and SDNN index $\leq$ 79.0 ms ($P < 0.05$).

Conclusion: Combined TR index $\leq$ 33.7 and SDNN index $\leq$ 79.0 ms were useful preliminary measures to predict therapeutic response to metoprolol in pediatric POTS.

Keywords: heart rate variability, children, postural tachycardia syndrome, metoprolol, therapy

INTRODUCTION

Postural tachycardia syndrome (POTS) is a common type of orthostatic intolerance (OI) and is characterized by excessive increase in heart rate (HR) when standing upright (Fedorowski et al., 2017). POTS is accompanied by symptoms of OI (Fedorowski, 2019) and results in serious physical and psychological problems in children (Bagai et al., 2011; Kizilbash et al., 2014). A beta-adrenoceptor blocker (β-blocker) is commonly used for treating POTS in children (Kernan and Tobias, 2010; Bryarly et al., 2019). It inhibits sympathetic nerve modulation, reducing HR and the stimulation of cardiac baroreceptors, thus blocking the action of increased catecholamine levels in circulation. Previous studies showed that β-blockers could improve symptoms only in some children with POTS (Lai et al., 2009; Chen et al., 2011). Additionally, β-blockers may impair the exercise tolerance of children (Ladage et al., 2013). Therefore, predicting the therapeutic effect of the β-blocker metoprolol on POTS before treatment is of great clinical importance to improve the effectiveness of the therapy.

In previous studies, we examined predictive indices of metoprolol efficacy before treating patients with POTS by detecting plasma levels of norepinephrine, copeptin and C-type natriuretic peptide (CNP) (Zhang et al., 2014; Zhao et al., 2014; Lin et al., 2015b). However, norepinephrine level in plasma is unstable, which limits its predictive accuracy, and the detection of plasma norepinephrine, copeptin, and CNP requires venipuncture to obtain blood samples for ELISA. Therefore, non-invasive and easy-to-measure indices are needed for predicting the therapeutic efficacy of metoprolol before POTS treatment.

HR variability (HRV) is an important measure that reflects the sympathetic and vagal modulation of the autonomic nervous system and its balance (Cygankiewicz and Zareba, 2013). It is primarily measured by 24-h dynamic Holter electrocardiography, which is non-invasive and easy-to-operate. Therefore, to improve the therapeutic effectiveness of metoprolol for pediatric POTS, we aimed to determine useful baseline HRV-based parameters to predict its efficacy for POTS.

MATERIALS AND METHODS

Study Population

From March 2012 to August 2018, 45 children with POTS admitted to the Pediatric Syncope Clinic of Peking University First Hospital were enrolled in the POTS group (23 males; mean age 12.2 ± 2.2 years). All received metoprolol. The control group consisted of 17 healthy children (11 males, mean age 11.5 ± 2.0 years) screened by medical history, physical examination, and laboratory investigations including ECG, Holter ECG, standing test, etc. This study was approved by the Ethics Committee of the First Hospital of Peking University (2018 [202]), and all parents or guardians of the children were informed of the research purpose and signed informed consent.

HRV Indices Analysis (Malik et al., 1989; Myers et al., 1992; Nguyen et al., 2017)

Heart rate variability was assessed by 3-channel 24-h Holter ECG (Mortara Dynamic ECG Recording Analyzer, United States), with sampling rate 10000 Hz and response band 0.05 to 60 Hz. All participants were required to be hospitalized during the recording and away from electronic products. Sitting, reading, walking, eating snacks, and drinking tea was allowed at the bedside. HRV indices were analyzed by using H scribe (Mortara Instruments). Each RR interval was validated visually before the analysis. Only normal-to-normal (NN) beats were considered for analysis with intervals. Interfering signal exclusion was performed by the analysis system automatically based on the normalized QRS peak detection, and abnormal heart beats were screened by an investigator who was blinded to the results. Abnormal heart beats included ventricular or supraventricular heart beats, artifacts and noise. We also excluded the recordings that provided $<$ 20 h of usable data ($\geq$240 of 288 5-min segments), requiring for time-domain analyses that at least 50% of each segment consisted of NN inter-beat intervals and for frequency-domain analyses at least 80%. After we checked manually, an automatic algorithm was applied to select the most stationary segments of 5-min duration, and 403 ± 92 beats were selected in each series. The time domain parameters were as follows: standard deviation of all NN intervals (SDNN), standard deviation of the averages of NN intervals in all 5-min segments of the entire recording (SDANN), mean of the standard deviation of NN intervals for each 5-min segment (SDNN index), root mean square of the successive NN interval difference (RMSSD), percentage difference between adjacent NN intervals $>$ 50 ms (pNN50) and triangular (TR) index.

The frequency domain parameters of HRV were calculated by spectral analysis performed by Fast Fourier Transform methods. Recordings were detrended and low-pass–filtered to remove frequencies $>$ 60 Hz. The power of frequency bands could be classified into four bands: ultra-low frequency (ULF; 0–0.003 Hz), very low frequency (VLF; 0.003–0.04 Hz), low frequency (LF; 0.04–0.15 Hz), high frequency (HF; 0.15–0.40 Hz), total power (TP; variance of all NN intervals, $\leq$0.4 Hz), and ratio of LF to HF (LF/HF). We defined 22:00–05:59 as the night time, and nighttime HRV indices were calculated. Participants were also asked to refrain from strenuous exercise and emotional excitement.

Standing Test and Basic Head-Up Tilt Test (BHUTT)

Standing Test (Liao et al., 2010; Wang et al., 2018)

The test environment requires dim light and a suitable temperature. The children first laid quietly for 10 min. The HR, blood pressure (BP), and ECG recordings were monitored by using a Dash 2000 multi-channel physiological monitor (General Electric, Co., New York, NY, United States) while children were lying supine. After HR and BP stabilized, children were then asked to stand for another 10 min, and HR, BP and ECG recordings were monitored dynamically during this process.

BHUTT (Lin et al., 2015a; Wang et al., 2018)

All drugs affecting autonomic function were discontinued for least five half-lives before the test. Children were required to fast for > 4 h before the test. Children were first asked to assume a supine position on the tilt bed (HUT-821; Beijing Juchi, Beijing) for 10 to 30 min. HR and ECG recordings were continuously monitored in a quiet, warm, and dim light environment with a multi-lead ECG monitor (General Electric, New York, NY, United States), and BP was monitored by using Finapres Medical System- FMS (FinometerPRO, FMS Company, Netherlands). After HR and BP stabilized, the tilt bed was raised to 60°, and HR, BP and ECG recordings were monitored until a positive reaction or until the children completed the entire 45-min examination.

Diagnosis of POTS

The diagnosis of POTS was mainly based on the following (Sheldon et al., 2015; Wang et al., 2018, 2019): (1) commonly seen in older children; (2) associated with inducements such as quick position change from supine to upright position, or long-term standing before the appearance of OI symptoms; (3) associated with OI symptoms such as dizziness, headache, fatigue, blurred vision, chest tightness, palpitations, hand tremors, and even syncope; (4) HR increased ≥ 40 bpm or the maximum HR ≥ 130 bpm (in children 6–12 years old) or ≥ 125 bpm (in adolescents 13–18 years old) without orthostatic hypotension (BP decrease > 20/10 mmHg) during the first 10 min of the standing test or BHUTT; and (5) exclusion of other diseases that cause OI symptoms such as cardiovascular diseases, metabolic diseases, neurologic diseases, or psychogenic disorders.

Symptom Score (SS) (Winker et al., 2005; Li et al., 2016)

SS was based primarily on symptoms of OI in children with POTS, including syncope, dizziness, chest tightness, nausea, palpitations, headache, hand tremors, sweating, blurred vision, and inattention. Scoring criteria were based on the frequency of an event during the observation: (0) no occurrence; (1) once per month; (2) 2 to 4 times per month; (3) 2 to 7 times per week; and (4) more than once per day. A child's total SS was the sum of his/her individual SS. The baseline SS was determined when the child was first diagnosed with POTS before treatment, and it was recorded again at the end of the first follow-up after treatment. A reduction in score by ≥ 2 points after the treatment as compared to baseline SS indicated that the treatment was effective and the patient was considered a "responder." Otherwise, an SS reduction < 2 points indicated that the treatment was ineffective, and the patient was considered a "non-responder."

Treatment and Follow-Up

First Follow-Up

Children with POTS received metoprolol. The standard dosage was 12.5 mg twice a day, but for a few children the dose was adjusted according to age and weight. The course of treatment was 1 to 3 months. After 3 months of treatment, children were followed up for the first time. The follow-up was conducted by questionnaire implemented in an outpatient setting or via telephone and was recorded by a trained responsible person. Drug adherence, frequency of OI symptoms and adverse drug reactions were the focus of the follow-up.

Second Follow-Up

The second telephone follow-up time was scheduled from January to February 2019. The follow-up involved Kaplan–Meier curve analysis of children with POTS at 3 to 48 months after discontinuation of treatment. The flowchart of study enrollment is in **Figure 1**. According to the cut-off values for predicting the therapeutic response to metoprolol in the first follow-up, together with the symptom scores before and after treatment, we plotted the Kaplan–Meier curve to determine whether the cut-off values derived from the first follow-up could predict the long-term therapeutic response to metoprolol in children with POTS.

Statistical Analysis

SPSS 23.0 (IBM, Armonk, NY, United States) was used for data analysis. Continuous data are expressed as mean ± SD. The data normality test was performed using the Shapiro–Wilk test. Independent sample *t*-test or Mann–Whitney *U*-test was used to compare other data between the two groups, and chi-square test was used for comparing categorical data. The Pearson correlation test was used to examine the correlation between normal distribution indices and the Spearman correlation test was used to examine the correlation between non-normal distribution indices. Receiver operator characteristic (ROC) curve analysis was used to evaluate the sensitivity and specificity of HRV indicators for predicting the short-term efficacy of metoprolol in children with POTS. An area under the ROC curve (AUC) 0.5 to 0.7 represented "low" predictive power, 0.7 to 0.9 "moderate" predictive power, and > 0.9 "high" predictive power. The optimal cutoff value was determined by the maximum Youden index, defined as sensitivity + specificity – 1, with sensitivity and specificity calculated as proportions (Schisterman et al., 2005).

According to the first follow-up-derived indices, children with POTS were divided into two groups. The OI symptoms and follow-up times were recorded at the second follow-up. The Kaplan–Meier curve was drawn, and symptom survival rate was compared by Log-rank test. The symptom rate over a certain period of time was defined as P (t) = 1 – (the number of asymptomatic cases after treatment that used to be symptomatic during this time/the number of cases observed at the beginning of this follow-up) × 100%, and cumulative symptom rate was calculated as S(t) = P(1) × P(2) × ... × P (t). Statistical significance was set at $P < 0.05$.

RESULTS

Comparison of Baseline Demographic and HRV Parameters Between POTS and Control Groups

The two groups did not significantly differ in sex, age, height, weight and body mass index (BMI) ($P > 0.05$) (**Table 1**).

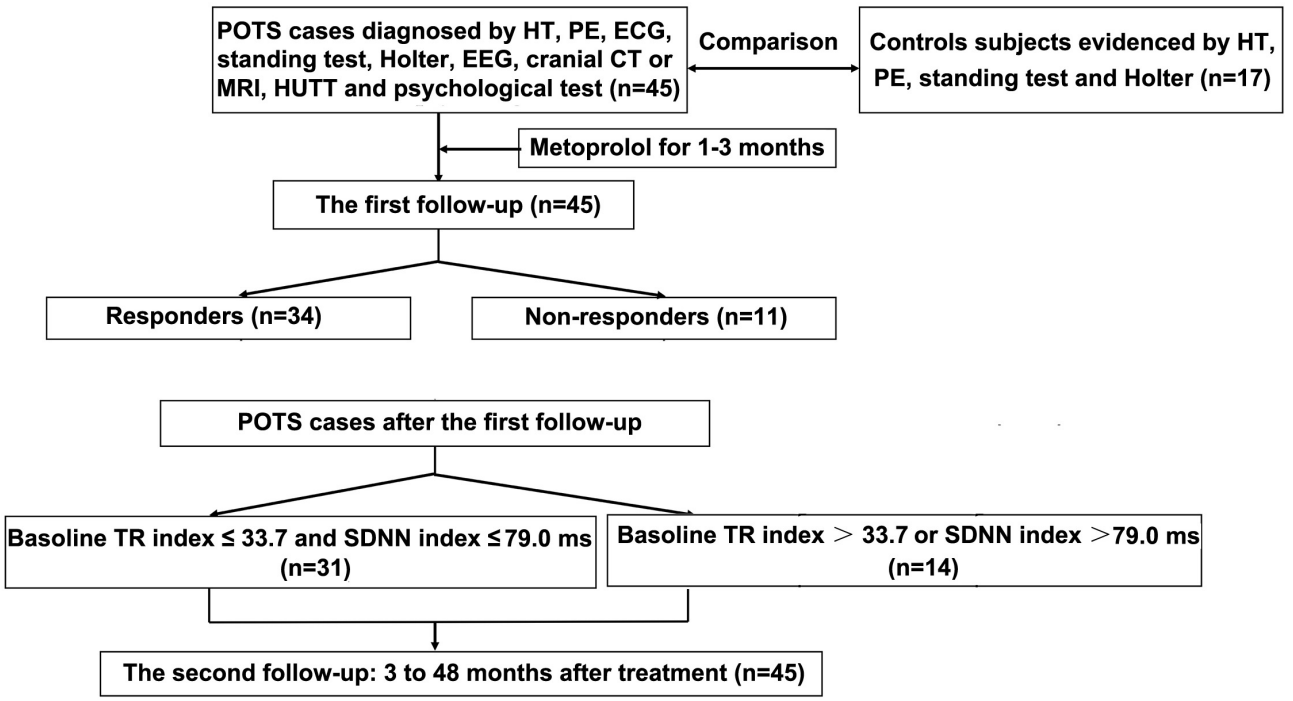

FIGURE 1 | Flowchart of enrollment of study population. POTS, postural tachycardia syndrome; HT, history taking; PE, physical examination; ECG, electrocardiography; EEG, electroencephalography; CT, computed tomography; MRI, magnetic resonance imaging; HUTT, head-up tilt test; TR index, triangular index.

However, SDNN index, pNN50, TR index, LF, and TP were significantly higher in POTS than control children all $P < 0.05$. The other HRV indicators were not significantly different between the two groups ($P > 0.05$) (**Table 2**).

Comparison of Baseline Demographic, Hemodynamics, Pre-treatment SS and HRV Parameters Between Responders and Non-responders to Metoprolol in Children With POTS

The two response groups did not significantly differ in sex, age, height, weight, BMI, systolic BP, diastolic BP, HR, and HR change from supine to standing (ΔHR), or pre-treatment SS ($P > 0.05$) (**Table 3**). The time domain indices, ULF, VLF, LF, HF, and TP, were markedly lower in responders than in non-responders; however, LF/HF were significantly higher in responders than non-responders ($P < 0.05$ for SDANN and LF/HF, and $P < 0.01$ for other parameters) (**Table 4**). Night-time HRV indices did not significantly differ between responders and non-responders (**Table 5**).

Baseline HRV Time-Domain Indices Predict Short-Term Therapeutic Response to Oral Metoprolol in Children With POTS

Before ROC curve analysis, the non-normal distribution of SDNN, SDANN, HF, TP, ULF, and LF/HF parameters was converted to a $\log_2$ that conformed to a normal distribution. The AUC for $\log_2$SDNN (**Figure 2A**), SDNN index (**Figure 2B**), RMSSD (**Figure 2C**), pNN50 (**Figure 2D**), and TR index (**Figure 2E**) was 0.811 (95% confidence interval [CI] 0.688–0.935), 0.820 (95% CI 0.671–0.968), 0.807 (95% CI 0.659–0.956), 0.813 (95% CI 0.673–0.952) and 0.807 (95% CI 0.659–0.956), respectively, in predicting the therapeutic response to metoprolol

TABLE 1 | Demographic characteristics of children with postural tachycardia syndrome (POTS) and control groups.

Groups	Case (*n*)	Sex (M/F)	Age (y)	Height (cm)	Weight (kg)	BMI (kg/m^2)
POTS	45	23/22	12.2 ± 2.2	158.0 ± 13.7	50.2 ± 17.1[a]	19.6 ± 4.2[a]
Control	17	11/6	11.5 ± 2.0	155.7 ± 11.9	48.3 ± 11.7	19.7 ± 2.9
$t/\chi^2/Z$	–	0.454	−1.235	−0.614	−0.197	−1.271
P	–	0.501	0.221	0.541	0.848	0.207

Data are mean ± SD. [a]Non-normal distribution.

TABLE 2 | Comparison of HRV indices between POTS and control groups.

Groups	SDNN (ms)	SDANN (ms)	SDNN index (ms)	RMSSD (ms)	pNN50 (%)	TR index	ULF (ms^2)	VLF (ms^2)	LF (ms^2)	HF (ms^2)	TP (ms^2)	LF/HF
POTS	143.2 ± 33.9	133.7 ± 42.5[a]	68.4 ± 16.9	49.3 ± 20.5[a]	20.6 ± 11.4	29.4 ± 7.3	15650.7 ± 7954.0[a]	2443.7 ± 965.3[a]	1075.3 ± 561.7[a]	901.4 ± 756.6[a]	3384.9 ± 1774.1[a]	1.6 ± 0.8[a]
Control	130.6 ± 31.7	144.5 ± 72.9[a]	55.0 ± 13.5	38.4 ± 13.2	14.4 ± 8.6	24.5 ± 7.0	13801.6 ± 8333.4[a]	1954.3 ± 856.2	747.7 ± 401.3[a]	554.7 ± 388.5[a]	2395.2 ± 1175.4[a]	1.6 ± 0.7[a]
t/Z	−1.317	−0.253	−2.934	−1.879	−2.038	−2.356	−1.034	−1.633	−2.012	−1.649	−1.996	−0.395
P	0.193	0.806	0.005	0.060	0.046	0.022	0.308	0.105	0.044	0.101	0.046	0.699

Data are mean ± SD. HRV, Heart rate variability; SDNN, standard deviation of all NN intervals during 24-h recording; SDANN, standard deviation of the average of NN intervals in all 5-min segments of the entire recording; SDNN index, mean of the standard deviation of NN intervals for each 5-min segment; RMSSD, root mean square of the successive NN interval difference; pNN50, percentage of adjacent RR intervals > 50 ms; TR index, triangular index; ULF, ultra low frequency; VLF, very low frequency; LF, low frequency; HF, high frequency; TP, total power; LF/HF, ratio of low to high frequency power. Data are mean ± SD. [a]Non-normal distribution.

TABLE 3 | Comparison of demographic, hemodynamics parameters and pre-treatment SS (symptom scores) between POTS children with response and non-response to metoprolol.

Groups	Cases (*n;* %)	Sex (M/F)	Age (y)	Height (cm)	Weight (kg)	BMI (kg/m^2)	HR (bpm)	SBP (mmHg)	DBP (mmHg)	ΔHR (bpm)	Pre-treatment SS (point)
Responders	34 (75.6)	18/16	12.0 ± 2.3	156.8 ± 15.2	49.8 ± 18.3	19.6 ± 4.3[a]	78 ± 13[a]	109 ± 12	63 ± 11	48 ± 8	6.6 ± 3.9[a]
Non-responders	11 (24.4)	5/6	12.9 ± 1.6	161.6 ± 7.2	51.4 ± 13.4	19.5 ± 4.1	74 ± 15	105 ± 8	62 ± 9	47 ± 8[a]	7.1 ± 4.4
t/Z/$\chi 2$	–	0.007	1.201	1.015	0.259	−0.092	−1.375	−0.805	−0.183	−0.595	−0.346
P-value	–	0.932	0.236	0.316	0.797	0.926	0.169	0.425	0.855	0.552	0.729

HR, heart rate; SBP, systolic blood pressure; DBP, diastolic blood pressure; ΔHR, heart rate change from supine to standing. Data are mean ± SD. [a]Non-normal distribution.

TABLE 4 | Comparison of HRV indices between POTS children with response and non-response to metoprolol.

Groups	SDNN (ms)	SDANN (ms)	SDNN index (ms)	RMSSD (ms)	pNN50 (%)	TR index	ULF (ms^2)	VLF (ms^2)	LF (ms^2)	HF (ms^2)	TP (ms^2)	LF/HF
Responders	134.6 ± 32.6[a]	128.4 ± 44.4[a]	63.2 ± 12.8	43.2 ± 15.2	17.5 ± 9.6	27.3 ± 6.1	14083.5 ± 8129.1[a]	2196.2 ± 770.7	883.4 ± 340.6	665.4 ± 478.2[a]	2811.5 ± 1147.9[a]	1.7 ± 0.8[a]
Non-responders	169.5 ± 23.5[a]	150.3 ± 32.3[a]	84.5 ± 18.3	67.9 ± 24.2	30.2 ± 11.5	35.7 ± 7.2	20494.8 ± 5112.6	3208.8 ± 1134.9	1630.7 ± 994.8	1630.7 ± 994.8	5257.3 ± 2219.8	1.2 ± 0.5
t/Z	−3.078	−2.206	4.305	4.013	3.634	3.779	−2.958	−2.588	5.013	−3.222	−3.143	−2.166
P	0.002	0.027	<0.001	<0.001	0.001	<0.001	0.003	0.010	<0.001	0.001	0.002	0.030

HRV, Heart rate variability; SDNN, standard deviation of all NN intervals during 24-h recording; SDANN, standard deviation of the average of NN intervals in all 5-min segments of the entire recording; SDNN index, mean of the standard deviation of NN intervals for each 5-min segment; RMSSD, root mean square of the successive NN interval difference; pNN50, percentage of adjacent RR intervals > 50 ms; TR index, triangular index; ULF, ultra low frequency; VLF, very low frequency; LF, low frequency; HF, high frequency; TP, total power; LF/HF, ratio of low to high frequency power. Data are mean ± SD. [a]Non-normal distribution.

TABLE 5 | Comparison of HRV indices for the night between POTS children with response and non-response to metoprolol.

Groups	nSDNN (ms)	nRMSSD (ms)	nPNN50 (%)	nTR index	nULF (ms^2)	nVLF (ms^2)	nLF (ms^2)	nHF (ms^2)	nTP (ms^2)	nLF/HF
Responders	73.1 ± 19.9	58.1 ± 25.3[a]	33.0 ± 17.0	11.7 ± 2.5	24.4 ± 7.1	999.0 ± 290.3	712.7 ± 280.5	909.5 ± 696.5[a]	2308.7 ± 1029.5	1.3 ± 0.6[a]
Non-responders	88.3 ± 30.1	80.3 ± 40.8	44.3 ± 20.8	13.3 ± 4.2	22.8 ± 6.0	997.4 ± 304.8	893.8 ± 496.9	1594.7 ± 1273.5	3188.5 ± 1920.3	1.2 ± 1.1[a]
t/Z	1.564	−1.664	1.812	1.270	−0.686	−0.016	1.522	−1.611	1.453	−1.604
P	0.142	0.096	0.077	0.228	0.497	0.988	0.135	0.107	0.172	0.109

HRV, Heart rate variability; nSDNN, night standard deviation of all NN intervals during 24-h recording; nRMSSD, night root mean square of the successive NN interval difference; npNN50, night percentage of adjacent RR intervals > 50 ms; nTR index, night triangular index; nULF, night ultra low frequency; nVLF, night very low frequency; nLF, night low frequency; nHF, night high frequency; nTP, night total power; nLF/HF, night ratio of low to high frequency power. Data are mean ± SD. [a]Non-normal distribution.

in POTS children. The cut-off values of the indices were 7.2 ms, 79.0 ms, 45.5 ms, 20.0 ms and 33.7 ms, respectively, yielding sensitivities of 73.5, 94.1, 61.8, 64.7, and 85.6%, respectively, and specificities of 100, 63.6, 90.9, 90.9, and 72.7%, respectively.

Baseline HRV Frequency-Domain Indices Predict Short-Term Therapeutic Response to Oral Metoprolol in Children With POTS

For the frequency-domain indices, the AUC values for HF (**Figure 3A**) and TP (**Figure 3B**) were 0.826 (95% CI 0.670–0.982) and 0.818 (95% CI 0.655–0.981), respectively, in predicting short-term therapeutic response to oral metoprolol. Cut-off values for the $\log_2$ indices were 10.1 and 11.8 ms^2, respectively, yielding sensitivities of 88.2 and 85.3%, respectively, and specificities of 72.7 and 72.7%, respectively.

Combined Baseline TR Index and SDNN Index for Predicting Outcome in Children With POTS

We showed that there was a strong correlation between HRV indicators. Please see the "**Supplementary Table 1**." To find indicators with high sensitivity and specificity, we used series-parallel analysis of those indicators and found that the baseline TR index $\leq$ 33.7 and SDNN index $\leq$ 79.0 ms yielded sensitivity 85.3%, specificity 81.8% and accuracy 84.4% to predict response to metoprolol.

In the second follow-up studies, based on the combined cut-off values for the TR index and SDNN index, the children with POTS were divided into those with TR index $\leq$ 33.7 and SDNN index $\leq$ 79.0 ms (group I; n = 31) and with TR index $>$ 33.7 and SDNN index $\leq$ 79.0 ms, TR index $\leq$ 33.7 and SDNN index $>$ 79.0 ms, or TR index $>$ 33.7 and SDNN index $>$ 79.0 ms (group II; n = 14). The Kaplan–Meier curves of the two groups were plotted. Cumulative symptom rates were 92.9, 78.6, 69.8, 69.8, and 69.8% at 3, 6, 9, 12 and 48 months, respectively, for children in group II and 64.5, 48.4, 39.6, 23.8, and 11.9% at 3, 6, 9, 12 and 48 months, respectively, for children in group I. Cumulative symptom rates were significantly higher for children with POTS in group II than group I (χ^2 = 5.952, P = 0.015) (**Figure 4**).

DISCUSSION

In this study, we found that values for the baseline HRV frequency domain indicators ULF, VLF, LF, HF, and TP and time domain indicators were significantly lower for responders than non-responders to metoprolol for POTS; however LF/HF values were markedly greater than those of non-responders. On further ROC curve analysis of HRV index, the baseline SDNN, SDNN index, RMSSD, pNN50, TR index, HF and TP were of value in predicting the efficacy of metoprolol. To improve the sensitivity and specificity of the prediction of drug efficacy, we used series-parallel analysis of the indicators. The combined baseline TR index $\leq$ 33.7 and SDNN index $\leq$ 79.0 ms as cut-off values yielded sensitivity, specificity and accuracy of 85.3, 81.8 and 84.4%, respectively, to predict the therapeutic response to metoprolol. The cumulative symptom rate in patients was significantly higher for group II than group I patients (TR index $\leq$ 33.7 and SDNN index $\leq$ 79.0 ms) ($P < 0.05$). Therefore, combined baseline TR index and SDNN index could be used as preliminary measures to predict responsiveness to metoprolol for POTS in children.

Postural tachycardia syndrome belongs to chronic OI in children, and patients often report dizziness, headache, palpitations and fatigue, believed to result from transient decreased blood flow to the brain (Stewart et al., 2018; Spahic et al., 2019). Metoprolol, a β-blocker, is considered an effective method for treating childhood POTS (Bryarly et al., 2019). Responders in our study showed marked reduction in SS on metoprolol as compared with non-responders. However, we also found that when we did not choose to use β-blockers in POTS, the effectiveness was limited. Additionally, hypotension, fatigue, and reduced exercise capacity are potential side effects of β-blockers. Therefore, exploring a non-invasive indicator of HRV is extremely important to predict the efficacy of metoprolol in the treatment of POTS.

Previous studies have shown that time domain indices of HRV are useful measures of the changes in HR over time or the intervals between successive normal cardiac cycles, and they reflect alterations in autonomic tone that are predominantly vagally mediated (Young and Benton, 2018). The ULF and VLF component was proposed as an auxiliary marker for sympathetic modulation (Kainuma et al., 2014). The interpretation of the LF component is controversial. Some authors consider it a combination of sympathetic and parasympathetic modulation, but others as a measure of sympathetic modulations. Research also shows that β-blockade resulted in a reduced LF power. Therefore, in practical terms, an increased LF component has been generally considered to result from sympathetic modulation (Sztajzel, 2004). The HF component is generally defined as a marker of vagal modulation (Zaravko et al., 2015).

According to previous literature, there are two types of POTS: neuropathic and hyperadrenergic. Neuropathic POTS is mainly characterized by vasodilation with over-enhanced vagal tone; nevertheless, hyperadrenergic POTS is mainly characterized by increased plasma noradrenaline level caused by sympathetic over-enhancement. Therefore, as compared with healthy controls, our POTS children presented increased vagal and sympathetic nerve tone. Our study showed that as compared with normal controls, SDNN index, pNN50, TR index, LF and TP were significantly increased, which suggests that vagal and sympathetic nerve tone in POTS patients was increased to a certain extent, which is consistent with previous research.

The pathogenesis of POTS is still unclear, possibly including autonomic dysfunction (Shannon et al., 2000), excessive vasodilation (Liao et al., 2013), and low central blood volume (Zhang et al., 2012). Providing active and effective treatment to children with POTS is an important

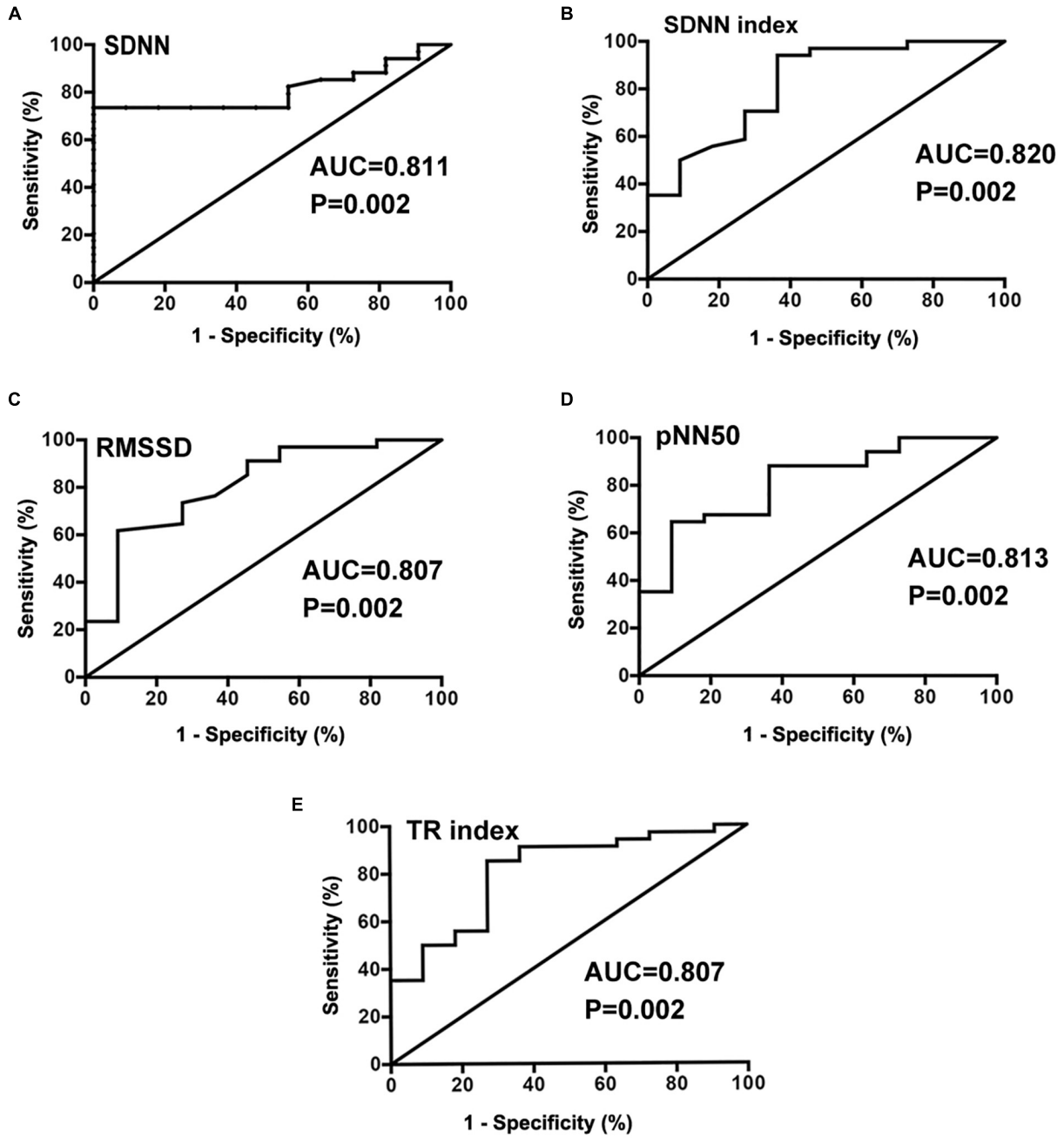

FIGURE 2 | Receiver operating characteristic (ROC) curve analysis of HRV time domain indexes of SDNN $_{(log2)}$ **(A)**, SDNN index **(B)**, RMSSD **(C)**, pNN50 **(D)**, and TR index **(E)** as predictors of therapeutic response to metoprolol in children with POTS.

clinical issue to investigate. Previous studies suggested that metoprolol could achieve better therapeutic effects in children with high catecholamine level, high adrenergic status, and β-receptor hypersensitivity (Thieben et al., 2007). To predict responders to metoprolol before treatment, we used to test plasma norepinephrine, copeptin and CNP levels, attempting to find predictive measures for therapeutic responders to metoprolol before treatment of children with POTS (Benditt and Chen, 2012; Zhang et al., 2014; Zhao et al., 2014; Lin et al., 2015b). However, the instability of plasma norepinephrine, the complexity of plasma copeptin detection and the invasiveness of CNP detection limited their clinical use to a certain extent.

Heart rate variability as a predictive measure reflecting the modulation of autonomic nervous function with the advantages of non-invasiveness and easy to perform was hypothesized to help in predicting the therapeutic response to metoprolol in treating POTS in children (Zygmunt and Stanczyk, 2004).

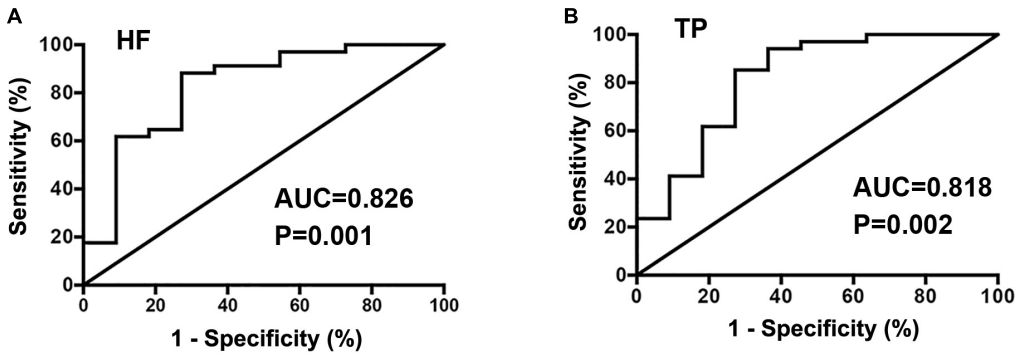

FIGURE 3 | Receiver operator characteristic curve analysis of HRV frequency domain indexes of HF **(A)** and TP **(B)** as predictors of therapeutic response to metoprolol in children with POTS.

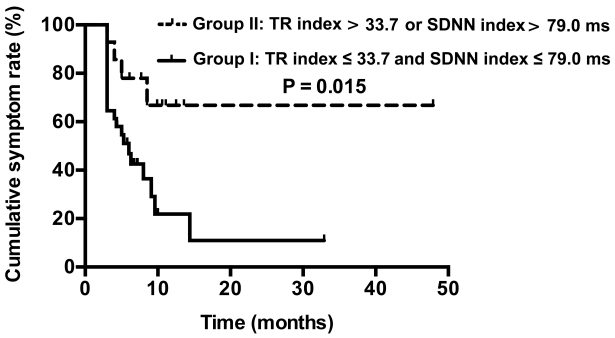

FIGURE 4 | Kaplan–Meier curve analysis of cumulative symptom rate between two groups of children with POTS. Group I: TR index $\leq$ 33.7 and SDNN index $\leq$ 79.0 ms, n = 31; Group II: TR index $>$ 33.7 and SDNN index $\leq$ 79.0 ms, TR index $\leq$ 33.7 and SDNN index $>$ 79.0 ms, or TR index $>$ 33.7 and SDNN index $>$ 79.0 ms, n = 14.

The immediate HR is the result of the interaction between the sympathetic and vagal nerves, which suggests that the two are constantly coordinated to produce a difference in HR. HRV reflects changes in HR over a long period. When the HRV is within a certain range, the vagal-sympathetic nerve system is well-regulated. That is to say, the child has a certain reserve capacity in the nervous system. Nevertheless, when it functions beyond the reserve capacity, it will manifest as a clinical symptom dominated by sympathetic or vagal nerves. In the present study, we employed 24-h HRV analysis to see if it is useful for predicting the therapeutic response to metoprolol in pediatric POTS. The reason that we used 24-h HRV analysis, including daytime HRV data, is that for POTS cases, the pathogenesis is closely related to postural change from supine to upright and such a postural change often occurs during the daytime. Actually, patients with POTS have the disproportionately enhanced sympathetic activity and vagal withdrawal during sitting or standing (Baker et al., 2018), which are often at daytime. Such alterations in autonomic nervous system function in children with POTS were also demonstrated during the HUTT (Stewart, 2000). While, we did not find any differences in nighttime HRV between POTS and normal controls, which accorded with the findings in previous studies (Mallien et al., 2014), nor between responders and non-responders to metoprolol. The above facts support us to use 24-h HRV recording to analyze the abnormal autonomic nervous function in children with POTS to predict therapeutic response to metoprolol in pediatric POTS. Of course, we should pay attention to the fact that 24-h HRV is also influenced by physical activities on daytime in the clinical evaluation.

To examine whether baseline 24-h HRV indices could predict the therapeutic response to metoprolol in children with POTS before treatment, we found that LF/HF ratio were higher in responders but other HRV indicators were lower than in non-responders before metoprolol treatment. The results suggested that the baseline indicators of sympathetic and vagal nervous tone were significantly lower in responders than non-responders before metoprolol treatment, but the ratio of sympathetic to vagal nervous modulation was significantly higher in responders than non-responders before metoprolol treatment. That is to say, before metoprolol treatment for POTS, responders to metoprolol had a predominant baseline sympathetic nervous modulation as compared with non-responders. Also, metoprolol achieves its therapeutic effects by inhibiting excessive sympathetic modulation by blocking beta receptors (Mizumaki, 2011).

Additionally, we further showed that when we combined TR index $\leq$ 33.7 and SDNN index $\leq$ 79.0 ms as the cut-off values to predict the short-term efficacy of metoprolol in children with POTS, the sensitivity, specificity, and accuracy were 85.3, 81.8, and 84.4%, respectively. We further confirmed that the combined TR index $\leq$ 33.7 and SDNN index $\leq$ 79.0 ms were useful as effective predictors for long-term outcome after metoprolol treatment. Therefore, HRV indicators may be non-invasive and easy-to-use predictors that could be used to predict the efficacy of metoprolol for POTS in children before the implication of the treatment.

However, our research still had limitations. This study was from a single center, and the case number was not sufficiently large. Also, sympathetic nervous activity was not directly measured. The 24-h HRV is influenced by the

physical activities on daytime, which needs the patients to avoid strenuous exercise and emotional excitement. The present study provided non-invasive and easy-to-use effective predictors for the therapeutic response to metoprolol in children with POTS, which would provide great help for deciding whether to choose metoprolol for pediatric POTS. In the future, multi-center studies should be conducted to validate the study findings.

DATA AVAILABILITY STATEMENT

The datasets generated for this study are available on request to the corresponding author.

ETHICS STATEMENT

The studies involving human participants were reviewed and approved by the Ethics Committee of the First Hospital of Peking University (2018 [202]). Written informed consent to participate in this study was provided by the participants legal guardian/next of kin.

AUTHOR CONTRIBUTIONS

JD, HJ, CT, and YYW conceived and designed the study. YYW, CZ, SC, and PL acquired the data. YYW and CZ analyzed and interpreted the data. YYW, HJ, and JD drafted the manuscript. CZ, SC, PL, and YLW revised the manuscript for important intellectual content. YYW, CZ, SC, PL, YLW, CT, JD, and HJ approved the final version to be submitted.

FUNDING

This study was supported by the Science and Technology Program of Beijing (Z171100001017253), Peking University Clinical Scientist Program (BMU2019LCKXJ001, Beijing), and Fundamental Research Funds for the Central Universities.

SUPPLEMENTARY MATERIAL

The Supplementary Material for this article can be found online at: https://www.frontiersin.org/articles/10.3389/fnins.2019.01214/full#supplementary-material

REFERENCES

Bagai, K., Song, Y., Ling, J. F., Malow, B., Black, B. K., Biaggioni, I., et al. (2011). Sleep disturbances and diminished quality of life in postural tachycardia syndrome. *J. Clin. Sleep Med.* 7, 204–210.

Baker, J., Racosta, J. M., and Kimpinski, K. (2018). Comparison fo heart rate variability parameters to the autonomic reflex screen in postural orthostatic tachycardia syndrome and neurogenic orthostatci hypotension. *J. Clin. Neurophysiol.* 35, 115–122. doi: 10.1097/WNP.0000000000000436

Benditt, D. G., and Chen, L. Y. (2012). Peptides in postural orthostatic tachycardia syndrome: players or epiphenomena? *J. Am. Coll. Cardiol.* 60, 321–333. doi: 10.1016/j.jacc.2012.04.021

Bryarly, M., Phillips, L. T., Fu, Q., Vernino, S., and Levine, B. D. (2019). Postural orthostatic tachycardia syndrome: JACC focus seminar. *J. Am. Coll. Cardiol.* 73, 1207–1228. doi: 10.1016/j.jacc.2018.11.059

Chen, L., Wang, L., Sun, J. H., Qin, J., Tang, C. S., Jin, H. F., et al. (2011). Midodrine hydrochloride is effective in the treatment of children with postural orthostatic tachycardia syndrome. *Circ. J.* 75, 927–931. doi: 10.1253/circj.cj-10-0514

Cygankiewicz, I., and Zareba, W. (2013). Heart rate variability. *Handb. Clin. Neurol.* 117, 379–393. doi: 10.1016/B978-0-444-53491-0.00031-6

Fedorowski, A. (2019). Postural orthostatic tachycardia syndrome: clinical presentation, aetiology and management. *J. Intern. Med.* 285, 352–366. doi: 10.1111/joim.12852

Fedorowski, A., Li, H., Yu, X., Koelsch, K. A., Harris, V. M., Liles, C., et al. (2017). Antiadrenergic autoimmunity in postural tachycardia syndrome. *Europace* 19, 1211–1219. doi: 10.1093/europace/euw154

Kainuma, M., Furusyo, N., Ando, S., Mukae, H., Ogawa, E., Toyoda, K., et al. (2014). Nocturnal difference in the ultra low frequency band of heart rate variability in patients stratified by kampo medicine prescription. *Circ. J.* 78, 1924–1927. doi: 10.1253/circj.cj-14-0362

Kernan, S., and Tobias, J. D. (2010). Perioperative care of an adolescent with postural orthostatic tachycardia syndrome. *Saudi J. Anaesth.* 4, 23–27. doi: 10.4103/1658-354X.62611

Kizilbash, S. J., Ahrens, S. P., Bruce, B. K., Chelimsky, G., Driscoll, S. W., Harbeck-Weber, C., et al. (2014). Adolescent fatigue, POTS, and recovery: a guide for clinicians. *Curr. Probl. Pediatr. Adolesc. Health Care* 44, 108–133. doi: 10.1016/j.cppeds.2013.12.014

Ladage, D., Schwinger, R. H., and Brixius, K. (2013). Cardio-selective beta-blocker: pharmacological evidence and their influence on exercise capacity. *Cardiovasc. Ther.* 31, 76–83. doi: 10.1111/j.1755-5922.2011.00306.x

Lai, C. C., Fischer, P. R., Brands, C. K., Fisher, J. L., Porter, C. J., Driscoll, S. W., et al. (2009). Outcomes in adolescents with postural orthostatic tachycardia syndrome treated with midodrine and β-blockers. *Pacing Clin. Electrophysiol.* 32, 234–238. doi: 10.1111/j.1540-8159.2008.02207.x

Li, H. X., Wang, Y. L., Liu, P., Chen, Y. H., Feng, X. L., Tang, C. S., et al. (2016). Body mass index (BMI) is associated with the therapeutic response to oral rehydration solution in children with postural tachycardia syndrome. *Pediatr. Cardiol.* 37, 1313–1318. doi: 10.1007/s00246-016-1436-1

Liao, Y., Chen, S., Liu, X. Q., Zhang, Q. Y., Ai, Y., Wang, Y. L., et al. (2010). Flow-mediated vasodilation and endothelium function in children with postural orthostatic tachycardia syndrome. *Am. J. Cardiol.* 106, 378–382. doi: 10.1016/j.amjcard.2010.03.034

Liao, Y., Yang, J., Zhang, F. W., Chen, S., Liu, X. Q., Zhang, Q. Y., et al. (2013). Flow-mediated vasodilation as a predictor of therapeutic response to midodrine hydrochloride in children with postural orthostatic tachycardia syndrome. *Am. J. Cardiol.* 112, 816–820. doi: 10.1016/j.amjcard.2013.05.008

Lin, J., Han, Z. H., Li, H. X., Chen, S. Y., Li, X. Y., Liu, P., et al. (2015a). Plasma C-type natriuretic peptide as a predictor for therapeutic response to metoprolol in children with postural tachycardia syndrome. *PLoS One* 10:e0121913. doi: 10.1371/journal.pone.0121913

Lin, J., Wang, Y. L., Ochs, T., Tang, C. S., Du, J. B., and Jin, H. F. (2015b). Tilt angles and positive response of head-up tilt test in children with orthostatic intolerance. *Cardiol. Young* 25, 76–80. doi: 10.1017/S1047951113001601

Malik, M., Farrell, T., Cripps, T., and Camm, A. J. (1989). Heart rate variability in relation to prognosis after myocardial infarction: selection of optimal processing techniques. *Eur. Heart J.* 10, 1060–1074. doi: 10.1093/oxfordjournals.eurheartj.a059428

Mallien, J., Lsenmann, S., Mrazek, A., and Haensch, C.-A. (2014). Sleep disturbances and autonomic dysfunction in patients with postural orthostatic tachycarida syndrome. *Front. Neurol.* 5:118. doi: 10.3389/fneur.2014.00118

Mizumaki, K. (2011). Postural orthostatic tachycardia syndrome (POTS). *J. Arrhythmia* 27, 289–306. doi: 10.1016/s1880-4276(11)80031-1

Myers, G., Workman, M., Birkett, C., Ferguson, D., and Kienzle, M. (1992). Problems in measuring heart rate variability of patients with congestive heart failure. *J. Electrocardiol.* 25, 214–219. doi: 10.1016/0022-0736(92)90105-9

Nguyen, N., Vandenbroucke, L., Hernandez, A., Pham, T., Beuchee, A., Pladys, P., et al. (2017). Early-onset neonatal sepsis is associated with a high heart rate during automatically selected stationary periods. *Acta Paediatr.* 106, 749–754. doi: 10.1111/apa.13782

Schisterman, E. F., Perkins, N. J., Liu, A., and Bondell, H. (2005). Optimal cut-point and its corresponding Youden index to discriminate individuals using pooled blood samples. *Epidemiology* 16, 73–81. doi: 10.1097/01.ede.0000147512.81966.ba

Shannon, J. R., Flattem, N. L., Jordan, J., Jacob, G., Jacob, G., Black, B. K., et al. (2000). Orthostatic intolerance and tachycardia associated with norepinephrine-transporter deficiency. *N. Engl. J. Med.* 324, 541–548. doi: 10.1056/NEJM200002243420803

Sheldon, R. S., Grubb, B. P., Olshansky, B., Shen, W.-K., Calkins, H., Brignole, M., et al. (2015). 2015 Heart Rhythm Society Expert consensus statement on the diagnosis and treatment of postural tachycardia syndrome, inappropriate sinus tachycardia, and vasovagal syncope. *Heart Rhythm.* 12, e41–e63. doi: 10.1016/j.hrthm.2015.03.029

Spahic, J. M., Ricci, F., Aung, N., Axelsson, J., Melander, O., Sutton, R., et al. (2019). Proconvertase furin is downregulated in postural orthostatic tachycardia syndrome. *Front. Neurosci.* 13:301. doi: 10.3389/fnins.2019.00301

Stewart, J. M. (2000). Autonomic nerous system dysfunction in adolescents with postural orthostatic tachycardia syndrome and chronic fatigue syndrome is characterized by attenuated vagal baroreflex and potentiated sympathetic vasomotion. *Pediatr. Res.* 48, 218–226. doi: 10.1203/00006450-200008000-00016

Stewart, J. M., Boris, J. R., Chelimsky, G., Fischer, P. R., Fortunato, J. E., Grubb, B. P., et al. (2018). Pediatric disorders of orthostatic intolerance. *Pediatrics* 141:e20171673. doi: 10.1542/peds.2017-1673

Sztajzel, J. (2004). Heart rate variability: a noninvasive electrocardiographic method to measure the autonomic nervous system. *Swiss Med. Wkly* 134, 514–522.

Thieben, M. J., Sandroni, P., Sletten, D. M., Benrud-Larson, L. M., Fealey, R. D., Vernino, S., et al. (2007). Postural orthostatic tachycardia syndrome: the Mayo clinic experience. *Mayo Clin. Proc.* 82, 308–313. doi: 10.4065/82.3.308

Wang, C., Li, Y., Liao, Y., Tian, H., Huang, M., Dong, X. Y., et al. (2018). 2018 Chinese Pediatric Cardiology Society (CPCS) guideline for diagnosis and treatment of syncope in children and adolescents. *Sci. Bull.* 63, 1558–1564. doi: 10.1016/j.scib.2018.09.019

Wang, Y., Zhang, C., Chen, S., Li, X., Jin, H., and Du, J. (2019). Frequency domain indices of heart rate variability are useful for differentiating vasovagal syncope and postural tachycardia syndrome in children. *J. Pediatr.* 207, 59–63. doi: 10.1016/j.jpeds.2018.11.054

Winker, R., Barth, A., Bidmon, D., Ponocny, I., Weber, M., Mayr, O., et al. (2005). Endurance exercise training in orthostatic intolerance: a randomized, controlled trial. *Hypertension* 45, 391–398. doi: 10.1161/01.HYP.0000156540.25707.af

Young, H. A., and Benton, D. (2018). Heart-rate variability: a biomarker to study the influence of nutrition on physiological and psychological health? *Behav. Pharmacol.* 29, 140–151. doi: 10.1097/FBP.0000000000000383

Zaravko, Z. T., Kiril, V. T., and Stefan, S. K. (2015). Heart rate variability as a method for assessment of the autonomic nervous system and the adaptations to different physiological and pathological conditions. *Folia Med.* 57, 173–180. doi: 10.1515/folmed-2015-0036

Zhang, Q. Y., Chen, X., Li, J. W., and Du, J. B. (2014). Orthostatic plasma norepinephrine level as a predictor for therapeutic response to metoprolol in children with postural tachycardia syndrome. *J. Transl. Med.* 12, 2–6. doi: 10.1111/j.1755-5922.2011.00306.x

Zhang, Q. Y., Liao, Y., Tang, C. S., Du, J. B., and Jin, H. F. (2012). Twenty-four-hour urinary sodium excretion and postural orthostatic tachycardia syndrome. *J. Pediatr.* 161, 281–284. doi: 10.1016/j.jpeds.2012.01.054

Zhao, J., Du, S. X., Yang, J. Y., Lin, J., Tang, C. S., Du, J. B., et al. (2014). Usefulness of plasma copeptin as a biomarker to predict the therapeutic effectiveness of metoprolol for postural tachycardia syndrome in children. *Am. J. Cardiol.* 114, 601–605. doi: 10.1016/j.amjcard.2014.05.039

Zygmunt, A., and Stanczyk, J. (2004). Heart rate variability in children with neurocardiogenic syncope. *Clin. Auton. Res.* 14, 99–106. doi: 10.1007/s10286-004-0168-0

Conflict of Interest: The authors declare that the research was conducted in the absence of any commercial or financial relationships that could be construed as a potential conflict of interest.

frontiers in Neuroscience

REVIEW
published: 12 November 2019
doi: 10.3389/fnins.2019.01197

Pubertal Hormonal Changes and the Autonomic Nervous System: Potential Role in Pediatric Orthostatic Intolerance

*Kassandra E. Coupal[1], Natalie D. Heeney[1], Brooke C. D. Hockin[1], Rebecca Ronsley[2], Kathryn Armstrong[3], Shubhayan Sanatani[3] and Victoria E. Claydon[1]**

[1] Department of Biomedical Physiology and Kinesiology, Simon Fraser University, Burnaby, BC, Canada, [2] Department of Pediatrics, BC Children's Hospital, Vancouver, BC, Canada, [3] Children's Heart Centre, BC Children's Hospital, Vancouver, BC, Canada

Puberty is initiated by hormonal changes in the adolescent body that trigger physical and behavioral changes to reach adult maturation. As these changes occur, some adolescents experience concerning pubertal symptoms that are associated with dysfunction of the autonomic nervous system (ANS). Vasovagal syncope (VVS) and Postural Orthostatic Tachycardia Syndrome (POTS) are common disorders of the ANS associated with puberty that are related to orthostatic intolerance and share similar symptoms. Compared to young males, young females have decreased orthostatic tolerance and a higher incidence of VVS and POTS. As puberty is linked to changes in specific sex and non-sex hormones, and hormonal therapy sometimes improves orthostatic symptoms in female VVS patients, it is possible that pubertal hormones play a role in the increased susceptibility of young females to autonomic dysfunction. The purpose of this paper is to review the key hormonal changes associated with female puberty, their effects on the ANS, and their potential role in predisposing some adolescent females to cardiovascular autonomic dysfunctions such as VVS and POTS. Increases in pubertal hormones such as estrogen, thyroid hormones, growth hormone, insulin, and insulin-like growth factor-1 promote vasodilatation and decrease blood volume. This may be exacerbated by higher levels of progesterone, which suppresses catecholamine secretion and sympathetic outflow. Abnormal heart rate increases in POTS patients may be exacerbated by pubertal increases in leptin, insulin, and thyroid hormones acting to increase sympathetic nervous system activity and/or catecholamine levels. Given the coincidental timing of female pubertal hormone surges and adolescent onset of VVS and POTS in young women, coupled with the known roles of these hormones in modulating cardiovascular homeostasis, it is likely that female pubertal hormones play a role in predisposing females to VVS and POTS during puberty. Further research is necessary to confirm the effects of female pubertal hormones on autonomic function, and their role in pubertal autonomic disorders such as VVS and POTS, in order to inform the treatment and management of these debilitating disorders.

Keywords: puberty, syncope, orthostatic intolerance, vasovagal, POTS

OPEN ACCESS

Edited by:
Maurizio Acampa, Siena University Hospital, Italy

Reviewed by:
Elisabeth Lambert, Swinburne University of Technology, Australia
Junbao Du, Peking University First Hospital, China

****Correspondence:***
Victoria E. Claydon
victoria_claydon@sfu.ca

Specialty section:
This article was submitted to Autonomic Neuroscience, a section of the journal Frontiers in Neuroscience

Received: *13 August 2019*
Accepted: *22 October 2019*
Published: *12 November 2019*

Citation:
Coupal KE, Heeney ND, Hockin BCD, Ronsley R, Armstrong K, Sanatani S and Claydon VE (2019) Pubertal Hormonal Changes and the Autonomic Nervous System: Potential Role in Pediatric Orthostatic Intolerance. Front. Neurosci. 13:1197. doi: 10.3389/fnins.2019.01197

INTRODUCTION

Puberty Is Associated With Orthostatic Intolerance

Puberty is a period of adolescence in which a child undergoes rapid changes that affect physical and mental functioning in order to reach adult maturation. During this time many adolescents experience substantial fatigue, mood swings, and stress (Larson et al., 1980). These symptoms of puberty are well-known and not generally worrisome (Larson et al., 1980; Wheeler, 1991; Viner and Christie, 2005; **Table 1**). However, other physical symptoms can occur at the onset of puberty that reflect autonomic nervous system (ANS) dysfunction, compromising the homeostatic regulation of basic bodily functions (Palma et al., 2017; **Table 2**). For example, puberty is associated with an increased incidence of syncope (fainting: transient loss of consciousness and postural tone) or presyncope (near-fainting), particularly in females (Walsh, 2001).

Syncope and presyncope are common across the lifespan, but have a particularly high incidence in adolescents, with a peak age of onset during puberty at age ∼10–15 years (**Figure 1**); approximately 1 in three adolescents with syncope experience recurrent and severe episodes (de Jong-de Vos van Steenwijk et al., 1995; Driscoll et al., 1997; McLeod, 2003; Kenny et al., 2010; Kanjwal and Calkins, 2015). However, this prevalence is likely underestimated because many do not report their symptoms (Wieling et al., 2004; Ganzeboom et al., 2006; Nordkamp et al., 2009). Episodes are often related to impaired autonomic function, and are associated with anxiety, fatigue, headaches, dizziness, abdominal discomfort, nausea, and weakness, with significant impairments in quality of life (Braune et al., 1999; Rose et al., 2000; Radtke et al., 2011; Anderson et al., 2012; Armstrong et al., 2017). In pediatric populations, morbidity is equivalent to patients with asthma, end-stage renal disease and structural heart disease (Linzer et al., 1991; Anderson et al., 2012). Recurrent episodes are associated with injury due to falls secondary to loss of postural control, and may indicate more widespread autonomic abnormalities (Hainsworth et al., 2012). Affected children find these episodes distressing and exhibit sleep disturbances and difficulty concentrating, attending and focusing at school (Carapetian et al., 2008), as well as problems with exercising and participating in activities of daily living (Braune et al., 1999; Rose et al., 2000; Radtke et al., 2011; Anderson et al., 2012; Raj, 2013; Armstrong et al., 2017). The burden on healthcare resources is also substantial, with frequent medical and emergency visits (Kanjwal and Calkins, 2015) and extensive investigation – up to 35% see 10–20 physicians before diagnosis (Armstrong et al., 2017) and 10% of individuals still do not have a diagnosis 1 year after presenting in clinic (Van Dijk et al., 2007). Given their high incidence, marked healthcare burden, and severe impact on quality of life, a better understanding of the predisposing factors to adolescent syncope and presyncope and the potential role for pubertal hormones is warranted.

TABLE 1 | Typical features of puberty.

Physical changes	Mental/Emotional changes
Breast, penis, testicle development	Mood swings – aggression, emotional surges, bouts of crying
Body hair – appearance in armpits and pubic area	Changes in sleep patterns and fatigue
Growth spurts and weight gain	Changes in social behavior
Menstruation and menstrual symptoms – nausea, cramps, bloating, diarrhea, aching in upper thighs, headache, backache, stomach ache	Menstrual symptoms – changes in appetite
Widening of the hips/shoulders	Risk-taking/novelty-seeking behaviors
Increased subcutaneous fat distribution/muscle development	Cognitive development

Typical physical and mental/emotional changes are shown. Adapted from Larson et al. (1980), Wheeler (1991), and Viner and Christie (2005).

TABLE 2 | Concerning features of puberty.

Physical changes
Dizziness and syncope upon standing
Exercise intolerance
Sweating abnormalities – hyperhidrosis or hypohidrosis
Digestive difficulties – loss of appetite, bloating unrelated to menstruation
Urinary problems – difficulty urinating, incontinence, incomplete bladder emptying
Sexual dysfunction
Vision problems – blurred vision or inability for pupils to react to light quickly

Concerning autonomic abnormalities associated with puberty are shown. Adapted from Palma et al. (2017).

Syncope has many causes, including structural heart disease, cardiac arrhythmia, and impaired orthostatic cardiovascular control (Hainsworth et al., 2012). Here we focus on orthostatic (postural) syncope and presyncope, the most common forms in children and adolescents (Hainsworth et al., 2012). The most common sub-type of orthostatic syncope associated with puberty is vasovagal syncope (VVS) (Da and da Silva, 2014), responsible for up to 80% of pediatric syncope cases (Massin et al., 2004). Another condition that often coincides with the onset of puberty and presents with similar symptoms to VVS is Postural Orthostatic Tachycardia Syndrome (POTS) (Stewart, 2009). Both these conditions are associated with orthostatic intolerance, where the ANS does not function properly during changes in position or orthostatic stress. In broad terms, VVS reflects an excessive decrease in blood pressure and/or heart rate during orthostasis (Medow et al., 2008), while POTS displays an excessive increase in heart rate with orthostatic stress, with variable changes in blood pressure (Low, 2014).

The hormonal factors that initiate the onset and maintenance of puberty must be considered as possible culprits in the associated increased susceptibility to disorders of orthostatic intolerance, considering the timing of increased incidence of POTS and VVS with puberty (Kenny et al., 2010; Shaw et al., 2019; **Figure 1**). The initiation of puberty is prompted by a rise in activity of the hypothalamic-pituitary-gonadal (HPG) axis following a prolonged period of suppression

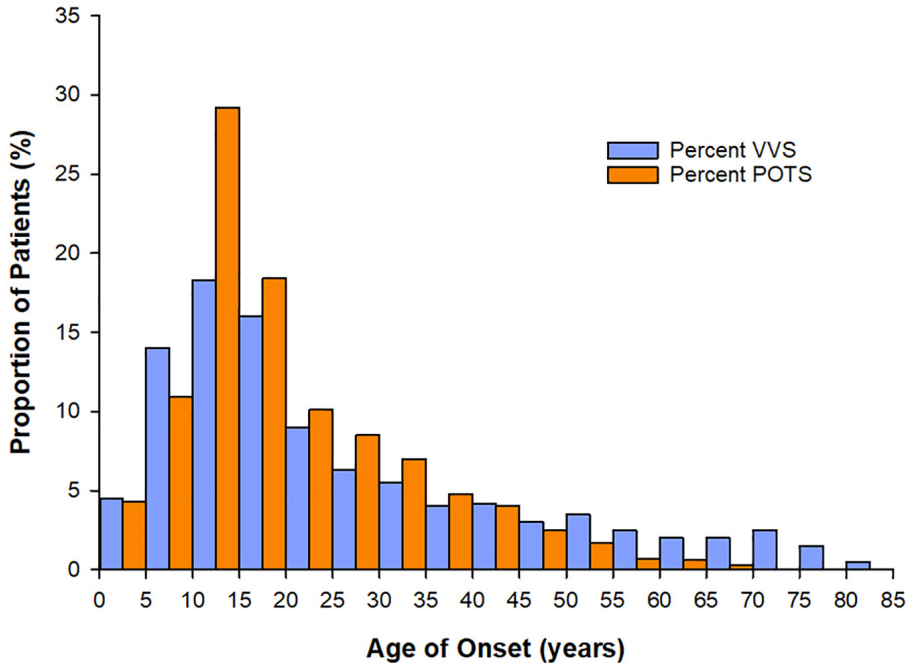

FIGURE 1 | Age at onset of vasovagal syncope (VVS) and Postural Orthostatic Tachycardia Syndrome (POTS). For both patients with VVS (n = 443) and POTS (n = 4835) the peak age of onset of symptoms is between 10–15 years – coinciding with the age of onset of puberty. Data sourced from Kenny et al. (2010), Shaw et al. (2019).

during childhood (Forbes and Dahl, 2010). The HPG axis increases pulsatile release of gonadotropin-releasing hormones (GnRHs), stimulating gonadal hormones, and inducing various changes throughout the body to stimulate sexual maturation (Forbes and Dahl, 2010). Puberty is further associated with changes in other non-gonadal hormones such as GH, thyroid hormone, leptin, cortisol, and melatonin, which facilitate physical growth and behavioral changes in adolescents (**Figure 2**).

Females are known to have lower orthostatic tolerance compared to males (Meendering et al., 2005), with a 5:1 predominance of POTS (Low et al., 2009) and more than twice the incidence of syncope (Wieling et al., 2004). Since the initiation of puberty is prompted by a rise in activity of the HPG axis inducing changes in sex hormones (Clemans et al., 2010), it may be that some of the increased susceptibility to autonomic dysfunction in pubertal females could be attributed to hormonal changes occurring during this stage. Indeed, females with known VVS are reported to experience significant improvements in their symptoms with the introduction of hormonal therapy (Boehm et al., 1997). Orthostatic tolerance also improves in women across the lifespan, and is highest in postmenopausal females (Protheroe et al., 2013). These observations support the potential role of pubertal hormones in increasing susceptibility to cardiovascular autonomic dysfunction. Accordingly, the purpose of this review is to identify the key hormonal changes associated with female puberty, their effects on the ANS, and their potential role in predisposing adolescent females to cardiovascular autonomic dysfunctions such as VVS and POTS.

Orthostasis Represents a Considerable Cardiovascular Challenge and Requires Compensation by the Autonomic Nervous System

Orthostasis is a common trigger for VVS and POTS because when a person is upright gravitational forces decrease arterial pressures in regions above the level of the heart, while simultaneously increasing lower body venous pooling and capillary filtration, reducing venous return (Hainsworth et al., 2012). If compensation for these hemodynamic consequences of orthostasis is inadequate, cardiac output is reduced and cerebral perfusion compromised, causing symptoms of presyncope that can progress to syncope (Hainsworth et al., 2012).

Orthostatic reductions in arterial pressure are sensed primarily by baroreceptors located in the aortic arch, coronary arteries, and carotid sinus (Hall and Guyton, 2011). The carotid sinus baroreceptors are particularly important in responding to orthostatic hemodynamic changes because of their location above the heart (carotid arterial pressure is about 15 mmHg lower than the pressure at the aortic root when upright, providing a potent stimulus to the carotid baroreceptors) (Hainsworth et al., 2012). Accordingly, during orthostasis these baroreceptors are unloaded, resulting in a reflex decrease in cardiac parasympathetic (vagal) tone, and increase in sympathetic outflow from the vasomotor center in the medulla

to the heart and blood vessels (Hall and Guyton, 2011). The combined effect of these compensatory influences on the heart are increases in heart rate and contractility, accompanied by sympathetically mediated vasoconstriction of the resistance and capacitance vessels in the splanchnic, musculocutaneous, and renal vascular beds (Smit et al., 1999; Hall and Guyton, 2011). These coordinated adaptations are, therefore, associated with increases in total peripheral resistance, stroke volume, and blood pressure, with the maintenance of cardiac output and consequently cerebral perfusion (Medow et al., 2008). Given that these compensatory mechanisms are chiefly mediated by the ANS, impaired autonomic responses can predispose to loss of orthostatic control (Medow et al., 2008), leading to presyncope or syncope.

Orthostatic Cardiovascular Responses Are Impaired in Patients With Vasovagal Syncope and Postural Orthostatic Tachycardia Syndrome

Ultimately, the cause of orthostatic presyncope or syncope is a failure of normal cardiovascular autonomic responses. However, different patterns of responses occur representing distinct autonomic syndromes, and this complicates their diagnosis and treatment. In POTS the primary problem is excessive orthostatic tachycardia, whereas in VVS it is impaired vasoconstriction and sudden hypotension, with or without reflex bradycardia or asystole (van Lieshout et al., 1991; McLeod, 2003; Hainsworth, 2004; Brignole, 2005; Mathias et al., 2012). These abnormalities can be subdivided further and may even coexist (Kurbaan et al., 1999; Brignole et al., 2000; Schroeder et al., 2011); however, the underlying mechanisms of these disorders remain unclear, particularly in children and adolescents.

Postural Orthostatic Tachycardia Syndrome is defined as "the development of orthostatic symptoms associated with a HR increment $\geq$30 bpm (beats per minute) [$\geq$40 bpm in children (Singer et al., 2012; Zhao et al., 2015)], usually to $\geq$120 bpm [$\geq$125 bpm in children aged 13–18 years or $\geq$130 bpm in children aged 6–12 years (Singer et al., 2012; Zhao et al., 2015)] without orthostatic hypotension" (Low et al., 2009). It is not clear what drives the change in cardiac responsiveness and the precise age at which this change occurs is unclear; pediatric POTS has been defined for chronological ages 12 years and younger (Kurbaan et al., 1999), but this definition does not reflect physiological age or pubertal status.

Postural Orthostatic Tachycardia Syndrome includes at least four subtypes: hyperadrenergic POTS with excessive sympathetic discharge; hypovolemic POTS (with compensatory tachycardia); neuropathic POTS with impaired vasoconstriction and compensatory tachycardia; and, rarely, noradrenaline transporter deficiency with synaptic noradrenaline accumulation (Low et al., 1995, 2009; Raj, 2013). Hemodynamic subtypes of VVS have also been recognized, and are characterized according to the relative contribution of hypotension and/or bradycardia to the event (Brignole et al., 2000). These distinctions provide mechanistic insight and may inform treatment, but present similarly, so are difficult to distinguish clinically. Whether adolescence is a time of general autonomic imbalance, and whether susceptibility to VVS and POTS are related to adolescence or pubertal hormone changes is unknown.

We and others demonstrated that in both patients with POTS and VVS, excessive venous pooling or capillary filtration (Brown and Hainsworth, 1999; Stewart et al., 2004), thermoregulatory vasodilation (Wilson et al., 2006; Hainsworth et al., 2012), low plasma or blood volumes (El-Sayed et al., 1995; Hoeldtke et al., 1995; El-Sayed and Hainsworth, 1996; Jacob et al., 1997; Mtinangi and Hainsworth, 1998, 1999; Lagi et al., 2003; Claydon et al., 2004), abnormal baroreflex responses (Thomson et al., 1997; Furlan et al., 1998; Gulli et al., 2001, 2005a,b; Cooper and Hainsworth, 2002), concurrent hypocapnia (Novak et al., 1998; Blaber et al., 2001; Carey et al., 2001; Lagi et al., 2001; Gisolf et al., 2004), excessive vascular responses to hypocapnia (Norcliffe-Kaufmann et al., 2007), and impaired cerebral autoregulation (Daffertshofer et al., 1991; Grubb et al., 1991; Claydon and Hainsworth, 2003) all increase susceptibility to orthostatic syncope in adults. In adults with VVS there is some evidence that the hypotension and reduced vascular resistance during hemodynamic collapse at presyncope may not be due to blunted sympathetic nerve activity *per se* but rather to other competing vasodilatory influences at that time (Vaddadi et al., 2010). There may also be an autoimmune component to susceptibility to both POTS and VVS in adults (Etienne and Weimer, 2006; Li et al., 2015; Ruzieh et al., 2017). These mechanistic insights have been central to the development of tailored management for affected adults; however, contributing mechanisms in children are less clear.

There may be a role for early excessive orthostatic cardiac sympathetic activation, and yet blunted vasoconstriction in children with POTS and VVS (Wieling et al., 1997; Moak et al., 2002; Laranjo et al., 2015; Wagoner et al., 2016), suggesting a disconnect between sympathetic outflow and the effector organ response. Indeed, some forms of POTS reflect selective neuropathy, with sympathetic denervation and impaired vascular resistance responses affecting the lower limbs (Raj, 2013). In children with VVS, initial increases in sympathetically–mediated vascular resistance responses are not sustained, and in fact abruptly reverse, precipitating hypotension (Moak et al., 2002). Orthostatic vasopressin and aldosterone are increased in children with VVS (Wagoner et al., 2016), presumably to compensate for impaired sympathetically–mediated vasoconstriction. Children with VVS and some forms of POTS have excessive venous pooling, particularly in the splanchnic vasculature (Stewart et al., 2004, 2006). Vitamin B12 deficiency (Wieling et al., 1997), low ferritin, and iron deficiency are reported in children with syncope (Antiel et al., 2011; Guven et al., 2013; Jarjour and Jarjour, 2013), presumably contributing to symptoms through anemia and low blood volumes.

Regardless of the underlying mechanism, orthostatic symptoms in children are associated with decreased cerebral blood flow velocity (Sung et al., 2000). Whether this is due to impaired cardiovascular control and compromised cerebral perfusion, or primary abnormalities in cerebral autoregulation is unclear. Interestingly, in adults with VVS cerebral pressure autoregulation is impaired (Claydon and Hainsworth, 2003)

and combined with orthostatic hyperventilation (via activation of the respiratory muscle pump), with subsequent hypocapnia and cerebral vasoconstriction (Novak et al., 1998; Blaber et al., 2001; Carey et al., 2001; Lagi et al., 2001; Gisolf et al., 2004) that is compounded by increased cerebral reactivity to hypocapnia (Norcliffe-Kaufmann et al., 2007). The role and relative contribution of hypocapnia and cerebral autoregulation in pediatric syncope remain unclear.

Another contributor to most forms of orthostatic syncope in adults is hypovolemia, which may be associated with impaired renal sodium reabsorption in patients with POTS (Raj, 2013). Plasma or blood volume expansion improves orthostatic tolerance in adults (Rosen and Cryer, 1982; El-Sayed et al., 1995; Hoeldtke et al., 1995; El-Sayed and Hainsworth, 1996; Jacob et al., 1997; Mtinangi and Hainsworth, 1998, 1999; Lagi et al., 2003; Claydon et al., 2004; Cooper and Hainsworth, 2008), so it is possible that low plasma volumes also contribute to orthostatic syncope in children with POTS or VVS.

Lastly, physical deconditioning of the heart due to conditions such as viral infections or chronic fatigue has also been recognized as a possible mechanism underlying POTS (Fu et al., 2010). There is an association between POTS and cardiac deconditioning, and this is thought to be the result of a decreased heart size and associated decrease in cardiac output (Fu et al., 2010). The reasons why adolescent females are particularly susceptible to POTS remain unknown but perhaps their lower cardiac mass compared to adolescent males is a contributing factor.

HORMONAL CHANGES DURING FEMALE PUBERTY AND THEIR INFLUENCES ON CARDIOVASCULAR AUTONOMIC CONTROL

There are many hormonal changes during puberty that may have implications for autonomic cardiovascular control. Certainly, puberty seems to be a time of considerable change in autonomic function and cardiovascular and cerebrovascular regulation, with increases in endothelial function (Deda et al., 2015), and reductions in high frequency heart rate variability (a marker of cardiac vagal tone) in healthy adolescents following puberty (Tanaka et al., 2000). Puberty is also associated with increases in blood pressure (Tanaka et al., 2000; Deda et al., 2015), although this occurs to a much lesser extent in females than in males (Moran et al., 2008), with associated decreases in arterial stiffness during puberty in females, but not in males (Ahimastos et al., 2003). Cerebral blood flow is higher in children than in adults, and decreases markedly during puberty, with the peak reduction occurring in mid-adolescence (aged 15–17 years) – coinciding with the timing of peak incidence of syncope (Satterthwaite et al., 2014). In females, there is a partial recovery of cerebral blood flow in late puberty such that in adulthood, cerebral blood flow is greater in females compared to males (Satterthwaite et al., 2014) – coinciding with a time at which the particularly high incidence of onset of syncope in female adolescents begins to decrease. Some of these alterations in cerebral blood flow may reflect alterations in carbon dioxide levels. Higher end tidal carbon dioxide levels ($P_{ET}CO_2$) act as a potent cerebral vasodilator, increasing cerebral blood flow (Norcliffe et al., 2002; Claydon and Hainsworth, 2003). Young women breathe with an increased minute ventilation compared to young males (White et al., 1983), thus resting $P_{ET}CO_2$ is significantly higher in young males relative to young females (Dhokalia et al., 1998). This may render young women more susceptible to cerebral hypoperfusion and syncope, particularly in the face of orthostatic activation of the respiratory muscle pump and further associated increases in ventilation.

Qualification of Pubertal Stages in Females

Tanner staging is a universally accepted means of qualifying pubertal development, with five proposed stages described by written criteria and illustrations (Marshall and Tanner, 1970; Swerdloff and Odell, 1975; **Table 3**). Tanner stage I refers to the preadolescent stage, while Tanner stage V represents the mature state (Marshall and Tanner, 1970). Normal timing of puberty varies and a child's chronological age is not necessarily an accurate measure of pubertal development. Therefore, where possible, hormone levels are compared based on biological maturation stages rather than age. Given that sex hormones fluctuate in females depending on the phase of the menstrual cycle, overall changes in pubertal hormones will be considered independently of menstrual timing. A summary of the key hormones involved in the regulation of female puberty is provided in **Figure 2**.

Initiation of Puberty

Given the common coincidental timing of onset of symptoms of autonomic impairment and puberty, it is pertinent to consider the factors at play in initiating puberty, as well as the pubertal hormones that are involved as puberty progresses. The ultimate trigger for the onset of puberty is the initiation of profound increases in pulsatile GnRH secretion from the hypothalamus. The pulsatile nature of GnRH secretion with the onset of puberty is important, tonic GnRH administration does not induce luteinizing hormone (LH) or follicle stimulating hormone (FSH) secretion and so prevents ovulation (Marshall and Tanner, 1970).

TABLE 3 | The Tanner stages of puberty in females.

Tanner stage	Description
I	Preadolescent
II	Breast budding; early labial hair growth
III	Increased breast size with palpable glandular tissue; no separating of breast contours; moderately dark coarser labial hair over mons pubis
IV	Further enlargement of breasts with projection of areola above breast plane; lateral spread of pubic hair
V	Adult breast size and pubic hair distribution

Typical stages of puberty in girls are defined according to breast development and distribution of pubic hair. Adapted from Swerdloff and Odell (1975).

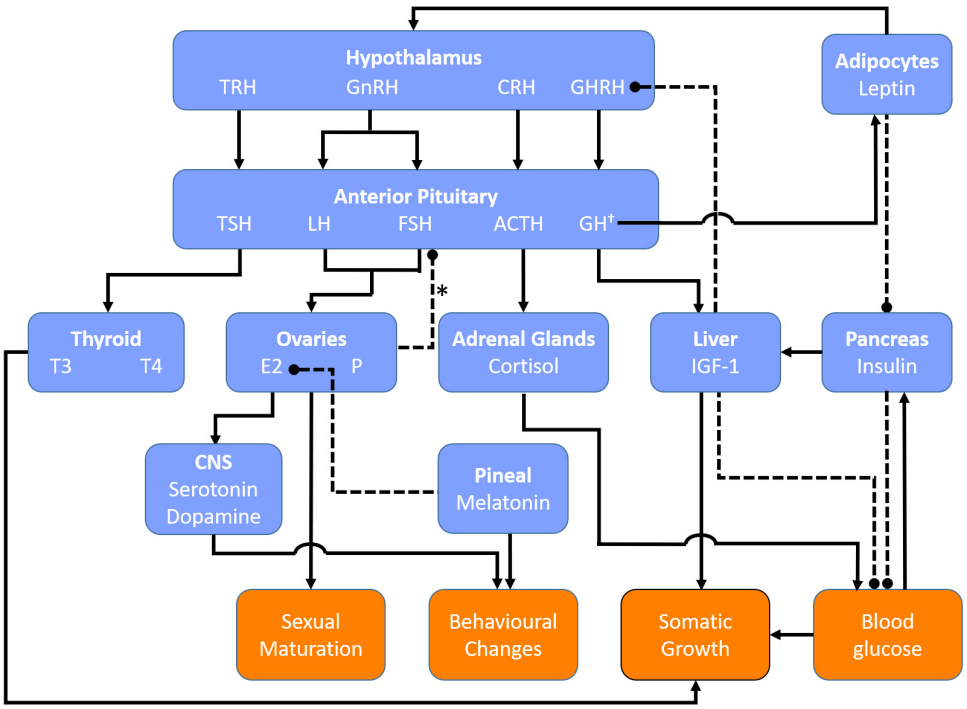

FIGURE 2 | Key regulatory hormones involved in female puberty. Blue boxes denote hormones and their source of release (bold). Orange boxes denote end organ responses. Solid lines indicate positive feedback. Dashed lines indicate negative feedback. *Negative feedback from the ovaries on FSH secretion is primarily mediated via inhibins secreted by ovarian follicles. †GH secretion is stimulated by estrogen and thyroid hormones. ACTH, adrenocorticotrophic hormone; CRH, corticotropin releasing hormone; CNS, central nervous system; E2, estradiol; GH, growth hormone; GHRH, growth hormone releasing hormone; GnRH, gonadotropin releasing hormone; IGF-1, insulin-like growth factor-1; P, progesterone, TRH, thyrotropin releasing hormone; TSH, thyroid stimulating hormone; T3, triiodothyronine; T4, thyroxine.

Numerous complementary mechanisms have been proposed to initiate the rise in pulsatile GnRH secretion (**Figure 3**). One key player is the loss of sensitivity to inhibition of GnRH secretion by ovarian sex steroids (such as estrogen and inhibins) (Gill et al., 2002; Shaw et al., 2010). Even very low levels of estrogen and inhibins block GnRH secretion in young children (Winter and Faiman, 1973). During puberty the levels of sex steroids required to block GnRH become progressively higher and this is permissive to increases in pulsatile GnRH, but not sufficient to trigger puberty (Messinis, 2006).

There may be a role for nutritional status and leptin in initiating puberty. Puberty starts earlier in overweight girls, and menstruation ceases with severe weight loss (Baker, 1985). Adiposity is linked to high leptin levels, and in animals leptin supplementation advances the onset of puberty compared to pair-fed animals (necessary because of the impact of leptin on appetite) – with leptin being permissive but not sufficient for the initiation of puberty (Cheung et al., 2001). This permissive role is likely via the indirect action of leptin (mediated via decreases in the antigonadotropic hormone, GnIH) on kisspeptin-expressing neurons that regulate GnRH secretion from the hypothalamus (Cunningham et al., 1999; Rhie, 2013). The arcuate nucleus contains abundant kisspeptin, a protein that is encoded by the Kiss1 gene, a GnRH pulse generating gene (Avendaño et al., 2017). Release of kisspeptin is inhibited until puberty when it rises and initiates increased pulsatile GnRH secretion. While it is likely that kisspeptin plays a major role in initiating puberty, the trigger for increased kisspeptin is unclear, with regulation suggested through either an internal "pubertal clock," or a "somatometer" that monitors somatic (perhaps skeletal) development and triggers kisspeptin secretion once a key developmental threshold is reached (Avendaño et al., 2017).

Melatonin secretion from the pineal gland also seems to regulate pubertal onset. Melatonin release occurs during sleep and darkness, with higher secretion during the winter when there are reduced daylight hours (Brainard et al., 1982). The human pineal gland produces a substance (s) that keeps sexual maturation in check, which may be melatonin and/or GnIH (Silman et al., 1979). Indeed, destructive tumors of the pineal gland are associated with precocious puberty, and hypersecretory tumors with delayed puberty (Kitay, 1954; Silman et al., 1979). At the onset of puberty, melatonin levels decrease and this is associated with initiation of pubertal development (Silman et al., 1979). Indeed, in children living near the equator, who have lower levels of melatonin because of the long daylight hours, puberty occurs earlier than in those at higher latitudes (Dossus et al., 2013), perhaps reflecting the role of melatonin in initiation of puberty (Murcia et al., 2002). Interestingly, the onset of pulsatile secretion of GnRH during puberty initially occurs only during rapid-eye-movement sleep (Shaw et al., 2015).

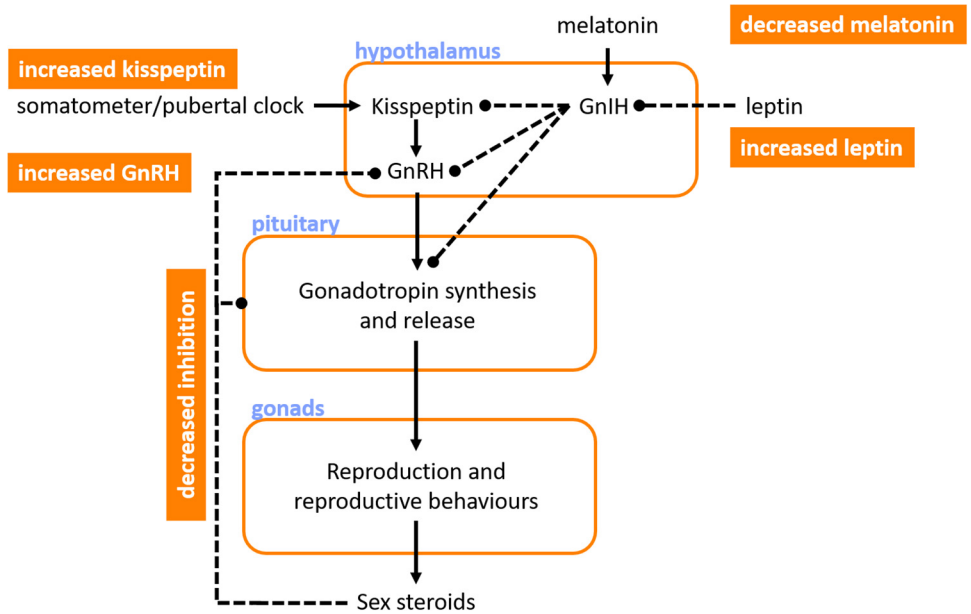

FIGURE 3 | Key hormones involved in the initiation of puberty. Ultimately, puberty is initiated by profound increases in gonadotropin releasing hormone (GnRH) that initiate cyclic synthesis and release of gonadotropins, which then regulate reproduction, reproductive behaviors and secondary sexual characteristics, and sex steroid levels. Several factors may promote the increase in GnRH that precedes puberty, including: reduced sensitivity to inhibition of GnRH secretion by the sex steroids; increased leptin, which reduces inhibition of gonadotropins and their releasing hormones by the gonadotropin inhibiting hormone (GnIH); decreases in melatonin, with an associated reduction in GnIH production; and increases in kisspeptin, perhaps triggered by a "somatometer" or "pubertal clock," which acts to further increase GnRH secretion. Orange boxes denote pubertal triggers. Blue text indicates sites of action or hormone release. Solid lines indicate positive feedback. Dashed lines indicate inhibitory influences.

The stimulus for this is unknown, but may involve nocturnal melatonin secretion or possibly a genetically programed state of maturity of GnRH secreting neurons – evidence for the latter is not yet available, but has been hypothesized given the strong correlation between the age of menses onset between mother and daughter (Kolarov et al., 2005).

Many of these key hormonal cues thought to be involved in the initiation of puberty also continue to be involved as puberty progresses, largely through their role in influencing the HPG axis.

The Hypothalamic-Pituitary-Gonadal Axis

Once puberty is initiated and the HPG axis is activated, GnRH is released from the hypothalamus (**Figure 2**), with peak levels at the onset of menstruation, after which its release becomes cyclical according to the phase of the menstrual cycle (Limonta et al., 2018). GnRH acts on the anterior pituitary to stimulate increases in LH and FSH production that induce sexual dimorphic changes in appearance as well as characteristic female behaviors (Limonta et al., 2018). The recent discovery of GnRH receptors in the ovary and endometrium raises the possibility of a role for GnRH outside of its hypothalamic functions (Limonta et al., 2018). LH and FSH levels increase with increases in GnRH pulse frequency and pulse amplitude during puberty. Levels of LH and FSH continue to increase until stage V for LH and stage IV for FSH, initially starting with undetectable levels of LH in prepubertal girls at stage I while low levels of FSH are detectable at this stage (Burger et al., 1988; **Figure 4**). During puberty, LH and FSH stimulate sex hormone secretion and regulate the menstrual cycle. LH acts on the ovaries to produce estrogen and facilitate egg maturation, while FSH is involved in follicle development and estrogen production (Limonta et al., 2018). LH also indirectly increases progesterone levels, secreted from the corpus luteum of mature follicles. Both LH and FSH appear to have indirect effects on the ANS, largely mediated through their effects on circulating estrogen and progesterone levels.

Estrogen

Increased activity of the gonads stimulated by LH and FSH during puberty results in an associated increased production of estrogen. During puberty, estrogen levels initially mirror LH and FSH changes, with the lowest levels in prepubertal girls at stage I (Wennink et al., 1990; **Figure 4**). However, similar to LH, estrogen levels continue to increase until stage V, during which time FSH levels begin to decline (Wennink et al., 1990). Estrogen is a sex steroid hormone that is secreted by the ovary and binds to estrogen receptors (Wennink et al., 1990). It contributes to breast, vaginal, and uterine development, as well as female fat distribution, linear growth velocity, and skeletal maturation (Swerdloff and Odell, 1975). In this review we only consider 17-β estradiol (E2) because this is the most abundant, active, and best studied form of estrogen (Rybaczyk et al., 2005; Lasiuk and Hegadoren, 2007). Other natural estrogens, estrone (E1), and estriol (E3), have weak estrogenic properties and must be

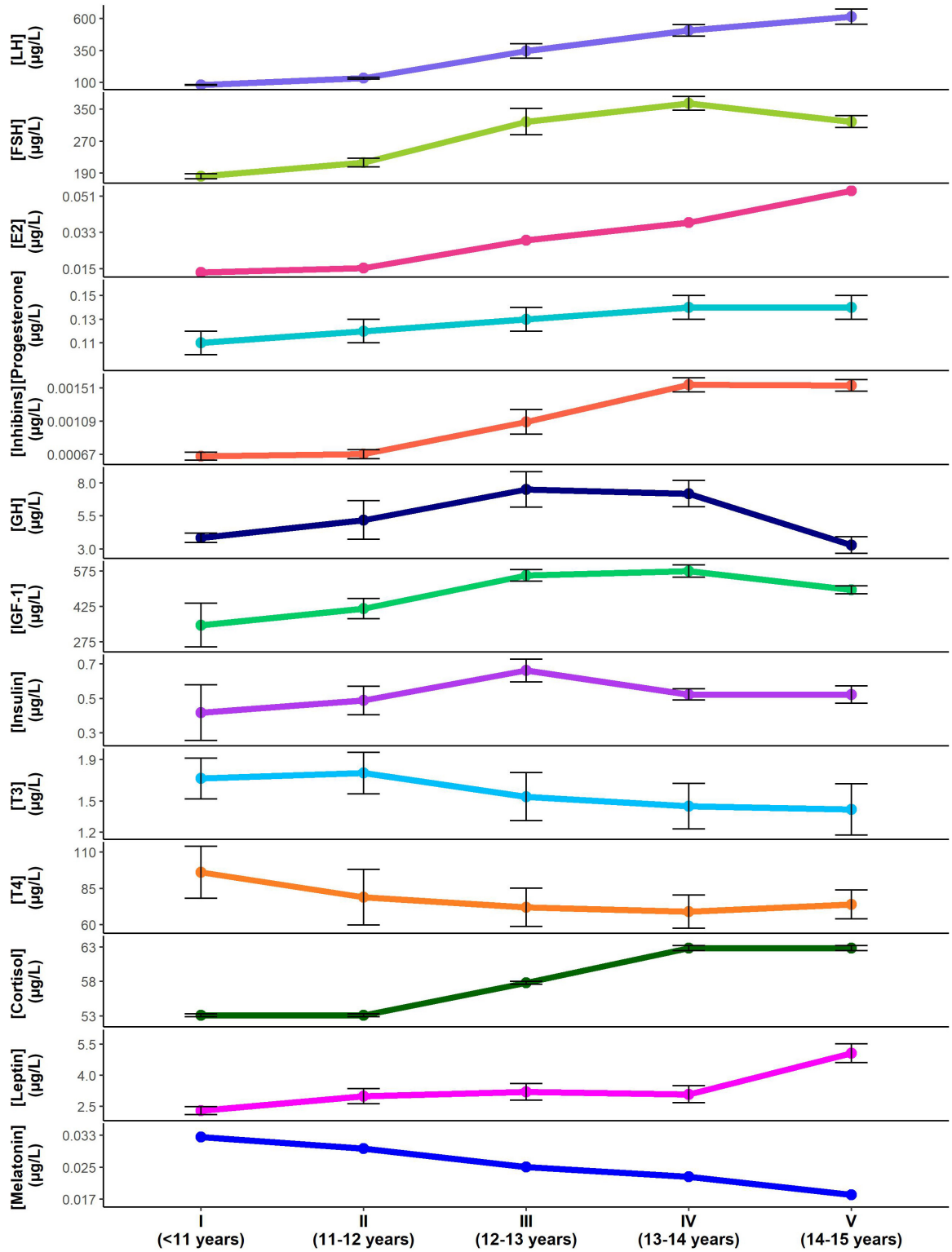

FIGURE 4 | Changes in pubertal hormone levels according to Tanner stage and approximate age (mean ± standard error). Hormone concentrations for luteinizing hormone (LH) (Burger et al., 1988). follicle stimulating hormone (FSH) (Burger et al., 1988), Estradiol (E2) (Wennink et al., 1990), progesterone (Apter, 1980), inhibins (Wennink et al., 1990), growth hormone (GH) (Rose et al., 1991), insulin-like growth factor-1 (IGF-1) (Moran et al., 2002), insulin (Moran et al., 2002), triiodothyronine (T3) (Elmlinger et al., 2001), thyroxine (T4) (Elmlinger et al., 2001), cortisol (Stroud et al., 2011), leptin (Ahmed et al., 1999), melatonin (Crowley et al., 2012) are shown through the Tanner stages for females. Note that standard errors were not available for estradiol or melatonin data. Standard errors for LH, FSH and inhibins were approximated based on data provided. Cyclical changes in hormone levels with menstruation are not reflected.

converted to E2 to have full estrogenic action; accordingly, they will not be considered further (Lasiuk and Hegadoren, 2007).

Estrogen Promotes Vasodilation and Hypocapnia, and Reduces Plasma Volume

Estrogen acts to acutely regulate vasomotor tone through endothelium-dependent and independent mechanisms (Mendelsohn and Karas, 1999; Maranon and Reckelhoff, 2013). E2 directly inhibits the influx of extracellular calcium into vascular smooth muscle via L-type calcium channels, preventing contraction and promoting vasodilatation (Mendelsohn and Karas, 1999). E2 also stimulates the opening of calcium-activated potassium channels through the nitric oxide (NO) and cyclic guanosine monophosphate-dependent pathways, relaxing smooth muscle and promoting vasodilatation (Mendelsohn and Karas, 1999). Lastly, E2 promotes rapid release of NO (Mendelsohn and Karas, 1999) and hydrogen sulfide (Dous et al., 2014), both of which are potent vasodilators. However, in addition to the acute effects on vasomotor tone, E2 also promotes chronic vasodilation through increased expression of endothelial nitric oxide synthase (eNOS), the enzyme that converts L-arginine to L-citrulline and NO, with a consequent vasodilatory response (Mendelsohn and Karas, 1999). In addition to promoting vasodilatation, E2 also acts to decrease plasma renin concentrations and angiotensin-converting-enzyme (ACE) with consequent reductions in plasma volume, accompanied by suppression of renal sympathetic activity, and ion and water reabsorption (Mendelsohn and Karas, 1999; Maranon and Reckelhoff, 2013). E2 also reduces circulating levels of the vasoconstrictor endothelin-1 (Mendelsohn and Karas, 1999). The net effect of these E2-mediated increases in vasodilatation and decreases in vasoconstriction and plasma volume, is a reduction in blood pressure, with the largest impact during stage V when E2 peaks. Interestingly, E2 enhances carotid vasomotor baroreflex sensitivity (but not cardiac baroreflex sensitivity), although this effect is likely mitigated by concurrent changes in progesterone levels, which blunt vasomotor baroreflex sensitivity (Brunt et al., 2013). Of note, estrogens have also been shown to increase cerebral blood flow in both animals and humans (Shamma et al., 1992; Belfort et al., 1995; Nevo et al., 2007), and loss of estrogens during menopause is associated with decreased cerebral reactivity (Matteis et al., 1998). The impact of vasodilation in the cerebral circulation secondary to increases in estrogen appears to be blunted in the face of estrogen and progesterone induced increases in respiration and hypocapnia, which would tend to reduce cerebral blood flow (Slatkovska et al., 2006; Preston et al., 2009).

Estrogen Has Indirect Effects on Central Nervous System Modulators That Regulate Behavior and Cardiovascular Control

Estradiol may also play a key role in regulating central nervous system factors that modulate adolescent behavior. For example, E2 may have the ability to modulate dopamine neurotransmission [dopaminergic neurons express estrogen receptors and mRNA (Purves-Tyson et al., 2012; Sinclair et al., 2014)], contributing to changes in dopamine signaling during adolescence (Sinclair et al., 2014). Dopamine is a catecholamine synthesized in dopaminergic neurons arising from the substantia nigra pars compacta and the ventral tegmental area and binds to dopamine receptor 1 (DR1) (Sinclair et al., 2014). Adult levels of DR1 mRNA and protein are attained during late adolescence/early adulthood, with coincidental timing to E2 levels (Sinclair et al., 2014). Dopamine influences control of movement, the ability to experience pleasure and pain, and emotional responses (Arain et al., 2013). In addition, dopamine inhibits noradrenaline release, and so acts to further amplify the vasodilatory effects of E2.

Increases in E2 have also been shown to increase serotonin concentrations by increasing the rate-limiting step in serotonin synthesis, as well as increasing the time that serotonin remains in the synapse and interstitial space (Rybaczyk et al., 2005). The latter is accomplished through the antagonistic action of E2 on the serotonin reuptake transporter (SERT) and down-regulation of SERT gene expression (Rybaczyk et al., 2005). Serotonin is an amine known to act as a neurotransmitter that is synthesized from tryptophan in serotoninergic neurons (Rybaczyk et al., 2005). Serotonin plays a role in arousal, anxiety, mood alterations and has also been shown to regulate various physiological functions including vasodilation (Arain et al., 2013). Thus, as E2 levels increase during female puberty, it is likely that these CNS modulators follow a similar increase, accounting for changes in behavior, and potentially exacerbating the vasodilatory effects of estrogen throughout puberty.

Progesterone

Progesterone secretion generally occurs in conjunction with E2, as it is regulated by gonadotropins and secreted by the ovaries and the placenta (Rossmanith et al., 1990). It binds to progesterone receptors to thicken the lining of the uterus and stimulate the formation of milk glands in the breast in preparation for pregnancy (Regidor, 2014). Progesterone remains at fairly low levels during childhood until adolescence where it is shown to increase in a cyclic manner depending on the phase of the menstrual cycle (Apter, 1980; **Figure 4**). Progesterone levels continue to increase and peak premenopausally, declining thereafter until reaching very low levels after menopause (O'Connor et al., 2009).

Progesterone Causes Vasodilatation, Increases Plasma Volume and Promotes Hypocapnia

The effects of progesterone in the absence of estrogen indicate that it promotes vasodilatation, blunts sympathetic outflow and increases plasma volume (Brunt et al., 2013). Progesterone stimulates NO synthesis through transcriptional and non-transcriptional pathways, promoting vasodilation (Miner et al., 2011). However, progesterone also acts to counteract the effects of estrogen on NO production, resulting in mixed evidence concerning the net role of progesterone in controlling vasomotor tone (Brunt et al., 2011). Progesterone also blunts carotid-vasomotor baroreflex sensitivity (Brunt et al., 2013), but without affecting the control of mean arterial pressure, perhaps because of concurrent augmentation of baroreflex control of stroke volume and/or the opposing action of estrogen on baroreflex

sensitivity (Brunt et al., 2011, 2013). Further research is needed to determine the precise role of progesterone in modulating vasomotor tone. However, the reported blunting of sympathetic outflow, which could account for decreases in heart rate and impaired vasoconstriction, may become relevant, particularly later in puberty.

Progesterone is a respiratory stimulant, with the consequence that $P_{ET}CO_2$ levels are reduced during times of high progesterone levels. For example, ventilation is increased during the luteal phase compared to the follicular phase of the menstrual cycle (White et al., 1983). This effect is enhanced during combined increases in both estrogen and progesterone (although estrogen alone is not closely correlated with cyclic fluctuations in ventilation during the menstrual cycle) (Regensteiner et al., 1989). Accordingly, higher estrogen and progesterone levels in younger women might contribute to their lower resting $P_{ET}CO_2$ in early life, and the age-related loss of estrogen would explain higher levels of $P_{ET}CO_2$ in later life (Regensteiner et al., 1989). These respiratory effects of estrogen and progesterone would be expected to promote reductions in $P_{ET}CO_2$ during puberty in females, particularly during the later stages, and might contribute to the reductions in cerebral blood flow that occur during female puberty.

Inhibins

Inhibin levels are increased at puberty due to increased FSH stimulation of the granulosa cells of ovarian follicles, which are the main source of circulating dimeric inhibins (Bergadá et al., 2001). During puberty, a progressive rise in inhibins accompanies an increased production of sex steroids (Bergadá et al., 2001) with the highest levels reached during stages IV–V (Burger et al., 1988; **Figure 4**). With the development of ovarian follicles, inhibin levels increase where they act largely to suppress FSH release (Bergadá et al., 2001). This negative feedback control of FSH secretion only occurs once adult inhibin levels are reached (Bergadá et al., 2001).

Inhibins Regulate Follicle Stimulating Hormone Levels and Indirectly Affect Estrogen Levels

Once adult inhibin levels are reached at around stage IV, inhibins indirectly modulate estrogen levels through negative feedback control of FSH (Bergadá et al., 2001), with a theoretical impact on cardiovascular regulation via estrogen (**Figure 2**). However, E2 continues to increase from stage IV to V, indicating that the role of inhibin on overall estrogen levels is small. Inhibins play a key role in regulating estrogen levels during the menstrual cycle, but do not appear to affect the overall estrogen levels during the stages of puberty. Direct effects of inhibins on cardiovascular regulation have not been demonstrated, although they may play a role in gestational hypertension and preeclampsia (Itoh et al., 2006).

Growth Hormone

Growth hormone (GH) increases substantially during the growth spurt of adolescence. It is secreted by the anterior pituitary gland in response to stimulation by GH releasing hormone from the hypothalamus (Soliman et al., 2014). GH levels more than double during puberty (Saenger, 2003), attaining peak levels at stage III–IV in females (Rose et al., 1991; Soliman et al., 2014; **Figure 4**). GH functions to promote lipolysis, increase protein synthesis, regulate energy metabolism in liver, muscle and adipose tissue, and is a potent insulin antagonist (Sakharova et al., 2008). GH levels are exquisitely regulated, with secretion enhanced by estrogen and thyroid hormones, and further regulation by somatostatin, ghrelin, and insulin-like growth factor 1 (IGF-1) levels. Circulating GH levels also regulate GH secretion through negative feedback (Romero et al., 2012).

Growth Hormone Is a Vasodilator and Induces Insulin-Resistance

Growth hormone acts as a vasodilator through activation of an endothelium-dependent component involving the NO pathway (Napoli et al., 2003) to improve arterial compliance, flow mediated dilation, and endothelial function (Napoli et al., 2003). Given its vasodilatory effects, GH would be expected to contribute to blood pressure lowering, particularly during stage III–IV where GH levels reach their peak. However, GH also acts to antagonize the hepatic and peripheral effects of insulin on glucose metabolism, preventing insulin uptake and inducing insulin resistance, thus increasing circulating insulin levels (Palmeiro et al., 2012). Furthermore, GH has a significant influence on adipocyte metabolism, increasing adipokines such as leptin (Palmeiro et al., 2012). Accordingly, GH contributes to increases in both insulin and leptin, increasing their impact on autonomic cardiovascular regulation.

Insulin-Like Growth Factor-1

Insulin-like growth factor-1 (IGF-1) production follows similar patterns to GH secretion during puberty; it is stimulated by GH in the liver and further enhanced by estrogen and thyroid hormones (Rozario et al., 2000). In females, IGF-1 levels peak during stage IV and are associated with increases in adiposity at this time (Moran et al., 2002; **Figure 4**). IGF-1 binds to the IGF-1 receptor and is a primary mediator of the actions of GH, promoting growth in almost every cell in the body by regulating cellular proliferation, differentiation and metabolism (Rozario et al., 2000).

Insulin-Like Growth Factor-1 Is a Vasodilator and Enhances Insulin Sensitivity

Insulin-like growth factor-1 induces vasodilation by enhancing NO and potassium channel activity, both of which reduce calcium release into vascular smooth muscle, blunting vasoconstriction (Conti et al., 2004). IGF-1 interacts with a tyrosine kinase membrane receptor that activates the serine/threonine kinase Akt signaling pathway, which in turn activates eNOS, increasing NO levels and promoting vasodilatation (Conti et al., 2004). By facilitating widespread vasodilatation, it is likely that IGF-1 reduces blood pressure, particularly during stage III–IV when IGF-1 levels peak. IGF-1 increases insulin sensitivity and prevents postprandial dyslipidemia by suppressing plasma free fatty acid levels, reducing fasting plasma triglyceride concentrations, and increasing oxidative and non-oxidative glucose metabolism

(Conti et al., 2004). Contrary to GH, IGF-1 helps to restore insulin and leptin levels to normal values (Conti et al., 2004). Thus, increases in IGF-1 are likely the result of, not the cause of, insulin resistance in puberty (Kelsey and Zeitler, 2016).

Insulin

During female puberty insulin levels generally coincide with changes in IGF-1 levels (Moran et al., 2002). Fasting insulin levels are highest in stage III, occurring one stage earlier than peak IGF-1 levels (Moran et al., 2002; **Figure 4**). Insulin is synthesized by beta cells in the pancreas following stimulation by blood glucose (Sliwowska et al., 2014)and primarily acts to facilitate cellular glucose entry for energy utilization and growth (Sliwowska et al., 2014). When this process is compromised, insulin resistance can develop, and if left untreated it can progress to type 2 diabetes mellitus.

Puberty is associated with a marked decrease in insulin sensitivity, on par with that seen during pregnancy. In otherwise healthy youth, insulin sensitivity reaches a nadir in mid-puberty (stage III) that recovers by stage V (Kelsey and Zeitler, 2016). In patients with POTS, increases in serum resistin have been documented, the significance of which is unclear, but it has been previously associated with insulin resistance (Bai et al., 2017). It is interesting to note that the decline in cerebral blood flow during puberty is tightly linked to the concurrent decreases in glucose metabolism (Satterthwaite et al., 2014).

In children with type 1 diabetes, profound insulin resistance associated with puberty is well documented, although effects on the ANS in these children are not well studied. In one study evaluating 73 diabetic children, abnormalities in heart rate variability (a marker of autonomic dysfunction) were correlated with poor glycemic control in pubertal children. This relationship was not seen in younger children (Massin et al., 1999).

Insulin Exhibits Opposing Roles in Regulating Vasomotor Tone

Insulin exhibits both central and peripheral effects on the ANS – insulin both promotes vasodilatation and prevents vasoconstriction, while also having the ability to stimulate sympathetic activity. Insulin diminishes arterial stiffness (Vehkavaara et al., 2000) and acts as a vasodilator by binding to an insulin receptor tyrosine kinase, activating the Akt pathway and further stimulating eNOS to increase NO production (Muniyappa et al., 2007). Insulin has further been shown to attenuate vascular smooth muscle contraction and decrease vasoconstrictor tone by inhibiting calcium influx (Muniyappa et al., 2007). In contrast, insulin can stimulate sympathetic activity and increase catecholamine levels (Muniyappa et al., 2007). The opposing roles of insulin essentially lead to little change in arterial diameter and blood pressure under normal circumstances in healthy individuals (Muniyappa et al., 2007). However, during acute increases in sympathetic nerve activity, different parts of the vascular tree respond differently to insulin, where distal arterioles vasodilate and proximal arterioles constrict (Muniyappa et al., 2007). This could contribute to enhanced venous pooling during sympathetic activation upon standing. Increases in sympathetic activity and catecholamine levels would tend to facilitate tachycardia.

Thyroid Hormones

The thyroid gland produces triiodothyronine (T3) and thyroxine (T4), both of which are stimulated by thyroid-stimulating hormone from the anterior pituitary gland secondary to release of thyrotropin-releasing hormone from the hypothalamus (Shahid and Sharma, 2019). The release of T3 and T4 from the thyroid gland is influenced by growth factors and modulated by sex steroids in females (Dunger et al., 1990). During puberty T3 increases, peaking during stage II, while T4 decreases at the onset of puberty and continues to decrease before leveling off after stage IV (Dunger et al., 1990; Elmlinger et al., 2001; **Figure 4**). The decrease in T4 is likely a result of its conversion into T3 in the periphery, as T3 is the more active, bioavailable form of thyroid hormone (Jørgensen et al., 1994). These hormones act to increase and regulate basal metabolic rate, as well as to increase heart rate, cardiac output, and ventilation, with decreases in peripheral resistance (Shahid and Sharma, 2019). Additional effects on the central nervous system and skeleton are crucial to normal development and growth (Shahid and Sharma, 2019).

Thyroid Hormones Act as Vasodilators While Increasing Heart Rate to Preserve Blood Pressure

Higher levels of thyroid hormones increase metabolism and heat production stimulating hypothalamic reflex responses (Thomas, 1957). These hypothalamic responses initiate vasodilation of arterioles, largely in the skin, to increase blood flow and dissipate heat, while simultaneously increasing heart rate and stroke volume to maintain a constant blood pressure (Thomas, 1957). T3 enhances endothelium-dependent relaxation through a cyclic adenosine monophosphate-mediated increase in endothelium-derived hyperpolarizing factor (EDHF), as well as through NO-mediated relaxation via up-regulation of eNOS (Büssemaker et al., 2003). EDHF prevents calcium influx through voltage-gated calcium channels, inhibiting contraction of vascular smooth muscle. T4 directly inhibits vascular contraction by inhibiting calcium/calmodulin-related regulatory mechanisms (Ishikawa et al., 1989). Cerebral blood flow remains unchanged during increases in thyroid hormones (Thomas, 1957).

Cortisol

Baseline cortisol levels increase during puberty, peaking at stage IV/V in females (Stroud et al., 2011; **Figure 4**). Cortisol is released by the adrenal gland following stimulation by adrenocorticotropic hormone, which is produced by the anterior pituitary (Lee et al., 2015). Cortisol binds to cortisol receptors and plays a role in maintaining blood glucose levels, central nervous system function, and cardiovascular function during fasting (Lee et al., 2015). Cortisol increases blood glucose levels during stress at the expense of muscle protein and one of its most important functions is to protect the body against self-injurious inflammatory and immune responses (Lee et al., 2015).

Cortisol Increases Plasma Volume and Increases Blood Pressure

Acute increases in cortisol levels blunt autonomic reactivity by suppressing the early effects of catecholamines in the brain (Teixeira et al., 2015), with subsequent decreases in arterial vasoconstriction (Theodorakis et al., 1998). However, chronic elevations in cortisol induce hypertension, independent of changes in sympathetic nervous system activity, likely mediated via increases in plasma volume, extracellular fluid and exchangeable sodium (Theodorakis et al., 1998).

Leptin

Leptin levels increase with the onset of puberty, but remain fairly steady following this initial rise until a late surge starting at stage IV in females (Ahmed et al., 1999; **Figure 4**). Leptin is secreted by adipocytes and is hypothesized to act on specific receptors at the level of the hypothalamus to regulate appetite, energy expenditure, the neuroendocrine axis, and weight (Ahmed et al., 1999). Differential changes in body composition between males and females during puberty are affected by the sexual dimorphism of leptin levels during this period (Ahmed et al., 1999). In females, leptin increases throughout puberty, with a prominent surge during stage IV–V, to reach adult concentrations, while in males it increases only transiently with the onset of puberty (Kelsey and Zeitler, 2016).

Leptin Activates the Sympathetic Nervous System and Increases Insulin Sensitivity

Leptin activates the sympathetic nervous system through hypothalamic mechanisms that are mediated by neuropeptide systems, including the melanocortin system and corticotropin-releasing hormone (Muniyappa et al., 2007). With increases in sympathetic activity, increases in heart rate and vasoconstriction are expected, particularly at stage V, when leptin levels peak. Leptin also increases insulin sensitivity which helps to prevent abnormally high levels of circulating insulin, and somewhat counteracts the role of GH in inducing insulin-resistance (Muniyappa et al., 2007). Higher leptin levels are also associated with impaired heart rate variability (a sign of autonomic dysfunction). In particular, increased low frequency heart rate variability, and an increased ratio of low to high frequency heart rate variability have been reported, suggesting that increased leptin levels may result in an autonomic imbalance with a sympathetic predominance in young females during puberty (Van De Wielle and Michels, 2017).

Melatonin

In the early stages of female puberty (I and II) melatonin secretion significantly decreases, with further successive decreases in the later stages (Murcia et al., 2002; Crowley et al., 2012; **Figure 4**). Melatonin is a lipophilic endocrine hormone that is synthesized in the pineal gland (Murcia et al., 2002). Melatonin secretion is largely regulated by light and dark information received by the suprachiasmatic nucleus from retinal photosensitive ganglionic cells (Murcia et al., 2002). It is secreted in a circadian pattern, with the greatest secretions occurring at night (Murcia et al., 2002), and functions in many regulatory processes including biological rhythms, metabolism, intestinal reflexes, and protection against inflammation (Chen et al., 2011).

Melatonin Inhibits Estrogen Receptor-Mediated Transcription

Melatonin interferes with E2 signaling by impairing estrogen receptor pathways via specific inhibition of E2-induced estrogen receptor alpha (ERα) mediated transcription of both estrogen response element and activator protein 1 containing promoters (Del Río et al., 2004). By reducing the transcription of one of the main estrogen receptors, ERα, the effects of estrogen are reduced. As melatonin levels decrease as puberty progresses, while estrogen increases, there is an inverse relationship between melatonin and estrogen. Thus, the inhibitory effect of melatonin on estrogen signaling is probably relatively minor during puberty.

Kisspeptin and Gonadotropin Inhibiting Hormone

Increases in kisspeptin levels and decreases in GnIH levels are thought to contribute to the initiation of puberty (**Figure 3**). However, data on kisspeptin and GnIH levels throughout

TABLE 4 | Impact of pubertal hormones on factors that predispose to syncope events.

Factors predisposing orthostatic intolerance	Pubertal hormones that exacerbate	Pubertal hormones that ameliorate
Vasodilatation	Estrogen	Progesterone (by inhibiting action of estrogen)
	Progesterone	Melatonin (by inhibiting action of estrogen)
	Growth hormone	
	IGF-1	
	Insulin	
	Thyroid hormones	
Impaired vasoconstriction	Insulin	Leptin
	Progesterone	
Hypotension	Estrogen	Cortisol
	Growth hormone	
	IGF-1	
Low sympathetic activity	Progesterone	Leptin
		Insulin
Excessive venous pooling	Insulin	
Hypovolemia	Estrogen	Cortisol
		Progesterone
Hypocapnia	Estrogen	
	Progesterone	
Decreased cerebral blood flow	Estrogen and progesterone (via hypocapnia)	Estrogen
Excessive tachycardia	Insulin	Progesterone
	Leptin	
	Thyroid hormones	
Decreased baroreflex sensitivity	Progesterone	Estrogen

IGF-1, insulin-like growth factor-1.

the phases of puberty, as well as any potential impact on cardiovascular responses or susceptibility to syncope are currently lacking.

PUBERTAL HORMONES AS POTENTIAL CONTRIBUTORS TO VASOVAGAL SYNCOPE AND POSTURAL ORTHOSTATIC TACHYCARDIA SYNDROME

There are numerous factors known to increase susceptibility to syncope. One key contributor is excessive vasodilatation and/or impaired vasoconstrictor responses, often associated with hypotension and blunted sympathetic outflow (Brown and Hainsworth, 2000; Bush et al., 2000). In addition, hypocapnia and cerebral hypoperfusion (Claydon and Hainsworth, 2003; Norcliffe-Kaufmann et al., 2007), hypovolemia (Cooper and Hainsworth, 2008), excessive tachycardia (Sandroni et al., 1999), or impaired baroreflex responses (Cooper and Hainsworth, 2002; Gulli et al., 2005a), will all impair orthostatic cardiovascular control. The potential impact of female pubertal hormones on these predisposing factors is summarized in **Table 4**.

The implications for these hormones as possible contributors to VVS and POTS can be considered based on the impact each has on cardiovascular control (**Table 4**), and the timing of their changes over the duration of puberty (Apter, 1980; Burger et al., 1988; Wennink et al., 1990; Rose et al., 1991; Ahmed et al., 1999; Elmlinger et al., 2001; Moran et al., 2002; Stroud et al., 2011; Crowley et al., 2012; **Figure 4**). Hormones promoting vasodilatation may exacerbate the inappropriate reductions in blood pressure that occur during VVS or the impaired vasoconstriction in POTS, placing increased reliance on orthostatic tachycardia for maintenance of blood pressure (**Figures 5**, **6**). Thyroid hormones, GH and IGF-1 largely act as vasodilators through their involvement with the NO pathway. Along with releasing NO and hydrogen sulfide, another vasodilator, E2 also promotes hyperpolarization in vascular smooth muscle, and decreases renal renin release with subsequent reductions in angiotensin-mediated vasoconstriction, culminating in a potent vasodilatory influence. Baseline blood

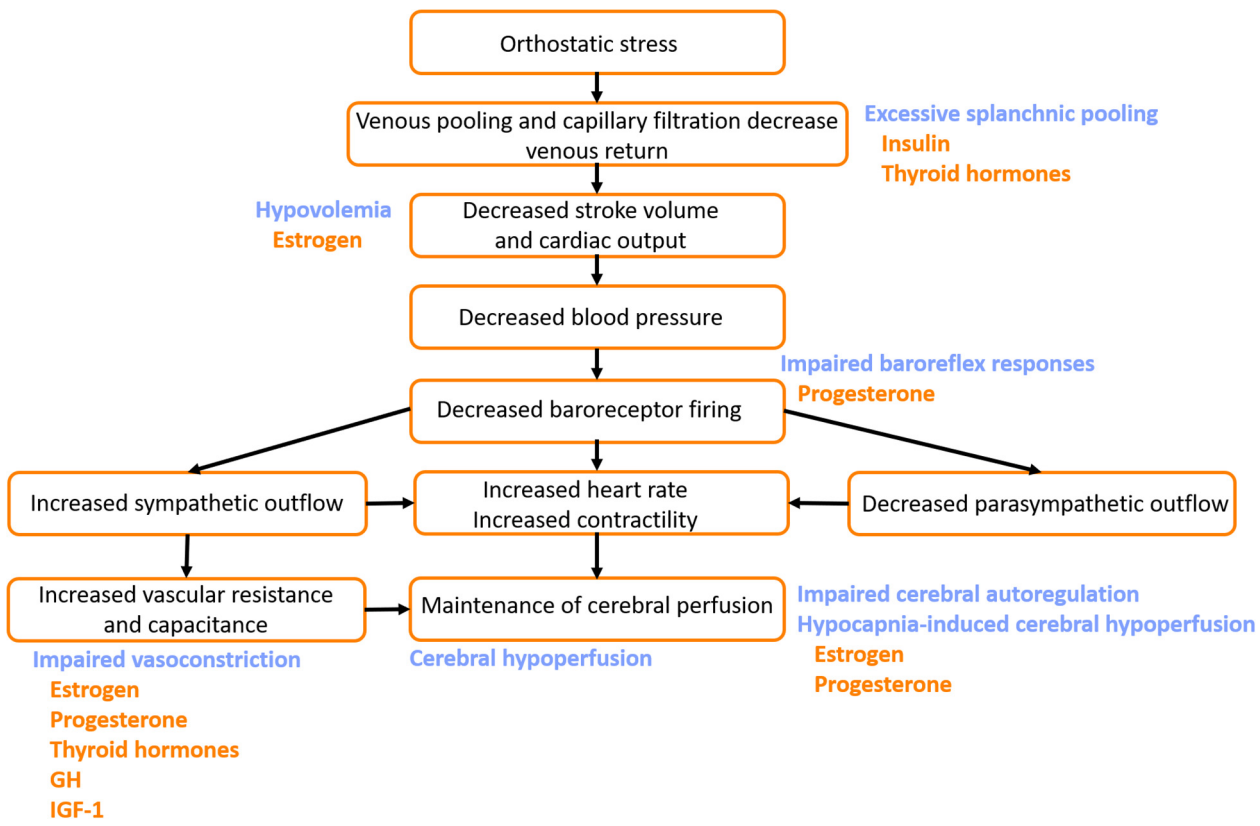

FIGURE 5 | Potential mechanisms by which pubertal hormones exacerbate susceptibility to vasovagal syncope (VVS). The normal cardiovascular response to orthostatic stress is shown (black text). In patients with VVS, hypovolemia and excessive venous pooling, particularly in the splanchnic vascular bed, combine to produce particularly large orthostatic reductions in stroke volume and cardiac output. Impaired baroreflex responses, and blunted orthostatic increases in vascular resistance and vascular capacitance fail to appropriately compensate, and ultimately blood pressure and cardiac output fall dramatically, with cerebral hypoperfusion and subsequent presyncope or syncope. Impairments in cerebral autoregulatory control and excessive reductions in cerebral blood flow in response to the hypocapnia during orthostasis further contribute to the decline in cerebral perfusion (blue text). Hormones that potentially exacerbate the impaired cardiovascular responses to orthostatic stress in patients with VVS are indicated (orange text). GH, growth hormone; IGF-1, insulin-like growth factor-1.

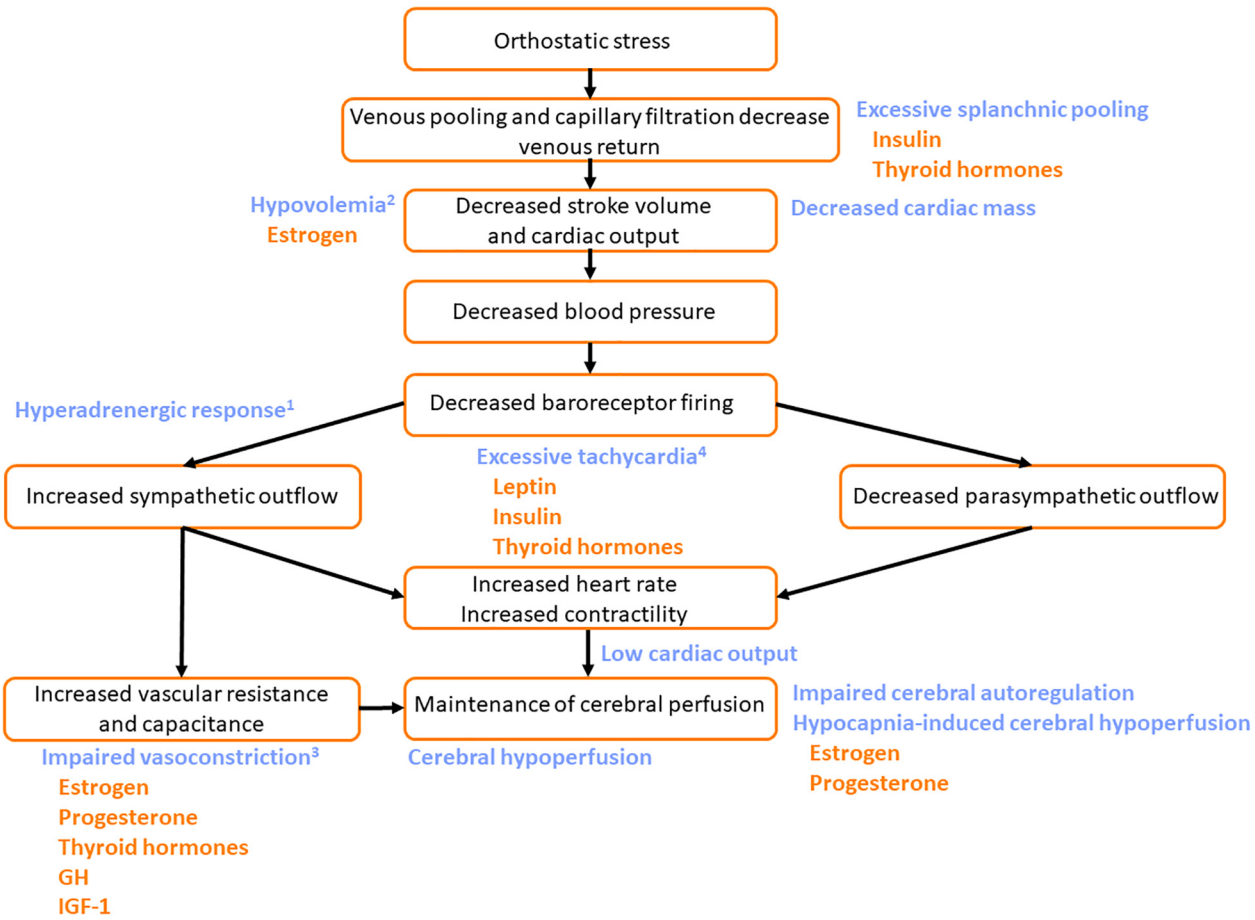

FIGURE 6 | Potential mechanisms by which pubertal hormones exacerbate susceptibility to the Postural Orthostatic Tachycardia Syndrome (POTS). The normal cardiovascular response to orthostatic stress is shown (black text). In patients with POTS, excessive venous pooling, particularly in the splanchnic vascular bed, contributes to particularly large orthostatic reductions in stroke volume and cardiac output. In those with hyperadrenergic POTS[1] central sympathetic outflow is excessive. In those with hypovolemic POTS[2], plasma volume is low exacerbating the impact of the orthostatic venous pooling. Patients with neuropathic POTS have impaired vasoconstrictor responses with compensatory tachycardia[3]. Those with noradrenaline transporter deficiency have a primary orthostatic tachycardia[4]. The common feature of all subtypes is excessive tachycardia (either primary tachycardia or secondary tachycardia to compensate for other impairments) with low venous return and stroke volume during orthostasis, reduced time for diastolic filling, and consequently low cardiac output. Cerebral perfusion is compromised and symptoms of presyncope are common. Impaired orthostatic increases in vascular resistance and vascular capacitance exacerbate the orthostatic tachycardia. Some patients with POTS are reported to have decreased cardiac mass, with low stroke volume, that also facilitates orthostatic tachycardia. Impairments in cerebral autoregulatory control and excessive reductions in cerebral blood flow in response to the hypocapnia during orthostasis further contribute to the decline in cerebral perfusion (blue text). Hormones that potentially exacerbate the impaired cardiovascular responses to orthostatic stress in patients with POTS are indicated (orange text). Leptin, insulin and thyroid hormones may exacerbate orthostatic tachycardia. GH, growth hormone; IGF-1, insulin-like growth factor-1.

pressures increase during puberty, but to a lesser degree in females than in males, suggesting that the vasodilatory actions of female pubertal hormones promote lower blood pressures in females, with an associated susceptibility to further orthostatic blood pressure decrements (Shankar et al., 2005). The differential influence of insulin in the presence of sympathetic stimulation may account for the abnormal blood perfusion and splanchnic pooling as a proposed mechanism of VVS and POTS (**Figures 5**, **6**). In the presence of high insulin and sympathetic activity, as seen with standing, distal vessels vasodilate while proximal vessels constrict, likely increasing blood flow to distal extremities while decreasing flow to the central regions of the body. This effect would predominate during stage III when insulin levels peak. Similarly, different organs in the body respond differently to the vasodilatory effects of thyroid hormones, and this may also promote splanchnic pooling (**Figures 5**, **6**). The presence of hypovolemia in POTS and VVS patients may be exacerbated by E2 as it acts to decrease renin concentrations with consequent decreases in blood volume mediated via the renin-angiotensin-aldosterone pathway. High levels of E2 and progesterone may promote hypocapnia and associated reductions in cerebral blood flow, increasing susceptibility to further cerebral compromise during orthostatic stress. While these hormones can account for some of the similar predisposing factors and symptoms of VVS and POTS, hormones that may contribute to the different profiles of VVS and POTS should further be considered.

The effects of these hormones on the ANS may be more prominent in some individuals, leading to a greater predisposition to POTS or VVS. As cortisol levels have been shown to increase during vasovagal reactions in patients with VVS (Stroud et al., 2011), peak levels of cortisol during stage IV/V may play a role in the manifestation of VVS. Progesterone may also be a contributor to VVS by blunting sympathetic outflow, and impairing baroreflex responses, exhibiting its greatest effects during stages IV–V, when progesterone is at its highest (**Figure 5**).

Central hyperadrenergic POTS and the abnormal heart rate increases in POTS patients could be exacerbated by hormones involved in increasing sympathetic activity and elevating norepinephrine levels (**Figure 6**). Both insulin and leptin have the ability to increase sympathetic activity and stimulate catecholamine release, and increases in leptin and insulin are associated with increases in heart rate. Insulin and leptin peak during puberty in stages III and V, respectively, and might be hypothesized to exacerbate orthostatic tachycardia at these times. Thyroid hormones also play a role in increasing heart rate to maintain blood pressure – with key rises in T3 during pubertal stage II.

While it is certainly not possible to imply causality between these pubertal hormone changes and disorders of orthostatic tolerance in adolescents, the coincidental timing of these profound hormonal changes – many of which have marked cardiovascular effects - and the timing of onset of VVS and POTS, together with the observation that many youth "grow out" of their symptoms (Kizilbash et al., 2014), is suggestive of a link between pubertal hormone changes and susceptibility to syncope in females. Certainly, orthostatic tolerance increases in women as they age, and is highest in postmenopausal women (Protheroe et al., 2013). It is conceivable that pubertal increases in these hormones, many of which have secondary actions to promote vasodilatation, impair vasoconstriction, decrease blood volume, promote hypocapnia and cerebral hypoperfusion, and contribute to excessive tachycardia, unmask a susceptibility to disorders of orthostatic intolerance in girls with a previously unknown predisposition to poor orthostatic tolerance. Further insight into the role of female sex hormones in susceptibility to VVS and POTS can also be gleaned from a case series in which fifteen women (including six adolescents) with refractory VVS/POTS experienced symptomatic benefit with complete resolution, or a marked reduction in the frequency, of orthostatic symptoms following ovarian hormone therapy (Boehm et al., 1997).

CONCLUSION

Hormone changes during puberty have the potential to impact cardiovascular autonomic control and as such may play a role in predisposing adolescent females to autonomic dysfunction, including disorders of orthostatic intolerance such as POTS and VVS. The peak incidence of VVS and POTS in young women occurs at approximately 10–15 years of age, a time where many hormones involved in puberty, capable of predisposing to disorders of orthostatic intolerance, are at peak levels. These pubertal hormones can act to promote vasodilatation, impair vasoconstriction, decrease plasma volume, promote hypocapnia and cerebral hypoperfusion, and contribute to excessive tachycardia. Additional research is necessary to examine the potential role that puberty, and in particular the hormonal changes that accompany it, may have in predisposing young females to orthostatic intolerance and autonomic dysfunction during their pubertal years.

AUTHOR CONTRIBUTIONS

KC, NH, BH, and VC wrote the manuscript. RR, KA, and SS provided critical analysis, insight, editing, and review of intellectual content.

FUNDING

This work was supported by a grant-in-aid (G-18-0022174) from the Heart and Stroke Foundation of Canada (VC).

ACKNOWLEDGMENTS

We are grateful to Ms. Rebekah Lee for her assistance in coordinating reference databases. We thank Dr. Shazan Amed for her help with conceptualization of the manuscript.

REFERENCES

Ahimastos, A. A., Formosa, M., Dart, A. M., and Kingwell, B. A. (2003). Gender differences in large artery stiffness pre- and post puberty. *J. Clin. Endocrinol. Metab.* 88, 5375–5380. doi: 10.1210/jc.2003-030722

Ahmed, M. L., Ong, K. K., Morrell, D. J., Cox, L., Drayer, N., Perry, L., et al. (1999). Longitudinal study of leptin concentrations during puberty: sex differences and relationship to changes in body composition. *J. Clin. Endocrinol. Metab.* 84, 899–905. doi: 10.1210/jc.84.3.899

Anderson, J. B., Czosek, R. J., Knilans, T. K., and Marino, B. S. (2012). The effect of paediatric syncope on health-related quality of life. *Cardiol. Young* 22, 583–588. doi: 10.1017/S1047951112000133

Antiel, R. M., Caudill, J. S., Burkhardt, B. E. U., Brands, C. K., and Fischer, P. R. (2011). Iron insufficiency and hypovitaminosis D in adolescents with chronic fatigue and orthostatic intolerance. *South. Med. J.* 104, 609–611. doi: 10.1097/SMJ.0b013e3182246809

Apter, D. (1980). Serum steroids and pituitary hormones in female puberty: a partly longitudinal study. *Clin. Endocrinol.* 12, 107–120. doi: 10.1111/j.1365-2265.1980.tb02125.x

Arain, M., Haque, M., Johal, L., Mathur, P., Nel, W., Rais, A., et al. (2013). Maturation of the adolescent brain. *Neuropsychiatr. Dis. Treat.* 9, 449–461. doi: 10.2147/NDT.S39776

Armstrong, K. R., De Souza, A. M., Sneddon, P. L., Potts, J. E., Claydon, V. E., and Sanatani, S. (2017). Exercise and the multidisciplinary holistic approach to adolescent dysautonomia. *Acta Paediatr.* 106, 612–618. doi: 10.1111/apa.13750

Avendaño, M. S., Vazquez, M. J., and Tena-Sempere, M. (2017). Disentangling puberty: novel neuroendocrine pathways and mechanisms for the control of mammalian puberty. *Hum. Reprod. Update* 23, 737–763. doi: 10.1093/humupd/dmx025

Bai, W., Han, Z., Chen, S., Li, H., Song, J., Qi, J., et al. (2017). Serum resistin negatively correlates with clinical severity of postural tachycardia syndrome in children. *Pediatr. Cardiol.* 38, 1639–1644. doi: 10.1007/s00246-017-1708-4

Baker, E. R. (1985). Body weight and the initiation of puberty. *Clin. Obstet. Gynecol.* 28, 573–579. doi: 10.1097/00003081-198528030-00013

Belfort, M. A., Saade, G. R., Snabes, M., Dunn, R., Moise, K. J., Cruz, A., et al. (1995). Hormonal status affects the reactivity of the cerebral vasculature. *Am. J. Obstet. Gynecol.* 172(4 Pt 1), 1273–1278. doi: 10.1016/0002-9378(95)91492-7

Bergadá, I., Bergadá, C., and Campo, S. (2001). Role of inhibins in childhood and puberty. *J. Pediatr. Endocrinol. Metab.* 14, 343–353.

Blaber, A. P., Bondar, R. L., Moradshahi, P., Serrador, J. M., and Hughson, R. L. (2001). Inspiratory CO2 increases orthostatic tolerance during repeated tilt. *Aviat. Space Environ. Med.* 72, 985–991.

Boehm, K. E., Kip, K. T., Grubb, B. P., and Kosinski, D. J. (1997). Neurocardiogenic syncope: response to hormonal therapy. *Pediatrics* 99, 623–625.

Brainard, G. C., Petterborg, L. J., Richardson, B. A., and Reiter, R. J. (1982). Pineal melatonin in syrian hamsters: circadian and seasonal rhythms in animals maintained under laboratory and natural conditions. *Neuroendocrinology* 35, 342–348. doi: 10.1159/000123405

Braune, S., Wrocklage, C., Schulte-Monting, J., Schnitzer, R., Lucking, C. H., Schulte-Mönting, J., et al. (1999). Diagnosis of tachycardia syndromes associated with orthostatic symptoms. *Clin. Auton. Res.* 9, 97–101. doi: 10.1007/bf02311766

Brignole, M. (2005). Neurally-mediated syncope. *Ital. Heart J.* 6, 249–255.

Brignole, M., Menozzi, C., Del Rosso, A., Costa, S., Gaggioli, G., Bottoni, N., et al. (2000). New classification of haemodynamics of vasovagal syncope: beyond the VASIS classification. Analysis of the pre-syncopal phase of the tilt test without and with nitroglycerin challenge. Vasovagal syncope international study. *Europace* 2, 66–76. doi: 10.1053/eupc.1999.0064

Brown, C. M., and Hainsworth, R. (1999). Assessment of capillary fluid shifts during orthostatic stress in normal subjects and subjects with orthostatic intolerance. *Clin. Auton. Res.* 9, 69–73. doi: 10.1007/bf02311762

Brown, C. M., and Hainsworth, R. (2000). Forearm vascular responses during orthostatic stress in control subjects and patients with posturally related syncope. *Clin. Auton. Res.* 10, 57–61. doi: 10.1007/bf02279892

Brunt, V. E., Miner, J. A., Kaplan, P. F., Halliwill, J. R., Strycker, L. A., and Minson, C. T. (2013). Short-term administration of progesterone and estradiol independently alter carotid-vasomotor, but not carotid-cardiac, baroreflex function in young women. *Am. J. Physiol. Heart Circ. Physiol.* 305, H1041–H1049. doi: 10.1152/ajpheart.00194.2013

Brunt, V. E., Miner, J. A., Meendering, J. R., Kaplan, P. F., and Minson, C. T. (2011). 17β-estradiol and progesterone independently augment cutaneous thermal hyperemia but not reactive hyperemia. *Microcirculation* 18, 347–355. doi: 10.1111/j.1549-8719.2011.00095.x

Burger, H. G., McLachlan, R. I., Bangah, M., Quigg, H., Findlay, J. K., Robertson, D. M., et al. (1988). Serum inhibin concentrations rise throughout normal male and female puberty. *Obstet. Gynecol. Surv.* 44, 379–380. doi: 10.1097/00006254-198905000-00024

Bush, V. E., Wight, V. L., Brown, C. M., and Hainsworth, R. (2000). Vascular responses to orthostatic stress in patients with postural tachycardia syndrome (POTS), in patients with low orthostatic tolerance, and in asymptomatic controls. *Clin. Auton. Res.* 10, 279–284. doi: 10.1007/bf02281110

Büssemaker, E., Popp, R., Fisslthaler, B., Larson, C. M., and Fleming, I. (2003). Hyperthyroidism enhances endothelium-dependent relaxation in the rat renal artery. *Cardiovasc. Res.* 59, 181–188. doi: 10.1016/s0008-6363(03)00326-2

Carapetian, S., Siedlarz, M., Jackson, S., and Perlmuter, L. C. (2008). Orthostatic blood pressure regulation predicts classroom effort in children. *Int. J. Psychophysiol.* 68, 70–74. doi: 10.1016/j.ijpsycho.2008.01.004

Carey, B. J., Eames, P. J., Panerai, R. B., and Potter, J. F. (2001). Carbon dioxide, critical closing pressure and cerebral haemodynamics prior to vasovagal syncope in humans. *Clin. Sci.* 101, 351–358. doi: 10.1042/cs1010351

Chen, C. Q., Fichna, J., Bashashati, M., Li, Y. Y., and Storr, M. (2011). Distribution, function and physiological role of melatonin in the lower gut. *World J. Gastroenterol.* 17, 3888–3898. doi: 10.3748/wjg.v17.i34.3888

Cheung, C. C., Thornton, J. E., Nurani, S. D., Clifton, D. K., and Steiner, R. A. (2001). A reassessment of leptin's role in triggering the onset of puberty in the rat and mouse. *Neuroendocrinology* 74, 12–21. doi: 10.1159/000054666

Claydon, V. E., and Hainsworth, R. (2003). Cerebral autoregulation during orthostatic stress in healthy controls and in patients with posturally related syncope. *Clin. Auton. Res.* 13, 321–329. doi: 10.1007/s10286-003-0120-8

Claydon, V. E., Norcliffe, L. J., Moore, J. P., Rivera-Ch, M., Leon-Velarde, F., Appenzeller, O., et al. (2004). Orthostatic tolerance and blood volumes in Andean high altitude dwellers. *Exp. Physiol.* 89, 565–571. doi: 10.1113/expphysiol.2004.027698

Clemans, K. H., DeRose, L. M., Graber, J. A., and Brooks-Gunn, J. (2010). "Gender in adolescence: applying a person-in-context approach to gender identity and roles," in *Handbook of Gender Research in Psychology: Volume 1: Gender Research in General and Experimental Psychology*, eds J. C. Chrisler, and D. R. McCreary, (New York, NY: Springer), 527–559.

Conti, E., Carrozza, C., Capoluongo, E., Volpe, M., Crea, F., Zuppi, C., et al. (2004). Insulin-like growth factor-1 as a vascular protective factor. *Circulation* 110, 2260–2265. doi: 10.1161/01.cir.0000144309.87183.fb

Cooper, V. L., and Hainsworth, R. (2002). Effects of head-up tilting on baroreceptor control in subjects with different tolerances to orthostatic stress. *Clin. Sci.* 103, 221–226. doi: 10.1042/cs1030221

Cooper, V. L., and Hainsworth, R. (2008). Head-up sleeping improves orthostatic tolerance in patients with syncope. *Clin. Auton. Res.* 18, 318–324. doi: 10.1007/s10286-008-0494-8

Crowley, S. J., Acebo, C., and Carskadon, M. A. (2012). Human puberty: salivary melatonin profiles in constant conditions. *Dev. Psychobiol.* 54, 468–473. doi: 10.1002/dev.20605

Cunningham, M. J., Clifton, D. K., and Steiner, R. A. (1999). Leptin's actions on the reproductive axis: perspectives and mechanisms. *Biol. Reprod.* 60, 216–222. doi: 10.1095/biolreprod60.2.216

Da, S. R., and da Silva, R. M. F. L. (2014). Syncope: epidemiology, etiology, and prognosis. *Front. Physiol.* 5:471. doi: 10.3389/fphys.2014.00471

Daffertshofer, M., Diehl, R. R., Ziems, G. U., and Hennerici, M. (1991). Orthostatic changes of cerebral blood flow velocity in patients with autonomic dysfunction. *J. Neurol. Sci.* 104, 32–38. doi: 10.1016/0022-510x(91)90212-p

de Jong-de Vos van Steenwijk, C. C., Wieling, W., Johannes, J. M., Harms, M. P., Kuis, W., and Wesseling, K. H. (1995). Incidence and hemodynamic characteristics of near-fainting in healthy 6- to 16-year old subjects. *J. Am. Coll. Cardiol.* 25, 1615–1621. doi: 10.1016/0735-1097(95)00056-a

Deda, L., Sochett, E. B., and Mahmud, F. H. (2015). Physiological changes in blood pressure impact peripheral endothelial function during adolescence. *Cardiol. Young* 25, 777–779. doi: 10.1017/S1047951114001024

Del Río, B., Garćia Pedrero, J. M., Martínez-Campa, C., Zuazua, P., Lazo, P. S., and Ramos, S. (2004). Melatonin, an endogenous-specific inhibitor of estrogen receptor α via calmodulin. *J. Biol. Chem.* 279, 38294–38302. doi: 10.1074/jbc.m403140200

Dhokalia, A., Parsons, D. J., and Anderson, D. E. (1998). Resting end-tidal CO2 association with age, gender, and personality. *Psychosom. Med.* 60, 33–37. doi: 10.1097/00006842-199801000-00007

Dossus, L., Kvaskoff, M., Bijon, A., Engel, P., Verdebout, J., Fervers, B., et al. (2013). Latitude and ultraviolet radiation dose in the birthplace in relation to menarcheal age in a large cohort of french women. *Int. J. Epidemiol.* 42, 590–600. doi: 10.1093/ije/dyt007

Dous, G. V., Grodman, R., Mornan, A., Otterbeck, P., and Grigos, A. (2014). Menopausal hormone treatment in postmenopausal women: risks and benefits. *South. Med. J.* 107, 689–695. doi: 10.14423/SMJ.0000000000000192

Driscoll, D. J., Jacobsen, S. J., Porter, C. J., and Wollan, P. C. (1997). Syncope in children and adolescents. *J. Am. Coll. Cardiol.* 29, 1039–1045.

Dunger, D. B., Perkins, J. A., Jowett, T. P., Edwards, P. R., Cox, L. A., Preece, M. A., et al. (1990). A longitudinal study of total and free thyroid hormones and thyroxine binding globulin during normal puberty. *Acta Endocrinol.* 123, 305–310. doi: 10.1530/acta.0.1230305

El-Sayed, H., Hainsworth, R., Sayed, H., and Hainsworth, R. (1995). El Relationship between plasma volume, carotid baroreceptor sensitivity and orthostatic tolerance. *Clin. Sci.* 88, 463–470. doi: 10.1042/cs0880463

El-Sayed, H., and Hainsworth, R. (1996). Salt supplement increases plasma volume and orthostatic tolerance in patients with unexplained syncope. *Hear* 75, 134–140. doi: 10.1136/hrt.75.2.134

Elmlinger, M. W., Kühnel, W., Lambrecht, H. G., and Ranke, M. B. (2001). Reference intervals from birth to adulthood for serum thyroxine (T4),

triiodothyronine (T3), free T3, free T4, thyroxine binding globulin (TBG) and thyrotropin (TSH). *Clin. Chem. Lab. Med.* 39, 973–979.

Etienne, M., and Weimer, L. H. (2006). Immune-mediated autonomic neuropathies. *Curr. Neurol. Neurosci. Rep.* 6, 57–64. doi: 10.1007/s11910-996-0010-2

Forbes, E. E., and Dahl, R. E. (2010). Pubertal development and behavior: hormonal activation of social and motivational tendencies. *Brain Cogn.* 72, 66–72. doi: 10.1016/j.bandc.2009.10.007

Fu, Q., Vangundy, T. B., Galbreath, M. M., Shibata, S., Jain, M., Hastings, J. L., et al. (2010). Cardiac origins of the postural orthostatic tachycardia syndrome. *J. Am. Coll. Cardiol.* 55, 2858–2868. doi: 10.1016/j.jacc.2010.02.043

Furlan, R., Jacob, G., Snell, M., Robertson, D., Porta, A., Harris, P., et al. (1998). Chronic orthostatic intolerance: a disorder with discordant cardiac and vascular sympathetic control. *Circulation* 98, 2154–2159. doi: 10.1161/01.cir.98.20.2154

Ganzeboom, K. S., Mairuhu, G., Reitsma, J. B., Linzer, M., Wieling, W., and van Dijk, N. (2006). Lifetime cumulative incidence of syncope in the general population: a study of 549 Dutch subjects aged 35-60 years. *J. Cardiovasc. Electrophysiol.* 17, 1172–1176. doi: 10.1111/j.1540-8167.2006.00595.x

Gill, S., Sharpless, J. L., Rado, K., and Hall, J. E. (2002). Evidence that GnRH decreases with gonadal steroid feedback but increases with age in postmenopausal women. *J. Clin. Endocrinol. Metab.* 8, 2290–2296. doi: 10.1210/jc.87.5.2290

Gisolf, J., Wilders, R., Immink, R. V., van Lieshout, J. J., and Karemaker, J. M. (2004). Tidal volume, cardiac output and functional residual capacity determine end-tidal CO2 transient during standing up in humans. *J. Physiol.* 554(Pt 2), 579–590. doi: 10.1113/jphysiol.2003.056895

Grubb, B. P., Gerard, G., Roush, K., Temesy-Armos, P., Montford, P., Elliott, L., et al. (1991). Cerebral vasoconstriction during head-upright tilt-induced vasovagal syncope. A paradoxic and unexpected response. *Circulation* 84, 1157–1164. doi: 10.1161/01.cir.84.3.1157

Gulli, G., Cooper, V. L., Claydon, V. E., and Hainsworth, R. (2005a). Prolonged latency in the baroreflex mediated vascular resistance response in subjects with postural related syncope. *Clin. Auton. Res.* 15, 207–212. doi: 10.1007/s10286-005-0273-8

Gulli, G., Claydon, V. E., Cooper, V. L., and Hainsworth, R. (2005b). R-R interval-blood pressure interaction in subjects with different tolerances to orthostatic stress. *Exp. Physiol.* 90, 367–375. doi: 10.1113/expphysiol.2004.029496

Gulli, G., Wight, V. L., Hainsworth, R., and Cevese, A. (2001). Spectral and cross-spectral autoregressive analysis of cardiovascular variables in subjects with different degrees of orthostatic tolerance. *Clin. Auton. Res.* 11, 19–27. doi: 10.1007/bf02317798

Guven, B., Oner, T., Tavli, V., Yilmazer, M. M., Demirpence, S., and Mese, T. (2013). Low iron storage in children with tilt positive neurally mediated syncope. *World J. Pediatr.* 9, 146–151. doi: 10.1007/s12519-012-0396-7

Hainsworth, R. (2004). Pathophysiology of syncope. *Clin. Auton. Res.* 14(Suppl. 1), 18–24.

Hainsworth, R., Claydon, V. E., Bannister, R., and Mathias, C. (2012). "Syncope and fainting," in *Autonomic Failure*, 5th Edn, eds R. Bannister, and C. Mathias, (Oxford: Oxford University Press).

Hall, J. E., and Guyton, A. C. (2011). *Guyton and Hall Textbook of Medical Physiology*, 12th Edn. Amsterdam: Elsevier.

Hoeldtke, R. D., Horvath, G. G., and Bryner, K. D. (1995). Treatment of orthostatic tachycardia with erythropoietin. *Am. J. Med.* 99, 525–529. doi: 10.1016/s0002-9343(99)80230-7

Ishikawa, T., Chijiwa, T., Hagiwara, M., Mamiya, S., and Hidaka, H. (1989). Thyroid hormones directly interact with vascular smooth muscle strips. *Mol. Pharmacol.* 35, 760–765.

Itoh, Y., Suzuki, Y., Yamamoto, T., Kojima, K., Murakami, I., and Suzumori, N. (2006). Increase in serum concentrations of inhibin in early onset pre-eclampsia with intrauterine growth restriction. *J. Obstet. Gynaecol. Res.* 32, 80–85. doi: 10.1111/j.1447-0756.2006.00355.x

Jacob, G., Robertson, D., Mosqueda-Garcia, R., Ertl, A. C., Robertson, R. M., and Biaggioni, I. (1997). Hypovolemia in syncope and orthostatic intolerance role of the renin-angiotensin system. *Am. J. Med.* 103, 128–133. doi: 10.1016/s0002-9343(97)00133-2

Jarjour, I. T., and Jarjour, L. K. (2013). Low iron storage and mild anemia in postural tachycardia syndrome in adolescents. *Clin. Auton. Res.* 23, 175–179. doi: 10.1007/s10286-013-0198-6

Jørgensen, J. O., Møller, J., Laursen, T., Orskov, H., Christiansen, J. S., and Weeke, J. (1994). Growth hormone administration stimulates energy expenditure and extrathyroidal conversion of thyroxine to triiodothyronine in a dose-dependent manner and suppresses circadian thyrotrophin levels: studies in GH-deficient adults. *Clin. Endocrinol.* 41, 609–614. doi: 10.1111/j.1365-2265.1994.tb01826.x

Kanjwal, K., and Calkins, H. (2015). Syncope in children and adolescents. *Cardiol. Clin.* 33, 397–409. doi: 10.1016/j.ccl.2015.04.008

Kelsey, M. M., and Zeitler, P. S. (2016). Insulin resistance of puberty. *Curr. Diab.* 16:64. doi: 10.1007/s11892-016-0751-5

Kenny, R. A., Fillit, H. M., Rockwood, K., and Woodhouse, K. (2010). "Syncope," in *Brocklehurst's Textbook of Geriatric Medicine and Gerontology*, 7th Edn, eds H. M. Fillit, K. Rockwood, and K. Woodhouse, (Philadelphia: Saunders), 338–347.

Kitay, J. I. (1954). Pineal lesions and precocious puberty: a review. *J. Clin. Endocrinol. Metab.* 14, 622–625. doi: 10.1210/jcem-14-6-622

Kizilbash, S. J., Ahrens, S. P., Bruce, B. K., Chelimsky, G., Driscoll, S. W., Harbeck-Weber, C., et al. (2014). Adolescent fatigue, POTS, and recovery: A guide for clinicians. *Curr. Probl. Pediatr. Adolesc. Health Care* 44, 108–133. doi: 10.1016/j.cppeds.2013.12.014

Kolarov, N., Cerni, M., and Jović, B. (2005). Correlation of age at menarche of mothers and daughters in Backa Palanka. *Med. Pregl.* 58, 208–210. doi: 10.2298/mpns0504208k

Kurbaan, A. S., Franzén, A. C., Bowker, T. J., Williams, T. R., Kaddoura, S., Petersen, M. E., et al. (1999). Usefulness of tilt test-induced patterns of heart rate and blood pressure using a two-stage protocol with glyceryl trinitrate provocation in patients with syncope of unknown origin. *Am. J. Cardiol.* 84, 665–670. doi: 10.1016/s0002-9149(99)00413-0

Lagi, A., Cencetti, S., Corsoni, V., Georgiadis, D., and Bacalli, S. (2001). Cerebral vasoconstriction in vasovagal syncope: any link with symptoms? A transcranial doppler study. *Circulation* 104, 2694–2698. doi: 10.1161/hc6172.099397

Lagi, A., Rossi, A., Sorelli, P., Cartei, A., and Cencetti, S. (2003). Plasma volume and hematocrit changes in recurrent fainters. *Clin. Auton. Res.* 13, 439–442.

Laranjo, S., Tavares, C., Oliveira, M., Trigo, C., Pinto, F., and Rocha, I. (2015). An insight into the autonomic and haemodynamic mechanisms underlying reflex syncope in children and adolescents: a multiparametric analysis. *Cardiol. Young* 25, 647–654. doi: 10.1017/S1047951114000511

Larson, R., Csikszentmihalyi, M., and Graef, R. (1980). Mood variability and the psychosocial adjustment of adolescents. *J. Youth Adolesc.* 9, 469–490. doi: 10.1007/BF02089885

Lasiuk, G. C., and Hegadoren, K. M. (2007). The effects of estradiol on central serotonergic systems and its relationship to mood in women. *Biol. Res. Nurs.* 9, 147–160. doi: 10.1177/1099800407305600

Lee, D. Y., Kim, E., and Choi, M. H. (2015). Technical and clinical aspects of cortisol as a biochemical marker of chronic stress. *BMB Rep.* 48, 209–216. doi: 10.5483/bmbrep.2015.48.4.275

Li, J., Zhang, Q., Liao, Y., Zhang, C., Hao, H., and Du, J. (2015). The value of acetylcholine receptor antibody in children with postural tachycardia syndrome. *Pediatr. Cardiol.* 36, 165–170. doi: 10.1007/s00246-014-0981-8

Limonta, P., Marelli, M. M., Moretti, R., Marzagalli, M., Fontana, F., and Maggi, R. (2018). GnRH in the human female reproductive axis. *Vitam. Horm.* 107, 27–66. doi: 10.1016/bs.vh.2018.01.003

Linzer, M., Pontinen, M., Gold, D. T., Divine, G. W., Felder, A., and Blair Brooks, W. (1991). Impairment of physical and psychosocial function in recurrent syncope. *J. Clin. Epidemiol.* 44, 1037–1043. doi: 10.1016/0895-4356(91)90005-t

Low, P., Sandroni, P., Joyner, M., and Shen, W. K. (2009). Postural orthostatic tachycardia syndrome (POTS). *J. Cardiovasc. Electrophysiol.* 20, 352–358.

Low, P. A. (2014). "Postural orthostatic tachycardia syndrome (POTS)," in *Encyclopedia of the Neurological Sciences*, eds M. J. Aminoff, and R. B. Daroff, (Amsterdam: Elsevier), 964–967. doi: 10.1016/b978-0-12-385157-4.00509-1

Low, P. A., Opfer-Gehrking, T. L., Textor, S. C., Benarroch, E. E., Shen, W. K., Schondorf, R., et al. (1995). Postural tachycardia syndrome (POTS). *Neurology* 45(4 Suppl. 5), S19–S25. doi: 10.1016/b978-0-12-385157-4.00509-1

Maranon, R., and Reckelhoff, J. F. (2013). Sex and gender differences in control of blood pressure. *Clin. Sci. Lond.* 125, 311–318. doi: 10.1042/CS20130140

Marshall, W. A., and Tanner, J. M. (1970). Variations in pattern of pubertal changes in girls. *Obstet. Gynecol. Surv.* 25, 694–695. doi: 10.1097/00006254-197007000-00018

Massin, M. M., Bourguignont, A., Coremans, C., Comté, L., Lepage, P., and Gérard, P. (2004). Syncope in pediatric patients presenting to an emergency department. *J. Pediatr.* 145, 223–228. doi: 10.1016/j.jpeds.2004.01.048

Massin, M. M., Derkenne, B., Tallsund, M., Rocour-Brumioul, D., Ernould, C., Lebrethon, M. C., et al. (1999). Cardiac autonomic dysfunction in diabetic children. *Diabetes* 22, 1845–1850. doi: 10.2337/diacare.22.11.1845

Mathias, C. J., Low, D. A., Iodice, V., Owens, A. P., Kirbis, M., and Grahame, R. (2012). Postural tachycardia syndrome-current experience and concepts. *Nat. Rev. Neurol.* 8, 22–34. doi: 10.1038/nrneurol.2011.187

Matteis, M., Troisi, E., Monaldo, B. C., Caltagirone, C., and Silvestrini, M. (1998). Age and sex differences in cerebral hemodynamics: a transcranial Doppler study. *Stroke* 29, 963–967. doi: 10.1161/01.str.29.5.963

McLeod, K. A. (2003). Syncope in childhood. *Arch. Dis. Child.* 88, 350–353. doi: 10.1136/adc.88.4.350

Medow, M. S., Stewart, J. M., Sanyal, S., Mumtaz, A., Sica, D., and Frishman, W. (2008). Pathophysiology. diagnosis, and treatment of orthostatic hypotension and vasovgal ayncope. *Cardiol. Rev.* 16, 4–20. doi: 10.1097/crd.0b013e31815c8032

Meendering, J. R., Torgrimson, B. N., Houghton, B. L., Halliwill, J. R., and Minson, C. T. (2005). Menstrual cycle and sex affect hemodynamic responses to combined orthostatic and heat stress. *Am. J. Physiol. Heart Circ. Physiol.* 289, H631–H642.

Mendelsohn, M. E., and Karas, R. H. (1999). The protective effects of estrogen on the cardiovascular system. *N. Engl. J. Med.* 340, 1801–1811. doi: 10.1056/nejm199906103402306

Messinis, I. E. (2006). From menarche to regular menstruation: endocrinological background. *Ann. N. Y. Acad. Sci.* 1092, 49–56. doi: 10.1196/annals.1365.004

Miner, J. A., Martini, E. R., Smith, M. M., Brunt, V. E., Kaplan, P. F., Halliwill, J. R., et al. (2011). Short-term oral progesterone administration antagonizes the effect of transdermal estradiol on endothelium-dependent vasodilation in young healthy women. *Am. J. Physiol. Heart Circ. Physiol.* 301, H1716–H1722. doi: 10.1152/ajpheart.00405.2011

Moak, J. P., Bailey, J. J., and Makhlouf, F. T. (2002). Simultaneous heart rate and blood pressure variability analysis. Insight into mechanisms underlying neurally mediated cardiac syncope in children. *J. Am. Coll. Cardiol.* 40, 1466–1474.

Moran, A., Jacobs, D. R., Steinberger, J., Cohen, P., Hong, C.-P., Prineas, R., et al. (2002). Association between the insulin resistance of puberty and the insulin-like growth factor-I/growth hormone axis. *J. Clin. Endocrinol. Metab.* 87, 4817–4820. doi: 10.1210/jc.2002-020517

Moran, A., Jacobs, D. R., Steinberger, J., Steffen, L. M., Pankow, J. S., Hong, C. P., et al. (2008). Changes in insulin resistance and cardiovascular risk during adolescence: establishment of differential risk in males and females. *Circulation* 117, 2361–2368. doi: 10.1161/CIRCULATIONAHA.107.704569

Mtinangi, B. L., and Hainsworth, R. (1998). Early effects of oral salt on plasma volume, orthostatic tolerance, and baroreceptor sensitivity in patients with syncope. *Clin. Auton. Res.* 8, 231–235. doi: 10.1007/bf02267786

Mtinangi, B. L., and Hainsworth, R. (1999). Effects of moderate exercise training on plasma volume, baroreceptor sensitivity and orthostatic tolerance in healthy subjects. *Exp. Physiol.* 84, 121–130. doi: 10.1111/j.1469-445x.1999.tb00077.x

Muniyappa, R., Montagnani, M., Koh, K. K., and Quon, M. J. (2007). Cardiovascular actions of insulin. *Endocr, Rev.* 28, 463–491. doi: 10.1210/er.2007-0006

Murcia, G. J., Muñoz, H. A., Molina, C. A., García, J. M. F., Narbona, L. E., Murcia Garcia, J., et al. (2002). Puberty and melatonin. *An. Esp. Pediatr.* 57, 121–126.

Napoli, R., Guardasole, V., Angelini, V., D'Amico, F., Zarra, E., Matarazzo, M., et al. (2003). Acute effects of growth hormone on vascular function in human subjects. *J. Clin. Endocrinol. Metab.* 88, 2817–2820. doi: 10.1210/jc.2003-030144

Nevo, O., Soustiel, J. F., and Thaler, I. (2007). Cerebral blood flow is increased during controlled ovarian stimulation. *Am. J. Physiol. Circ. Physiol.* 293, H3265–H3269.

Norcliffe, L. J., Bush, V. E., and Hainsworth, R. (2002). Patients with posturally related syncope have increased responsiveness of the cerebral circulation to carbon dioxide. *Clin. Auton. Res.* 12, 316.

Norcliffe-Kaufmann, L. J., Kaufmann, H., and Hainsworth, R. (2007). Enhanced vascular responses to hypocapnia in neurally mediated syncope. *Ann. Neurol.* 63, 288–294. doi: 10.1002/ana.21205

Nordkamp, L. R. O., Van, D. N., Ganzeboom, K. S., Reitsma, J. B., and Luitse, J. S. (2009). Syncope prevalence in the ED compared to general practice and population: a strong selection process. *Am. J. Emerg. Med.* 27, 271–279. doi: 10.1016/j.ajem.2008.02.022

Novak, V., Spies, J. M., Novak, P., McPhee, B. R., Rummans, T. A., and Low, P. A. (1998). Hypocapnia and cerebral hypoperfusion in orthostatic intolerance. *Stroke* 29, 1876–1881. doi: 10.1161/01.str.29.9.1876

O'Connor, K. A., Ferrell, R., Brindle, E., Trumble, B., Shofer, J., Holman, D. J., et al. (2009). Progesterone and ovulation across stages of the transition to menopause. *Menopause* 16, 1178–1187. doi: 10.1097/gme.0b013e3181aa192d

Palma, J. A., Norcliffe-Kaufmann, L., Fuente-Mora, C., Percival, L., Spalink, C. L., and Kaufmann, H. (2017). "Disorders of the autonomic nervous system: autonomic dysfunction in pediatric practice," in *Swaiman's Pediatric Neurology: Principles and Practice, Sixth Edition*, eds K. F. Swaiman, S. Ashwal, and M. I. Shevell, Amsterdam: Elsevier.

Palmeiro, C. R., Anand, R., Dardi, I. K., Balasubramaniyam, N., Schwarcz, M. D., and Weiss, I. A. (2012). Growth hormone and the cardiovascular system. *Cardiol. Rev.* 20, 197–207.

Preston, M. E., Jensen, D., Janssen, I., and Fisher, J. T. (2009). Effect of menopause on the chemical control of breathing and its relationship with acid-base status. *Am. J. Physiol. Regul. Integr. Comp. Physiol.* 296, R722–R727. doi: 10.1152/ajpregu.90865.2008

Protheroe, C. L., Ravensbergen, H. R., Inskip, J. A., and Claydon, V. E. (2013). Tilt Testing with combinedlLower body negative pressure: a "gold standard" for measuring orthostatic tolerance. *J. Vis. Exp.* 73:e4315. doi: 10.3791/4315

Purves-Tyson, T. D., Handelsman, D. J., Double, K. L., Owens, S. J., Bustamante, S., and Weickert, C. S. (2012). Testosterone regulation of sex steroid-related mRNAs and dopamine-related mRNAs in adolescent male rat substantia nigra. *BMC Neurosci.* 13:95. doi: 10.1371/journal.pone.0091151

Radtke, A., Lempert, T., von, B. M., Feldmann, M., Lezius, F., Neuhauser, H., et al. (2011). Prevalence and complications of orthostatic dizziness in the general population. *Clin. Auton. Res.* 21, 161–168. doi: 10.1007/s10286-010-0114-2

Raj, S. R. (2013). Postural tachycardia syndrome (POTS). *Circulation* 127, 2336–2342. doi: 10.1161/circulationaha.112.144501

Regensteiner, J. G., Woodard, W. D., Hagerman, D. D., Weil, J. V., Pickett, C. K., Bender, P. R., et al. (1989). Combined effects of female hormones and metabolic rate on ventilatory drives in women. *J. Appl. Physiol.* 66, 808–813.

Regidor, P. A. (2014). Progesterone in peri- and postmenopause: a review. *Geburtshilfe Frauenheilkd.* 74, 995–1002.

Rhie, Y. J. (2013). Kisspeptin/G protein-coupled receptor-54 system as an essential gatekeeper of pubertal development. *Ann. Pediatr. Endocrinol. Metab.* 18, 55–59. doi: 10.6065/apem.2013.18.2.55

Romero, C. J., Pine-Twaddell, E., Sima, D. I., Miller, R. S., He, L., Wondisford, F., et al. (2012). Insulin-Like Growth Factor 1 Mediates Negative Feedback to Somatotroph GH Expression via POU1F1/CREB Binding Protein Interactions. *Mol. Cell Biol.* 32, 4258–4269. doi: 10.1128/MCB.00171-12

Rose, M. S., Koshman, M. L., Spreng, S., and Sheldon, R. (2000). The relationship between health-related quality of life and frequency of spells in patients with syncope. *J. Clin. Epidemiol.* 53, 1209–1216. doi: 10.1016/s0895-4356(00)00257-2

Rose, S. R., Municchi, G., Barnes, K. M., Kamp, G. A., Uriarte, M. M., Ross, J. L., et al. (1991). Spontaneous growth hormone secretion increases during puberty in normal girls and boys. *J. Clin. Endocrinol. Metab.* 73, 428–435. doi: 10.1210/jcem-73-2-428

Rosen, S. G., and Cryer, P. E. (1982). Postural tachycardia syndrome. Reversal of sympathetic hyperresponsiveness and clinical improvement during sodium loading. *Am. J. Med.* 72, 847–850.

Rossmanith, W. G., Laughlin, G. A., Mortola, J. F., and Yen, S. S. (1990). Secretory dynamics of oestradiol (E2) and progesterone (P4) during periods of relative pituitary LH quiescence in the midluteal phase of the menstrual cycle. *Clin. Endocrinol.* 32, 13–23. doi: 10.1111/j.1365-2265.1990.tb03745.x

Rozario, K. S., Lloyd, C., and Ryan, F. (2000). "GH and IGF-1 physiology in childhood," in *Endotext*, eds L. J. De Groot, G. Chrousos, K. Dungan, K. R. Feingold, and A. Grossman, (South Dartmouth, MA: MDText.com).

Ruzieh, M., Batizy, L., Dasa, O., Oostra, C., and Grubb, B. (2017). The role of autoantibodies in the syndromes of orthostatic intolerance: a systematic review. *Scand. Cardiovasc. J.* 51, 243–247. doi: 10.1080/14017431.2017.1355068

Rybaczyk, L. A., Bashaw, M. J., Pathak, D. R., Moody, S. M., Gilders, R. M., and Holzschu, D. L. (2005). An overlooked connection: serotonergic mediation of estrogen-related physiology and pathology. *BMC Womens Health* 5:12. doi: 10.1186/1472-6874-5-12

Saenger, P. (2003). Dose effects of growth hormone during puberty. *Horm. Res.* 60(Suppl. 1), 52–57. doi: 10.1159/000071226

Sakharova, A. A., Horowitz, J. F., Surya, S., Goldenberg, N., Harber, M. P., Symons, K., et al. (2008). Role of growth hormone in regulating lipolysis, proteolysis, and hepatic glucose production during fasting. *J. Clin. Endocrinol. Metab.* 93, 2755–2759. doi: 10.1210/jc.2008-0079

Sandroni, P., Opfer-Gehrking, T. L., McPhee, B. R., and Low, P. A. (1999). Postural tachycardia syndrome: clinical features and follow-up study. *Mayo Clin. Proc.* 74, 1106–1110. doi: 10.4065/74.11.1106

Satterthwaite, T. D., Shinohara, R. T., Wolf, D. H., Hopson, R. D., Elliott, M. A., Vandekar, S. N., et al. (2014). Impact of puberty on the evolution of cerebral perfusion during adolescence. *Proc. Natl. Acad. Sci. U.S.A.* 111, 8643–8648. doi: 10.1073/pnas.1400178111

Schroeder, C., Tank, J., Heusser, K., Diedrich, A., Luft, F. C., and Jordan, J. (2011). Physiological phenomenology of neurally-mediated syncope with management implications. *PLoS One* 6:e26489. doi: 10.1371/journal.pone.0026489

Shahid, M. A., and Sharma, S. (2019). *Physiology, Thyroid Hormone*. Treasure Island, FL: StatPearls.

Shamma, F. N., Fayad, P., Brass, L., and Sarrel, P. (1992). Middle cerebral artery blood velocity during controlled ovarian hyperstimulation. *Fertil. Steril.* 57, 1022–1025. doi: 10.1016/s0015-0282(16)55020-1

Shankar, R. R., Eckert, G. J., Saha, C., Tu, W., and Pratt, J. H. (2005). The change in blood pressure during pubertal growth. *J. Clin. Endocrinol. Metab.* 90, 163–167. doi: 10.1210/jc.2004-0926

Shaw, B. H., Stiles, L. E., Bourne, K., Green, E. A., Shibao, C. A., Okamoto, L. E., et al. (2019) The face of postural tachycardia syndrome – insights from a large cross-sectional online community-based survey. *J. Intern. Med.* 286, 438–448. doi: 10.1111/joim.12895

Shaw, N. D., Butler, J. P., Nemati, S., Kangarloo, T., Ghassemi, M., Malhotra, A., et al. (2015). Accumulated deep sleep is a powerful predictor of LH pulse onset in pubertal children. *J. Clin. Endocrinol. Metab.* 100, 1062–1070. doi: 10.1210/jc.2014-3563

Shaw, N. D., Histed, S. N., Srouji, S. S., Yang, J., Lee, H., and Hall, J. E. (2010). Estrogen negative feedback on gonadotropin secretion: evidence for a direct pituitary effect in women. *J. Clin. Endocrinol. Metab.* 95, 1955–1961. doi: 10.1210/jc.2009-2108

Silman, R. E., Leone, R. M., Hooper, R. J., and Preece, M. A. (1979). Melatonin, the pineal gland and human puberty. *Nature* 282, 301–303. doi: 10.1038/282301a0

Sinclair, D., Purves-Tyson, T. D., Allen, K. M., and Weickert, C. S. (2014). Impacts of stress and sex hormones on dopamine neurotransmission in the adolescent brain. *Psychopharmacology* 231, 1581–1599. doi: 10.1007/s00213-013-3415-z

Singer, W., Sletten, D. M., Opfer-Gehrking, T. L., Brands, C. K., Fischer, P. R., and Low, P. A. (2012). Postural tachycardia in children and adolescents: what is abnormal? *J. Pediatr.* 160, 222–226. doi: 10.1016/j.jpeds.2011.08.054

Slatkovska, L., Jensen, D., Davies, G. A. L., and Wolfe, L. A. (2006). Phasic menstrual cycle effects on the control of breathing in healthy women. *Respir. Physiol. Neurobiol.* 154, 379–388. doi: 10.1016/j.resp.2006.01.011

Sliwowska, J. H., Fergani, C., Gawałek, M., Skowronska, B., Fichna, P., and Lehman, M. N. (2014). Insulin: its role in the central control of reproduction. *Physiol. Behav.* 133, 197–206. doi: 10.1016/j.physbeh.2014.05.021

Smit, A. A. J., Halliwill, J. R., Low, P. A., and Wieling, W. (1999). Pathophysiological basis of orthostatic hypotension in autonomic failure. *J. Physiol.* 519, 1–10. doi: 10.1111/j.1469-7793.1999.0001o.x

Soliman, A., Sanctis, V. D., Elalaily, R., and Bedair, S. (2014). Advances in pubertal growth and factors influencing it: can we increase pubertal growth? *Indian J. Endocrinol. Metab.* 18, 53–62. doi: 10.4103/2230-8210.145075

Stewart, J. M. (2009). Postural tachycardia syndrome and reflex syncope: similarities and differences. *J. Pediatr.* 154, 481–485. doi: 10.1016/j.jpeds.2009.01.004

Stewart, J. M., McLeod, K. J., Sanyal, S., Herzberg, G., and Montgomery, L. D. (2004). Relation of postural vasovagal syncope to splanchnic hypervolemia in adolescents. *Circulation* 110, 2575–2581. doi: 10.1161/01.cir.0000145543.88293.21

Stewart, J. M., Medow, M. S., Cherniack, N. S., and Natelson, B. H. (2006). Postural hypocapnic hyperventilation is associated with enhanced peripheral vasoconstriction in postural tachycardia syndrome with normal supine blood flow. *Am. J. Physiol. Heart Circ. Physiol.* 291, H904–H913.

Stroud, L. R., Papandonatos, G. D., Williamson, D. E., and Dahl, R. E. (2011). Sex differences in cortisol response to corticotropin releasing hormone challenge over puberty: pittsburgh pediatric neurobehavioral studies. *Psychoneuroendocrinology* 36, 1226–1238. doi: 10.1016/j.psyneuen.2011.02.017

Sung, R. Y., Du, Z. D., Yu, C. W., Yam, M. C., and Fok, T. F. (2000). Cerebral blood flow during vasovagal syncope induced by active standing or head up tilt. *Arch. Dis. Child.* 82, 154–158. doi: 10.1136/adc.82.2.154

Swerdloff, R. S., and Odell, W. D. (1975). Hormonal mechanisms in the onset of puberty. *Postgrad. Med. J.* 51, 200–208. doi: 10.1136/pgmj.51.594.200

Tanaka, H., Borres, M., Thulesius, O., Tamai, H., Ericson, M. O., and Lindblad, L. E. (2000). Blood pressure and cardiovascular autonomic function in healthy children and adolescents. *J. Pediatr.* 137, 63–67. doi: 10.1067/mpd.2000.108098

Teixeira, R. R., Díaz, M. M., Santos, T. V., da, S., Bernardes, J. T. M., Peixoto, L. G., et al. (2015). Chronic stress induces a hyporeactivity of the autonomic nervous system in response to acute mental stressor and impairs cognitive performance in business executives. *PLoS One* 10:e0119025. doi: 10.1371/journal.pone.0119025

Theodorakis, G. N., Markianos, M., Livanis, E. G., Zarvalis, E., Flevari, P., and Kremastinos, D. T. (1998). Central serotonergic responsiveness in neurocardiogenic syncope: a clomipramine test challenge. *Circulation* 98, 2724–2730. doi: 10.1161/01.cir.98.24.2724

Thomas, H. M. (1957). Effect of thyroid hormone on circulation. *J. Am. Med. Assoc.* 163, 337–341.

Thomson, H. L., Wright, K., and Frenneaux, M. (1997). Baroreflex sensitivity in patients with vasovagal syncope. *Circulation* 95, 395–400. doi: 10.1161/01.cir.95.2.395

Vaddadi, G., Esler, M. D., Dawood, T., and Lambert, E. (2010). Persistence of muscle sympathetic nerve activity during vasovagal syncope. *Eur. Heart J.* 31, 2027–2033. doi: 10.1093/eurheartj/ehq071

Van De Wielle, R. V., and Michels, N. (2017). Longitudinal associations of leptin and adiponectin with heart rate variability in children. *Front. Physiol.* 8:498. doi: 10.3389/fphys.2017.00498

Van Dijk, N., Sprangers, M. A., Boer, K. R., Colman, N., Wieling, W., and Linzer, M. (2007). Quality of life within one year following presentation after transient loss of consciousness. *Am. J. Cardiol.* 100, 672–676. doi: 10.1016/j.amjcard.2007.03.085

van Lieshout, J. J., Wieling, W., Karemaker, J. M., and Eckberg, D. L. (1991). The vasovagal response. *Clin. Sci. Lond.* 81, 575–586.

Vehkavaara, S., Westerbacka, J., Hakala-Ala-Pietilä, T., Virkamäki, A., Hovatta, O., and Yki-Järvinen, H. (2000). Effect of estrogen replacement therapy on insulin sensitivity of glucose metabolism and preresistance and resistance vessel function in healthy postmenopausal women. *J. Clin. Endocrinol. Metab.* 85, 4663–4670. doi: 10.1210/jc.85.12.4663

Viner, R., and Christie, D. (2005). Fatigue and somatic symptoms. *BMJ* 330, 1012–1015. doi: 10.1136/bmj.330.7498.1012

Wagoner, A. L., Shaltout, H. A., Fortunato, J. E., and Diz, D. I. (2016). Distinct neurohumoral biomarker profiles in children with hemodynamically defined orthostatic intolerance may predict treatment options. *Am. J. Physiol. Heart Circ. Physiol.* 310, H416–H425. doi: 10.1152/ajpheart.00583.2015

Walsh, C. A. (2001). Syncope and sudden death in the adolescent. *Adolesc. Med.* 12, 105–132.

Wennink, J. M., Delemarre-van de Waal, H. A., Schoemaker, R., Schoemaker, H., and Schoemaker, J. (1990). Luteinizing hormone and follicle stimulating hormone secretion patterns in girls throughout puberty measured using highly sensitive immunoradiometric assays. *Clin. Endocrinol.* 33, 333–344. doi: 10.1111/j.1365-2265.1990.tb00498.x

Wheeler, M. D. (1991). Physical changes of puberty. *Endocrinol. Metab. Clin. North Am.* 20, 1–14.

White, D. P., Douglas, N. J., Pickett, C. K., Weil, J. V., and Zwillich, C. W. (1983). Sexual influence on the control of breathing. *J. Appl. Physiol.* 54, 874–879. doi: 10.1152/jappl.1983.54.4.874

Wieling, W., Ganzeboom, K. S., and Saul, J. P. (2004). Reflex syncope in children and adolescents. *Heart* 90, 1094–1100. doi: 10.1136/hrt.2003.022996

Wieling, W., Smit, A. A., de Jong-de Vos van Steenwijk, C. C., van Lieshout, J. J., and Karemaker, J. M. (1997). Pathophysiological mechanisms underlying vasovagal syncope in young subjects. *Pacing Clin. Electrophysiol.* 20(8 Pt 2), 2034–2038. doi: 10.1111/j.1540-8159.1997.tb03622.x

Wilson, T. E., Cui, J., Zhang, R., and Crandall, C. G. (2006). Heat stress reduces cerebral blood velocity and markedly impairs orthostatic tolerance in humans. *Am. J. Physiol. Regul. Integr. Comp. Physiol.* 291, R1443–R1448.

Winter, J. S. D., and Faiman, C. (1973). The development of cyclic pituitary-gonadal function in adolescent females. *J. Clin. Endocrinol. Metab.* 37, 714–718. doi: 10.1210/jcem-37-5-714

Zhao, J., Han, Z., Zhang, X., Du, S., Liu, A. D., Holmberg, L., et al. (2015). A cross-sectional study on upright heart rate and BP changing characteristics: basic data for establishing diagnosis of postural orthostatic tachycardia syndrome and orthostatic hypertension. *BMJ Open* 5:95. doi: 10.1136/bmjopen-2014-007356

Conflict of Interest: The authors declare that the research was conducted in the absence of any commercial or financial relationships that could be construed as a potential conflict of interest.

frontiers in Neuroscience

ORIGINAL RESEARCH
published: 19 November 2019
doi: 10.3389/fnins.2019.01217

Leptin-Mediated Sympathoexcitation in Obese Rats: Role for Neuron–Astrocyte Crosstalk in the Arcuate Nucleus

*Xuefei Liu and Hong Zheng**

Division of Basic Biomedical Sciences, Sanford School of Medicine, University of South Dakota, Vermillion, SD, United States

Introduction: Accumulated evidence indicates that obesity is associated with enhanced sympathetic activation. Hypothalamic leptin-mediated signaling may contribute to the exaggerated sympathoexcitation of obesity. The goal of this study was to investigate the "neuron–astrocyte" interaction affecting leptin-mediated sympathoexcitation within the arcuate nucleus (ARCN) of the hypothalamus in obese rats.

Methods and Results: Obesity was induced by high-fat diet (HFD, 42% of calories from fat) in Sprague Dawley rats. Twelve weeks of HFD produced hyperleptinemia, hyperlipidemia, and insulin resistance. In anesthetized rats, microinjections of leptin into the ARCN induced increases in heart rate (HR), renal sympathetic nerve activity (RSNA), and mean arterial pressure (MAP) in both control and HFD rats. However, microinjections of leptin in HFD rats elicited higher responses of RSNA and arterial pressure than control-fed rats. It also caused the inhibition of astrocytes within the ARCN using an astrocytic metabolic inhibitor, fluorocitrate, and reduced leptin-induced sympathetic activity and blood pressure responses. Moreover, the expression of the leptin receptor in the ARCN of HFD-fed rats was significantly increased compared to rats fed a control diet. Immunohistochemistry analysis revealed leptin receptor localization from both neurons and astrocytes of the ARCN. HFD rats exhibited increased protein expression of glial fibrillary acidic protein (GFAP) in the ARCN. We also found that the expression of astrocyte-specific glutamate transporters and excitatory amino acid transporter 1 (EAAT1) and 2 (EAAT2) were decreased within the ARCN of the HFD rats. In cultured astrocytic C6 cells, 24 h of leptin treatment increased the protein expression of GFAP and reduced the expression of EAAT1 and EAAT2.

Conclusion: The results suggest that central leptin signaling occurs via neuron-astrocyte interactions in the ARCN and contributing to the exaggerated sympathoexcitation observed in obese rats. The effects may be mediated by the action of leptin on regulating astrocytic glutamate transporters within the ARCN of the hypothalamus.

Keywords: sympathetic nerve activity, obesity, glial cells, hypothalamus, leptin

OPEN ACCESS

Edited by:
Valdir Andrade Braga,
Federal University of Paraíba, Brazil

Reviewed by:
Julie A. Chowen,
Niño Jesús University Children's Hospital, Spain
Youichirou Ootsuka,
Flinders University, Australia

***Correspondence:**
Hong Zheng
hong.zheng@usd.edu

Specialty section:
This article was submitted to Autonomic Neuroscience, a section of the journal Frontiers in Neuroscience

Received: *04 June 2019*
Accepted: *28 October 2019*
Published: *19 November 2019*

Citation:
Liu X and Zheng H (2019) Leptin-Mediated Sympathoexcitation in Obese Rats: Role for Neuron–Astrocyte Crosstalk in the Arcuate Nucleus. Front. Neurosci. 13:1217. doi: 10.3389/fnins.2019.01217

INTRODUCTION

Accumulated evidence indicates that obesity is associated with enhanced sympathetic activation (Kalil and Haynes, 2012; Head et al., 2014; Vaneckova et al., 2014; Hall et al., 2019). Chronic sympathetic activation increases cardiovascular risks, such as heart failure, hypertension, arrhythmia, atherosclerosis, and subsequent mortality in obesity (Corry and Tuck, 1999; Balasubramanian et al., 2019). The central nervous system plays a critical role in integrating peripheral afferent signals to regulate sympathetic outflow and cardiovascular function (Prior et al., 2010; Ward et al., 2011). The levels of circulating leptin have been found to be elevated in the obese condition and therefore may be related to the onset and maintenance of a hyper-sympathetic state during obesity (Bell and Rahmouni, 2016). Central leptin administration increases renal sympathetic nerve activity (RSNA), arterial pressure, and heart rate (HR) in conscious animals (Matsumura et al., 2000). The precise central mechanisms linking obesity with sympathetic overactivation are not entirely understood.

Leptin is an adipose-derived hormone that links to sympathetic activation in obesity-related hypertension (Haynes et al., 1997; Lim et al., 2013; Hall et al., 2019). Importantly, leptin can cross the blood–brain barrier to interact with a leptin receptor (OBR) in the hypothalamic nuclei. Central leptin action mainly affects feeding, thermogenesis, and sympathetic activation of the kidneys, hind limbs, and adrenal glands (Rahmouni and Haynes, 2002). Leptin can exert pressor effects through its action at the hypothalamic nuclei–the arcuate nucleus (ARCN), paraventricular nucleus, and ventromedial hypothalamus–resulting in sympathetic activation in animals (Badoer and Ryan, 1999; Rahmouni and Morgan, 2007; Habeeballah et al., 2016). The OBR is widely expressed in all these hypothalamic nuclei (Ghamari-Langroudi et al., 2011). Thus far, the central hypothalamic leptin-mediated pathways have not been fully elucidated.

The hypothalamus, including the ARCN, is a heterogeneous area comprised of different types of cells, including neurons, astrocytes, oligodendrocytes, microglia, endothelial cells, and ependymal cells (Thaler et al., 2010). The function of astrocytes in the brain extends beyond providing structural and metabolic support to the neurons. Astrocytes can also affect neuronal activity in a variety of ways, including influencing the action of glutamate and other neurotransmitters (Gordon et al., 2009). Indeed, it has been recently revealed that astrocytes serve as active mediators of various complex central mechanisms (Pan et al., 2012; Marina et al., 2016). OBR has been found in both neurons and astrocytes in the hypothalamus (Hsuchou et al., 2009b) and is responsible for leptin-induced calcium signaling in astrocytes (Hsuchou et al., 2009a). Further, it has been shown that metabolic changes can alter OBR expression and astrocytic activity in obese mice (Hsuchou et al., 2009a). Pan et al. have reported that leptin actions on astrocytic cells played an essential role in affecting metabolism and neuronal activity in obesity (Pan et al., 2012). We, therefore, proposed that defining the role of astrocytes on leptin signaling would provide an understanding of the central mechanisms involved in the sympathetic over-activation exhibited during HFD-induced obesity.

MATERIALS AND METHODS

This protocol was approved by the Institutional Animal Care and Use Committee of the University of South Dakota and was conducted in accordance with the guidelines of the National Institutes of Health Guide for the Care and Use of Laboratory Animals.

High Fat Diet-Induced Obese Rats

Male Sprague Dawley rats (130–150 g, age 6–7 weeks) were obtained from Envigo and housed in a room with a 12-h light-dark cycle with free access to water. Rats were fed with the HFD (TD 0.88137, 42% of calories are from fat, 42% of calories from carbohydrate, 15% of calories from protein, Harlan) ($n = 30$). Rats fed a standard diet served as non-HFD controls ($n = 30$). Body weight, food consumption and blood glucose were monitored weekly. The blood glucose sample was obtained by a nick on the tail and a small drop of blood was collected to measure blood glucose by a commercial handheld glucometer (Accu-Chek, Roche).Using blood samples collected from the tail vein, levels of plasma insulin, leptin (ALPCO, Salem, NH, United States), and angiotensin II (LifeSpan BioSciences, Seattle, WA, United States) were measured by commercial ELISA kits. A total of 33 plasma samples (16 from control and 17 from HFD rats) were tested. The absorbance was measured with a microplate reader at 450 nm (PerkinElmer, Waltham, MA, United States). The plasma triglyceride level was measured by a quantification kit (BioVision, Milpitas, CA, United States). The insulin sensitivity index was calculated as 1/[log (fasting insulin) + log (fasting glucose)].

Urinary norepinephrine excretion was measured as an index of overall sympathetic nerve activity. After 12 weeks of HFD, rats were placed in metabolic cages, and 24-h urine was collected, and urine volume was measured. Urinary norepinephrine concentration was measured using an ELISA kit (LifeSpan BioSciences) and calculated as urinary norepinephrine concentration multiplied by urine volume over a 24-h period.

Acute experiments and tissue collections were performed after 12 weeks of exposure to the HFD or control diet (18-week-old rats).

In vivo Electrophysiological Studies

General Surgery for the Recording of Renal Sympathetic Nerve Activity and Arterial Pressure

Rats were anesthetized with a cocktail of urethane (0.75–1.5 g/kg, i.p) and α-chloralose (140 mg/kg, i.p). Adequate depth of anesthesia was assessed by the absence of a corneal reflex and paw withdrawal response to a noxious pinch. The femoral vein was cannulated with PE20 tubing for administration of additional anesthesia and 0.9% saline. The femoral artery was cannulated and connected to the MacLab (ADInstruments, Colorado Springs, CO, United States) for a computer-based recording of arterial pressure and HR.

The left kidney was exposed through a retroperitoneal flank incision. A renal nerve bundle was isolated from fat and connective tissue. The nerve bundle was placed on a bipolar electrode and fixed with Wacker Silgel. The electrical signal was amplified with a Grass amplifier (gain, 10,000) with high- and low-frequency cutoffs of 1,000 and 100 Hz, respectively. The rectified output from the amplifier was displayed, using the PowerLab system to record and integrate the raw nerve discharge (full-wave rectified and integrated with a 0.5 s time constant) (Kleiber et al., 2008).

Basal nerve activity was determined at the beginning of the acute experiment. The background noise was determined by the RSNA recorded at the end of the experiment after a ganglionic blocker hexamethonium (30 mg/kg, iv) injection. The value of RSNA during the experiment was calculated by subtracting the background noise from the actual recorded value. The changes of RSNA were expressed as a percentage of the basal value of RSNA.

Microinjections Into the ARCN

An incision was made on the midline of the scalp. The coordinates of the ARCN were 2.3 mm posterior to the bregma, 0.5 mm lateral to the midline, and 9.6–9.9 mm ventral to the dura (Harlan et al., 2011; Kawabe et al., 2013). 30 min after the surgical procedure, a microsyringe needle (0.2 mm OD) was inserted into the ARCN for drug delivery. At the end of the experiment, blue dye (2% Chicago blue, 30 nL) was injected into the brain for histological verification.

Microinjection Experimental Protocols

Experiment 1: In the control and HFD groups (n = 8–9/group), leptin (R&D Systems, Minneapolis, MN, United States) (50, 100, and 200 ng in 50 nL yielding concentrations of 1, 2, and 4 mg/ml, respectively) (Rahmouni and Morgan, 2007; Shi et al., 2015) dissolved in the vehicle consisting of artificial cerebrospinal fluid was microinjected into the ARCN. The responses of RSNA, mean arterial pressure (MAP), and HR over the following 30 min were recorded. Microinjections into the ARCN with 50 nL of vehicle were also performed and recorded accordingly.

Experiment 2: In the separate groups of control and HFD rats (n = 8/group), astrocytic metabolic inhibitor fluorocitrate (20 mM, 1 nmol in 50 nL, MilliporeSigma) (Pan et al., 2011) dissolved in the artificial cerebrospinal fluid vehicle was pre-microinjected into the ARCN. A total of 30 min later, leptin (200 ng in 50 nL) was microinjected into the ARCN. The responses of RSNA, MAP, and HR over the next 30 min were recorded. Microinjections into the ARCN of the vehicle (50 nL) and, 30 min later, leptin (200 ng in 50 nL) were performed. The responses of RSNA, MAP, and HR were recorded.

Immunohistochemistry

Under deep anesthesia with isoflurane, rats were perfused through the left cardiac ventricle with heparinized saline followed by 4% paraformaldehyde. The brain was removed, post-fixed with paraformaldehyde, and then placed in 30% sucrose. Brain sections of the ARCN (each section 30 μm thick) were cut with a cryostat according to a stereotaxic atlas and preserved in cryoprotectant.

The floating brain sections (control and HFD, n = 4/group) were incubated with 10% normal donkey serum for 1 h and then incubated in the primary antibody against OBR, (anti-rabbit, 1:200∼500, Abcam, Cambridge, MA, United States) with neuronal marker NeuN, (anti-mouse, 1:500, MilliporeSigma, Burlington, MA, United States) or glial marker glial fibrillary acidic protein (GFAP) (anti-mouse, 1:500, MilliporeSigma) antibody overnight at 4°C. Negative control for dual labeling included the sections with NeuN or GFAP primary antibody only. OBR block peptide and OBR siRNA (**Supplementary Figure 1**) was used in the dual labeling staining to test the specificity of the OBR primary antibody. On the second day, the sections were incubated with Alexa Fluor 594 donkey anti-rabbit secondary antibody and Alexa Fluor 488 donkey anti-mouse secondary antibody (1:200, Jackson ImmunoResearch, West Grove, PA, United States) for 2 h. After washing, the sections were mounted on glass slides and cover slipped with Vectashield mounting medium (Vector Laboratories, Burlingame, CA, United States). The images of OBR with NeuN or GFAP immunofluorescence, respectively, within the ARCN (sections from −2.3 to −2.8 mm to bregma) were viewed by a Leica fluorescence microscope and captured by a digital camera (Leica, Germany). Quantification of the intensity of OBR fluorescence in the ARCN area was done using NIH ImageJ software. Six sections of the ARCN were averaged for each rat. The number of GFAP immunoreactive ($GFAP^+$) cells and the number of projections from $GFAP^+$ cells were measured in five randomly chosen high-power (400X magnification) fields within the ARCN using ImageJ software.

Micropunch of the ARCN of the Hypothalamus for Protein Measurements

In the separate groups of control (n = 6) and HFD (n = 6), under deep anesthesia with isoflurane, rats were sacrificed, and brains were removed and frozen on dry ice. Serial coronal sections (100 μm/section) of the ARCN (total 15 sections, from −2.0 to −3.5 mm to bregma) were cut with a cryostat according to a stereotaxic atlas. The sections were bilaterally punched using the Palkovits and Brownstein technique (Palkovits and Brownstein, 1983). The punches were homogenized and placed in 100 μl of radioimmunoprecipitation assay (RIPA) buffer containing 1% protease inhibitor cocktail (Promega, Madison, WI, United States), and protein samples were stored at −80°C.

Western Blot Measurements

The total protein concentrations were measured with a bicinchoninic acid assay kit (Pierce, Rockford, IL, United States). Samples were adjusted to contain the same total protein concentrations. 4× loading buffer was added, and samples were loaded onto sodium dodecyl sulfate polyacrylamide electrophoresis gel, subjected to electrophoresis, and transferred to a polyvinylidene difluoride membrane (MilliporeSigma). Then, the membrane was incubated with primary antibody [rabbit anti-OBR (1:300, Abcam), mouse anti-GFAP (1:500, MilliporeSigma), rabbit anti-excitatory amino acid transporter 1 (EAAT1), rabbit anti-EAAT2, rabbit anti-vesicular glutamate transporter 2 (vGLUT2) (1:200, Cell Signaling, Danvers, MA, United States), or mouse anti-β-actin (1:1000, Santa Cruz

Biotechnology, Santa Cruz, CA, United States)] overnight. After the incubation with secondary antibody conjugated with fluorescent dye (1:10000, Thermo Fisher Scientific), the membrane was visualized by the Odyssey Imaging System (LI-COR Biosciences, Lincoln, NE, United States). The intensity of the band was quantified using NIH ImageJ software. The protein expression was calculated as the ratio of the intensity of the protein to the intensity of β-actin.

In vitro Studies

GFAP Protein and Glutamate Transporter Levels in Response to Leptin in Astrocytes

Stock cultures of the astrocytic cell line C6 were purchased from American Type Culture Collection (ATCC CCL-107, Manassas, VA, United States). Cells were grown in 60 mm culture dishes in ATCC-formulated F-12K medium supplemented with 2.5% fetal bovine serum and 15% horse serum, and they were maintained at 37°C and 5% CO_2 until 60–70% confluence before treatment with leptin. Cells were then maintained in the medium without serum for differentiation purposes. Subsequently, cells were treated with leptin at the concentration of 25–200 ng/ml or vehicle for 24 h. Each treatment was performed for four times (n = 4). Cultured cells prepared were subjected to immunohistochemistry study for GFAP and OBR staining, protein extraction procedure, and Western blot studies for GFAP, EAAT1, and EAAT2 protein measurements.

Statistical Analysis

All data are presented as Means ± SE. Statistical data analysis was performed with Graph Pad Prism 7 (GraphPad Software, La Jolla, CA, United States). For the dose response studies in the electrophysiological experiments and *in vitro* experiments, log dose-response linear analysis was used first to assess the dose-dependent responses. Values of $P < 0.05$ were considered as displaying a significant linear trend. Then factorial one-way or two-way analysis of variance (ANOVA) was used, followed by the Tukey post-test or Sidak's post-test for multiple comparisons when appropriate, to assess the difference in response between doses and the differences between experimental groups. Other measurements were compared between the groups using two tailed unpaired Student's t tests. $P < 0.05$ was considered statistically significant.

RESULTS

General Characteristics of Control and HFD Rats

General characteristics of control and HFD rats used in the experiments are summarized in **Table 1**. Twelve weeks of HFD increased animal body weight, retroperitoneal fat pad weight, and epididymal fat pad weight. The HFD rats also had increased brown adipose tissue weight. The levels of plasma leptin, insulin, and triglyceride were significantly higher in the HFD rats than in control rats. Although the plasma glucose levels were not significantly different between the groups, the HFD rats had a lower mean insulin sensitivity index. These data confirmed that 12 weeks of HFD induced hyperlipidemia, hyperleptinemia, hyperinsulinemia, and insulin resistance.

As can be seen in **Table 1**, the level of plasma angiotensin II was significantly elevated, while the basal RSNA and 24-h urinary norepinephrine levels were significantly increased in the HFD group, suggesting that overall sympathetic activity was elevated. The basal MAP was also significantly increased in the HFD rats compared to control rats. There was no significant difference in HR in the two groups.

Sympathetic Responses to Leptin Injections Into the ARCN of the HFD Rats

In anesthetized rats, microinjections of leptin (50, 100, and 200 ng) into the ARCN induced dose-dependent increases of RSNA [linear regression analysis, control: $F(1,2) = 94.83$, $R^2 = 0.979$, $P = 0.010$; HFD: $F(1,2) = 43.05$, $R^2 = 0.956$, $P = 0.022$], MAP [control: $F(1,2) = 31.25$, $R^2 = 0.940$, $P = 0.031$; HFD: $F(1,2) = 48.51$, $R^2 = 0.960$, $P = 0.020$], and HR [control: $F(1,2) = 12.27$, $R^2 = 0.890$, $P = 0.042$; HFD: $F(1,2) = 25.95$, $R^2 = 0.929$, $P = 0.036$] in both control and HFD rats (**Figure 1**). Leptin administration (200 ng) in the ARCN of HFD rats elicited significantly higher increases in RSNA and MAP (reaching RSNA: 46 ± 7%, ΔMAP: 35 ± 5 mmHg) compared with control rats (ΔRSNA: 29 ± 5%, ΔMAP: 22 ± 4 mmHg) [RSNA: $F(7,7) = 5.656$, $P = 0.036$; MAP: $F(7,7) = 2.265$, $P = 0.034$]. There was no significant difference in the increase in HR seen in control and HFD groups. Vehicle injections did not affect the sympathetic responses in either group.

TABLE 1 | General characteristics of control and HFD rats.

	Control (n = 16)	HFD (n = 17)		Control (n = 16)	HFD (n = 17)
Body weight (g)	415 ± 10	454 ± 17*	Plasma glucose (mmol/L)	4.7 ± 0.6	5.5 ± 0.9
Retroperitoneal fat pad (g)	4.3 ± 0.5	8.7 ± 1.2*	Plasma insulin (mU/L)	14.3+2.7	78.0 ± 15.6*
Epididymal fat pad (g)	4.3 ± 0.2	9.0 ± 1.2*	Insulin sensitivity index	0.54 ± 0.06	0.38 ± 0.04*
Brown adipose tissue (g)	0.28 ± 0.03	0.61 ± 0.08*	Plasma leptin (ng/ml)	358 ± 37	2577 ± 356*
Plasma triglyceride (mmol/L)	1.1 ± 0.3	5.3 ± 1.3*	Plasma angiotensin II (pg/ml)	92.5 ± 34.1	298.5 ± 31.4*
Basal MAP (mmHg)	93 ± 4	103 ± 5	Basal heart rate (beat/min)	347 ± 26	366 ± 19
Basal Int. RSNA (μv.s)	2.2 ± 0.3	4.2 ± 0.4*	24 h urinary NE (μg)	2.0 ± 0.3	6.2 ± 0.8*

*Values are mean ± SE. *P < 0.05 vs. control group. MAP, mean arterial pressure; Int RSNA, integrated renal sympathetic nerve activity; NE, norepinephrine.*

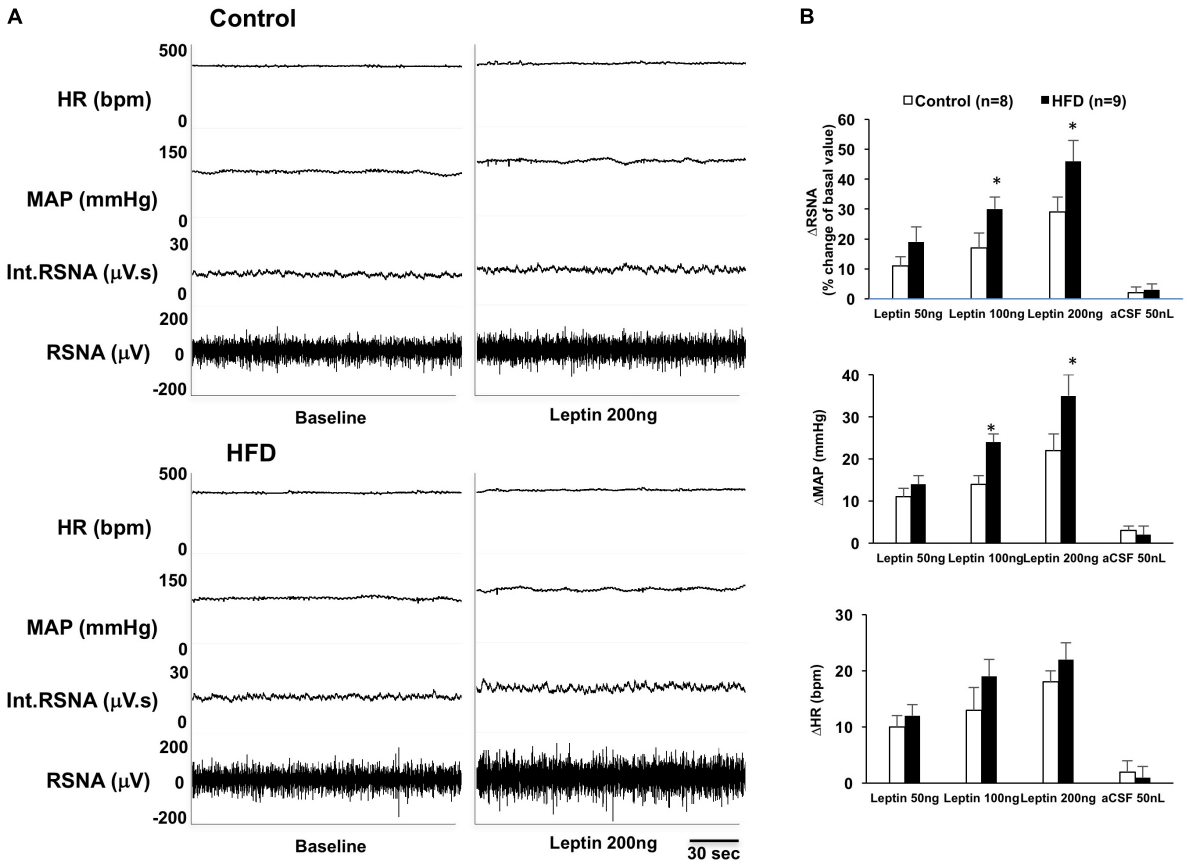

FIGURE 1 | (A) Representative tracer of renal sympathetic nerve activity (RSNA), integrative RSNA (int.RSNA), mean arterial pressure (MAP), and heart rate (HR) responses to microinjection of leptin in the ARCN of the control and HFD rat. **(B)** Mean changes in RSNA, MAP, and HR to microinjection of leptin (50, 100, 200 ng) in the ARCN. *$P < 0.05$ vs. control group. aCSF: artificial cerebrospinal fluid.

Pre-inhibition of Astrocytes With Astrocytic Metabolic Inhibitor Fluorocitrate Reduced Leptin-Induced Sympathetic Responses in the ARCN

Inhibition of astrocytes in the ARCN with the astrocytic metabolic inhibitor fluorocitrate significantly inhibited leptin-induced increases of RSNA, MAP, and HR in the ARCN in both control and HFD rats (ΔRSNA: 12 ± 3% vs. 29 ± 5% in control, 15 ± 6% vs. 46 ± 7% in HFD; ΔMAP: 8 ± 2 mmHg vs. 22 ± 4 mmHg in control, 10 ± 3 mmHg vs. 35 ± 5 mmHg in HFD; ΔHR: 11 ± 3 bpm vs. 18 ± 2 bpm in control, 11 ± 8 bpm vs. 22 ± 3 bpm in HFD, $P < 0.05$) (**Figure 2**). The HFD rats had more reductions of RSNA, MAP, and HR responses to the leptin with fluorocitrate microinjections. Fluorocitrate itself did not affect RSNA, MAP, and HR responses in either group of rats (**Figure 2**).

Increased Leptin Receptor (OBR) Expression in the ARCN of the HFD Rats

Immunohistochemistry staining confirmed the expression of OBR within the ARCN in control and HFD rats (**Figure 3**). The OBR immunofluorescent signal co-localized with neuronal marker NeuN (**Figure 3A**) as well as with glial cell marker GFAP (**Figure 3B**) within the ARCN. The immunofluorescent signal for OBR was found to be increased in the ARCN from rats fed on an HFD compared to control rats ($P = 0.021$, **Figure 3C**). In addition, Western blot analysis showed the HFD rats had a significantly higher protein level of OBR (ratio of intensity: 0.84 ± 0.08 vs. 0.39 ± 0.02, $P < 0.001$) in the ARCN compared to the controls (**Figure 3D**).

Increased Astrocyte Structural Protein (GFAP) Levels in the ARCN of the HFD Rats

Western blot analysis showed the HFD rats had a significantly higher protein level of GFAP (ratio of intensity: 0.97 ± 0.10 vs. 0.64 ± 0.06, $P = 0.021$) in the ARCN (**Figure 4A**). The morphology of $GFAP^+$ cells in the ARCN of HFD rats was different from the controls (**Figure 4B**). Morphological analysis demonstrated that there were increases in the number of primary projections from $GFAP^+$ cells in the ARCN of HFD rats ($P = 0.021$). However, there were no significant changes in the number of $GFAP^+$ cells in the ARCN of HFD rats ($P = 0.665$, **Figure 4B**).

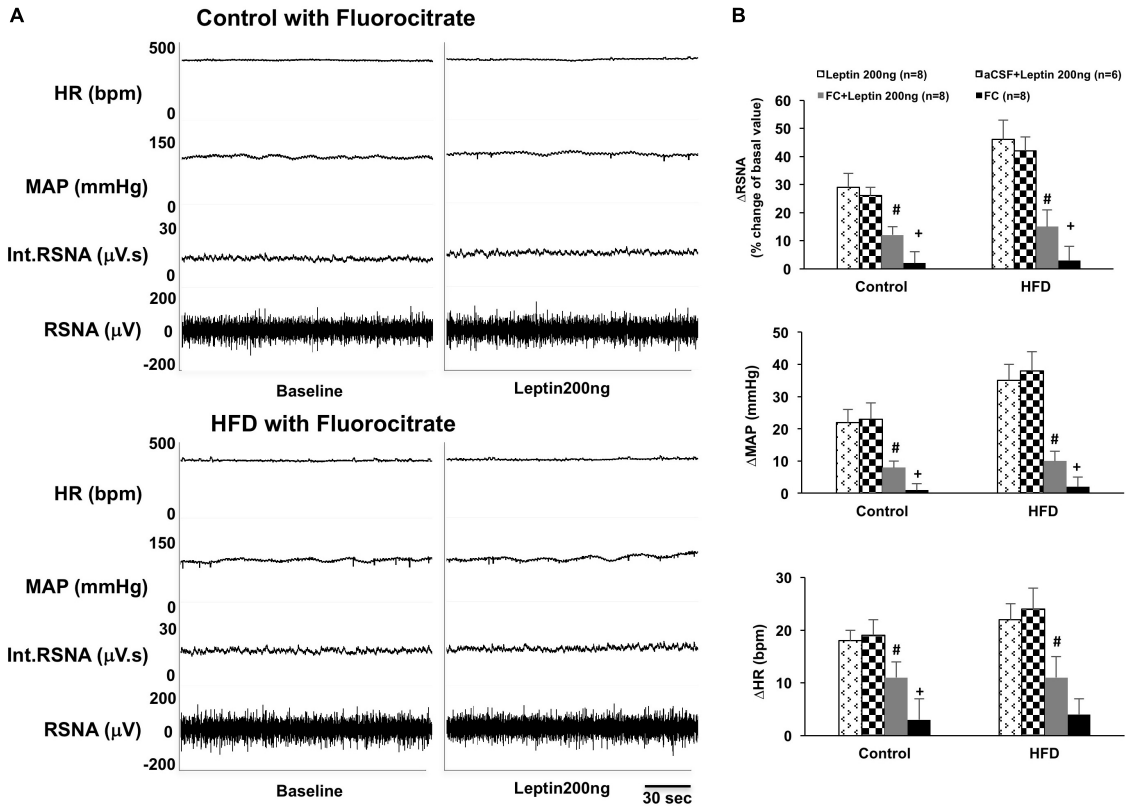

FIGURE 2 | (A) Representative tracer of RSNA, int.RSNA, MAP, and HR responses to microinjection of leptin with fluorocitrate in the ARCN of the control and HFD rat. **(B)** Mean changes in RSNA, MAP, and HR to microinjection of leptin (200 ng) with and without fluorocitrate in the ARCN. # $P < 0.05$ vs. the leptin group without fluorocitrate. +$P < 0.05$ vs. the FC + leptin group. FC: fluorocitrate.

Altered Glutamate Transporter Levels in the ACRN of the HFD Rats

Western blot analysis showed the HFD rats had significantly lower protein levels of astrocyte-specific glutamate transporters, EAAT1 (ratio of intensity: 0.15 ± 0.03 vs. 0.34 ± 0.08, $P = 0.026$) and EAAT2 (ratio of intensity: 0.50 ± 0.06 vs. 0.86 ± 0.14, $P = 0.031$) in the ARCN (**Figures 5A,B**). There was no significant difference in the level of vGLUT2 protein (ratio of intensity: 0.74 ± 0.05 vs. 0.80 ± 0.08, $P = 0.497$) in the ARCN in the HFD rats (**Figure 5C**).

GFAP Protein and Glutamate Transporter Levels in Response to Leptin in Astrocytes (*in vitro* Study)

Immunohistochemistry staining revealed GFAP staining was increased after 24 h of leptin treatment in the cultured astrocytic C6 cells (**Figure 6A**). Western blot analysis showed increased GFAP protein expression with leptin incubation (25–200 ng/ml) [linear regression analysis, $F(1,3) = 9.455$, $R^2 = 0.759$, $P = 0.05$] increasing by 2.9 folds at a concentration of 200 ng/ml [$F(3,3) = 4.334$, $P < 0.001$] (**Figure 6B**). After 24 h, *in vitro* exposure to leptin (25–200 ng/ml) reduced EAAT1 protein expression [linear regression analysis, $F(1,3) = 2.442$, $R^2 = 0.449$, $P = 0.22$], decreasing it by 38% at a concentration of 200 ng/ml [$F(3,3) = 1.34$, $P = 0.016$] (**Figure 7A**). *In vitro* exposure to leptin also reduced EAAT2 protein expression [linear regression analysis, $F(1,3) = 5.066$, $R^2 = 0.628$, $P = 0.11$], decreasing it by 39% at a concentration of 200 ng/ml [$F(3,3) = 2.014$, $P = 0.022$] (**Figure 7B**) in the astrocytes. *In vitro* exposure of leptin had no significant effects on the EAAT1 and EAAT2 protein expression in a neuronal cell line CLU (**Supplementary Figure 2**).

Brain Histology

Supplementary Figure 3 depicts the brain histological verifications for the injection sites. There was a total of 38 injections within the ARCN area. Among them, 19 injection sites belonged to control group rats, and 19 injection sites belonged to the HFD rats. There were five injections that missed the ARCN area. Data from these five missed injections was excluded from the analysis.

DISCUSSION

In the HFD obese rat model used in this study, we observed the elevation of 24-h urinary norepinephrine excretion, which suggests an increased overall sympathetic tone in this HFD rat model. Twelve weeks of HFD also produced

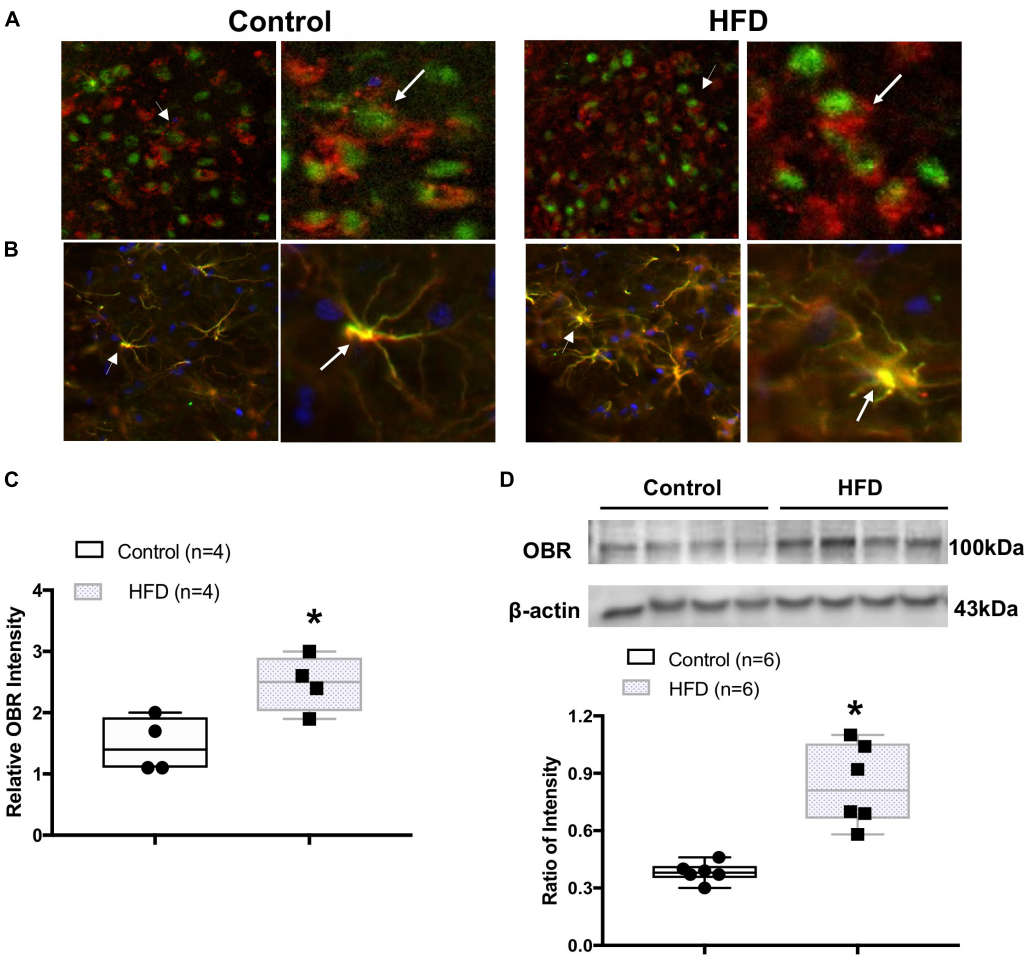

FIGURE 3 | (A) Immunofluorescent photomicrographs from the sections of the ARCN region stained for leptin receptor (OBR, in red), neuronal marker NueN (in green), and 4′,6-diamidino-2-phenylindole (DAPI, in blue) in a control and an HFD rat (X200). Amplified images are shown in the right panel. Arrow indicates the localization of OBR in the NeuN-labeled cell. **(B)** Immunofluorescent photomicrographs from the sections of the ARCN region stained for OBR (in red), glial marker glial fibrillary acidic protein (GFAP, in green), and DAPI (in blue) in a control and an HFD rat (X200). Amplified images are shown in the right panel. Arrow indicates the colocalization of OBR and GFAP. **(C)** Mean intensity of OBR staining signal in the ARCN of control and HFD rats. **(D)** Representative gel of OBR and mean protein expressions in the ARCN of control and HFD rats. $^*P < 0.05$ vs. control group.

hyperleptinemia, hyperlipidemia, hyperinsulinemia, and insulin resistance in the rats. Hyperleptinemia, as well as higher levels of insulin and angiotensin II, have been reported to be associated with sympathoexcitation in obese conditions (Hilzendeger et al., 2012; Xue et al., 2016; Hall et al., 2019). The role of leptin in activating the sympathetic drive through the central nervous system has been highlighted in many reviews (Kalil and Haynes, 2012; Mark, 2013; Head et al., 2014). The present study confirms the critical role of leptin in relation to the sympathetic over-activation in HFD obese rats.

Leptin, an adipokine, is able to elicit a myriad of physiologic effects including, but not limited to, sympathetic activation and blood pressure regulation. The ARCN in the hypothalamus has been shown as an important gateway for the actions of leptin signaling for controlling sympathetic activity (Dampney, 2011). In our animal studies, we observed that direct leptin administration into the ARCN increased RSNA, MAP, and HR. These results were consistent with our previous study and other reports that centrally administered leptin increased sympathetic nerve activity and blood pressure (Dunbar et al., 1997; Rahmouni and Morgan, 2007; Zheng et al., 2017). More importantly, we observed that OBR protein expression in the ARCN was upregulated in the HFD rats, indicating enhanced endogenous leptin signaling after HFD feeding. Further, our electrophysiological study functionally confirmed that central stimulation with leptin resulted in elevated sympathetic activation in obese rats. Taken together, these results suggest that the up-regulation of OBR and leptin signaling within the hypothalamus could be one possible mechanism for the enhanced leptin-mediated excitatory action on sympathetic outflow elemental to the obese condition.

The hypothalamus including the ARCN is comprised of different types of cells (Gordon et al., 2009). Our dual labeling

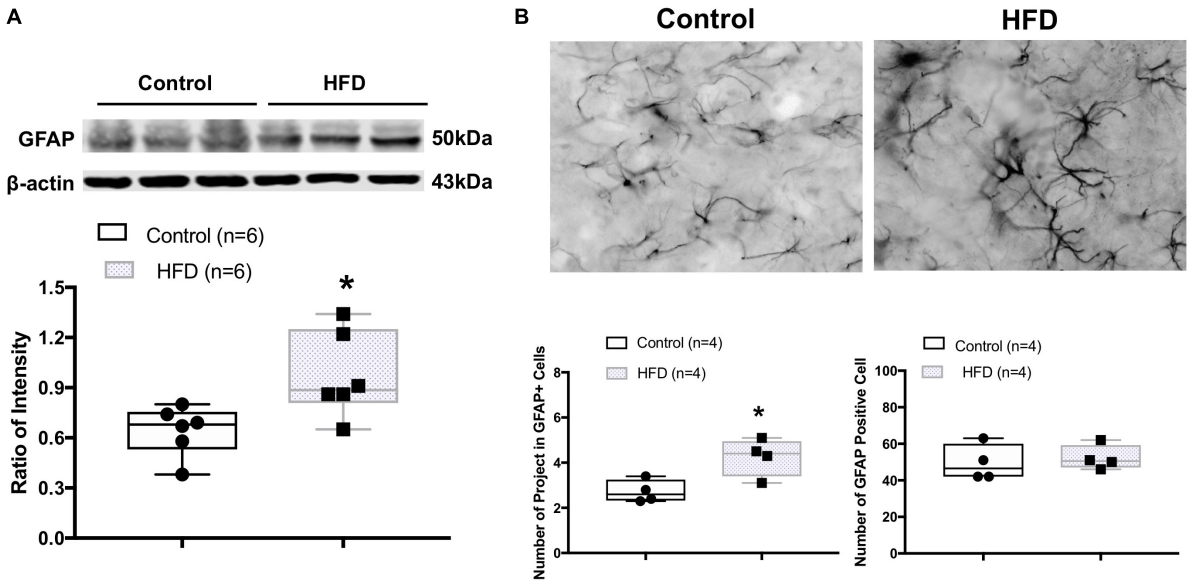

FIGURE 4 | (A) Representative gel of GFAP and mean protein expressions in the ARCN of control and HFD rats. **(B)** Immunofluorescent photomicrographs from the sections of the ARCN region stained for GFAP positive ($GFAP^+$) cells in a control and an HFD rat (X400). Bottom panel shows the mean number of projects in $GFAP^+$ cells and mean number of $GFAP^+$ cells. $^*P < 0.05$ vs. control group.

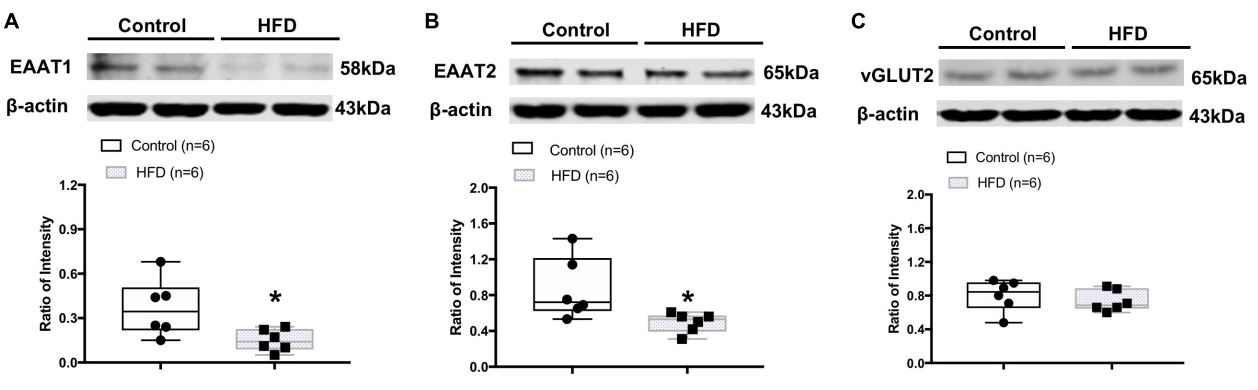

FIGURE 5 | Representative gel and mean protein expressions of **(A)** excitatory amino acid transporter 1 (EAAT1), **(B)** EAAT2, and **(C)** vesicular glutamate transporter 2 (vGLUT2) in the ARCN of the control and HFD rats. $^*P < 0.05$ vs. control group.

immunohistochemistry staining showed that both neurons and astrocytes in the ARCN expressed OBR. Interestingly, in the HFD obese rats, the expression of OBR was increased in the ARCN. Furthermore, we found that the HFD rats had increased levels of astrocyte structural protein GFAP and an increased number of primary projection of $GFAP^+$ cells in the ARCN. This is consistent with other previous reports that increased gliosis in the ARCN is related to the enhanced leptin signaling in obesity (Pan et al., 2012). HFD-induced weight gain also results in hypothalamic gliosis and changes in the glial coverage of neurons and vasculature (Horvath et al., 2010). Our data provides further evidence of the role of astrocyte involvement in the alteration of leptin signaling. This may contribute to the leptin-mediated sympathetic over-activation in the obese condition.

Astrocytes have recently emerged as an important constituent of central sympathetic activation mechanisms (Park et al., 2009; Guo et al., 2010). It is reported the astrocytes are potential cellular substrates of angiotensin (1–7), mediating effects on local metabolism and microcirculation in the rostral ventrolateral medulla, resulting in changes in the activity of pre-sympathetic neurons and blood pressure (Guo et al., 2010). Astrocytic GABA transporters have been shown to regulate tonic GABA inhibitory function, pre-sympathetic neuronal activity, and sympathetic outflow from the paraventricular nucleus (Park et al., 2009). Indeed, in our functional study, we observed that metabolic inhibition of astrocytes significantly reduced leptin-induced RSNA, MAP, and HR. Particularly in the HFD rats, there were further reductions of RSNA, MAP, and HR after astrocytic

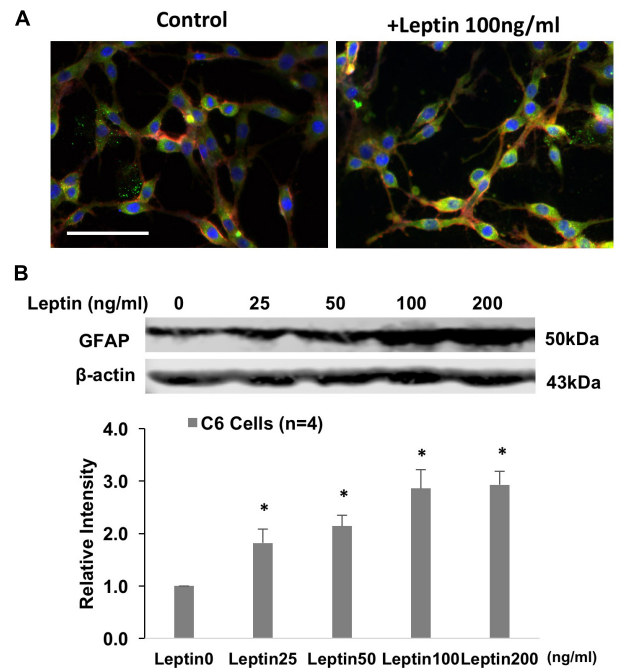

FIGURE 6 | (A) Immunofluorescent photomicrographs from the cultured astrocytic C6 cells stained for GFAP (green), OBR (red), and DAPI (blue) with/without leptin treatment. Bar = 50 μm. **(B)**. Representative gel and mean protein expressions of GFAP in the C6 cells with leptin treatment. *$P < 0.05$ vs. control without leptin treatment.

inhibition. As described, rats in our experiments were pre-inhibited with the gliotoxin fluorocitrate, a metabolic inhibitor of reactive astrocytes. Fluorocitrate has been effectively used *in vivo* and *in vitro* to study the effects of astrocyte function on particular signaling pathways (Fonnum et al., 1997; Gordon et al., 2005). In the brain, fluorocitrate is selectively taken up by the astrocytes, blocking the activity of the enzyme aconitase, and leading to depletion of ATP stores. We did not expect fluorocitrate to produce precise changes to astrocyte remodeling. However, we anticipated that using fluorocitrate would provide a useful approach to determine the effects of altered astrocytic function in the central nervous system. In the study, the injection of fluorocitrate *per se* into the ARCN had no significant effects on sympathetic activity and blood pressure. This may support evidence that fluorocitrate does not cause significant direct effects on the excitability of neurons in the ARCN. However, further evidence needs to be provided by a direct neuronal activity recording from the ARCN.

Astrocytes participate in neuroendocrine function partially through the modulation of synaptic input density in the hypothalamus (Garcia-Caceres et al., 2011). Leptin modulates synaptic input in the hypothalamus, but whether astrocytes participate in this action is not fully known. It is reported that chronic leptin exposure increases astrocytic activation in the hypothalamus (Garcia-Caceres et al., 2011). Some studies have indicated astrocytic activity may modulate neuronal uptake and leptin signaling in obese mice (Hsuchou et al., 2009a). In the central nervous system, astrocytes participate in the control of obesity by the upregulation of their associated OBRs. Progression of obesity may be associated with a shift of the neuronal predominant expression pattern to an astrocytic preference in mice (Pan et al., 2008). In the HFD rats, we observed that astrocyte structural protein GFAP was increased and that there were morphologic changes in astrocytes in the ARCN, suggesting astrocytes may play an important role in the pathology of obesity.

Glutamate, the excitatory amino acid, plays a central role in astrocyte–neuronal interactions (Simard and Nedergaard, 2004) and contributes to sympathetic activation (Li et al., 2003, 2008). Glutamate is cleared from the neuronal synapses by astrocytes via glutamate transporters, and it is then converted into glutamine, which is released and taken up by neurons (Simard and Nedergaard, 2004). Excitatory amino acid transporters, EAAT1 and EAAT2, are the major glutamate transporters; they are expressed predominantly in astrocytic cells and are

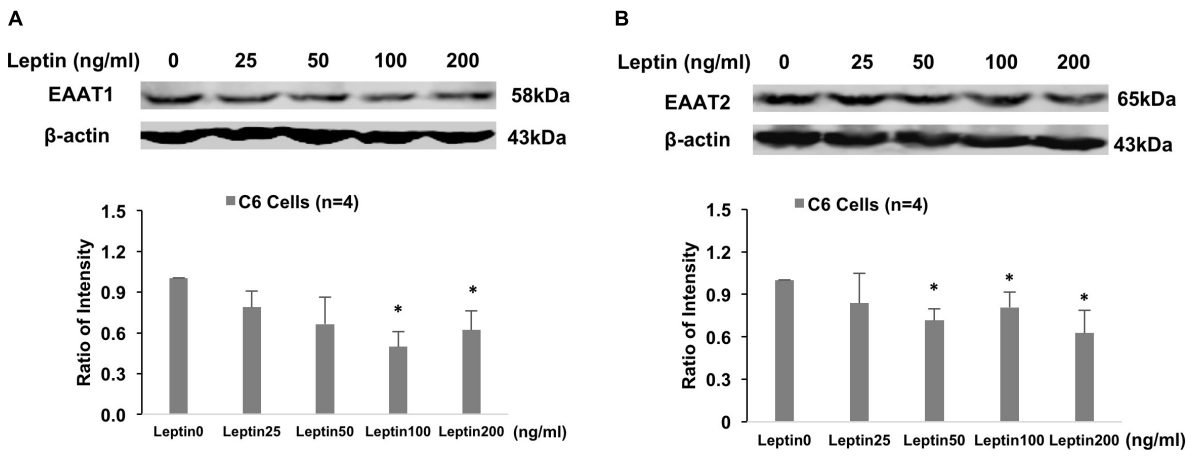

FIGURE 7 | Representative gel and mean protein expressions of panels **(A)** EAAT1 and **(B)** EAAT2 in the astrocytic C6 cells with leptin treatment. *$P < 0.05$ vs. control without leptin treatment.

responsible for glutamate uptake (Kim et al., 2011). EAATs are responsible for regulating glutamate concentration in the synaptic cleft. When the astrocyte-mediated clearance of glutamate from the extracellular space is altered, it may cause an increased concentration of the excitatory amino acid in the extracellular space (Carney et al., 2014). Dysfunction of EAAT and accumulation of excessive extracellular glutamate has been implicated in the development of several neurodegenerative diseases (Kim et al., 2011; Zhang et al., 2016). In the present study, we observed reduced EAAT1 and EAAT2 expression in the ARCN when the rats were chronically exposed to the HFD. Additionally, our *in vitro* study showed that the expression of both EAAT1 and EAAT2 was downregulated by leptin stimulation in the cultured astrocytes. These results suggest that astrocytes play important roles in the relationship of leptin signaling within the ARCN. We propose that these important roles may be due to the effects of EAATs on astrocytic glutamate uptake. Therefore, in obese rats, reduced efficacy of EAATs in the astrocytes may result in increased sympathetic activation of leptin signaling from the ARCN. It is noted that Cano et al. (2014) reported astrocytes from HFD mice showed longer and less abundant projections accompanied by the upregulation of both glutamate transporter 1 and astrocyte glutamate transporter in the area of the hippocampus (Cano et al., 2014). The differential responses of astrocytes from the hypothalamus and outside the hypothalamus may be due to their origin in a specific brain area.

In the central nervous system, leptin has shown to exert its effects on sympathetic activity and blood pressure through a number of mediators, including glutamate (Ghamari-Langroudi et al., 2011). Both leptin and glutamate are important neuromodulators in the central nervous system. A higher glutamatergic tone also has been shown in several hyper-sympathetic disease conditions, such as chronic heart failure, hypertension, and diabetes (Luo et al., 2002; Li et al., 2003, 2008). Previously, we have reported that central leptin–glutamate signaling interactions contributed to sympathetic activation (Zheng et al., 2017). The present study provides evidence that, in the obese condition, there are alterations in the astrocytic glutamate transporter expression in the ARCN. Furthermore, the *in vitro* study indicates that leptin directly inhibits the expression of EAATs, suggesting an important role for the involvement of leptin–glutamate signaling in the obese condition.

CONCLUSION

These studies provide evidence that, within the hypothalamic nuclei, leptin signaling via neuron–astrocyte interactions in the ARCN may contribute to the exaggerated sympathoexcitation observed in HFD obese rats. The effects are potentially mediated by the actions of leptin on the regulation of astrocytic glutamate transporters within the ARCN of the hypothalamus.

DATA AVAILABILITY STATEMENT

The datasets generated for this study are available on request to the corresponding author.

ETHICS STATEMENT

The animal study was reviewed and approved by Institutional Animal Care and Use Committee of the University of South Dakota.

AUTHOR CONTRIBUTIONS

XL and HZ conceived and designed the experiments, performed the experiments, analyzed the data, and drafted and finalized the manuscript.

FUNDING

The study was supported by the author's faculty start-up fund from Sanford School of Medicine of the University of South Dakota Department of Basic Biomedical Sciences.

SUPPLEMENTARY MATERIAL

The Supplementary Material for this article can be found online at: https://www.frontiersin.org/articles/10.3389/fnins.2019.01217/full#supplementary-material

REFERENCES

Badoer, E., and Ryan, A. (1999). Effects of leptin on spinally projecting neurons in the PVN of the hypothalamus. *Brain Res.* 844, 210–215. doi: 10.1016/s0006-8993(99)01902-2

Balasubramanian, P., Hall, D., and Subramanian, M. (2019). Sympathetic nervous system as a target for aging and obesity-related cardiovascular diseases. *Geroscience* 41, 13–24. doi: 10.1007/s11357-018-0048-5

Bell, B. B., and Rahmouni, K. (2016). Leptin as a mediator of obesity-induced hypertension. *Curr. Obes. Rep.* 5, 397–404. doi: 10.1007/s13679-016-0231-x

Cano, V., Valladolid-Acebes, I., Hernandez-Nuno, F., Merino, B., Del Olmo, N., Chowen, J. A., et al. (2014). Morphological changes in glial fibrillary acidic protein immunopositive astrocytes in the hippocampus of dietary-induced obese mice. *Neuroreport* 25, 819–822. doi: 10.1097/WNR.0000000000000180

Carney, K. E., Milanese, M., van Nierop, P., Li, K. W., Oliet, S. H., Smit, A. B., et al. (2014). Proteomic analysis of gliosomes from mouse brain: identification and investigation of glial membrane proteins. *J. Proteom. Res.* 13, 5918–5927. doi: 10.1021/pr500829z

Corry, D. B., and Tuck, M. L. (1999). Obesity, hypertension, and sympathetic nervous system activity. *Curr. Hypertens Rep.* 1, 119–126. doi: 10.1007/s11906-999-0005-x

Dampney, R. A. (2011). Arcuate nucleus - a gateway for insulin's action on sympathetic activity. *J. Physiol.* 589(Pt 9), 2109–2110. doi: 10.1113/jphysiol.2011.208579

Dunbar, J. C., Hu, Y. G., and Lu, H. Q. (1997). Intracerebroventricular leptin increases lumbar and renal sympathetic nerve activity and blood pressure in normal rats. *Diabetes* 46, 2040–2043. doi: 10.2337/diab.46.12.2040

Fonnum, F., Johnsen, A., and Hassel, B. (1997). Use of fluorocitrate and fluoroacetate in the study of brain metabolism. *Glia* 21, 106–113. doi: 10.1002/(sici)1098-1136(199709)21:1<106::aid-glia12>3.3.co;2-v

Garcia-Caceres, C., Fuente-Martin, E., Burgos-Ramos, E., Granado, M., Frago, L. M., Barrios, V., et al. (2011). Differential acute and chronic effects of leptin on hypothalamic astrocyte morphology and synaptic protein levels. *Endocrinology* 152, 1890–1898. doi: 10.1210/en.2010-1252

Ghamari-Langroudi, M., Srisai, D., and Cone, R. D. (2011). Multinodal regulation of the arcuate/paraventricular nucleus circuit by leptin. *Proc. Natl. Acad. Sci. U.S.A.* 108, 355–360. doi: 10.1073/pnas.1016785108

Gordon, G. R., Baimoukhametova, D. V., Hewitt, S. A., Pajapaksha, W. R., Fisher, T. E., and Bains, J. S. (2005). Norepinephrine triggers release of glial ATP to increase postsynaptic efficacy. *Nat. Neurosci.* 8, 1078–1086. doi: 10.1038/nn1498

Gordon, G. R., Iremonger, K. J., Kantevari, S., Ellis-Davies, G. C., MacVicar, B. A., and Bains, J. S. (2009). Astrocyte-mediated distributed plasticity at hypothalamic glutamate synapses. *Neuron* 64, 391–403. doi: 10.1016/j.neuron.2009.10.021

Guo, F., Liu, B., Lane, S., Souslova, E. A., Chudakov, D. M., Paton, J. F., et al. (2010). Astroglia are a possible cellular substrate of angiotensin(1-7) effects in the rostral ventrolateral medulla. *Cardiovasc. Res.* 87, 578–584. doi: 10.1093/cvr/cvq059

Habeeballah, H., Alsuhaymi, N., Stebbing, M. J., Jenkins, T. A., and Badoer, E. (2016). Central administration of insulin and leptin together enhance renal sympathetic nerve activity and fos production in the arcuate nucleus. *Front. Physiol.* 7:672. doi: 10.3389/fphys.2016.00672

Hall, J. E., do Carmo, J. M., da Silva, A. A., Wang, Z., and Hall, M. E. (2019). Obesity, kidney dysfunction and hypertension: mechanistic links. *Nat. Rev. Nephrol.* 15, 367–385. doi: 10.1038/s41581-019-0145-4

Harlan, S. M., Morgan, D. A., Agassndian, K., Guo, D. F., Cassell, M. D., Sigmund, C. D., et al. (2011). Ablation of the leptin receptor in the hypothalamic arcuate nucleus abrogates leptin-induced sympathetic activation. *Circ. Res.* 108, 808–812. doi: 10.1161/CIRCRESAHA.111.240226

Haynes, W. G., Sivitz, W. I., Morgan, D. A., Walsh, S. A., and Mark, A. L. (1997). Sympathetic and cardiorenal actions of leptin. *Hypertension* 30(3 Pt 2), 619–623. doi: 10.1161/01.hyp.30.3.619

Head, G. A., Lim, K., Barzel, B., Burke, S. L., and Davern, P. J. (2014). Central nervous system dysfunction in obesity-induced hypertension. *Curr. Hypertens Rep.* 16:466. doi: 10.1007/s11906-014-0466-4

Hilzendeger, A. M., Morgan, D. A., Brooks, L., Dellsperger, D., Liu, X., Grobe, J. L., et al. (2012). A brain leptin-renin angiotensin system interaction in the regulation of sympathetic nerve activity. *Am. J. Physiol. Heart Circ. Physiol.* 303, H197–H206. doi: 10.1152/ajpheart.00974.2011

Horvath, T. L., Sarman, B., Garcia-Caceres, C., Enriori, P. J., Sotonyi, P., Shanabrough, M., et al. (2010). Synaptic input organization of the melanocortin system predicts diet-induced hypothalamic reactive gliosis and obesity. *Proc. Natl. Acad. Sci. U.S.A.* 107, 14875–14880. doi: 10.1073/pnas.1004282107

Hsuchou, H., He, Y., Kastin, A. J., Tu, H., Markadakis, E. N., Rogers, R. C., et al. (2009a). Obesity induces functional astrocytic leptin receptors in hypothalamus. *Brain* 132(Pt 4), 889–902. doi: 10.1093/brain/awp029

Hsuchou, H., Pan, W., Barnes, M. J., and Kastin, A. J. (2009b). Leptin receptor mRNA in rat brain astrocytes. *Peptides* 30, 2275–2280. doi: 10.1016/j.peptides.2009.08.023

Kalil, G. Z., and Haynes, W. G. (2012). Sympathetic nervous system in obesity-related hypertension: mechanisms and clinical implications. *Hypertens Res.* 35, 4–16. doi: 10.1038/hr.2011.173

Kawabe, T., Kawabe, K., and Sapru, H. N. (2013). Tonic gamma-aminobutyric acid-ergic activity in the hypothalamic arcuate nucleus is attenuated in the spontaneously hypertensive rat. *Hypertension* 62, 281–287. doi: 10.1161/HYPERTENSIONAHA.113.01132

Kim, K., Lee, S. G., Kegelman, T. P., Su, Z. Z., Das, S. K., Dash, R., et al. (2011). Role of excitatory amino acid transporter-2 (EAAT2) and glutamate in neurodegeneration: opportunities for developing novel therapeutics. *J. Cell Physiol.* 226, 2484–2493. doi: 10.1002/jcp.22609

Kleiber, A. C., Zheng, H., Schultz, H. D., Peuler, J. D., and Patel, K. P. (2008). Exercise training normalizes enhanced glutamate-mediated sympathetic activation from the PVN in heart failure. *Am. J. Physiol. Regul. Integr. Comp. Physiol.* 294, R1863–R1872. doi: 10.1152/ajpregu.00757.2007

Li, D. P., Yang, Q., Pan, H. M., and Pan, H. L. (2008). Pre- and postsynaptic plasticity underlying augmented glutamatergic inputs to hypothalamic presympathetic neurons in spontaneously hypertensive rats. *J. Physiol.* 586, 1637–1647. doi: 10.1113/jphysiol.2007.149732

Li, Y. F., Cornish, K. G., and Patel, K. P. (2003). Alteration of NMDA NR1 receptors within the paraventricular nucleus of hypothalamus in rats with heart failure. *Circ. Res.* 93, 990–997. doi: 10.1161/01.res.0000102865.60437.55

Lim, K., Burke, S. L., and Head, G. A. (2013). Obesity-related hypertension and the role of insulin and leptin in high-fat-fed rabbits. *Hypertension* 61, 628–634. doi: 10.1161/HYPERTENSIONAHA.111.00705

Luo, Y., Kaur, C., and Ling, E. A. (2002). Neuronal and glial response in the rat hypothalamus-neurohypophysis complex with streptozotocin-induced diabetes. *Brain Res.* 925, 42–54. doi: 10.1016/s0006-8993(01)03258-9

Marina, N., Teschemacher, A. G., Kasparov, S., and Gourine, A. V. (2016). Glia, sympathetic activity and cardiovascular disease. *Exp. Physiol.* 101, 565–576. doi: 10.1113/EP085713

Mark, A. L. (2013). Selective leptin resistance revisited. *Am. J. Physiol. Regul. Integr. Comp. Physiol.* 305, R566–R581. doi: 10.1152/ajpregu.00180.2013

Matsumura, K., Abe, I., Tsuchihashi, T., and Fujishima, M. (2000). Central effects of leptin on cardiovascular and neurohormonal responses in conscious rabbits. *Am. J. Physiol. Regul. Integr. Comp. Physiol.* 278, R1314–R1320.

Palkovits, M., and Brownstein, M. (1983). "Brain microdissection techniques," in *Brain Microdissection Techniques*, ed. A. E. Cuello, (Chichester: John Wiley & Sons).

Pan, W., Hsuchou, H., He, Y., Sakharkar, A., Cain, C., Yu, C., et al. (2008). Astrocyte leptin receptor (ObR) and leptin transport in adult-onset obese mice. *Endocrinology* 149, 2798–2806. doi: 10.1210/en.2007-1673

Pan, W., Hsuchou, H., Jayaram, B., Khan, R. S., Huang, E. Y., Wu, X., et al. (2012). Leptin action on nonneuronal cells in the CNS: potential clinical applications. *Ann. N. Y. Acad. Sci.* 1264, 64–71. doi: 10.1111/j.1749-6632.2012.06472.x

Pan, W., Hsuchou, H., Xu, C., Wu, X., Bouret, S. G., and Kastin, A. J. (2011). Astrocytes modulate distribution and neuronal signaling of leptin in the hypothalamus of obese A vy mice. *J. Mol. Neurosci.* 43, 478–484. doi: 10.1007/s12031-010-9470-6

Park, J. B., Jo, J. Y., Zheng, H., Patel, K. P., and Stern, J. E. (2009). Regulation of tonic GABA inhibitory function, presympathetic neuronal activity and sympathetic outflow from the paraventricular nucleus by astroglial GABA transporters. *J. Physiol.* 587(Pt 19), 4645–4660. doi: 10.1113/jphysiol.2009.173435

Prior, L. J., Elkelis, N., Armitage, J. A., Davern, P. J., Burke, S. L., Montani, J. P., et al. (2010). Exposure to a high-fat diet alters leptin sensitivity and elevates renal sympathetic nerve activity and arterial pressure in rabbits. *Hypertension* 55, 862–868. doi: 10.1161/HYPERTENSIONAHA.109.141119

Rahmouni, K., and Haynes, W. G. (2002). Leptin and the central neural mechanisms of obesity hypertension. *Drugs Today* 38, 807–817.

Rahmouni, K., and Morgan, D. A. (2007). Hypothalamic arcuate nucleus mediates the sympathetic and arterial pressure responses to leptin. *Hypertension* 49, 647–652. doi: 10.1161/01.hyp.0000254827.59792.b2

Shi, Z., Li, B., and Brooks, V. L. (2015). Role of the paraventricular nucleus of the hypothalamus in the sympathoexcitatory effects of leptin. *Hypertension* 66, 1034–1041. doi: 10.1161/HYPERTENSIONAHA.115.06017

Simard, M., and Nedergaard, M. (2004). The neurobiology of glia in the context of water and ion homeostasis. *Neuroscience* 129, 877–896. doi: 10.1016/j.neuroscience.2004.09.053

Thaler, J. P., Choi, S. J., Schwartz, M. W., and Wisse, B. E. (2010). Hypothalamic inflammation and energy homeostasis: resolving the paradox. *Front. Neuroendocrinol.* 31, 79–84. doi: 10.1016/j.yfrne.2009.10.002

Vaneckova, I., Maletinska, L., Behuliak, M., Nagelova, V., Zicha, J., and Kunes, J. (2014). Obesity-related hypertension: possible pathophysiological mechanisms. *J. Endocrinol.* 223, R63–R78. doi: 10.1530/JOE-14-0368

Ward, K. R., Bardgett, J. F., Wolfgang, L., and Stocker, S. D. (2011). Sympathetic response to insulin is mediated by melanocortin 3/4 receptors in the hypothalamic paraventricular nucleus. *Hypertension* 57, 435–441. doi: 10.1161/HYPERTENSIONAHA.110.160671

Xue, B., Yu, Y., Zhang, Z., Guo, F., Beltz, T. G., Thunhorst, R. L., et al. (2016). Leptin mediates high-fat diet sensitization of angiotensin II-elicited hypertension

by upregulating the brain renin-angiotensin system and inflammation. *Hypertension* 67, 970–976. doi: 10.1161/HYPERTENSIONAHA.115.06736

Zhang, Y., Tan, F., Xu, P., and Qu, S. (2016). Recent advance in the relationship between excitatory amino acid transporters and parkinson's disease. *Neural Plast.* 2016:8941327. doi: 10.1155/2016/8941327

Zheng, H., Liu, X., Li, Y., and Patel, K. P. (2017). A hypothalamic leptin-glutamate interaction in the regulation of sympathetic nerve activity. *Neural Plast.* 2017:2361675. doi: 10.1155/2017/2361675

Conflict of Interest: The authors declare that the research was conducted in the absence of any commercial or financial relationships that could be construed as a potential conflict of interest.

frontiers in Neuroscience

BRIEF RESEARCH REPORT
published: 25 May 2020
doi: 10.3389/fnins.2020.00530

Cutaneous Aβ-Non-nociceptive, but Not C-Nociceptive, Dorsal Root Ganglion Neurons Exhibit Spontaneous Activity in the Streptozotocin Rat Model of Painful Diabetic Neuropathy *in vivo*

Laiche Djouhri[1], Asad Zeidan[1], Seham A. Abd El-Aleem[2,3] and Trevor Smith[4]*

[1] Department of Basic Medical Sciences, College of Medicine, QU Health, Qatar University, Doha, Qatar, [2] Department of Histology and Cell Biology, University of Manchester, Manchester, United Kingdom, [3] Department of Pathology, Faculty of Medicine, Minia University, Minya, Egypt, [4] Medical Physics and Biomedical Engineering, University College London, London, United Kingdom

OPEN ACCESS

Edited by:
Jan D. Huizinga, McMaster University, Canada

Reviewed by:
Hamid I. Akbarali, Virginia Commonwealth University, United States
Yong Fang Zhu, McMaster University, Canada

***Correspondence:**
Laiche Djouhri
ldjouhri@qu.edu.qa

Specialty section:
This article was submitted to Autonomic Neuroscience, a section of the journal Frontiers in Neuroscience

Received: *19 February 2020*
Accepted: *29 April 2020*
Published: *25 May 2020*

Citation:
Djouhri L, Zeidan A, Abd El-Aleem SA and Smith T (2020) Cutaneous Aβ-Non-nociceptive, but Not C-Nociceptive, Dorsal Root Ganglion Neurons Exhibit Spontaneous Activity in the Streptozotocin Rat Model of Painful Diabetic Neuropathy in vivo. Front. Neurosci. 14:530. doi: 10.3389/fnins.2020.00530

Diabetic peripheral neuropathic pain (DPNP) is the most devastating complication of diabetes mellitus. Unfortunately, successful therapy for DPNP remains a challenge because its pathogenesis is still elusive. However, DPNP is believed to be due partly to abnormal hyperexcitability of dorsal root ganglion (DRG) neurons, but the relative contributions of specific functional subtypes remain largely unknown. Here, using the strepotozotocin (STZ) rat model of DPNP induced by a STZ injection (60 mg/kg, i.p), and intracellular recordings of action potentials (APs) from DRG neurons in anesthetized rats, we examined electrophysiological changes in C-and Aβ-nociceptive and Aβ-low threshold mechanoreceptive (LTM) neurons that may contribute to DPNP. Compared with control, we found in STZ-rats with established pain hypersensitivity (5 weeks post-STZ) several significant changes including: (a) A 23% increase in the incidence of spontaneous activity (SA) in Aβ-LTMs (but not C-mechanosensitive nociceptors) that may cause dysesthesias/paresthesia suffered by DPNP patients, (b) membrane hyperpolarization and a ∼85% reduction in SA rate in Aβ-LTMs by K_v7 channel activation with retigabine (6 mg/kg, i.v.) suggesting that K_v7/M channels may be involved in mechanisms of SA generation in Aβ-LTMs, (c) decreases in AP duration and in duration and amplitude of afterhyperpolarization (AHP) in C-and/or Aβ-nociceptors. These faster AP and AHP kinetics may lead to repetitive firing and an increase in afferent input to the CNS and thereby contribute to DPNP development, and (d) a decrease in the electrical thresholds of Aβ-nociceptors that may contribute to their sensitization, and thus to the resulting hypersensitivity associated with DPNP.

Keywords: action potential, diabetic neuropathy, nociception, primary sensory neurons, K^+ channels

INTRODUCTION

Diabetic peripheral neuropathic pain (DPNP) is the most debilitating complication of diabetes mellitus with up to 50% of people with diabetic neuropathy (DN) having some degree of PNP (e.g., Lee-Kubli and Calcutt, 2014). Patients with DPNP usually experience a range of unpleasant positive symptoms such as spontaneous/ongoing pain, mechanical and cold hypersensitivity and dysesthesias/paresthesias, as well as negative symptoms notably heat hypoalgesia (e.g., Schreiber et al., 2015). Successful therapy for DPNP remains a challenge because currently available drugs have either limited efficacy and/or adverse side effects. Despite its high prevalence and clinical importance, the pathophysiology of DPNP is still illusive. However, several mechanisms have been implicated in its pathogenesis including mechanisms that involve structural changes in the peripheral nervous system (Polydefkis et al., 2004; Shun et al., 2004), and functional changes such as abnormal hyperexcitability of dorsal root ganglion (DRG) and CNS neurons (see (Baron et al., 2010)). Like other models of PNP, the hypersensitivity and/or ongoing pain associated with DPNP are likely to result from changes in excitability of the primary afferent neurons (Burchiel et al., 1985; Hong et al., 2004; Jagodic et al., 2007; Serra et al., 2012). Several animal studies using rodent models of DPNP have shown that both C- and A-fiber DRG neurons exhibit aberrant spontaneous activity (SA), the key characteristic of neuronal hyperexcitability (Burchiel et al., 1985; Ahlgren et al., 1992; Chen and Levine, 2001; Khan et al., 2002). While these studies suggest that both A-and C-fiber afferent fibers are involved in DPNP pathogenesis, the relative contributions of specific functional afferent subtypes that are likely to mediate different aspects of DPNP remain unknown. Indeed, little is known about the sensory receptive properties (sensory modality) of the afferent neurons involved in development and/or maintenance DPNP pathogenesis.

The primary aim of this *in vivo* study was to examine in the streptozotocin (STZ) rat model of DPNP electrophysiological changes in physiologically identified C- and A-fiber DRG neurons that might contribute to their hyperexcitability, and thereby to DPNP development. We found (5 weeks post-STZ) several significant changes in both nociceptive and non-nociceptive DRG neurons in STZ rats. These include SA in A/β-LTMs (but not in C-mechanosensitive nociceptors) that may cause dysesthesias/paresthesias experienced by many patients with DPNP. Interestingly, we also found that activation of Kv7 channels with retigabine caused membrane hyperpolarization and marked suppression of the SA in Aα/β-LTMs suggesting that these channels may be involved in mechanisms of SA generation in this subtype of Aβ-LTMs. It should be note that a decrease in expression or a change in activation properties of Kv7 channels that underlie the M current that normally acts as a "dynamic brake" on repetitive action potential discharges (see Brown and Passmore, 2009) could result in membrane depolarization, and render neurons more prone to action potential firing.

METHODS

The Animal Model of DPNP and *in vivo* Preparation

Male Sprague–Dawley rats (250–300 g) were used in the present study. They were housed in groups of 4 per cage, in a room (with room temperature maintained between 21 and 24°C) in the animal house of Liverpool University (UK), under standard laboratory conditions with 12-h light\dark cycles. The experimental protocols were approved by the University of Liverpool Ethical review committee, and complied throughout with the UK Animals (Scientific Procedures) Act 1986. The terminal surgery and recordings were conducted under deep anesthesia (sodium pentobarbitone 60 mg/kg i.p.). At the end of experiments, animals were humanely killed with an overdose of sodium pentobarbitone. We used the STZ rat model of DPNP that involves a single injection of STZ (60 mg/kg, i.p.) after an overnight fast to reduce competition between glucose and STZ for uptake into pancreatic β-cells as reported previously (see Djouhri et al., 2019). It is noteworthy that hypoinsulinemia and hyperglycemia caused by STZ is due to its cytotoxicity to pancreatic β cells. The STZ model (model of type 1 diabetes) is more commonly used than other models of DPNP because of its low cost, rapid induction, greater stability and relative lack of toxicity to other organs (Skovso, 2014). More imoprtantly, the STZ model is known to exhibit long lasting behavioral signs of DPNP including mechanical and heat hypersensitivity (see Djouhri et al., 2019 and section "Discussion").

Pain Behavioral Testing

Pain behavioral testing was conducted on 10 STZ rats by an experimenter blind to the various treatment animal groups as reported recently (Djouhri et al., 2019). Briefly, paw withdrawal threshold (PWT), paw withdrawal latency (PWL), and cold escape/nocifensive behavior, were assessed on the left hind paw of each STZ rat. Mechanical hypersensitivity was indicated by a significant decrease in the mean PWT, whereas heat hypersensitivity was indicated by a significant decrease in the mean PWL to a noxious heat. Cold hypersensitivity was assessed using a hot/cold plate analgesiometer (Ugo Basile, Milan, Italy) and a stop watch to record the duration (in seconds) of the escape/nocifensive behavior (licking, lifting, guarding, shaking or biting of the hind paw, or jumping) in a 2 min period in rats before and after STZ treatment. Cold hypersensitivity was indicated by a significant decrease in the duration of cold-evoked responses as reported previously (e.g., Orio et al., 2009). STZ rats were also assessed for the presence of spontaneous foot lifting (SFL), a behavioral sign of spontaneous/ongoing pain as described previously (Djouhri et al., 2019).

In vivo Electrophysiological Recordings

Intracellular recordings were made in deeply anesthetized STZ rats (n = 28) 5 weeks post-STZ or in control (vehicle treated) rats (n = 18 rats) of similar age/weight. General anesthesia

was induced by sodium pentobarbitone (60 mg/kg. i.p.). The relatively large number of rats used is due to the low percentage (about 23%) of neurons with SA (see section "Results"). This means finding a spontaneously firing neuron requires 4 or more successful experiments with at least 4 neurons in each experiment. Full details of the animal preparation were as reported previously (Djouhri et al., 2018). Briefly, to allow artificial ventilation and monitoring of end-tidal CO_2, a tracheotomy was performed. CO_2 was maintained between 3 and 4% by adjusting the volume and rate of the respiratory pump. The left jugular vein and carotid artery were tabulated to enable, respectively, regular injections of additional doses of anesthetic (sodium pentobaribtone 10mg/kg) and monitoring of blood pressure (normally ∼80–100 mmHg). A laminectomy was performed from vertebrae L2-L6 as reported previously (Djouhri et al., 2018). Intracellular voltage recordings from somata of L4 or L5 DRG neurons were obtained using sharp glass microelectrodes filled with 3M or 1M KCl. Somatic action potentials (APs) were antidromically evoked by dorsal root stimulation with single rectangular pulses (0.03 ms duration for A-fiber neurons or 0.3 ms for C-fiber neurons). The electrical threshold (the minimum stimulus (in volts) applied to the dorsal root that evoked a somatic AP) was measured. The stimulus intensity (up to 25 V) was adjusted to twice threshold for A-fiber neurons and between 1 and 1.5 times threshold for C-fiber neurons. As reported previously (Djouhri et al., 2006), spontaneous firing/activity (SA) which is the ongoing firing in the absence of any known stimulus, was recoded (when present) before modality testing to avoid the search stimuli influencing such firing. In all neurons, the assessment period for SA was initially 2 min. The recording time was extended up to 5 min for neurons exhibiting SA during this initial observation period to calculate the rate of SA. SA rate was calculated by counting the number of action potentials during the recording period.

Conduction Velocity, Action Potential Recordings, and Selection Criteria

The conduction velocity (CV, m/s) of each neuron was calculated by dividing the conduction distance between the recording and stimulating sites by the latency to onset of the evoked AP. Neurons were classified according to their dorsal root CVs as C ($\leq$ 0.8m/s), Aδ (1.5–6.5 m/s) or Aα/β (>6.5 m/s) (see Fang et al., 2002). These borderlines were relatively low, for reasons discussed previously including inclusion of utilization time (Djouhri and Lawson, 2001). As reported previously (e.g., Fang et al., 2002; Djouhri et al., 2018), APs were recorded online with a CED (Cambridge Electronics Design) 1401 plus interface and the spike II programs from CED and were subsequently analyzed offline using CED Spike II program. For each neuron, various variables were measured as described previously (see (Djouhri et al., 2012)). These include CV, resting membrane potential (Em), durations of AP at base, rise time (RT) and fall time (FT) as well as AP height and AP overshoot. AHP duration to 80% recovery (AHP80%) and AHP amplitude (between Em and maximum AHP depth). were also measured. Neurons were included in the analysis only if their Ems were equal to, or more negative, than −40 mV, and an AHP.

Sensory Receptive Properties

The sensory receptive properties of DRG neurons were identified using natural innocuous and noxious mechanical and thermal stimuli as described previously (Fang et al., 2005; Djouhri et al., 2018). Briefly, non-nociceptive neurons including low threshold mechanorecptive (LTMs) were those units that responded to non-noxious mechanical stimuli including light brushing of limb fur with a fine paint-brush, skin contact and light pressure with blunt objects. Only cutaneous Aβ-LTMs were included in the current study; they were classed as slowly adapting units or rapidly adapting units (see Fang et al., 2005; Djouhri et al., 2018). Slowly conducting C-, Aδ-fiber LTMs were not encountered in the present study. Nociceptive neurons were those that failed to respond to the non-noxious mechanical stimuli but responded either to noxious mechanical stimuli (applied with a needle, fine forceps or coarse toothed forceps) only, or to both noxious mechanical and noxious heat stimuli (hot water at 50–65°C applied with a syringe). These are referred to as C-mechano-sensitive nociceptors. C-mechano-insensitive nociceptors were not included in the present study.

Statistical Tests

The behavioral data are normally distributed (Shapiro–Wilk normality test) and are therefore presented as the mean ± SEM. Comparisons between values before and after STZ treatment were made with paired *t*-tests (**Figure 1**). Comparisons of percentage change were made using the Fisher exact test (**Figure 2**). Most of the electrophysiological data (not normally distributed) are presented as medians and compared with the nonparametric Mann–Whitney *U* test (**Figures 3**, **4**). All tests were made using GraphPad Prism software, version 8 (GraphPad, San Diego, CA, United States), and were two-tailed. Values of $P < 0.05$ were considered significant. Statistical significance: $^{*}P < 0.05$, $^{**}P < 0.01$, and $^{***}P < 0.001$.

RESULTS

STZ Rats Exhibit Behavioral Sings of Mechanical and Heat, but Not Cold, Hypersensitivity or Spontaneous Pain

We have previously shown that STZ-diabetic rats exhibit behavioral signs of mechanical and heat hypersensitivity, but not cold hypersensitivity or spontaneous/ongoing pain (Djouhri et al., 2019). To confirm that the STZ-rats on which the present electrophysiological experiments were conducted also show behavioral indices of DPNP, we assessed pain behaviors in 10 rats including 7 STZ-rats from which the spontaneously firing Aβ-LTMs were recorded (see below). Consistent with our previous study (Djouhri et al., 2019), we found 5 weeks post-STZ that all STZ-rats exhibited: (1) significant decreases in the mean PWT and PWL ($P < 0.01$) indicating that they developed behavioral signs of mechanical and heat

hypersensitivity respectively (**Figure 1**), and (2) no behavioral signs of cold hypersensitivity or spontaneous/ongoing pain (data not shown).

In vivo Intracellular Voltage Recordings in Control and STZ Rats

In vivo intracellular voltage recordings were made from 125 physiologically identified DRG neurons that met the acceptance criteria defined in the methods. Only C-mechano-sensitive nociceptors, Aβ-nociceptors and cutaneous Aβ-LTMs were included in the present study. Other subtypes were either not included (e.g., Aα/β-muscle spindle afferent neurons) or not encountered including C-LTMs, C-cooling, Aδ-nociceptors and Aδ-LTMs. Of the 125 neurons recorded, 67 neurons (20 C-nociceptors, 20 Aβ-nociceptors, and 27 cutaneous Aβ-LTMs) were recorded from L4/L5 DRGs in control rats, and 58 neurons (15 C-nociceptors, 13 Aβ-nociceptors, and 30 cutaneous Aβ-LTMs) were recorded from STZ rats.

STZ Induces Spontaneous Firing in Aβ-Nociceptors and Aβ-LTMs but Not C-Mechanosensitive Nociceptors

None of control C-nociceptors (0/20), Aβ-nociceptors (0/20) or cutaneous Aβ-LTMs (0/27) exhibited spontaneous activity (SA). Of the STZ neurons, none of the C-nociceptors (0/15) fired spontaneously, but 23% (7/30) and 15% (2/13) of cutaneous Aβ-LTMs and Aβ-nociceptors showed SA, respectively (**Figure 2**). **Figure 2** also shows example records of three typical Aβ-LTMs with SA. These neurons fired spontaneously at a rate of 0.15 Hz (**Figure 2A**), 0.53 Hz (**Figure 2B**), and 0.59 Hz (**Figure 2C**). As shown in **Figure 2D** the incidence of Aβ-LTMs, but not Aβ-nociceptors with SA is significant ($P < 0.05$ Fisher exact test). The median SA rate for the whole sample of Aβ-LTMs was 0.59 Hz (**Figure 2E**).

Activation of K_v7 Channels With Retigabine Suppressed STZ-Induced SA in Aβ-LTMs

We have recently shown that retigabine given intraperitoneally at a dose of 15mg/kg attenuated mechanical hypersensitivity in STZ rats (Djouhri et al., 2019). Given that PNP is due partly to SA in DRG neurons (see section "Introduction"), we sought to determine whether activation of K_v7 channels with retigabine modulates SA in Aβ-LTMs that we see in STZ-rats. Interestingly, we found that intravenous administration of retigabine at a dose of 6 mg/kg substantially reduced SA rate in all Aβ-LTMs examined ($n = 7$) as illustrated for the three Aβ-LTMs shown in **Figures 2A–C**. Indeed, 15 min after retigabine injection, the rate of SA in the neuron shown in **Figure 2A** was reduced by ∼80% (from 0.15 to 0.03 Hz), whereas in the other two neurons, the SA rate was reduced by 58% (from 0.53 to 0.22, **Figure 2B**) and 91% (from 0.59 to 0.05 Hz **Figure 2C**). The median SA rate for the whole sample of Aβ-LTMs tested was significantly ($P < 0.01$) reduced by ∼85% (from 0.59 to 0.09 Hz) 15 min after retigabine administration (**Figure 2E**). Only one of the two spontaneously firing Aβ-nociceptors was examined for the effects of retigabine; its SA rate was also reduced (by ∼70%) 15 min after by retigabine injection (not shown). The other Aβ-nociceptive neuron was lost before testing.

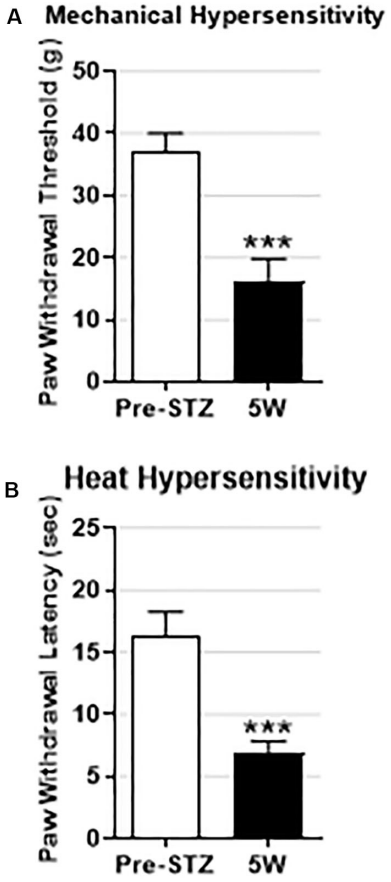

FIGURE 1 | Behavioral signs of mechanical and heat hypersensitivity in STZ-diabetic rats. Data are presented as mean ± SEM. STZ treatment significantly decreased the mean paw withdrawal threshold (PWT) **(A)** and the mean paw withdrawal latency (PWL) **(B)** in STZ rats ($n = 10$) 5 weeks post-STZ. The decrease in both PWT and PWL was highly significant ($P < 0.001$) indicating that the STZ-treated rats developed mechanical and heat hypersensitivity. Comparisons are between values before STZ treatment (pre-STZ, *open bars*) and 5 weeks post-STZ (5W, *black bars*). Statistical tests were made with paired *t*-test. The level of statistical significance is: $^{***}P < 0.001$.

Retigabine Causes Membrane Hyperpolarization in Spontaneously Active Aβ-LTMs

We compared resting membrane potential (Em) in STZ Aβ-LTMs with those of control Aβ-LTMs because EM could influence SA. As shown in **Figure 2F**, there was no significant difference in the median Ems of Aβ-LTMs between STZ and control rats. However, the Ems of Aβ-LTMs were significantly hyperpolarized 15 min after retigabine administration ($P < 0.001$, paired *t*-test). The median Em decreased from −51 to −71 mV

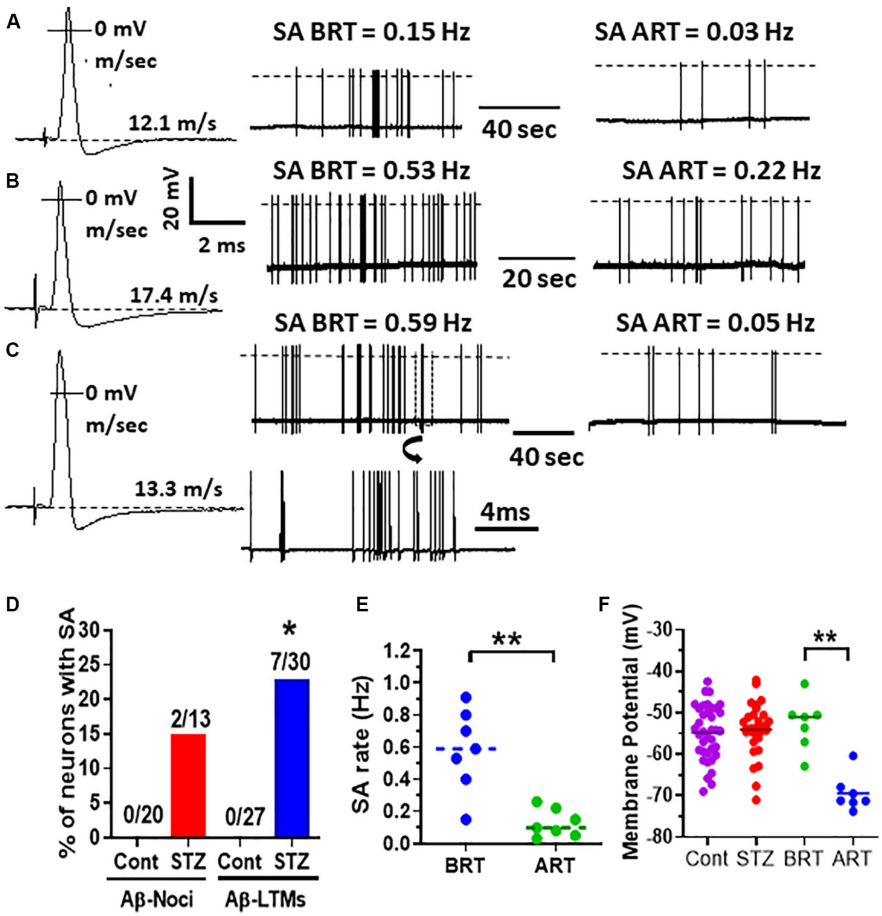

FIGURE 2 | Effects of retigabine on spontaneous activity (SA) and membrane potential (Em) in Aβ-LTMs in STZ rats. Shown in panels **(A–C)** are example records of three typical spontaneously active Aβ-LTMs recorded from STZ rats before and 15 min after systemic administration of retigabine (6 mg/kg, i.v.). The left traces **(A,B** and **C,B)** are somatic APs evoked by dorsal root electrical stimulation and recorded intracellularly from these three Aβ-LTMs; the CV (m/s) of each neuron is given above the Ems shown by dotted lines. The middle traces in panels **(A–C)** are original records of these neurons firing spontaneously at different rates before retigabine administration (BRT). The traces on the right in panels **(A–C)** illustrate that 15 min after retigabine (ART), the SA rate of these neurons was reduced from 0.15 to 0.03 Hz, 0.53 to 0.22 Hz, and 0.59 to 0.05 Hz, respectively. Shown below the middle trace in panel **(C)** is part of the trace shown in panel **(C)** (in a box) on an expanded time scale (note different time scales). Panel **(D)** shows that the percentage of Aβ-LTMs with SA (but not Aβ-nociceptors) is significantly greater (Fisher exact test, $P < 0.05$) than that of control Aβ-LTMs. Panel **(E)** shows that the median SA rate (0.59 Hz) for the whole sample of Aβ-LTMs tested ($n = 7$) was significantly ($P < 0.01$) reduced to 0.09 Hz 15 min after retigabine (ART) administration. Panel **(F)** shows that retigabine (6 mg/kg, i.v.) caused a highly significant decrease (hyperpolarization) in the median resting membrane potential (Em) of the Aβ-LTMs in STZ rats ($P < 0.001$, paired t-test). Note that there was no significant difference in the median Em between STZ and control Aβ-LTMs. The voltage and time scales to the right of AP shown in panel **(B)** are for all three evoked APs. The dotted lines on the traces indicate AP overshoot. $^*P < 0.05$; $^{**}P < 0.01$.

(**Figure 2F**). Retigabine had no significant effects on other AP variables in Aβ-LTMs (**Supplementary Figure S1**).

STZ Induces Decreased Electrical Thresholds in Aβ-but Not C-Nociceptors

To avoid the risk of sensitizing and/or losing the recorded DRG neurons, we did not measure their mechanical thresholds (see section "Discussion"). However, we compared the dorsal root electrical thresholds of control and STZ C-and Aβ-nociceptors, and found that the median electrical threshold of Aβ-nociceptors (**Figure 4A**) (but not C-nociceptors, **Figure 3A**) was significantly ($P < 0.05$) lower than that of control Aβ-nociceptors.

STZ Induces Other Changes in Electrophysiological Properties of C-and Aβ-Nociceptors and Aβ-LTMs

Several changes in electrophysiological variables were found in both C-and Aβ-nociceptors in STZ-rats. These include significant decreases in: (1) AP and rise time (RT) durations in C-nociceptors (**Figures 3F,G**) and Aβ-nociceptors (**Figures 4F,G**) and (2) AHP duration and amplitude in Aβ- nociceptors (**Figures 4H,I**). The decreased AP duration in both C-and Aβ-nociceptors was largely due to a significant decrease in the duration of RT (**Figures 3G**, **4G**) but not in fall time (data not shown). There was no significant changes in the other variables measured including CV, Em, AP fall time, AP amplitude, AP

overshoot and electrical threshold exhibited in C-nociceptors (**Figure 3**). However, there was a highly significant ($P < 0.001$) decrease (by 80%) in the median electrical threshold in Aβfiber nociceptors (**Figure 4A**). Furthermore, as shown in **Figure 4** there was significant decreases in the CV, AP duration, RT AHP duration and AHP amplitude in Aβ-nociceptors. We also examined whether the aforementioned variables also change in subtypes of cutaneous Aα/β-LTMs. The significant changes found in cutaneous Aβ-LTMs (grouped together) were decreased CV, AHP duration and AHP amplitude (**Supplementary Figure S1**). The faster AP and AHP kinetics and decreased AHP amplitude induced by STZ in A-fiber nociceptive and LTMs are likely to cause repetitive firing in these neurons resulting in increased afferent input to the CNS.

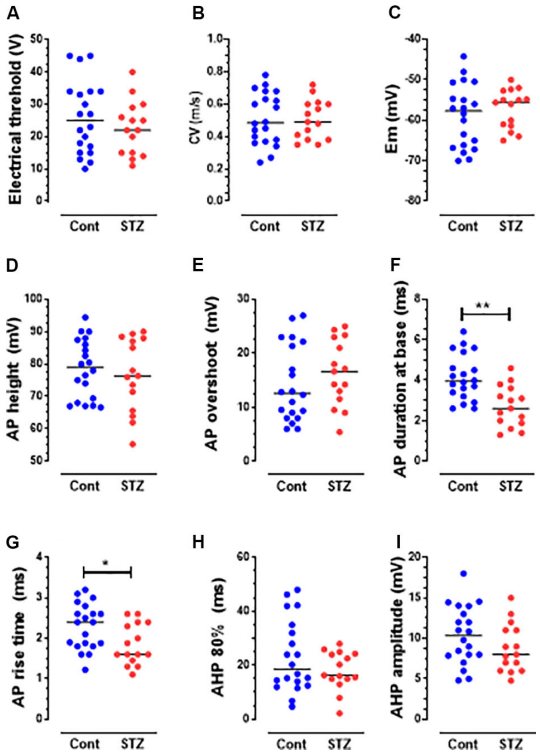

FIGURE 3 | Changes in AP variables in C-fiber mechano-sensitive nociceptors in STZ rats. The graphs **(A–I)** show scatterplots of variables measured 5 weeks post-STZ. These variables are: electrical threshold **(A)**, CV **(B)**, Em **(C)**, AP height **(D)**, AP overshoot **(E)**, AP duration at base **(F)**, Rise time (RT) **(G)**, AHP duration (AHP 80%, **H**) and AHP amplitude **(I)**. Each dot in these graphs and in those shown in **Figure 4** represents a value from one neuron. Medians are superimposed. Note the significant decreases in the durations of AP **(F)** and RT **(G)**, but not in other variables. Comparisons between medians in columns 1 (control, blue dots) and column 2 (STZ, red dots) were with the Mann–Whitney *U* test. The level of statistical significance is as follows: $^{*}P < 0.05$; $^{**}P < 0.01$.

DISCUSSION

We report several novel electrophysiological changes in Aβ-LTMs, and C-and Aβ-nociceptors in STZ-rats that are likely to contribute to DPNP pathogenesis. These include: (1) increased incidence of SA in Aβ-LTMs that may result in dysesthesias/paresthesias associated with DPNP, and (2) faster AP and AHP kinetics, and reduced electrical thresholds (C-and/or Aβ-nociceptors) that may lead to their repetitive firing and sensitization respectively, and thereby contribute to development of DPNP. Furthermore, we found that activation of K_v7 channels with retigabine suppressed STZ-induced SA, and caused membrane hyperpolarization in Aβ-LTMs, suggesting that the reduction in SA rate was a direct consequence of the hyperpolarizing effects of retigabine.

We used the STZ model, a well-established model of DPNP, that has been shown by numerous studies to exhibit long lasting behavioral signs of DPNP including mechanical and heat hypersensitivity (see Djouhri et al., 2019 and references therein). Consistent with those studies and with our recent study (Djouhri et al., 2019) we found that STZ-diabetic rats developed mechanical and heat hypersensitivity 5 weeks post-STZ. However, unlike other models of PNP such as those induced by traumatic nerve injury or chemotherapy that exhibit spontaneous/ongoing pain behavior and cold hypersensitivity (Djouhri et al., 2006, 2012; Al-Mazidi et al., 2018), we found that STZ-diabetic rats do not show these behaviors, in agreement with our recent study (Djouhri et al., 2019). It is noteworthy, however, that STZ model validity as a model of DPNP was challenged by a number of investigators (Romanovsky et al., 2004; Cunha et al., 2009; Bishnoi et al., 2011).

One of the interesting and novel findings of the present study is that Aβ-LTMs, but not C-mechanosensitive nociceptors, exibited signficant SA in STZ rats. Serra and his co-workers (Serra et al., 2012) also found, using microneurographic recordings from patients with diabetic neuropathy and STZ rats, significant SA in C-mechanoinsensitive, but not C-mechanosensitive nociceptors, but they did not record from afferent A-fibers. Other studies that investigated the impact of diabetes on excitability of primary afferent neurons/fibers have been inconsistent. Indeed, some studies reported that SA occurs almost exclusively in C-fibers in diabetic BB/Wistar rats (Burchiel et al., 1985), while other studies found no SA in this subtype of afferent fibers in STZ rats (Ahlgren et al., 1992; Chen and Levine, 2001). A significant increase in incidence of C-fibers with SA but not in Aδ-or Aβ-afferents was also reported by another study (Khan et al., 2002). However, these co-workers found that all CV groups in STZ-rats exhibited a significant increase in SA frequency and lower activation thresholds and augmented responses to mechanical stimuli. In contrast, another study (Chen and Levine, 2001) found no significant change in mechanical thresholds in STZ-diabetic rats. The causes for the apparent discrepancy between these various studies are not clear, but might be due to differences in the nerve type used for recordings, rat strains, time interval post-STZ and/or different recording methodologies.

Another interesting finding of the present study is that activation of K_v7 channels with retigabine caused membrane hyperpolarization and profound suppression of SA in Aβ-LTMs. These findings suggest that retigabine exerts its anti-allodynic effects in STZ rats (Djouhri et al., 2019) by causing membrane

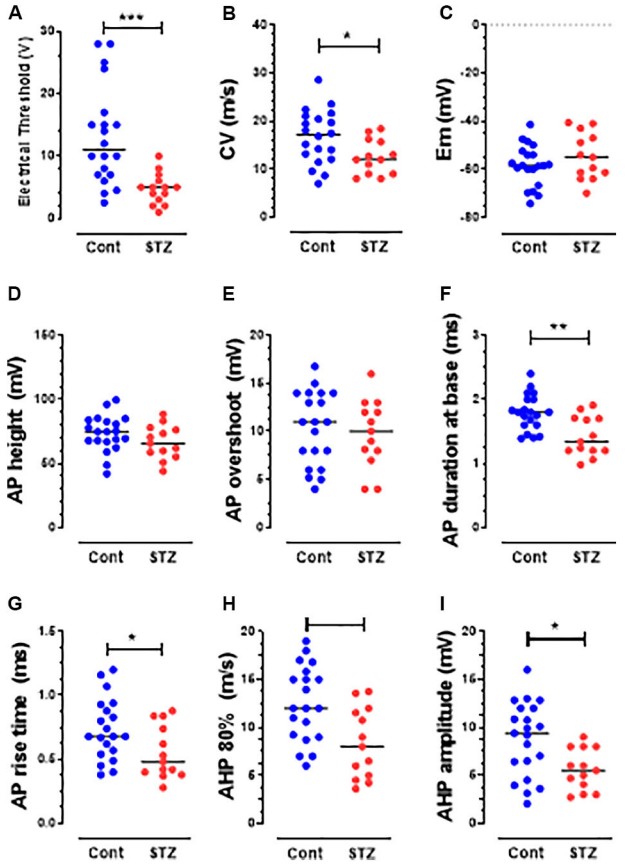

FIGURE 4 | Changes in AP variables in Aβ-nociceptors in STZ rats. The variables shown are the same as those shown in **Figure 3**. Note the significant decreases in the CV **(B)**, durations of AP **(F)**, RT **(G)**, and AHP **(H)** and in AHP amplitude **(I)**. Details are as in **Figure 2**. Note that there was no significant change in the other variables: electrical threshold **(A)**, resting membrane potential **(C)**, AP height **(D)**, AP overshoot **(E)** and afterhyperpolarization duration to 80% recovery **(H)**.

hyperpolarization in this subpopulation of DRG neurons. Retigabine has also been shown to induce membrane hyperpolarization in several neuronal types, including DRG (Passmore et al., 2003) and spinal cord (Rivera-Arconada and Lopez-Garcia, 2005) neurons, as well as axotomized afferent neurons in mice (Roza and Lopez-Garcia, 2008). The hyperpolarizing effect of retiagbine is likely to be due to a shift in the K^+ channel opening to more negative potentials (Rundfeldt and Netzer, 2000; Tatulian et al., 2001; Schwarz et al., 2006; Vervaeke et al., 2006). Although previous studies have implicated Aβ-afferent neurons (Xu et al., 2015), but not capsaicin-sensitive C-nociceptors (Khan et al., 2002) in STZ-induced mechanical hypersensitivity in mice, our current findings extend those findings and show that the functional identity of those Aβ-afferent neurons, at least in the rat, is Aβ-LTMs and probably not Aβ-nociceptors.

Retigabine has also been shown to block or reduce: (1) SA induced by saphenous nerve injury in almost all C-fibers and two putative Aβ-LTMs tested (Bernal et al., 2016), (2) SA in small dissociated DRG neurons following spinal cord injury (Wu et al., 2017), and in axotomized sensory fibers (Roza and Lopez-Garcia, 2008), (3) excitability of C- fibers in humans suffering from polyneuropathy (Lang et al., 2008), and (4) C- and Aδ-fiber discharges induced by heat stimuli (see (Brown and Passmore, 2009)). It is known that retigabine works by activating Kv7 channels mediating the low threshold and non-inactivating outward K^+ (M) current that results from homo- or heteromeric assemblies of KCNQ proteins (Brown and Adams, 1980; Jentsch, 2000). The exact site of retigabine action remains to be determined, but it could be any of the anatomical compartments of DRG neuron because: (a) Kv7 channels are expressed in the somata of DRG neurons, and in their peripheral and central terminals (see (Du et al., 2018)), and (b) retigabine effects have been described at the nodal membrane of myelinated axons in peripheral nerve (Devaux et al., 2004; Schwarz et al., 2006) as well as at the somata level and at peripheral and central terminals of primary afferent neurons (see (Brown and Passmore, 2009).

It is noteworthy that retigabine exhibits non-Kv7 channel effects including positive allosteric modulation of GABA subtypes as well as blockade of voltage-gated Ca^{2+} and Kv2.1 channels (see Stas et al., 2016 and refrences therein). The Kv7 channel inhibitor XE991 also has been shown to have off-target effect on Na^+ channels (Sun et al., 2019). Therefore, the possibility that changes in neuronal excitability caused by these Kv7 channels modulators are due to their non-Kv7 channel effects cannot be excluded. To ensure that the observed effects of retigabine on SA are mediated by K_v7 channels, ideally one should conduct further experiments using a K_v7 inhibitor such as XE991 to show that the effects of retigabine on SA in Aβ-LTMs are prevented by pre- or co-treatment with a K_v7 channel blocker. However, since XE991 has been found to induce repetitive AP firing in rat lumbar DRG neurons (Barkai et al., 2017), administration of XE991 before or with retigabine is likely to induce SA in non-spontaneously firing DRG neurons. This would make interpreting the findings of such experiments very difficult. Nevertheless, further experiments are required to determine whether the other electrophysiological changes in Aβ-nociceptors and Aβ-LTMs including changes in AP and AHP variables are mediated by KV7 channels. However, the findings of such experiments should be interpreted with caution because, as noted above, both retigabine and XE991, the most widely used modulators of KV7 channels, have off-target effects. Indeed, XE991 may not be an ideal compound to evaluate the influence of blocking channels on nerve excitability, as suggested previously (Sun et al., 2019).

Our current findings of changes in AP and AHP variables in Aβ-nociceptors or Aβ-LTMs are in agreement with those of a previous *in vitro* study (Kriz and Padjen, 2003) that also reported other changes in Aβ-fibers from isolated sural nerves in STZ-rats. These *in vitro and in vivo* preclinical findings are consistent with the clinical findings of impaired perception of vibration (see Garrow and Boulton, 2006) which is known to be mediated by Aβ-fibers (e.g., Claus et al., 1993). Our results of decreased CV in Aβ-nociceptors in STZ rats which is likely to result for demyelination, are also in agreement with those of other animal studies (e.g., Chen and Levine, 2001) and

with clinical studies that showed slowing of CV in A-fibers in patients with DN (Herrmann et al., 2002). In contract, another clinical study reported a reduction in CV of C mechano-sensitive fibers, but not C-mechano-insensitive fibers in patients with DN (Orstavik et al., 2006). The findings that Aβ-LTMs exhibit SA in STZ-rats may result in unpleasant sensations (dysesthesias/paresthesias) experienced by many patients with DPNP. Furthermore, SA in primary afferent neurons is believed to trigger and/or maintain central sensitization (see e.g., Baron et al., 2010), promoting hypersensitivity to normally innocuous stimulus (allodynia). In the presence of central sensitization during PNP conditions, nerve impulses carried centrally from the periphery along Aβ-LTMs are believed to be amplified and acquire access to the central nociceptive system, and thereby contribute to mechanical hypersensitivity associated with PNP. Normally central sensitization is driven by inputs from C-nociceptors (see Latremoliere and Woolf, 2009; von Hehn et al., 2012), but during chronic pain states, Aβ-LTMs are thought to exhibit phenotypic changes that would render them capable of triggering or maintaining central sensitization (Liu et al., 2000). On the other hand, spontaneous firing in Aβ-LTMs is expected, under normal conditions, to reduce transmission of pain signals at the spinal cord level via the gate control mechanism (Melzack and Wall, 1965). However, it is possible that this inhibitory mechanism is overridden by facilitatory spinal mechanisms involved in chronic pain conditions.

One of the major strengths of this study is that it is the first *in vivo* study that investigated electrophysiological changes in different subtypes of physiologically identified DRG neurons. We believe this is important because, as noted above, subtypes of DRG neuron are likely to contribute to different aspects of DPNP. We also believe that it is important to investigate these DRG neurons *in vivo* in their native environment that changes during chronic pain states in a complex way that cannot be readily mimicked *in vitro* (see Djouhri et al., 2018). Indeed, loss *in vitro* of the chemical environment including target-derived trophic factors such as NGF and BDNF, and dissociation-induced damage of DRG neurons profoundly alters properties of these neurons including their normal electrophysiological values against which comparisons are made (Kerekes et al., 2000). One limitation of the present study is that we did not routinely measure the mechanical thresholds of neurons, but precise determination of thresholds requires application of more stimuli to tissues that increases the risk of losing the recording. Another potential limitation of our study is the use of the general anesthetic pentobarbital that my affect the excitability of DRG neurons via modulating some ion channels. However, changes in the excitability of DRG neurons that we see in STZ rats are unlikely to be due to effects of pentobarbital because it was used in both control and STZ rats and because pentobarbital has been shown to have negligible effects on excitability of cutaneous Aβ-mechanoreceptive afferents (Cheng et al., 2013).

In conclusions, we have shown, in an established rat model of DPNP, that Aβ-LTMs, but not C-mechanosensitive nociceptors, exhibit significant SA, and that activation of K_v7 channels with systemic retigabine causes membrane hyperpolarization and suppression of SA in this subpopulation of DRG neurons in STZ-rats. These findings suggest that K_v7 channels are involved in mechanisms of SA generation in Aβ-LTMs, and taken together with our previous findings of significant attenuation of mechanical hypersensitivity (allodynia) in STZ rats (Djouhri et al., 2019) suggest that retigabine exerts its antiallodynic effects probably by causing membrane hyperpolarization in Aβ-LTMs.

DATA AVAILABILITY STATEMENT

The datasets generated for this study are available on request to the corresponding author.

ETHICS STATEMENT

The experimental protocols were approved by the University of Liverpool Ethical review committee, and complied throughout with the UK Animals (Scientific Procedures) Act 1986.

AUTHOR CONTRIBUTIONS

LD designed the research, conducted some of the electrophysiological experiments, and wrote the first draft of the manuscript. AZ helped in analyzing the behavioral data, writing, editing, and revising the manuscript. TS helped in conducting the behavioral and electrophysiological experiments, writing, editing, and revising the manuscript. SA helped in writing, editing, and revising the MS. All authors approved final version of the manuscript.

FUNDING

This research work was supported by a Medical Research Council grant (G0700420) and a Ph.D. studentship from Biotechnology and Biological Sciences Research Council to LD.

ACKNOWLEDGMENTS

We thank staff at BSU of University of Liverpool for their technical support and help.

SUPPLEMENTARY MATERIAL

The Supplementary Material for this article can be found online at: https://www.frontiersin.org/articles/10.3389/fnins.2020.00530/full#supplementary-material

FIGURE S1 | Changes in AP variables in cutaneous Aβ-LTMs in STZ rats and the effects of retigabine on those variables in Aβ-LTMS with SA. The variables shown are the same as those shown in **Figure 3**. Note the significant decreases in the CV **(B)** and AHP duration **(H)** and AHP amplitude **(I)**. Note that administration of retigabine (6 mg/kg, i.v.) had not significant effects on all the variables. Details are as in **Figure 3**. Note that there was no significant changes in the other variables: electrical threshold **(A)**, AP height **(C)**, AP overshoot **(D)**, AP duration **(E)**, AP rise time **(F)**, and AP fall time **(G)**.

REFERENCES

Ahlgren, S. C., White, D. M., and Levine, J. D. (1992). Increased responsiveness of sensory neurons in the saphenous nerve of the streptozotocin-diabetic rat. *J. Neurophysiol.* 68, 2077–2085. doi: 10.1152/jn.1992.68.6.2077

Al-Mazidi, S., Alotaibi, M., Nedjadi, T., Chaudhary, A., Alzoghaibi, M., and Djouhri, L. (2018). Blocking of cytokines signalling attenuates evoked and spontaneous neuropathic pain behaviours in the paclitaxel rat model of chemotherapy-induced neuropathy. *Eur. J. Pain* 22, 810–821. doi: 10.1002/ejp.1169

Barkai, O., Goldstein, R. H., Caspi, Y., Katz, B., Lev, S., and Binshtok, A. M. (2017). The role of Kv7/M potassium channels in controlling ectopic firing in nociceptors. *Front. Mol. Neurosci.* 10:181. doi: 10.3389/fnmol.2017.00181

Baron, R., Binder, A., and Wasner, G. (2010). Neuropathic pain: diagnosis, pathophysiological mechanisms, and treatment. *Lancet Neurol.* 9, 807–819. doi: 10.1016/S1474-4422(10)70143-5

Bernal, L., Lopez-Garcia, J. A., and Roza, C. (2016). Spontaneous activity in C-fibres after partial damage to the saphenous nerve in mice: effects of retigabine. *Eur. J. Pain* 20, 1335–1345. doi: 10.1002/ejp.858

Bishnoi, M., Bosgraaf, C. A., Abooj, M., Zhong, L., and Premkumar, L. S. (2011). Streptozotocin-induced early thermal hyperalgesia is independent of glycemic state of rats: role of transient receptor potential vanilloid 1(TRPV1) and inflammatory mediators. *Mol. Pain* 7:52. doi: 10.1186/1744-8069-7-52

Brown, D. A., and Adams, P. R. (1980). Muscarinic suppression of a novel voltage-sensitive K+ current in a vertebrate neurone. *Nature* 283, 673–676. doi: 10.1038/283673a0

Brown, D. A., and Passmore, G. M. (2009). Neural KCNQ (Kv7) channels. *Br. J. Pharmacol.* 156, 1185–1195. doi: 10.1111/j.1476-5381.2009.00111.x

Burchiel, K. J., Russell, L. C., Lee, R. P., and Sima, A. A. (1985). Spontaneous activity of primary afferent neurons in diabetic BB/Wistar rats. A possible mechanism of chronic diabetic neuropathic pain. *Diabetes* 34, 1210–1213. doi: 10.2337/diab.34.11.1210

Chen, X., and Levine, J. D. (2001). Hyper-responsivity in a subset of C-fiber nociceptors in a model of painful diabetic neuropathy in the rat. *Neuroscience* 102, 185–192. doi: 10.1016/s0306-4522(00)00454-1

Cheng, J. W., Weber, A. I., and Bensmaia, S. J. (2013). Comparing the effects of isoflurane and pentobarbital on the responses of cutaneous mechanoreceptive afferents. *BMC Anesthesiol.* 13:10. doi: 10.1186/1471-2253-13-10

Claus, D., Mustafa, C., Vogel, W., Herz, M., and Neundorfer, B. (1993). Assessment of diabetic neuropathy: definition of norm and discrimination of abnormal nerve function. *Muscle Nerve* 16, 757–768. doi: 10.1002/mus.880160711

Cunha, J. M., Funez, M. I., Cunha, F. Q., Parada, C. A., and Ferreira, S. H. (2009). Streptozotocin-induced mechanical hypernociception is not dependent on hyperglycemia. *Braz. J. Med. Biol. Res.* 42, 197–206. doi: 10.1590/s0100-879x2009000200008

Devaux, J. J., Kleopa, K. A., Cooper, E. C., and Scherer, S. S. (2004). KCNQ2 is a nodal K+ channel. *J. Neurosci.* 24, 1236–1244. doi: 10.1523/JNEUROSCI.4512-03.2004

Djouhri, L., Fang, X., Koutsikou, S., and Lawson, S. N. (2012). Partial nerve injury induces electrophysiological changes in conducting (uninjured) nociceptive and nonnociceptive DRG neurons: Possible relationships to aspects of peripheral neuropathic pain and paresthesias. *Pain* 153, 1824–1836. doi: 10.1016/j.pain.2012.04.019

Djouhri, L., Koutsikou, S., Fang, X., McMullan, S., and Lawson, S. N. (2006). Spontaneous pain, both neuropathic and inflammatory, is related to frequency of spontaneous firing in intact C-fiber nociceptors. *J. Neurosci.* 26, 1281–1292. doi: 10.1523/JNEUROSCI.3388-05.2006

Djouhri, L., and Lawson, S. N. (2001). Increased conduction velocity of nociceptive primary afferent neurons during unilateral hindlimb inflammation in the anaesthetised guinea-pig. *Neuroscience* 102, 669–679. doi: 10.1016/s0306-4522(00)00503-0

Djouhri, L., Malki, M. I., Zeidan, A., Nagi, K., and Smith, T. (2019). Activation of Kv7 channels with the anticonvulsant retigabine alleviates neuropathic pain behaviour in the streptozotocin rat model of diabetic neuropathy. *J. Drug Target.* 27, 1118–1126. doi: 10.1080/1061186X.2019.1608552

Djouhri, L., Smith, T., Ahmeda, A., Alotaibi, M., and Weng, X. (2018). Hyperpolarization-activated cyclic nucleotide-gated channels contribute to spontaneous activity in L4 C-fiber nociceptors, but not Abeta-non-nociceptors, after axotomy of L5-spinal nerve in the rat in vivo. *Pain* 159, 1392–1402. doi: 10.1097/j.pain.0000000000001224

Du, X., Gao, H., Jaffe, D., Zhang, H., and Gamper, N. (2018). M-type K(+) channels in peripheral nociceptive pathways. *Br. J. Pharmacol.* 175, 2158–2172. doi: 10.1111/bph.13978

Fang, X., Djouhri, L., Black, J. A., Dib-Hajj, S. D., Waxman, S. G., and Lawson, S. N. (2002). The presence and role of the tetrodotoxin-resistant sodium channel Na(v)1.9 (NaN) in nociceptive primary afferent neurons. *J. Neurosci.* 22, 7425–7433. doi: 10.1523/JNEUROSCI.22-17-07425.2002

Fang, X., McMullan, S., Lawson, S. N., and Djouhri, L. (2005). Electrophysiological differences between nociceptive and non-nociceptive dorsal root ganglion neurones in the rat in vivo. *J. Physiol.* 565(Pt 3), 927–943. doi: 10.1113/jphysiol.2005.086199

Garrow, A. P., and Boulton, A. J. (2006). Vibration perception threshold–a valuable assessment of neural dysfunction in people with diabetes. *Diabetes Metab. Res. Rev.* 22, 411–419. doi: 10.1002/dmrr.657

Herrmann, D. N., Ferguson, M. L., and Logigian, E. L. (2002). Conduction slowing in diabetic distal polyneuropathy. *Muscle Nerve* 26, 232–237. doi: 10.1002/mus.10204

Hong, S., Morrow, T. J., Paulson, P. E., Isom, L. L., and Wiley, J. W. (2004). Early painful diabetic neuropathy is associated with differential changes in tetrodotoxin-sensitive and -resistant sodium channels in dorsal root ganglion neurons in the rat. *J. Biol. Chem.* 279, 29341–29350. doi: 10.1074/jbc.M404167200

Jagodic, M. M., Pathirathna, S., Nelson, M. T., Mancuso, S., Joksovic, P. M., Rosenberg, E. R., et al. (2007). Cell-specific alterations of T-type calcium current in painful diabetic neuropathy enhance excitability of sensory neurons. *J. Neurosci.* 27, 3305–3316. doi: 10.1523/JNEUROSCI.4866-06.2007

Jentsch, T. J. (2000). Neuronal KCNQ potassium channels: physiology and role in disease. *Nat. Rev. Neurosci.* 1, 21–30. doi: 10.1038/35036198

Kerekes, N., Landry, M., Lundmark, K., and Hokfelt, T. (2000). Effect of NGF, BDNF, bFGF, aFGF and cell density on NPY expression in cultured rat dorsal root ganglion neurones. *J. Auton. Nerv. Syst.* 81, 128–138. doi: 10.1016/s0165-1838(00)00115-6

Khan, G. M., Chen, S. R., and Pan, H. L. (2002). Role of primary afferent nerves in allodynia caused by diabetic neuropathy in rats. *Neuroscience* 114, 291–299. doi: 10.1016/s0306-4522(02)00372-x

Kriz, J., and Padjen, A. L. (2003). Intra-axonal recording from large sensory myelinated axons: demonstration of impaired membrane conductances in early experimental diabetes. *Diabetologia* 46, 213–221. doi: 10.1007/s00125-002-1026-z

Lang, P. M., Fleckenstein, J., Passmore, G. M., Brown, D. A., and Grafe, P. (2008). Retigabine reduces the excitability of unmyelinated peripheral human axons. *Neuropharmacology* 54, 1271–1278. doi: 10.1016/j.neuropharm.2008.04.006

Latremoliere, A., and Woolf, C. J. (2009). Central sensitization: a generator of pain hypersensitivity by central neural plasticity. *J. Pain* 10, 895–926. doi: 10.1016/j.jpain.2009.06.012

Lee-Kubli, C. A., and Calcutt, N. A. (2014). Painful neuropathy: mechanisms. *Handb. Clin. Neurol.* 126, 533–557. doi: 10.1016/B978-0-444-53480-4.00034-5

Liu, C. N., Wall, P. D., Ben-Dor, E., Michaelis, M., Amir, R., and Devor, M. (2000). Tactile allodynia in the absence of C-fiber activation: altered firing properties of DRG neurons following spinal nerve injury. *Pain* 85, 503–521. doi: 10.1016/s0304-3959(00)00251-7

Melzack, R., and Wall, P. D. (1965). Pain mechanisms: a new theory. *Science* 150, 971–979. doi: 10.1126/science.150.3699.971

Orio, P., Madrid, R., de la Pena, E., Parra, A., Meseguer, V., Bayliss, D. A., et al. (2009). Characteristics and physiological role of hyperpolarization activated currents in mouse cold thermoreceptors. *J. Physiol.* 587(Pt 9), 1961–1976. doi: 10.1113/jphysiol.2008.165738

Orstavik, K., Namer, B., Schmidt, R., Schmelz, M., Hilliges, M., Weidner, C., et al. (2006). Abnormal function of C-fibers in patients with diabetic neuropathy. *J. Neurosci.* 26, 11287–11294. doi: 10.1523/JNEUROSCI.2659-06.2006

Passmore, G. M., Selyanko, A. A., Mistry, M., Al-Qatari, M., Marsh, S. J., Matthews, E. A., et al. (2003). KCNQ/M currents in sensory neurons: significance for pain therapy. *J. Neurosci.* 23, 7227–7236. doi: 10.1523/JNEUROSCI.23-18-07227.2003

Polydefkis, M., Hauer, P., Sheth, S., Sirdofsky, M., Griffin, J. W., and McArthur, J. C. (2004). The time course of epidermal nerve fibre regeneration: studies

in normal controls and in people with diabetes, with and without neuropathy. *Brain* 127(Pt 7), 1606–1615. doi: 10.1093/brain/awh175

Rivera-Arconada, I., and Lopez-Garcia, J. A. (2005). Effects of M-current modulators on the excitability of immature rat spinal sensory and motor neurones. *Eur. J. Neurosci.* 22, 3091–3098. doi: 10.1111/j.1460-9568.2005.04507.x

Romanovsky, D., Hastings, S. L., Stimers, J. R., and Dobretsov, M. (2004). Relevance of hyperglycemia to early mechanical hyperalgesia in streptozotocin-induced diabetes. *J. Periph. Nerv. Syst.* 9, 62–69. doi: 10.1111/j.1085-9489.2004.009204.x

Roza, C., and Lopez-Garcia, J. A. (2008). Retigabine, the specific KCNQ channel opener, blocks ectopic discharges in axotomized sensory fibres. *Pain* 138, 537–545. doi: 10.1016/j.pain.2008.01.031

Rundfeldt, C., and Netzer, R. (2000). Investigations into the mechanism of action of the new anticonvulsant retigabine. Interaction with GABAergic and glutamatergic neurotransmission and with voltage gated ion channels. *Arzneimittelforschung* 50, 1063–1070. doi: 10.1055/s-0031-1300346

Schreiber, A. K., Nones, C. F., Reis, R. C., Chichorro, J. G., and Cunha, J. M. (2015). Diabetic neuropathic pain: Physiopathology and treatment. *World J. Diabetes* 6, 432–444. doi: 10.4239/wjd.v6.i3.432

Schwarz, J. R., Glassmeier, G., Cooper, E. C., Kao, T. C., Nodera, H., Tabuena, D., et al. (2006). KCNQ channels mediate IKs, a slow K+ current regulating excitability in the rat node of Ranvier. *J. Physiol.* 573(Pt 1), 17–34. doi: 10.1113/jphysiol.2006.106815

Serra, J., Bostock, H., Sola, R., Aleu, J., Garcia, E., Cokic, B., et al. (2012). Microneurographic identification of spontaneous activity in C-nociceptors in neuropathic pain states in humans and rats. *Pain* 153, 42–55. doi: 10.1016/j.pain.2011.08.015

Shun, C. T., Chang, Y. C., Wu, H. P., Hsieh, S. C., Lin, W. M., Lin, Y. H., et al. (2004). Skin denervation in type 2 diabetes: correlations with diabetic duration and functional impairments. *Brain* 127(Pt 7), 1593–1605. doi: 10.1093/brain/awh180

Skovso, S. (2014). Modeling type 2 diabetes in rats using high fat diet and streptozotocin. *J. Diabetes Invest.* 5, 349–358. doi: 10.1111/jdi.12235

Stas, J. I., Bocksteins, E., Jensen, C. S., Schmitt, N., and Snyders, D. J. (2016). The anticonvulsant retigabine suppresses neuronal KV2-mediated currents. *Sci. Rep.* 6:35080. doi: 10.1038/srep35080

Sun, H., Lin, A. H., Ru, F., Patil, M. J., Meeker, S., Lee, L. Y., et al. (2019). KCNQ/M-channels regulate mouse vagal bronchopulmonary C-fiber excitability and cough sensitivity. *JCI Insight.* 4:124467. doi: 10.1172/jci.insight.124467

Tatulian, L., Delmas, P., Abogadie, F. C., and Brown, D. A. (2001). Activation of expressed KCNQ potassium currents and native neuronal M-type potassium currents by the anti-convulsant drug retigabine. *J. Neurosci.* 21, 5535–5545. doi: 10.1523/JNEUROSCI.21-15-05535.2001

Vervaeke, K., Gu, N., Agdestein, C., Hu, H., and Storm, J. F. (2006). Kv7/KCNQ/M-channels in rat glutamatergic hippocampal axons and their role in regulation of excitability and transmitter release. *J. Physiol.* 576(Pt 1), 235–256. doi: 10.1113/jphysiol.2006.111336

von Hehn, C. A., Baron, R., and Woolf, C. J. (2012). Deconstructing the neuropathic pain phenotype to reveal neural mechanisms. *Neuron* 73, 638–652. doi: 10.1016/j.neuron.2012.02.008

Wu, Z., Li, L., Xie, F., Du, J., Zuo, Y., Frost, J. A., et al. (2017). Activation of KCNQ channels suppresses spontaneous activity in dorsal root ganglion neurons and reduces chronic pain after spinal cord injury. *J. Neurotrauma* 34, 1260–1270. doi: 10.1089/neu.2016.4789

Xu, Z. Z., Kim, Y. H., Bang, S., Zhang, Y., Berta, T., Wang, F., et al. (2015). Inhibition of mechanical allodynia in neuropathic pain by TLR5-mediated A-fiber blockade. *Nat. Med.* 21, 1326–1331. doi: 10.1038/nm.3978

Conflict of Interest: The authors declare that the research was conducted in the absence of any commercial or financial relationships that could be construed as a potential conflict of interest.

Advantages of publishing in Frontiers

OPEN ACCESS
Articles are free to read for greatest visibility and readership

FAST PUBLICATION
Around 90 days from submission to decision

HIGH QUALITY PEER-REVIEW
Rigorous, collaborative, and constructive peer-review

TRANSPARENT PEER-REVIEW
Editors and reviewers acknowledged by name on published articles

Frontiers
Avenue du Tribunal-Fédéral 34
1005 Lausanne | Switzerland

Visit us: www.frontiersin.org
Contact us: frontiersin.org/about/contact

REPRODUCIBILITY OF RESEARCH
Support open data and methods to enhance research reproducibility

DIGITAL PUBLISHING
Articles designed for optimal readership across devices

FOLLOW US
@frontiersin

IMPACT METRICS
Advanced article metrics track visibility across digital media

EXTENSIVE PROMOTION
Marketing and promotion of impactful research

LOOP RESEARCH NETWORK
Our network increases your article's readership